ELECTRIC ENERGY SYSTEMS THEORY:

# ELECTRIC ENERGY SYSTEMS THEORY:

## AN INTRODUCTION

OLLE I. ELGERD

T M H EDITION

**ELECTRIC ENERGY SYSTEMS THEORY : An Introduction**



**T M H Edition 1973**
Reprinted **1975**
Reprinted **1976**

The paper used in printing this book was made available by the Government of India at concessional rate.

*Printed in India by arrangement with McGraw-Hill, Inc. New York.*

This edition can be exported from India only by the Publishers, Tata McGraw-Hill Publishing Company Ltd.

Published by Tata McGraw-Hill Publishing Company Limited and Printed by Mohan Makhijani at Rekha Printers Pvt. Ltd., New Delhi-110020

TO
Margaret,
Erik,
Andy,
and
Lisa

Motto: Think MKS

# Preface

The United States electric utility industry rates number one in many respects:

With a total plant and equipment investment of about 90 billion dollars (1970 figure) it is the largest industry in the country and the world.

With an annual production figure of almost 2 trillion kilowatthours, it not only outproduces every other country in the world, but actually accounts for more than one-third of the total world production of electric energy.

It leads the world in peaceful use of the atom; as of this writing the industry has under development and construction more nuclear plant capacity than the rest of the world put together.

It is the only United States industry that has been able to maintain an average 7 to 8 percent annual growth rate for almost four decades, and from all indications will continue to expand at the same rate for the next three decades.

And yet, somewhere along the line, it has ended up at the bottom of the academic totem pole.

In 1970 only a handful of United States universities can claim well-established and modern programs in power systems engineering. In fact, most universities offer neither undergraduate courses nor graduate research opportunities in the field.

This situation has developed gradually since World War II. It would serve no useful purpose to try here to affix the blame.

The picture did not always look so dismal. During the thirties and forties most colleges offered good power programs, well attuned to the need of the time.† Some of today's power courses are actually remnants from those days. A large percentage of today's practicing power systems engineers is of pre-World War II vintage.

Since these engineers are leaving the scene through natural attrition, the elec-

† The terms "power" and "energy" are both in use and appear interchangeably in this book. The former has "historical" precedence, but since the electric utilities undoubtedly concern themselves with electric *energy*, we consider this latter term more proper.

tric utility industry will find itself in somewhat of a manpower crisis. And this happens at a time when the industry is in the midst of a "nuclear revolution," is encountering an "environmental barrier," and faces a whole new set of technological problems due to its ever-increasing power density.

Nowhere is the academic pariah role of the electric utility industry more glaringly obvious than in the textbook field. At a time when dozens of new texts are published annually in specialty areas like computer technology, control theory, networks, etc., a professor offering a course in electric energy systems theory must be content with undergraduate texts which are anywhere from ten to twenty years old.

On the assumption that a radically new teaching approach is long overdue in the energy systems field, the author set out to develop a set of class notes reflecting such a modern teaching philosophy. The present text grew out of these notes. Upon consulting a great many engineers and educators, it was possible to identify a set of desirable features which should characterize a modern undergraduate energy systems text. These are:

1. The main objectives of the electric energy system should be clearly presented against a background of the national energy situation and predicted future demands.
2. A *systems* approach should be followed, with primary emphasis placed on the essential overall operational features.
3. Mathematical models of all main system components should be included. The models should be accurate enough to be useful for both steady-state and dynamic systems studies.
4. A clear demonstration should be given of the interplay between the frequency, voltage, and real and reactive power flow variables which characterize the quasi-static steady-state operation of a system.
5. A thorough discussion must be included of the systems control problem.
6. All aspects of system stability should be given ample emphasis.
7. Fault analysis and unbalanced operation should be treated.

There are diverging opinions in regard to the need for inclusion of peripheral topics like

Distribution technology
Systems protection
Systems communication

In the final analysis they were all dropped for the simple reason of space limitations.

The end product is a *systems text* intended for use by the senior undergraduate and first-year graduate student. The reader is expected to have taken an



introductory circuits course, and it is desirable, but not necessary, to have had a machinery course. He should also have been exposed to Laplace transforms, elementary control theory, and linear differential equations.

Due to the complexity of even the smallest power system, it is possible to derive analytical solutions of system models only under the rarest of circumstances. It is therefore imperative to provide the reader with an ample repertoire of computer solution methods. Such methods have been presented in the form of computational flow charts. Most undergraduate students have taken programming courses and should have no problem in writing the necessary computer programs from these flow charts. However, a detailed computer program is presented in Appendix B for the important load flow analysis case.

Matrix analysis is used throughout the text. However, the simplest of matrix operations suffice, and they are summarized in Appendix A for those readers not familiar with this tool.

The complete emphasis on computer analysis methods is only one of many novel features of the text. The profusion of system variables which determine both the static and dynamic states of a power system† constitutes a formidable roadblock for the student who wishes to gain even an intuitive understanding of what goes on in the system. We have tried to remove this roadblock by making extensive use of simple analogs.

We have also tried to put order in the picture by the method (developed by control people) of classifying the vast number of system variables into "state," "control," and "disturbance" variables. We have attempted to clarify the cause-effect relationships by use of modern sensitivity analysis.

In the extensive chapter on system control, we have introduced the methods of optimum control and we have critically examined (and found flaws in) existing control practices. We have suggested alternative control strategies.

Linear graph theory, general programming, and use of state-variable models in formulating the stability problem are also novel in an undergraduate text.

The book can easily be covered in two semesters or three quarters. In some instances the material in Chapters 4 to 6 may be covered in depth in other electrical engineering courses, in which case these chapters may be skipped altogether.

Assistance and encouragement were received from many sources during the preparation of this manuscript. My colleague Professor Erv Priem tested the early versions of the manuscript in our undergraduate program. I had, also, the help of dedicated students, without which no project of this nature could have been completed. I remember with special pleasure and gratitude the many stimulating discussion sessions (many in canoe in the Florida backwoods) with Charles Fosha, Bob Sullivan, Charles Durick, Jim Dickenson, and Don Smith. These students have proofread the manuscript, tested the computer flow charts, obtained computer recordings, and suggested many improvements throughout the text.

† A simple two-bus system operating in steady state is characterized by 12 variables.

This book project is part of a broadly based program in electric energy engineering, jointly sponsored by the Florida Power and Light Co., Florida Power Corp., Tampa Electric Co., and Gulf Power Co. Much assistance in the form of data, feedback, and advice was obtained from these companies, and I wish, in particular, to acknowledge my indebtedness to Messrs. T. F. Thompson, T. L. Jones, W. C. Summers, A. N. Aldredge, Jr., J. K. Wiley, and G. E. Marks.

The harmonious climate in our department provided the proper academic setting, due in great measure to the energetic, diplomatic, and intelligent leadership of our chairman, Dr. Wayne Chen.

Miss Edwina Huggins typed the whole manuscript, and her expert work is fully appreciated.

**Olle I. Elgerd**

# Contents

# 1
# Introduction

*Your task is nothing less than the creation of a whole new civilized industrial technology to replace the brute machine that raised so much ecological hell.*

WALTER J. HICKEL
*Secretary of Interior*

(In a speech to the graduating class of Stevens Institute of Technology, May 1970.)

Electric energy systems engineering (EESE) is that special branch of electrical engineering which concerns itself with the technology of generation, transmission, and distribution of electric energy. The vast electric energy systems that span every modern nation represent the largest and most expensive of man-made systems. To the electric energy systems engineer whose job it is to design and operate them, they offer some of the most challenging problems to be found in any branch of engineering.

The objective of an electric energy system is simply stated: It shall generate electric energy in sufficient quantities at the most suitable generating locality, transmit it in bulk quantities to the load centers, and then distribute it to the individual customers in proper form and quality and at the lowest possible ecological and economic price.

## 1-1 ELECTRIC ENERGY—ITS IMPACT ON SOCIETY

To appreciate some of the problems that will face the electric energy systems engineer in the final third of the twentieth century, it is appropriate to look first at some of the characteristic features of the electric energy demand.

In Fig. 1-1 are plotted versus time in semilogarithmic scale the growth of the electric energy production and generating capacity in the United States for the last three decades, extrapolated to the year 1980.† The curves are straight lines, indicating that the electric energy demand is an *exponential* growth function.‡ An exponential time function has the property of constantly doubling its value at regular time intervals, in this case approximately every 10 years, which corresponds to an annual growth rate of about 7 percent. If we assume that this growth rate will persist, it means that we

† All the statistical data presented in this introductory chapter are obtained from Edison Electric Institute and apply to the U.S. electric utility industry.

‡ A function of this nature is held in great respect by most engineers and scientists since it signifies a situation that is of the *unstable*, or *runaway*, nature. Obviously, an exponential growth can never be permitted to prevail for more than a limited period of time. Sooner or later we must apply external control to avoid destructive consequences.

Our population growth, which greatly influences the growth of our energy consumption, is unfortunately also exponential. As we enter the last third of the century, we are being reminded in many ways of the conflicts between an exponentially growing society and its demands on a finite supply of environmental space and resources.

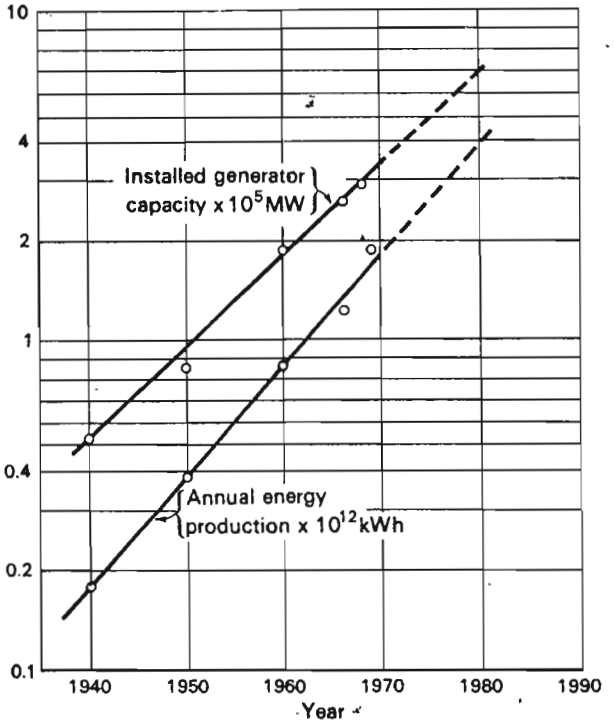


**Fig. 1-1** Growth of U.S. electric energy demand.



must, in the next 10 years, install as much generating capacity as was built since the beginning of the age of technology.

If we were to extrapolate the curves in Fig. 1-1 to the year 2000, we would conclude that we must increase the electric output by 700 percent, based upon the 1970 figure. However, due to increased attractiveness of electric energy compared with other energy forms (see next section), this figure is probably very conservative.

As of this writing (1970) the annual U.S. electricity demand is approaching 2 trillion kilowatthours. The installed generator capacity exceeds 300 gigawatts (GW), or about 1.5 kW for every U.S. citizen. What is the significance of these figures? To put them in proper perspective we will, in comparison, mention the fact that a person performing vigorous manual labor averages a power output of 25 to 50 W. We are therefore permitted to state that electric power constitutes the "muscle" of our industrialized society. Abundant availability of this commodity assures the strength of our industry—and thus our standard of living.

The United States, with only 6 percent of the world's population, accounts for 36 percent of the electric energy produced in the entire world.† It is interesting to note that the net output of goods and services of the United States likewise constitutes about 35 percent of the world's total. Certainly, there is a correlation between these two figures.

There is, however, another side to the coin. As sure as the abundant availability of electric energy has greatly contributed to the affluence of our nation it holds the potential for our own destruction.

As a nation we presently consume about one-third of the world's nonrenewable resources and produce about half of its waste products. And these rates increase exponentially!

No other nation can match our per capita impact on our environment—and the ability to upset nature's delicate ecological balance. It is estimated that this "ecological impact factor" of the average U.S. citizen is fifty times that of the citizen of India.

## 1-2 ELECTRIC ENERGY SOURCES

Two trillion kilowatthours is a figure of staggering proportions, but large as it is, it still constitutes only about one-fifth of the total U.S. annual energy consumption, 80 percent of which is still of the nonelectrical form. Transportation, home, and industrial heating fall in this latter category. It is estimated, however, that by the turn of the century, as a result of cheap nuclear power (see below) and stringent antipollution measures, these markets will "go electric." Imagine, for example, what the electric

† Norway and Sweden have the highest per capita generations.

automobile will mean in annual energy. It is probably not unrealistic to predict that the electric share of our total energy consumption by the turn of the century will be in excess of 50 percent.

In view of these predictions, the U.S. electric energy demand by the year 2000 will probably be considerably in excess of what we would obtain by "linear" extrapolation of the curves in Fig. 1-1. Maybe a reasonable figure is 3000 GW of generating capacity and an annual energy production of 20 trillion kilowatthours.

From what energy sources will these fantastic amounts of electricity have to come? For a clue, let us see where we *presently* (1970) get it. As Fig. 1-2 shows, fossil fuels (coal, natural gas, and oil) make up the lion's

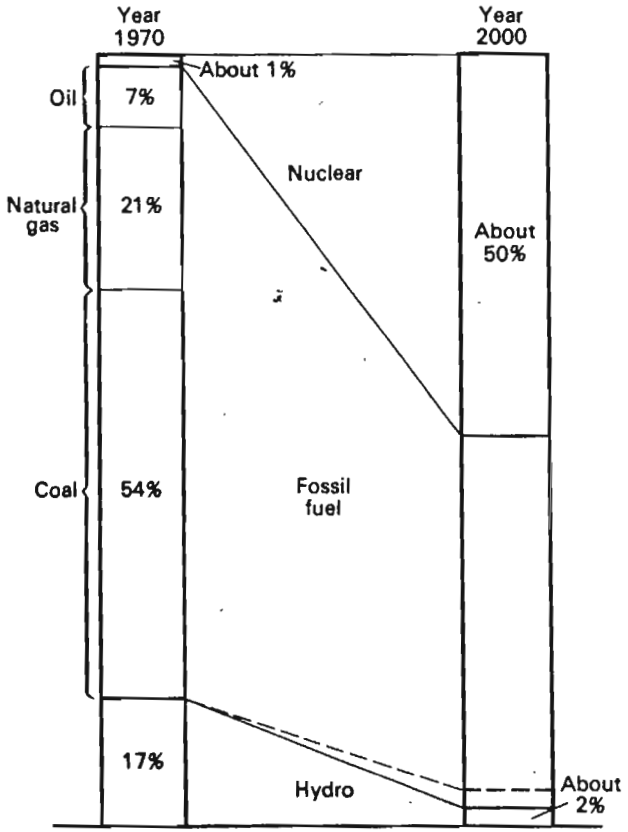


**Fig. 1-2** Relative importance of primary energy resources in the United States: present and predicted future figures. Note future dominance of nuclear energy and insignificance of hydropower. [Even if all remaining hydro resources were to be developed, hydropower would account for only 4 percent of the total in the year 2000 (dotted lines).]



share, with hydropower and nuclear power playing only secondary roles. To estimate the future trends, let us investigate each individual potential energy source.

### 1-2.1 HYDROPOWER

Historically, hydropowered generator stations played the major role as sources of electric energy. In many countries they still do. In our own nation we have harnessed, in 1970, close to half of our available hydro resources. It is estimated that the total hydro resources in the United States (not including Alaska) amount to about 130,000 MW. We are therefore talking about a very scarce resource indeed. Let us contemplate the following facts:

1. *The remaining undeveloped hydropower in the United States corresponds to only about two years' increase in our total electric demand.*
2. Development of the hydropower potential of a wild free-flowing river means a complete and permanent destruction of the river valley and a complete upset of the regional ecology.

At a time when an exploding population takes inventory of its shrinking supply of unspoiled wilderness *and at a time when alternative energy sources are available*, it must be judged as extremely poor and short-sighted engineering to contemplate further hydro development. Our country is fortunate to have at least half of its rivers essentially unspoiled. Let us keep them that way—because we can afford to.

### 1-2.2 FOSSIL FUELS

Coal, natural gas, and oil presently account for four-fifths of the total U.S. electric generation. With the exception of natural gas, which already is made available for power generation only on a rationed basis, fossil fuels are relatively abundant. The Department of Interior estimates that the "recoverable reserves" of coal, the present "workhorse," amount to about 830 billion tons. In comparison, the annual coal demand will be about 900 million tons by the year 1980.

The chemical energy stored in the fossil fuels is transformed into electric energy in steam-electric power plants. By burning the fuel in the combustion chamber, heat energy is released, and this energy is being used to produce steam in the boiler. The steam is passed through the steam turbine, where it gives off some of its energy in mechanical form. The steam turbine drives the electric generator.

The efficiency of the overall process is poor, considerably less than 50 percent. The heat losses in the combustion gases and the condenser cooling water dominate.

Whereas the poor efficiency can be tolerated, the *air* and *thermal pollution* problems associated with steam generation are of major proportion. The air pollutants are emitted via the exhaust gases,† and the thermal pollution is associated with the vast amounts of heat losses in the condenser cooling water. For example, a 1000-MW plant utilizes about 40 $m^3$ ($\approx$1300 $ft^3$) of coolant per second, with a temperature rise of 6 to 10°C. For a seaside plant the thermal pollution will probably have negligible effect on the aquatic life, but a large power plant on a small river or lake poses severe problems.

It should be added that both the air and thermal pollution problems are, in practice, solvable if sufficient capital is invested. Air pollutants *can* be removed, and the cooling water *can* be cooled in cooling towers. It should also be pointed out that because a steam plant is a "point source" for pollution, it is much more amenable to pollution control than the myriad of small pollution sources on our highways.

Strip mining of coal, if permitted to be performed with present standards, poses a potentially much greater environmental threat than air and thermal pollution. Serious massive damage is presently being done to the landscape of several of our Eastern states.

### 1-2.3 NUCLEAR POWER

Figure 1-2 indicates that the third type of energy source, nuclear energy, presently accounts for only about 1 percent of the electric production. This figure is very misleading, since the nuclear power is a latecomer to the arena. The most recent authoritative prediction indicates that by the year 1980 we shall have 150 GW of installed nuclear capacity. By the turn of the century it should actually be the dominant source—in fact, fossil fuel plants would probably then no longer be built.

In a nuclear plant the controlled nuclear reactor replaces the conventional boiler as the heat source. The heat released in the fission process is led via a primary coolant to a "steam generator," which is essentially a heat exchanger. The steam is then used in a "conventional" manner to produce electricity.

† Broadly classified, air pollutants consist of particulates and gases. In fossil-fueled power plants fly ash and polycyclic hydrocarbons constitute the important ingredients in the particulates group, oxides of sulfur and nitrogen in the gases. Generally, sulfur dioxide ($SO_2$) is considered the most troublesome agent. Sulfur is present in all fossil fuels in various quantities, and it is extremely hard to remove it from the fuel, particularly coal.

Sulfur dioxide will therefore appear in the stack emission, and after further oxidation to sulfur trioxide ($SO_3$) in the combustion and heat transfer processes, it will combine with atmospheric water $H_2O$ into sulfuric acid ($H_2SO_4$). This is an extremely active compound which poses serious health and material hazards.



The nuclear power has many advantages over fossil fuel:

1. It is perfectly air pollution–free.
2. The relatively small amount of nuclear fuel needed poses no transportation problems.
3. It compares very favorably with coal from an economic point of view.

Its greatest drawback is its potential for thermal pollution. In this respect it is about 30 percent worse than a conventional steam plant of comparable size. However, of all environmental threats posed by any practicable electric bulk power production process known, this is certainly the one we can most easily tolerate and protect against. Nuclear power thus stands out as our certain choice in the decades to come. It should, hopefully, completely replace all other methods within the next forty years, and remain our basic source of electricity until the controlled fusion process takes over, sometime next century—if homo sapiens still is around by that time.

## 1-3 THE STRUCTURE AND ECONOMY OF THE ELECTRIC ENERGY INDUSTRY

With the humble beginning of the installation of a waterwheel-driven generator by the Rochester (New York) Electric Light Co. in 1880, the U.S. electric energy industry, known also as the *electric utility industry*, has grown into the world's largest industry. The private segment of the electric utility industry represents about 12 percent of the total U.S. industrial investment. The structure of this industry is of a pluralistic nature, as can be expected in a nation that gives its citizens a wide range of choice. The overall industry is made up of four distinct ownership segments, representing more than 3600 separate subsystems, which vary greatly in size. Table 1-1 gives a breakdown. We note that more than three-fourths of the industry is privately owned. The great majority of the systems are small; actually, the 100 largest systems account for about 90 percent of the total generation.

**Table 1-1**

| *Ownership* | *Generating capacity, percent of total* |
|---|---|
| Investor-owned | 76 |
| Federal | 13 |
| Municipal (public) | 10 |
| Cooperative | 1 |

The size of capital investment is of such proportions that we cannot afford duplications of service, and the industry is therefore, in a sense, a monopoly. However, through regulatory bodies, the state and Federal governments have power to exert rate control.

For economical and technological reasons, to be discussed in more detail in later chapters, most of the systems are electrically interconnected into regional operating groups called *power pools*. Each individual power system within such a pool operates technically and economically independently, but is contractually tied to the other pool members in respect to certain generation and scheduling features. As the size, complexity, and energy density of the overall system increase, we shall see an increased trend toward pool operation.

It is obvious that the best geographical location of the generating plants would be close to the electrical *load centers*, i.e., the regions where the major energy demand exists. However, the locations of the primary conventional energy sources do not coincide with the nation's population centers, and we are therefore faced with the following choice:

1. Build the power plants close to the energy sources and then transport the electric energy to the load centers.
2. Build the power plants close to the load centers and transport the fuel from the source locality.

The electric transmission network makes the first alternative technically feasible. However, in reality, the actual choice will be based upon a combination of technical, economical, and environmental factors. As we will see later, the voltage level of a transmission line determines its energy transmission capacity. By constantly increasing the voltage level and physical length of our transmission grid, we are developing a "superhighway system" for large blocks of electric energy that more and more widens our choice in this respect.

It is also worthwhile to point out that the trend toward nuclear power will mean, in an increased number of cases, that we will find the power stations close to the population centers. This is due to the absence of atmospheric pollution, and also, of course, to the absence of a fuel-transport problem.

## 1-4 THE FUTURE OF EESE

What does the future hold in store for the electric energy systems engineer? Anybody venturing to author a book on energy systems theory must consider very carefully the trends of the technology, or he may very well end up with a product that is outmoded before it is put on the market. The author, on



consulting a large number of authoritative sources, makes the following predictions for the next thirty years.

1. The demand for electricity in the United States will increase at even a faster pace than the present as both new and presently nonelectric markets open up. By the year 2000 we should find a demand figure of, perhaps, 10 to 15 times the 1970 figure.
2. Nuclear power will outcompete all conventional primary energy sources.
3. The safety and control of a nuclear power station permits no error margins. The design and operation of a nuclear station is therefore very complex compared with a conventional power plant. For economical reasons the size of nuclear plants will therefore be very large (1000 MW and up), and this makes it impractical for small companies to stay in the generating business. The trend will therefore be to leave the generation to the big companies. To preserve fair rate schedules we will in all probability see more Federal control.
4. The three-phase generation and transmission system will continue to dominate. Transmission voltages will probably level off at around 1,000,000 V, the reason being that nuclear power makes it possible to place the generator stations close to the load centers.
5. Since the power densities will increase ten- to fifteenfold, the power lines will have to go underground in metropolitan areas.
6. A disadvantage of the pluralistic U.S. power system structure has been a tendency toward total regional control and self-sufficiency. With the present U.S. network, characterized by a very weak interconnected grid, we are not operating at maximum national efficiency, neither from an economical nor a safety point of view. It is hoped that the utility industry on its own initiative will develop plans for a continental control center and a continent-spanning grid system on par with the future load densities.
7. As the U.S. system grows in size, strength, and complexity, there will be a continued need to improve its stability. The present load frequency control strategy (Chap. 9) is not optimal, nor is it necessarily the best one in terms of large-scale disturbances. The author feels strongly that the whole question of system control should be made subject to a penetrating, unbiased study directed toward the objective of developing a dual-mode control system which is optimal both for small and large disturbances. (See discussion in Chap. 12.)

In conclusion, we can state unequivocally that there seems little likelihood that electric energy systems engineering is facing obsolescence. The modern energy systems engineer, however, must be cast in an entirely different mold than his predecessor. True, the objective of a power system

is the same in 1970 as it was in 1930, but the performance requirements, energy magnitudes, and the equipments are vastly different. Perhaps more important: modern society is dependent upon the uninterrupted electric service to a much higher degree. In fact, whereas a blackout in 1930 could be joked about, in 1970 it could spell disaster.

Ecological awareness is the one characteristic that will make the new generation of engineers—and particularly energy engineers—different from their predecessors. Too often in the past engineering projects were justified solely on economic criteria without regard for their impact upon the environment.

As the professed custodian for his nation's resources the engineer must take major responsibility for their optimum and balanced use.

## REFERENCES

1. "National Power Survey," pts. I and II, U.S. Government Printing Office, Washington D.C., 1964.
2. Federal Power Commission: "Prevention of Power Failures," vols. I–III, U.S. Government Printing Office, Washington, D.C., 1967.
3. Vogely, W. A., and W. E. Morrison: Patterns of U.S. Energy Consumption to 1980, *IEEE Spectrum*, September, 1967, pp. 81–86.
4. Edison Electric Institute: "Statistical Yearbook of the Electric Utility Industry," New York.
5. Hicks, B. C.: The Future of Energy Supply, *IEEE Spectrum*, October, 1966, pp. 82–84.,
6. Kusko, A.: A Prediction of Power System Development, 1968–2030, *IEEE Spectrum*, April, 1968, pp. 75–80.
7. Dillard, J. K., C. J. Baldwin, and N. H Woodley,: The Future Role of Breeder Reactors in Utility Planning, *IEEE Spectrum*, March, 1969, pp. 100–107.
8. Dubos, R.: "So Human an Animal," Charles Scribner's Sons, New York, 1968.

(References 1 and 2, although somewhat outdated, are highly recommended to those who wish to obtain a good background picture of the U.S. power situation. Reference 6 gives a very interesting and believable prediction to the year 2030. Reference 8 should be required reading for every U.S. engineer.)

# 2
# Fundamental Concepts of Electric Energy Systems Engineering

The electric communications engineer uses the medium of electricity for the purpose of transmitting data and messages, or in general, information. The vast information communications networks that today span our nation and the world are designed to meet certain minimum criteria in regard to:

1. Information-transmission capacity
2. Transmission quality
3. Reliability
4. Economy

The electric *energy* transmission systems are designed to meet certain minimum requirements in respect to:

1. Energy-transmission capacity
2. Transmission quality
3. Reliability
4. Economy

Obviously, there are many surface similarities between electric communication and energy systems engineering; however, these are only superficial, and any attempt to draw useful parallels between the two generally fails. This is due to the vast dissimilarities between the central physical commodities concerned, *information* and *energy*. The concept of information is vague and hard to define. Energy, on the contrary, is a well-defined and well-accepted physical concept. The reader is most certainly already well acquainted with the elementary aspects of electric energy, its various forms, the factors affecting its magnitude, etc. Since it will be subject to our continued attention throughout the book, it may be appropriate to review, at this time, some of its basic characteristics.

First, we point out that, for various reasons, we shall find it convenient on most occasions to turn our attention not to the energy $w$ itself, but to its *time rate*, or *power* $p$. By definition we have

$$p \triangleq \frac{dw}{dt} \quad \text{W} \tag{2-1}$$

A few words must be said about our choice of notation. We use lowercase symbols throughout† to indicate time functions or instantaneous values. The symbol $p$ therefore indicates the magnitude of electric power at the running moment $t$, and should therefore, strictly, be symbolized $p(t)$. However, we shall often prefer the shorter symbol $p$.

From Eq. (2-1) is obtained upon integration

$$w = \int_{t_0}^{t} p\, dt \quad \text{Ws (or J)} \tag{2-2}$$

Note that $w$ will depend upon the arbitrarily chosen initial time $t_0$. This is not the case with power, and constitutes the basic reason why we prefer its use.

The units for electric energy and electric power in the mks system (which is adhered to throughout the book) are wattsecond (Ws) and watt (W), respectively. These units are very small, and the more practical units kilowatt (kW), megawatt (MW), gigawatt (GW), and kilowatthour (kWh) are preferred. The conversion constants are as follows:

$$1 \text{ GW} = 10^3 \text{ MW} = 10^6 \text{ kW} = 10^9 \text{ W}$$

$$1 \text{ kWh} = 3.6 \times 10^6 \quad \text{Ws}$$

† Except for symbols representing electric and magnetic field vectors, in which instance it would be impractical to differ from the well-established practice of using capital-letter symbols.



## 2-1 THE FUNDAMENTAL POWER FORMULA—ELECTROMAGNETIC ENERGY

The entire technology of EESE is based upon the physical reality that it is possible to transform the "raw" energy forms available in nature into electric form, transmit this electric form of energy to the potential user, and then finally transform it back into useful energy forms of various types. These energy transformations take place often in a rather roundabout fashion.

Take, for example, the chemical energy stored in coal. In pulverized form the coal is mixed with air in the combustion chamber of the boiler, where the chemical energy is released into thermal, or heat, energy. In a sequence of heat exchangers, this thermal energy is transmitted to another medium, water, which upon absorption of the energy changes its phase into steam. The steam, upon passing through the turbine, gives off some of this thermal energy in *mechanical* energy. Finally, in the electric generator, the mechanical energy is transformed into *electric* energy.

In each of the above steps, the energy transformations take place at the expense of losses that may be of considerable size. In the process just described, the largest loss energies are found in the combustion gases emitted from the stack and in the condenser cooling water.

Practically 100 percent of the electric energy that is produced today is obtained from rotating generators, where the last energy-transformation step is mechanical to electrical. Intensive research efforts are being expended in *direct energy conversion* (DEC) methods. The outstanding feature of all DEC techniques is that one tries to eliminate the intermediate mechanical energy step and thus seeks to obtain electric energy *directly* from either thermal, solar, or chemical energy forms.

Although many DEC devices (thermoelectric, thermionic, fuel cells, MHD, and others) have found important applications in the low-power area, it is highly doubtful that they will compete the conventional rotating generator out of a market in the high-power field within the next two or three decades.

In this section we shall discuss the characteristics of the energy once it has reached the electric form. However, it is unimportant *how* it reached there. Our starting assumption is therefore the availability of a device, referred to as a *generator*, having a minimum of two output terminals, from which we are able to draw a *sustained* current $i$ at a *sustained* terminal potential $v$. We shall make the additional assumption that $v$ and $i$ are *quasi-static;* i.e., their variations are relatively slow, which in practice means that they should not contain frequency components in excess of a few kilocycles.

The *fundamental power formula* now states that the generator supplies energy at the rate

$$p = vi \quad \text{W} \tag{2-3}$$

If the generator is connected via two conductors to a *load*, as shown in Fig. 2-1*a*, then we haye, in fact, the simplest prototype of a *transmission system*. The only assumption we need to make at this time about the load is that it will "accept" the current $i$ at the voltage level $v$.

*It is perfectly proper to consider Eq.* (2-3) *as an elementary physical law, the validity of which is experimentally proved beyond doubt.* As often in physics, we may, of course, postulate "still simpler" elementary laws, and then try to derive the formula from these. If, for example, we postulate (as is commonly done in field theory) the so-called *Maxwell's field equations*, the above formula can be derived from these. From an engineering viewpoint this is really hairsplitting, and does not in any significant way add to one's understanding of the process in question.

Actually, we can give Eq. (2-3) added credibility if we view the process in Fig. 2-1*a* as a "charge-pumping" mechanism. The current represents as we know, the electric charge flow per time unit, and the generator is thus a "charge pump" that is capable of sustaining the flow $i$ against the pressure, or potential, $v$.

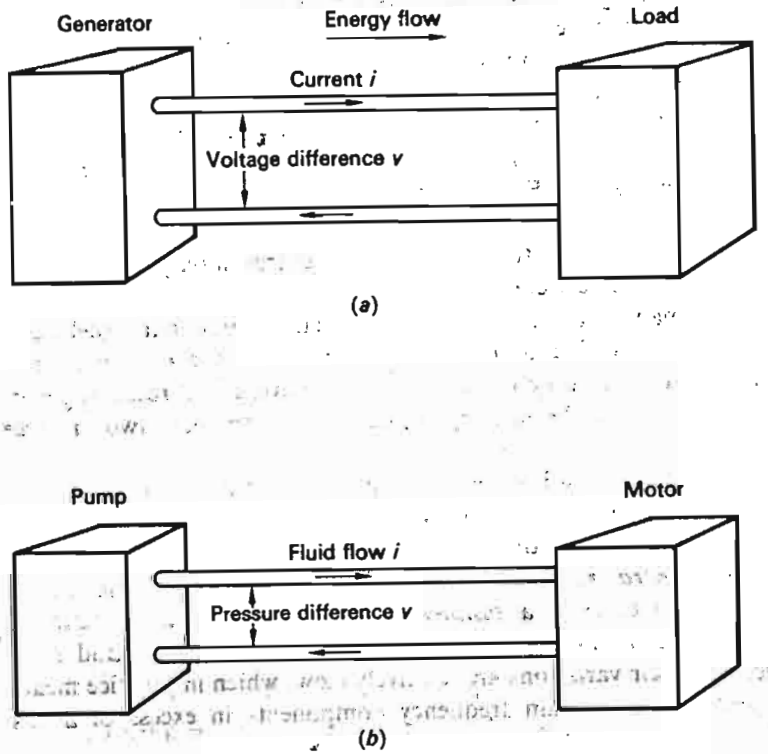


**Fig. 2-1** Elementary energy transmission systems: (*a*) Electric case; (*b*) hydraulic case.



The student may gain a still better feel for its meaning by drawing parallels with the hydraulic power transmission system in Fig. 2-1*b*. The electric conductors correspond to the hydraulic pressure lines carrying an incompressible fluid. The hydraulic pump, corresponding to the generator, supplies a fluid flow of $i$ m³/s and maintains a pressure difference of $v$ N/m². If the sectional area of the pressure lines is $A$ m², the fluid velocity will therefore be $i/A$ m/s, and the total force (as felt by the motor piston) $Av$ N. By using the formula

$$\text{Mechanical power} = \text{force} \times \text{velocity}$$

we obtain the following expression for the mechanical power transmitted by this system:

$$p_{\text{mech}} = Av \times \frac{i}{A} = vi \qquad \text{W} \tag{2-4}$$

i.e., the same result as in Eq. (2-3). There are, to be sure, fundamental differences between the two systems in Fig. 2-1*a* and *b*.

For example, there is no doubt that in the hydraulic system the energy transfer between the pump and motor actually takes place *inside* the pressure lines. We have no such guarantee in the electric transmission system. Although Eq. (2-3) places the emphasis on the *current* which no doubt is localized inside the conductors, the modern physical view tends to place the energy flow *outside* the conductors in the electromagnetic field that surrounds them. Supporters of this view delegate to the conductors the role of *waveguides*. If we accept this interpretation, we designate the transmitted energy as *electromagnetic* energy $w_{em}$. We would not, of course, expect to find the energy uniformly distributed in the outside space, but rather having a *volume density* that would increase in some proportion to the intensity of the field vectors. The phenomenon is beautifully and compactly described by the *Poynting vector* $\mathbf{P}$,

$$\mathbf{P} = \mathbf{E} \times \mathbf{H} \qquad \text{W/m}^2 \tag{2-5}$$

In this formula the vector symbols represent

$\mathbf{E}$ = electric field strength, V/m

$\mathbf{H}$ = magnetic field strength, A/m

The vector $\mathbf{P}$ defined by Eq. (2-5) evidently has a direction perpendicular to the plane containing $\mathbf{E}$ and $\mathbf{H}$ and a magnitude $|\mathbf{P}|$ equaling $|\mathbf{E}|\,|\mathbf{H}| \sin \alpha$, where $\alpha$ is the angle between $\mathbf{E}$ and $\mathbf{H}$. It has the dimension of watts per meter squared.

The interpretation of Eq. (2-5) is as follows:

The electromagnetic energy *travels*, or *radiates*, in a direction coinciding with the direction of $\mathbf{P}$. The amount of energy that penetrates a unit area

(oriented perpendicular to the radiation direction) per time unit is given by the magnitude $|\mathbf{P}|$.

To exemplify, let us apply the concept of electromagnetic energy radiation to the simple system in Fig. 2-1*a*. The electromagnetic field picture around the wires, which are assumed straight and relatively long, is depicted in Fig. 2-2. The magnetic field lines are actually perfect nonconcentric circles, and the electric field lines constitute segments of circles that are orthogonal to the magnetic ones.

Since $\mathbf{E}$ and $\mathbf{H}$ are both located in a plane perpendicular to the conductors, $\mathbf{P}$ will be directed along the wires and (following the rule of a vector cross product) toward the load. Due to the orthogonality of $\mathbf{E}$ and $\mathbf{H}$, the magnitude of $\mathbf{P}$ equals

$$|\mathbf{P}| = |\mathbf{E}|\,|\mathbf{H}| \qquad \text{W/m}^2$$

and since $\mathbf{E}$ and $\mathbf{H}$ have their largest intensities close to the conductors, the energy density is highest in the immediate neighborhood of the conductors,

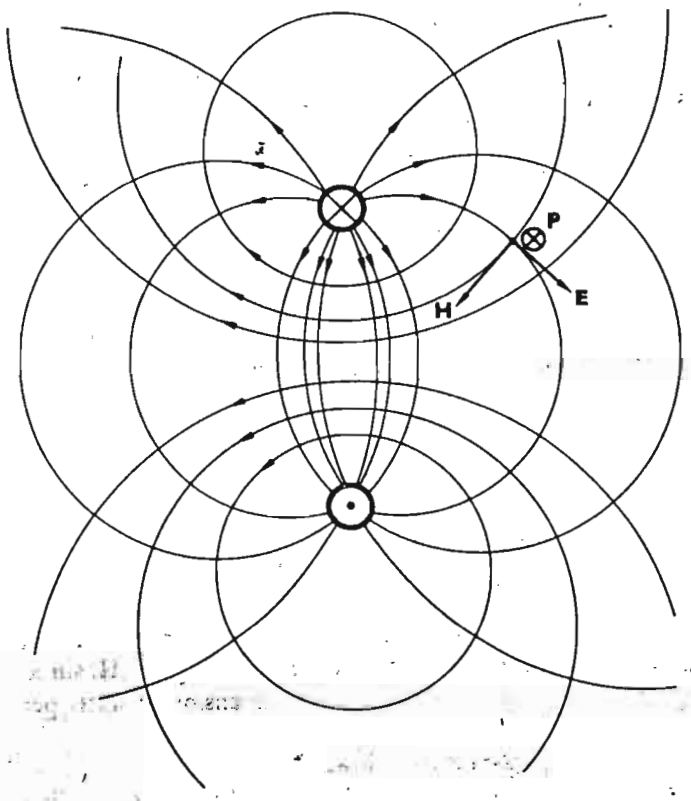


**Fig. 2-2** Electromagnetic field picture around wires of Fig. 2-1*a*.



rapidly diminishing with the distance from the conductors. Note that if the conductors are perfect, the electric field $\mathbf{E}$ will be zero inside the conductors, and thus no energy travels inside the conductors.

The totally radiated energy is obtained by integration over the total sectional area in Fig. 2-2. This is not particularly difficult in view of the simple geometry, and if we actually perform the necessary operations, we obtain the result

$$p = iv \qquad \text{W}$$

i.e., the same result as given directly by the fundamental power equation (2-3).

We are free to adopt whatever interpretation appeals most to us; the end result is the same. The energy *is* present; it *does* travel from generator to load and in magnitudes that *do* agree with Eq. (2-3).

We shall, finally, discuss one additional and important aspect of the electromagnetic energy, its speed of travel. Consider, first, for comparison, the hydraulic analog in Fig. 2-1*b*. How fast does the energy travel in that system? Obviously, with the same velocity with which a pressure disturbance propagates through the hydraulic fluid, i.e., the velocity of sound for the fluid in question.

In the electric system of Fig. 2-1*a* the speed of energy travel equals the speed with which a voltage (or current) perturbation propagates along the line. This velocity varies somewhat with the line parameters, but is always slightly less than the velocity of light.† We can therefore conclude that, for all practical purposes, the energy transmission takes place instantaneously. This fact has important practical consequences, to be discussed in later chapters.

## 2-2 ADDITIONAL FORMS OF ELECTRIC ENERGY

In addition to electromagnetic energy, we are concerned in EESE with three additional forms of electric energy:

1. Electric field energy $w_{ef}$
2. Magnetic field energy $w_{mf}$
3. Ohmic, or dissipative, energy $w_{\Omega}$

### 2-2.1 ELECTRIC FIELD ENERGY $w_{ef}$

This form of energy exists wherever in space there is present an electric field, for instance, between the plates of a plate capacitor or surrounding the

† Compare the discussion on wave propagation in Chap. 10.

wires of a transmission line. It is found in *volume densities* that can be computed from†

$$\frac{dw_{ef}}{d(\text{vol})} = \tfrac{1}{2}\varepsilon\varepsilon_0 |\mathbf{E}|^2 \quad \text{Ws/m}^3 \tag{2-6}$$

where $\mathbf{E}$ = electric field strength, as before

$\varepsilon_0 = \dfrac{1}{36\pi} \times 10^{-9}$ = dielectric constant for vacuum

$\varepsilon$ = relative dielectric constant of medium in question

We use the terminology that the electric field energy is *stored* in the field.

**Example 2-1** Let us study the field energy situation in the plate capacitor in Fig. 2-3. We shall assume a plate area of $A$ m² and a distance between the plates of $d$ m. The capacitor is charged to the voltage $v$ V. We shall neglect the fringe effect, and thus assume that the electric field strength is constant $= v/d$ throughout the entire space between the plates. If we assume a linear dielectric with a relative dielectric constant $\varepsilon$, we obtain from Eq. (2-6) the following expression for the energy volume density:

$$\frac{dw_{ef}}{d(\text{vol})} = \tfrac{1}{2}\varepsilon\varepsilon_0\left(\frac{v}{d}\right)^2 \quad \text{Ws/m}^3$$

Since this density is constant throughout the total volume $Ad$, we thus obtain for the total energy

$$w_{ef} = \tfrac{1}{2}\varepsilon\varepsilon_0\left(\frac{v}{d}\right)^2 Ad = \tfrac{1}{2}\varepsilon\varepsilon_0\frac{v^2}{d}A \quad \text{Ws}$$

† The formula actually reads

$$\frac{dw_{ef}}{d(\text{vol})} = \tfrac{1}{2}\mathbf{E}\cdot\mathbf{D} \quad \text{Ws/m}^3 \tag{2-7}$$

where $\mathbf{D}$ is the electric flux density measured in Vs/m². We will be exclusively concerned with *isotropic* and *linear* media, where we have the relationship

$$\mathbf{D} = \varepsilon\varepsilon_0\mathbf{E} \tag{2-8}$$

and in this case Eq. (2-7) reduces to the simpler Eq. (2-6).

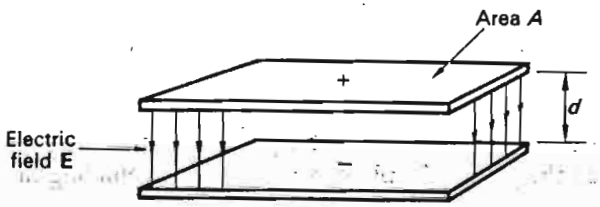


**Fig. 2-3** Simple plate capacitor.



The capacitance $C$ of the capacitor is

$$C = \varepsilon\varepsilon_0\frac{A}{d} \quad \text{F}$$

and we thus obtain

$$w_{ef} = \tfrac{1}{2}Cv^2 \quad \text{Ws} \tag{2-9}$$

This formula can actually be proved valid for any capacitor geometry, and is thus general.

### 2-2.2 MAGNETIC FIELD ENERGY $w_{mf}$

Magnetic field energy $w_{mf}$ is found everywhere in space where there is a magnetic field present. Its energy volume density is computed from†

$$\frac{dw_{mf}}{d(\text{vol})} = \tfrac{1}{2}\mu\mu_0 |\mathbf{H}|^2 \quad \text{Ws/m}^3 \tag{2-10}$$

where $\mathbf{H}$ = magnetic field strength, as before

$\mu_0 = 4\pi \times 10^{-7}$ = magnetic permeability of vacuum

$\mu$ = relative magnetic permeability of medium in question

Just as in the case of the electric field energy, we obtain the *total* magnetic field energy by integration over the total volume where the field exists.

For a circuit element (coil) having the inductance $L$ and carrying the current $i$, we can easily derive the formula

$$w_{mf} = \tfrac{1}{2}Li^2 \quad \text{Ws} \tag{2-11}$$

representing the total magnetic field energy *stored* in the coil.‡ The two symmetric equations (2-9) and (2-11) are quite useful in finding the inductance and capacitance for various circuit elements. We shall later use them for

† The formula actually reads

$$\frac{dw_{mf}}{d(\text{vol})} = \tfrac{1}{2}\mathbf{B}\cdot\mathbf{H} \quad \text{Ws/m}^3 \tag{2-12}$$

where $\mathbf{B}$ is the magnetic flux density measured in Wb/m². In isotropic and linear media we have

$$\mathbf{B} = \mu\mu_0\mathbf{H} \quad \text{Wb/m}^2 \tag{2-13}$$

and in this case Eq. (2-12) reduces to the simpler Eq. (2-10).

‡ The magnetic field energy formula for a system of magnetically coupled coils will contain additional terms due to the mutual inductance $M$. For example, for a system of two coils carrying the currents $i_1$ and $i_2$, we get

$$w_{mf} = \tfrac{1}{2}L_1i_1^2 + \tfrac{1}{2}L_2i_2^2 + Mi_1i_2 \tag{2-14}$$

(Note the absence of the factor $\frac{1}{2}$ in the last term.)

that purpose. We shall also return to those formulas in our discussion of *reactive* power, in Sec. 2-3.

### 2-2.3 OHMIC, OR DISSIPATIVE, ENERGY $w_\Omega$

This form of energy is dissipated into heat whenever a current flows in a resistive medium. On a per-volume basis this energy dissipation takes place at a time rate†

$$\frac{dp_\Omega}{d(\text{vol})} = \frac{dw_\Omega}{d(\text{vol})} = \rho\,|\mathbf{I}|^2 \qquad \text{W/m}^3 \tag{2-15}$$

where $\mathbf{I}$ = current density vector, A/m²
$\rho$ = specific resistivity, $\Omega \cdot$ m, of medium in question

**Example 2-2** In a conductor of length $L$ m and sectional area $A$ m² carrying a total current of $i$ A (of *uniform* current density $i/A$ A/m²), we obtain for the total dissipation in the volume $LA$

$$p_\Omega = \rho\left(\frac{i}{A}\right)^2 LA = \rho\frac{L}{A}i^2 \qquad \text{W} \tag{2-16}$$

The *resistance* of the conductor is

$$R = \frac{\rho L}{A} \qquad \Omega$$

and this gives us the well-known formula for heat dissipation,

$$p_\Omega = Ri^2 \qquad \text{W} \tag{2-17}$$

In many instances this heat dissipation represents a *useful* energy form, as, for example, in an electrically heated oven. In most instances, however, the ohmic energy must be considered a *loss* energy. This is particularly true in a transmission system.

**Example 2-3** Assume that we wish to transmit a given amount of power $p_{tr}$ in the system in Fig. 2-1*a*. Due to line resistance $R$, this transmission will be associated with an unavoidable power loss

$$p_{\text{loss}} = Ri^2$$

† The formula actually reads

$$\frac{dp_\Omega}{d(\text{vol})} = \mathbf{I}\cdot\mathbf{E} \qquad \text{W/m}^3 \tag{2-18}$$

In an isotropic and linear medium we have

$$\mathbf{E} = \rho\mathbf{I} \qquad \text{V/m}$$

and Eq. (2-18) reduces to the simpler Eq. (2-15).



By making use of Eq. (2-3), we eliminate the current and obtain

$$p_{\text{loss}} = R\left(\frac{p_{tr}}{v}\right)^2 \tag{2-19}$$

By putting the power loss in relation to transmitted power, we get

$$\frac{p_{\text{loss}}}{p_{tr}} = R\frac{p_{tr}}{v^2} \tag{2-20}$$

This formula teaches us an important lesson: *The relative loss of power is inversely proportional to the square of the transmission voltage.*

The last example brings into focus the need for high transmission voltages. As an extra bonus, a high transmission voltage also results in increased "transmission capacity," a concept we shall explain in the next chapter.

## 2-3 DC VERSUS AC POWER—CONCEPTS OF REAL AND REACTIVE POWERS

The first power transmission systems put into operation in the early 1880s (including the historic Pearl Street, New York, plant built by Edison) were operated on direct current. Single-phase alternating current came into use in the United States in 1890, polyphase alternating current a few years later. Three-phase alternating current has dominated the scene since. In the last decade high-voltage direct current has reentered the picture, and as of this writing several important direct current links are in operation around the world. It is safe to say, however, that three-phase alternating current will remain the dominant transmission method for the foreseeable future.

Direct current has some inherent advantages that make it the ideal transmission medium in certain instances. Alternating current, on the other hand, can be easily generated and conveniently transformed to high voltage levels, and since cheap and effective ac motors can be built, this has naturally become our most common form of electric energy.

### 2-3.1 SINGLE-PHASE TRANSMISSION

We shall proceed to present some of the fundamental characteristics of ac power. We shall start with single-phase and demonstrate later the advantages of the three-phase technique.

Consider, therefore, the case where the voltage and current in the system depicted in Fig. 2-1*a* are of the sinusoidal form

$$v = v_{\max}\sin\omega t$$
$$i = i_{\max}\sin(\omega t - \phi) \tag{2-21}$$

By using Eq. (2-3) we thus obtain the following expression for the transmitted power:

$$p = vi = v_{\max} i_{\max} \sin \omega t \sin (\omega t - \phi)$$

or

$$p = \frac{v_{\max} i_{\max}}{2} [\cos \phi - \cos (2\omega t - \phi)] \tag{2-22}$$

We introduce at this juncture† the *effective*, or *rms*, values of current and voltage in accordance with

$$|V| \triangleq \frac{1}{\sqrt{2}} v_{\max}$$
$$|I| \triangleq \frac{1}{\sqrt{2}} i_{\max} \tag{2-23}$$

and can then write Eq. (2-22) as follows:

$$p = |V||I| \cos \phi - |V||I| \cos (2\omega t - \phi) \tag{2-24}$$

The transmitted power evidently *pulsates* (Fig. 2-4*a*) around an *average power* ($|V||I| \cos \phi$) at double radian frequency $2\omega$. During certain periods the power actually is *negative*, indicating that the energy flow during these intervals is in the negative direction.

† Whenever we work with sinusoidal time variables we shall always make use of *phasors* and phasor notation. The reader is assumed to be acquainted with these concepts, but we give this brief account in order to remove any symbol confusion.

Consider the sinusoidal voltage function

$$v = v_{\max} \sin (\omega t + \alpha)$$

If by the symbol Im $\{\cdots\}$ we mean "the imaginary part of," then we can write

$$v = \text{Im} \{v_{\max} e^{j(\omega t + \alpha)}\} = \sqrt{2} \, \text{Im} \left\{ \frac{v_{\max}}{\sqrt{2}} e^{j\alpha} e^{j\omega t} \right\}$$

We now *define* the *phasor* $V$ as the complex number

$$V \triangleq \frac{v_{\max}}{\sqrt{2}} e^{j\alpha}$$

and have, then,

$$v = \sqrt{2} \, \text{Im} \{V e^{j\omega t}\}$$

We note the following features about phasors:

1. We symbolize them by capital-letter symbols.
2. A phasor has a magnitude $|V| = v_{\max}/\sqrt{2}$ that equals the rms value of the corresponding time function.
3. A phasor has a phase $\angle V = \alpha$ that equals the phase angle of the time function.



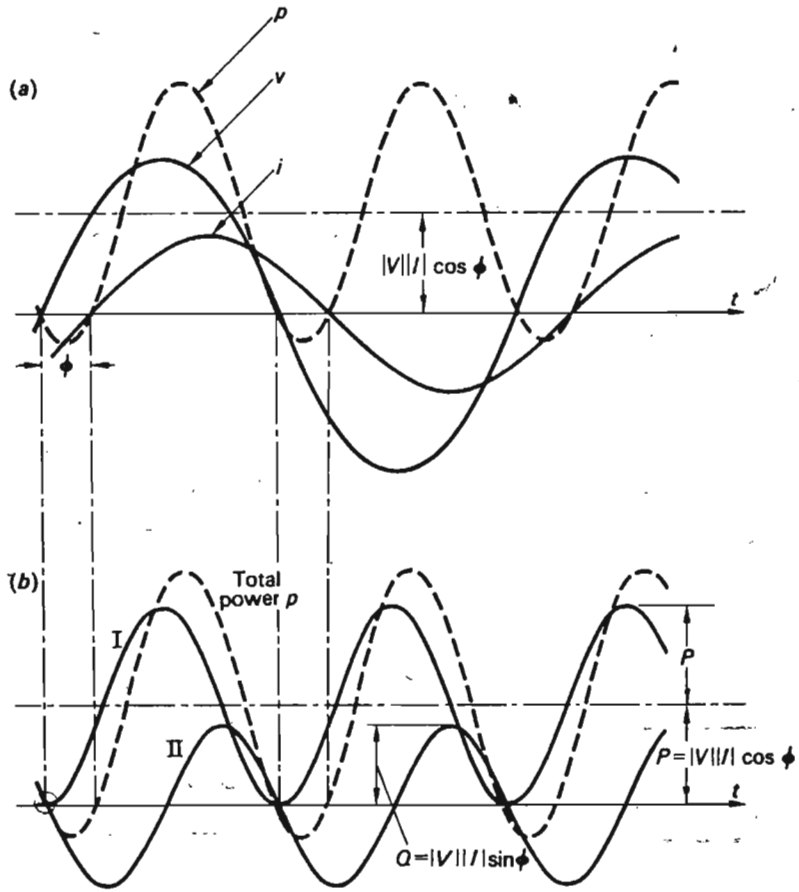


**Fig. 2-4** Voltage, current, and power in single-phase circuit.

Equation (2-24) can be transformed into

$$p = \underbrace{|V||I| \cos \phi (1 - \cos 2\omega t)}_{\text{I}} - \underbrace{|V||I| \sin \phi \sin 2\omega t}_{\text{II}} \tag{2-25}$$

We have actually decomposed the power into two components (marked I and II in Fig. 2-4*b*): the first pulsates around the same average value as before *but never goes negative*, and the second has a zero average value.

We introduce here the following two quantities:

$$P \triangleq |V||I| \cos \phi \quad \textit{real}, \text{ or } \textit{active}, \text{ power}$$
$$Q \triangleq |V||I| \sin \phi \quad \textit{reactive} \text{ power} \tag{2-26}$$

and can then write Eq. (2-25) more compactly.

$$p = P(1 - \cos 2\omega t) - Q \sin 2\omega t \tag{2-27}$$

These newly defined concepts are of such fundamental importance in EESE that we find it appropriate to say a few words about their meaning:

1. The real power $P$ is *defined* as the average value of $p$ and therefore, physically, means the *useful* power being transmitted. Its magnitude depends very strongly on the *power factor* $\cos\phi$.
2. The reactive power $Q$ is *by definition* equal to the *peak* value of that power component that travels back and forth on the line, resulting in zero average, and therefore capable of no useful work.

$P$ and $Q$ both have dimension watts, but to emphasize the fact that the latter represents a "nonactive," or "reactive," power, it is measured in

**Table 2-1**

| Load type | Phasor relation | Phase angle | Power absorbed by load | |
|---|---|---|---|---|
| | | | $P$ | $Q$ |
| 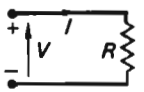 | 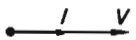 | $\phi = 0$ | $P > 0$ | $Q = 0$ |
|  | 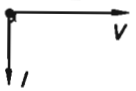 | $\phi = +90°$ | $P = 0$ | $Q > 0$ |
| 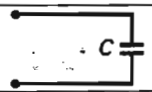 |  | $\phi = -90°$ | $P = 0$ | $Q < 0$ |
| 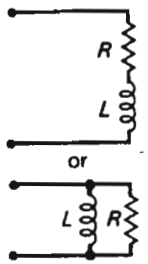 | 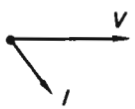 | $0 < \phi < +90°$ | $P > 0$ | $Q > 0$ |
| 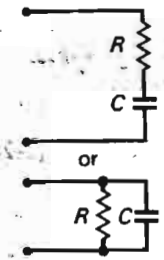 | 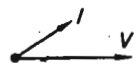 | $-90 < \phi < 0$ | $P > 0$ | $Q < 0$ |



*voltamperes reactive* (*vars*). Larger and more practical units are kilovars and megavars, related, as follows, to the basic unit.

$$1 \text{ Mvar} = 10^3 \text{ kvar} = 10^6 \text{ vars}$$

Table 2-1 summarizes the real and reactive powers for the most commonly encountered load types. Note, in particular, that an inductive load absorbs positive $Q$. In power lingo, we say that an inductor *consumes* reactive power. A capacitive load, on the other hand, absorbs negative $Q$. We say that a capacitor *generates* reactive power. The sign situation should not present any mystery to the attentive reader, who will realize that a sign change in $Q$ simply means a 180° phase shift in the second power component in Eq. (2-25).

In the following example we demonstrate the physical relationship between "reactive power" and the magnetic field energy.

**Example 2-4** Consider the fourth entry in Table 2-1, i.e., the series $RL$ circuit. If the voltage is of the form

$$v = \sqrt{2}\,|V| \sin \omega t$$

then we know from simple circuit analysis that the current will be of the form

$$i = \sqrt{2}\,|I| \sin(\omega t - \phi)$$

with

$$|I| = \frac{|V|}{\sqrt{R^2 + (\omega L)^2}}$$

and

$$\phi = \tan^{-1}\frac{\omega L}{R}$$

Thus

$$\cos\phi = \frac{R}{\sqrt{R^2 + (\omega L)^2}}$$

$$\sin\phi = \frac{\omega L}{\sqrt{R^2 + (\omega L)^2}}$$

By substitution into Eq. (2-26) we therefore get

$$P = \frac{|V|^2 R}{R^2 + (\omega L)^2}$$

$$Q = \frac{|V|^2 \omega L}{R^2 + (\omega L)^2} \qquad (2\text{-}28)$$

It is possible to relate the reactive power to the stored magnetic field energy in the coil. In accordance with Eq. (2-13), this energy equals

$$w_{mf} = \tfrac{1}{2}Li^2 = \tfrac{1}{2}L\left[\sqrt{2}\,\frac{|V|}{\sqrt{R^2 + (\omega L)^2}}\sin(\omega t - \phi)\right]^2 \tag{2-29}$$

The rate of change of this stored energy is

$$\frac{dw_{mf}}{dt} = 2\omega L\,\frac{|V|^2}{R^2 + (\omega L)^2}\sin(\omega t - \phi)\cos(\omega t - \phi)$$

$$= \omega L\,\frac{|V|^2}{R^2 + (\omega L)^2}\sin 2(\omega t - \phi) = Q\sin 2(\omega t - \phi) \tag{2-30}$$

The last step follows from Eq. (2-28), We conclude:

The magnetic field energy *rate* varies harmonically with a frequency of $2\omega$, zero average value, *and a peak value that exactly equals* $Q$.

*This, of course, fully identifies the reactive power component in Eq.* (2-25) *as that component that periodically, and twice per voltage cycle, fully stores and discharges the coil with its magnetic field energy.*

An identical analysis (see Exercise 2-I) of the capacitive circuits would reveal a similar relationship between the reactive power and the stored electric field energy in the capacitor.

*The student should carefully consider these observations since they fully explain the physical nature of reactive power.*

**Example 2-5** Let us study the power situation in the case where the load consists of a parallel combination of a coil and a capacitor, as shown in Fig. 2-5. A simple application of Eq. (2-25) tells us that the instantaneous powers $p_L$ and $p_C$ absorbed by the coil and capacitors, respectively, are

$$p_L = -|V|\,|I_L|\sin 2\omega t$$

$$p_C = |V|\,|I_C|\sin 2\omega t$$

As we can expect, the powers are 180° out of phase. The total line power $p$ will be obtained as the sum of $p_L$ and $p_C$:

$$p = p_L + p_C = |V|\,(|I_C| - |I_L|)\sin 2\omega t$$

Note that all three powers, $p$, $p_L$, and $p_C$, are purely reactive.

An interesting special case is obtained if the circuit is *tuned to resonance*. The currents $|I_L|$ and $|I_C|$ are now equal, and therefore the powers $p_L$ and $p_C$ will

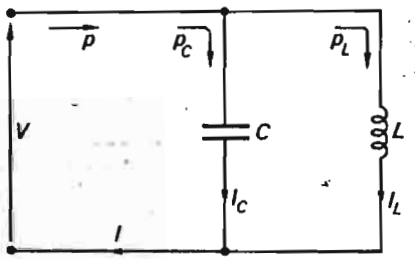


**Fig. 2-5** Power flow in $LC$ circuit.



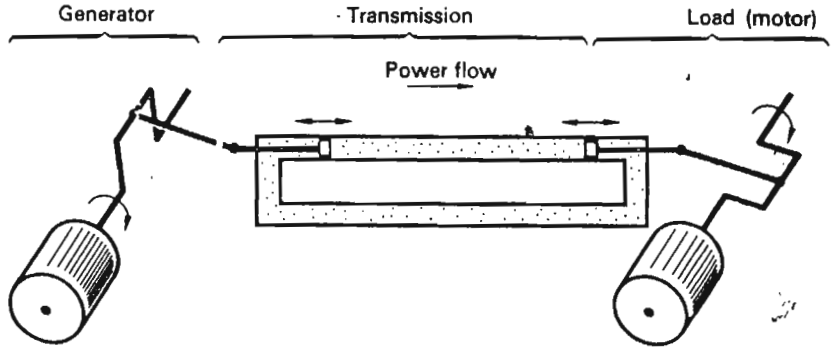


**Fig. 2-6** Hydraulic analog of single-phase system.

now have equal magnitudes. The line power $p$ will therefore be zero. Physically, this means that the energy travels back and forth between the coil and the capacitor. At one moment the coil is stored to a maximum with magnetic field energy, and the capacitor is fully discharged. Half a voltage cycle later the capacitor is fully charged, and the coil is empty.

### 2-3.2 THREE-PHASE TRANSMISSION

The transmission system just described is referred to as *single-phase*. It probably has occurred to the reader that the great drawback of this arrangement is the *pulsating* character of the power. We may draw a useful parallel with the hydraulic system in Fig. 2-6, characterized by a pulsating motor shaft torque. Considerable torque improvement can be obtained by an

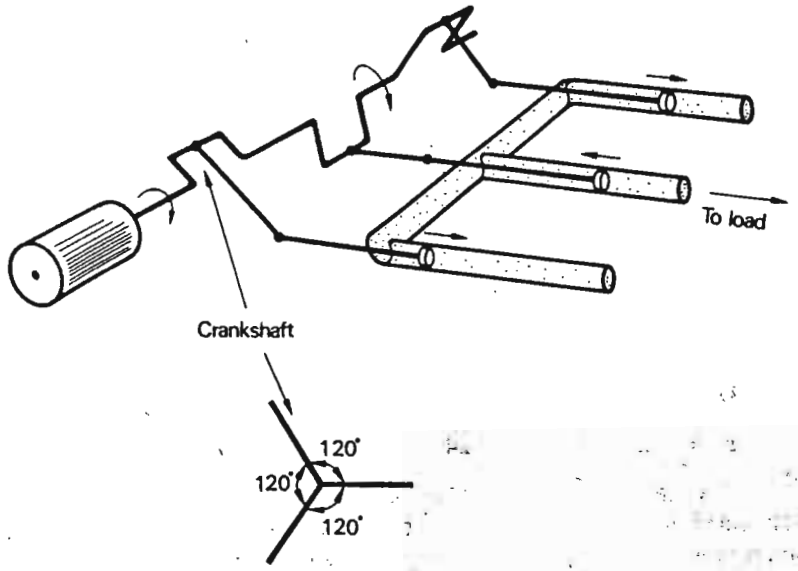


**Fig. 2-7** Hydraulic analog of three-phase systems.

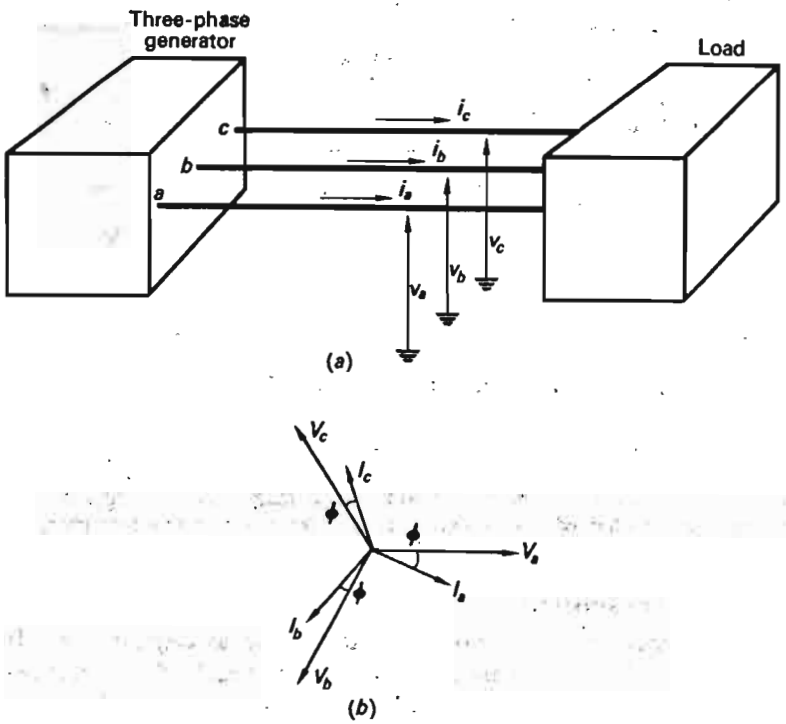


**Fig. 2-8** Three-phase transmission system.

arrangement of the type shown in Fig. 2-7, consisting of three parallel-operating single-phase systems. Note that if the crankshaft has the particular design shown in the figure, then the instantaneous total fluid flow is zero. *This means that we can discard the three individual return pipes.* Note also that we very well could have used a larger number of pistons to achieve the same smoothing effect on the shaft torque.

By taking a cue from the above hydraulic analog, we arrive at the classic three-phase transmission system depicted in Fig. 2-8*a*. The three-phase generator supplies the three sinusoidal phase voltages

$$\begin{aligned} v_a &= \sqrt{2}\,|V| \sin \omega t \\ v_b &= \sqrt{2}\,|V| \sin (\omega t - 120°) \\ v_c &= \sqrt{2}\,|V| \sin (\omega t - 240°) \end{aligned} \tag{2-31}$$

Internally, in the three-phase generator (Chap. 4), the three phases are connected to a *neutral* point, which usually is *grounded*. The three *phase voltages* $v_a$, $v_b$, and $v_c$ are therefore usually measured relative to ground.



If the load is *balanced*, or *symmetrical*, the three phase currents will then be of the symmetrical form

$$\begin{aligned} i_a &= \sqrt{2}\,|I| \sin (\omega t - \phi) \\ i_b &= \sqrt{2}\,|I| \sin (\omega t - 120° - \phi) \\ i_c &= \sqrt{2}\,|I| \sin (\omega t - 240° - \phi) \end{aligned} \tag{2-32}$$

If we utilize the phasor method of characterizing voltages and currents, we obtain the phasor diagram shown in Fig. 2-8*b*.

The total transmitted three-phase power equals the sum of the individual phase powers:

$$p_{3\phi} = v_a i_a + v_b i_b + v_c i_c \tag{2-33}$$

By using Eqs. (2-31) and (2-32) and after some simple trigonometric manipulations, we obtain for the *balanced* case

$$p_{3\phi} = 3\,|V|\,|I| \cos \phi \tag{2-34}$$

We note that the total instantaneous three-phase power is *constant*, having a magnitude of three times the real power per phase. We thus have

$$p_{3\phi} = 3P \tag{2-35}$$

In these two last formulas $P$, $|V|$, and $|I|$ represent *per-phase* values.

We make the following easily confirmed observations about the *balanced* three-phase transmission system:

1. The algebraic sum of the three phase currents equals zero. No return conductor is therefore needed in a balanced three-phase system.
2. The algebraic sum of the three phase voltages also equals zero.
3. The three *line voltages* (measured between the three phases) are of equal magnitude $|V_L|$. The following relationship exists between the line and phase voltages:

$$|V_L| = \sqrt{3}\,|V| \tag{2-36}$$

*When referring to the voltage level of a three-phase system, one invariably understands the line voltage.* In terms of the line voltage, the power equation (2-34) reads

$$p_{3\phi} = \sqrt{3}\,|V_L|\,|I| \cos \phi \tag{2-37}$$

4. Since the instantaneous power is constant, we are tempted to assume that the reactive power is of no importance in a three-phase system. This is *not* the case. Note that the power in each phase still is of "single-phase type," as described by Eq. (2-27).

*Compare:* The three phase currents add up to zero, but they are still very much in evidence in each phase.

5. Equation (2-35) tells us that the three-phase *real* power equals three times the single-phase real power. We are thus led to ask whether a similar formula, i.e.,

$$Q_{3\phi} = 3Q \qquad (2\text{-}38)$$

is applicable for the *reactive* power.

We realize immediately that the concept of "three-phase reactive power" $Q_{3\phi}$ makes as little physical sense as would the concept of a "three-phase current" $I_{3\phi} \triangleq 3I$. *Nevertheless*, when we refer to reactive power in a three-phase system, we *always* express it as a "three-phase power" in accordance with Eq. (2-38). The *only* reason for this "strange custom" is to obtain symmetry between real and reactive powers. (Compare Example 2-6, below.) It should be added, however, that the use of per-unit values (see below) eliminates any confusion between "phase" and "three-phase" values.

6. Due to the complete symmetry between the three phases, it is sufficient, in analysis, to determine the current, voltage, and power in one phase, the "reference phase," only. The knowledge of these variables in one phase immediately implies knowledge in all phases. We refer to this as *per-phase analysis*.

We exemplify some of the above points by the following example.

**Example 2-6** The equivalent induction motor load on a section of a 138-kV transmission network can be represented by an impedance

$$Z = 80 + j60 \ \Omega \text{ per phase}$$

as shown in Fig. 2-9. (See also discussion of load representation in Chap. 3.)

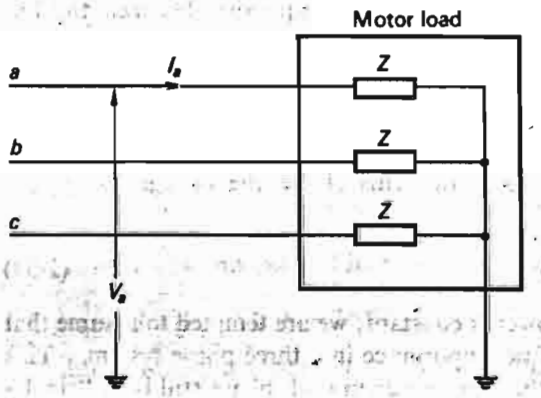


**Fig. 2-9** Equivalent three-phase motor load.



We wish to determine the real and reactive powers absorbed by this load per phase and total three-phase.

Since there is complete symmetry between the phases, we limit our analysis to phase *a* only. We obtain for the current in this reference phase

$$I_a = \frac{V_a}{Z} = \frac{138/\sqrt{3}}{80 + j60} = 0.798e^{-j36.9^\circ} \quad \text{kA}$$

also

$$\cos\phi = \frac{80}{\sqrt{(60)^2 + (80)^2}} = 0.800$$

and

$$\sin\phi = \frac{60}{\sqrt{(60)^2 + (80)^2}} = 0.600$$

By using Eq. (2-37), we then obtain for the *total* real power

$$P_{3\phi} = \sqrt{3} \times 138 \times 0.798 \times 0.800 = 153 \text{ MW} \qquad \text{(or 51 MW per phase)}$$

(Note that if voltage and current in this formula are inserted in *kilo* values, the resulting power will come out directly in megawatts.) From Eq. (2-26) we then obtain for the reactive power per phase

$$Q = \frac{138}{\sqrt{3}} \times 0.798 \times 0.600 = 38.2 \text{ Mvar/phase} \qquad \text{(or 114.6 Mvar } \textit{total} \text{ three-phase)}$$

## 2-4 CONCEPT OF COMPLEX POWER

Consider the simple circuit shown in Fig. 2-10*a*, which may, for example, represent one phase of the three-phase circuit in Fig. 2-9. We have for the

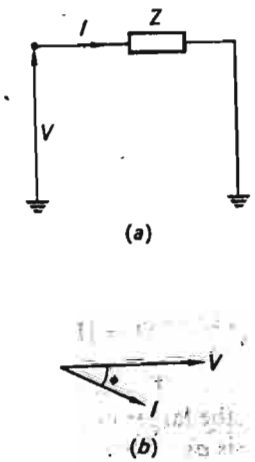


**Fig. 2-10** Per-phase representation of three-phase circuit.

voltage and current phasors

$$V = |V|\, e^{j\angle V}$$
$$I = |I|\, e^{j\angle I}$$

We introduce now the *conjugate* current defined by

$$\dot{I}^* \triangleq |I|\, e^{-j\angle I} \tag{2-39}$$

whereupon we form the product

$$S = VI^* \tag{2-40}$$

This product has a very useful property, which we may confirm by substituting $I^*$ into Eq. (2-40).

We get

$$S = VI^* = |V|\, e^{j\angle V}\, |I|\, e^{-j\angle I} = |V|\,|I|\, e^{j(\angle V - \angle I)}$$

The phase angle $\angle V - \angle I$ is the earlier introduced $\phi$ angle (Fig. 2-10*b*), and we thus get

$$S = |V|\,|I|\, e^{j\phi} = |V|\,|I| \cos\phi + j\,|V|\,|I| \sin\phi = P + jQ \tag{2-41}$$

The last step follows directly from the definition of $P$ and $Q$. We can write Eq. (2-40) in two alternative forms by using the relationships

$$V = ZI \quad \text{and} \quad I = YV$$

we obtain

$$S = VY^*V^* = Y^*\,|V|^2$$

or

$$S = ZII^* = Z\,|I|^2$$

By summarizing, we thus have the three alternative power expressions

$$S = P + jQ = VI^* = Z\,|I|^2 = Y^*\,|V|^2 \tag{2-42}$$

The complex number $S$ defined by Eqs. (2-40) is referred to as *complex power*. Upon computing $S$ from either of the three alternative expressions (2-42), we obtain $P$ and $Q$ simply as the real and imaginary parts of $S$, respectively.

The magnitude $|S|$ of the complex power is referred to as *apparent power*. It can be expressed in any one of several ways:

$$|S| = |VI^*| = |V|\,|I| = \sqrt{P^2 + Q^2} \tag{2-43}$$

The unit of $|S|$ is obviously voltamperes (VA), but in EESE we prefer the larger units kVA or MVA. The practical significance of apparent power is *as a rating unit* for generators and transformers (Chaps. 4 and 5).



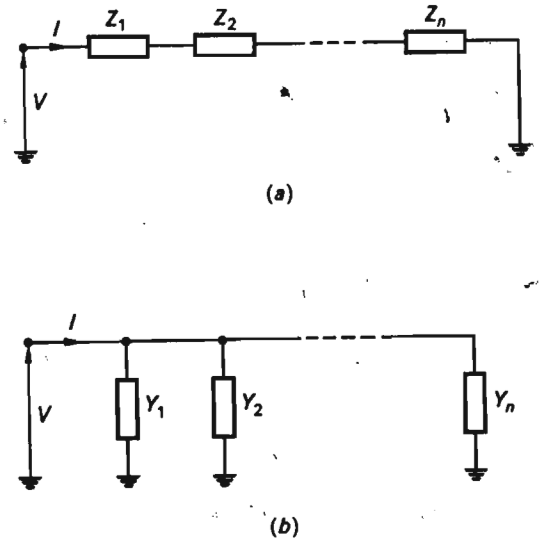


**Fig. 2-11** Multiload cases.

Very often we find it convenient to use the *summation rule for complex powers*. Consider the two cases shown in Fig. 2-11. In the series circuit the individual series elements absorb, according to Eq. (2-42), the individual powers

$$S_1 = |I|^2 Z_1$$
$$S_2 = |I|^2 Z_2$$
$$\cdots\cdots\cdots$$
$$S_n = |I|^2 Z_n$$

The *total* power equals

$$S_{tot} = VI^*$$

Since we have

$$V = IZ_1 + IZ_2 + \cdots + IZ_n$$

we can write the total power as

$$S_{tot} = (IZ_1 + IZ_2 + \cdots + IZ_n)I^* = |I|^2 Z_1 + |I|^2 Z_2 + \cdots + |I|^2 Z_n$$

We therefore obtain the summation rule

$$S_{tot} = \sum_{i=1}^{n} S_i \tag{2-44}$$

where $S_i$ is the power absorbed by the $i$th impedance.

The reader will easily verify that this summation rule also applies to the parallel circuit in Fig. 2-11, where $S_i$ now means the power absorbed by the $i$th admittance.

Let us give examples of the use of complex power.

**Example 2-7** Let us compute the real and reactive powers that we found by other means in Example 2-6.

Since we know, in this example, the voltage and impedance *but not the current*, it is convenient to use the third form of Eq. (2-42).

We have

$$Y = \frac{1}{Z} = \frac{1}{80 + j60} = \frac{80 - j60}{10{,}000} = 0.008 - j0.006$$

Thus

$$Y^* = 0.008 + j0.006$$

From Eq. (2-42) we then get directly

$$P + jQ = \left(\frac{138}{\sqrt{3}}\right)^2 (0.008 + j0.006) = 51.0 + j38.2$$

These, then, are the *per-phase values* of $P$ and $Q$. Since the voltage is in kilovolts, the power values come out in megavalues. If, instead, we use the *line* voltage directly, we immediately obtain the total, or three-phase, values

$$P_{3\phi} + jQ_{3\phi} = (138)^2(0.008 + j0.006) = 153 + j114.6$$

The reader should compare this analysis method with the one used in Example 2-6.

**Example 2-8** Consider as a second example the transmission link depicted in Fig. 2-12. This link could represent a transmission line connecting two buses, $i$ and $j$, of a larger system.†

† For a discussion of the symbols used in Fig. 2-12 and for the definition of "bus," see Chap. 3.

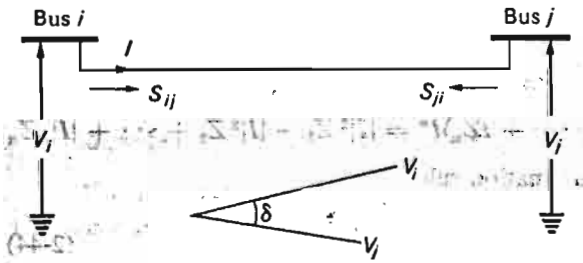


**Fig. 2-12** Per-phase representation of simple three-phase transmission link.



We shall give an expression for the power (real and reactive) being transmitted across this link, on the following assumptions:

1. The two bus voltages $V_i$ and $V_j$ are known and expressed in phase values.
2. The link has a series impedance $Z = R + jX$ per phase.
3. The line current $I$ is the same throughout the line. For "long" lines this is not quite accurate (Chap. 6).
4. Due to the line losses, the transmitted powers as measured in each end of the line will not be equal. We have designated the line powers $S_{ij}$ and $S_{ji}$ as measured at the end points $i$ and $j$, respectively. *Note that both are defined positive directed away from the respective buses.*

Since we have

$$I = \frac{V_i - V_j}{Z}$$

we obtain for the line powers

$$S_{ij} = P_{ij} + jQ_{ij} = V_i I^* = V_i \frac{V_i^* - V_j^*}{Z^*} = \frac{|V_i|^2 - |V_i||V_j| e^{j(\angle V_i - \angle V_j)}}{R - jX}$$
$$S_{ji} = P_{ji} + jQ_{ji} = V_j(-I)^* = \frac{|V_j|^2 - |V_i||V_j| e^{j(\angle V_j - \angle V_i)}}{R - jX} \tag{2-45}$$

We introduce now the *power angle*

$$\delta \triangleq \angle V_i - \angle V_j \tag{2-46}$$

i.e., the phase angle between the two bus voltages. Upon substitution of $\delta$ into Eqs. (2-45), and after separating the equations into real and imaginary parts, we get

$$P_{ij} = \frac{1}{R^2 + X^2}(R|V_i|^2 - R|V_i||V_j|\cos\delta + X|V_i||V_j|\sin\delta)$$
$$Q_{ij} = \frac{1}{R^2 + X^2}(X|V_i|^2 - X|V_i||V_j|\cos\delta - R|V_i||V_j|\sin\delta)$$
$$P_{ji} = \frac{1}{R^2 + X^2}(R|V_j|^2 - R|V_i||V_j|\cos\delta - X|V_i||V_j|\sin\delta) \tag{2-47}$$
$$Q_{ji} = \frac{1}{R^2 + X^2}(X|V_j|^2 - X|V_i||V_j|\cos\delta + R|V_i||V_j|\sin\delta)$$

Note that if all voltages are inserted in these formulas in *line values* and *kilovalues*, then all powers will come out as *three-phase megavalues*.

The formulas thus arrived at are important and will be used later, in our discussion of transmission capacity.

## 2-5 PER-UNIT REPRESENTATION OF IMPEDANCES, CURRENTS, VOLTAGES, AND POWERS

The electric power systems engineer prefers to express impedances, currents, voltages, and powers in per-unit values rather than in ohms, amperes,

kilovolts, and megavars or megawatts. Several advantages can be gained by this practice:

1. Per-unit value representation results in more meaningful and easily correlated data.
2. There will be less chance of mixup between phase and line voltages, single-phase or three-phase powers, and, in the case of transformers, between primary and secondary voltages.

Assume we are informed that the armature resistance of a dc machine equals 5.3 Ω. What does this piece of information communicate to us about the relative magnitude of the resistance? Really, very little! If the machine is large, the given numerical value could indicate an unusually high resistance value. If the machine happens to be small, the opposite will be true.

Assume now that we are informed about the resistance in question in the following roundabout manner: "The resistance has such a value that if *rated* machine current is passed through it, the voltage across the impedance will amount to 11 percent or 0.11 per unit of the rated machine voltage."

At a first glance the second alternative would seem to be an unnecessary complication. Certainly "5.3 Ω" is a more concise statement than the 33-word sentence. However, let us now, instead of using the given sentence, simply define that the resistance equals "0.11 per unit," or "11 percent."

The two alternatives are now equally concise, but the per-unit value gives, in addition, a *relative-magnitude information* missing in the first alternative.

In system studies, when many machines of different ratings are involved, it is more practical to choose a common *base value* for current and voltage, to which we then can refer our actual values. Let $|I_b|$ and $|V_b|$ represent the *base current* and *base voltage*, expressed in kiloamperes and kilovolts, respectively. The product

$$|S_b| = |I_b|\,|V_b| \quad \text{MVA} \tag{2-48}$$

is then referred to as our *base MVA*. Note that, of the three base values thus defined, only two are independent. Rather than choose the $|I_b|$, $|V_b|$ pair as we did, we could have chosen (and this is far more often done) the $|S_b|$, $|V_b|$ pair.

In terms of the chosen base values, we then *define*† the *base impedance* $|Z_b|$:

$$|Z_b| \triangleq \frac{|V_b|}{|I_b|} = \frac{|V_b|^2}{|S_b|} \quad \Omega \tag{2-49}$$

† Note that, defined in this manner, the base impedance is simply that impedance across which we can measure the voltage $|V_b|$ if the current through it equals $|I_b|$.



[The second step follows directly from Eq. (2-48).]

The last formula can be written

$$|Z_b| = \frac{(\sqrt{3}\,|V_b|)^2}{3\,|S_b|}$$

and this then signifies that our results come out the same whether we use per-phase values for $|V_b|$ and $|S_b|$ or line values and three-phase values. But we must always be consistent.

In terms of the four base values thus defined we can now compute per-unit values of voltages, currents, powers, and impedances. Let us, for example, express the ohmic impedance $Z_\Omega$ in per-unit value $Z_{pu}$.

From the definition of per-unit impedance we have the following alternative conversion formulas:

$$Z_{pu} \triangleq \frac{Z_\Omega}{|Z_b|} = \frac{Z_\Omega\,|I_b|}{|V_b|} = \frac{Z_\Omega\,|I_b|\,|V_b|}{|V_b|^2} = \frac{Z_\Omega\,|S_b|}{|V_b|^2} \quad \text{pu} \tag{2-50}$$

When we work with admittances, the last conversion formula reads

$$Y_{pu} \triangleq \frac{1}{Z_{pu}} = \frac{|V_b|^2}{Z_\Omega\,|S_b|} = Y_\mho\,\frac{|V_b|^2}{|S_b|} \tag{2-51}$$

We sometimes need to convert an impedance from one base system, $|V_b'|$, $|S_b'|$, to another one, $|V_b''|$, $|S_b''|$. From Eq. (2-50) we get

$$Z_{pu}' \triangleq Z_\Omega\,\frac{|S_b'|}{|V_b'|^2}$$

$$Z_{pu}'' \triangleq Z_\Omega\,\frac{|S_b''|}{|V_b''|^2}$$

By eliminating $Z_\Omega$, we get our conversion formula:

$$Z_{pu}'' = Z_{pu}'\,\frac{|S_b''|\,|V_b'|^2}{|S_b'|\,|V_b''|^2} \tag{2-52}$$

**Example 2-9** We have defined in a particular system study the following base values:

$|V_b| \triangleq 10$ kV

$|S_b| \triangleq 1$ MVA

We want to express in per-unit values the following voltages, currents, powers, impedances and admittances:

1. $|V| = 12.0$ kV
2. $V = 13.3 + j6.0$ kV
3. $I = 513 + j203$ A
4. $S = 200 + j300$ kW and kvar
5. $|S| = 9.3$ MVA
6. $Z = 80 + j40\ \Omega$
7. $Y = 0.1 - j0.3\ \mho$

We first compute the base current and base impedance:

$$|I_b| = \frac{|S_b|}{|V_b|} = \frac{1}{10} = 0.1 \text{ kA}$$

$$|Z_b| = \frac{|V_b|}{|I_b|} = \frac{10}{0.1} = 100\ \Omega$$

and also

$$|Y_b| = \frac{1}{100} = 0.01\ \mho$$

We get then directly:

1. $|V| = \dfrac{12.0}{10} = 1.20$ pu

2. $V = \dfrac{13.3 + j6.0}{10} = 1.33 + j0.6$ pu

3. $I = \dfrac{513 + j203}{100} = 5.13 + j2.03$ pu

4. $S = \dfrac{200 + j300}{1000} = 0.2 + j0.3$ pu

5. $|S| = \dfrac{9.3}{1} = 9.3$ pu

6. $Z = \dfrac{80 + j40}{100} = 0.8 + j0.4$ pu

7. $Y = \dfrac{0.1 - j0.3}{0.01} = 10.0 - j30.0$ pu

Since all our problems in this book will be worked in per-unit values, the student will get ample opportunity to get acquainted with this practice.

## 2-6 SUMMARY

We have attempted in this chapter to give a brief demonstration of the basic physical laws upon which the EESE technology is based. In particular, the various electric energy forms with which we shall be concerned have been discussed. The practically important three-phase transmission technique has been presented, and its basic advantage, the constancy of transmitted power, has been stressed.

The concepts of real and reactive powers have been reviewed and related to the three-phase system. These concepts are of such fundamental importance that the reader should not proceed until he has gained a thorough understanding of them. We have also reviewed the concept of complex power and introduced the reader to the practically important per-unit



representation of electrical quantities. Both will prove invaluable throughout the book.

## EXERCISES

**2-1.** For the purely capacitive load type in Table 2-1 (item 3), derive an expression for the reactive power. Then prove that this value is identical with the peak rate of change of the electric field energy stored in the capacitor. (Compare with Example 2-4.)

**2-2.** The power equation (2-34) was obtained on the assumption that the three-phase load was *balanced*. Analyze the situation when we have a slight load unbalance as depicted in

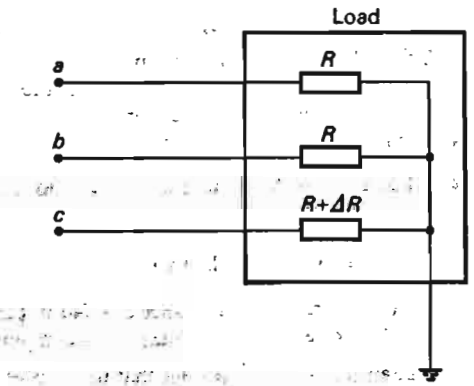


**Fig. 2-13** Unbalanced three-phase load.

Fig. 2-13. Show in particular that the total power will now have a small pulsating component, the amplitude of which is proportional to the unbalance $\Delta R$. We make the assumption that the unbalance is relatively small, i.e.,

$$\Delta R \ll R$$

The load voltage is assumed symmetrical.

**2-3.** For each one of the seven circuits in Table 2-1 find the actual values for $P$ and $Q$. Your answers should be expressed in terms of $|V|$ (that is, the rms value of the terminal voltage) and the circuit parameters $R$, $L$, and $C$.

**2-4.** Consider the transmission line in Fig. 2-12. Its "nominal" voltage rating is 345 kV (line voltage). The line is relatively short, only 50 miles, and has an impedance of $Z = 5 + j40\ \Omega$ per phase.

Let us assume that the voltage magnitudes of both terminal buses, $i$ and $j$, can be controlled. (This presupposes that we have controllable sources of reactive power at each bus. This matter will be penetratingly discussed in later chapters.) We assume that we hold the terminal voltages at the following levels:

$$|V_i| = 345.0 \text{ kV}$$
$$|V_j| = 360.0 \text{ kV}$$

Let us also assume that $V_i$ leads $V_j$ by 10°. In accordance with Eq. (2-46), we thus have $\delta = +10°$. (How this phase angle can actually be controlled will also be discussed later.)

(*a*) Compute the real and reactive line powers in each end of the line.

(*b*) Compute the total line losses $P_{loss} + jQ_{loss}$. Express all powers in total three-phase values.

(*c*) Let us then assume a "flat voltage profile" $|V_i| = |V_j| = 345.0$ and $\delta = 10°$ (unchanged). Compute again the line and loss powers.

(*d*) Change the voltage levels back to their original values, i.e.,

$$|V_i| = 345 \text{ kV}$$
$$|V_j| = 360 \text{ kV}$$

and increase the angle $\delta$ to the new value $\delta = 15°$.

Find real and reactive line powers.

*Note:* Your results should demonstrate the following important facts:

1. Although $|V_j| > |V_i|$, the *real* power flow is still in the direction $i \rightarrow j$.
2. The real losses are relatively small compared with the real power flow in the line.
3. A change in the voltage level of a bus affects the flow of reactive power but leaves the real power flow relatively unaffected.
4. A change in the phase angle $\delta$ affects the *real* line flow strongly.

**2-5.** For Exercise 2-4 let us choose the following base values:

$|S_b| \triangleq 100$ MVA — three-phase
$|V_b| \triangleq 345$ kV — line voltage

(*a*) Express the impedance $5 + j40$ in per units of these base values.

(*b*) Express all given voltages and computed powers in per units of those base values.

**2-6.** Example 2-4 demonstrates that under normal conditions the line losses are relatively small. The power leaving bus $i$ thus approximately equals the power entering bus $j$. We shall refer to this power (computed, for example, as the average value of the values at each end) as the "transmitted power" and symbolize it $S_{tr} = P_{tr} + jQ_{tr}$.

The line voltage likewise changes very little from one end of the line to the other. Let us therefore, in a first approximation, set the "transmission voltage" $|V_{tr}|$ equal for the whole line.

(*a*) Prove that the transmission losses may be computed from the approximate formulas

$$P_{loss} \approx R \frac{P_{tr}^2 + Q_{tr}^2}{|V_{tr}|^2} \tag{2-53}$$

$$Q_{loss} \approx X \frac{P_{tr}^2 + Q_{tr}^2}{|V_{tr}|^2} \tag{2-54}$$

(*b*) Show that if $S_{tr}$ and $V_{tr}$ are given in per-phase values, the loss formulas render per-phase losses, but if $S_{tr}$ represents three-phase power and $V_{tr}$ line-to-line voltage, then the loss powers come out as three-phase values.

(*c*) Compare the loss powers computed from the approximate equations (2-53) and (2-54) with the *exact* values computed earlier in Exercise 2-4*b*.

*Note:* Equations (2-53) and (2-54) tell us that the transmitted *real* and *reactive* powers contribute *equally* to the losses. Since in a practical situation we are interested primarily in the transmission of *real* power, we can evidently minimize the transmission losses by reducing $Q_{tr}$. This can be accomplished by "producing" the reactive power "locally," where the need exists.



Equations (2-53) and (2-54) also confirm our earlier findings that the losses are inversely proportional to the square of the transmission voltage.

**2-7.** Consider the cable depicted in Fig. 2-14. Hold the inner conductor at the potential $v$. The outer shield is grounded.

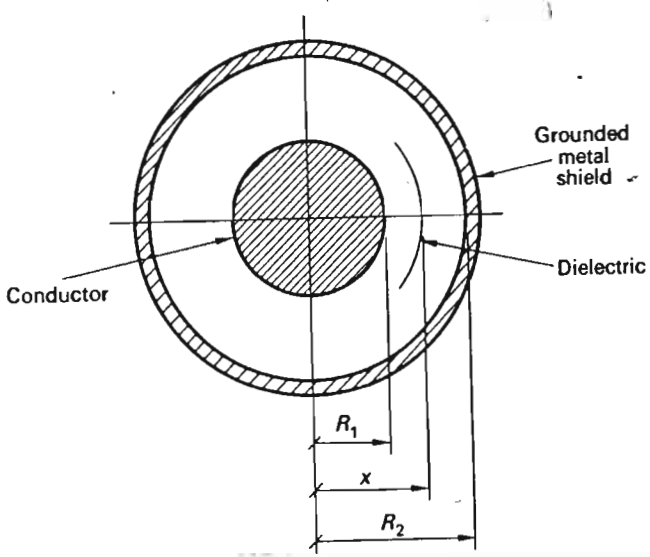


**Fig. 2-14** Cable section.

(*a*) Find a formula for the electric field energy stored in the cable, expressed as joules per meter cable.

*Hint:* The electric field is radially directed, and its magnitude is proportional to $x^{-1}$.

(*b*) Use Eq. (2-9) to find an expression for the cable capacitance, expressed in farads per meter cable.

(*c*) Consider the following numerical case:

$R_1 = 1.5$ cm

$R_2 = 4.0$ cm

$\varepsilon = 5$ *relative* dielectric constant

If the cable is used for three-phase transmission at 138 kV (line to line) and 60 Hz, compute the reactive power generated per mile of cable. (1 mile = 1609 m.)

(*d*) What would your preceding answer be if we doubled the voltage and decreased the frequency to 50 Hz?

**2-8.** Consider again the cable in the previous exercise. Assume that a 60-Hz current is led through the cable using the shield as return path. Neglect "skin effect" and assume that the current is uniformly distributed in both conductors.

(*a*) Find the reactance per meter of the cable operated in this manner.

(*b*) Assume that shield thickness is 5 mm and $\mu = 1$ in all three media. Compute the reactance per mile.

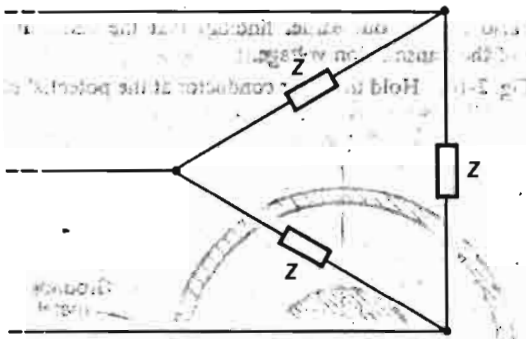


**Fig. 2-15** Delta-connected load.

**2-9.** Consider the system in Fig. 2-15. The load consists of three equal impedances of $Z = 0.103 + j0.051$ pu each, forming a balanced *delta*-connected load. The symmetrical three-phase voltage is 1.00 pu. Compute the power consumed by this load expressed in per units.

**2-10.** As we shall see in Chap. 5, a power transformer can be represented by an equivalent network consisting simply of a series impedance. Two transformers working in parallel therefore can be represented by the simple parallel circuit shown in Fig. 2-16. From this

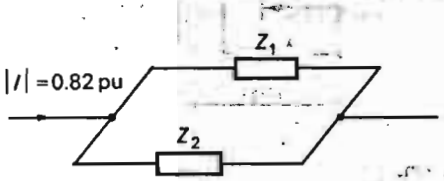


**Fig. 2-16** Equivalent circuit of two parallel working transformers.

circuit compute the total transformer losses if you know that the total current equals 0.82 pu, based upon 100 MVA and 220 kV.

The transformer impedances are

$Z_1 = 0.0051 + j0.103$ pu, based upon 220 kV and 50 MVA.

$Z_2 = 0.0063 + j0.0861$ pu, based upon 220 kV and 75 MVA.

(50 and 75 MVA are the ratings of each transformer.)

Express the power losses in per units of the base 100 MVA.

**2-11.** In the circuit in Fig. 2-17 the voltage of point $A$ is kept at a magnitude of 1 pu rms. Compute the powers (real and reactive) absorbed by the nine impedance elements. Their impedances (based on our selected MVA-kV base) are

$Z_1 = 0.015$ pu

$Z_2 = j0.100$ pu

$Z_3 = 0.21$ pu

$Z_4 = -j0.100$ pu

$Z_5 = j0.200$ pu

$Z_6 = j0.300$ pu

$Z_7 = -j0.201$ pu

$Z_8 = j0.40$ pu

$Z_9 = 0.600$ pu



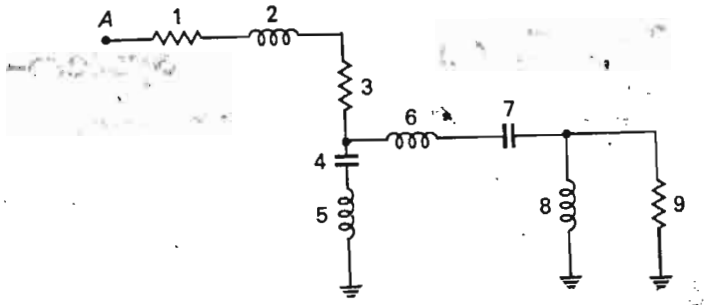


**Fig. 2-17** Circuit used in Ex. 2-11.

**2-12.** In a symmetrical $n$-phase system the $n$ phase voltages are of the form

$$v_1 = \sqrt{2}\,|V| \sin \omega t$$

$$v_2 = \sqrt{2}\,|V| \sin\left(\omega t - \frac{360°}{n}\right) \tag{2-55}$$

$$\cdots\cdots\cdots\cdots$$

$$v_n = \sqrt{2}\,|V| \sin\left(\omega t - \frac{(n-1)360°}{n}\right)$$

Compute the total power consumed by a balanced load consisting of $n$ star-connected equal impedances. Prove in particular that the power is constant.

## REFERENCES

**Books**

1. Meisel, J.: "Principles of Electromechanical Energy Conversion," McGraw-Hill Book Company, New York, 1966.
2. Fitzgerald, A. E., and C. Kingsley, Jr.: "Electric Machinery," 2d ed., McGraw-Hill Book Company, 1961.
3. Woodson, H. H., and J. R. Melcher.: "Electromechanical Dynamics," vols. I–III, John Wiley & Sons, Inc., New York, 1968.
4. Hallén, E.: "Electromagnetic Theory," John Wiley & Sons, Inc., New York, 1962.

(The introductory chapters of Refs. 1 to 3 constitute excellent supplementary reading for this chapter. Reference 4 treats field theory in a manner very appealing to a power major.)

# 3

# The Electric Energy System—Operational Considerations

## 3-1 OBJECTIVES

The basic objective of an electric energy system is to supply electric energy to the various loads throughout a given service area. Properly designed and operated, it should meet the following requirements:

1. It must supply energy practically everywhere the customer demands.
2. The load demands for real and reactive power vary with time. The system must be able to supply this ever-changing demand.
3. The delivered energy must meet certain minimum requirements in regard to "quality." Three basic factors determine this quality: (*a*) constant frequency; (*b*) constant voltage; (*c*) high reliability.
4. It should deliver energy at minimum economic and ecological costs.

In this chapter we examine those factors that closely affect these objectives. We start by discussing the system *structure* as being of basic importance in regard to the geographic availability of electric energy. We next define the *transmission capacity*, which concept determines the power-transmission capabilities of the network.

The character of the typical "load" is investigated, followed by a discussion of those factors that determine frequency and voltage constancy. Lastly, we concern ourselves with the questions of reliability and economy





## 3-2 THE STRUCTURE OF THE ELECTRIC ENERGY SYSTEM

An electric power system is never as simple as the one depicted in Fig. 2-8, characterized by one generator, one load, and one transmission line. Indeed, even the smallest power system constitutes an electric network of vast complexity. The one factor that determines the system structure more than any others is system *size*. The largest individual power company in the United States has an operating area covering seven states and has a peak demand of 10,600 MW and an annual production in excess of 67 billion kWh (1970 figures). The engineering objectives underlying the design of its 86,000-mile network must of necessity be very different from those that govern the construction of the system for a small municipal company with a load less than 1 MW. We shall not here enter into a discussion of the reasons of economical, political, historical, and technological nature that lie behind the present size distribution. By pointing out the great diversity in system magnitude, we wish to make it clear that there are no general rules regarding system structure that apply to *all* systems. It is possible, however, to discern certain similarities characterizing the majority, indeed most, of the systems.

All systems do one thing in common: operate at various voltage levels separated by transformers. Starting with the lowest voltage level, we can distinguish the following layers:

1. Distribution level (secondary and primary)
2. Subtransmission level
3. Transmission and pool level

Figure 3-1 shows schematically how a typical system is structured from a voltage-level point of view.

### 3-2.1 DISTRIBUTION LEVEL

The distribution circuits constitute the finest meshes in the overall network. Usually, two distribution voltage levels are used:

1. The *primary*, or *feeder*, voltage (for instance, 13,200 V)
2. The *secondary*, or *consumer*, voltage (for instance, 120/240 V).

The distribution circuits, fed from the *distribution substations* (transformer stations), supply energy to the small (domestic) or medium-sized (small industrial and commercial) customers.

Distribution engineering is in itself a subtechnology of considerable importance and variety, covering the problems of overhead or underground

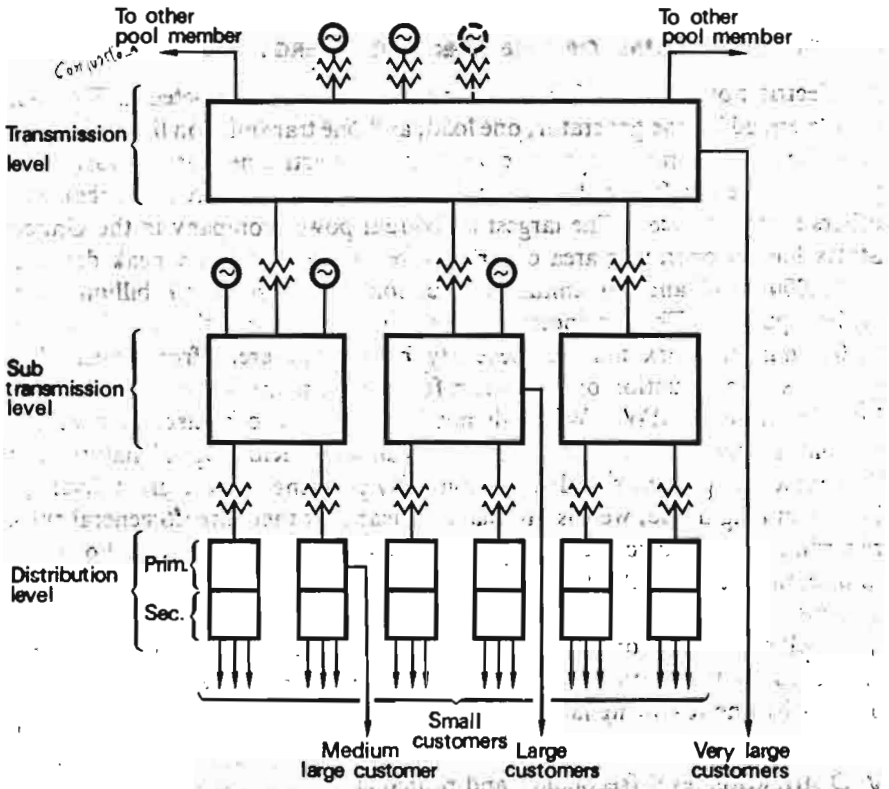


**Fig. 3-1** Power system structure.

service, metering, switching, and fusing. A typical system may have half its capital investment in distribution circuits.

### 3-2.2 SUBTRANSMISSION LEVEL

The subtransmission circuit distributes energy to a number of distribution substations in a certain geographical area at a voltage level that typically varies between 11 and 138 kV. It receives the energy directly from the generator bus in a generator station or via *bulk power substations*. Large customers are served directly from those stations.

The role of a subtransmission system is mainly the same as that of a distribution system, except that it serves a larger geographical area and distributes energy in larger blocks at higher power and voltage levels. It should be pointed out that in many systems there are no clear demarcation lines between subtransmission and transmission circuits. Increased load density makes it necessary and economical to superimpose a new and higher-voltage grid on the existing one. In this way yesterday's transmission network becomes part of tomorrow's subtransmission network.



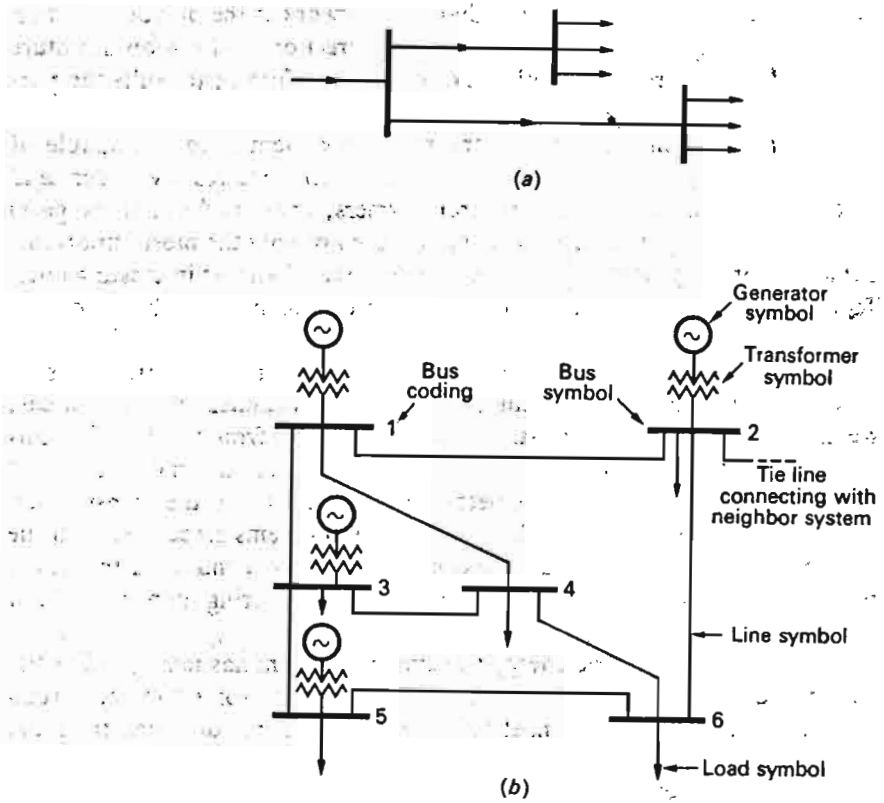


**Fig. 3-2** Radial- and loop-structured systems.

### 3-2.3 TRANSMISSION LEVEL

The transmission system is distinctly different in both its operation and characteristics from the distribution and subtransmission systems. Whereas the latter two simply draw energy from a single source and transmit it to individual loads, the function of the transmission system is quite different. Not only does it handle the largest blocks of power, it also interconnects all the generator stations and all the major loading points in the system. The energy can be routed, generally, in any desired direction on the various links of the transmission system in a way that corresponds to best overall operating economy or best serves a technical objective. Via *interties*, transport of energy can take place to or from other power systems belonging to the same *power pool*.

The fundamental difference in the purpose of the transmission system as compared with the subtransmission and distribution systems shows up in the network *structure*. Whereas the latter two generally (but not always) are of *radial* structure (Fig. 3-2*a*), the former tends to obtain a *loop* structure,

as exemplified in Fig. 3-2*b*.† A radial-type network is the obvious solution where the energy flow has a predominant direction. The loop structure obviously gives more path combinations, and therefore better suits the purpose of the transmission level.

Because, as mentioned, the transmission system is to be capable of handling the largest blocks of power in the system, we readily understand that the components (generators, transformers, lines, and switching gear) that make up this part of the power system are not only the most important, but also, from a systems engineering point of view, the most interesting ones. Transmission voltages used in this country are as high as 765 kV as of this writing.

Although the design and operation of distribution and subtransmission networks entail many important and interesting technical problem areas, we are forced, for reasons of space, to exclude them from the scope of this book. The most sophisticated engineering problems, and certainly the most important from the system engineers' viewpoint, involve the transmission level almost exclusively. We refer here to the problems associated with the control and routing of the large blocks of energy that move on this level, both during normal steady-state operation and during abnormal fault conditions.

Designing an electric energy transmission system has many similarities with the design of any other transportation system, for example, a road system. Many constraints must be taken into account, of which the more important are:

1. Existing system.
2. Geographical location of present and projected future load centers.
3. Suitable geographical location for generator stations. In particular, availability of fuel and cooling water for the condenser must be considered.

It is worth pointing out that the development of a power transmission system is a gradual growth process. In designing new links for the system, we must always base the design on predicted growth patterns of the population density and industry of the area. Power companies, by providing guarantees for cheap and abundant power for an undeveloped region, can actually strongly affect the growth of that region.

Within the given constraints, and after decisions of economical and often political nature have been made for expansion of the system, it is up

† Figure 3-2*b* represents a so-called "one-line" diagram of a transmission system. The symbols for generators, transformers, buses, lines, and loads that we shall use throughout the book are introduced in this figure. A nodal point of a transmission network is referred to as a "bus."



to the energy systems engineer to develop designs that are sound from a technoeconomical-ecological viewpoint.

Just as the geographical structure and the traffic-handling capacity of our interstate superhighway system must be determined by present and *future* traffic flow patterns and volume, so must the design of an electric transmission system be governed by present and *future* load flow patterns and load volume.

## 3-3 TRANSMISSION CAPACITY

A critical factor in the design and operation of a transmission system is the load capacity of a specific transmission link.

Quite clearly, in attempting to transmit electric energy via a transmission link, we would expect, if for no other reason than purely intuitional, that we would reach a limit beyond which no more energy can be "jammed into the line." In this section we shall investigate the limits for energy transmission under *static* conditions; i.e., we shall derive the *static transmission capacity*, or the *static stability limit*, of a transmission link. The assumption we make is that, by *slowly* increasing the load, we force a *slow* increase of the energy that is being transmitted via the link under study. To be specific, let us consider the link in Fig. 2-12, for which we have already derived expressions for the transmitted power.

To make the situation as simple and as clean-cut as possible, we shall initially make the additional assumption that the line is loss-free; i.e., we shall neglect the line resistance $R$ besides the reactance $X$. This is a reasonable practical assumption, the validity of which we shall confirm in Chaps. 4 to 6. With no real losses along the line,† the "sending-end" and the "receiving-end" real powers must be equal. For $R = 0$, Eqs. (2-47) actually give, for the transmitted real power,

$$P_{ij} = -P_{ji} = \frac{|V_i|\,|V_j|}{X} \sin \delta \tag{3-1}$$

We remember that $\delta$ represented the phase angle between $V_i$ and $V_j$. If the bus voltages are kept constant,‡ we can write the above equation as

$$P_{ij} = P_{\max} \sin \delta \tag{3-2}$$

where

$$P_{\max} \triangleq \frac{|V_i|\,|V_j|}{X} = \text{const} \tag{3-3}$$

† We still of course have *reactive* losses in the series reactance $X$.

‡ This is being accomplished by manipulation of the reactive power, as will be demonstrated in Example 3-2.

(Note that $P_{max}$ is obtained in three-phase megawatt units if the voltages are inserted in the formula in kilovolt line voltages.)

*The only way in which we can affect the magnitude of the transmitted power is, clearly, by changing the phase angle* $\delta$. When increased load forces the transmitted power upward, this takes place by an increase of the phase angle between $V_i$ and $V_j$. Figure 3-3 shows the relationship between the transmitted power and $\delta$. Note that the power reverses sign by sign reversal of $\delta$; that is, the direction of power flow is determined simply by which of the voltages, $V_i$ or $V_j$, is leading the other.

When we force the transmitted power to reach the value $P_{max}$, the angle $\delta$ has reached the value 90°, and any added increment to the load will not result in a corresponding increase in the transmitted power. Actually, when the added load forces $\delta$ beyond 90°, the transmitted power starts to *decrease*. At this point, referred to as the *static stability limit*, the system "pulls apart electrically"; i.e., we lose synchronism between the buses *i* and *j*.

We may obtain a good analogy by considering the mechanical transmission gear in Fig. 3-4. Torque transmission between the two shafts *i* and *j* (corresponding to buses *i* and *j*) takes place via two spring-coupled disks.

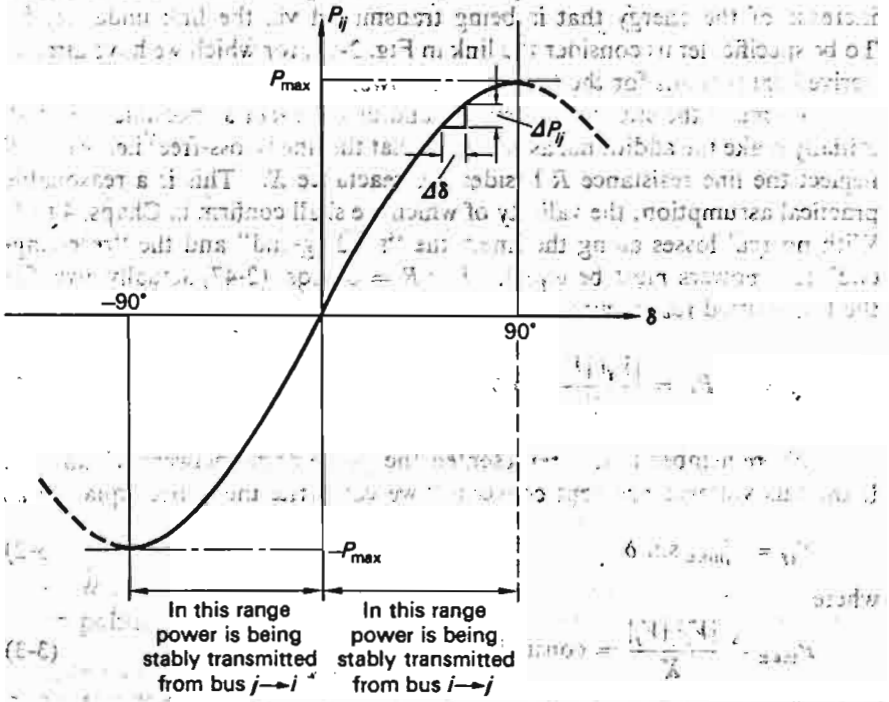


**Fig. 3-3** Line power versus power angle.



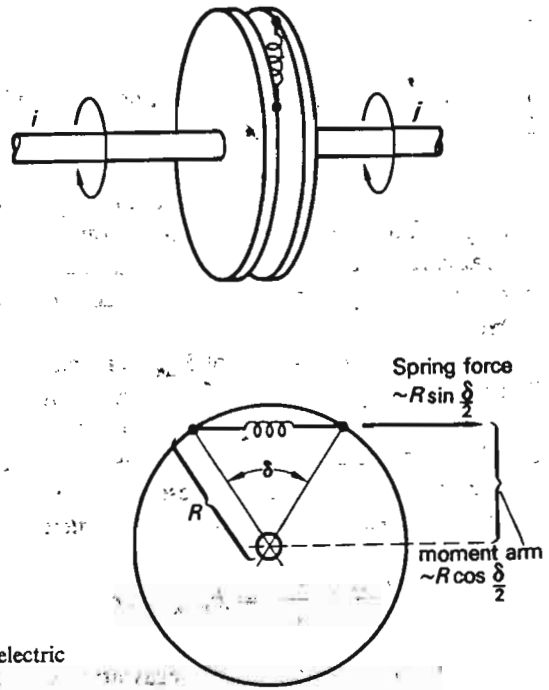


**Fig. 3-4** Mechanical analog of electric transmission link.

If we assume that the distance between the disks is negligible, and if the spring force is proportional to the length of the spring, then the *torque* $T$ maintained between the shafts equals

$$T = \text{force} \times \text{moment arm} = kR \sin \frac{\delta}{2} \times R \cos \frac{\delta}{2}$$
$$= \frac{kR^2}{2} \sin \delta \quad \text{N} \cdot \text{m} \tag{3-4}$$

where $k$ is the spring constant, measured in newtons per meter elongation. Transmitted mechanical power $P_{mech}$ equals $\omega_{mech} T$, and we thus have

$$P_{mech} = \omega_{mech} \frac{kR^2}{2} \sin \delta = P_{max} \sin \delta \quad \text{W} \tag{3-5}$$

A comparison of Eqs. (3-2) and (3-5) should confirm the analogy between the electrical and mechanical transmission systems. The reader will easily understand what happens in the mechanical case when we attempt to transmit power in excess of $P_{max}$.

The maximum real power $P_{max}$ in Eq. (3-2) represents the *static transmission capacity* of the link if operated as assumed (i.e., with constant

bus voltages). We note two important characteristics of $P_{max}$:

1. It increases as the square of transmission voltage.
2. It is inversely proportional to line reactance.

We therefore again have found a good reason for high transmission voltage. Low series reactances in our transmission systems are also a desirable feature. They may be obtained by paralleling lines, using "bundle conductors" or insertion of series capacitors. We shall discuss these matters in Chap. 6.

The above derivation of $P_{max}$ was made for a lossless transmission link. The student is invited to perform the analysis for the lossy case in Exercise 3-2.

The *incremental* increase in transmitted power, $\Delta P_{ij}$, as caused by a small increment $\Delta\delta$ in the angle $\delta$, is a measure of the "electrical stiffness" of the transmission link. These increments are shown in Fig. 3-3. We define a stiffness, or synchronizing, coefficient

$$T_{ij} \triangleq \frac{\Delta P_{ij}}{\Delta\delta} \approx \frac{dP_{ij}}{d\delta} = P_{max} \cos\delta \tag{3-6}$$

$T_{ij}$ is obviously measured in megawatts per radian, and the reader should appreciate its close analogy with a spring constant. Note that, as $\delta$ approaches $\pm 90°$, the stiffness goes to zero. This is the reason why we seldom operate our lines with power angles $\delta$ in excess of about 30 to 45°. The system is getting electrically "softer" the closer we approach the stability limit. (The mechanical system in Fig. 3-4 has the same feature.)

**Example 3-1** To obtain a feel for the magnitudes involved, let us compute the transmission capacity for two different lines, both having an assumed length of 100 miles.

*Case A* This line is designed for a nominal voltage of 140 kV and consists of one conductor per phase. Line reactance is 0.8 Ω/mile for a total reactance of 80 Ω (Chap. 6). From Eq. (3-3), we thus get

$$P_{max} = \frac{(140)^2}{80} = 245 \text{ MW} \qquad \text{three-phase}$$

*Case B* This line is designed for a nominal voltage of 765 kV and consists of four conductors ("bundle") per phase. Line reactance is 0.55 Ω/mile for a total reactance of 55 Ω. Thus

$$P_{max} = \frac{(765)^2}{55} = 10{,}600 \text{ MW} \qquad \text{three-phase}$$

The 765-kV line would thus handle the same power as 43 lines rated at 140 kV.



## 3-4 LOAD CHARACTERISTICS

We have on several occasions referred to "load," "load impedance," etc., without giving much justification for our assumptions. For example, we have assumed symmetry between the phases, which presupposes that whatever the load is, it is equally distributed between the three phases. It is appropriate at this time to present a more detailed discussion of typical load characteristics.

Generally, the term *load* shall refer to a device or a conglomeration of devices that tap energy from the network. In a practical situation the load devices may range from a few-watt night lamp to a multimegawatt induction motor. The power system, if properly designed, shall be capable of supplying energy to all of them. It is possible to divide the various load devices we may encounter into the following categories:

1. Motor devices (including stationary ones in the industry and portable ones in transportation equipment, i.e., trains, etc.)
2. Heating equipment
3. A diversity of electronic gear
4. Lighting equipment

From an electrical point of view the multitude of devices are characterized by vast differences in regard to:

1. Size
2. Symmetry (single- or three-phase)
3. Load constancy (in respect to time, frequency, and voltage)
4. Use cycle (regular or random use)

For example, industrial loads may have few, if any, resemblances to domestic loads in respect to all the above categories. A certain type of industry load may be made up to 95 percent of large three-phase motors with considerable load constancy and very predictable duty cycle (on at 8 A.M., off at 5 P.M.). A typical domestic load, on the contrary, may consist mostly of single-phase apparatus operated in random manner by housewives. How does one logically go about putting any order in such a picture? The fact is that the situation is not as hopeless as it appears at a first glance. *The laws of statistics are on our* (the system engineers') *side.* Whereas the *individual* loads may be entirely random in character, a certain average pattern is recognizable already at the distribution transformers. At the subtransmission level, this averaging effect is still more pronounced. Finally, at the transmission level, we reach an almost predictable situation.

To be fair, we must admit that we "help" the law of statistics to work their way. For example, on the distribution level we always distribute, by design, the single-phase loads between the three phases.

In summary fashion we give the following rules characterizing typical system loads:

1. Although individually of random type, the *lumped*, or *composite*, loads, as we encounter them at subtransmission or transmission levels, are of highly predictable character.
2. These lumped loads vary in a *predictable* fashion *with time*. Figure 3-5 shows some typical load variations for a medium-sized company. In general, there is considerable variation, not only throughout the hours of the day, but also between weekdays and Sundays and holidays and also between different seasons.
3. Although the loads are time-variant, the variations are relatively *slow*. From *minute to minute* we have an almost *constant* load. *A minute is a long time period compared with the electrical time constants of the power system, and this permits us to consider the system operating in steady state—a steady state that slowly "shifts" throughout the hours of the day* ("quasi-static" operation).

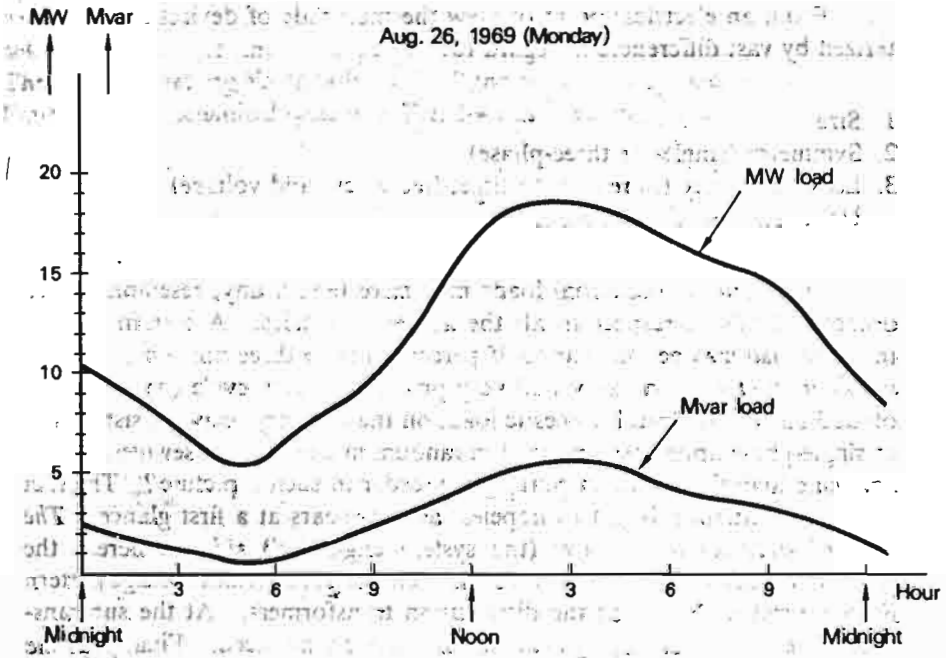


**Fig. 3-5** Typical load variation with time.



4. The typical load always *consumes* reactive power. The reason for this is that motor load is an important (actually *the* most important) ingredient in most cases. Motors are *always* (with the exception of overexcited synchronous machines) *inductive*.
5. The typical load is always *symmetric*. In the case of large motors (greater than a few horsepowers), this symmetry is automatic, since they are always designed for balanced three-phase operation.

   In the case of single-phase devices, the symmetry comes about by intentional distribution between phases and statistical effects.

### 3-4.1 VOLTAGE AND FREQUENCY LOAD DEPENDENCY

We shall find in later chapters that it is necessary in certain system studies to know how the various bus loads vary with frequency and voltage. If the load consists of an impedance, it is simple to find these relationships *analytically*. For example, consider the series $RL$ load in Table 2-1. From the formula

$$P + jQ = |V|^2 Y^*$$

we obtain the following load formulas in this case:

$$P = \frac{R|V|^2}{R^2 + (2\pi fL)^2}$$
$$Q = \frac{2\pi fL|V|^2}{R^2 + (2\pi fL)^2} \tag{3-7}$$

The formulas reveal that both $P$ and $Q$ increase as the square of the voltage magnitude, a feature characterizing all "impedance loads."

The formulas furthermore tell us that $P$ decreases but $Q$ increases with increasing frequency. Equations (3-7) are of the form

$$P = P(f, |V|)$$
$$Q = Q(f, |V|) \tag{3-8}$$

Composite loads, which constitute the vast majority of actual loads, also vary with voltage and frequency, and can therefore also be written in the form of Eqs. (3-8). However, for this type of load the functional relationships cannot as a rule be found analytically. The best we can hope for in a practical situation is to estimate, measure, or by some empiric method find the voltage and frequency dependency.

In most practical situations we shall be concerned with the changes $\Delta P$ and $\Delta Q$ in the real and reactive loads as caused by relatively *small* variations

$\Delta f$ and $\Delta |V|$ in frequency and voltage. From Eq. (3-8) we obtain, in this case,

$$\Delta P \approx \frac{\partial P}{\partial f}\Delta f + \frac{\partial P}{\partial |V|}\Delta |V|$$
$$\Delta Q \approx \frac{\partial Q}{\partial f}\Delta f + \frac{\partial Q}{\partial |V|}\Delta |V| \qquad (3\text{-}9)$$

The four partial derivatives in these expressions cannot be determined analytically for composite loads; they must be found empirically. These partial derivatives take on the role of load parameters which fully describe the nature of the load around the nominal voltage and frequency levels. They vary widely with the physical character of the load. For example, a load composed mainly of induction motors has very different parameters compared with a heating-type load.

A number of studies have been made about the frequency and voltage dependency of "typical" composite loads. In taking the average of a number of such studies, we define an "average load" as one having the following *approximate* composition:

Induction motors, 60 percent
Synchronous motors, 20 percent
Other "ingredients," 20 percent

Such a load would have the following *approximate* parameters:

$$\frac{\partial P}{\partial |V|} \approx 1.0 \qquad \text{percent/percent}$$
$$\frac{\partial Q}{\partial |V|} \approx 1.3$$
$$\frac{\partial P}{\partial f} \approx 1.0$$

($\partial Q/\partial f$ is not available and is of less practical importance.)

We make the following important observations:

1. A composite load is characterized by much lower voltage dependency than impedance load (1 versus 2 percent).
2. Whereas an *RL* impedance load in accordance with Eqs. (3-7) actually decreases with increasing frequency, a composite load will *increase*. This is due to the predominance of motors, which *always* will experience increased load as frequency (and speed) increases.



## 3-5 THE REAL POWER BALANCE AND ITS EFFECT ON SYSTEM FREQUENCY

There are at least three good reasons why we should keep strict limits on the system frequency fluctuations:

1. Most types of ac motors run at speeds that are directly related to the frequency.
2. A large number of electrically operated clocks are used. They are all driven by *synchronous* motors, and the accuracy of these clocks is a function not only of the frequency error but, actually, of the *integral* of this error.
3. The overall operation of a power system can be much better controlled if we keep the frequency error within strict limits.

The first of the above reasons does not put particularly strict bounds on the frequency swings. The vast majority of ac motor-driven loads probably would not be sensitive to frequency fluctuations of the order of $60 \pm 2$ Hz.

The second and third reasons are the really important ones. It is a fact that unusual deviations in frequency indicate that something is basically wrong with a system. When the system becomes "sick," our frequency sensors serve as "fever thermometers." (The analogy is not too good—a sick body increases its temperature, whereas the frequency of a faulty system usually drops.) By reducing *normal* frequency fluctuations to a faint ripple, we are able to detect the frequency disturbances following a fault at an early stage. In modern energy systems the frequency constancy is normally kept within $\pm 0.05$ Hz.

### 3-5.1 LOAD-FREQUENCY MECHANISM

Before we attempt to explain the means we have at our disposal to control the system frequency, it is appropriate that we should examine the reasons why it tends to vary in the first place.

*The frequency is closely related to the real power balance in the overall network.* Under normal operating conditions the system generators run *synchronously* and generate together the power that at each moment is being drawn by all loads, *plus* the real transmission losses. The latter, amounting usually to a few percent, consist of ohmic losses in the various transmission components, corona losses on the lines, and core losses in transformers and generators. We must remember that the energy is being transmitted at the velocity of light, and since it is not being stored† somewhere in the system,

† The storage that actually takes place in the *reactive* elements (coils and capacitors) at the rate of twice per cycle amounts, as we recall, to zero average, and therefore does not enter into our discussion.

*we conclude that the energy production rate must equal the consumption rate (plus losses).*

It should be pointed out (and this will be explained more carefully in Chap. 4, in our discussion of synchronous generators) that the synchronous operation of generators represents a *stable* system state. By that we mean that once a generator has been synchronized onto a network, electromechanical forces build up within the machine that tend to keep it running at the same speed as the rest of the network. Once the speed of the generator has been thus *locked* to that of the rest of the system, we may control its real-power generation by controlling the torque from its prime mover. By opening the steam valve and thus increasing the steam pressure on the turbine blades, or in the case of a hydroturbine, by opening the water gates, we apply greater torque to the generator, thereby tending to accelerate the generator. However, its speed is tied to the rest of the system, and what happens is that its rotor advances its running angle a few degrees. This results in an increase in delivered current and power, and at the same time the current builds up a decelerating torque within the machine that exactly counteracts the increase in accelerating torque.

Within each generator we thus have a delicate and automatic torque-balancing mechanism. If all generators have a perfect torque balance, their speed, and thus frequency, must remain constant. The ideal way to operate the system would therefore be to instruct the machine operators to set all water gates and steam valves of the various generators at values that would *exactly* correspond to the load demand. We would then have a perfect real-power balance with constant speed and frequency, and the operators could take a coffee break.

Unfortunately, reality is not so accommodating. As we remember from a previous section, the system load can be predicted only to within certain limits. Its fluctuations are entirely random in character, and it is indeed impossible to accomplish a perfect instant-by-instant match between generation and demand. There will *always be* a small surplus or deficiency in the generation, *and this everpresent mismatch will cause frequency fluctuations.*

To understand this important fact let us consider what would happen if we were running at 60.00 Hz perfectly power-matched and suddenly experienced a small load drop. The prime mover valve settings would be unchanged (since they are ignorant about the load change), meaning, in effect, that the driving torques were unchanged. The decrease in load results in a current decrease that would be distributed among all generators, resulting in a slight decrease in the electromechanical torques in every machine. Every generator would thus experience a small surplus accelerating torque, with an ensuing speed (and frequency) increase.



The rate at which the speed (and frequency) increased would depend upon the total moment of inertia of the running equipment. All tens of thousands of motors which during these moments were being supplied by the network would likewise experience the frequency increase. Their speeds would go up, and they would all meet higher load torques, thus requiring the motors to pull more power from the network. The resulting load increase would soon balance out the load decrease that started the whole chain of events, and the frequency would level off at a new higher value.

We have chosen to discuss this *load-frequency* interrelationship in great detail because it constitutes one of the most important basic phenomena in the power system. The example just discussed is realistic in all respects except one: in real life the prime mover power settings would not remain fixed in face of the shifting frequency. The attentive reader probably has already reached the important conclusion that *inasmuch as the frequency constitutes a sensitive indicator of the energy balance in the system, it should indeed be used as the sensor portion of the control system, the job of which is to provide such a balance automatically.*

### 3-5.2 A MECHANICAL ANALOG

Let us for a moment digress from our topic in order to study a mechanical system that constitutes a very good model, or analog, of a power system. Consider a freight train consisting of several engines and a string of freight cars. It is desired to keep the velocity of the train automatically controlled at $60.00 \pm 0.05$ miles/h, in spite of the fact that the train will experience fluctuating grades along its course. The obvious way to accomplish this job would be to measure the speed with a sensor, accurate to the desired degree, and let the amplified signal from this sensor command increased or decreased engine power whenever the speed deviated from the reference setting of 60.00 miles/h. This is an example of the classical control problem.

When posing control problems, there is the problem of *control strategy:* in this case we must ask ourselves *how* the *speed-error signal* should affect a change in engine power. Should the error signal command an engine power change proportional to the speed error (*proportional* control) or should we be more sophisticated and let the power increase be on the job *ahead* of an actual speed change by using *derivative* control? Or should we use some other strategy? Also, there is the important question: Should we command appropriate changes in the engine power for all engines or should we let one or possibly two engines take on the role of speed regulators, keeping the throttles constant on the remaining engines? Whatever strategy we settle on, there is finally the problem of *stability* of the selected control loop.

The reader realizes, of course, the analogy between the speed-regulation

problem of the train and the frequency-regulation problem of the energy system. This so-called *load frequency control problem* occupies a central position in EESE, and we shall devote considerable attention to it in Chap. 9.

## 3-6 THE REACTIVE POWER BALANCE AND ITS EFFECT ON SYSTEM VOLTAGE

Just as constancy of the system frequency is our best guarantee that real power balance is being maintained in the system, so does an unchanged bus voltage profile represent the criterion that balance is kept between produced and consumed reactive power. Whenever the magnitude of a particular bus voltage undergoes variations, this means that $Q$ balance is not kept at the bus in question.

To understand this situation, consider the two-bus system in Fig. 3-6*a*. The load $P + jQ$ is tapped from *load bus* 2. Since no generator exists at this bus, the load must be transmitted via the line from bus 1.

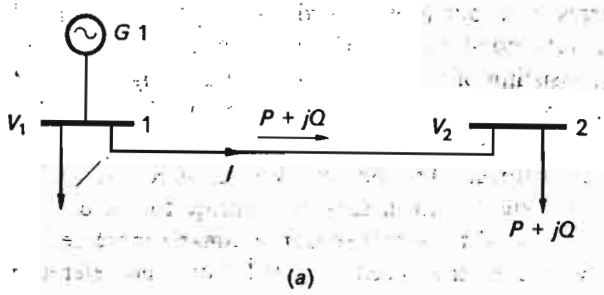


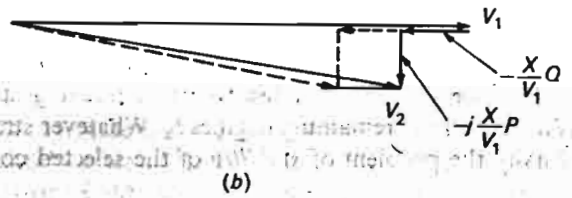


**Fig. 3-6** Change in voltage profile as a function of reactive line flow.



For the following analysis we shall make these simplifying but reasonable assumptions:

1. The bus voltage $V_1$ is kept at constant magnitude by field control of $G1$. We choose $V_1$ as reference voltage.
2. The transmission line impedance is purely inductive, i.e.,

$$Z = jX \tag{3-10}$$

3. The line power is set equal to $P + jQ$. Since we have neglected the line resistance, this implies no approximation as far as $P$ is concerned. However, due to reactive losses in the line reactance, the reactive line power is somewhat greater at the sending end.

Due to the voltage drop along the line, we have the following voltage relation:

$$V_2 = V_1 - IZ \tag{3-11}$$

The line current $I$ satisfies the relationship

$$V_1 I^* \approx P + jQ \tag{3-12}$$

Thus

$$I \approx \frac{P - jQ}{V_1^*} = \frac{P - jQ}{V_1}$$

The last step follows as a consequence of our choosing $V_1$ as reference phasor, i.e., $\underline{/V_1} = 0$. From Eq. (3-11) we therefore have

$$V_2 = V_1 - \frac{P - jQ}{V_1} jX = V_1 - \frac{X}{V_1} Q - j\frac{X}{V_1} P \tag{3-13}$$

We have identified these three voltage terms in the phasor diagram in Fig. 3-6*b*. The following facts should be immediately clear from this diagram:

1. A change in the *real* load $P$ affects the voltage-drop phasor which is *perpendicular to* $V_1$. No appreciable change in the *magnitude* of $V_2$ will thus ensue.
2. A change in the *reactive* load $Q$ affects the voltage-drop phasor which is *in phase* with $V_1$. The change in the magnitude of $V_2$ is therefore essentially proportional to $Q$. (The dotted voltage phasors illustrate the change in $V_2$ if the reactive load is doubled.)

*If we wish to keep the magnitude $|V_2|$ constant, we must arrange to have the shifting $Q$ demands matched locally at bus 2 so that they need not be transported on the line, with accompanying strong effects on the voltage.*

Such local $Q$ generation can be achieved by shunt capacitors and/or synchronous condensers (Chap. 4). We mentioned in our discussion of composite loads that typical loads are *inductive*. As the real load increases, the reactive load thus follows. There is therefore a tendency in a normal system for the voltages to drop during periods of peak load.

The opposite effect is discernible during light-load periods in the early morning hours. Due to the ever-present shunt capacitance in lines, and particularly in cables, we may actually have a *surplus* of reactive power on our hands. This means that the $Q$ flow in Fig. 3-6 reverses direction, and so does the phasor $XQ/V_1$ in Fig. 3-6*b*, with the result that the voltage drop changes to a voltage *rise*. It may actually be necessary, during light-load hours, to connect $Q$-consuming elements, i.e., shunt reactors to certain points in the network, to keep the voltage from going too high.

We should also point out that there is really no practical need for any *excessive* rigidity in our requirements for voltage constancy. Let us see why we want voltage control in the first place.

Practically all equipment used in a power system is designed to operate at a certain voltage level, the *rated*, or *nameplate*, voltage. If the system voltage should deviate from that value, the performance of the device suffers, and its life expectancy drops. For example, the torque of an induction motor is proportional to the square of the terminal voltage; the light flux from a lamp varies strongly with the voltage; etc.

The motivations for controlling the voltage level on a power system are thus strong. However, there is no need to regulate it to within the same narrow margins as was the case with system frequency. Industry-wide standards exist, specifying favorable and tolerable voltage variations on a network. In most practical situations we will actually tolerate a higher voltage profile on the transmission system during the light-load hours than during the peak hours. By changing the transformation ratio on the most important transformers, we can compensate for this changing primary voltage profile and still keep the secondary voltage level constant at the customer levels. Such tap changes can be performed either manually or automatically.

**Example 3-2** Add a generator to bus 2 in the two-bus system in Fig. 3-6. We wish to find the required outputs of the generators at each bus in order to maintain a specified voltage profile. In Fig. 3-7*a* we define the powers at the various points in the system. We shall work the problem on the basis of the following data and assumptions:

1. The desired voltage profile is flat. The two bus voltages must be kept at
$$|V_1| = |V_2| = 1.00 \quad \text{pu}$$
2. The line reactance equals 0.03 pu. Resistance is neglected.



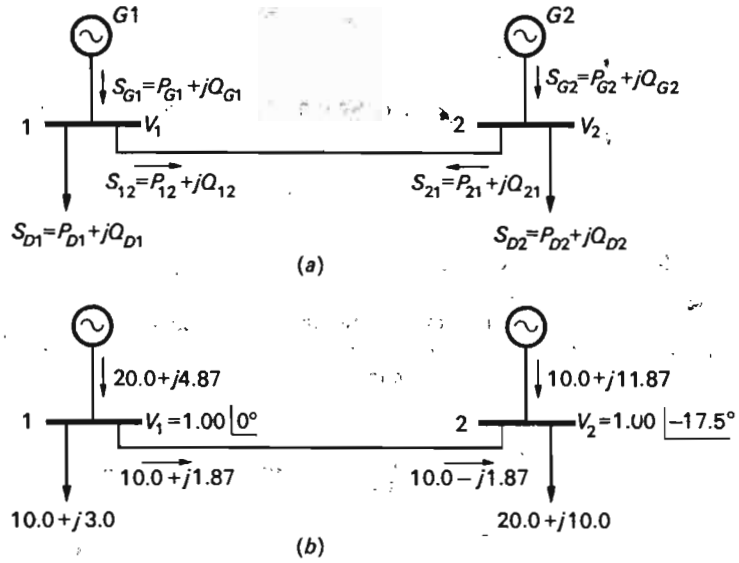


**Fig. 3-7** Two-bus system.

3. The load demands at the two buses are
$$S_{D1} = 10.0 + j3.0 \quad \text{pu}$$
$$S_{D2} = 20.0 + j10.0 \quad \text{pu}$$
4. Of the total real load (= 30.0 pu), only 10.0 pu can be generated in $G2$, due to generator size. Therefore a real load of 10.0 pu must be exported from $G1$ via the line. Since the real line losses are zero, the total real generation in $G1$ will be 20.0 pu.

Before we proceed with the analysis, we first need the following formulas for the line powers, obtained directly from Eqs. (2-47) by setting $R = 0$.

$$P_{12} = -P_{21} = \frac{|V_1|\,|V_2|}{X} \sin\delta$$
$$Q_{12} = \frac{1}{X}(|V_1|^2 - |V_1|\,|V_2| \cos\delta) \tag{3-14}$$
$$Q_{21} = \frac{1}{X}(|V_2|^2 - |V_1|\,|V_2| \cos\delta)$$

Since we know the magnitude of the real line power and the magnitudes of the bus voltages, we obtain from the first of these equations

$$10.0 = \frac{1 \times 1}{0.03} \sin\delta$$

Thus

$$\delta = 17.5°$$

derivatives in per-unit megawatts or megavars per hertz or volt. (For example, find $\partial P/\partial f$ in per-unit megawatts per hertz.)

(*b*) Compute from Eqs. (3-9) the total change in $P$ and $Q$ if voltage and frequency both increase by 1 percent each.

**3-2.** The static transmission capacity given in Eq. (3-3) was derived on the assumption of zero real line losses. Repeat the analysis *without* this assumption. (Note that the sending-end and receiving-end real powers are *not* equal in this case. Find the maximum for the receiving-end power.) Assume that the terminal voltages are kept at constant magnitude.

**3-3.** Consider Example 3-2. Compute the required reactive output from each generator if we wish to hold a voltage profile characterized by

$$|V_1| = 1.00 \quad \text{pu}$$
$$|V_2| = 0.95 \quad \text{pu}$$

Use the same line data and assumptions about load and real generation as was used in the text. What does the exercise teach you?

**3-4.** A transmission line is characterized by a series reactance of 30 Ω per phase. To increase the power transmission capacity, we wish to reduce this impedance by 40 percent per phase by inserting series capacitors in each phase (so-called "series compensation"). The largest-magnitude current that is expected to flow in the line is 1 kA per phase. Frequency is 60 Hz.

(*a*) Determine the capacitance per phase that must be installed in order to accomplish the desired compensation.

(*b*) It is assumed that commercially available capacitors have a voltage and current rating of 2 kV and 50 A per unit. How would you combine such units into a bank to achieve the desired compensation? What must the individual capacitance per unit be?

(*c*) How many kilovars would each unit produce if maximum current flowed in the line? How many kilovars would be produced totally in all three phases?

**3-5.** A power system has an installed generator capacity of 2000 MW. The total synchronous rotating inertia of the system (generators and motors) represents at a certain hour of the day a total kinetic energy of 10,000 MWs (or 2780 kWh). The frequency is 60.00 Hz, and the system is in perfect energy balance. At this moment we experience a sudden load increase of 50 MW (= 2.5 percent of installed capacity). At what initial rate, expressed in hertz per second, will the frequency decrease *if we do not compensate by increasing the production*? (This is actually the system deceleration that we experience during the initial instants of time when, due to time lags in the control loop, the steam valves have not yet started to open.)

**3-6.** Consider a transmission line characterized by $R = 0$. The line is operated at its maximum capacity, that is, $\delta = 90°$, and with both terminal voltages equal to 1 pu. Define $P_{max}$ as base power = 1 pu.

(*a*) Prove that the reactive losses in the line amount to the staggering amount of 2 pu.

(*b*) Prove that the voltage as measured midline is only 0.71 pu.

**3-7.** If in Exercise 3-6 we could "support" the "sagging" voltage midline, we could increase the transmission capacity of the line. Specifically, prove that $P_{max}$ of the line can be increased by 100 percent by keeping (by means of a synchronous condenser or a shunt capacitor) the midline voltage at 1 pu, i.e., the same voltage as at the ends.

(Note that the role of the synchronous condenser is to inject reactive power in the midpoint. Compare also Example 3-2.)

**3-8.** The three Eqs. (3-14) contain six variables, $|V_1|$, $|V_2|$, $\delta$, $P_{12}$, $Q_{12}$, and $Q_{21}$. Therefore, if we want to solve the equations, we must specify *three* of the variables; then the remaining three will follow as solutions of the equations. For example, in Example 3-2 we had



specified $|V_1| = |V_2| = 1$ pu and $P_{12} = 10$ pu. We then could solve for $\delta$, $Q_{12}$, and $Q_{21}$.

(*a*) Specify $\delta = 30°$, $|V_1| = |V_2| = 1$ pu. You should not have any difficulty solving for the three unknowns $P_{12}$, $Q_{12}$, and $Q_{21}$. (Assume $X = 0.03$ pu.)

(*b*) Specify $P_{12} = 10$ pu and $Q_{12} = Q_{21} = 0$ pu. Now you will have difficulty finding the unknowns $\delta$, $|V_1|$, and $|V_2|$. Explain why.

**3-9.** In deriving Eq. (3-13), we based our analysis on the approximate assumption that the line power is equal throughout the line. If we require that our results be *exact*, we run into some computational difficulties when we attempt to find the current. If we use Eq. (3-12) and apply it to the sending end, we know $V_1$ *but not* the power (since we do not know the line losses). If, instead, we apply the formula to the receiving end, we know the power *but not* the voltage $V_2$ (since we do not know the size of the voltage drop).

We can approach the problem in the following way. We *assume* a reasonable value for $V_2$, and based upon this assumption, we can obtain an *approximate* solution for $I$.

On the basis of this $I$ value, we compute the voltage drop and then obtain an approximate *but better* value for $V_2$ than we originally assumed. With this value of $V_2$ we compute a second, and better, value for $I$, and we can then repeat the whole process. This is called an *iterative* computational process, and is often used in conjunction with a digital computer. The iterative process is stopped when we converge on a solution. (How do we know when to stop?)

Use this technique to find a value for $V_2$ based upon the following data: Line impedance:

$$0.005 + j0.03 \quad \text{pu}$$
$$V_1 = 1.00 \angle 0° \quad \text{pu}$$

Load at bus 2: $10.0 + j5.0$ pu

If you have the opportunity, program the iterative computations on a computer.

**3-10.** Consider the *RC* series impedance load (item 6) in Table 2-1. We have

$$R = 10\,\Omega$$
$$\frac{1}{\omega C} = 10\,\Omega \quad \text{at } f = 60.00 \text{ Hz}$$

The voltage is 10 kV rms.

Compute $\partial P/\partial f$, $\partial P/\partial |V|$, $\partial Q/\partial f$, and $\partial Q/\partial |V|$ for this load.

**3-11.** Assume that the load in Exercise 3-5 has the characteristic

$$\frac{\partial P}{\partial f} = 20 \text{ MW/Hz}$$

If we assume that no change is taking place in the prime mover settings, at what new frequency will the system level off following the 50-MW load increase? Compute and plot the change in frequency versus time following the sudden load increase.

**3-12.** Consider the transmission line in Fig. 2-12. The line has a reactance of 0.095 pu and a negligible resistance.

Generators are feeding both buses, and automatic voltage regulators working in the field circuits of these generators are keeping the two bus voltages constant at the values

$$|V_i| = 1.00 \quad \text{pu}$$
$$|V_j| = 0.95 \quad \text{pu}$$

The static stability limit of the line is evidently 10 pu MW.

We consider now three operational cases characterized by the following real line powers:

*Case I.* $P_{ij} = 1$ pu MW
*Case II.* $P_{ij} = 5$ pu MW
*Case III.* $P_{ij} = 8$ pu MW

The three cases correspond to a light, moderate, and heavy line load.

(*a*) Compute the reactive line flows $Q_{ij}$ and $Q_{ji}$ in the three cases.

(*b*) Increase the real loads by 1 percent in each case and determine, in each case, the percentage change in the reactive flows.

The bus voltages are kept constant throughout.

(*c*) A change in the $P$ flow evidently affects the $Q$ flow. Differently stated, the $Q$ flow is sensitive to changes in the $P$ flow. Does the degree of real line load affect this sensitivity? How?

## REFERENCES


### Books

1. Zaborszky, J., and J. W. Rittenhouse.: "Electric Power Transmission," The Ronald Press Company, New York, 1954.
2. Mortlock, J. R., and M. W. Humprey Davies.: "Power System Analysis," Chapman and Hall, Ltd., London, 1952.
3. Stevenson, W. D.: "Elements of Power System Analysis," 2d ed., McGraw-Hill Book Company, New York, 1962.
4. Tarboux, J. G.: "Introduction to Electric Power Systems," International Textbook Company, Inc., Scranton, Pa., 1944.
5. Rothe, F. S.: "An Introduction to Power Systems Analysis," John Wiley & Sons, Inc., New York, 1953.
6. Stagg, G. W., and A. H. El-Abiad: "Computer Methods in Power Systems Analysis," McGraw-Hill Book Company, New York, 1968.
7. Weedy, B. M.: "Electric Power Systems," John Wiley & Sons, Inc., New York, 1967.
8. Waddicor, H.: "Principles of Electric Power Transmission," Chapman and Hall, Ltd., London, 1964.
9. Knable, A. H.: "Electrical Power Systems Engineering Problems and Solutions," McGraw-Hill Book Company, New York, 1967.
10. Dineley, J. L. (ed.): "The Use of Digital Computers in Electric Power Systems," Oriel Press, Newcastle upon Tyne, England, 1967.
11. Skrotzki, B. G. A. (ed.): "Electric Transmission and Distribution," McGraw-Hill Book Company, New York, 1954.
12. Hore, R. A.: "Advanced Studies in Electrical Power System Design," Chapman & Hall, Ltd., London, 1966.

(References 1 to 3 are the "classics" in the power systems field. Although of "precomputer" age, these books still convey relevant information, and should deserve a place in a complete power system library. Reference 6, although not claiming to be an undergraduate text, must be given credit for stirring new academic interest in the power field. Reference 7 caters to the undergraduate student but suffers the disadvantage of being far too superficial.)

### Technical papers and reports

13. Kent, M. H. et al.: "Dynamic Modeling of Loads in Stability Studies," paper 68, TP 706-PWR, ASME/IEEE Joint Power Generation Conference, San Francisco, Sept. 15–19, 1968.





14. Stone & Webster Engineering Corporation: Northeast Interconnection Study, Boston, November, 1966.
15. *Proc. Instr. Soc. Am., Tenth Natl. Power Instrumentation Symp.*, vol. 10, May 8–10, 1967, Dallas, Texas.
16. Editors of *Power*: "Power Generation Systems," McGraw-Hill Book Company, New York, 1966.
17. The Effect of Frequency and Voltage on Power System Load, IEEE Committee Report, presented at IEEE Winter Power Meeting, New York, 1966.

# 4

# The Synchronous Machine—System Model Representation

## 4-1 INTRODUCTION

The synchronous generator, the three-phase transformer, and the high-energy transmission line constitute the basic components of an electric energy system. The reader has no doubt been exposed to the theory of all these devices in his previous course work. It is tempting, therefore, to skip these topics altogether and proceed with our main business, the study of the overall system. However, we will not take this approach, for the following reasons:

1. If the reader is a junior- or senior-level student, he will most probably have been exposed to the theory of some or all of these devices in an *elementary* way only.
2. If the reader is a practicing engineer, he most probably has a thorough knowledge of the operating characteristics of these devices in terms of *classical steady-state* models. From a system-analysis point of view, these models are not powerful enough, particularly if we are concerned with the *dynamic* system behavior.





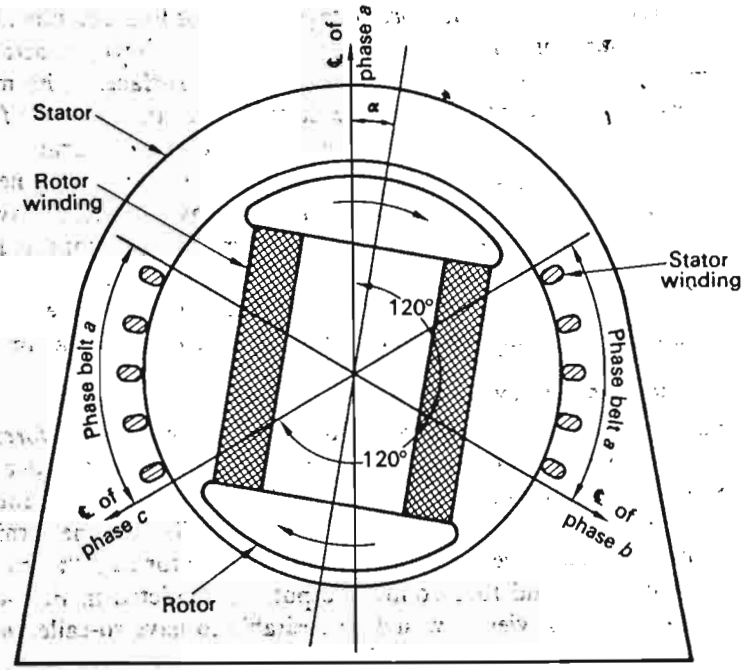


**Fig. 4-1** Schematic design of 3-phase synchronous machine.

Our discussion of synchronous machines in this chapter, and of the transformer and transmission lines in the next, does not pretend to be a comprehensive treatment. We are focusing attention on only those characteristics that are important from a *systems* point of view. Indeed, we will assume that the reader is familiar with these devices to the extent corresponding to a modern introductory course.

A note of caution before we proceed. A synchronous machine is not a simple device. The multitude of windings all characterized by time-varying self-inductances and mutual inductances tend to complicate matters and obscure the physical behavior. Whenever possible we shall try to make use of simple analogs.

## 4-2 ELEMENTARY MODELS AND ANALOGS

It is fruitful to consider the *physical* behavior of the synchronous machine before we present its *mathematical* model. When the machine is operated in a balanced steady state, it is possible to expose some of its most important characteristics by means of simple *analogs*. We first remind the reader of the basic design features of the machine, as sketched in Fig. 4-1. If the machine is operated as a generator, which will most often be the case in our story, the

rotor is driven by a *prime mover* (steam-, gas-, or hydroturbine, for example). The *armature*, or *stator*, *winding* (only phase *a* is shown), is arranged in three symmetrical *phase belts* in slots in the stator surface. The magnetic field intensity can be controlled via the dc current in the *rotor*, or *field*, *winding*.

A synchronous generator may conceivably be operated alone with a single load or in parallel with other generators into a large network. The latter arrangement is most common. We have depicted a typical system arrangement in Fig. 4-2. A total of $n$ generators are connected to a system, each generator via a *generator bus*. The $\nu$th generator $G\nu$ supplies the complex power $S_{G\nu} = P_{G\nu} + jQ_{G\nu}$ to the system. Its bus is kept at the voltage magnitude $|V_\nu|$, and the system is running *synchronously* at the frequency $f$.

### 4-2.1 CONTROL OF SYNCHRONOUS MACHINES

Each machine may be controlled by means of two *control forces*, or *inputs*, the *rotor* (or *field*) current $i_{r\nu}$ and the mechanical *shaft torque* $\tau_{m\nu}$. When either one or both of these inputs are changed, all the above four quantities, $P_{G\nu}$, $Q_{G\nu}$, $|V_\nu|$, and $f$, will generally change. To use the terminology of a control engineer, we may represent each generator as a "plant" having two control inputs and four control outputs, as depicted in Fig. 4-3. From a systems point of view it would be desirable to have so-called *noninteracting control*; i.e., by manipulation of one input, we would wish one, and only one, output to change. This is not generally possible. In the first place, we have four outputs but only two inputs. Furthermore, because of the inherent physical behavior of the machine, there will always be *cross coupling* between the two inputs and the four outputs. *The degree of cross coupling depends upon the system size and structure.* The best degree of noninteraction is

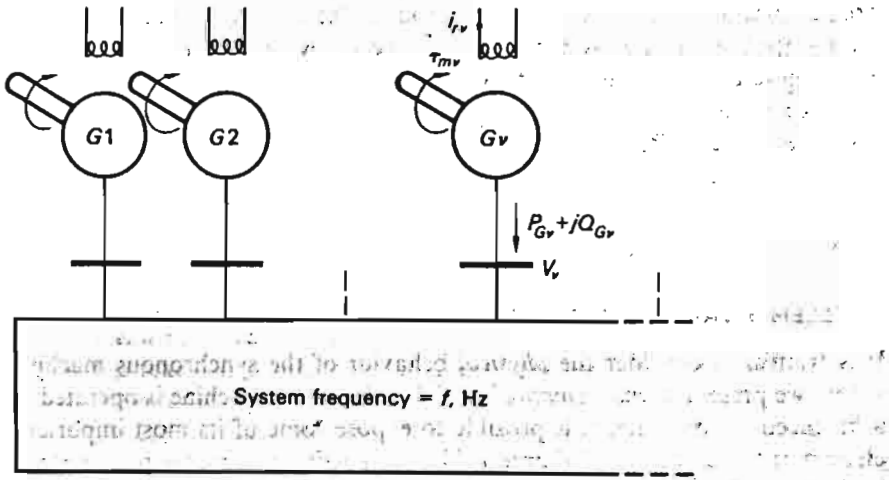


**Fig. 4-2** Typical parallel operation of generators.




**Fig. 4-3** Input-output representation of individual synchronous generator.

obtained when the system is *very large*—in the limit case we talk about an "infinitely strong network." Such a network (and in reality many networks come close to this theoretical ideal) represents a very large moment of inertia† in comparison with any one of the individual machines. It is obvious, therefore, that by manipulation of the torque input of an individual machine little change will take place in the system speed, or frequency, $f$. Also, since the large network as viewed from the individual generator represents a zero impedance source, the individual bus voltage magnitude $|V_\nu|$ will be fixed and beyond control by the field current $i_{r\nu}$.

In the case of an infinitely strong network, the system frequency $f$ and the individual bus voltages $|V_\nu|$ are therefore beyond the influence of the individual control inputs, and in such a case the four outputs of Fig. 4-3 reduce to two, the real and reactive machine outputs $P_{G\nu}$ and $Q_{G\nu}$. In this special case the conditions for noninteraction are almost satisfied. Manipulation of the field current will affect the reactive power output only, whereas a change in the shaft torque initiated by a change in the valve or gate settings in the prime mover will mainly affect the real power output. The torque change will also, in a *relatively minor way*, affect the reactive power output; i.e., we have a weak cross coupling between $\tau_{m\nu}$ and $Q_{G\nu}$.

The "infinitely strong" network represents one extreme case of network size. The other extreme is represented by one single generator supplying energy to one single load.

Let us for simplicity assume this to be an "impedance load," as defined in Chap. 3. Assume now that we increase the torque input. What will happen? Since no large external system acts as a restraint, the increased torque will mean increased speed and thus increased frequency. The increased speed means increased emf, and therefore increased bus voltage, and we conclude that both the reactive and real powers will change. In summary, the torque change sets in motion changes in all four outputs. The reader should similarly examine what happens when we perform a change in the field current input.

It should be clear from this discussion that we may expect in the general case a fairly complicated interplay between the inputs and outputs of the individual machines. Our mathematical models must be accurate enough to tell the full story.

† Compare with the "train analog" in Chap. 3.

### 4-2.2 A MECHANICAL ANALOG

The relationship between the torque input and the real power output of a synchronous machine operated in a large system may be demonstrated by means of the mechanical analog depicted in Fig. 4-4. Here we have a number of "drives" which, via a big gear box, are together pulling a large mechanical load. Assume, first, that one of the mechanical drives is disconnected from the system (which is running at a constant speed) and we are about to connect it to the system. How would this be accomplished?

Clearly, three conditions must be satisfied before we can mesh the gears:

1. The drive gear $A$ must run with a speed equal to the system gear $B$ and in proper direction.
2. The gears must have matching teeth.
3. The gears must have a matching relative position (phase). Clearly, we cannot mesh the gears if they run tooth to tooth.

If the above three conditions are satisfied, we can smoothly lock the drive gear to the system by just pushing the gears together.

After this "synchronization" has been accomplished, we can force the individual drive either to deliver power to the system ("generator") or to take power from the system ("motor") simply by controlling its torque. If we arrange it so that the torque tends to accelerate the big system, then the machine is operating as a generator supplying power into the system. If, on the contrary, the machine "loads" the system by a torque that tends to decelerate it, then we have motor action.

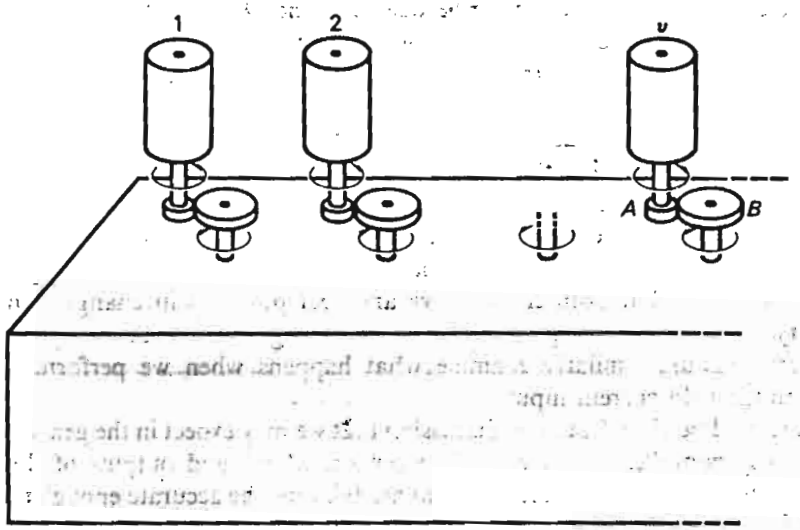


**Fig. 4-4** Mechanical analog of electric system in Fig. 4-2.



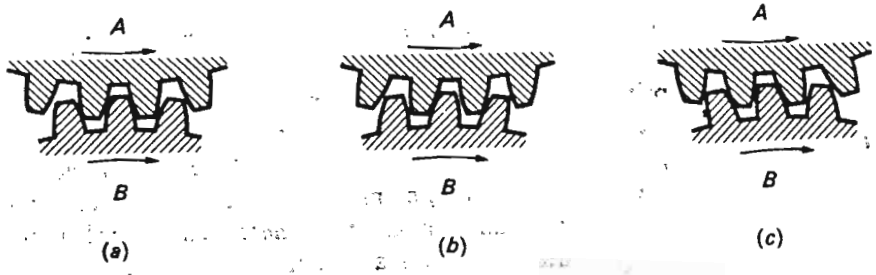


**Fig. 4-5** Mechanical analog of power angle. (*a*) No load; (*b*) generator case; (*c*) motor case.

If we assume, in order to make this a still better analogy, that the gears are *elastic* (for example, made of hard rubber), then we can determine just by viewing the gears via a *stroboscope* whether we have generator or motor action and also the degree of each. The picture we see is the one in Fig. 4-5. In the "generator case," shown in Fig. 4-5*b*, the drive gear $A$ is running a certain angle ahead of the system gear $B$. The magnitude of the angle depends upon the magnitude of the torque, i.e., the power delivered to the system. In the "motor case," the situation is reversed. In either the motor or generator case, if the torque (or power) is too large, we start to "skip teeth," with destructive results. The magnitude of this limit (or "pullout") torque depends upon (1) size of teeth and (2) stiffness of gear material.

### 4-2.3 THE TORQUE–POWER ANGLE MECHANISM

After this excursion into the mechanical domain, let us now return to the electric system and try to interpret the lessons we have learned.

As in the mechanical case, we first must connect or "synchronize" our machine to the network. This is done by closing the generator circuit breaker. Three conditions must be satisfied before we can close this breaker:

1. The generator must run with a speed equal to that of the system, and in proper direction. This is accomplished when the generator voltage has a frequency equal to that of the system voltage and the two are of equal phase sequence.
2. The machine and system voltage phasors must be of equal magnitude (i.e., we must adjust by means of the field current the generator emfs to match the network voltages).
3. The machine and system voltages must have equal phase.

With a little imagination we can correlate these conditions one by one with those that we had to satisfy for mechanical synchronization. Once they *all* are satisfied, we can close the circuit breaker, and the machine is smoothly locked to the system.

When thus locked to the big system, the machine can be operated either as a generator or a motor, depending upon how we treat it torquewise. If by means of the prime mover we apply an accelerating torque that tends to speed up the big system, then we have *generator* action. If, on the contrary, we apply a breaking torque, then we force the machine to operate as a motor. In either of these cases we can actually, by means of a stroboscope, confirm that the rotor runs a certain mechanical angle, *power angle*, leading or lagging the network. In the generator case the machine tries to pull the network; in the motor case the network pulls the machine. The magnitude of the angle depends upon the magnitude of the torque (or power). If we exceed a certain limit-value (or "pullout") torque, the machine starts to "jump poles" (or "skip electrical teeth"), with destructive results.

The above analog is of course not perfect. For example, it does not tell us anything about the reactive power. However, the synchronous machine is a fairly complicated device, and we should not discard a useful analog just because it fails in certain details.

### 4-2.4 TORQUE CREATION

When either an accelerating or decelerating torque is applied to the drive gear $A$ in Fig. 4-5, an immediate internal counterbalancing torque is built up by means of mechanical forces inside the gear. The resulting stresses in the material cause the deformation depicted in Fig. 4-5. A somewhat similar situation prevails in the electrical case, but the balancing torque no longer is obtained by means of mechanical forces. In the synchronous machine the required forces are *electromagnetic* in nature, caused by interaction between the rotor flux and the currents in the armature winding.

It is helpful to draw analogies between the situation as existing inside the synchronous machine and the simple setup depicted in Fig. 4-6. Here we have a current-carrying coil free to rotate in the constant magnetic flux of assumed uniform density $B$ Wb/m². The interaction between this flux and the coil current $i$ results in the two vertical forces $F = BiL$ N, which together result in a *couple* acting on the coil. If no external load torque is applied to the coil system, the coil will clearly assume a vertical equilibrium position. If a load torque is applied, the coil will assume a tilted position at the angle $\alpha$ corresponding to an electrodynamic restoring torque

$$\tau_e = FD \sin \alpha = BiLD \sin \alpha \quad \text{N} \cdot \text{m} \tag{4-1}$$

Since the magnetic field $B$ is proportional to the battery emf $E$ and the current $i = V/R$, where $R$ is the resistance of the movable coil, we get

$$\tau_e \sim \frac{VE}{R} \sin \alpha \quad \text{N} \cdot \text{m} \tag{4-2}$$

(For definition of $V$ and $E$ see Fig. 4-6.)



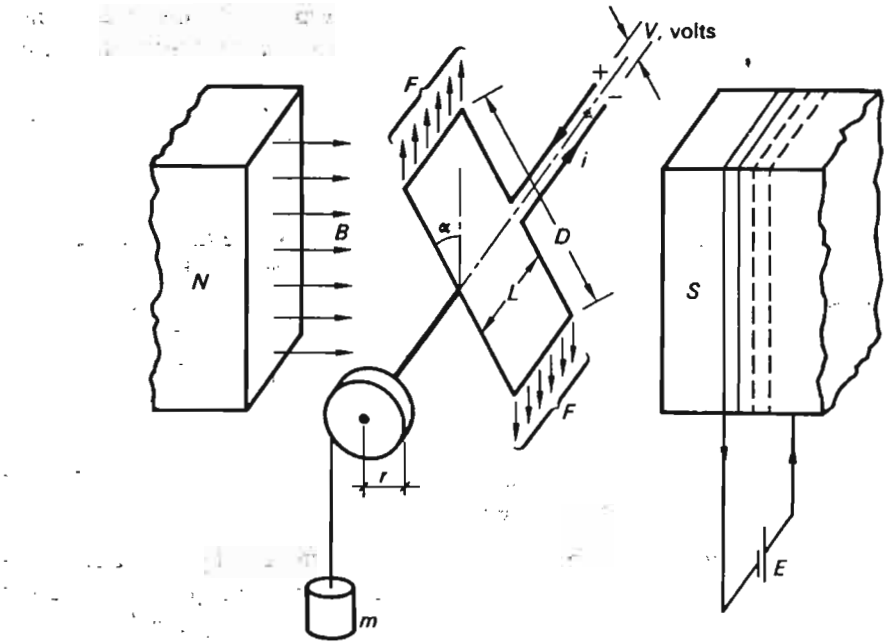


**Fig. 4-6** Movable coil in magnetic field.

If the load torque is increased, the tilt angle $\alpha$ will increase until, for $\alpha = 90°$, we reach the *pullout torque*. Clearly, by increasing $V$ and $E$, we can obtain a greater pullout torque.

The torque-balancing mechanism inside the synchronous machine is quite similar in nature *although different in detail.*

## 4-3 DEVELOPMENT OF GENERAL MACHINE EQUATIONS

To develop a full understanding of the behavior of the synchronous machine under *both* steady state and dynamic conditions, we have no recourse but to attack the full-scale problem of deriving machine equations valid for the most general of operating conditions. To make the machine amenable to reasonably simple analysis, we must (as always) make certain simplifying assumptions. We shall point out these assumptions as the analysis proceeds.

Classically, the theory of the synchronous machine was presented in terms of traveling air gap flux, current, and emf waves. This theory has the advantage of close adherence to the physical realities within the machine and serves excellently the limited purpose of explaining its elementary steady-state operating characteristics. This approach becomes extremely impractical when it becomes necessary, as in our case, to expose the behavior of the

machine under transient conditions and its interplay with the external network. For this purpose we know of no more powerful analysis method than the one that follows. The central feature of this method is the exclusive use of the circuit concept; the machine is considered as a set of magnetically coupled circuits the main parameters of which are time-variant.

### 4-3.1 THE BASIC MACHINE PARAMETERS

The machine (Fig. 4-1) contains four basic windings: the three identical and symmetrically placed distributed stator windings (identified by the subscripts $a$, $b$, and $c$) and the rotor, or field, winding (subscript $r$). An actual machine may be equipped, in addition, with *damper* windings, consisting of a short-circuited squirrel cage winding placed in slots on the rotor surface. Since we wish at this time to expose the *basic* features of the machine, we shall make out first simplifying assumption:

*Assumption* 1 *Neglect the influence of damper windings.*† (We shall later qualitatively discuss their effect.)

Each of the four windings is characterized by resistance, self-inductance, and mutual inductance, relative to the other three windings (Fig. 4-7). For the $i$th winding these parameters are symbolized $r_i$, $l_{ii}$, and $l_{ij}$, respectively. The reader should note that in making the assumption that these inductance parameters exist, we have tacitly made

*Assumption* 2 *The machine is assumed to be magnetically linear.* The concept of inductance makes sense only if we assume direct proportionality between currents and fluxes.

At this point we make the following important observations in regard to these parameters:

1. The stator resistances $r_a$, $r_b$, and $r_c$ are all equal and of relatively small magnitude by design. Henceforth we shall proceed with the analysis on the basis that $r_a = r_b = r_c \triangleq r_s$.
2. As can immediately be ascertained from Fig. 4-1, all 16 inductance elements, with the single exception of $l_{rr}$, depend upon the position of the rotor and are therefore functions of the time-varying angle $\alpha$.‡ (For definition of $\alpha$ see Fig. 4-1.)
3. Should the rotor be *nonsalient* (or *round*), as is approximately the case for a turbogenerator, then all inductance elements will be constant except those *mutual* elements containing $r$ in their subscripts.

† In balanced steady-state operation the damper winding is inoperative.
‡ This statement is true only if the rotor is of *salient* design.



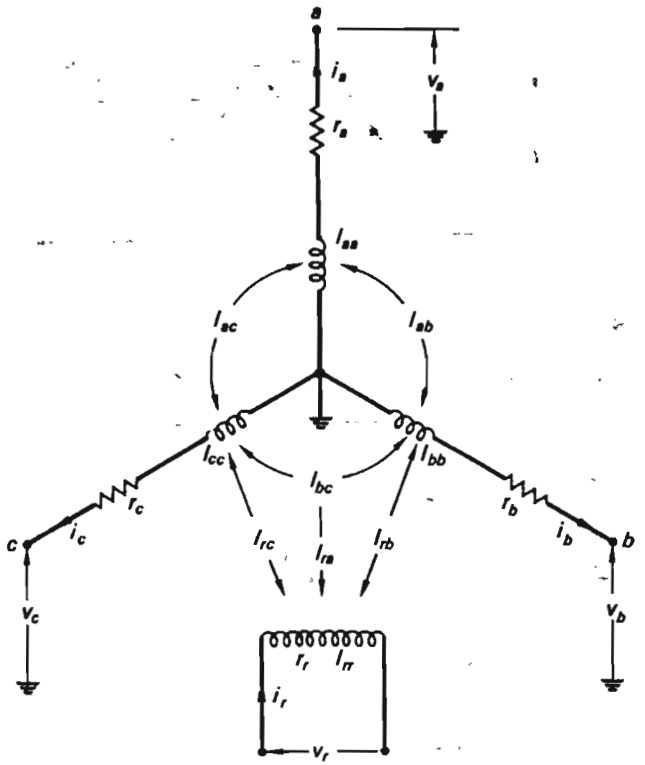


**Fig. 4-7** Winding inductance and resistance parameters.

The self-inductance $l_{aa}$ of stator winding $a$ varies periodically with position angle $\alpha$, as shown in Fig. 4-8*a*, reaching a peak when the rotor axis coincides with the winding axis, that is, for $\alpha = 0$ *and* $\alpha = \pi$, that is, *twice* during one full revolution of the rotor.

At this juncture we make

*sumption* 3 *The inductance variation depicted in Fig. 4-8a is considered harmonic;* i.e., we may write $l_{aa}$ as follows:

$$l_{aa} = L_1 + L_2 \cos 2\alpha \tag{4-3}$$

where the positive inductance parameters $L_1$ and $L_2$ are defined in the figure. *Note that $L_2$ is zero for round rotor.*

(This assumption is very good. We wish, actually, to eliminate higher harmonics, and therefore the pole surfaces are shaped so as to obtain as sinusoidal reluctance as possible.)

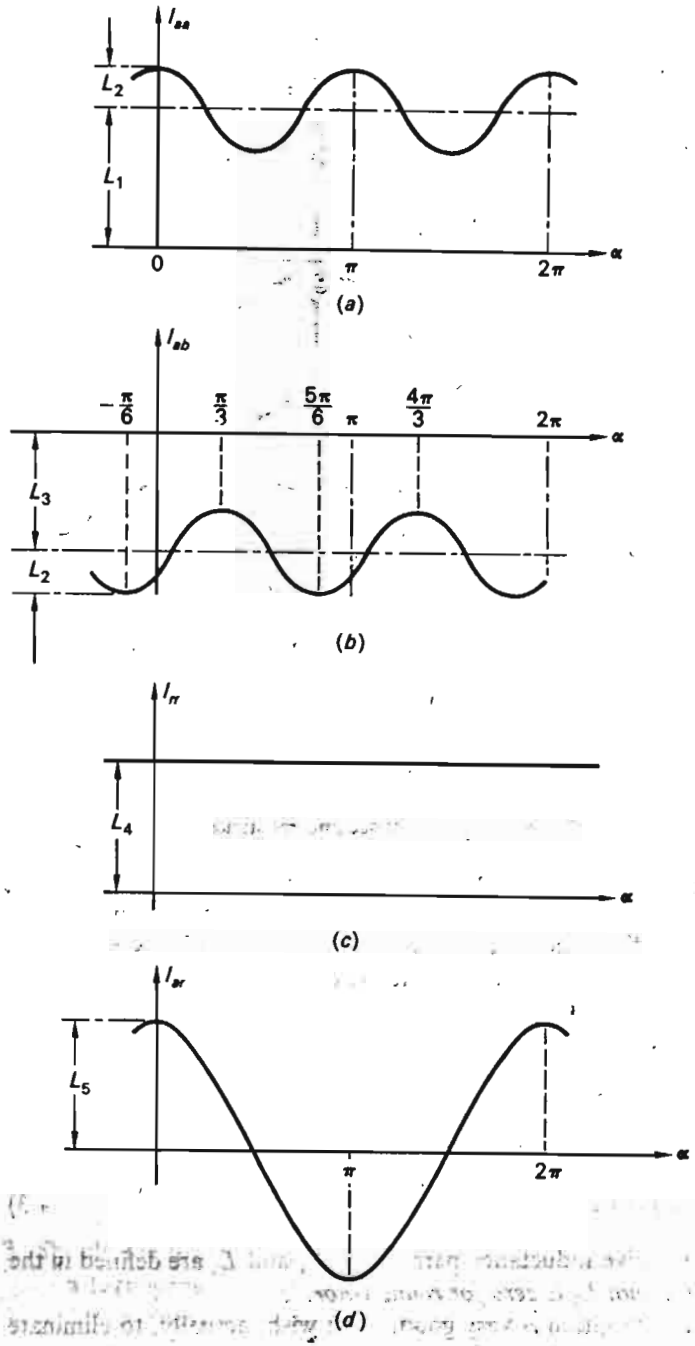


**Fig. 4-8** Variation in inductance parameters with angular rotor position.





5. The self-inductances $l_{bb}$ and $l_{cc}$ will look identical with $l_{aa}$, but since the stator windings $b$ and $c$ are spaced $2\pi/3$ and $4\pi/3$ spatial radians displaced from winding $a$, we must replace in our formulas the angular coordinate $\alpha$ with $(\alpha - 2\pi/3)$ and $(\alpha - 4\pi/3)$, respectively.

   By making use of assumption 3, we therefore have

$$l_{bb} = L_1 + L_2 \cos 2\left(\alpha - \frac{2\pi}{3}\right)$$
$$l_{cc} = L_1 + L_2 \cos 2\left(\alpha - \frac{4\pi}{3}\right) \tag{4-4}$$

6. The mutual inductances $l_{ij}$ satisfy the equations

$$l_{ij} = l_{ji} \tag{4-5}$$

   and the stator inductances $l_{ab}$, $l_{ac}$, $l_{bc}$ are all *negative.*

Equation (4-5) is a consequence of the fact that a current in winding $i$ will give a linked flux in winding $j$ of a magnitude and direction identical with the flux which an equal current in $j$ would give rise to in winding $i$. We note also from Fig. 4-1 that a positive† current in *stator* winding $i$ will give a negative flux linkage component in the two remaining *stator* windings. This, then, means that the three stator mutual inductances are negative.

7. The flux linked to *stator* winding $b$ by a given current in winding $a$ will have its largest magnitude when the rotor angle $\alpha$ is either $-30$ or $+150°$, since the rotor in these two positions offers the least magnetic reluctance.

Similarly, the flux will be at minimum magnitude for $\alpha = 60$ or $240°$. The mutual inductance $l_{ab}$ will therefore look as depicted in Fig. 4-8*b*. *Note that the double-frequency component will have the same amplitude as in the case of the self-inductance.* We therefore have

$$l_{ab} = -L_3 - L_2 \cos 2\left(\alpha + \frac{\pi}{6}\right) \tag{4-6}$$

where $L_3$ is defined in Fig. 4-8*b*. Note that $L_3$ is positive.

† For definition of "positive" current see Fig. 4-7. See also discussion of current polarity on page 83.

8. A similar reasoning reveals that $l_{bc}$ will have a numerical maximum for $\alpha = 90$ and 270° and $l_{ac}$ for $\alpha = 30$ and 210°. We therefore have

$$l_{bc} = -L_3 - L_2 \cos 2\left(\alpha - \frac{\pi}{2}\right)$$
$$l_{ac} = -L_3 - L_2 \cos 2\left(\alpha - \frac{\pi}{6}\right) \tag{4-7}$$

9. In regard to the *rotor* inductance elements, we note that
   (*a*) The rotor *self*-inductance $l_{rr}$ is constant (as was mentioned above). We symbolize it $L_4$ (Fig. 4-8*c*).
   (*b*) The *mutual* inductances between the rotor and stator windings vary between positive and negative maxima. One cycle corresponds to 360° of the rotor position. We can therefore, if we again make use of assumption 3, write

$$l_{ra} = L_5 \cos \alpha$$
$$l_{rb} = L_5 \cos\left(\alpha - \frac{2\pi}{3}\right) \tag{4-8}$$
$$l_{rc} = L_5 \cos\left(\alpha - \frac{4\pi}{3}\right) = L_5 \cos\left(\alpha + \frac{2\pi}{3}\right)$$

   where $L_5$ is defined as in Fig. 4-8*d*.

10. In all the above formulas the angle $\alpha$ must be understood to represent the *electrical* angle. As shown in Fig. 4-1, the electrical and mechanical angles are identical for a two-pole machine, but for $p > 2$, we have

$$\alpha_{el} = \frac{p}{2} \alpha_{\text{mech}} \tag{4-9}$$

11. In summary, we may conclude that all the 16 inductance elements can be expressed in terms of a set of five *positive* inductance parameters $L_1, \ldots, L_5$ (all defined in Fig. 4-8) and the rotor position angle $\alpha$. In the following analysis we shall assume these parameters known, either by test or from manufacturers' data. Note also that in the case of a round rotor the inductance parameter set reduces to four ($L_1$, $L_3$, $L_4$, $L_5$).

#### 4-3.2 THE GENERAL MACHINE EQUATIONS

At this point we possess full knowledge of all circuit parameters pertaining to the problem. We shall now proceed to write the general set of circuit equations, from which we subsequently shall be able to deduce all information relating to our systems studies.

If we write the Kirchhoff's voltage equations for the four separate



circuits in Fig. 4-7, we get directly

$$\begin{aligned}
v_a &= -i_a r_s - \frac{d}{dt}(l_{aa} i_a) - \frac{d}{dt}(l_{ab} i_b) - \frac{d}{dt}(l_{ac} i_c) + \frac{d}{dt}(l_{ar} i_r) \\
v_b &= -i_b r_s - \frac{d}{dt}(l_{ba} i_a) - \frac{d}{dt}(l_{bb} i_b) - \frac{d}{dt}(l_{bc} i_c) + \frac{d}{dt}(l_{br} i_r) \\
v_c &= -i_c r_s - \frac{d}{dt}(l_{ca} i_a) - \frac{d}{dt}(l_{cb} i_b) - \frac{d}{dt}(l_{cc} i_c) + \frac{d}{dt}(l_{cr} i_r) \\
v_r &= \quad i_r r_r - \frac{d}{dt}(l_{ra} i_a) - \frac{d}{dt}(l_{rb} i_b) - \frac{d}{dt}(l_{rc} i_c) + \frac{d}{dt}(l_{rr} i_r)
\end{aligned} \tag{4-10}$$

In Fig. 4-7 the *stator* currents are defined positive in the direction of positive potential, i.e., in *generator sense*. The rotor current is defined positive in opposite sense. These mixed definitions agree with the normal mode of operation of the respective windings. However, they cause a mixed-sign situation in Eq. (4-10). This we are forced to tolerate.

It would be prohibitively impractical to proceed from here without resorting to the compact notation features and "bookkeeping" abilities of matrices. The majority of the students should be familiar with matrix analysis; those readers who are not must at this juncture avail themselves† of this tool. We shall be concerned with large-scale circuits throughout our story, and the reader will fairly soon, as he gains familiarity with this analytical tool, agree with us that in handling equations of the above complexity, *and in particular as we program our problems on computers*, we would be unwise, indeed, not to *adopt matrix methods* at this juncture. Nevertheless, we assure the reader that we shall not get more sophisticated than necessary; indeed, it will prove sufficient to be familiar with only the most elementary matrix operations.

Having thus explained the necessity for temporarily obscuring matters in a new and unfamiliar mathematical clothing, we define the following matrices:

$$\mathbf{v} \triangleq \begin{bmatrix} v_a \\ v_b \\ v_c \\ \cdots \\ v_r \end{bmatrix} \qquad \mathbf{i} \triangleq \begin{bmatrix} i_a \\ i_b \\ i_c \\ \cdots \\ -i_r \end{bmatrix} \tag{4-11}$$

$$\mathbf{R} \triangleq \left[\begin{array}{ccc:c} r_s & 0 & 0 & 0 \\ 0 & r_s & 0 & 0 \\ 0 & 0 & r_s & 0 \\ \hdashline 0 & 0 & 0 & r_r \end{array}\right] \tag{4-12}$$

† See Appendix A, for example.

It is important to realize that in the case of a *round rotor*, all stator self- and mutual-inductance elements are *independent of the rotor angle* $\alpha$, which is tantamount to saying that the inductance coefficient $L_2$ in Fig. 4-8 is zero. In this case the inductance matrix assumes the simpler value

$$\mathbf{L} = \left[\begin{array}{ccc:c} L_1 & -L_3 & -L_3 & L_5\cos\alpha \\ -L_3 & L_1 & -L_3 & L_5\cos\left(\alpha-\frac{2\pi}{3}\right) \\ -L_3 & -L_3 & L_1 & L_5\cos\left(\alpha+\frac{2\pi}{3}\right) \\ \hdashline L_5\cos\alpha & L_5\cos\left(\alpha-\frac{2\pi}{3}\right) & L_5\cos\left(\alpha+\frac{2\pi}{3}\right) & L_4 \end{array}\right] \tag{4-14}$$

(Note that the **v** and **i** matrices contain only one column. We shall always symbolize such a *column matrix*, or *vector*, with *lowercase* boldface letter symbols. All other matrices will be symbolized with *capital* boldface letter symbols. The dashed *partition lines* shown in all the matrices will be explained later.)

In terms of the above matrices we can then write the system (4-10) very compactly:

$$\mathbf{v} = -\mathbf{R}\mathbf{i} - \frac{d}{dt}(\mathbf{L}\mathbf{i}) \tag{4-15}$$

We hope the reader already is impressed with the usefulness of matrices. Once we have made the "tabulations" (4-11) to (4-14), we can work with compact *vector equations*, and whenever we wish detailed data we need only look up the "tables."

Before proceeding further with our analysis, we shall make a few remarks in regard to Eq. (4-10) [or (4-15)]:

1. Note that, because the elements of the **L** matrix depend upon $\alpha$ (and thus upon time $t$), we *cannot* write the second term

$$\frac{d}{dt}(\mathbf{L}\mathbf{i}) = \mathbf{L}\frac{d\mathbf{i}}{dt}$$

The differential equations therefore are not of the constant-parameter type, and for this reason we are *not* able to use Laplace transforms directly for their solution.

(4-13)

$$\mathbf{L} \triangleq \left[\begin{array}{ccc:c} l_{aa} & l_{ab} & l_{ac} & l_{ar} \\ l_{ba} & l_{bb} & l_{bc} & l_{br} \\ l_{ca} & l_{cb} & l_{cc} & l_{cr} \\ \hdashline l_{ra} & l_{rb} & l_{rc} & l_{rr} \end{array}\right] = \left[\begin{array}{ccc:c} L_1+L_2\cos 2\alpha & -L_3-L_2\cos 2\left(\alpha-\frac{\pi}{6}\right) & -L_3-L_2\cos 2\left(\alpha+\frac{\pi}{6}\right) & L_5\cos\alpha \\ -L_3-L_2\cos 2\left(\alpha+\frac{\pi}{6}\right) & L_1+L_2\cos 2\left(\alpha-\frac{2\pi}{3}\right) & -L_3-L_2\cos 2\left(\alpha-\frac{\pi}{2}\right) & L_5\cos\left(\alpha-\frac{2\pi}{3}\right) \\ -L_3-L_2\cos 2\left(\alpha-\frac{\pi}{6}\right) & -L_3-L_2\cos 2\left(\alpha-\frac{\pi}{2}\right) & L_1+L_2\cos 2\left(\alpha-\frac{4\pi}{3}\right) & L_5\cos\left(\alpha-\frac{4\pi}{3}\right) \\ \hdashline L_5\cos\alpha & L_5\cos\left(\alpha-\frac{2\pi}{3}\right) & L_5\cos\left(\alpha-\frac{4\pi}{3}\right) & L_4 \end{array}\right]$$

$$= \left[\begin{array}{ccc:c} L_1+L_2\cos 2\alpha & -L_3+L_2\cos\left(2\alpha-\frac{2\pi}{3}\right) & -L_3+L_2\cos\left(2\alpha+\frac{2\pi}{3}\right) & L_5\cos\alpha \\ -L_3+L_2\cos\left(2\alpha-\frac{2\pi}{3}\right) & L_1+L_2\cos\left(2\alpha+\frac{2\pi}{3}\right) & -L_3+L_2\cos 2\alpha & L_5\cos\left(\alpha+\frac{2\pi}{3}\right) \\ -L_3+L_2\cos\left(2\alpha+\frac{2\pi}{3}\right) & -L_3+L_2\cos 2\alpha & L_1+L_2\cos\left(2\alpha-\frac{2\pi}{3}\right) & L_5\cos\left(\alpha-\frac{2\pi}{3}\right) \\ \hdashline L_5\cos\alpha & L_5\cos\left(\alpha-\frac{2\pi}{3}\right) & L_5\cos\left(\alpha+\frac{2\pi}{3}\right) & L_4 \end{array}\right]$$

2. Consider a typical term in Eq. (4-10), for example,

$$\frac{d}{dt}(l_{aa}i_a)$$

By performing the derivation called for, we obtain terms of the types

$$i_a \frac{d\alpha}{dt} \sin 2\alpha \qquad \text{and} \qquad \frac{di_a}{dt} \cos 2\alpha$$

If the rotor angular velocity $d\alpha/dt$ is *constant* (which is usually the case, since the machine has large inertia), then we can write

$$\frac{d\alpha}{dt} = \omega = \text{const} \tag{4-16}$$

and

$$\alpha = \omega t + \alpha_0$$

and the above terms will therefore reduce to

$$\omega \sin 2(\omega t + \alpha_0) i_a \qquad \text{and} \qquad \cos 2(\omega t + \alpha_0) \frac{di_a}{dt}$$

We conclude that our general differential equation in this case is of the *linear* type with *time-varying* coefficients. In that case we shall be able to obtain solutions for the system of Eqs. (4-15). On the other hand, under the influence of the electrodynamical torque (of which we have not yet spoken), should the speed $\dot{\alpha}$ change, then the differential equations (4-15) obviously would be *nonlinear*, and general *analytical* solutions cannot be found. In such a case it would still be possible, of course, to obtain *numerical* solutions by computer. In Sec. 4-3.4 we shall return to the problem of solution of Eqs. (4-15).

### 4-3.3 THE GENERAL POWER EQUATION

By making use of the fundamental power formula presented in Chap. 2, we have the following expression for the total generated power *delivered* by the *stator* windings:

$$p = i_a v_a + i_b v_b + i_c v_c \qquad \text{W} \tag{4-17}$$

We emphasize that $p$ is defined positive in a generator sense.

We note that this $p$ formula contains those elements of the $\mathbf{v}$ and $\mathbf{i}$ matrices that are associated with the stator.† At this point we therefore find reason to work with only *parts* of the matrices earlier defined. If we then, for a moment, return to the defining equations (4-11) to (4-14), we note

† If we had added the term $-i_r v_r$ to Eq. (4-17), we would simply have obtained the total power delivered by the machine, *including the rotor winding*. We are not generally interested in this total power.



that they have been *partitioned* so as to make a distinction between the *rotor* and *stator* portions. In view of these partitions we define the following new *submatrices:*

$$\mathbf{v}_s \triangleq \begin{bmatrix} v_a \\ v_b \\ v_c \end{bmatrix} \qquad \mathbf{i}_s \triangleq \begin{bmatrix} i_a \\ i_b \\ i_c \end{bmatrix} \tag{4-18}$$

$$\mathbf{R}_s \triangleq \begin{bmatrix} r_s & 0 & 0 \\ 0 & r_s & 0 \\ 0 & 0 & r_s \end{bmatrix} \tag{4-19}$$

$$\mathbf{L}_s \triangleq \begin{bmatrix} l_{aa} & l_{ab} & l_{ac} \\ l_{ba} & l_{bb} & l_{bc} \\ l_{ca} & l_{cb} & l_{cc} \end{bmatrix} \qquad \mathbf{l}_{rs} \triangleq \begin{bmatrix} l_{ar} \\ l_{br} \\ l_{cr} \end{bmatrix} \tag{4-20}$$

Clearly, the *total* matrices $\mathbf{v}$, $\mathbf{i}$, $\mathbf{R}$, and $\mathbf{L}$ are composed of the submatrices in the following manner:

$$\mathbf{v} = \begin{bmatrix} \mathbf{v}_s \\ v_r \end{bmatrix} \qquad \mathbf{i} = \begin{bmatrix} \mathbf{i}_s \\ -i_r \end{bmatrix} \tag{4-21}$$

$$\mathbf{R} = \begin{bmatrix} \mathbf{R}_s & \mathbf{0} \\ \mathbf{0} & r_r \end{bmatrix} \qquad \mathbf{L} = \begin{bmatrix} \mathbf{L}_s & \mathbf{l}_{rs} \\ \mathbf{l}_{rs}^T & l_{rr} \end{bmatrix} \tag{4-22}$$

Superscript $T$ indicates transposition (see App. A).

Returning now to our power equation (4-17), we conclude immediately that we can write it in terms of the $\mathbf{v}_s$ and $\mathbf{i}_s$ matrices as follows:

$$p = [i_a, i_b, i_c] \begin{bmatrix} v_a \\ v_b \\ v_c \end{bmatrix} = \mathbf{i}_s^T \mathbf{v}_s \qquad \text{W} \tag{4-23}$$

We shall find it convenient in the following analysis to express the general equation (4-15) in terms of the submatrices defined above. We get directly, by substitution,

$$\begin{bmatrix} \mathbf{v}_s \\ v_r \end{bmatrix} = -\begin{bmatrix} \mathbf{R}_s & \mathbf{0} \\ \mathbf{0} & r_r \end{bmatrix} \begin{bmatrix} \mathbf{i}_s \\ -i_r \end{bmatrix} - \frac{d}{dt} \left\{ \begin{bmatrix} \mathbf{L}_s & \mathbf{l}_{rs} \\ \mathbf{l}_{rs}^T & l_{rr} \end{bmatrix} \begin{bmatrix} \mathbf{i}_s \\ -i_r \end{bmatrix} \right\} \tag{4-24}$$

We may write this equation in "component" form:

$$\begin{aligned} \mathbf{v}_s &= -\mathbf{R}_s\mathbf{i}_s - \frac{d}{dt}(\mathbf{L}_s\mathbf{i}_s - \mathbf{l}_{rs}i_r) \\ v_r &= r_r i_r - \frac{d}{dt}(\mathbf{l}_{rs}{}^T\mathbf{i}_s - l_{rr}i_r) \end{aligned} \tag{4-25}$$

Note that the first "component" is actually a three-vector. The reader should perform all the matrix operations in these last two equations and satisfy himself that they are indeed identical with Eqs. (4-10).

#### 4-3.4 THE BLONDEL TRANSFORMATION

We have indicated that it is possible to obtain analytical solutions to the system of differential equations (4-10) on the assumption that the speed $\dot{\alpha}$ is constant. Although we could arrive at these solutions directly from the equations as they stand, it is possible to simplify these equations to a great extent by means of a special technique, which we shall here refer to as the *Blondel transformation*† (*BT*). The technique involves the introduction of a new set of voltage and current variables or components, the so-called *direct axis* (*d*), *quadrature axis* (*q*), and *zero-sequence* (0) *components*.

These Blondel currents are *defined* as follows:‡

$$\begin{aligned} i_d &\triangleq \frac{2}{3}\cos\alpha i_a + \frac{2}{3}\cos\left(\alpha - \frac{2\pi}{3}\right)i_b + \frac{2}{3}\cos\left(\alpha + \frac{2\pi}{3}\right)i_c \\ i_q &\triangleq -\frac{2}{3}\sin\alpha i_a - \frac{2}{3}\sin\left(\alpha - \frac{2\pi}{3}\right)i_b - \frac{2}{3}\sin\left(\alpha + \frac{2\pi}{3}\right)i_c \\ i_0 &\triangleq \tfrac{1}{3}i_a + \tfrac{1}{3}i_b + \tfrac{1}{3}i_c \end{aligned} \tag{4-26}$$

† The initial idea stems from André Blondel in France, but much of the development of the method was carried out by Doherty, Nickle, Park, and others.

‡ It is perfectly possible to proceed with the analysis by viewing the Blondel currents as *mathematical artifices*. However, the reader will gain a better understanding of what these mathematical operations really do by trying to attach physical significance to them. From electrical machine theory the reader knows that the stator currents due to the spatial distribution of the stator winding give rise to an mmf wave proportional to the currents in question. In a coordinate system *fixed* with respect to the *stator* and having its origin coinciding with the axis of the *a* winding (Fig. 4-1), the mmf caused by the *a* current is therefore directly proportional to $i_a$. For example, if the current pulsates with frequency $f$, so does the mmf.

For a coordinate system *fixed* with respect to the *rotor* and having the origin coinciding with the midpoint of the pole (Fig. 4-1), the *same mmf* wave has an intensity proportional to $i_a \cos\alpha$. Looked at from this point of view, the current $i_d$ is therefore a measure of the *total* mmf (i.e., caused by all three stator currents) *as measured in* the midpole (= direct-axis) direction. Similarly, $i_q$ gives the mmf in quadrature pole direction.



or in compact matrix notation,

$$\mathbf{i}_B \triangleq \mathbf{B}\mathbf{i}_s \tag{4-27}$$

where $\mathbf{i}_s$ is the stator current vector earlier introduced, defined by Eqs. (4-18), and the $\mathbf{i}_B$ and $\mathbf{B}$ matrices are defined by

$$\mathbf{i}_B \triangleq \begin{bmatrix} i_d \\ i_q \\ i_0 \end{bmatrix} \tag{4-28}$$

$$\mathbf{B} \triangleq \tfrac{2}{3}\begin{bmatrix} \cos\alpha & \cos\left(\alpha - \frac{2\pi}{3}\right) & \cos\left(\alpha + \frac{2\pi}{3}\right) \\ -\sin\alpha & -\sin\left(\alpha - \frac{2\pi}{3}\right) & -\sin\left(\alpha + \frac{2\pi}{3}\right) \\ 0.5 & 0.5 & 0.5 \end{bmatrix} \tag{4-29}$$

The currents $i_d$, $i_q$, and $i_0$ are called the *direct-axis*, *quadrature-axis*, and *zero-sequence* components, respectively. Collectively, we refer to them as *Blondel currents*. Equation (4-27) is referred to as the *direct Blondel transformation*. By solving for the stator currents in accordance with

$$\mathbf{i}_s = \mathbf{B}^{-1}\mathbf{i}_B \tag{4-30}$$

we have, in effect, introduced the *inverse Blondel transformation*.

It is readily checked by the methods of matrix inversion presented in Appendix A that

$$\mathbf{B}^{-1} = \begin{bmatrix} \cos\alpha & -\sin\alpha & 1 \\ \cos\left(\alpha - \frac{2\pi}{3}\right) & -\sin\left(\alpha - \frac{2\pi}{3}\right) & 1 \\ \cos\left(\alpha + \frac{2\pi}{3}\right) & -\sin\left(\alpha + \frac{2\pi}{3}\right) & 1 \end{bmatrix} \tag{4-31}$$

Equation (4-27) defines the BT of the stator *currents*. We similarly *B*-transform the stator *voltages:*

$$\mathbf{v}_B \triangleq \mathbf{B}\mathbf{v}_s \tag{4-32}$$

with the associated inverse transformation

$$\mathbf{v}_s = \mathbf{B}^{-1}\mathbf{v}_B \tag{4-33}$$

Upon substitution of the Blondel voltages and currents for the actual stator voltages and currents in Eqs. (4-25), we obtain

$$\begin{aligned}\mathbf{B}^{-1}\mathbf{v}_B &= -\mathbf{R}_s\mathbf{B}^{-1}\mathbf{i}_B - \frac{d}{dt}(\mathbf{L}_s\mathbf{B}^{-1}\mathbf{i}_B - \mathbf{l}_{rs}i_r) \\ v_r &= r_r i_r - \frac{d}{dt}(\mathbf{l}_{rs}{}^T\mathbf{B}^{-1}\mathbf{i}_B - l_{rr}i_r)\end{aligned} \tag{4-34}$$

Upon premultiplying the first of these equations with $\mathbf{B}$, Eqs. (4-34) take on the form

$$\begin{aligned}\mathbf{v}_B &= -\mathbf{B}\mathbf{R}_s\mathbf{B}^{-1}\mathbf{i}_B - \mathbf{B}\frac{d}{dt}(\mathbf{L}_s\mathbf{B}^{-1}\mathbf{i}_B - \mathbf{l}_{rs}i_r) \\ v_r &= r_r i_r - \frac{d}{dt}(\mathbf{l}_{rs}{}^T\mathbf{B}^{-1}\mathbf{i}_B - l_{rr}i_r)\end{aligned} \tag{4-35}$$

It is not immediately realized from these equations that a simplification has been achieved; indeed, it looks as if the new Eqs. (4-35) are more complex than Eqs. (4-25). If the called-for matrix operations are performed (they are straightforward but somewhat tedious), Eqs. (4-35) reduce to the following component form:

$$\begin{aligned}v_d &= -r_s i_d - L_d\frac{di_d}{dt} + L_5\frac{di_r}{dt} + L_q i_q\frac{d\alpha}{dt} \\ v_q &= -r_s i_q - L_q\frac{di_q}{dt} - (L_d i_d - L_5 i_r)\frac{d\alpha}{dt} \\ v_0 &= -r_s i_0 - L_0\frac{di_0}{dt} \\ v_r &= r_r i_r + L_4\frac{di_r}{dt} - \tfrac{3}{2}L_5\frac{di_d}{dt}\end{aligned} \tag{4-36}$$

In shorter form, we have introduced the following new parameters:

$$\begin{aligned}L_d &\triangleq L_1 + L_3 + \tfrac{3}{2}L_2 \\ L_q &\triangleq L_1 + L_3 - \tfrac{3}{2}L_2 \\ L_0 &\triangleq L_1 - 2L_3\end{aligned} \tag{4-37}$$

These new inductances are referred to as the *direct-axis synchronous inductance*, the *quadrature-axis synchronous inductance*, and the *zero-sequence inductance*, respectively.

Without exception, we shall be concerned with cases where the rotor speed is constant, or at least almost constant. We can then set

$$\frac{d\alpha}{dt} = \omega = \text{const} \tag{4-38}$$



and the differential Eqs. (4-36) are then recognized as *linear with constant coefficients*. We can actually write them in matrix form:

$$\begin{bmatrix} v_d \\ v_q \\ v_0 \\ v_r \end{bmatrix} = -\begin{bmatrix} r_s & -\omega L_q & 0 & 0 \\ \omega L_d & r_s & 0 & \omega L_5 \\ 0 & 0 & r_s & 0 \\ 0 & 0 & 0 & r_r \end{bmatrix}\begin{bmatrix} i_d \\ i_q \\ i_0 \\ -i_r \end{bmatrix} - \begin{bmatrix} L_d & 0 & 0 & L_5 \\ 0 & L_q & 0 & 0 \\ 0 & 0 & L_0 & 0 \\ \tfrac{3}{2}L_5 & 0 & 0 & L_4 \end{bmatrix}\frac{d}{dt}\begin{bmatrix} i_d \\ i_q \\ i_0 \\ -i_r \end{bmatrix} \tag{4-39}$$

The Blondel transformation has reduced the complexity of our Eqs. (4-10) in two ways:

1. It has transformed a set of differential equations with *time-varying* coefficients to a set characterized by *constant* parameters. (This means, for example, that the equations are now made amenable to the extremely powerful Laplace transform analysis technique.)
2. The new transformed equations contain comparatively few terms. This means that the parameter matrices (4-39) contain many zeros (we refer to them as *sparse*). Whereas the physical stator currents $\mathbf{i}_s$ are *strongly* coupled to each other, the Blondel currents $\mathbf{i}_B$ are only *weakly* coupled.

We proceed now to investigate what the Blondel transformation has done to the power equation (4-23). Since we have

$$\mathbf{i}_s = \mathbf{B}^{-1}\mathbf{i}_B$$

we get, by using Eq. (A-30) in Appendix A,

$$\mathbf{i}_s{}^T = \mathbf{i}_B{}^T(\mathbf{B}^{-1})^T \tag{4-40}$$

Thus, by substitution into Eq. (4-23),

$$p = \mathbf{i}_B{}^T(\mathbf{B}^{-1})^T\mathbf{B}^{-1}\mathbf{v}_B \tag{4-41}$$

It is easy to confirm by direct multiplication that

$$(\mathbf{B}^{-1})^T\mathbf{B}^{-1} = \begin{bmatrix} \tfrac{3}{2} & 0 & 0 \\ 0 & \tfrac{3}{2} & 0 \\ 0 & 0 & 3 \end{bmatrix} \tag{4-42}$$

and thus we can write Eq. (4-41)

$$p = \tfrac{3}{2}(v_d i_d + v_q i_q + 2v_0 i_0) \tag{4-43}$$

This, then, is our power formula in terms of the Blondel current and voltage variables.

## 4-4 STEADY-STATE MACHINE MODELS

We have developed our preceding machine equations under very generalized assumptions. Now we shall apply them to some special but important operating conditions. It is logical to start with an analysis of the machine when operated in static *steady state.*

### 4-4.1 THE MACHINE AT NO LOAD

The simplest form of steady-state operation is characterized by *zero* stator currents and constant rotor current and speed. This type of operation is obtained when the alternator is either disconnected from the network and running by itself or connected to the network but delivering neither real nor reactive power. Since the stator currents are zero, the power and torques are, of course, also zero.

With $\mathbf{i}_s = \mathbf{0}$ and $i_r = i_r^0 = \text{const}$,† Eqs. (4-25) reduce to

$$\begin{aligned} \mathbf{v}_s &= \frac{d}{dt}(\mathbf{l}_{rs} i_r^0) = \frac{d}{dt}(\mathbf{l}_{rs}) i_r^0 \\ v_r^0 &= r_r i_r^0 = \text{const} \end{aligned} \tag{4-44}$$

[The term $(d/dt)(l_{rr} i_r^0) = 0$ because $l_{rr} = \text{const}$.]

Since

$$\mathbf{l}_{rs} = \begin{bmatrix} L_5 \cos\alpha \\ L_5 \cos\left(\alpha - \frac{2\pi}{3}\right) \\ L_5 \cos\left(\alpha + \frac{2\pi}{3}\right) \end{bmatrix}$$

and since $\alpha = \omega t$ (where $\omega$ is constant), we can write the first of Eqs. (4-44) as follows:

$$\begin{bmatrix} v_a \\ v_b \\ v_c \end{bmatrix} = -\omega L_5 i_r^0 \begin{bmatrix} \sin\omega t \\ \sin\left(\omega t - \frac{2\pi}{3}\right) \\ \sin\left(\omega t + \frac{2\pi}{3}\right) \end{bmatrix} \triangleq \begin{bmatrix} e_a \\ e_b \\ e_c \end{bmatrix} \tag{4-45}$$

† Throughout the book the superscript 0 designates a constant steady-state variable.



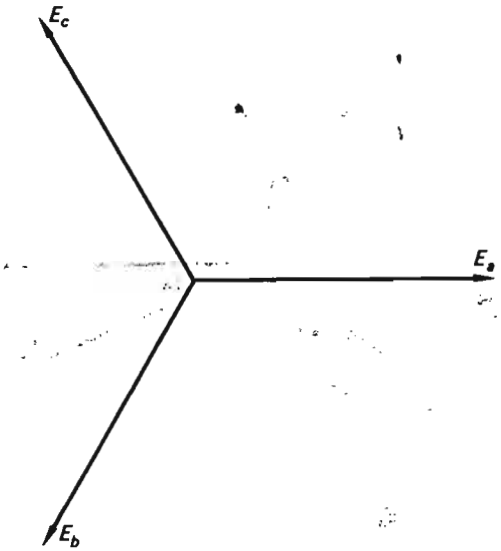


**Fig. 4-9** The three stator emfs represented in phasor form.

We conclude that the stator voltages are *sinusoidal* and the voltages in phases $b$ and $c$ lag the voltages in phase $a$ by 120 and 240°, respectively; i.e., *they are characterized by three-phase symmetry.* We refer to these voltages as the *stator emfs*, and shall henceforth symbolize them by the letter symbols $e_a$, $e_b$, and $e_c$. Since they are harmonic time functions, we can symbolize them as *phasors*, as in Fig. 4-9. The emfs reach their maximums in order $a, b, c, \ldots$, and we refer to this as the *phase sequence* of the machine. The emf in phase $a$ can be written

$$e_a = -\omega L_5 i_r^0 \sin\omega t = \sqrt{2}\,\text{Im}\{E_a e^{j\omega t}\}$$

where the emf phasor $E_a$ is defined by

$$E_a \triangleq -\frac{\omega L_5 i_r^0}{\sqrt{2}} \tag{4-46}$$

Note that the magnitude $|E_a|$ is proportional to the field current magnitude $i_r^0$ and rotor speed $\omega$.

### 4-4.2 THE MACHINE UNDER SYMMETRICAL LOADING CONDITIONS

**Derivation of voltage and current relations** The most important mode of operation is the symmetrically loaded machine. This case occurs in normal operation of the alternator when connected to a three-phase bus, the voltages of which, $v_a$, $v_b$, and $v_c$, *possess three-phase symmetry.* We shall

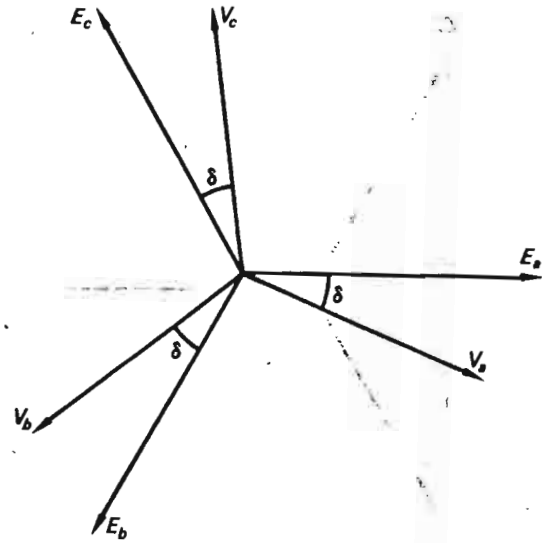


**Fig. 4-10** Machine emfs and terminal voltages represented in phasor form.

assume that the field current is constant, $i_r^0$, which guarantees a set of machine emfs $e_a$, $e_b$, $e_c$, also possessing three-phase symmetry and having constant magnitudes. The machine is running synchronously, which means that the bus voltages $v$ and the emfs $e$ are of identical frequencies. The $E$ and $V$ phasors are thus separated by a *constant* angle $\delta$, as shown in Fig. 4-10.

Since both the emfs and bus voltages have three-phase symmetry, the same also applies to the stator currents, which are therefore of the form

$$\begin{aligned} i_a &= \sqrt{2}\,|I| \cos(\omega t + \Psi) \\ i_b &= \sqrt{2}\,|I| \cos\left(\omega t - \frac{2\pi}{3} + \Psi\right) \\ i_c &= \sqrt{2}\,|I| \cos\left(\omega t + \frac{2\pi}{3} + \Psi\right) \end{aligned} \tag{4-47}$$

where $|I|$ is the rms value of the stator current and $\Psi$ is the as yet undetermined phase angle of the current.

By substitution of Eqs. (4-47) into Eqs. (4-26) we get

$$\begin{aligned} i_d &= \sqrt{2}\,|I| \cos\Psi \\ i_q &= \sqrt{2}\,|I| \sin\Psi \\ i_0 &= 0 \end{aligned} \tag{4-48}$$



i.e., the zero-sequence component of stator current is *zero* and the *direct- and quadrature-axis components are constant.*† The machine equations (4-36) now take on the following simple forms:

$$\begin{aligned} v_d &= -r_s i_d + \omega L_q i_q \\ v_q &= -r_s i_q + \omega L_5 i_r^0 - \omega L_d i_d \\ v_0 &= 0 \\ v_r &= r_r i_r^0 \end{aligned} \tag{4-49}$$

We define at this juncture the *direct-* and *quadrature-axis synchronous reactances:*

$$\begin{aligned} X_d &\triangleq \omega L_d \\ X_q &\triangleq \omega L_q \end{aligned} \tag{4-50}$$

and can then write the first two of Eqs. (4-49) as follows:

$$\begin{aligned} v_d &= -r_s i_d + X_q i_q \\ v_q &= -r_s i_q - X_d i_d + \omega L_5 i_r^0 \end{aligned} \tag{4-51}$$

We make the important observation that $v_d$ and $v_q$, just like $i_d$ and $i_q$, are *constant.* From the general power equation (4-43), we thus conclude that *the power is constant.*‡

Upon making use of the inverse $B$ transformation (4-33) and remembering that $\alpha = \omega t$, we get for the stator voltages $v_a$, $v_b$, and $v_c$

$$\begin{aligned} v_a &= v_d \cos\omega t - v_q \sin\omega t \\ &= -(r_s i_d - X_q i_q)\cos\omega t + (r_s i_q + X_d i_d - \omega L_5 i_r^0)\sin\omega t \\ v_b &= -(r_s i_d - X_q i_q)\cos(\omega t - 120^\circ) \\ &\quad + (r_s i_q + X_d i_d - \omega L_5 i_r^0)\sin(\omega t - 120^\circ) \\ v_c &= -(r_s i_d - X_q i_q)\cos(\omega t + 120^\circ) + (r_s i_q + X_d i_d \\ &\quad - \omega L_5 i_r^0)\sin(\omega t + 120^\circ) \end{aligned} \tag{4-52}$$

† The physical significance of this fact is that the mmf wave caused by the stator currents is *constant* as measured relative to the rotor. We can express this situation differently. The armature-current mmf wave has constant amplitude and travels with the same speed and direction as the rotor. As the flux caused by this wave ("armature reaction") thus is stationary with respect to the rotor, no voltage is induced by it in the rotor winding. (This confirms our assumption that the rotor current is constant $= i_r^0$.)

‡ As we pointed out in the introductory chapter, the symmetrical three-phase system *transmits a constant power.* Now we find that a symmetrically operated synchronous machine produces (or consumes) a *constant* power (and torque). (The same applies to a three-phase induction motor.)

**Table 4-1 Synchronous machine reactances (in pu of rated MVA)**

| | *Synchronous motors* | | | | |
|---|---|---|---|---|---|
| *Reactances* | *High-speed* | *Low-speed* | *Synchronous condensers* | *Hydro generators* | *Turbine generators* |
| $X_d$ | 0.80 | 1.10 | 1.60 | 1.00 | 1.15 |
| $X_q$ | 0.65 | 0.80 | 1.00 | 0.65 | 1.00 |
| $X'_d$ | 0.30 | 0.35 | 0.40 | 0.30 | 0.15 |
| $X''_d$ | 0.18 | 0.20 | 0.25 | 0.20 | 0.10 |
| $X_-$ | 0.19 | 0.35 | 0.25 | 0.20 | 0.13 |
| $X_0$ | 0.05 | 0.07 | 0.08 | 0.07 | 0.04 |

At this point we shall neglect the resistive voltage drops in Eqs. (4-52). The armature resistance $r_s$ is very small (usually less than 0.01 pu in terms of the machine ratings), compared with the reactances $X_d$ and $X_q$. Table 4-1 gives average values for those reactances for various types of practical synchronous machines. (The last four rows in the table refer to transient reactances, introduced in Chap. 10.)

Upon dropping the two resistive terms from Eqs. (4-52), we have the simpler form

$$v_a \approx X_q i_q \cos \omega t + (X_d i_d - \omega L_5 i_r^0) \sin \omega t \tag{4-53}$$

We also have, for the current,

$$i_a = i_d \cos \omega t - i_q \sin \omega t \tag{4-54}$$

Because of the existing three-phase symmetry, we do not care to write out the current and voltage relations for phases $b$ and $c$.

**Phasor diagrams** Since both $v_a$ and $i_a$ are *harmonic*, it is instructive to represent the foregoing equations in *phasor* form. For this purpose we write them in complex form.

$$\begin{aligned} v_a &= \text{Im}\,\{(X_d i_d - \omega L_5 i_r^0)e^{j\omega t} + jX_q i_q e^{j\omega t}\} \\ i_a &= \text{Im}\,\{j i_d e^{j\omega t} - i_q e^{j\omega t}\} \end{aligned} \tag{4-55}$$

We have made use of the relations

$$\begin{aligned} \sin \omega t &= \text{Im}\,\{e^{j\omega t}\} \\ \cos \omega t &= \text{Im}\,\{j e^{j\omega t}\} \end{aligned}$$



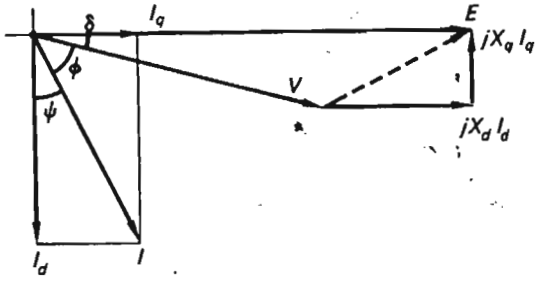


**Fig. 4-11** Phasor diagram of symmetrically operated machine. Only phase $a$ is shown.

At this juncture we introduce the following phasors:

$$\begin{aligned} I_q &\triangleq -\frac{i_q}{\sqrt{2}} \\ I_d &\triangleq j\frac{i_d}{\sqrt{2}} \end{aligned} \tag{4-56}$$

From Eqs. (4-55) we then get

$$\begin{aligned} v_a &= \sqrt{2}\,\text{Im}\left\{\left(-jX_d I_d - \frac{\omega L_5 i_r^0}{\sqrt{2}} - jX_q I_q\right)e^{j\omega t}\right\} \\ i_a &= \sqrt{2}\,\text{Im}\,\{(I_d + I_q)e^{j\omega t}\} \end{aligned} \tag{4-57}$$

and we can, obviously, represent $v_a$ and $i_a$ by the phasors

$$\begin{aligned} V_a &\triangleq E_a - jX_d I_d - jX_q I_q \\ I_a &\triangleq I_d + I_q \end{aligned} \tag{4-58}$$

Note that we have identified the second term in Eqs. (4-57) as the stator emf $E_a$ defined by Eq. (4-46).

All the above phasors are shown in Fig. 4-11. This is an extremely important diagram, since it is possible to obtain from it all essential information relating to the symmetrical operation of synchronous machines. Before we discuss these matters we shall make a few observations in regard to the phasor diagram:

1. Since complete symmetry exists between the three phases, we have dropped the subscript $a$ on phasors $V$, $E$, and $I$.
2. We have identified the *power angle* $\delta$, introduced in Fig. 4-10. *We shall define $\delta$ positive when $E$ leads $V$.*
3. We have also identified both the phase angle $\Psi$ introduced in Eqs. (4-47) and also the more important one, $\phi$, that is, the phase angle between

stator voltage and current. As usual, $\phi$ is defined positive when voltage leads current, as in Fig. 4-11.

**Power relations** When operating the machine under symmetrical conditions, the questions that most often are asked relate to the real and reactive powers consumed by or delivered from the alternator. We have already observed that the real power is *constant*. We could readily obtain an expression for it by using Eq. (4-43), but instead prefer to use our well-known formula for complex power, which will render both the real and reactive powers.

We have

$$S_G = P_G + jQ_G = |V|\,|I| \cos\phi + j\,|V|\,|I| \sin\phi$$

We have made use of Eqs. (2-26), which state that

$$\begin{aligned} P_G &= |V|\,|I| \cos\phi \qquad \text{MW/phase} \\ Q_G &= |V|\,|I| \sin\phi \qquad \text{Mvar/phase} \end{aligned} \tag{4-59}$$

$V$, $I$, and $\phi$ are all defined and appear in Fig. 4-11. Note that because $I$ is defined positive out from the machine, Eqs. (4-59) *define $P_G$ and $Q_G$ positive in a generator sense.* Note also that the equations give us *per-phase* values of power. Since Eqs. (4-59) contain the current, which is seldom known explicitly, we shall write the equations in different form. From the phasor diagram in Fig. 4-11 we obtain upon projection along and perpendicular to $E$

$$\begin{aligned} |E| - |I_d|\,X_d &= |V| \cos\delta \\ |I_q|\,X_q &= |V| \sin\delta \end{aligned} \tag{4-60}$$

We also have

$$\begin{aligned} |I_q| &= |I| \sin\Psi \\ |I_d| &= |I| \cos\Psi \end{aligned} \tag{4-61}$$

and for the angles:

$$\phi + \delta + \Psi = 90^\circ \tag{4-62}$$

From the last equation we derive

$$\cos\phi = \sin\Psi \cos\delta + \cos\Psi \sin\delta$$

and therefore

$$|I| \cos\phi = |I| \sin\Psi \cos\delta + |I| \cos\Psi \sin\delta \tag{4-63}$$

By making use of Eqs. (4-61), we have, from the last equation,

$$|I| \cos\phi = |I_q| \cos\delta + |I_d| \sin\delta \tag{4-64}$$



and by substituting this expression for $|I| \cos\phi$ into Eqs. (4-59), and at the same time making use of Eqs. (4-60), we arrive, after some simple algebra at the following formula for the real power:

$$P_G = \frac{|V|\,|E|}{X_d} \sin\delta + \frac{|V|^2}{2}\left(\frac{1}{X_q} - \frac{1}{X_d}\right) \sin 2\delta \tag{4-65}$$

The importance of this formula is due to the fact that the bus voltage $|V|$ is a fairly constant quantity if the network is of reasonably large size.† The magnitude $|E|$ of the emf is constant if we hold the field current constant. *We conclude therefore that, for all practical purposes, $P_G$ is a function only of the power angle $\delta$.*

The power formula becomes simple for a machine lacking rotor saliency. In such a case $X_d = X_q \triangleq X_d$, and we get

$$P_G = \frac{|V|\,|E|}{X_d} \sin\delta \tag{4-66}$$

The second term‡ in Eq. (4-65) is referred to as the *saliency*, or the *reluctance*, component of torque, and is as a rule relatively small (10 to 20 percent), in comparison with the first term.

In the following discussion where we shall place more emphasis on qualitative than quantitative behavior, we shall therefore use the "round-rotor" equation (4-66) as a basis. We need, first, a similar formula for the *reactive* power and obtain it readily from the second of Eqs. (4-59). A derivation analogous to that of Eq. (4-66) gives

$$Q_G = \frac{|E|\,|V|}{X_d} \cos\delta - \frac{|V|^2}{X_d} \tag{4-67}$$

Again, the reactive power out from the machine is defined as positive. Also, the formula applies to the nonsalient case, with $X_q = X_d$.

It should be noted that *both* Eqs. (4-66) and (4-67) give $P_G$ and $Q_G$ per phase. If, however, $|E|$ and $|V|$ are expressed in *line* voltages and *kilovolts*, the results are *total* three-phase powers in *megavalues*.

**Real generator power $P_G$** Let us now first display some of the characteristics of the real power $P_G$. If the network is very large ("infinite"), we can consider $|V|$ practically constant. If we do not vary the field current $i_f$,

† For an "infinite" network we concluded earlier that $|V|$ is absolutely constant.

‡ Note that the reluctance torque component is independent of $|E|$; that is, it will be present even when the rotor field current is zero. A torque, albeit a weak one, can thus be had with a salient piece of iron as a rotor. This type of synchronous motor is often used in electric clocks.

the emf $|E|$ will also be constant, and we can then write

$$P_G = P_{\max} \sin \delta \tag{4-68}$$

where

$$P_{\max} \triangleq \frac{|E|\,|V|}{X_d} \tag{4-69}$$

$P_G$ is plotted versus the *power angle* $\delta$ in Fig. 4-12. Positive $P_G$, indicating generator action, is obtained for $\delta > 0$, that is, for $E$ leading $V$. Negative $P_G$, corresponding to motor action, is obtained for negative $\delta$. The *pullout power* $P_{po}$, that is, the power at which the machine steps out of synchronization, equals

$$P_{po} = \pm P_{\max} = \pm \frac{|E|\,|V|}{X_d} \quad \text{MW} \tag{4-70}$$

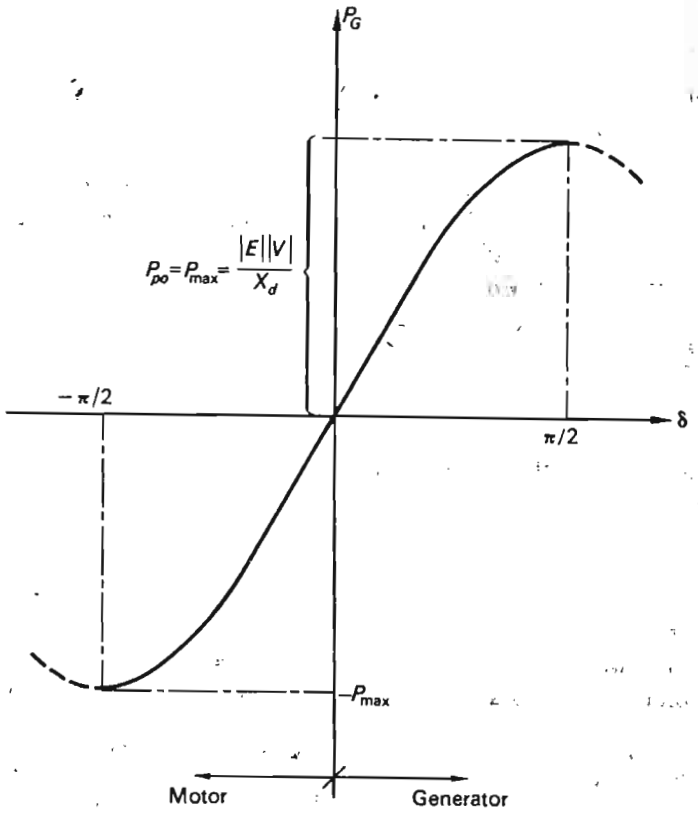


**Fig. 4-12** Real generated power versus power angle for nonsalient machine.



The *stiffness* of the machine is defined as

$$\frac{dP_G}{d\delta} = \frac{|E|\,|V|}{X_d} \cos \delta \quad \text{MW/rad} \tag{4-71}$$

and indicates the differential power increase obtained per differential power angle increase. Note that the stiffness is zero at the point of pullout. *We can evidently make our machine stiffer by either increasing* $|E|$, *that is, using high-magnitude pole flux, or by decreasing the synchronous reactance* $X_d$. The latter method can, of course, be employed only as a *design tool.* The most effective way of building a machine with low-magnitude $X_d$ is by using relatively large air gaps.† (We pay a price for this: a very powerful dc excitation source must be used to overcome the air gap reluctance in order to obtain required flux density.)

The reader, at this point, must have noticed the great similarities between the concept of "pullout power" for a generator and "transmission capacity" for a transmission line. Compare, in particular, Eqs. (3-2) and (4-68).

We know now how $P_G$ varies as a function of $\delta$, and the next question is: How is $\delta$ made to vary?

This is where the *torque* enters the picture. Since the speed is constant, we know that the mechanical driving torque emanating from the prime mover $\tau_m$ must equal the electrodynamic torque $\tau_e$. The powers being constant, so are the torques, and if we neglect the losses, we can most conveniently obtain them from the equation

$$\tau_e = \tau_m = \frac{P_G}{\omega_{\text{mech}}} \quad \text{MN} \cdot \text{m} \tag{4-72}$$

i.e., there is a direct proportionality between the torque and power. We realize now how the power angle, and thus the power, will change. When, by means of the prime mover, added positive torque is applied (a "positive" torque would tend to accelerate the generator if decoupled from the network), the rotor will advance a certain angle (compare Fig. 4-5). This means, in effect, that the phasor $E$, the phase of which depends upon the rotor position, will pull away from $V$, resulting in an increase in $\delta$, and thus an increase in $P_G$. The new $\delta$ value will correspond to exactly the power needed to balance out the added torque in accordance with Eq. (4-72). If the torque is increased beyond the value $P_{\max}/\omega_{\text{mech}}$, then a further increase will not result in a corresponding increase in $P_G$, and the machine will step out of synchronism and "skip poles." The process just described can be easily viewed by means of a stroboscope.

† The reader should confirm this statement by going back to the definition of $X_d$ and convince himself that the air gap dimensions greatly affect this reactance.

If, by means of some mechanical load, we applied a *negative* torque to our machine, then emf $E$ would lag behind $V$, and we would have motor action. Too large negative torque could again cause desynchronization.

It is important that the student fully understand the torque-power mechanism just described, because it is basic to the operation of a power system. Clearly, the question whether an alternator behaves like a generator or motor depends entirely upon how we treat it torquewise. Once synchronized onto a network, it stands ready to serve us in either way.

Before we leave this topic, it is of interest once more to make a comparison between the torque situation in the synchronous machine and the system depicted in Fig. 4-6.

Returning to Eq. (4-2), we note the great similarity between that formula and Eq. (4-66). The only basic difference is that in the one case our variables are of dc type and in the other of the ac variety.

**The reactive power $Q_G$** We have so far said nothing about the *reactive power* $Q_G$ delivered by the machine. In the discussion that follows we shall make use of Eq. (4-67). The $Q_G$ formula for a salient-pole machine is somewhat more complicated, and we have not bothered to derive it. However, what we are about to say will apply also to a salient-pole machine, in a *qualitative* sense. The $Q_G$ formula tells us that if

$$|E| \cos \delta > |V| \tag{4-73}$$

then $Q_G > 0$, and the generator *produces* reactive power, i.e., acts, from the network point of view, as a capacitor. Equation (4-73) evidently depends upon $\delta$, that is, upon the *real* power $P_G$.† Generally, however, the inequality is satisfied for high-magnitude $|E|$, that is, for *strong* excitation. We refer to this as *overexcitation*.

We therefore have the following important rule:

*An overexcited synchronous machine (operated either as motor or generator) produces reactive power and acts as a shunt capacitor as viewed from the network.*

An *underexcited* machine, on the contrary, *consumes* reactive power from the network and acts, consequently, as a shunt coil, if viewed from the network. Underexcitation is defined by the inequality

$$|E| \cos \delta < |V| \tag{4-74}$$

This feature of an overexcited synchronous machine, of actually generating reactive power, is taken advantage of in a so-called *synchronous condenser*. In this mode of operation the machine usually carries no real load; that is, $\delta = 0$. From Eq. (4-67) we then have

$$Q_G = \frac{|V|\,(|E| - |V|)}{X_d} \quad \text{Mvar} \tag{4-75}$$

The beauty of this arrangement is that $Q_G$ can be *continuously* and *simply* controlled by changing $|E|$, that is, by varying the dc excitation current.

A bank of capacitors, used for the same purpose of generating megavars, can be controlled only discontinuously (in steps) and only in a positive direction.

We are now in a position to verify what we said earlier, in Sec. 4-2, about means for controlling the real and reactive powers in an alternator. Clearly, a change in the field current will affect the magnitude of $|E|$, and thus the magnitude and direction of $Q_G$, as Eq. (4-67) indicates. The change will also affect the magnitude of $P_{\max}$, and thus the stiffness of the machine. This means that the power angle $\delta$, *but not the power* $P_G$, will vary. For example, a reduction in the field current will increase the magnitude of $\delta$, even possibly to the point of pullout (compare Example 4–3).

A change in the shaft torque, as earlier reasoned, will immediately affect the power $P_G$. At the same time the power angle $\delta$ will also change, and since $Q_G$ depends on cos $\delta$, we therefore also experience a change in $Q_G$. We usually work with power angles below 30°. For such small angles, cos $\delta$ is rather insensitive to changes in $\delta$, and therefore we do not experience too large a fluctuation in $Q_G$. We say that the cross coupling is weak.

**Equivalent diagram representation of alternator** Consider the voltage difference between $V$ and $E$ (shown dotted) in the phasor diagram of Fig. 4-11. If we assume that the alternator has a round rotor, so that $X_q = X_d$, then it is found by simple geometry that the voltage difference in question leads the current $I$ by 90°. The phasor diagram now takes on the simplified form shown in Fig. 4-13. Since the magnitude of the voltage difference under consideration equals

$$X_d \sqrt{|I_q|^2 + |I_d|^2} = X_d\,|I|$$

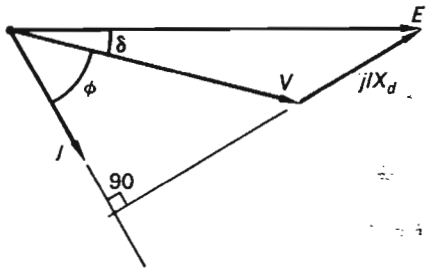


**Fig. 4-13** Phasor diagram for nonsalient synchronous machine. Resistive voltage drop neglected.

† However, since cos $\delta$ is an *even* function of $\delta$, it does not matter whether we have motor or generator action.

then it is clear that we can consider the voltage in question a "drop" across the reactance $X_d$ caused by the current $I$, in accordance with the phasor equation

$$V = E - jIX_d \tag{4-76}$$

This is tantamount to saying that the machine *when operated in symmetrical steady state* may be viewed from the terminal as a source emf $E$ behind an internal impedance $jX_d$. The corresponding equivalent diagram is depicted in Fig. 4-14. The impedance $jX_d$ is referred to as the "synchronous impedance" of the machine.

Equations (4-53), (4-54), and (4-76) prove that

1. The voltages in all three phases are characterized by three-phase symmetry.
2. The voltage drop in each phase is proportional to the current in that phase only.

We can actually write for the three phases

$$V_a = E_a - jI_aX_d$$
$$V_b = E_b - jI_bX_d$$
$$V_c = E_c - jI_cX_d$$

or in vector form,

$$\mathbf{V} = \mathbf{E} - \mathbf{Z}_i\mathbf{I} \tag{4-77}$$

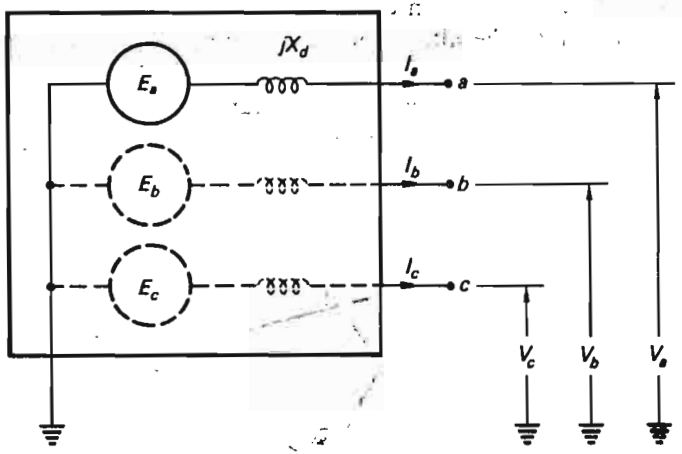


**Fig. 4-14** Equivalent network representation of symmetrically operated machine. Nonsaliency assumed.



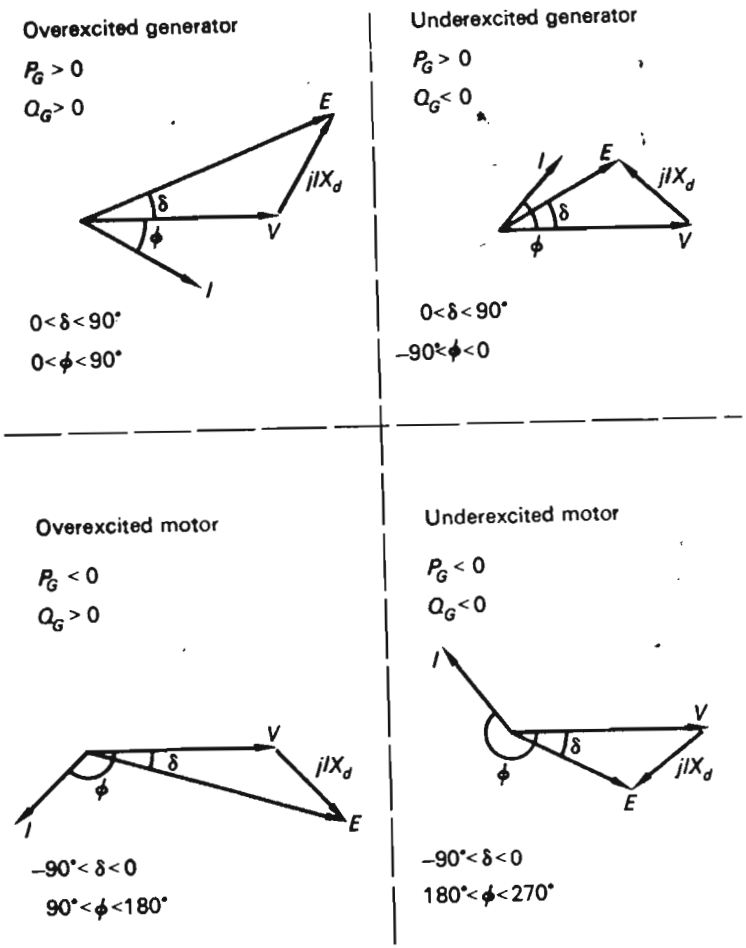


**Fig. 4-15** The four possible operating cases of a synchronous machine.

where the *internal impedance matrix* $\mathbf{Z}_i$ is defined by

$$\mathbf{Z}_i \triangleq \begin{bmatrix} jX_d & 0 & 0 \\ 0 & jX_d & 0 \\ 0 & 0 & jX_d \end{bmatrix} \tag{4-78}$$

and the $\mathbf{V}$, $\mathbf{E}$, and $\mathbf{I}$ vectors by

$$\mathbf{V} \triangleq \begin{bmatrix} V_a \\ V_b \\ V_c \end{bmatrix} \qquad \mathbf{E} \triangleq \begin{bmatrix} E_a \\ E_b \\ E_c \end{bmatrix} \qquad \mathbf{I} \triangleq \begin{bmatrix} I_a \\ I_b \\ I_c \end{bmatrix}$$

The fact that $\mathbf{Z}_i$ is *diagonal* means *zero coupling* between phases, and is our real guarantee that we can treat the symmetrically loaded alternator on a per-phase basis. This *cannot* be done in the case of unbalanced load (Chap. 11).

In Fig. 4-15 we summarize the four possible operational cases of a synchronous machine: over- and underexcited generator, over- and underexcited motor. Note that in all four cases the voltage drop $jIX_d$ leads the current by 90°. Note also that the positive directions for $P_G$ and $Q_G$ in these diagrams are those corresponding to Eqs. (4-59); i.e., they are both positive in the generator sense.

We shall work a few examples to illustrate the results arrived at in this section.

**Example 4-1** A generator has the following ratings:

$|S_r| = 400$ MVA total three-phase

$|V_r| = 20$ kV line to line

$f = 60$ Hz

We may consider its rotor round, and therefore assume $X_d = X_q$. Its measured synchronous reactance amounts to 100 percent (based on rated megavoltamperes). Compute its real and reactive power output, assuming the power angle $\delta = 30°$ and its field excitation is set at a value corresponding to an emf of 125 percent. (This means that if the machine were running open-circuited, we could measure $|E| = 1.25 \times 20 = 25$ kV between its phases.)

Using Eq. (2-50), we first compute the ohmic value of the synchronous reactance.

$$X_d = \frac{20^2 \times 1.00}{400} = 1.00\ \Omega/\text{phase}$$

From Eqs. (4-66) and (4-67), we then get directly

$$P_G = \frac{|E|\,|V|}{X_d} \sin\delta = \frac{25 \times 20}{1.0} \sin 30° = 250 \text{ MW}$$

$$Q_G = \frac{|V|\,|E|}{X_d} \cos\delta - \frac{|V|^2}{X_d} = \frac{25 \times 20}{1.0} \cos 30° - \frac{(20)^2}{1.0} = 33 \text{ Mvar}$$

(Note that we have inserted the *line* voltages into the formulas and thereby directly obtained the *total three-phase powers*.)

If, instead, we insert per-unit values in the above formulas, we obtain

$$P_G = \frac{1.25 \times 1.0}{1.0} \sin 30° = 0.625 \quad \text{pu}$$

$$Q_G = \frac{1.25 \times 1.0}{1.0} \cos 30° - \frac{(1.0)^2}{1.0} = 1.0825 - 1.0 = 0.0825 \quad \text{pu}$$



If we wish to translate these per-unit values into megawatts and megavars, we remember that 1.0 pu corresponds to *rated* Mvar = 400 MVA. Thus

$P_G = 0.625 \times 400 = 250$ MW

$Q_G = 0.0825 \times 400 = 33$ Mvar

which is in agreement with earlier results.

**Example 4-2** A salient-pole generator is characterized by the following synchronous reactances:

$X_d = 100\%$

$X_q = 60\%$

Assume the machine is operated at a power angle of 45° and at $|V| = |E| =$ 100 percent. How many percent of the total power output is contributed by the reluctance term in Eq. (4-65)?

We have

$$P_G = \frac{1.0 \times 1.0}{1.00} \sin 45° + \frac{(1.0)^2}{2}\left(\frac{1}{0.6} - \frac{1}{1.0}\right) \sin 90°$$

Hence

$$P_G = 0.707 + 0.333 = 1.040 \quad \text{pu}$$

The second term contributes

$$\frac{0.333}{1.040} \times 100 = 31\% \text{ of total power}$$

We note, by the way, that the generator delivers 104 percent power, which means that it is 4 percent overloaded, powerwise. Is the machine overloaded currentwise?

**Example 4-3** In this example we study how the real and reactive power outputs of a generator change when the machine is subject to manipulation of the two control inputs, the shaft torque and the excitation current.

Consider a turbogenerator feeding into a network which, for all practical purposes, we may consider "infinite." As we explained earlier, this means that, viewed from the generator, the network appears impedanceless, and the bus voltage will therefore remain constant, independent of what happens inside the generator. We shall, for our analysis, consider the bus voltage to be equal to 1 pu, i.e., the rated machine voltage. We shall choose the rated power of the generator as our base power, and perform all our computations in per-unit values.

Let us assume that the generator initially runs overexcited, with $|E| = 1.50$ pu and a real power output corresponding to $P_G = 0.25$ pu. We shall assume the synchronous reactance to equal 1.0 pu.

From the $P_G$ equation (4-66) we can now compute the power angle $\delta$.

$$0.25 = \frac{1.5 \times 1.0}{1.0} \sin\delta \quad \text{MW}$$

We obtain

$\sin\delta = 0.1667$

and thus

$\delta = 9.60°$

From the $Q_G$ equation (4-67), we then compute the reactive power output.

$$Q_G = \frac{1.5 \times 1.0}{1.0} \cos 9.60° - \frac{(1.0)^2}{1.0} = 0.48 \quad \text{pu Mvar}$$

The megavoltampere output of the generator is thus

$$\sqrt{(0.25)^2 + (0.48)^2} = 0.54 \quad \text{pu MVA}$$

indicating that the generator is running at slightly above half current load.

We shall now subject the machine to (*a*) torque control and, (*b*) excitation control, and study the output changes in both cases.

*Case a. Torque control* Let us assume that we open the steam valve corresponding to a 100 percent increase in the turbine torque; i.e., the real power output will increase to 0.5 pu. The power angle will now increase, and we compute the new value

$$0.5 = \frac{1.5 \times 1.0}{1.0} \sin \delta$$

i.e.,

$$\delta = 19.5°$$

For this new rotor position the reactive power will *decrease* to

$$Q_G = \frac{1.5 \times 1.0}{1.0} \cos 19.5° - \frac{(1.0)^2}{1.0} = 0.41 \quad \text{pu Mvar}$$

We thus conclude that a 100 percent *increase* in the torque input (and thus the $P_G$ output) results in a $[(0.48 - 0.41)/0.48] \times 100 = 15$ percent *decrease* in the $Q_G$ output. We have here, obviously, a cross coupling between the $\tau$ input and the $Q$ output, but a weak one.

*Case b. Excitation control* Let us now assume that we start from the same initial state as before, keeping the steam valve setting unchanged but varying the field current. For example, let us assume a 20 percent increase of field current, which (if we assume no saturation) means that $|E|$ increases to $1.20 \times 1.50 = 1.8$ pu. This increase of the pole flux results in a stiffer machine, and from the $P_G$ equation we compute the new and smaller power angle.

$$0.25 = \frac{1.8 \times 1.0}{1.0} \sin \delta$$

i.e.,

$$\delta = 8.00°$$

There will, of course, be no change in the $P_G$ output. The new $Q_G$ output will be

$$Q_G = \frac{1.8 \times 1.0}{1.0} \cos 8.00° - \frac{(1.0)^2}{1.0} = 0.78 \quad \text{pu Mvar}$$

i.e., a 63 percent increase from the original value of 0.48 pu.

The generator reactive output is thus very sensitive to changes in excition level.



## 4-5 MACHINE RATINGS

The rating of a synchronous machine is limited by the losses, which are of two types, ohmic losses $P_\Omega$ in the rotor and stator winding, and core or iron losses $P_{Fe}$ in the stator iron. For the former we have

$$P_\Omega \sim |I|^2 \tag{4-79}$$

The latter consist of *eddy current* $P_{ec}$ and *hysteresis losses* $P_{hyst}$; that is,

$$P_{Fe} = P_{ec} + P_{hyst} \tag{4-80}$$

By direct application of Faraday's law, the eddy currents $I_{ec}$ are related to the frequency $f$ and stator flux $\Phi$ through the relation

$$|I_{ec}| \sim f|\Phi| \tag{4-81}$$

Since the eddy current losses are proportional to $I_{ec}^2$, we therefore have

$$P_{ec} \sim f^2 |\Phi|^2 \tag{4-82}$$

For the flux $\Phi$, we have

$$|\Phi| \sim i_r \sim \frac{|E|}{f} \tag{4-83}$$

[The last step follows from Eq. (4-46).]

From Eq. (4-82) we thus have

$$P_{ec} \sim |E|^2 \tag{4-84}$$

The hysteresis losses are directly proportional to frequency and increase *empirically* with $\Phi$ in an exponential manner:

$$P_{hyst} \sim f|\Phi|^\kappa \tag{4-85}$$

where

$$1.5 < \kappa < 2.0$$

By using Eq. (4-83), we have

$$P_{hyst} \sim \frac{|E|^\kappa}{f^{\kappa-1}} \tag{4-86}$$

We conclude from Eqs. (4-84) and (4-86) that *the core losses vary strongly with the emf, i.e., the degree of excitation.*

To summarize our findings, we conclude that the stator *current* and stator *emf both* determine the losses. As the megavoltampere loading thus is more representative for the heat losses than the megawatt load,† it makes sense *to rate a synchronous machine in megavoltamperes.*

† Note that a synchronous condenser may be operating at its loss limit and delivers zero megawatts.

## 4-6 SUMMARY

The three-phase synchronous generator is the basic component of an electric energy system. We have attempted to give a brief exposition of its operational characteristics as viewed from a systems point of view. Thus we have concentrated upon the response of the machine to variations in the two basic control inputs, the prime mover torque and the field current. We have concluded that these two inputs are *essentially* decoupled; i.e., a change in torque affects the real power output, whereas a change in the field current controls the reactive output.

We have formulated general equations for the machine, but in this chapter we have solved these equations only for balanced steady-state operation. This analysis has confirmed that the machine torque and power are constants. We shall make use of the general mathematical models in later chapters to analyze the behavior of the machines under unbalanced operation and transient conditions.

The models developed in this chapter were all based upon the simplifying assumption of linearity. Since all synchronous machines operate in a region of magnetic saturation, the models must of necessity be characterized by some approximation. We do not, in our introductory type of presentation, enter into a detailed discussion of the effect of these nonlinearities. We wish to point out, however, that the linear models presented form the basis for *all* practical system studies. It is possible to take account of the nonlinear effects by adding first-order corrective terms to our linear parameters. Some comments on these procedures will be given in Chap. 12.

## EXERCISES

**4-1.** We found in the text an expression for the pullout torque based on the assumption that $X_d = X_q$. Find, using Eq. (4-65), an expression for the pullout torque for a machine when we do not assume nonsaliency.

(*a*) Does pullout occur for $\delta = 90°$?

(*b*) Prove that your equation for $P_{po}$ renders values in excess of $P_{max}$ defined in the text. Explain.

**4-2.** A generator having a synchronous reactance of 0.90 pu based on its own rating is connected via a transmission line to a remote bus, the voltage of which we may assume is kept constant at a value of 100 percent. The line has an impedance of $j0.15$ pu per phase, based upon the machine megavoltamperes. The internal emf $E$ of the machine is kept at a constant magnitude of 135 percent.

(*a*) Compute the pullout power of the machine if operated as a generator.

(*b*) At the moment of pullout, determine magnitude and direction of the reactive power at both the generator terminal and the remote bus.

(*c*) At the moment of pullout, what is the terminal voltage?

(*d*) Is the machine current overloaded at pullout?



**4-3.** Consider a synchronous machine running open-circuited. Equation (4-10) tells us that the terminal voltages in this case are

$$v_a = \frac{d}{dt}(l_{ra} i_r)$$

$$v_b = \text{etc.}$$

Assume, then, that the mutual inductances $l_{ra}$, $l_{rb}$, and $l_{rc}$ are *not* sinusoidal in accordance with Eqs. (4-8) but contain, owing to poor air gap design, a third harmonic.

(*a*) Prove now that each phase voltage will contain a 180-Hz component.

(*b*) Prove also that this 180-Hz component is *not* present in the line voltages. (Explain this fact physically.)

**4-4.** A synchronous machine is running overexcited with $|E| = 150$ percent. The synchronous reactance has the value 120 percent, and the machine delivers a real power of 0.4 pu.

If the prime mover torque is increased by 1 percent, with how many percents will $P_G$ and $Q_G$ change?

**4-5.** Consider the two-bus system shown in Fig. 4-16. The load $S_{D2}$ drawn from bus 2 is in its entirety supplied by generator 1 and transported via the line. The latter, as will be

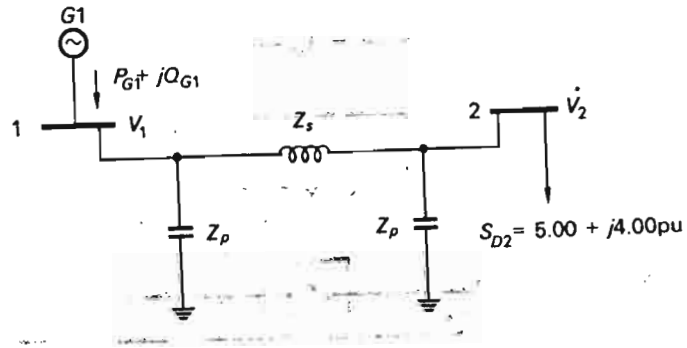


**Fig. 4-16** Example system.

demonstrated in Chap. 6, may be represented by an equivalent $\pi$ network, the impedances of which are as follows:

$$Z_s = j0.05 \quad \text{pu}$$

$$Z_p = -j3.00 \quad \text{pu}$$

The synchronous reactance equals 110 percent.

The magnitude $|V_2|$ of the voltage of bus 2 must equal 1.00 pu.

(*a*) Determine the voltage that we must maintain at bus 1 in order to achieve the above objective.

(*b*) Compute the required reactive generation $Q_G$.

(*c*) Compute the generator emf $|E|$.

(*d*) With this degree of generator excitation, what would be the pullout torque?

(*e*) Assume now that the load of bus 2 decreases to a night load which is approximately zero. We still wish to maintain $|V_2| = 1.00$.

Find the answers to questions (*a*) to (*d*) and confirm that the generator pullout torque will be considerably reduced (= reduced stability limit).

**4-6.** A synchronous machine has been synchronized onto a big network. All three conditions for a smooth "lock-in" were satisfied. Without changing the field current, we now make the machine generate real power. Will it, at the same time, generate or consume reactive power? Explain.

**4-7.** Equation (4-67) for $Q_a$ was derived for a nonsalient rotor. Find a formula valid for the salient-rotor case.

Use your formula to find the generated reactive power for the following set of numerical values:

$|E| = 1.60$ pu
$|V| = 1.00$ pu
$X_d = 1.10$ pu
$X_q = 0.90$ pu
$\delta = 30°$

How approximate would your answer be if you used Eq. (4-67)?

**4-8.** Figure 4-17 depicts a simple arrangement for synchronization of a generator to a network. *A*, *B*, and *C* are three light bulbs (or voltmeters). If the generator speed

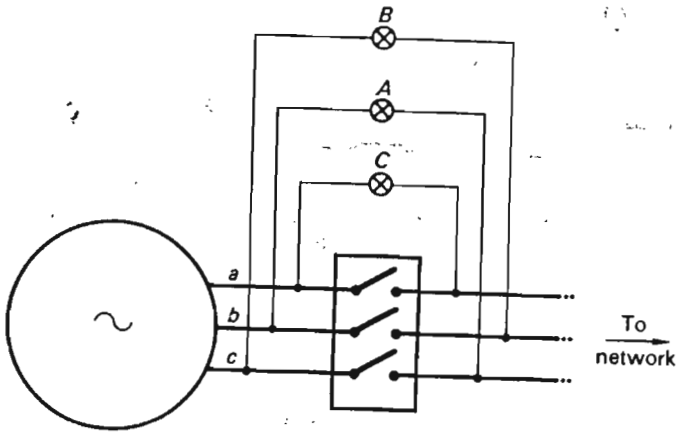


**Fig. 4-17** Simple synchronizing arrangement.

(or frequency) is different from that of the network, the lights of each bulb will pulsate in sequence $ABCA \cdots$ or $ACBA \cdots$.

(*a*) Relate the pulsation sequence with over- or underspeed.
(*b*) State the conditions that must be satisfied for closing the breaker.

## REFERENCES

**Books**

1. Kron, G.: "Tensor Analysis of Networks," MacDonald & Co., Publishers, Ltd., London, 1964.
2. Electrical Transmission and Distribution Reference Book, Westinghouse Electric and Manufacturing Co., East Pittsburgh, Pa., 1964.



3. Adkins, B.: "The General Theory of Electrical Machines," John Wiley & Sons, Inc., New York, 1957.
4. Concordia, C.: "Synchronous Machines," John Wiley & Sons, Inc., New York, 1951.
5. Meisel, J.: "Principles of Electromechanical Energy Conversion," McGraw-Hill Book Company, New York, 1966.
6. Fitzgerald, A. E., and C. Kingsley: "Electric Machinery," 2d ed., McGraw-Hill Book Company, New York 1961.
7. Woodson, H. H., and J. R. Melcher: "Electromechanical Dynamics," vols. I–III, John Wiley & Sons, Inc., New York, 1968.

(References 3 to 7 give excellent detailed treatment of the synchronous machine. Reference 2 contains a wealth of machine and systems data. Dr. Krons's work, although hard to digest, should be familiar to any electrical engineer, particularly a power man.)

**Technical papers and reports**

8. Woodson, H. H. et al.: A Study of Alternators with Superconducting Field Windings, *IEEE Trans.*, vol. PAS-85, no. 3, pp. 264–280, March, 1966.
9. Erdelyi, E. A. et al.: Nonlinear Theory of Synchronous Machines On-load, *IEEE Trans.*, vol. PAS-85, no. 7, pp. 792–801, July, 1966.
10. Doherty, R. E., and C. A. Nickle: Synchronous Machines: An Extension of Blondel's Two-reaction Theory, pts. I and II, *Trans. AIEE*, vol. 44, pp. 403–418, 1925. (A classic paper.)
11. Garver, L. L.: Effective Load Carrying Capability of Generator Units, *IEEE Trans.*, vol. PAS-85, no. 8, pp. 910–919, August, 1966.

# 5

# The Power Transformer

We have demonstrated, in Chaps. 2 and 3, that the need for high power transmission capacity and effective reduction of transmission losses requires high transmission voltages. It is not practically feasible to generate voltages of magnitudes in the hundreds of kilovolts directly in synchronous generators. The necessary insulation thickness prohibits generation in excess of about 25 kV. To achieve the transmission capabilities called for in the systems of today and the near future, we must make use of transmission voltages in the range of 500 to 1000 kV. The role of the power transformer is therefore an important one. The power transformer also serves in its capacity as a *regulating transformer* the additional important purpose of *voltage and load flow control device.* In this chapter we describe some of the important characteristics of this apparatus. Our philosophy in presenting the material is the same as in the preceding chapter: we concentrate on bringing about an understanding of the basic operation and develop simple but adequate mathematical models useful in subsequent system analysis. We avoid getting involved in design details which are relatively unimportant from the systems engineer's viewpoint.





Chances are that the reader is already familiar with the transformer as a device used in various aspects of communication engineering. In such applications the transformed power may range, usually, in watts or kilowatts. He may have been acquainted with the transformer used as a matching device between an output amplifier stage and a loudspeaker. In any event, he will have been impressed with the need of designing a transformer where the major specifications concern the frequency transfer characteristics. For example, a flat response over the entire audio range 20 to 15,000 Hz is a feature much more sought after than a few percent saved in efficiency.

A power transformer, on the contrary, will always be operated at *one* frequency, 60 Hz, and its performance is mainly based upon its characteristics in the following respects:

1. Reliability of service, when operated within its ratings
2. Overall economics

Let us comment on both these points. The high-voltage terminals of a transformer always constitute the end point of a transmission line. A line is a very *exposed* system component, and there will always be a risk that transient overvoltages caused by atmospheric disturbances will be propagated along the lines as waves, having steep voltage fronts and high velocity (slightly less than the velocity of light). Since those waves are being reflected at the transformer terminals, high-voltage amplitudes will be built up which will stress the insulation of the transformer. A breakdown can mean a severely damaged transformer—and interrupted service.

Transformation of power is always associated with unavoidable losses, *core losses* in the transformer and *copper losses* in its windings. Those losses may amount to no more than a fraction of one percent of transformed power in the case of a large transformer. But even one percent of 1000 MW is a respectable loss; over time, it accumulates in considerable energy and money losses.

## 5-1 PRACTICAL DESIGN CONSIDERATIONS

Power transformers come in sizes ranging from distribution transformers rated at a few kilovoltamperes to huge transmission transformers with ratings (three-phase) in excess of 1000 MVA. Since we are concerning ourselves with the transmission level of power systems, we will be talking about transformers with ratings in the hundreds of megavoltamperes. As such we shall distinguish between

1. Generator transformers
2. Transmission transformers
3. Regulating (or control) transformers

The first type, having a typical voltage rating of, say, 20/345 kV, serves as a step-up device, transforming the power from generator level to transmission level. The second type, having a typical voltage rating of, say, 345/500 kV, is used for transformation of power between the different voltage levels in the transmission system. The third type of transformer is used as a load flow and voltage control device.

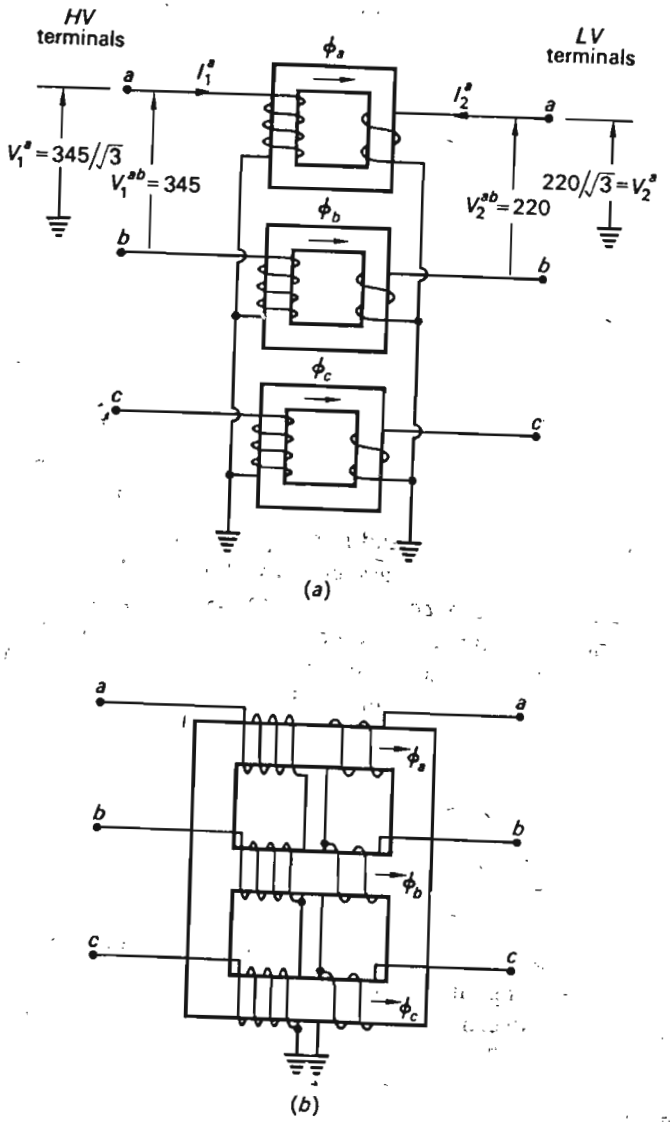


**Fig. 5-1** Three-phase transformation. (*a*) Bank arrangement; (*b*) core arrangement.



### 5-1.1 DIFFERENT TYPES OF CORE ARRANGEMENTS

Figure 5-1 depicts two different transformer schemes used in three-phase systems. Figure 5-1*a* depicts the so-called *bank* arrangement, consisting simply of three separate single-phase units, each transforming one-third of the throughpower. Figure 5-1*b* shows a *core* or *three-phase* transformer. In this latter design we make use of the fact that the three fluxes $\phi_a$, $\phi_b$, $\phi_c$, because of their three-phase symmetry, *add up to zero, and there is therefore no need for a magnetic return path.* Clearly, this design saves transformer core, and consequently also core losses, and one core transformer therefore has an economic advantage over a bank of three single-phase units. The bank arrangement has the advantage that, in case of breakdown, only one-third of the equipment needs to be replaced.

### 5-1.2 DIFFERENT WINDING ARRANGEMENTS AND ELECTRICAL CONNECTIONS

The winding arrangement depicted in Fig. 5-1 is only schematic. The *physical* arrangement of the different windings varies considerably, depending upon size, voltage rating, and the manufacturer. We shall not here enter into a discussion of the pros and cons of "concentric," "pancake," or other coil design. We will, however, briefly comment on winding *connections.*

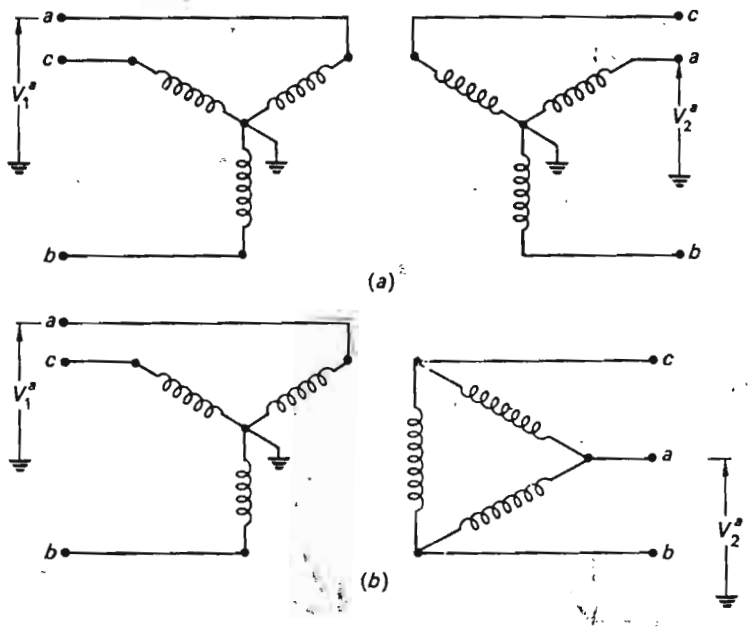


**Fig. 5-2** Typical winding connections. (*a*) YY type; (*b*) Y$\Delta$ type. As to the transformer symbols we make the following comments: The three-phase symbol is drawn so that the windings actually constitute a true picture of the voltage phasors both in *phase* and *phase sequence* (but not magnitude). Note that all windings located on the same core leg have their voltages in phase and will therefore always be shown parallel.

Two different connection schemes are used predominantly in transmission level transformers, the so-called YY and YΔ types shown in Fig. 5-2. The neutral point of the Y is usually solidly grounded. The voltage relations in those two transformer types are depicted in phasor form in Fig. 5-3. The following rules will be adhered to in regard to symbols:

1. The superscripts $a$, $b$, and $c$ will be used when there is a need to distinguish between phases. When no such need exists, they will be deleted.
2. The subscripts 1, 2, 3, . . . will be used to identify "primary," "secondary," "tertiary," etc., variables.
3. Line voltages will, *when needed*, be symbolized by double superscripts. The order of the superscripts defines polarity, for example,

$$V_1^{ab} \triangleq V_1^a - V_1^b$$

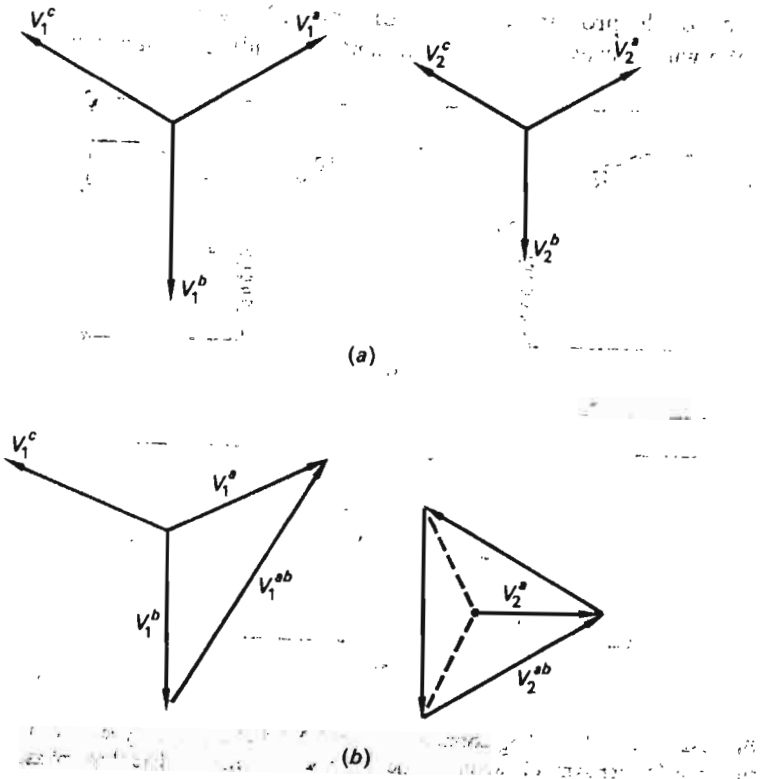


**Fig. 5-3** Phasor representation of primary and secondary voltages of transformers in Fig. 5-2. Note that Δ winding introduces a 30° phase shift in phase voltages.



When the transformers are operated under *balanced* steady-state conditions *there is no basic difference between the* YY *and the* YΔ *transformer*, except that the latter introduces a $\pm 30°$ phase shift between primary and secondary phase and line voltages, as shown in Fig. 5-3.† Under *unbalanced* operating conditions the two are quite different. We shall postpone a discussion of these matters until Chap. 11. As long as we tacitly assume balanced operation, we shall not make any distinction (except in regard to the phase shift) between the various connection types.

#### 5-1.3 RATINGS

Transformer losses are related to winding currents and emfs in the same manner as we found to be the case in a synchronous machine. We conclude, therefore, that a transformer must be rated in megavoltamperes rather than megawatts.

## 5-2 EQUIVALENT CIRCUITS FOR TWO-WINDING TRANSFORMERS

### 5-2.1 EXACT EQUIVALENT CIRCUIT OF YY-CONNECTED TRANSFORMERS

Consider the YY-connected transformer shown in Fig. 5-1. (We shall concern ourselves with phase $a$ only, so we will discard superscripts.) For the two windings we can write the following well-known voltage equations:

$$\begin{aligned} V_1 &= I_1 R_1 + I_1 j\omega L_1 + I_2 j\omega M_{12} \\ V_2 &= I_2 R_2 + I_2 j\omega L_2 + I_1 j\omega M_{12} \end{aligned} \tag{5-1}$$

where $R_1$ and $R_2$ = winding resistances
$L_1$ and $L_2$ = self-inductances
$M_{12}$ = mutual inductance between windings on same core

Consider next the circuit in Fig. 5-4*a*. It consists of two impedances, $Z_m$ and $Z_L$, and a "blackbox" characterized by the following properties:

1. A voltage $V_1$ applied at the input terminal will appear at the output terminal in the reduced magnitude $V_1/a$.
2. A current $I_1$ injected into its input terminal will exit from the output terminal magnified to $aI_1$.

The blackbox shall be regarded as a *mathematical* artifice rather than a physical device. It sometimes is referred to as an "ideal transformer."

The output variables $aI_1$ and $V_1/a$ are said to represent the current and voltage of winding 1 "referred to winding 2."

† If the Δ winding has the polarity shown in Fig. 5-2*b*, then, as explained by Fig. 5-3*b*, we introduce a phase shift of $-30°$. Change the polarity of the Δ winding and show that the phase shift now will be $+30°$.

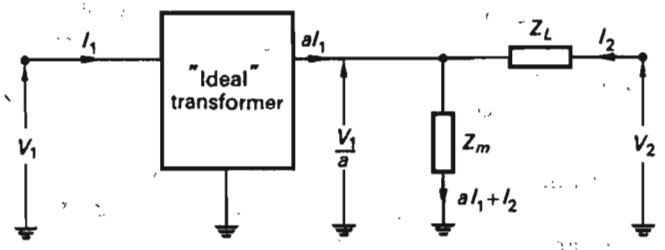


(*a*)

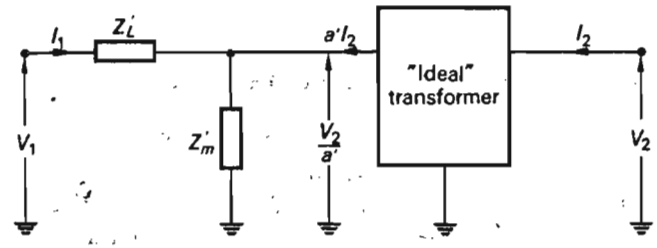


(*b*)

**Fig. 5-4** Equivalent transformer circuit. (*a*) Leakage and magnetizing impedances referred to secondary side. (*b*) Impedances now referred to primary side.

The impedances $Z_m$ and $Z_L$ are referred to as the "magnetizing" and "leakage" impedances, respectively. We have arbitrarily chosen to place the impedances on the right side of the ideal transformer, and we say that they have been "referred to winding 2." We could equally well have represented the transformer as shown in Fig. 5-4*b*. The parameters in Fig. 5-4*b* will, of course, not be equal to those in Fig. 5-4*a*.

We show now that with proper choice of the three parameters $a$, $Z_m$, and $Z_L$, the circuit in Fig. 5-4*a* obeys Eqs. (5-1), which is tantamount to saying that we have found an *equivalent circuit* for our transformer.

**Proof** For the circuit in Fig. 5-4*a* we can write

$$\frac{V_1}{a} = Z_m(aI_1 + I_2) \tag{5-2}$$

$$V_2 = Z_m(aI_1 + I_2) + Z_L I_2$$



We confirm readily that Eqs. (5-1) and (5-2) are identical if we choose the following values for our three parameters:†

$$a \triangleq \frac{R_1 + j\omega L_1}{j\omega M_{12}}$$

$$Z_m = -\frac{\omega^2 M_{12}^2}{R_1 + j\omega L_1} \tag{5-3}$$

$$Z_L = R_2 + j\omega L_2 + \frac{\omega^2 M_{12}^2}{R_1 + j\omega L_1}$$

### 5-2.2 APPROXIMATE EQUIVALENT CIRCUITS FOR YY-CONNECTED TRANSFORMERS

For the inductances $L_1$, $L_2$, and $M_{12}$, we have the formulas

$$L_1 = b\mu N_1^2$$

$$L_2 = b\mu N_2^2 \tag{5-4}$$

$$M_{12} = k\sqrt{L_1 L_2} = k\mu b N_1 N_2$$

where $N_1$ = primary-winding turns
$N_2$ = secondary-winding turns
$\mu$ = permeability for the core
$b$ = constant, depending upon core geometry
$k$ = leakage coefficient

$\mu$ being very high for the iron core, all three inductances are very large, and since, by design, we make the resistances small, we have

$$\omega L_1 \gg R_1 \tag{5-5}$$

$$\omega L_2 \gg R_2$$

If we make use of these inequalities, we obtain from Eqs. (5-3) the following approximate parameters for our equivalent circuit:

$$a \approx \frac{L_1}{M_{12}} = \frac{N_1}{kN_2}$$

$$Z_m \approx j\omega \frac{M_{12}^2}{L_1} = j\omega k^2 L_2 \tag{5-6}$$

$$Z_L \approx R_2 + \frac{R_1}{a^2} + j\omega L_2(1 - k^2) \triangleq R_L + jX_L$$

For a normal power transformer the leakage impedance is essentially reactive. Since, in addition, $k$ is very close to unity, we have the inequality

$$R_L \ll X_L \lll |Z_m| \tag{5-7}$$

† The easiest way to prove this statement is to substitute the parameter values defined by Eqs. (5-3) into Eqs. (5-2) and note that the equations become identical with Eqs. (5-1).

and

$$a \approx \frac{N_1}{N_2} = \text{phase voltage ratio} \tag{5-8}$$

In system studies it is customary, in view of Eq. (5-7), to set

$$|Z_m| = \infty$$

and thus obtain the simple equivalent circuit shown in Fig. 5-5. [Note that if we can also set $k = 1$ (exactly) and neglect the resistances, then the leakage impedance vanishes and our power transformer equivalent is *identical* with the "ideal" transformer.]

From Fig. 5-5 we conclude that

$$I_2 \approx -aI_1$$

In view of Eq. (5-8), we have for the currents

$$N_1 I_1 + N_2 I_2 \approx 0 \tag{5-9}$$

We also conclude from Fig. 5-5 that if we operate the transformer at no load (that is, $I_1 = I_2 = 0$), there is no voltage drop across $Z_L$, and we then have

$$V_2 = \frac{V_1}{a}$$

or

$$\frac{V_1}{V_2} = a \approx \frac{N_1}{N_2} \tag{5-10}$$

This means that the $a$ parameter is obtained most conveniently by means of an open-circuit test.

Should we prefer to express voltages and currents in per units of rated values, then the approximate equivalent diagram of Fig. 5-5 reduces to the one in Fig. 5-6. The reason that the "ideal transformer" disappears from the picture is that its input and output variables have equal values when expressed in per units.

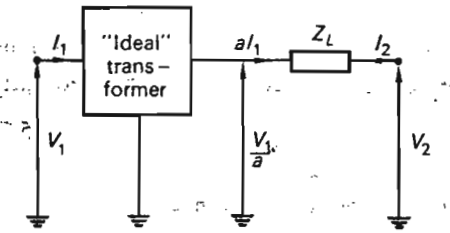


**Fig. 5-5** Approximate equivalent transformer circuit.



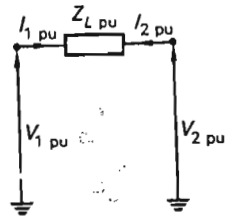


**Fig. 5-6** Equivalent circuit for YY-connected transformer. Voltages and impedance expressed in per units.

**Example 5-1** A single-phase unit of the three-phase bank shown in Fig. 5-1 has the following ratings:

200 MVA, 60 Hz

Primary voltage: $\frac{345}{\sqrt{3}}$ kV

Secondary voltage: $\frac{220}{\sqrt{3}}$ kV

To find the leakage impedance of the transformer, the low-voltage side is short-circuited and the high-voltage side is fed from a 60-Hz source. It is determined from test that in order to circulate a 100 percent short-circuit current in the windings, the source voltage must be increased to 21.3 kV. At this point the transformer consumes 703 kW in losses. From these data determine the transformer leakage impedance.

*Solution*

$$21.3 \text{ kV} = \frac{21.3}{345/\sqrt{3}} = 0.107 \quad \text{pu voltage}$$

Since the current is 1.00 pu, we obtain directly from Fig. 5-6, by short-circuiting the secondary,

$$|Z_L| = \frac{0.107}{1.00} = 0.107 \quad \text{pu}$$

The test voltage being only about 10 percent of rated voltage, the core losses can be completely neglected.† The measured loss represents, therefore, for all practical purposes, winding losses. Since the current is 1.00 pu, we thus have

$$R_L \times (1.00)^2 = \frac{0.703}{200}$$

Thus

$$R_L = 0.00352 \quad \text{pu}$$

We find, then, $X_L$:

$$X_L = \sqrt{(0.107)^2 - (0.00352)^2} \approx 0.107 \quad \text{pu}$$

† Because the flux is only about 10 percent of normal value.

The load ratio is thus

$$\frac{(\text{MVA})'}{(\text{MVA})''} = \frac{|Z_L''|}{|Z_L'|} \tag{5-14}$$

If the impedances are expressed in per units based upon respective MVA ratings, then we have

$$\frac{(\text{MVA})'}{(\text{MVA})''} = \frac{|Z_L''|}{|Z_L'|} = \frac{|Z_{\text{pu}}''|\,(V^2/|S_r''|)}{|Z_{\text{pu}}'|\,(V^2/|S_r'|)} = \frac{|S_r'|\,|Z_{\text{pu}}''|}{|S_r''|\,|Z_{\text{pu}}'|} \tag{5-15}$$

It is clearly desired that the transformers divide the load in the ratio $|S_r'|/|S_r''|$, and we conclude, therefore, that proper load division requires

$$|Z_{\text{pu}}'| = |Z_{\text{pu}}''| \tag{5-16}$$

If this impedance equality is not satisfied, one transformer is overloaded (which one?) and the other one underloaded when both of them together deliver the sum of their rated powers.

### 5-2.4 EQUIVALENTS

For many purposes, particularly load flow studies, it is convenient to represent a two-winding transformer with a $\pi$ equivalent of the type depicted in Fig. 5-9. For this circuit we obtain from inspection

$$I_1 = \frac{V_1 - V_2}{Z_\pi} + V_1 Y_1 = \left(\frac{1}{Z_\pi} + Y_1\right) V_1 - \frac{1}{Z_\pi} V_2$$
$$I_2 = -\frac{V_1 - V_2}{Z_\pi} + V_2 Y_2 = -\frac{1}{Z_\pi} V_1 + \left(\frac{1}{Z_\pi} + Y_2\right) V_2 \tag{5-17}$$

For the circuit in Fig. 5-5 we have

$$aI_1 = \frac{V_1/a - V_2}{Z_L}$$
$$I_2 = -aI_1 = -\frac{V_1/a - V_2}{Z_L} \tag{5-18}$$

The latter equations can be written

$$I_1 = \frac{1}{a^2 Z_L} V_1 - \frac{1}{aZ_L} V_2$$
$$I_2 = -\frac{1}{aZ_L} V_1 + \frac{1}{Z_L} V_2 \tag{5-19}$$

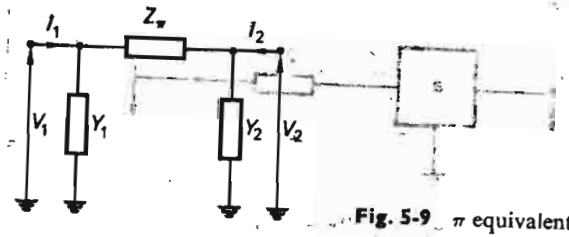


**Fig. 5-9** $\pi$ equivalent of transformer.



Clearly, Eqs. (5-17) and (5-19) can be made identical if we set

$$\frac{1}{Z_\pi} + Y_1 = \frac{1}{a^2 Z_L}$$
$$\frac{1}{Z_\pi} = \frac{1}{aZ_L}$$
$$\frac{1}{Z_\pi} + Y_2 = \frac{1}{Z_L} \tag{5-20}$$

We thus obtain for our $\pi$ parameters

$$Z_\pi = aZ_L$$
$$Y_1 = \frac{1}{Z_L}\frac{1-a}{a^2}$$
$$Y_2 = \frac{1}{Z_L}\frac{a-1}{a} = -aY_1 \tag{5-21}$$

In the foregoing equations the $a$ parameter may be complex, as would be the case if one of the windings were $\Delta$ type.

**Example 5-4** The three-phase transformer in Fig. 5-10*a* has the following ratings:

100 MVA, 60 Hz
220/138 kV (line to line)

One of the windings is $\Delta$ type, with the result that the low-side voltage ($V_2$) leads the high side by 30°. Since the voltage ratings tell the open-circuit voltage ratio, we get

$$a = \frac{220}{138} e^{-j30^\circ} = 1.60e^{-j30^\circ} = 1.38 - j0.798$$

From a short-circuit test of the type discussed in Example 5-1, we have determined the leakage impedance:

$$Z_L = j0.100 \quad \text{pu}$$

(The resistance is neglected.)

We express this impedance in ohms referred to the low side.

$$Z_L = j0.100 \times \frac{(138)^2}{100} = j19.1 \quad \Omega$$

The values for $a$ and $Z_L$ that we have thus computed are those of the circuit in Fig. 5-10*b*.

From Eqs. (5-21) we get directly

$$Z_\pi = aZ_L = (1.38 - j0.798)j19.1 = 15.2 + j26.3$$
$$Y_1 = \frac{1}{Z_L}\frac{1-a}{a^2} = \frac{1}{j19.1}\frac{1-(1.38-j0.798)}{(1.38-j0.798)^2} = 0.0183e^{-j55^\circ} \quad \text{℧}$$
$$Y_2 = -aY_1 = 0.0292e^{j95^\circ} \quad \text{℧}$$

These are the parameters of Fig. 5-10*c* expressed in ohms and mhos.

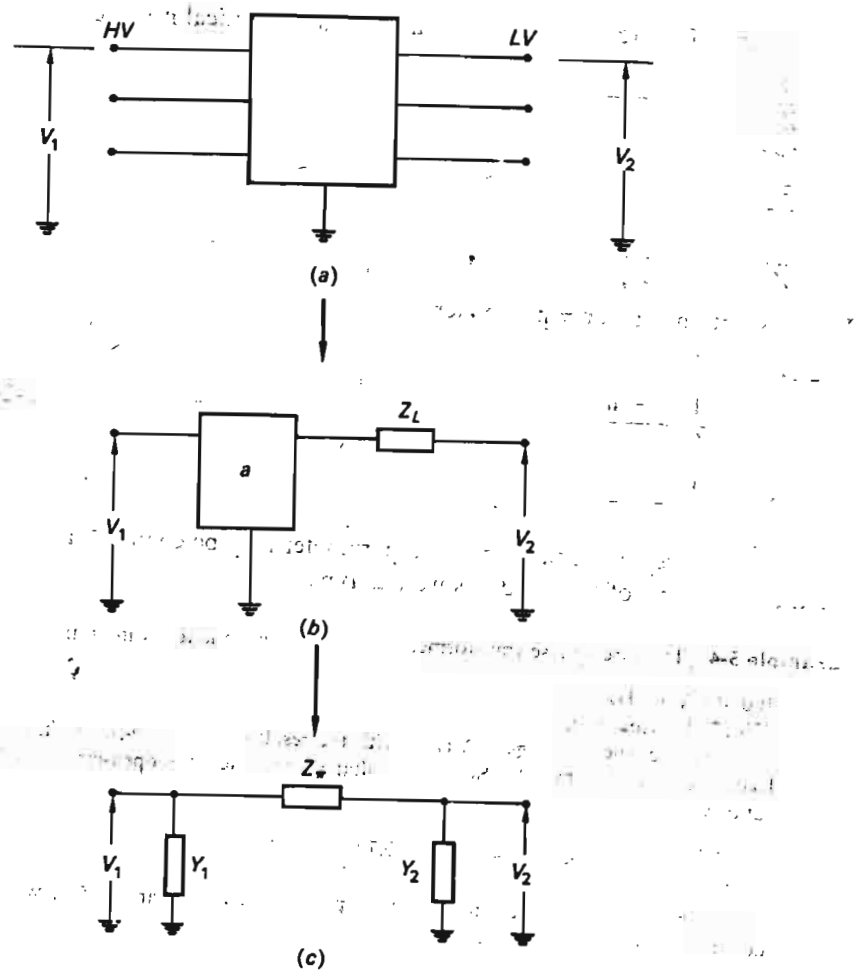


**Fig. 5-10** Two possible circuit representations of transformer in Example 5-4.

### 5-2.5 THE IMPEDANCE MATRIX OF A SYMMETRICALLY OPERATED THREE-PHASE TRANSFORMER

From the equivalent network in Fig. 5-5 we obtain for phases $a$, $b$ and $c$

$$\begin{aligned}
\frac{1}{a}V_1^a - aI_1^a Z_L &= V_2^a \\
\frac{1}{a}V_1^b - aI_1^b Z_L &= V_2^b \\
\frac{1}{a}V_1^c - aI_1^c Z_L &= V_2^c
\end{aligned} \qquad (5\text{-}22)$$



In vector form this equation can be written

$$\mathbf{V}_1' - \mathbf{Z}_L\mathbf{I}_1' = \mathbf{V}_2 \qquad (5\text{-}23)$$

Here we have defined the following vectors and matrix:

$$\mathbf{V}_1' \triangleq \frac{1}{a}\begin{bmatrix} V_1^a \\ V_1^b \\ V_1^c \end{bmatrix} \qquad \mathbf{I}_1' \triangleq a\begin{bmatrix} I_1^a \\ I_1^b \\ I_1^c \end{bmatrix} \qquad \mathbf{V}_2 \triangleq \begin{bmatrix} V_2^a \\ V_2^b \\ V_2^c \end{bmatrix}$$

$$\mathbf{Z}_L \triangleq \begin{bmatrix} Z_L & 0 & 0 \\ 0 & Z_L & 0 \\ 0 & 0 & Z_L \end{bmatrix} \qquad (5\text{-}24)$$

The vector $\mathbf{V}_2$ represents the secondary-phase voltage vector. The vectors $\mathbf{V}_1'$ and $\mathbf{I}_1'$ represent the primary phase voltage and current vectors *referred to the secondary*. The matrix $\mathbf{Z}_L$ is the leakage impedance matrix of the transformer. It is *diagonal*, indicating *noninteraction* between the phases. Compare the analogous situation for the symmetrically operated synchronous machine. [Compare Eqs. (4-77) and (4-78).]

## 5-3 EQUIVALENT CIRCUITS FOR MULTIWINDING TRANSFORMERS

It is common to design power transformers with more than two windings per phase. The different windings have different kilovolt and megavoltampere ratings and provide means for transforming power between more than two voltage levels. Also, a regular two-winding transformer is usually provided with a Δ-connected tertiary which, under normal balanced operation, is idle, but which, under unbalanced conditions, will carry so-called "zero-sequence currents." More will be said about such matters in Chap. 11.

Consider the $n$-winding transformer depicted in Fig. 5-11. The core represents phase $a$ of a three-phase arrangement. The $\nu$th winding obeys the following voltage equilibrium equation:

$$V_\nu = I_1 j\omega M_{1\nu} + I_2 j\omega M_{2\nu} + \cdots + I_\nu(R_\nu + j\omega L_\nu) + \cdots + I_n j\omega M_{\nu n} \qquad \text{for } \nu = 1, 2, \ldots, n \qquad (5\text{-}25)$$

It is easy in principle, although considerably more complicated in detail, to extend our previous two-winding analysis to the $n$-winding case. We shall limit ourselves to summarizing the results of such an analysis. Figure 5-12 depicts the equivalent network for a multiwinding transformer. Whereas the two-winding transformer is characterized by only one leakage impedance, the $n$-winding transformer has a total of $[n(n-1)]/2$ impedance elements connected between the $n$ terminals. The network in Fig. 5-12 refers

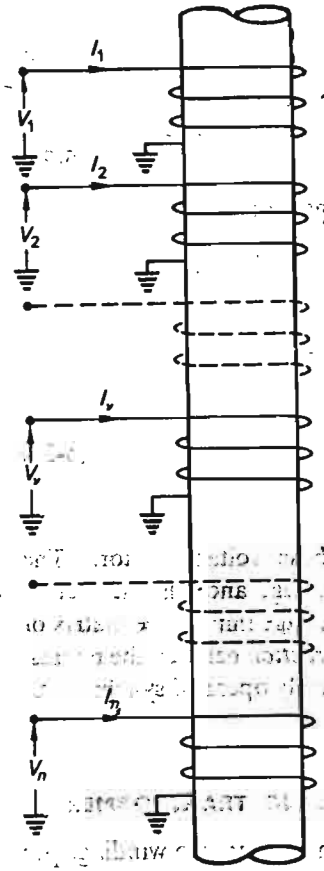


**Fig. 5-11** Multiwinding transformer.

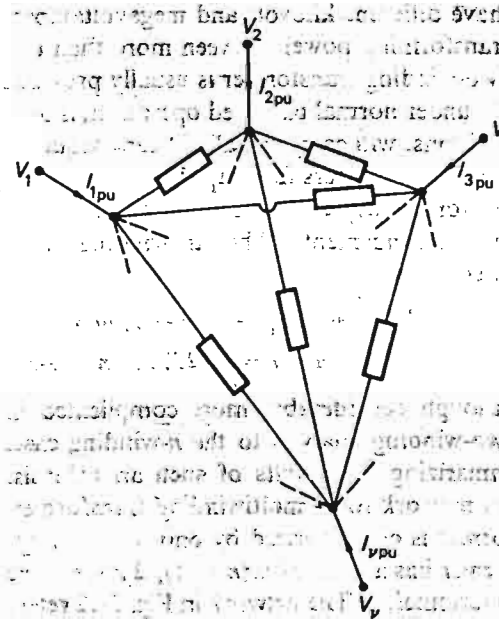


**Fig. 5-12** Equivalent circuit for multiwinding transformer.





to the case where all parameters and variables are expressed in per-unit values. If we wish to express voltages and currents in volts and amperes and/or if Δ windings are present, we must add "ideal transformers" to our network.

**Example 5-5** We shall construct a mathematical model for the practically important three-winding transformer depicted in Fig. 5-13*a*. It is equipped with Y-connected primaries (1) and secondaries (2) and a Δ-connected tertiary (3). We have in this case a total of $(3 \cdot 2)/2 = 3$ leakage impedances, as shown in Fig. 5-13*b*. In accordance with a well-known network theorem, we can replace the three impedances in Fig. 5-13*b* with the three "star-connected" impedances shown in Fig. 5-13*c*.† On the

† This *cannot* be done for $n > 3$.

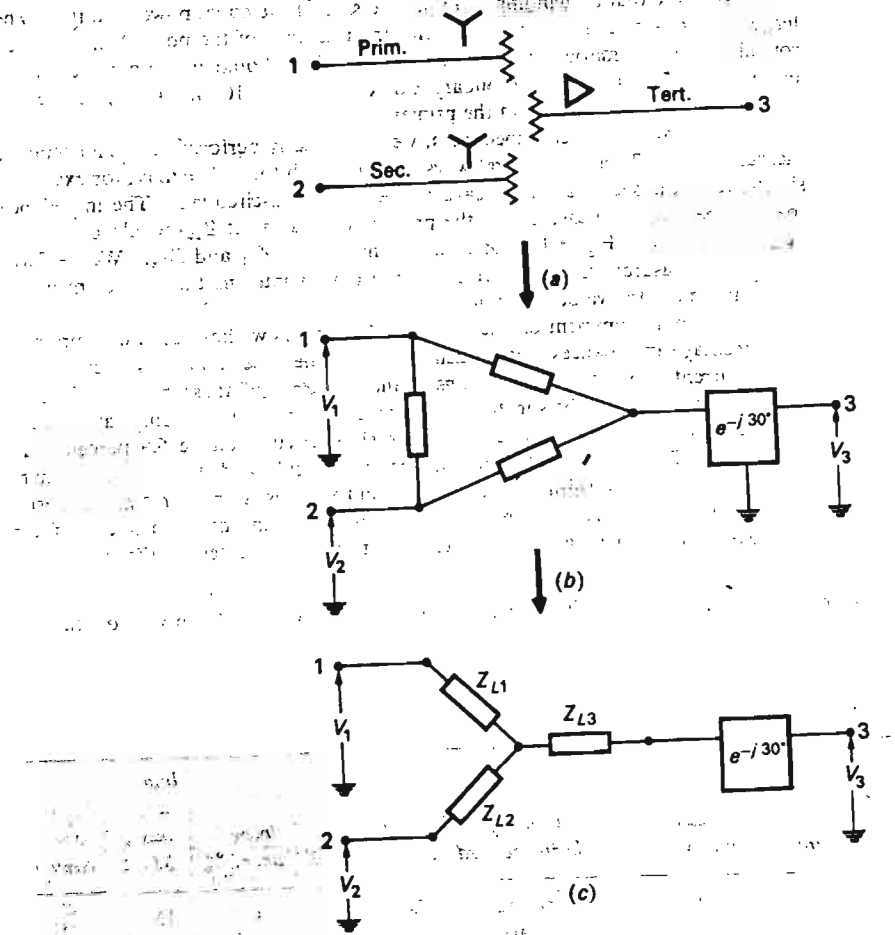


**Fig. 5-13** Three-winding transformer and its circuit equivalent.

**Table 5-1**

| *Winding* | *Rated voltage, line to line, kV* | *Rated megavoltamperes total three-phase* |
|---|---|---|
| Primary (1) | 14.85 | 15.0 |
| Secondary (2) | 66.0 | 15.0 |
| Tertiary (3) | 4.80 | 5.25 |

basis of experimentally obtained short-circuit data, we shall determine the leakage impedances $Z_{L1}$, $Z_{L2}$, and $Z_{L3}$. We shall neglect the resistive parts of all impedances, and furthermore express them in percentage values.

The winding data are obtained from Table 5-1.

We note that all windings do not necessarily have equal power ratings. The tertiary, in this case, is designed for only about a third of the power† that may be routed via the primaries and the secondaries. We should also note that if the tertiary is full-loaded, the secondary can deliver only 10 MVA; any increased secondary load would overload the primary.

To obtain the three impedances, we must clearly perform three independent measurements. There are several ways to accomplish this. We may, for example, short-circuit the secondary and leave the tertiary open-circuited. The impedance that we then would measure into the primary (let us call it $Z_{12}$) would obviously, in accordance with Fig. 5-13*c*, be equal to the sum of $Z_{L1}$ and $Z_{L2}$. We perform three such measurements, measuring the impedances into the three different windings, and obtain the values given in Table 5-2.

We should comment on the different MVA bases we have used in expressing the percentage impedances. In measurement 1, when the tertiary is open, short-circuit currents flow only in windings 1 and 2. *Both* of these have a 15-MVA rating, and we increase the short-circuit voltage until both the windings are current full-loaded, at which point we measure the short-circuit voltage 6.9 percent. In measurement 2, clearly, the tertiary will be current full-loaded when the primary carries only about one-third of rated current, but we must stop at this point (corresponding to 5.25 MVA) and read a short-circuit voltage of 5.6 percent of the lower base. The same argument applies to the third measurement. *We must, later,*

† Which physically means that its copper weight is only about a third of that of the two other windings. Why?

**Table 5-2**

| *Measurement* | *Impedance measured into winding* | *Winding short-circuited* | *Winding open-circuited* | *Impedance, %* | *Impedance base, MVA* | *Impedance symbol* |
|---|---|---|---|---|---|---|
| 1 | Primary | Secondary | Tertiary | 6.9 | 15 | $Z_{12}$ |
| 2 | Primary | Tertiary | Secondary | 5.6 | 5.25 | $Z_{13}$ |
| 3 | Secondary | Tertiary | Primary | 3.8 | 5.25 | $Z_{23}$ |



*remember that the percentage impedances refer to different MVA bases*, and in our equivalent diagram we are about to develop, we must refer the impedances to *one common* base.

From the equivalent diagram we obtain now the following equations between the leakage impedances $Z_{L1}$, $Z_{L2}$, and $Z_{L3}$ and the measured impedances $Z_{12}$, $Z_{13}$, and $Z_{23}$:

$$\begin{aligned} Z_{L1} + Z_{L2} &= Z_{12} \\ Z_{L1} + Z_{L3} &= Z_{13} \\ Z_{L2} + Z_{L3} &= Z_{23} \end{aligned} \tag{5-26}$$

From Eqs. (5-26) we readily solve

$$\begin{aligned} Z_{L1} &= \tfrac{1}{2}(Z_{12} + Z_{13} - Z_{23}) \\ Z_{L2} &= \tfrac{1}{2}(Z_{12} + Z_{23} - Z_{13}) \\ Z_{L3} &= \tfrac{1}{2}(Z_{13} + Z_{23} - Z_{12}) \end{aligned} \tag{5-27}$$

Introducing numerical values and referring all impedance values to the common base 15 MVA, we get

$$Z_{L1} = \tfrac{1}{2}\left(j6.9 + j5.6 \times \frac{15.0}{5.25} - j3.8 \times \frac{15.0}{5.25}\right) = j6.02\%$$

$$Z_{L2} = \tfrac{1}{2}\left(j6.9 + j3.8 \times \frac{15.0}{5.25} - j5.6 \times \frac{15.0}{5.25}\right) = j0.88\%$$

$$Z_{L3} = \tfrac{1}{2}\left(j5.6 \times \frac{15.0}{5.25} + j3.8 \times \frac{15.0}{5.25} - j6.9\right) = j9.97\%$$

This completes the example. Note that the tertiary branch contains an ideal transformer having a complex ratio $a$ characterized by

$$|a| = 1$$
$$\angle a = -30°$$

This transformer accounts for the fact that the tertiary phase-to-ground voltages lead the phase voltages of the two other windings by 30°.

**Example 5-6** The transformer in Example 5-5 acts as shown in Fig. 5-14, as a connecting link between three buses in a substation. Another 30-MVA transformer is also connected between the 66.0- and 14.85-kV buses. Energy is fed from the 66-kV bus to the two other buses. The 66-kV bus can, for practical purposes, be considered "infinite."† Assume that a symmetric solid three-phase short circuit occurs on the 4.8-kV bus. Find the short-circuit current fed to the faulted bus

† We talk in power lingo of an *infinite bus*. Such a bus will maintain a 100 percent voltage *independently of how much current we drain from it*. In other words, it is assumed to be connected to a perfect, i.e., impedanceless, voltage source. No physical network bus is, of course, that strong. There is a great need in EESE to know just how strong a bus really is. This information has important bearing upon the magnitude of fault currents that the system will experience in that particular locality, and thus is determining for the dimension of bus bars, circuit breakers, switches, etc. The so-called *short-circuit capacity* (SCC) is a measure of the strength of a bus. We shall return to this concept later, in Chap. 10, in connection with network fault studies.

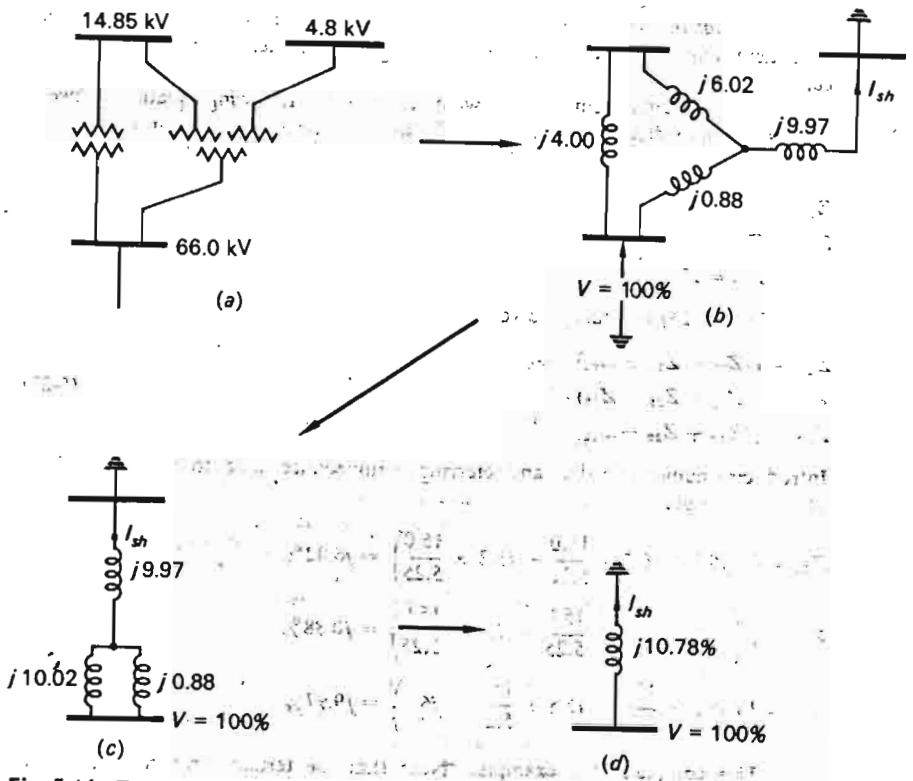


**Fig. 5-14** Example system—reduction of equivalent circuit.

from the tertiary winding. We assume that the 30-MVA transformer has an impedance of $j8.00$ percent, based on its own rating.

If all impedances are based on 15 MVA, the equivalent network will be the one shown in Fig. 5-14*b*. We have reduced this network in two self-explanatory steps to the one in Fig. 5-14*d*. From this latter network we compute the short-circuit current

$$|I_{sh}| = \frac{100}{10.78} = 9.26 \text{ pu}$$

This current value is based on 15 MVA. In terms of the rated megavoltamperes of the tertiary, we have

$$|I_{sh}| = 9.26 \times \frac{15}{5.25} = 26.4 \text{ pu}$$

In other words, the short-circuit current is 26.4 times the rated value. This example demonstrates a conflicting feature of transformer impedances:

From a voltage-drop point of view, we wish the impedances to be small.

From a short-circuit point of view, we would like them to be large.



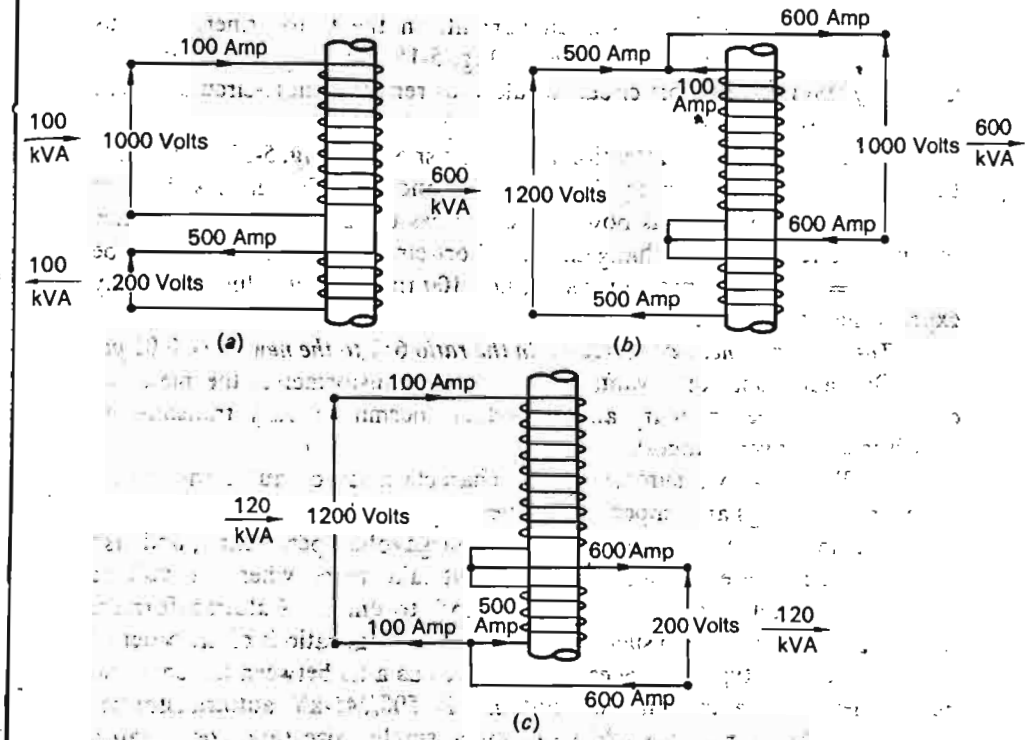


**Fig. 5-15** Autotransformer connections.

## 5-4 AUTOTRANSFORMERS

Consider the two-winding single-phase transformer depicted in Fig. 5-15*a*. It has a power rating of 100 kVA and a voltage rating of 1000/200 V. The rated currents are thus 100 and 500 A in the high-voltage and low-voltage windings, respectively, as indicated in the figure. Let us now interconnect the windings as shown in Fig. 5-15*b* and *c*. *Without changing the voltage per turn, and thus the core flux*, we obviously have now obtained a 1200-V winding.

We can then designate the former 1000-V terminals as our "secondaries" and thus obtain a 1200/1000-V *autotransformer*, or we can use the former 200-V terminals for the same purpose and obtain a 1200/200-V autotransformer. In either case we can load these new terminals with maximum 600 A and still limit the coil currents to their rated values, as shown in Fig. 5-15*b* and *c*. *Without increasing the core and copper losses, and thus not overloading the transformer, we have in effect increased its rating to* 600 *and* 120 *kVA, respectively, i.e., with* 600 *and* 20 *percent, respectively.*

This substantial gain in power rating is bought at a price. To appreciate this let us study the effect that the interconnection of windings has had

on the impedance and short-circuit currents in the transformer. Let us assume that the original transformer in Fig. 5-15*a* has a typical impedance value of $j0.06$ pu. A short circuit would thus render a short-circuit current of $1/0.06 = 16.7$ pu.

Let us then turn our attention to the case shown in Fig. 5-15*b*. Assume that a short-circuit occurs on the 1000-V secondary. This means that the primary voltage, 1200 V, is now applied across the 200-V winding. Since the impedance has not changed, the short-circuit current will now be $1200/200 = 6$ times its previous value, i.e., 100 times rated value. We may express the situation thus:

*The pu impedance has decreased in the ratio* 6:1 *to the new value* 0.01 *pu.*

One additional disadvantage of the autotransformer is the metallic† connection between primary and secondary (permitting easy transmission of disturbance overvoltages).

In Table 5-3 we summarize the characteristics of autotransformers in regard to ratings and impedance values.

We note that the greatest increase in megavoltampere rating, and also the greatest increase in short-circuit current take place when the voltage ratio of the resulting autotransformer is close to unity. Autotransformers are used with advantage in such cases when the voltage ratio is of the order of 2:1 or lower. A typical application would be as a tie between the 550- and 345-kV levels of a transmission system. A 500/345-kV autotransformer with a 1000-MVA rating would be of much smaller size (and cost) than a two-winding transformer of equal ratings.

† It is this metallic connection that explains the increased power rating of the autotransformer. As the reader probably has already realized, we do not really increase the *power transformation ability* of a transformer by connecting it "auto." For example, when we increased the *rating* from 100 to 600 kVA in the above example, the autotransformer is actually only *transforming* 100 kVA (i.e., the old value). $600 - 100 = 500$ kVA is simply passing the transformer untransformed.

**Table 5-3**

| *Transformer type* | *MVA rating* | *Voltage ratio* | *Impedance in per units of ratings* |
|---|---|---|---|
| Two-winding type | $\lvert S_r \rvert$ | $a$:1 | $Z_L$ |
| Autotransformer, case I | $(a+1)\lvert S_r \rvert$ | $\frac{a+1}{a}:1$ | $\frac{1}{1+a}Z_L$ |
| Autotransformer, case II | $\frac{a+1}{a}\lvert S_r \rvert$ | $(a+1)$:1 | $\frac{a}{1+a}Z_L$ |



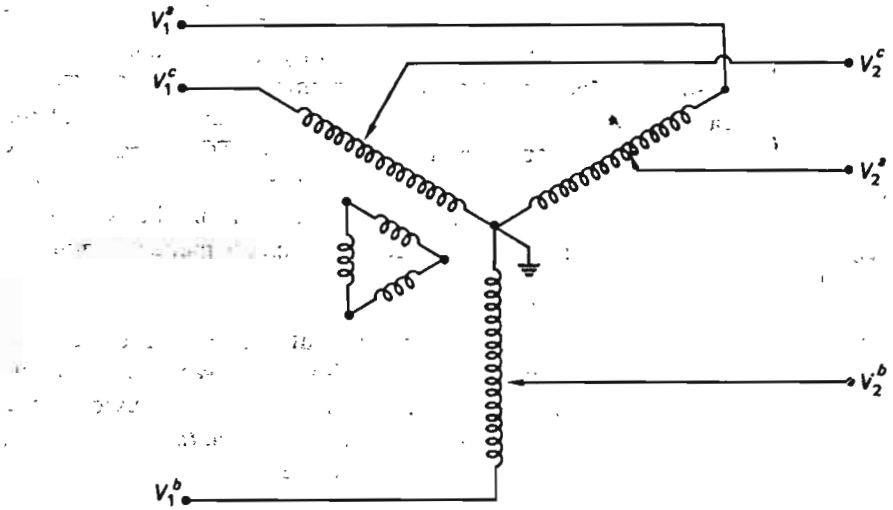


**Fig. 5-16** Three-phase autotransformer.

All the foregoing discussions have referred to single-phase transformers. They can be directly applied to the per-phase situation in three-phase systems. Figure 5-16 shows the winding connections for the most common three-phase arrangement. Usually, a Δ-connected tertiary is added which will be idle under normal balanced operation but gets into operation in unbalanced fault and loading situations (Chap. 11).

## 5-5 THE TRANSFORMER AS A CONTROL DEVICE

### 5-5.1 TCUL TRANSFORMERS

Transforming energy between different voltage levels is the primary job of a power transformer. Practically every transformer is provided with taps for ratio control, and is thus equipped to perform a secondary duty, i.e., controlling the secondary voltage level. On most transformers these taps can be changed only in deenergized state. In many instances this ratio control can be performed by *tap changing under load* (TCUL).

We recall from our discussions in Chap. 3 that, due to the changing load flow, the voltage profile of the transmission network tends to vary slowly throughout the day, dropping during peak load hours and rising during night hours. It is theoretically possible, of course, to maintain the level perfectly constant by providing every bus of the transmission system with controllable $Q$ sources. However, this is neither a practical nor an economical approach, and as a result the transmission voltage profile will vary within certain tolerable limits. TCUL transformers make it possible to maintain a constant

voltage level on important subtransmission- and distribution-level buses, in spite of fluctuations in the voltage level of the transmission system.

For example, a 5 percent drop of the primary voltage of a TCUL transformer can be completely compensated by a 5 percent decrease of the transformation ratio. The tap-changing equipment of TCUL transformers is usually motor-operated, and by letting the motors be commanded from voltage sensors, we can provide closed loop control of the secondary voltage level. A less sophisticated arrangement employs manual command.

### 5-5.2 REGULATING TRANSFORMERS

Regular ratio control, as discussed, is a feature that can be incorporated into any transformer, including distribution transformers. We now turn our attention to a type of transformer which is almost exclusively used on the transmission levels of our systems, the so-called *regulating*, or *control*, transformer. The primary job of these transformers is not to transform a

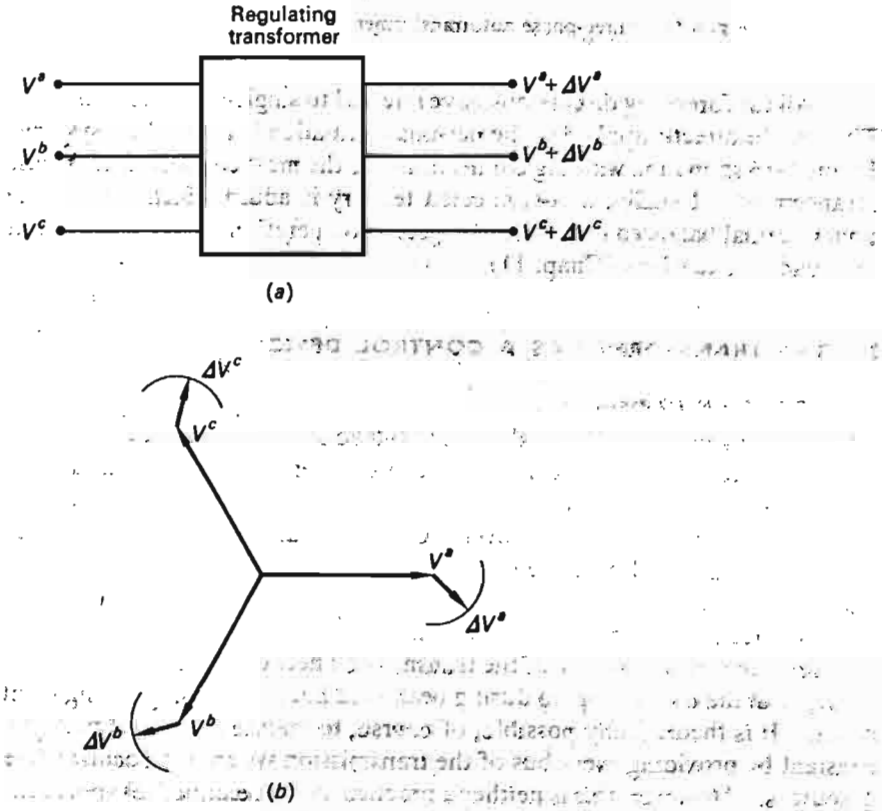


**Fig. 5-17** A three-phase control transformer adds a voltage increment to the system.



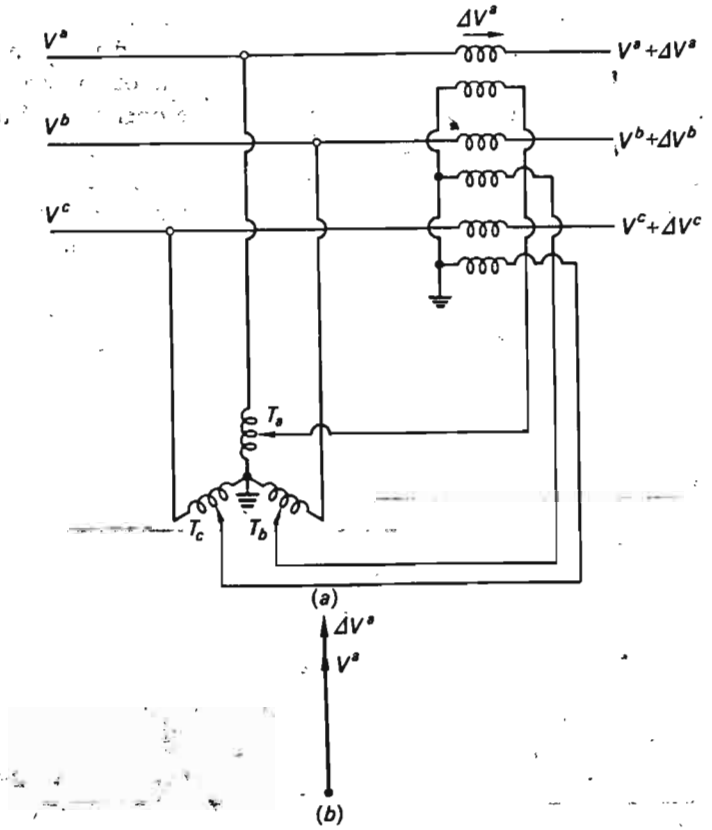


**Fig. 5-18** Regulating transformer for voltage magnitude control.

large amount of energy. Indeed, their megavoltampere ratings are often quite limited. The primary function of these devices is to change, by usually a *small* amount, the voltage in a point of the system, as shown in Fig. 5-17. The voltage change $\Delta V$, introduced by these devices, can in general be changed in both magnitude and phase.

As we shall see, the added voltage $\Delta V$, although of small magnitude, will have a drastic effect on the *load flow* in the link in question. *Regulating transformers are therefore in effect means for controlling the load flow in our system.*

Before we prove this statement, let us present some typical examples on regulating transformers.

**Regulating transformer for voltage magnitude control** There are a number of different schemes by means of which it is possible to obtain *magnitude* control of the added voltage $\Delta V$. Figure 5-18*a* depicts one

common arrangement. From a three-phase autotransformer (*exciting transformer*) an adjustable voltage is picked off and used as a primary voltage in a series transformer which is placed at the point in our network where we wish to add the voltage $\Delta V$. To comprehend the operation of the device, consider phase $a$ of the system. The voltage picked off by means of the tap changer $T_a$ is obviously in phase with $V^a$. Therefore the series transformer in phase $a$ must add a voltage $\Delta V^a$ to $V$ which is in phase with $V^a$ itself, illustrated by the phasor diagram in Fig. 5-18*b*. The magnitude $|\Delta V|$ is obviously dependent upon the tap changer position.

We shall confirm later that the effect of this type of regulating transformer is to control the flow of *reactive* power in the link in question.

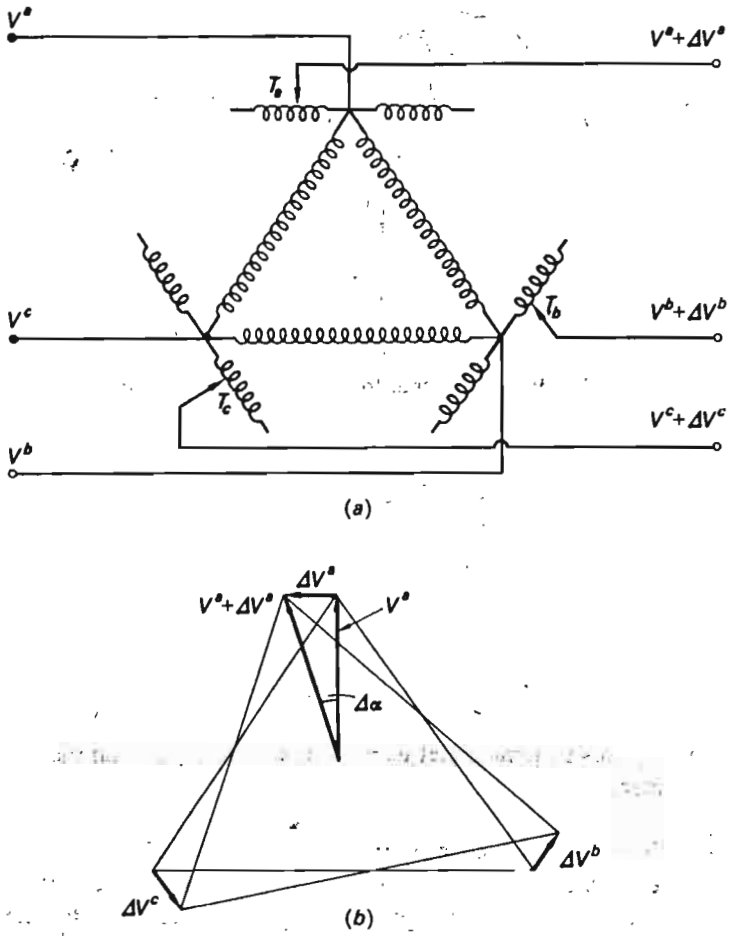


**Fig. 5-19** Regulating transformer for voltage phase angle control.



**Regulating transformer for voltage phase angle control** If the added voltage $\Delta V$ has a phase of $\pm 90°$ relative to the system voltage $V$, then the effect of the added voltage is to change the phase angle of the system voltage, as depicted in the phasor diagram of Fig. 5-19*b*. A possible arrangement to accomplish this type of control is shown in Fig. 5-19*a*. The operation of the device should be self-explanatory. The associated phasor diagram indicates that the phase angle adjustment $\Delta\alpha$ is approximately proportional to the magnitude of the added regulator voltage $\Delta V$. The approximation is better, the smaller the adjustments we work with. It is also easily confirmed from the geometry of the phasor diagram that, for small angular adjustments, the arrangement leaves the voltage magnitude practically unaffected. Later examples will confirm that this type of device will control the *real power* flow in the line.

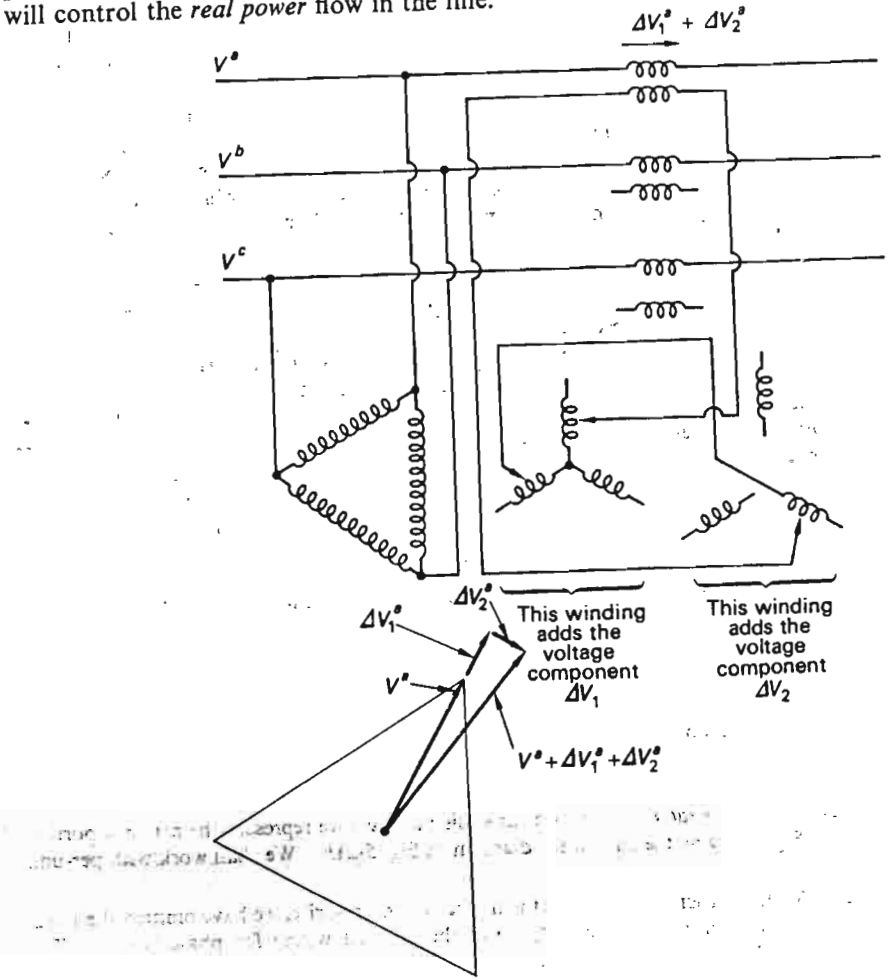


**Fig. 5-20** Regulating transformer for voltage magnitude and phase angle control.

**Regulating transformer for independent magnitude and phase angle control** In many instances it becomes necessary to exert independent control of voltage magnitude and phase angle. The regulating transformer shown in Fig. 5-20 permits us to adjust these two variables separately.† The exciting transformer is equipped with two sets of secondaries. It is easy to confirm that the voltage component picked off from the one set of secondaries, $\Delta V_1$, is in phase with the system phase voltage $V$, and the voltage component $\Delta V_2$, obtained from the second set, is 90° out of phase with $V$. By adjusting the magnitude of $\Delta V_1$, we thus have magnitude control, whereas adjustment of $\Delta V_2$ provides phase angle control.

**Example 5-7** We shall work in detail a simple example on power flow control by means of voltage regulation. The example should demonstrate some of the results that can be achieved by relatively simple means. A more exhaustive treatment of the general topic of load flow analysis and control will have to be postponed to Chap. 7, when we have developed more systematic techniques for power network analysis.

Consider the network portion depicted in Fig. 5-21*a*. Two transformers, designated 1 and 2, are operated in parallel and transforming power between an 11-kV generator bus and a 60-kV substation bus, from which a load of $S_L = 80$ MW $+ j60$ Mvar must be supplied. The 60-kV bus must be kept at 60.0 kV exactly.

The two transformers, both YY-connected, have identical megavoltampere ratings of 50 MVA each, and their voltage ratings, 11/60 kV, are of course also equal.

The load corresponds to $\sqrt{(80)^2 + (60)^2} = 100$ MVA, and it would therefore seem feasible for the transformers mutually to supply it. However, there is a complication: the two transformers have different impedances, $j6$ and $j8$ percent, respectively, and in accordance with Example 5-3 [Eq. (5-15)], they will therefore *not* divide their loads in the proper ratio 1:1. Transformer 1 will, in effect, be overloaded; the other one, underloaded. We wish to see to what extent we can improve the load division by manipulation of the transformer ratios. Each transformer ratio can be varied from 95 to 105 percent of the nominal value‡ in discrete steps of 0.5 percent. Clearly, this ratio change will provide us with voltage *magnitude* control only, which of course right away puts constraints on us.

We approach this problem in the following manner:

1. We determine the load division with no corrective action taken.
2. We make appropriate tap changes, within the limits given, and investigate the effects on the load division.

*Load division before ratio change* For analysis purposes we represent the network portion in Fig. 5-21*a* by the equivalent diagram in Fig. 5-21*b*. We shall work with per-unit

† In Fig. 5-20, in order not to clutter the diagram unnecessarily, we have omitted the interconnections for phases *b* and *c* and shown the detailed wiring for phase *a* only. The student should complete the diagram.

‡ Nominal ratio is $a = 11.0/60.0$.



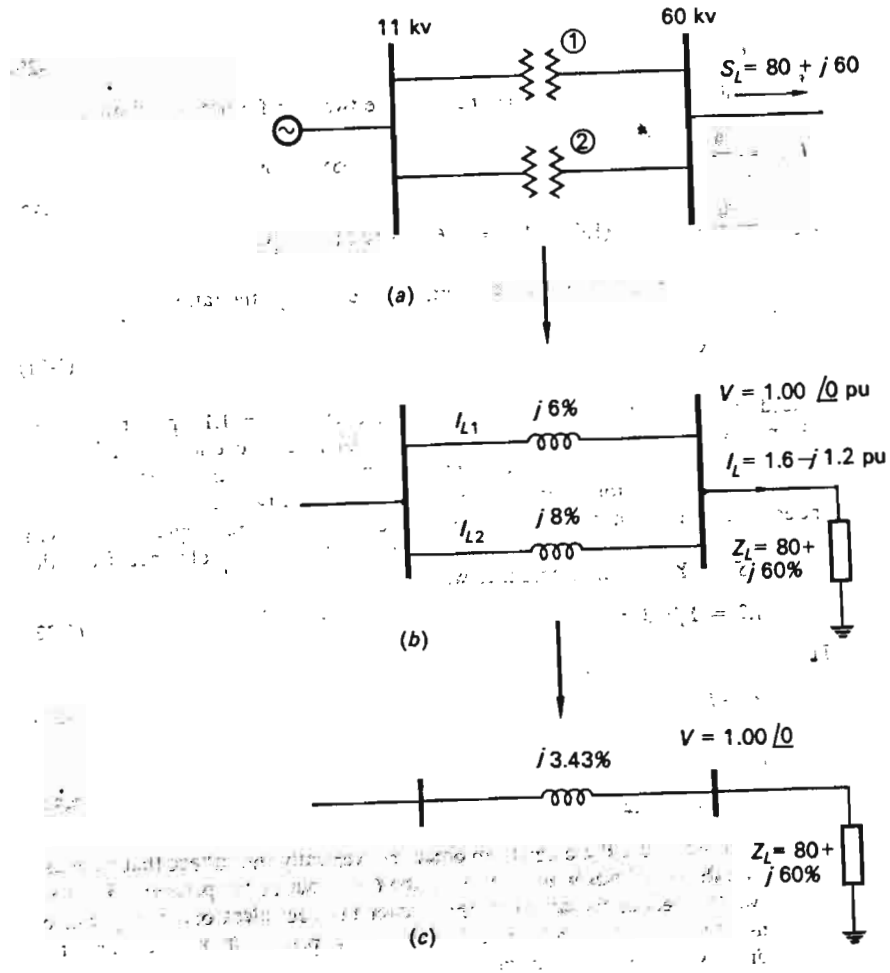


**Fig. 5-21** Two parallel-working transformers.

(or percentage) values and settle first for the following base values:
Power base = 50 MVA
Voltage base = 60 kV
(The 60-kV bus voltage is also chosen as our reference phasor.)

The actual load is therefore

$$S_L = \frac{80}{50} + j\frac{60}{50} = 1.6 + j1.2 \quad \text{pu}$$

and since the 60-kV bus is held at 100 percent voltage, the corresponding load current is calculated from the formula $S_L = VI_L^*$, as follows:

$$1.6 + j1.2 = 1.0I_L^* \tag{5-28}$$

Hence

$$I_L = 1.6 - j1.2 \quad \text{pu} \tag{5-29}$$

This load current is divided between the two transformers as follows:

$$I_{L1} = \frac{j8}{j6 + j8} I_L = \tfrac{8}{14}(1.6 - j1.2) = 0.914 - j0.685 \quad \text{pu}$$
$$I_{L2} = \frac{j6}{j6 + j8} I_L = \tfrac{6}{14}(1.6 - j1.2) = 0.686 - j0.515 \quad \text{pu} \tag{5-30}$$

The two transformer load currents have, evidently, the ratio

$$\frac{|I_{L2}|}{|I_{L1}|} = \frac{6}{8} = 0.75 \tag{5-31}$$

instead of the desired ratio 1.00. Actually, since $|I_{L1}| = 1.14$ pu and $|I_{L2}| = 0.86$ pu, we note that transformer 1 would be 14 percent overloaded, and transformer 2, 14 percent underloaded. This is an intolerable situation, and we now set out to correct it. Before doing so, we wish to point out two additional features in the equivalent diagram in Fig. 5-21*b*. First, we note that we may represent the given load by a load impedance $Z_L$ (or admittance $Y_L$) that may be obtained from the formula $S_L = Y_L^* |V|^2$ in accordance with

$$1.6 + j1.2 = Y_L^*(1.0)^2 \tag{5-32}$$

Thus

$$Y_L = 1.6 - j1.2 \tag{5-33}$$

or

$$Z_L = \frac{1}{Y_L} = \frac{1}{1.6 - j1.2} = 0.8 + j0.6 \quad \text{pu} \tag{5-34}$$

We may also use the diagram to obtain conveniently the voltage that we must maintain on the 11-kV bus in order to keep the 60-kV bus at 100 percent. For this purpose we first reduce the circuit to the simpler but equivalent one of Fig. 5-21*c*. The transformers are now represented by the 3.43 percent impedance, and the voltage drop $\Delta V$ across this impedance amounts to

$$\Delta V = j0.0343(1.6 - j1.2) = 0.041 + j0.055 \quad \text{pu} \tag{5-35}$$

The 11-kV bus must thus be kept at the voltage

$$1.00 + j0 + 0.041 + j0.055 = 1.041 + j0.055 \quad \text{pu} \tag{5-36}$$

or at the voltage level

$$|1.041 + j0.055| = 1.041 \text{ pu (or 104.1 percent)}$$

Expressed in kilovolts, this amounts to

$$1.041 \times 11.0 = 11.45 \text{ kV}$$

*Effects of ratio change* We will now make an analysis of the effects of adjusting the transformer ratios. What we will be doing, in effect, is *deliberately* to make the ratios of the two transformers different. This results in a *circulating current* in the



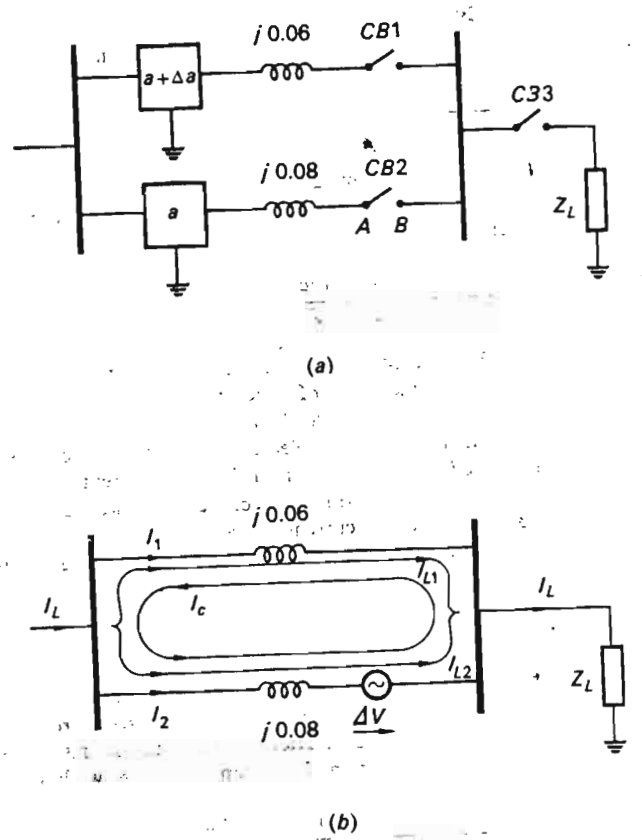


**Fig. 5-22** Equivalent circuit of system of Fig. 5-21.

transformers, a current that will be present should even the common load be disconnected. To explain this fact let us refer to the equivalent diagram in Fig. 5-22*a*. We have here included two ideal transformers, one of which (transformer 2) has the nominal transformation ratio $a = 11.0/60.0$, and the other one the same ratio plus an adjustment $\Delta a$.

We have also included the individual transformer circuit breakers *CB*1 and *CB*2, and also the load breaker *CB*3. With *CB*3 open, we now first parallel-connect the two transformers by closing *CB*1 and *CB*2. If we first close *CB*1, *there will be a potential difference across CB*2 *of* $\Delta V$ *volts*, the magnitude of which we find as follows:

$$\Delta V \triangleq V_A - V_B = \frac{V_1}{a} - \frac{V_1}{a + \Delta a} \approx \frac{V_1}{a}\frac{\Delta a}{a}$$

If we express $\Delta V$ in pu of our voltage base, we get

$$\Delta V \approx V_1 \frac{\Delta a}{a} \tag{5-37}$$

where $V_1$ (i.e., the voltage of the 11-kV bus) must be expressed in pu.

By invoking the well-known Thévenin's circuit theorem,† we know that when we close *CB*2, we obtain a current $I_C$ through the breaker that equals

$$I_C = \frac{\Delta V}{Z_{loop}}$$

where $Z_{loop}$ is the impedance as viewed into the network from the breaker terminals. This impedance obviously equals the sum of the transformer impedances, and we therefore get

$$I_C = \frac{\Delta V}{Z_1 + Z_2} \approx \frac{V_1 \, \Delta a/a}{Z_1 + Z_2} \tag{5-38}$$

We evidently obtain a current $I_C$ that circulates through the two transformers (Fig. 5-22*b*), the value of which is equivalent to what would be the case had we placed an emf $= \Delta V$ into the loop.

Having thus paralleled the transformers, we close, next, the load circuit via breaker *CB*3, which gives rise to the load current $I_L$ found earlier [Eq. (5-29)]. As before, this current will divide between the two transformers, as expressed by Eqs. (5-30), into the two currents $I_{L1}$ and $I_{L2}$. Upon using the superposition theorem, we conclude that the transformer currents in the new state equal

$$\begin{aligned} I_1 &= I_{L1} - I_C \\ I_2 &= I_{L2} + I_C \end{aligned} \tag{5-39}$$

*We note that, since we can control $I_C$ within certain limits, we may be able to arrange it so that these new transformer currents result in a better loading of the transformers.* Before we attempt to accomplish this, let us look closer at the nature of the circulating current $I_C$. From Eq. (5-38) we have

$$I_C = \frac{\Delta V}{j0.06 + j0.08} = \frac{\Delta V}{j0.14} = \frac{V_1 \, \Delta a/a}{j0.14} \quad \text{pu} \tag{5-40}$$

The voltage differential $\Delta V$ is in phase with our reference voltage (= the phase voltage of the 60-kV bus) if $\Delta a > 0$. Should $\Delta a < 0$ then $\Delta V$ would be of opposite phase relative to our reference. From Eq. (5-40) we therefore conclude that the circulating current will be either 90° lagging our reference voltage or 90° leading, depending upon the ratio settings. Positive $\Delta a$ corresponds to lagging current.

In the current phasor diagram of Fig. 5-23, we have drawn to proper scale the currents $I_{L1}$ and $I_{L2}$ from Eqs. (5-30). The circle represents 1 pu current. A current phasor extending outside of this circle thus represents an *overloaded* transformer. By adding and subtracting the circulating current vector $I_C$ to $I_{L2}$ and from $I_{L1}$, respectively, in accordance with Eqs. (5-39), we find that the new currents $I_1$ and $I_2$ tend toward the circle from the outside and inside, respectively. By trial and error (or more sophisticated analysis if we wish), we find that if $|I_C|$ is chosen approximately equal to 0.25 pu, the currents $I_1$ and $I_2$ fall slightly outside (about 1 percent) the circle.‡ This slight overload is certainly acceptable in a practical situation, and we therefore settle for this solution.

† For a discussion of this theorem see Chap. 10.

‡ This case is shown in Fig. 5-23.



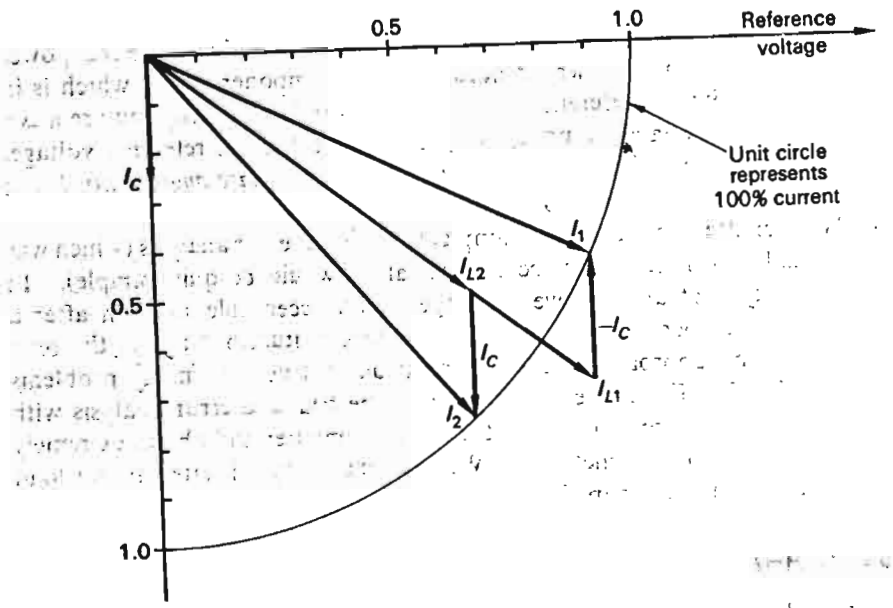


**Fig. 5-23** Phasor diagram depicting currents in circuit of Fig. 5-22.

We need $|I_C| = 0.25$ pu, and this means, in accordance with Eq. (5-40), that

$$\frac{V_1 \, \Delta a}{a} = 0.14 \times 0.25 \text{ pu}$$

As $V_1 = 1.041$, we therefore get

$$\frac{\Delta a}{a} = 0.0336 \text{ pu} \quad \text{or} \quad 3.36\%$$

As the adjustments can be made only in 0.5 percent steps, the proper thing to do is to *increase* the ratio of transformer 1 by 3.5 percent. A still better solution would be to increase it only by 2 percent and *reduce* the ratio of transformer 2 by 1.5 percent. This would give the same $\Delta V$ as before, but also result in a 60-kV bus voltage closer to the required 100 percent. Why?

Having completed our solution, we make a few important observations:

1. Since the phase angle of the circulating current $I_C$ is either $\pm 90°$, we can control only the *reactive component* of the transformer current. This is tantamount to saying that we can control only the *reactive* power flow; the *real* power flow is beyond our control. It is worthwhile to realize that the $\pm 90°$ phase angle was due to two assumptions:
   *a.* Purely reactive transformer impedances (which is generally a good assumption)
   *b.* Voltage *magnitude* control

2. If, in the above example, we would like to have control over the real power flow also, then we would need to add a component to $I_C$ which is in phase with our reference voltage. This would obviously require a $\Delta V$ component having a phase of $\pm 90°$ in respect to our reference voltage. *Such a component could clearly be obtained by phase angle control* (not available in the present case).
3. We submitted, in the above example, to trial-and-error analysis (which was really not necessary since *exact* analysis would be quite simple). In this type of analysis we converge on an acceptable solution after a finite number of trial solutions. In many situations this is the *only* workable approach, and this is particularly true with many problems in EESE. Fortunately, we can combine trial-and-error analysis with the computational ability of the digital computer and obtain extremely powerful analysis methods. We shall exemplify this later, in our load flow studies in Chap. 7.

## 5-6 SUMMARY

In this chapter we have exposed the essential features of the power transformer to the extent that this device concerns the systems engineer. We have followed the same philosophy as we applied in our discussion of synchronous machines; relatively unimportant design details have been left out of our story.

The systems engineer is particularly interested in simple models of the transformer, and we have presented those equivalent diagrams that are of particular value in subsequent systems studies.

The advantages and disadvantages of autotransformers have been pointed out. Considerable emphasis has been placed on the transformer as a control device. We have noted that phase-angle- and voltage-magnitude-regulating transformers can be used in controlling the routing of real and reactive power within the network. More will be said about this aspect of transformers in Chap. 7. Little emphasis has been placed on various types of transformer connections since this topic is of importance only under unbalanced loading conditions, which will be discussed in Chap. 11.

## EXERCISES

**5-1.** Consider the equivalent $\pi$ network in Fig. 5-10c. If the secondary terminals are open-circuited, the voltage $V_2$ is obtained simply by "voltage division":

$$V_2 = V_1 \frac{1/Y_2}{Z_x + 1/Y_2} = V_1 \frac{1}{1 + Z_x Y_2}$$

Use the parameter values computed in Example 5-4 and check the value for $V_2$ if we apply an input voltage of $V_1 = 220/\sqrt{3}$ kV. Note that you should obtain $V_2 = (138/\sqrt{3})e^{j30°}$.



**5-2.** A three-phase transformer has the ratings

100 kVA, 60 Hz
13,200/200 V

Explain what would happen if, by mistake, the transformer were to be used at rated voltage but at 50 Hz.

**5-3.** The transformer in Exercise 5-2 has impedance $0.0050 + j0.061$ pu. The core losses are found to be 340 W. (The simplest way to measure these is by an open-circuit test at 100 percent voltage. Why?)

(*a*) Compute the efficiency of this transformer if operated at 50 percent current load, rated voltage and frequency, and a load power factor of 0.8.

(*b*) Write a formula for the efficiency if the transformer is operated at $x$ percent current load and constant power factor.

(*c*) Prove that the efficiency reaches a maximum for a particular $x$ value. Compute this maximum value for the given transformer and power factor 0.8.

**5-4.** Consider the 100-kVA two-winding transformer depicted in Fig. 5-15*a*. We wish to connect it as an autotransformer. The two windings obviously can be connected together in four different ways, *only two of which are correct.*

Assume that we make the *wrong* connection. In the belief that we have a 1200/1000 V autotransformer, we connect our "autotransformer" to a 1200-V source.

(*a*) What voltage will we measure across the "1000-V" terminals?

(*b*) Explain the effect that our mistake will have on the device.

**5-5.** The U.S. Navy possesses a self-cooled transformer type, intended for use in arctic surroundings and having the hypothetical ratings

500 kVA, 60 Hz
1000/500 V

What will be the new ratings of this transformer if used in tropical climate with the same voltage as before but at 50 Hz? Work with the following assumptions:

1. In the new installation we tolerate only 80 percent of the total losses accepted in the arctic installation.
2. In the original installation the total losses amounted to 0.5 percent of rated power and were distributed as follows:

| | | |
|---|---|---|
| Copper losses | 1.25 kW | measured at 100% current. |
| Eddy current losses | 0.625 kW | measured at 100% voltage. |
| Hysteresis losses | 0.625 kW | measured at 100% voltage. |

3. The parameter $\kappa$ in Eq. (4-85) equals 1.6.

**5-6.** Assume that each of the three series transformers in Fig. 5-18 has a turns ratio of unity. The system voltage is 220 kV (line to line), and we wish to be able to boost this value by a maximum of 5 percent. The maximum line current is 1 kA per phase. Calculate the necessary ratings for the series and exciting transformers.

**5-7.** Refer to Example 5-6.

(*a*) How much of the computed short-circuit current will flow via the 30-MVA transformer?

(*b*) Will it be current-overloaded?

(*c*) We wish to decrease the short-circuit current in the tertiary winding from the computed value of 926 percent to not more than 400 percent by placing series reactors

between the 66-kV bus and the 66-kV winding of the three-winding transformer. Prove that this is not possible. Explain.

(*d*) Prove that the objective of part (*c*) can be achieved by adding series reactors to the high-voltage terminals of the 30-MVA transformer *also*.

(*e*) Assume that we insert six identical reactors in accordance with part (*d*). Compute the minimum reactance, expressed in ohms per reactor, needed to do the job.

**5-8.** Consider Example 5-7. Assume that we wish to divide the total load current into two equal currents

$$I_{L1} = I_{L2} = 0.8 - j0.6$$

by means of a regulating transformer (RT) placed as shown in Fig. 5-24. We assume we

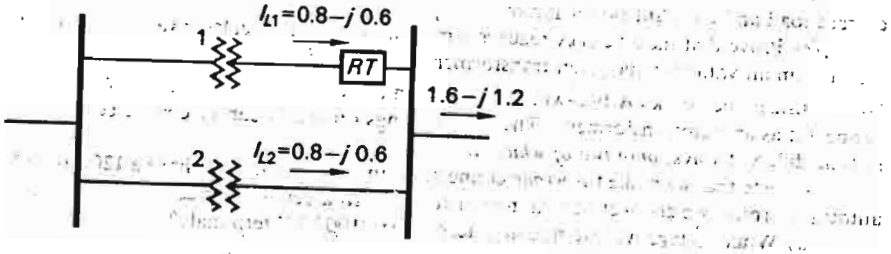


**Fig. 5-24** Load flow control by means of regulating transformer.

have available an RT of the type shown in Fig. 5-20. Compute the voltage components $\Delta V_1$ and $\Delta V_2$ needed to do the job.

Assume that the two 50-MVA transformers have equal voltage ratio = 11:60 kV and neglect the impedance of the RT.

**5-9.** For metering and relaying purposes one makes use of *current and potential transformers* (CT and PT, respectively) connected to the high-voltage bus, to be monitored as shown in Fig. 5-25. Answer the following questions in regard to these devices:

(*a*) If, as usual, we define the transformation ratio in accordance with Eq. (5-8),

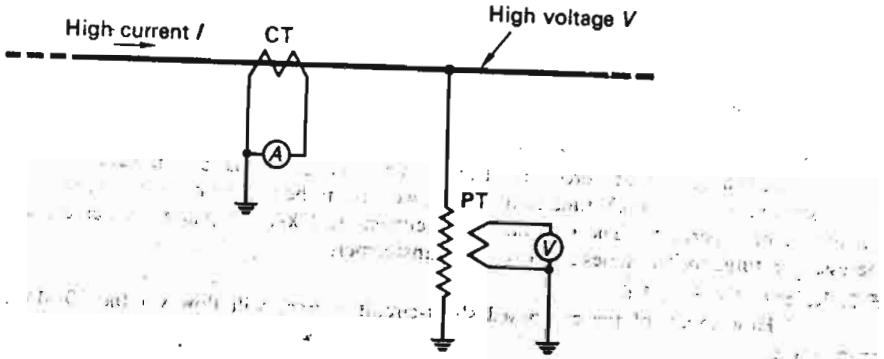


**Fig. 5-25** Typical connection of potential and current transformers.



why is it normally true that

$a \gg 1$ for a PT

$a \ll 1$ for a CT

(*b*) Why should one strive to load a CT with as small, and a PT with as large, an impedance as possible?

(*c*) If a CT is accidentally open-circuited, the device will be momentarily destroyed, due to excessive core losses. If a PT is accidentally short-circuited, it will be destroyed due to excessive copper losses. Explain.

**5-10.** A three-phase transformer of the core type depicted in Fig. 5-1*b* has a voltage rating of 11,000/220 V. Feed the middle phase of the HV winding from a *single-phase* 5-kV source.

(*a*) What voltages can be measured across the five remaining open-circuited windings?

(*b*) Prove that we can transform power between the above source and only one of the remaining five windings. Which are?

## REFERENCES


### Books

1. Blume, L. F., A. Boyajian, G. Camilli, T. C. Lennox, S. Minneci, and V. M. Montsinger: "Transformer Engineering," John Wiley & Sons, Inc., New York, 1951.
2. Connelly, F. C.: "Transformers," Sir Isaac Pitman & Sons, Ltd., London, 1950.
3. Staff members of M.I.T.: "Magnetic Circuits and Transformers," The Technology Press of the Massachusetts Institute of Technology, Cambridge, Mass., 1943.

### Technical papers and reports

4. Älgbrandt, A., et al.: Switching Surge Testing of Transformers, *IEEE Trans.*, vol. PAS-85, no. 1, pp. 54–61, January, 1966.
5. Alexander, G. W., and W. J. McNutt.: EHV Application of Autotransformers, *IEEE Trans.*, vol. PAS-86, no. 8, pp. 995–1000, August, 1967.
6. Whitman, L. C.: Transient Temperature Cooling of Transformers, *IEEE Trans.*, vol. PAS-86, no. 11, pp. 1293–1311, November, 1967.
7. Switching Surge Tests for Oil-insulated Power Transformers, IEEE Committee Report, *IEEE Trans.*, vol. PAS-86, no. 2, February, 1967.
8. Kurita, K.: Mechanical Strength of Transformer Windings under Short-circuit Conditions, *IEEE Trans.*, vol. PAS-88, no. 3, pp. 222–230, March, 1969.

# 6
# The High-energy Transmission Line

## 6-1 INTRODUCTION

The transmission lines constitute the arteries of the electric energy system. The availability of a well-developed, high-capacity system of transmission lines makes it technically and economically feasible to move large blocks of electric energy over large distances.

Historically, long high-voltage transmission lines were used for the transport of electric energy from remote hydroelectric stations. The pioneering efforts to develop *extra-high-voltage* (EHV) transmission lines were consequently made in countries (Sweden,† U.S.S.R., Canada) which depended heavily upon hydroelectric energy for their industrial development. The relative abundance of fossil fuels in the United States has made this country comparatively independent of the need for long-distance energy transmission. However, the economic and operational advantages that can be realized by the availability of a high-capacity transmission network have

† Sweden already operated successfully a 380-kV, 400-mile line in 1952. The designation EHV usually refers to voltages in excess of 230 kV.





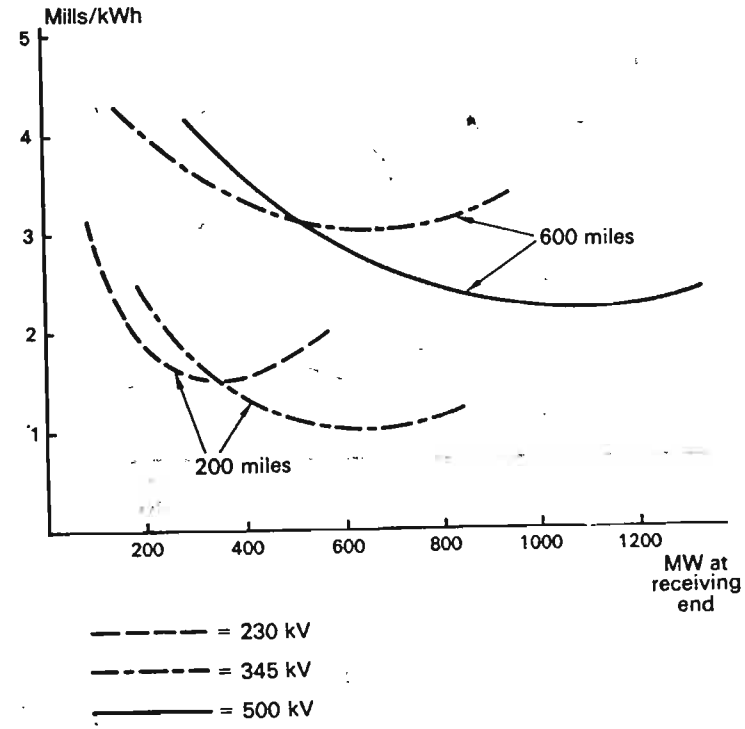


**Fig. 6-1** Transmission costs as function of voltage level, line length, and line power.

changed the picture radically. As of this writing (1970), 765-kV lines are in operation and 1000-kV lines are in the planning stages.

Recalling the formula

$$P_{ij} = \frac{|V_i|\,|V_j|}{X} \sin \delta$$

we realize the role of EHV in achieving high transmission capacities. For example, we can transmit of the order of 1 GW across 600 miles using one line operated at 500 kV. In addition, the reduced line losses make it more economical to operate at these extremely high voltages, as indicated in the graphs of Fig. 6-1. These graphs give the cost of transmission expressed in mills per kilowatthour.† The curves clearly indicate that the

† The total transmission costs are made up of two components:

1. Fixed costs for towers, conductors, insulators, and right-of-way plus terminal equipment. These costs increase rapidly with voltage level (Fig. 6-2).
2. Cost for lost energy. These costs are inversely proportional to the square of the voltage level [Eq. (2-20)].

(*Continued on page 154*)

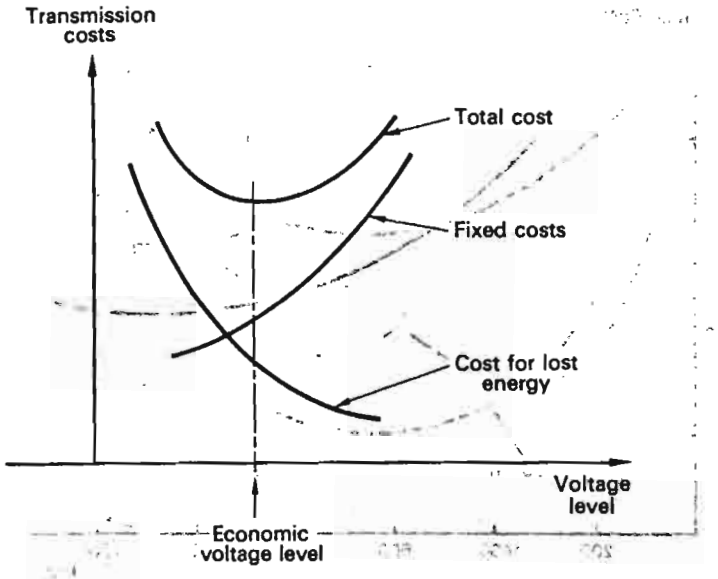


**Fig. 6-2** Graphs for finding "economic voltage level."

longer the transmission distance, the more favorable are the higher voltage levels.

There has been a tendency in the past for the individual electric utility companies to operate essentially independently of each other. For example, relatively large utilities, having peak demands of several thousands of megawatts, may be connected to their neighboring systems with only relatively weak tie lines. Looking into the future, we see an increased role to be played by *pooling* and *area coordination*, which will require a superimposed transmission grid of great strength. We summarize the functions visualized for such a grid:

1. Its existence will permit the construction of larger and more economical generating units and the transmission of large blocks of energy from the generating sources to major load centers.
2. It will permit reduced reserve requirements by sharing of capacity between areas and sectors.
3. It will provide capacity savings by seasonal exchange of capacity between areas which have opposing winter and summer needs. (See Fig. 6-3.)

The total transmission costs will obviously be characterized by a minimum occurring at one particular voltage value, the "economic voltage level." Before selecting this particular voltage, one must of course check that it will correspond to sufficient transmission capacity.



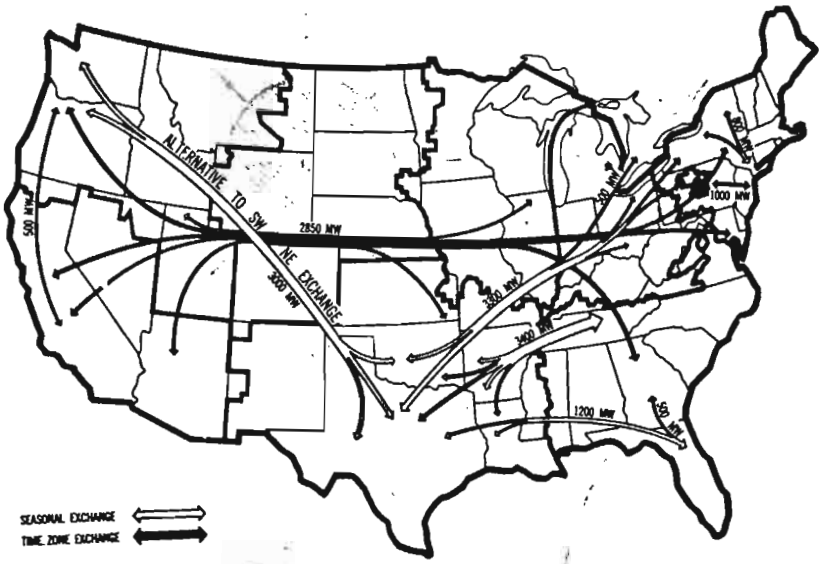


**Fig. 6-3** Estimated seasonal and time-zone exchanges by 1980.

4. It will permit capacity savings from time zone and random diversity. (The load peak in California occurs 3 h later than in New York.) (See Fig. 6-3.)
5. It will facilitate transmission of off-peak energy.
6. It will provide the flexibility to meet unforeseen emergency demands.

## 6-2 DESIGN CONSIDERATIONS

Although copper has almost twice the conductivity of aluminum, the latter is almost exclusively used for today's conductors. Not only is it characterized by a weight and price advantage, but perhaps more important is the fact that an aluminum conductor has a larger diameter than a copper conductor of equivalent resistance and/or weight.

Figure 6-4 shows the electric field picture around three different conductor types:

(*a*) Single copper conductor
(*b*) Single aluminum conductor
(*c*) "Bundled" aluminum conductor

To make the three cases comparable, we have assumed that all are characterized by the same resistance and voltage (note the equal number of electric flux lines). The closeness of the flux lines at the conductor surface is

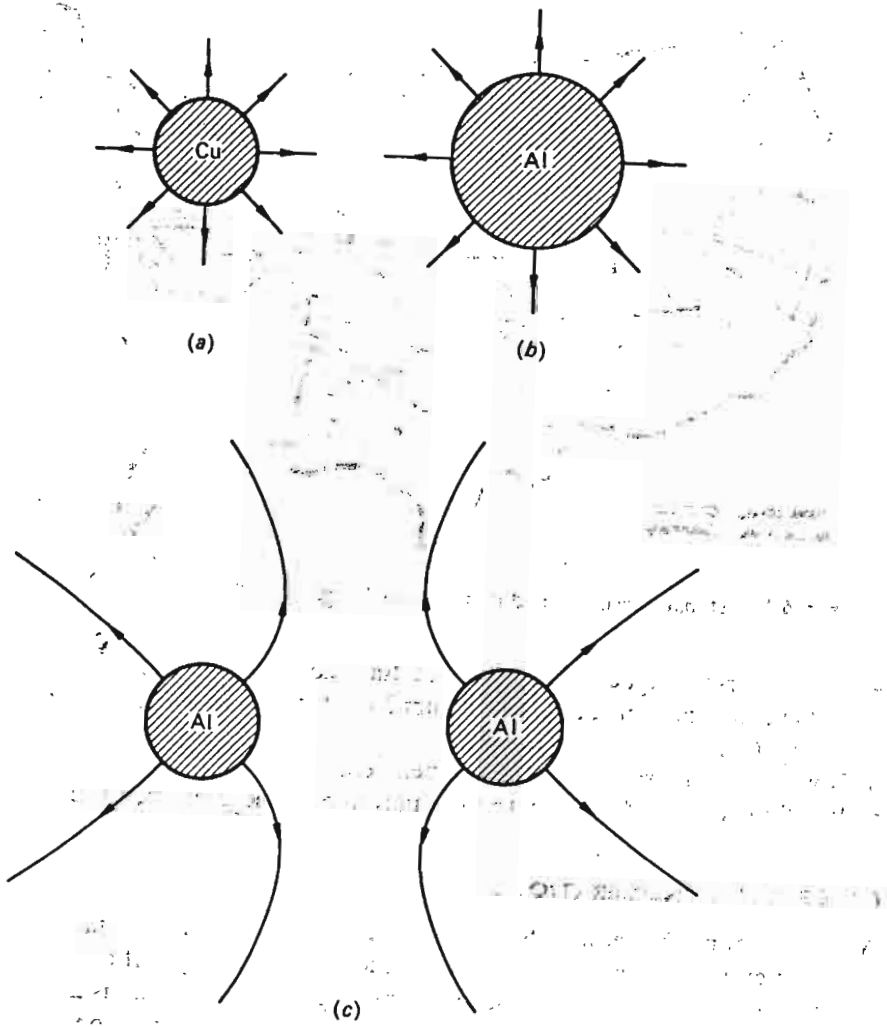


**Fig. 6-4** Electric field picture around three different conductor types. Voltage is the same in all 3 cases.

a measure of the electric field intensity $|E|$. Note the decrease of $|E|$ as we move from $a \rightarrow b \rightarrow c$. This results in less chance for *corona* in the latter cases. This phenomenon is a serious problem in EHV technology. It is caused by a breakdown or ionization of the atmosphere when a certain field intensity ($\approx$ 3000 kV/m) is reached. Corona is associated with energy loss, will cause communication interference, and is generally not tolerated. For voltages in excess of about 230 kV it is in fact not possible to use a round single conductor. Instead of going to a hollow conductor, it is more practical



to use bundle conductors of two, three, and four conductors per phase spaced about 1½ ft apart. As we shall see, bundling of conductors also reduces to a considerable extent the line reactance, and therefore gives the added advantage of increased transmission capacity.

For the conductor sizes in use (up to about 1,000,000 cmil) it is not practical to use solid design. *Aluminum-cable steel-reinforced* (ACSR) conductors, consisting of a central core of *stranded* steel wires for the mechanical strength, surrounded by the current-carrying layers of aluminum strands, are the most common design. The conductors are suspended from the tower crossarms by flexible insulator strings.

It used to be that the transmission towers were designed with only one objective in mind: to provide adequate conductor support and insulation for minimum cost. Our countryside abounds with ugly monuments from this era. Fortunately, our society is awakening to the fact that it pays to design with beauty in mind.

## 6-3 ELECTRIC LINE PARAMETERS

From a systems point of view, we are interested primarily in the electric performance characteristics of the transmission line. We shall show that these can be expressed in terms of the following four line parameters, listed in order of importance:

1. Line inductance, expressed in henrys per meter
2. Line shunt capacitance, expressed in farads per meter
3. Line resistance, expressed in ohms per meter
4. Line shunt conductance, expressed in mhos per meter

We shall symbolize these parameters by $L$, $C$, $R$, and $G$, respectively, and shall in most practical cases express them per length unit (meter) and per phase of the transmission line. If the transmission line is unsymmetrical (*nontransposed*), it is in general not *theoretically* possible to express some of the parameters on a per-phase basis. However, if we tolerate some slight approximations, it can be done as a *practical* convenience. We shall comment on these matters as we proceed.

### 6-3.1 LINE RESISTANCE AND SHUNT CONDUCTANCE

The reason why we classify $R$ and $G$ as "least important" is that they affect the equivalent line impedances, and thus the transmission capacity, to a relatively unimportant degree. They do, of course, *completely* determine the real transmission *losses*, and to the extent that we are interested in the transmission *economy*, we must consider their presence.

The *resistance*, measured in ohms per phase and meter, is obtained from the formula

$$R = \frac{\delta}{A} \tag{6-1}$$

where $\delta$ = resistivity of conductor material, $\Omega \cdot m$
$A$ = effective conductor area, $m^2$

(In the case of an ACSR cable we must compute the resistance per meter of both the Fe and Al sections and then parallel them. The easiest way out is to use manufacturers' tables.†)

In attempting to reduce the resistance, we increase the cost of conductors, and we reach a point of diminishing returns.

For the *shunt conductance* $G$, there is no reliable formula. The shunt conductance accounts for the leakage current between the phases and ground, and this leakage, which takes place mainly along the insulator strings, varies strongly with the weather, atmospheric humidity, and salt content. It is customary to neglect its presence under normal operating conditions, partly because it usually is of negligible magnitude, partly because of our ignorance.

### 6-3.2 LINE INDUCTANCE

The inductance of a power line is by far the most important line parameter from a systems engineer's viewpoint. For normal line designs the reactance is the dominating impedance element, and we have seen in earlier chapters how the reactance directly affects the transmission capacity of the line. It is important, therefore, that we give this parameter proper attention, in particular, as we are concerned about the possible means we have at our disposal to reduce its magnitude.

**The single-phase line** The *single-phase* transmission line (Fig. 2-1) serves as an appropriate point of departure in our analysis. The line

† It should also be added that, because the conductors are of considerable size, the effective ac resistance will be somewhat higher than the dc value, due to "skin effect."

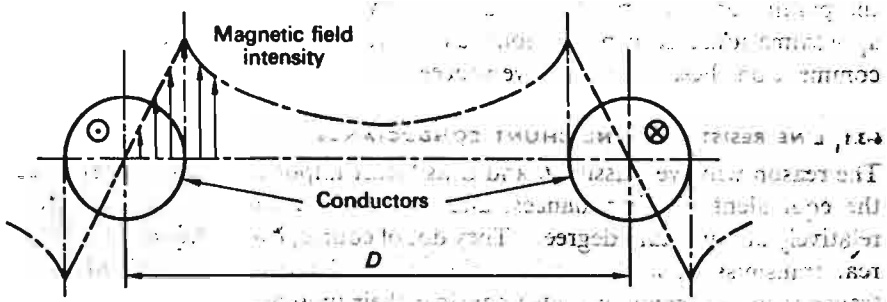


**Fig. 6-5** Magnetic field distribution around a single-phase line.



inductance is directly associated with the magnetic flux *inside* and *around* the two conductors. In Fig. 6-5 we show the distribution of this flux. We make two significant observations in regard to this distribution:

1. Although the *inside* volume is comparatively small, the field densities are of *high magnitude*, and the magnetic field energy stored inside the conductor is therefore not negligible.
2. The presence of the earth will affect the magnetic† field geometry insignificantly. Not only is the relative permeability of earth about the same as that of air, but its electric conductivity is relatively small; i.e., the surface currents induced are generally so small that they have very little effect on the magnetic field.

In computing the total inductance per meter line, we shall distinguish between the inductance due to the magnetic field energy *inside* the conductors ($L_i$) and *outside* the conductors ($L_o$). We then have

$$L = L_i + L_o \tag{6-2}$$

*Inside inductance* $L_i$ If the total conductor current is $i$ A, the current inside radius $x$, where $x < R$ (Fig. 6-6*a*), will equal $(x/R)^2 i$. By performing a line integration $\int H\,dl$ around the circle of radius $x$, we thus obtain

$$|H|\,2\pi x = \left(\frac{x}{R}\right)^2 i \tag{6-3}$$

Hence

$$|H| = \frac{x}{2\pi R^2} i \qquad \text{A/m} \tag{6-4}$$

i.e., the magnetic field intensity increases linearly with $x$, as shown in Fig. 6-5.

The volume element shown shaded in Fig. 6-6*a* has the volume $2\pi x\,dx$ m³/m of line, and the total magnetic field energy *inside both* conductors is thus, in accordance with Eq. (2-10),

$$w_{mf} = 2 \times \tfrac{1}{2}\mu\mu_0 \int_0^R \left(\frac{x}{2\pi R^2} i\right)^2 2\pi x\,dx = \frac{\mu\mu_0}{8\pi} i^2 \qquad \text{J/m} \tag{6-5}$$

From Eq. (2-13), we thus have

$$\tfrac{1}{2} L_i i^2 = \frac{\mu\mu_0}{8\pi} i^2$$

† The *electric* field geometry will, on the contrary, be very much affected.

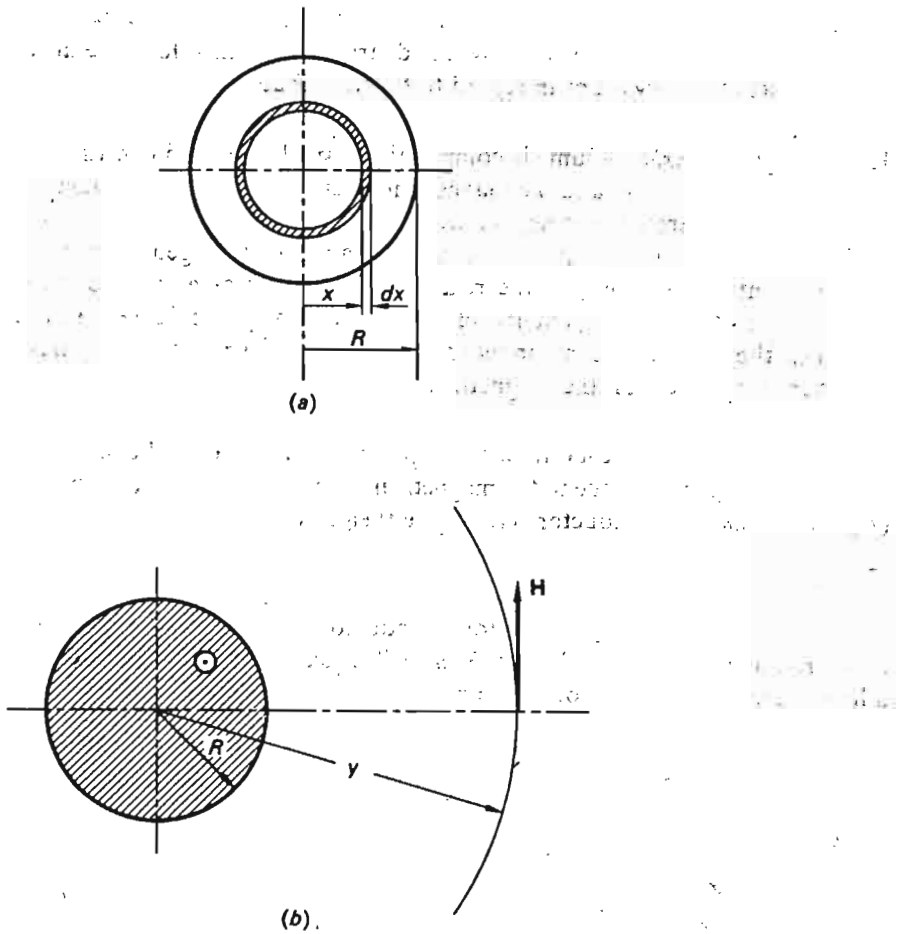


**Fig. 6-6** Computation of field intensity inside and outside single conductor due to its own current.

Hence

$$L_i = \frac{\mu\mu_0}{4\pi} \quad \text{H/m} \tag{6-6}$$

Note that this component of the inductance is *independent* of wire size.

*Outside inductance* $L_o$ We could obtain the outside inductance in the same manner as we computed $L_i$. It is *considerably* simpler† to approach the problem of finding $L_o$ in the following manner.

† Using Eq. (2-10), we would obtain formidable integrals.



We compute the total *outside* magnetic flux $\phi_o$ inside the loop formed by the two conductors. The inductance $L_o$ is then (from the definition of inductance) obtained, simply, as

$$L_o = \frac{\phi_o}{i} \tag{6-7}$$

The magnetic flux lines due to the current in *one* conductor form concentric circles, as depicted in Fig. 6-6*b*. By performing a line integration around a circle of radius $y$, where $y > R$, we therefore obtain for the $|H|$ contribution from *one* conductor

$$2\pi y\,|H| = i$$

The flux density due to *one* conductor is therefore

$$|B| = \mu_0\,|H| = \mu_0 \frac{i}{2\pi y} \quad \text{Wb/m}^2 \tag{6-8}$$

The total magnetic flux per meter of line between the two conductors due to the current in *one* conductor is thus

$$\int_R^{D-R} \mu_0 \frac{i}{2\pi y}\,dy = \mu_0 \frac{i}{2\pi} \ln \frac{D-R}{R} \approx \mu_0 \frac{i}{2\pi} \ln \frac{D}{R} \quad \text{Wb/m of line} \tag{6-9}$$

where $D$ is the distance between conductors. The approximation is valid, since we usually have $D \gg R$. The total flux contributed by *both* conductor currents is finally obtained:

$$\phi_o \approx \mu_0 \frac{i}{\pi} \ln \frac{D}{R} \quad \text{Wb/m of line} \tag{6-10}$$

From Eq. (6-7) we then have

$$L_o = \frac{\mu_0}{\pi} \ln \frac{D}{R} \quad \text{H/m of line} \tag{6-11}$$

For the *total* line inductance of a *single-phase* line we finally have

$$L = L_i + L_o = \frac{\mu\mu_0}{4\pi} + \frac{\mu_0}{\pi} \ln \frac{D}{R} \quad \text{H/m of line} \tag{6-12}$$

Since $\mu_0 = 4\pi \times 10^{-7}$, we can write Eq. (6-12)

$$L = 4 \times 10^{-7}\left(\frac{\mu}{4} + \ln \frac{D}{R}\right) \quad \text{H/m of line} \tag{6-13}$$

**Example 6-1** To get a feel for the order of magnitudes involved, let us compute the inductance of a single-phase transmission line having the following data:

$R = 0.5$ in. (copper conductor, $\mu = 1$)
$D = 20$ ft†

we get

$$L = 4 \times 10^{-7}\left(\frac{1}{4} + \ln\frac{240}{0.5}\right)$$
$$= 25.7 \times 10^{-7} \text{ H/m of line}$$
$$= 41.3 \times 10^{-4} \text{ H/mile of line}$$

Multiplying by $\omega = 377$, we obtain the corresponding reactance:

$$X = \omega L = 1.56\ \Omega\text{/mile of line}$$

*It is interesting to note that, because of the relative "insensitivity" of the logarithmic function, a change of line dimensions will only slightly change the inductance.* For example, a 100 percent increase of the conductor spacing $D$ will result in only a 11 percent increase of the reactance in the case just given.

**The three-phase line** The results obtained for the single-phase case can be readily applied to a three-phase line. Equation (6-12) can be written in a different form:

$$L = \frac{\mu_0}{2\pi}\left[\left(\frac{\mu}{4} + \ln\frac{1}{R}\right) + \left(\frac{\mu}{4} + \ln\frac{1}{R}\right) - 2\ln\frac{1}{D}\right] \tag{6-14}$$

We introduce now the *apparent self-inductances* and *mutual inductances* of the wires, defined, respectively, as follows:

$$L_1 = L_2 \triangleq \frac{\mu_0}{2\pi}\left(\frac{\mu}{4} + \ln\frac{1}{R}\right) \tag{6-15}$$

$$M_{12} \triangleq \frac{\mu_0}{2\pi}\ln\frac{1}{D}$$

The inductance of the line may then be written in the more familiar-looking form

$$L = L_1 + L_2 - 2M_{12} \quad \text{H/m} \tag{6-16}$$

The reader will recognize this as the formula for the "effective" inductance of two series-connected magnetically coupled coils, each having the self-inductance $L_1$ and $L_2$, respectively, and characterized by a mutual inductance $M_{12}$. In looking at the line inductance from this point of view, we must make the following observations:

† In Chap. 2 we assured the reader that we were sticking to the mks system. In this chapter we temporarily succumb to the British units (presently being abandoned even by the British), for the following reasons:

1. In Eq. (6-12) and others to follow, line and conductor dimensions appear in *ratios* of the type $D/R$. It is therefore of little importance what unit system we use.
2. For the present generation of U.S. power engineers, it is probably very awkward to measure conductor diameters in centimeters, and phase spacing in meters.



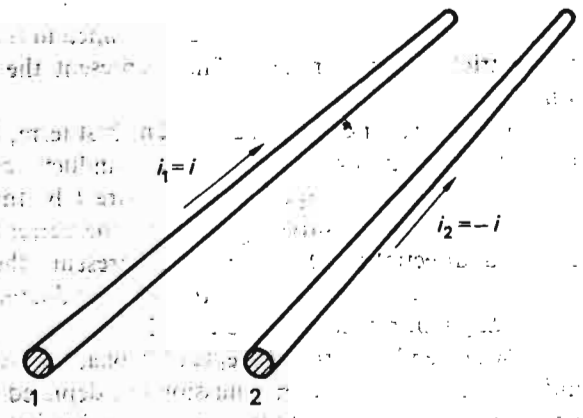


**Fig. 6-7** Conductor currents defined for two-wire line.

1. The apparent inductances defined by Eq. (6-15) contain an "error of dimension," since the logarithmic arguments have the dimension $(\text{length})^{-1}$. They must therefore be considered individually as mathematical artifices that will attain physical meaning only when appearing together, in which case the dimensionality error disappears.
2. $L_1$ and $L_2$ turned out identical because the wires had equal radii $R$. Had the wire radii been different, then $L_1$ and $L_2$ would have been different also [the reader is encouraged to check this by going back to the original derivation of Eq. (6-12).]
3. The last term in Eq. (6-16) will have a *negative* sign because the current directions in the wires are *opposite*.

If we were to inject a current $i$ into the single-phase line, as shown in Fig. 6-7, we would obviously be able to measure an inductive voltage drop $\Delta v$ per meter of line of magnitude.

$$\Delta v = L\frac{di}{dt} = (L_1 + L_2 - 2M_{12})\frac{di}{dt} \quad \text{V/m} \tag{6-17}$$

We can rewrite Eq. (6-17) as follows:

$$\Delta v = \left(L_1\frac{di}{dt} - M_{12}\frac{di}{dt}\right) + \left(L_2\frac{di}{dt} - M_{12}\frac{di}{dt}\right) \tag{6-18}$$

If we here introduce the conductor currents $i_1$ and $i_2$ defined† in Fig. 6-7, we can write Eq. (6-18) as follows:

$$\Delta v = \underbrace{\left(L_1\frac{di_1}{dt} + M_{12}\frac{di_2}{dt}\right)}_{\Delta v_1} - \underbrace{\left(L_2\frac{di_2}{dt} + M_{12}\frac{di_1}{dt}\right)}_{\Delta v_2} \quad \text{V/m} \tag{6-19}$$

† Note that $i_1 + i_2 = 0$.

The voltage drops $\Delta v_1$ and $\Delta v_2$, defined in this manner, are completely symmetrical in appearance. They represent the reactance drops in each wire.

Consider, for example, $\Delta v_1$. The first term, $L_1(di_1/dt)$, can be thought of as the voltage drop across the self-inductance $L_1$. The second term, $M_{12}(di_2/dt)$, is the voltage induced in wire 1 by the current in wire 2. The second term has a positive sign because the currents $i_1$ and $i_2$ have the same assumed directions. $\Delta v_1$ therefore represents the total inductive voltage drop measured per meter of length along conductor 1. The same holds true about $\Delta v_2$ with respect to conductor 2.

We extend now the concepts of "apparent" self-inductance and mutual inductance to the $n$-wire transmission line depicted in Fig. 6-8. It should be noted that the single- and three-phase lines are but special cases of this more general case. Taking a cue from Eq. (6-15), we thus define

$$L_\nu \triangleq \frac{\mu_0}{2\pi}\left(\frac{\mu_\nu}{4} + \ln\frac{1}{R_\nu}\right) \quad \text{H/m}$$
$$M_{\nu\mu} \triangleq \frac{\mu_0}{2\pi}\ln\frac{1}{D_{\nu\mu}} \quad \text{H/m} \tag{6-20}$$

$L_\nu$ is the apparent self-inductance of wire $\nu$, and $M_{\nu\mu}$ is the apparent mutual inductance between the wires $\nu$ and $\mu$.

In terms of these "mathematical" inductances we can specify completely the inductive voltage drops in each of the $n$ parallel wires. Specifically, the inductive voltage drop $\Delta v_\nu$ per meter of wire $\nu$ can be written, in analogy with Eq. (6-19),

$$\Delta v_\nu = L_\nu\frac{di_\nu}{dt} + \sum_{\mu=1}^{n} M_{\nu\mu}\frac{di_\mu}{dt} \quad \text{V/m} \tag{6-21}$$

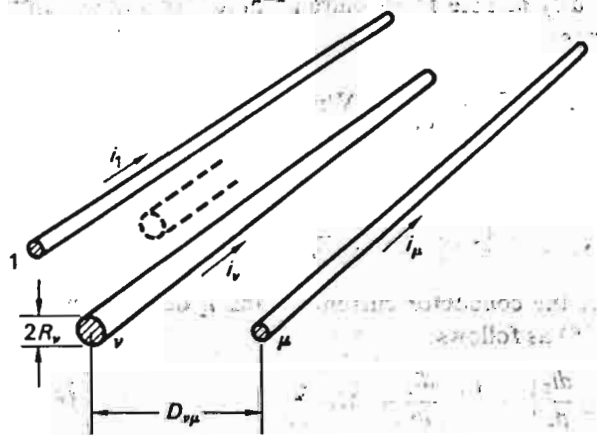


**Fig. 6-8** $n$-wire transmission line.



or in the case of *sinusoidal* currents,

$$\Delta V_\nu = L_\nu j\omega I_\nu + \sum_{\mu=1}^{n} M_{\nu\mu} j\omega I_\mu \quad \text{V/m} \tag{6-22}$$

In using these formulas, we must observe the following rules:

1. They can be proved correct only in the case where $\sum i_\nu = 0$; i.e., we cannot apply them to a line where return currents are flowing in the ground.
2. In adding the contributions of all mutually induced voltage drops in the formulas, we must extend the summation over all $\mu$, except, of course, $\mu = \nu$.

**Example 6-2** We shall demonstrate the usage of the above technique in finding the line inductance of a three-phase line. The line consists of three equal conductors of radii $R$, placed in a horizontal plane, with a phase spacing of $D$ m, as depicted in Fig. 6-9*a*.

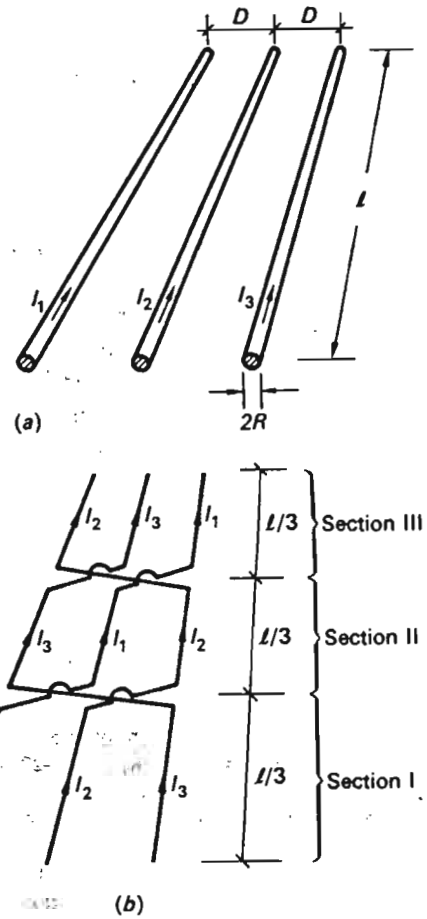


**Fig. 6-9** Three-phase transmission line. (*a*) Nontransposed; (*b*) transposed.

For the sake of completeness and for the purpose of exposing some important points, we shall compare the *untransposed* and *transposed* cases depicted in Fig. 6-9*a* and *b*, respectively.

*Case I. Untransposed line* Using Eq. (6-22), we obtain, for the total voltage drop in phase 1,

$$\Delta V_1 = j\omega I_1 \frac{\mu_0}{2\pi}\left(\frac{1}{4} + \ln\frac{1}{R}\right) + j\omega I_2 \frac{\mu_0}{2\pi}\ln\frac{1}{D} + j\omega I_3 \frac{\mu_0}{2\pi}\ln\frac{1}{2D} \quad \text{V/m} \tag{6-23}$$

By using the current relation

$$I_1 + I_2 + I_3 = 0 \tag{6-24}$$

we can eliminate, for example, $I_3$ from Eq. (6-23) and obtain then, upon collecting terms,

$$\Delta V_1 = I_1 j\omega \frac{\mu_0}{2\pi}\left(\frac{1}{4} + \ln\frac{2D}{R}\right) + I_2 j\omega \frac{\mu_0}{2\pi}\ln 2 \quad \text{V/m} \tag{6-25}$$

If, in a similar fashion, we compute the voltage drops per meter of phases 2 and 3, we get

$$\Delta V_2 = I_2 j\omega \frac{\mu_0}{2\pi}\left(\frac{1}{4} + \ln\frac{D}{R}\right) \tag{6-26}$$

$$\Delta V_3 = I_3 j\omega \frac{\mu_0}{2\pi}\left(\frac{1}{4} + \ln\frac{2D}{R}\right) + I_3 j\omega \frac{\mu_0}{2\pi}\ln 2 \tag{6-27}$$

By using *matrix* notation, we can summarize the results of Eqs. (6-25) to (6-27) in a more compact *tabular* form:

$$\begin{bmatrix}\Delta V_1\\ \Delta V_2\\ \Delta V_3\end{bmatrix} = j\omega\frac{\mu_0}{2\pi}\begin{bmatrix}\frac{1}{4}+\ln\frac{2D}{R} & \ln 2 & 0\\ 0 & \frac{1}{4}+\ln\frac{D}{R} & 0\\ 0 & \ln 2 & \frac{1}{4}+\ln\frac{2D}{R}\end{bmatrix}\begin{bmatrix}I_1\\ I_2\\ I_3\end{bmatrix} \tag{6-28}$$

Before we comment on this result we treat case II for comparison.

*Case II. The transposed (or phase-symmetrical) line* We must consider separately the three different sections of the line.

In section I we obtain the same voltage drop per meter and phase as we earlier computed in Eq. (6-23).

Similarly, the drops per meter and phase in sections II and III may be obtained directly from Eqs. (6-26) and (6-27) by renaming the currents in accordance with Fig. 6-9*b*. Specifically, if we wish to obtain the voltage drop per meter in phase 1 of section II, we replace the current $I_2$ in Eq. (6-26) by $I_1$. The voltage drop per meter in phase 1 and section III is obtained from Eq. (6-27) by replacing the currents $I_2$ and $I_3$ in the formula by $I_3$ and $I_1$, respectively. By using Eqs. (6-25) to (6-27) with these modifications and by taking the *average* of the drops thus computed, we



obtain the following formula for the voltage drop in phase 1 per meter of the transposed line:

$$\Delta V_1 = \tfrac{1}{3}\left[I_1 j\omega\frac{\mu_0}{2\pi}\left(\tfrac{1}{4}+\ln\frac{2D}{R}\right) + I_2 j\omega\frac{\mu_0}{2\pi}\ln 2\right] + \tfrac{1}{3}\left[I_1 j\omega\frac{\mu_0}{2\pi}\left(\tfrac{1}{4}+\ln\frac{D}{R}\right)\right] + \tfrac{1}{3}\left[I_1 j\omega\frac{\mu_0}{2\pi}\left(\tfrac{1}{4}+\ln\frac{2D}{R}\right) + I_3 j\omega\frac{\mu_0}{2\pi}\ln 2\right] \tag{6-29}$$

We can readily reduce this expression to the following simple one:

$$\Delta V_1 = I_1 j\omega\frac{\mu_0}{2\pi}\left[\tfrac{1}{4}+\ln\frac{\sqrt[3]{2}D}{R}\right] \quad \text{V/m} \tag{6-30}$$

Because of the complete symmetry between phases, we can write directly the expressions for the voltage drops per meter for phases 2 and 3:

$$\Delta V_2 = I_2 j\omega\frac{\mu_0}{2\pi}\left[\tfrac{1}{4}+\ln\frac{\sqrt[3]{2}D}{R}\right] \quad \text{V/m} \tag{6-31}$$

$$\Delta V_3 = I_3 j\omega\frac{\mu_0}{2\pi}\left[\tfrac{1}{4}+\ln\frac{\sqrt[3]{2}D}{R}\right] \quad \text{V/m} \tag{6-32}$$

Or by summarizing in matrix form,

$$\begin{bmatrix}\Delta V_1\\ \Delta V_2\\ \Delta V_3\end{bmatrix} = j\omega\frac{\mu_0}{2\pi}\begin{bmatrix}\frac{1}{4}+\ln\frac{\sqrt[3]{2}D}{R} & 0 & 0\\ 0 & \frac{1}{4}+\ln\frac{\sqrt[3]{2}D}{R} & 0\\ 0 & 0 & \frac{1}{4}+\ln\frac{\sqrt[3]{2}D}{R}\end{bmatrix}\begin{bmatrix}I_1\\ I_2\\ I_3\end{bmatrix} \tag{6-33}$$

We pause here to make some observations and comparisons of the transposed and untransposed cases.

1. In the transposed line the voltage drops in *each* phase are directly proportional to the own phase current *but independent of the currents in the other phases*. We can actually write the voltage drops in the form

$$\Delta V_\nu = j\omega L I_\nu = jX I_\nu \qquad \text{for } \nu = 1, 2, 3 \tag{6-34}$$

where $X$ has the *same value for all three phases* and has the dimension of reactance per meter. We refer to $X$ as the *reactance per phase* of the line, expressed in ohms per meter.

Clearly, if the three phase currents possess three-phase symmetry, so will the three voltage drops. As a consequence, if the voltages (measured either to ground or between the lines) in the sending end of the line possess three-phase symmetry, so will the voltages of the other end.

2. In the untransposed line, only the voltage drop in the middle (symmetrical) phase can be expressed in the form of Eq. (6-34). As a consequence, the inductive voltage drops will *not* possess three-phase symmetry even if the currents do.

It is interesting to see what this unsymmetry amounts to for a specific case. Let us, for demonstration purposes, assume

$R = 0.5$ in.

$D = 20$ ft

For these specific conductor and spacing dimensions the two $3 \times 3$ matrices in Eqs. (6-33) and (6-28) take on the respective numerical values

$$\begin{bmatrix} 6.66 & 0 & 0 \\ 0 & 6.66 & 0 \\ 0 & 0 & 6.66 \end{bmatrix} \quad \text{and} \quad \begin{bmatrix} 7.12 & 0.69 & 0 \\ 0 & 6.42 & 0 \\ 0 & 0.69 & 7.12 \end{bmatrix}$$

We note that the coupling between the phases, as measured by the elements of value 0.69 in the second matrix, is relatively insignificant as compared with the elements along the main diagonal. Also, we note that these latter elements do not have too wide a spread and have an average value close to that of the transposed line. For this reason we do not introduce too great an error if, even in the untransposed case, we treat the voltage drop on a per-phase basis.

The inductance per phase, defined in Eq. (6-34), will in the above numerical example be

$$L = \frac{\mu_0}{2\pi} \times 6.66 = 1.332 \times 10^{-6} \text{ H/m}$$

and the reactance per phase will have the value

$X = 377 \times 1.332 \times 10^{-6} = 5.02 \times 10^{-4}\ \Omega$/m and phase

or 0.807 Ω/mile and phase. For comparison, the resistance of this conductor, if we assume ACSR design, would be about 0.14 Ω/mile and phase, thus confirming what we mentioned earlier about the dominance of the reactance.

**Example 6-3** As a second example, on finding the line reactance for a three-phase line, we shall turn our attention now to the *bundle conductor* transmission line, a section of which is shown in Fig. 6-10. The transmission line has the same phase spacing, $D$, as the one in Fig. 6-9, but for reasons of reducing corona, we use two conductors per phase, placed the distance $d$ apart, and each carrying half the phase current. We will assume that the line is transposed identically with the line in Fig. 6-9*b*.

In finding the inductive voltage drop in, say, phase 1, we can now consider either one of two conductors of that phase (we designate them $a$ and $b$ in Fig. 6-10). The voltage drops along either one will be practically† the same. We choose

† The student should check this statement, and he will find that the drops along conductors $a$ and $b$ are practically, *but not exactly*, the same. The slight difference will in effect give rise to a small circulating current which will have as effect that the phase current $I_1$ does not divide exactly 50-50 between the two conductors. The effect is of negligible practical importance.



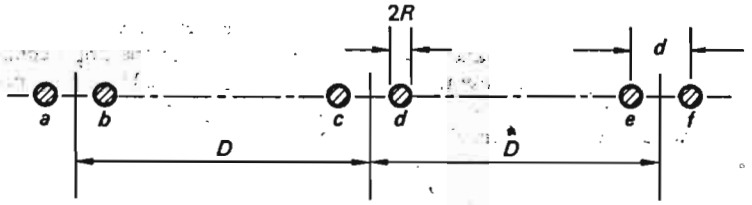


**Fig. 6-10** Bundled three-phase transmission line.

conductor $a$ and obtain the following expression for the voltage drop per meter in section I.

$$\Delta V_a = \underbrace{j\omega \frac{I_1}{2}\frac{\mu_0}{2\pi}\left(\tfrac{1}{4} + \ln\frac{1}{R}\right)}_{1} + \underbrace{j\omega \frac{I_1}{2}\frac{\mu_0}{2\pi}\ln\frac{1}{d}}_{2} + \underbrace{j\omega \frac{I_2}{2}\frac{\mu_0}{2\pi}\ln\frac{1}{D}}_{3} + \underbrace{j\omega \frac{I_2}{2}\frac{\mu_0}{2\pi}\ln\frac{1}{D+d}}_{4}$$

$$+ \underbrace{j\omega \frac{I_3}{2}\frac{\mu_0}{2\pi}\ln\frac{1}{2D}}_{5} + \underbrace{j\omega \frac{I_3}{2}\frac{\mu_0}{2\pi}\ln\frac{1}{2D+d}}_{6} \quad \text{V/m} \qquad (6\text{-}35)$$

The six terms in this expression represent the contributions to the total drop by the currents in the six conductors $a$ to $f$, respectively. Since $d \ll D$, we realize that terms 3 and 4 and also 5 and 6 are practically equal, and we can therefore reduce the expression to the following one:

$$\Delta V_a \approx j\omega \frac{I_1}{2}\frac{\mu_0}{2\pi}\left(\tfrac{1}{4} + \ln\frac{1}{R} + \ln\frac{1}{d}\right) + j\omega I_2 \frac{\mu_0}{2\pi}\ln\frac{1}{D}$$

$$+ j\omega I_3 \frac{\mu_0}{2\pi}\ln\frac{1}{2D} \quad \text{V/m} \qquad (6\text{-}36)$$

If we now proceed to find the corresponding voltage drops in sections II and III, for the conductors occupying the positions $c$ (or $d$) and $e$ (or $f$), respectively, we get

$$\Delta V_c \approx j\omega I_1 \frac{\mu_0}{2\pi}\left(\tfrac{1}{8} + \ln\frac{D}{\sqrt{Rd}}\right) \quad \text{V/m} \qquad (6\text{-}37)$$

$$\Delta V_e \approx j\omega \frac{I_1}{2}\frac{\mu_0}{2\pi}\left(\tfrac{1}{4} + \ln\frac{1}{R} + \ln\frac{1}{d}\right) + j\omega I_2 \frac{\mu_0}{2\pi}\frac{1}{2D}$$

$$+ j\omega I_3 \frac{\mu_0}{2\pi}\ln\frac{1}{D} \quad \text{V/m} \qquad (6\text{-}38)$$

By taking the average of $\Delta V_a$, $\Delta V_c$, and $\Delta V_e$, we obtain the total inductive voltage drop per meter in phase 1:

$$\Delta V_1 = \frac{\Delta V_a + \Delta V_c + \Delta V_e}{3} = j\omega \frac{\mu_0}{2\pi} I_1 \left[\tfrac{1}{8} + \ln\frac{\sqrt[3]{2}D}{\sqrt{Rd}}\right] \quad \text{V/m} \qquad (6\text{-}39)$$

The reactance per phase is, obviously,

$$X = \omega \frac{\mu_0}{2\pi}\left[\tfrac{1}{8} + \ln\frac{\sqrt[3]{2}D}{\sqrt{Rd}}\right] \quad \Omega\text{/m} \qquad (6\text{-}40)$$

2. In the untransposed line, only the voltage drop in the middle (symmetrical) phase can be expressed in the form of Eq. (6-34). As a consequence, the inductive voltage drops will *not* possess three-phase symmetry even if the currents do.

It is interesting to see what this unsymmetry amounts to for a specific case. Let us, for demonstration purposes, assume

$R = 0.5$ in.

$D = 20$ ft

For these specific conductor and spacing dimensions the two $3 \times 3$ matrices in Eqs. (6-33) and (6-28) take on the respective numerical values

$$\begin{bmatrix} 6.66 & 0 & 0 \\ 0 & 6.66 & 0 \\ 0 & 0 & 6.66 \end{bmatrix} \quad \text{and} \quad \begin{bmatrix} 7.12 & 0.69 & 0 \\ 0 & 6.42 & 0 \\ 0 & 0.69 & 7.12 \end{bmatrix}$$

We note that the coupling between the phases, as measured by the elements of value 0.69 in the second matrix, is relatively insignificant as compared with the elements along the main diagonal. Also, we note that these latter elements do not have too wide a spread and have an average value close to that of the transposed line. For this reason we do not introduce too great an error if, even in the untransposed case, we treat the voltage drop on a per-phase basis.

The inductance per phase, defined in Eq. (6-34), will in the above numerical example be

$$L = \frac{\mu_0}{2\pi} \times 6.66 = 1.332 \times 10^{-6} \text{ H/m}$$

and the reactance per phase will have the value

$$X = 377 \times 1.332 \times 10^{-6} = 5.02 \times 10^{-4} \ \Omega/\text{m and phase}$$

or 0.807 Ω/mile and phase. For comparison, the resistance of this conductor, if we assume ACSR design, would be about 0.14 Ω/mile and phase, thus confirming what we mentioned earlier about the dominance of the reactance.

**Example 6-3** As a second example, on finding the line reactance for a three-phase line, we shall turn our attention now to the *bundle conductor* transmission line, a section of which is shown in Fig. 6-10. The transmission line has the same phase spacing, $D$, as the one in Fig. 6-9, but for reasons of reducing corona, we use two conductors per phase, placed the distance $d$ apart, and each carrying half the phase current. We will assume that the line is transposed identically with the line in Fig. 6-9*b*.

In finding the inductive voltage drop in, say, phase 1, we can now consider either one of two conductors of that phase (we designate them $a$ and $b$ in Fig. 6-10). The voltage drops along either one will be practically† the same. We choose

† The student should check this statement, and he will find that the drops along conductors $a$ and $b$ are practically, *but not exactly*, the same. The slight difference will in effect give rise to a small circulating current which will have as effect that the phase current $I_1$ does not divide exactly 50-50 between the two conductors. The effect is of negligible practical importance.



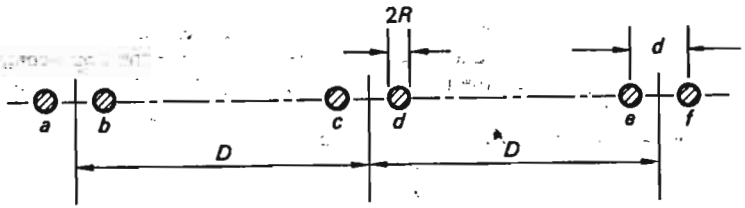


**Fig. 6-10** Bundled three-phase transmission line.

conductor $a$ and obtain the following expression for the voltage drop per meter in section I.

$$\Delta V_a = \underbrace{j\omega \frac{I_1}{2}\frac{\mu_0}{2\pi}\left(\tfrac{1}{4} + \ln\frac{1}{R}\right)}_{1} + \underbrace{j\omega \frac{I_1}{2}\frac{\mu_0}{2\pi}\ln\frac{1}{d}}_{2} + \underbrace{j\omega \frac{I_2}{2}\frac{\mu_0}{2\pi}\ln\frac{1}{D}}_{3} + \underbrace{j\omega \frac{I_2}{2}\frac{\mu_0}{2\pi}\ln\frac{1}{D+d}}_{4}$$
$$+ \underbrace{j\omega \frac{I_3}{2}\frac{\mu_0}{2\pi}\ln\frac{1}{2D}}_{5} + \underbrace{j\omega \frac{I_3}{2}\frac{\mu_0}{2\pi}\ln\frac{1}{2D+d}}_{6} \quad \text{V/m} \qquad (6\text{-}35)$$

The six terms in this expression represent the contributions to the total drop by the currents in the six conductors $a$ to $f$, respectively. Since $d \ll D$, we realize that terms 3 and 4 and also 5 and 6 are practically equal, and we can therefore reduce the expression to the following one:

$$\Delta V_a \approx j\omega \frac{I_1}{2}\frac{\mu_0}{2\pi}\left(\tfrac{1}{4} + \ln\frac{1}{R} + \ln\frac{1}{d}\right) + j\omega I_2 \frac{\mu_0}{2\pi}\ln\frac{1}{D}$$
$$+ j\omega I_3 \frac{\mu_0}{2\pi}\ln\frac{1}{2D} \quad \text{V/m} \qquad (6\text{-}36)$$

If we now proceed to find the corresponding voltage drops in sections II and III, for the conductors occupying the positions $c$ (or $d$) and $e$ (or $f$), respectively, we get

$$\Delta V_c \approx j\omega I_1 \frac{\mu_0}{2\pi}\left(\tfrac{1}{8} + \ln\frac{D}{\sqrt{Rd}}\right) \quad \text{V/m} \qquad (6\text{-}37)$$

$$\Delta V_e \approx j\omega \frac{I_1}{2}\frac{\mu_0}{2\pi}\left(\tfrac{1}{4} + \ln\frac{1}{R} + \ln\frac{1}{d}\right) + j\omega I_2 \frac{\mu_0}{2\pi}\frac{1}{2D}$$
$$+ j\omega I_3 \frac{\mu_0}{2\pi}\ln\frac{1}{D} \quad \text{V/m} \qquad (6\text{-}38)$$

By taking the average of $\Delta V_a$, $\Delta V_c$, and $\Delta V_e$, we obtain the total inductive voltage drop per meter in phase 1:

$$\Delta V_1 = \frac{\Delta V_a + \Delta V_c + \Delta V_e}{3} = j\omega \frac{\mu_0}{2\pi} I_1 \left[\tfrac{1}{8} + \ln\frac{\sqrt[3]{2D}}{\sqrt{Rd}}\right] \quad \text{V/m} \qquad (6\text{-}39)$$

The reactance per phase is, obviously,

$$X = \omega \frac{\mu_0}{2\pi}\left[\tfrac{1}{8} + \ln\frac{\sqrt[3]{2D}}{\sqrt{Rd}}\right] \quad \Omega/\text{m} \qquad (6\text{-}40)$$

It is interesting to see how this value compares numerically with the reactance value (0.807 Ω/mile and phase) that we obtained for the single-conductor line in Fig. 6-9. We shall use the same phase spacing, $D = 20$ ft, and to make the comparison meaningful, we shall assume the same copper area per phase in both cases, which therefore means that we shall use

$$R = \frac{1}{\sqrt{2}} \times 0.5 = 0.354 \text{ in.}$$

Finally, let us assume a conductor spacing $d$ of 12 in. From Eq. (6-40), we now get

$$X = 377 \times \frac{4\pi \times 10^{-7}}{2\pi} \left[ \frac{1}{4} + \ln \frac{\sqrt[4]{2} \times 240}{\sqrt{12 \times 0.354}} \right]$$

$$= 3.85 \times 10^{-4} \ \Omega/\text{m and phase (or } 0.62 \ \Omega/\text{mile and phase)}$$

*The bundling has therefore resulted in a 23 percent reduction of the line reactance, a circumstance that we appreciate, in view of the accompanying 31 percent increase in transmission capacity.*

### 6-3.3 LINE CAPACITANCE

The line resistance and inductance constitute the elements that make up the *series* impedance of the transmission line.

The capacitance that we will now discuss, together with the conductance, forms the *shunt*, or *parallel*, admittance of the line.

The series elements, of which the inductance is the dominating one, set a limit to the current that can flow through the line and therefore physically determine the power transmittability. The parallel elements, of which the capacitance is the dominating one, represent a "leakage" path for the line currents. These leakage currents are proportional to the line voltage, and the importance of these shunt elements increases, therefore, with the magnitude of the operating voltage. For line voltages of the order 300 to 500 kV and line lengths in excess of 200 miles, the impact of these shunt elements becomes of primary concern for the systems engineer. In a high-voltage *cable*, where the close proximity of the conductors results in a very large shunt capacitance per mile, it becomes, in effect, practically impossible to transmit large energy amounts beyond 20 to 30 miles, without special compensation.

**Capacitance of single-phase line** As in the case of the line inductance we find it convenient to start with a study of the capacitance of the single-phase line. We shall investigate two long parallel wires (Fig. 6-11), which we initially shall consider very thin; indeed, we shall view them as "mathematical" lines. The wires are charged with electric charges of opposite signs to the extent of $\pm Q$ C/m of wire. Since it will serve our purpose, we shall first derive an expression for the electric potential $v_P$ at an arbitrary point $P$



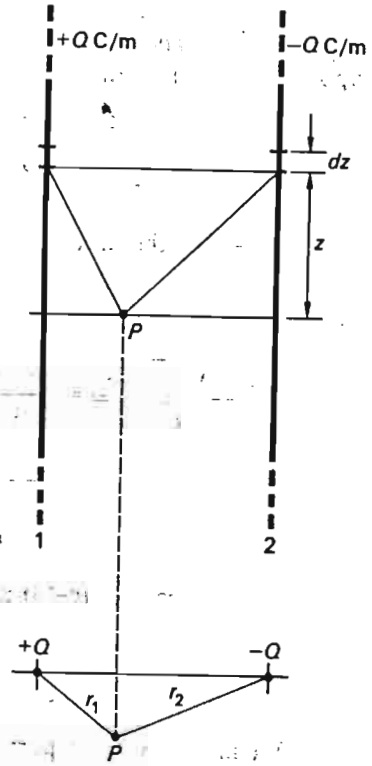


**Fig. 6-11** Finding the shunt capacitance for single-phase line.

located at a distance of $r_1$ and $r_2$ from the two wires, respectively. (Note that $P$ is not necessarily located in the plane containing the two wires.)

Consider two opposite line elements of differential length $dz$. They may be considered as electric *point charges* containing the charges $\pm Q\,dz$, respectively. An elementary law of electric field theory states that the potential $v$ at the distance $r$ from a point charge $q$ equals†

$$v = \frac{q}{4\pi\varepsilon_0 r} \text{ V} \tag{6-41}$$

where

$\varepsilon_0 = 8.85 \times 10^{-12}$ dielectric constant for vacuum

Since the distances from the line elements to the point $P$ equal, respectively, $\sqrt{z^2 + r_1^2}$ and $\sqrt{z^2 + r_2^2}$, we obtain by summation for the potential in point $P$

$$v_P = \int_{-L}^{+L} \frac{Q\,dz}{4\pi\varepsilon_0\sqrt{z^2 + r_1^2}} + \int_{-L}^{+L} \frac{-Q\,dz}{4\pi\varepsilon_0\sqrt{z^2 + r_2^2}} \text{ V} \tag{6-42}$$

† $q$ is in general a function of time. This applies to all variables introduced in this section.

We have integrated over the total line length $2L$. We shall later let $L$ approach $\infty$. The integrals of Eq. (6-42) are easily evaluated, and we get upon substitution of the integration limits,

$$v_P = \frac{Q}{4\pi\varepsilon_0} \ln \left[ \frac{(L + \sqrt{L^2 + r_1^2})}{(L + \sqrt{L^2 + r_2^2})} \frac{(-L + \sqrt{L^2 + r_2^2})}{(-L + \sqrt{L^2 + r_1^2})} \right] \quad \text{V} \qquad (6\text{-}43)$$

If $L \to \infty$, the ratio $(L + \sqrt{\ })/(L + \sqrt{\ })$ clearly approaches 1, but the second ratio, $(-L + \sqrt{\ })/(-L + \sqrt{\ })$, takes on an indeterminate value, and we must therefore study it more carefully. We can write

$$\frac{-L + \sqrt{L^2 + r_2^2}}{-L + \sqrt{L^2 + r_1^2}} = \frac{-1 + [1 + (r_2/L)^2]^{1/2}}{-1 + [1 + (r_1/L)^2]^{1/2}}$$

$$= \frac{-1 + [1 + \frac{1}{2}(r_2/L)^2 + \cdots]}{-1 + [1 + \frac{1}{2}(r_1/L)^2 + \cdots]} = \left(\frac{r_2}{r_1}\right)^2 + \cdots$$

(terms which vanish with increasing $L$)

For $L \to \infty$, Eq. (6-43) therefore takes on the limit value

$$v_P = \frac{Q}{4\pi\varepsilon_0} \ln \left[ 1 \left(\frac{r_2}{r_1}\right)^2 \right] = \frac{Q}{2\pi\varepsilon_0} \ln \frac{r_2}{r_1} \quad \text{V} \qquad (6\text{-}44)$$

We make several important observations in regard to this result:

1. The potential $v_P$ is constant along contours for which the ratio $r_2/r_1$ is unchanging. From an important geometrical rule we know that these contours are the so-called *harmonic* circles, a few of which are sketched in Fig. 6-12. The *equipotential surfaces* (i.e., surfaces of same potential) thus are cylinders. (The electric *field* lines are orthogonal to the equipotential surfaces. They are also circles, some of which are shown dotted in Fig. 6-12.)
2. In close proximity to the line charges, the ratio $r_2/r_1$ is either very large or very small. Consider, for example, the immediate neighborhood of the positive wire. The ratio is now very large, and since we can write

$$\frac{r_2}{r_1} \approx \frac{D}{r_1} \qquad (D = \text{distance between wires})$$

we realize that $v_P$ depends, approximately, only upon $r_1$, and *the equipotential surfaces adjacent to the conductor therefore form concentric cylinders with centers in the wire.* In Fig. 6-12 we have drawn in boldface one such surface of radius $r_1 = R_1$.



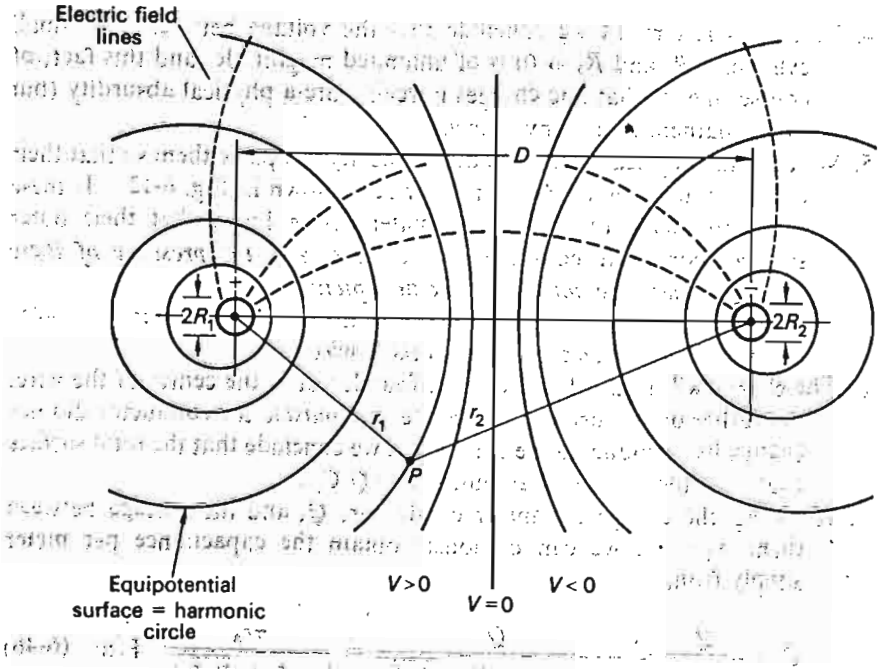


**Fig. 6-12** Electric field and potential picture around a single-phase transmission line.

In the immediate neighborhood of the negative line charge we have

$$\frac{r_2}{r_1} \approx \frac{r_2}{D}$$

and we conclude that, even here, the equipotential surfaces have the above-indicated features. In Fig. 6-12 we show one of radius $r_2 = R_2$.

3. The potential $v_1$ on the cylinder of radius $R_1$ equals, in accordance with Eq. (6-44),

$$v_1 \approx \frac{Q}{2\pi\varepsilon_0} \ln \frac{D}{R_1}$$

Likewise, for the potential $v_2$ on the cylinder of radius $R_2$, we have

$$v_2 \approx \frac{Q}{2\pi\varepsilon_0} \ln \frac{R_2}{D}$$

The potential *difference* between these two cylindrical surfaces is therefore

$$v_1 - v_2 \approx \frac{Q}{2\pi\varepsilon_0} \left( \ln \frac{D}{R_1} - \ln \frac{R_2}{D} \right) \approx \frac{Q}{\pi\varepsilon_0} \ln \frac{D}{\sqrt{R_1 R_2}} \qquad (6\text{-}45)$$

4. From this last result we conclude that the voltage between very small cylinders ($R_1$ and $R_2 \to 0$) is of unlimited magnitude, and this fact, of course, means that line charges in reality are a physical absurdity (but still a mathematical convenience).
5. We can take physical wires of radii $R_1$ and $R_2$ and place them so that their outer surfaces coincide with the surfaces shown in Fig. 6-12. If these wires are made of conducting material, we know that their outer surfaces constitute equipotential surfaces, and *the presence of these wires will therefore not change the field picture.*

   *We draw from this fact the important conclusion that Eq.* (6-45) *indeed tells us the voltage between these wires.*
6. The charge will in this latter case be found, not in the center of the wire, but rather on its surface. Since the field *outside* the conductor did not change by introducing the conductor, we conclude that the total surface charge of the wires still amounts to $\pm Q$ C/m.
7. Knowing the charge per meter conductor, $Q$, and the voltage between them, $v_1 - v_2$, we can obviously obtain the capacitance per meter simply from

$$C_\ell \triangleq \frac{Q}{v_1 - v_2} = \frac{Q}{(Q/\pi\varepsilon_0)\ln(D/\sqrt{R_1R_2})} = \frac{\pi\varepsilon_0}{\ln(D/\sqrt{R_1R_2})} \quad \text{F/m} \quad (6\text{-}46)$$

If the conductors have equal radii, $R = R_1 = R_2$, then the formula for the line capacitance will simply be

$$C = \frac{\pi\varepsilon_0}{\ln(D/R)} \quad (6\text{-}47)$$

**Example 6-4** To get a feel for the magnitudes involved, consider a single-phase transmission line characterized by

$D = 10$ ft

$R = 0.5$ in.

Its capacitance will be

$$C = \frac{\pi 8.85 \times 10^{-12}}{\ln 240} = 5.07 \times 10^{-12} \text{ F/m}$$

(or $8.13 \times 10^{-9}$ F/mile)

Assume that the line is operated at 100 kV and 60 Hz. It will then have a total capacitive shunt *reactance* of

$$X_c = \frac{1}{\omega C} = \frac{1}{377 \times 8.13 \times 10^{-9}} = 3.27 \times 10^5 \ \Omega\text{/mile}$$



At the assumed operating voltage the line will take a "charging" current of

$$\frac{100 \times 10^3}{3.27 \times 10^5} = 0.306 \text{ A/mile}$$

and it will *generate* reactive power $Q$ in the amount of†

$$Q = \frac{|V|^2}{X_c} = \frac{10^{10}}{3.27 \times 10^5} = 30{,}600 \text{ vars/mile or } 30.6 \text{ kvar/mile}$$

**Influence of earth** The field picture in Fig. 6-12 is valid only if the two wires are far removed from any other conductors, particularly the surface of earth. The presence of earth will change the electric flux lines and equipotential surfaces considerably, which in effect will change the effective capacitance between the wires. Since in the case of normal power lines the distances between the phases and between phases and ground are of the same order of magnitude, these effects cannot be neglected. If the two conductors in Fig. 6-12 are placed over ground, the changes in the electric field picture are as demonstrated in Figure 6-13. Note that the equipotential surfaces no longer are cylinders.

It turns out that the effect of the presence of ground can be accounted for in a very simple way by means of so-called *image charges*. These

† There is an unfortunate "symbol collision" between line charge $Q$ and reactive power $Q$, which should not be confused.

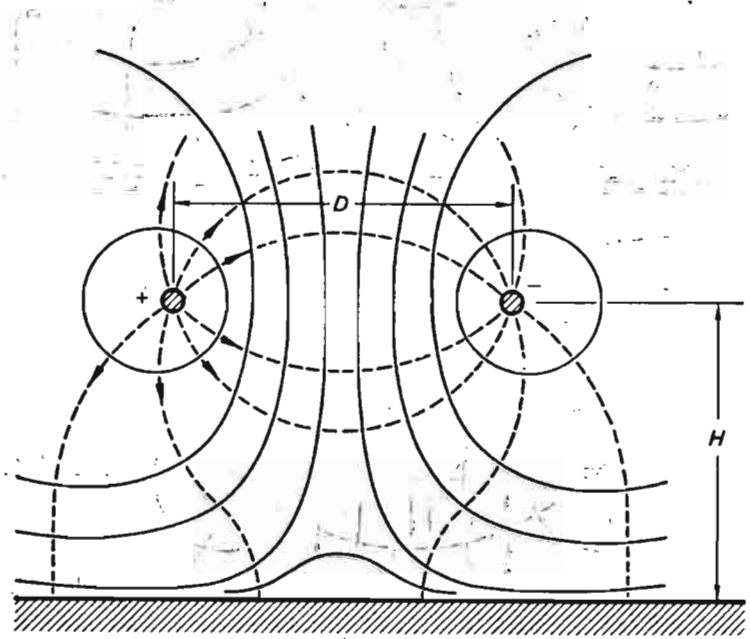


**Fig. 6-13** Disturbance of field picture in Fig. 6-12 due to presence of ground.

*imaginary* charges are of the same magnitude as the actual physical charges, but of opposite sign, and placed as far underground as the actual charges are placed overhead. The situation is depicted in Fig. 6-14. In making use of this concept the following steps should be followed:

1. Place the image charges in proper location.
2. Remove the ground. Actual and image charges are now surrounded by air.
3. Compute the potential in a general point $P$ by adding the contributions from *both* the actual and image charges. (How this is actually accomplished will be shown in the next section.)

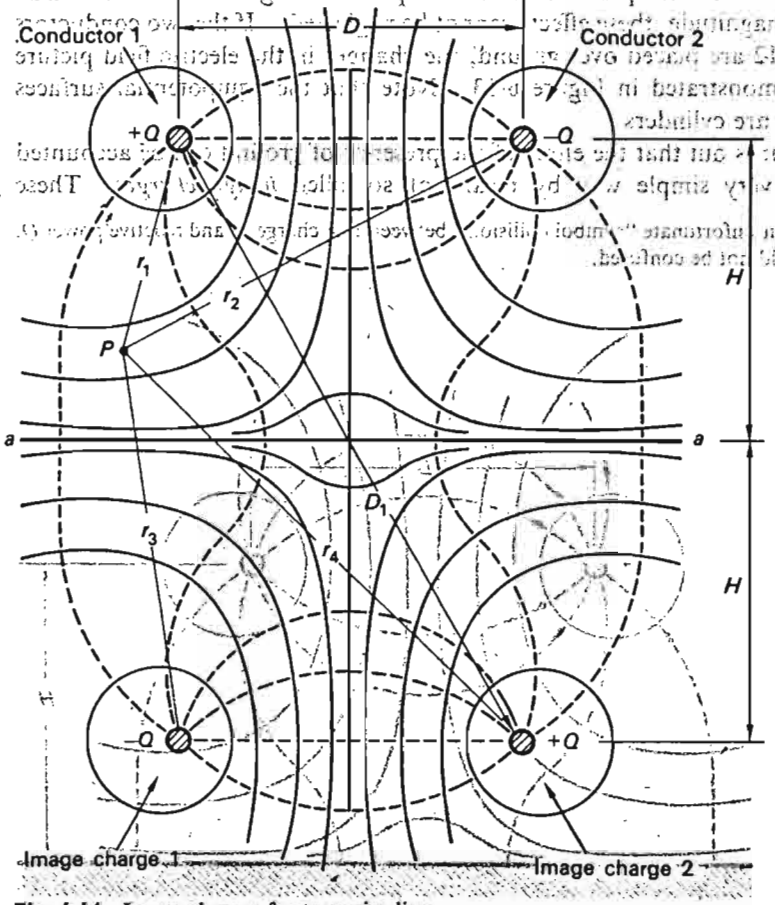


**Fig. 6-14** Image charges for two-wire line.



4. The potential as computed in step 3 will, *for any point above the ground level*, be identical with the *actual* potential caused by the two actual charges plus the ground.

The proof of the validity of the above method is very simple.

The ground level is an equipotential surface in Fig. 6-13. In Fig. 6-14 the level *aa* is likewise an equipotential surface, for *symmetry*. In addition, the conductor configuration above the ground level being identical in both cases, the field configurations *above* this level *must* be the same, since there cannot be two different fields satisfying these same boundary conditions.†

**Capacitance of multiple conductor lines** If the effect of ground is taken into account, the two-wire problem evidently grows into a four-wire problem. Computing the capacitance for a three-phase line is clearly a three-wire problem, and if the effect of ground must be taken into account, a six-wire problem (including the three image charges). There is clearly a need here to expand our two-wire theory to include $n$ parallel long conductors.

We remember that the line-inductance derivations valid for a single-phase line could be extended to an $n$-wire line by introduction of the concepts of "apparent self-inductance and mutual inductance." We can likewise extend our single-phase capacitance derivations to the $n$-wire case by use of similar concepts.

The potential $v_P$ resulting from the two line charges $+Q$ and $-Q$ can, in accordance with Eq. (6-44), be written

$$v_P = \frac{Q}{2\pi\varepsilon_0} \ln \frac{1}{r_1} + \frac{-Q}{2\pi\varepsilon_0} \ln \frac{1}{r_2} \tag{6-48}$$

The two individual terms in this expression are referred to as *logarithmic potentials*‡ and can be viewed as the individual contributions by each line charge to the total potential in point $P$.

We now consider a system of $n$ parallel and very long conductors that carry the line charges $Q_1, Q_2, \ldots, Q_n$ C/m, respectively. A point $P$ having the distances $r_1, r_2, \ldots, r_n$ to the conductors in question has a potential $v_P$ that contains contributions from each line charge, in accordance with the formula

$$v_P = \sum_{\nu=1}^{n} \frac{Q_\nu}{2\pi\varepsilon_0} \ln \frac{1}{r_\nu} \tag{6-49}$$

† As is known from the theory of electric fields, the Laplace differential equation

$$\Delta V = 0$$

has *one* solution only for given boundary conditions.

‡ Note that the logarithmic potential thus defined is characterized by the same error of dimension as we found in the case of "apparent inductance." As, in reality, the line charges *always* appear in pairs, this dimensionality error will automatically disappear.

It is understood that the algebraic sum of all the line charges, including those of the image charges, equals zero; i.e.,

$$\sum_{\nu=1}^{n} Q_\nu = 0 \tag{6-50}$$

If this were not true, we would have (because of the infinite length of the conductors) an infinite surplus of charge, which is physically impossible.

**Example 6-5** In our first example on use of logarithmic potentials we shall recompute the capacitance of a single-phase line, taking account of the effect of ground. In the following analysis the symbols refer to those given in Fig. 6-14.

In accordance with Eq. (6-49), and by obeying rules 3 and 4 with respect to using the image charges, we obtain the following expression for the potential in a point $P$ *above* ground level:

$$v_P = \frac{Q}{2\pi\varepsilon_0}\ln\frac{1}{r_1} + \frac{-Q}{2\pi\varepsilon_0}\ln\frac{1}{r_2} + \frac{-Q}{2\pi\varepsilon_0}\ln\frac{1}{r_3} + \frac{Q}{2\pi\varepsilon_0}\ln\frac{1}{r_4} \tag{6-51}$$

If, in particular, the point $P$ is chosen on the surface of conductor 1, the potential $v_P$ will equal $v_1$, and we get

$$v_1 = \frac{Q}{2\pi\varepsilon_0}\ln\frac{1}{R} - \frac{Q}{2\pi\varepsilon_0}\ln\frac{1}{D} - \frac{Q}{2\pi\varepsilon_0}\ln\frac{1}{2H} + \frac{Q}{2\pi\varepsilon_0}\ln\frac{1}{D_1} \tag{6-52}$$

If $P$ is moved to the surface of conductor 2, we have

$$v_2 = \frac{Q}{2\pi\varepsilon_0}\ln\frac{1}{D} - \frac{Q}{2\pi\varepsilon_0}\frac{1}{R} - \frac{Q}{2\pi\varepsilon_0}\ln\frac{1}{D_1} + \frac{Q}{2\pi\varepsilon_0}\ln\frac{1}{2H} \tag{6-53}$$

We thus get, after some algebra,

$$v_1 - v_2 = \frac{Q}{\pi\varepsilon_0}\ln\left(\frac{D}{R}\frac{2H}{D_1}\right) \tag{6-54}$$

and finally, for the capacitance,

$$C = \frac{Q}{v_1 - v_2} = \frac{\pi\varepsilon_0}{\ln\left(\dfrac{D}{R}\dfrac{2H}{D_1}\right)} \quad \text{F/m} \tag{6-55}$$

The result should be compared with Eq. (6-47). Since $2H < D_1$, it is clear that the proximity to ground has resulted in an *increase* of the line capacitance.† Let us see the numerical effect by considering the line discussed in Example 6-4. We shall assume that the distance above ground, $H$, equals the spacing between the conductors; i.e., we have

$$H = D$$

† The reader should ask himself why, on physical ground, we get an increase.



and

$$D_1 = \sqrt{D^2 + 4H^2} = \sqrt{5D^2} = \sqrt{5}D$$

Since we had, in Example 6-4,

$$\frac{D}{R} = 240$$

we now obtain

$$C = \frac{\pi\varepsilon_0}{\ln(240 \times 2/\sqrt{5})} = \frac{\pi 8.85 \times 10^{-12}}{5.37} = 5.18 \times 10^{-12} \text{ F/m}$$

The presence of ground has thus resulted in a 2.2 percent increase of the capacitance.†

**Example 6-6** In our second example we consider the practically very important case of finding the line capacitance of a three-phase line. We shall choose the same conductor configuration as we used previously, in Example 6-2, to study the line inductance. The line with its image charges is shown in Fig. 6-15. We shall distinguish between the transposed and the untransposed cases.

† The relatively insignificant effect of the presence of earth demonstrated by this example gives us a good excuse to neglect it on occasion.

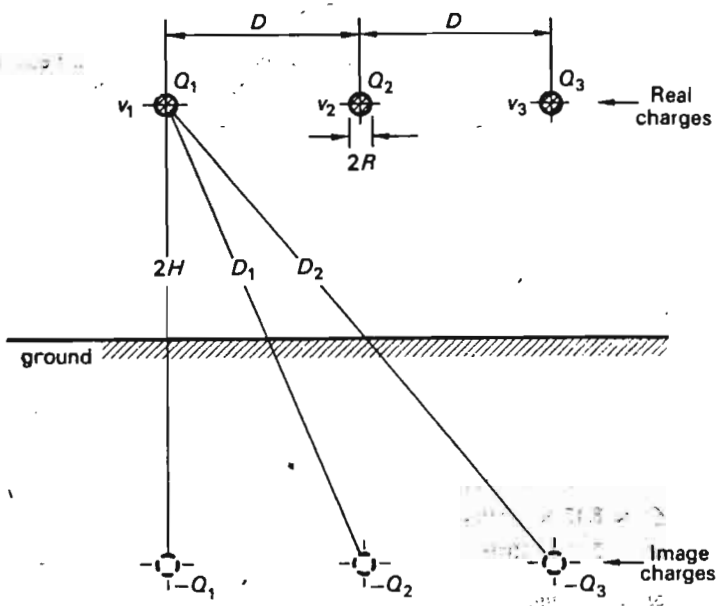


**Fig. 6-15** A three-phase transmission line with its image charges.

*Case I. Line untransposed* If the potentials of the three conductors relative to ground are in order $v_1$, $v_2$, and $v_3$, we obtain, by using the method of logarithmic potentials,

$$v_1 = \frac{Q_1}{2\pi\varepsilon_0}\ln\frac{2H}{R} + \frac{Q_2}{2\pi\varepsilon_0}\ln\frac{D_1}{D} + \frac{Q_3}{2\pi\varepsilon_0}\ln\frac{D_2}{2D}$$

$$v_2 = \frac{Q_1}{2\pi\varepsilon_0}\ln\frac{D_1}{D} + \frac{Q_2}{2\pi\varepsilon_0}\ln\frac{2H}{R} + \frac{Q_3}{2\pi\varepsilon_0}\ln\frac{D_1}{D} \qquad (6\text{-}56)$$

$$v_3 = \frac{Q_1}{2\pi\varepsilon_0}\ln\frac{D_2}{2D} + \frac{Q_2}{2\pi\varepsilon_0}\ln\frac{D_1}{D} + \frac{Q_3}{2\pi\varepsilon_0}\ln\frac{2H}{R}$$

Distances $D_1$, $D_2$, and $H$ are defined in Fig. 6-15.

Since it would be very unwieldy to work in general dimensions in our continued analysis, we shall at this point introduce numerical values, as follows:

$R = 0.5$ in.

$D = 20$ ft $= 240$ in.

$2H = 50$ ft

$D_1 = \sqrt{(50)^2 + (20)^2} = 53.8$ ft

$D_2 = \sqrt{(50)^2 + (40)^2} = 64.0$ ft

For these numerical values we can write Eq. (6-56) in the form

$$\begin{bmatrix} v_1 \\ v_2 \\ v_3 \end{bmatrix} = 1.8 \times 10^{10} \begin{bmatrix} 7.10 & 0.99 & 0.47 \\ 0.99 & 7.10 & 0.99 \\ 0.47 & 0.99 & 7.10 \end{bmatrix} \begin{bmatrix} Q_1 \\ Q_2 \\ Q_3 \end{bmatrix} \qquad (6\text{-}57)$$

It will prove useful to solve for the charges in this last equation (which can be done most effectively by inverting the matrix). We obtain

$$\begin{bmatrix} Q_1 \\ Q_2 \\ Q_3 \end{bmatrix} = 10^{-12} \begin{bmatrix} 7.98 & -1.06 & -0.38 \\ -1.06 & 8.12 & -1.06 \\ -0.38 & -1.06 & 7.98 \end{bmatrix} \begin{bmatrix} v_1 \\ v_2 \\ v_3 \end{bmatrix} \qquad (6\text{-}58)$$

or in matrix form,

$$\mathbf{Q} = \mathbf{C}\mathbf{v}$$

where C is the "capacitance matrix" of the line.

We make the important observation that the *diagonal* elements of the matrices in both Eqs. (6-57) and (6-58) are *dominating*, which means that we can write, *approximately*,

$$\begin{aligned} Q_1 &\approx 7.98 \times 10^{-12} v_1 \\ Q_2 &\approx 8.12 \times 10^{-12} v_2 \\ Q_3 &\approx 7.98 \times 10^{-12} v_3 \end{aligned} \qquad (6\text{-}59)$$

or after a slight "averaging,"

$$Q_\nu \approx 8.03 \times 10^{-12} v_\nu \qquad \text{for } \nu = 1, 2, 3 \qquad (6\text{-}60)$$



By differentiating these last equations and taking note of the fact that the time derivative $dQ/dt$ is identical with the "charging current" expressed in amperes per meter line, we obtain

$$i_\nu = \frac{dQ_\nu}{dt} \approx 8.03 \times 10^{-12}\frac{dv_\nu}{dt} \qquad \text{A/m line} \qquad \text{for } \nu = 1, 2, 3 \qquad (6\text{-}61)$$

In our case we are particularly interested in *sinusoidal* phenomena, so we make the usual introductions to phasors:

$i_\nu \to I_\nu$

$v_\nu \to V_\nu$

and

$$\frac{d}{dt} \to j\omega = j377$$

By substitution into Eq. (6-61),

$$I_\nu \approx j377 \times 8.03 \times 10^{-12} V_\nu \approx j3.03 \times 10^{-9} V_\nu \qquad \text{A/m} \qquad \text{for } \nu = 1, 2, 3 \qquad (6\text{-}62)$$

or

$$I_\nu \approx j4.9 \times 10^{-6} V_\nu \qquad \text{A/mile} \qquad \text{for } \nu = 1, 2, 3$$

The fact that we have been able, albeit approximately, to write the current in each phase proportional to the voltage (as measured to ground) of that phase alone means that we can treat each phase individually; i.e., we can analyze the situation on a per-phase basis.

We can write Eq. (6-62)

$$\frac{V_\nu}{I_\nu} \approx \frac{1}{j\omega 8.03 \times 10^{-12}} \triangleq \frac{1}{j\omega C}, \qquad \text{for } \nu = 1, 2, 3 \qquad (6\text{-}63)$$

where

$$C \triangleq 8.03 \times 10^{-12}$$

represents the shunt capacitance expressed in farads per meter and phase of the transmission line.

To get a feel for the magnitudes involved, let us consider a 220-kV transmission line. The voltage per phase would then be $220/\sqrt{3} = 127$ kV. From Eq. (6-62) we would obtain a charging current of

$|I| = 4.9 \times 0.127 = 0.62$ A/mile and phase

If operated at this voltage, the line would *generate*

$0.62 \times 127 = 79$ kvar/phase and mile

or

$3 \times 79 = 237$ kvar/mile total three-phase

*Case II. Line transposed* For completeness we shall also consider the above line transposed. We shall assume the particular transposition shown earlier in Fig. 6-9*b*. Equations (6-57) and (6-58) are now valid for line section I only. The corresponding

equations for sections II and III are obtained simply by changing the subscripts in the columa vectors v and Q to correspond with the transposition. Summarizing the results,

$$\begin{bmatrix} Q_1^{\mathrm{I}} \\ Q_2^{\mathrm{I}} \\ Q_3^{\mathrm{I}} \end{bmatrix} = \mathbf{C} \begin{bmatrix} v_1 \\ v_2 \\ v_3 \end{bmatrix} \quad \text{for section I}$$

$$\begin{bmatrix} Q_2^{\mathrm{II}} \\ Q_1^{\mathrm{II}} \\ Q_3^{\mathrm{II}} \end{bmatrix} = \mathbf{C} \begin{bmatrix} v_3 \\ v_1 \\ v_2 \end{bmatrix} \quad \text{for section II} \qquad (6\text{-}64)$$

$$\begin{bmatrix} Q_3^{\mathrm{III}} \\ Q_2^{\mathrm{III}} \\ Q_1^{\mathrm{III}} \end{bmatrix} = \mathbf{C} \begin{bmatrix} v_2 \\ v_3 \\ v_1 \end{bmatrix} \quad \text{for section III}$$

C in these formulas is the earlier defined capacitance matrix of the line. The superscripts in these formulas refer to the three line sections, respectively. Note that there is no need for superscripts for the phase voltages since they are the same in all sections.

Let us study the expressions for $Q_1^{\mathrm{I}}$, $Q_1^{\mathrm{II}}$, and $Q_1^{\mathrm{III}}$, that is, the line charges belonging to phase 1. From the above equations we get

$$\begin{aligned} 10^{12}Q_1^{\mathrm{I}} &= 7.98v_1 - 1.06v_2 - 0.38v_3 \\ 10^{12}Q_1^{\mathrm{II}} &= -1.06v_3 + 8.12v_1 - 1.06v_2 \\ 10^{12}Q_1^{\mathrm{III}} &= -0.38v_2 - 1.06v_3 + 7.98v_1 \end{aligned} \qquad (6\text{-}65)$$

and upon summing these equations we get

$$10^{12}(Q_1^{\mathrm{I}} + Q_1^{\mathrm{II}} + Q_1^{\mathrm{III}}) = (7.98 + 8.12 + 7.98)v_1 - 2.50(v_2 + v_3) \qquad (6\text{-}66)$$

In a *balanced* three-phase system we have

$$v_1 + v_2 + v_3 = 0$$

and eliminating $(v_2 + v_3)$ from Eq. (6-66) by using this last equation, we finally get

$$\frac{Q_1^{\mathrm{I}} + Q_1^{\mathrm{II}} + Q_1^{\mathrm{III}}}{3} = 8.86 \times 10^{-12}v_1 \qquad (6\text{-}67)$$

The left side of Eq. (6-67) represents the *average* value, $Q_{1,\mathrm{av}}$, of the line charge per meter in phase 1, and we therefore have

$$Q_{1,\mathrm{av}} = 8.86 \times 10^{-12}v_1 \qquad (6\text{-}68)$$

Identical equations can easily be derived for phases 2 and 3.

The *exact* equation (6-68) should be compared with the *approximate* equation (6-60) that we arrived at for the untransposed line.

The transposition has resulted in a complete "decoupling" of the phases, and whereas we suggested an approximate per-phase capacitance in the untransposed case, we can now with confidence work with an *exact* value. From Eq. (6-68) we have

$C = 8.86 \times 10^{-12}$ F/m and phase



The student should compare carefully the similar situations that existed with respect to line inductance in the transposed and untransposed cases.

## 6-4 LONG-LINE THEORY

The line parameters presented in preceding sections were derived on a per-phase basis and were obtained per meter or mile of the line. It would seem reasonable, therefore, if we are interested in the performance of a specific line of length $l$, simply to multiply these parameters by the actual line length in order to obtain the total parameter values for the line. This can indeed be done, up to a certain limit value of $l$. Beyond this value the accuracy of this procedure becomes impaired because of our neglect of the *distributed* effect of the parameters.

In this section we shall study this "distribution effect" of the line. We shall develop exact models for lines of arbitrary length, and also approximate models valid under specified conditions. We start out with a compilation of the assumptions used in subsequent analysis:

1. The transmission line is assumed transposed. The formulas and models derived may, however, be used even for untransposed lines if a certain approximation is tolerated.
2. The line is assumed operated with voltages and currents satisfying conditions $\sum_{p=1}^{3} v_p = 0$ and $\sum_{p=1}^{3} i_p = 0$ respectively.
3. All *time* variations of variables are assumed *sinusoidal*.

The reason for the first two assumptions is that they permit us to analyze the line on a per-phase basis. As we remember, only if these two conditions are satisfied is it possible to define in accurate fashion per-phase values of inductance and capacitance.

### 6-4.1 LONG-LINE EQUATIONS

Figure 6-16 depicts a differential section of our transmission line. On the basis of previously made assumptions, we consider one phase of the line and

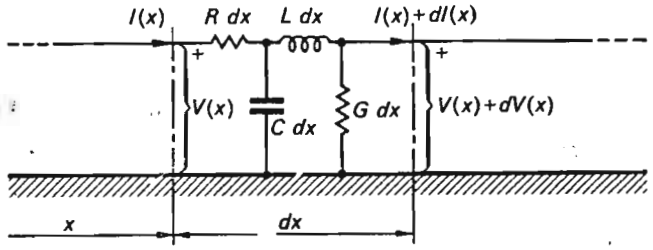


**Fig. 6-16** Differential line element.

conclude that the section has a series impedance of

$$dZ = (R + j\omega L)\,dx \qquad \Omega/\text{phase}$$

and a shunt admittance of

$$dY = (G + j\omega C)\,dx \qquad \mho/\text{phase}$$

The voltage (measured from phase to ground) and current phasors at the distance coordinate $x$ equal $V(x)$ and $I(x)$, respectively. At the other end of the element, they have grown to $V(x) + dV(x)$ and $I(x) + dI(x)$, respectively. The difference in voltage and current must be due to the voltage drop over $dZ$ and the current leakage through $dY$, respectively, and expressing this mathematically, we have

$$\begin{aligned} V(x) - [V(x) + dV(x)] &= dZ\,I(x) \\ I(x) - [I(x) + dI(x)] &= dY\,V(x) \end{aligned} \tag{6-69}$$

or, upon substitution of $dZ$ and $dY$,

$$\begin{aligned} \frac{dV(x)}{dx} &= -(R + j\omega L)I(x) \\ \frac{dI(x)}{dx} &= -(G + j\omega C)V(x) \end{aligned} \tag{6-70}$$

By separation of variables we obtain the following "long-line" differential equations for $V(x)$ and $I(x)$:

$$\begin{aligned} \frac{d^2V(x)}{dx^2} &= (R + j\omega L)(G + j\omega C)V(x) \\ \frac{d^2I(x)}{dx^2} &= (R + j\omega L)(G + j\omega C)I(x) \end{aligned} \tag{6-71}$$

We introduce at this juncture the *propagation constant* $\gamma$ and *wave* (or *characteristic*) *impedance* $Z_w$, defined as follows:

$$\begin{aligned} Z_w &\triangleq \sqrt{\frac{R + j\omega L}{G + j\omega C}} \qquad (\text{dimension} = \text{ohms}) \\ \gamma &\triangleq \sqrt{(R + j\omega L)(G + j\omega C)} \qquad (\text{dimension} = \text{m}^{-1}) \end{aligned} \tag{6-72}$$

We can now write the differential equations (6-71) in shorter form.

$$\begin{aligned} \frac{d^2V}{dx^2} &= \gamma^2 V \\ \frac{d^2I}{dx^2} &= \gamma^2 I \end{aligned} \tag{6-73}$$



Before we attempt to solve these equations, we shall comment briefly on the question of *initial*, or *boundary*, *conditions*. Equations (6-70) are two first-order coupled ordinary differential equations. Therefore we have a right to specify *two* independent "initial" conditions for $V(x)$ and/or $I(x)$.† We could choose these in an *infinite* number of ways. For example, we may settle for any two of the following pairs:

$$\begin{aligned} &V(0), I(0) \\ &V(0), V(l) \\ &V(l|2), I(l) \\ &I(l), I(l|2) \end{aligned} \tag{6-74}$$

We shall find it particularly useful to choose combinations of the *end-point* values $V(0)$, $V(l)$, $I(0)$, and $I(l)$.

In reality, we are of course basically interested in the magnitudes of the real and reactive *powers* along the line. These powers are obtained directly from $V(x)$ and $I(x)$ by the usual formula

$$P(x) + jQ(x) = S(x) = V(x)\,I^*(x)$$

Equations (6-73) are easily integrated. The reader can, by back substitution, convince himself that the general solutions are of the form

$$\begin{aligned} V(x) &= A \cosh \gamma x + B \sinh \gamma x \\ I(x) &= C \cosh \gamma x + D \sinh \gamma x \end{aligned} \tag{6-75}$$

Of the integration constants $A$, $B$, $C$, and $D$, only two can be chosen independently, for reasons stated above. Let us, for example, choose the first pair of the boundary conditions (6-74). Then, by setting $x = 0$, we obtain from Eqs. (6-75)

$$\begin{aligned} V(0) &= A \cdot 1 + B \cdot 0 \\ I(0) &= C \cdot 1 + D \cdot 0 \end{aligned}$$

Hence

$$\begin{aligned} A &= V(0) \\ C &= I(0) \end{aligned} \tag{6-76}$$

† We are tempted to conclude that because Eqs. (6-73) represent two coupled second-order ordinary differential equations, we have a right to assign *four* initial conditions. What is the fallacy in this thinking?

We can also find the constants $B$ and $D$ by substituting Eqs. (6-75) into (6-70) and then letting $x = 0$. These operations yield

$$B = -Z_w I(0)$$
$$D = -\frac{V(0)}{Z_w} \tag{6-77}$$

In terms of $V(0)$ and $I(0)$, our solutions thus are

$$V(x) = V(0)\cosh \gamma x - Z_w I(0)\sinh \gamma x$$
$$I(x) = I(0)\cosh \gamma x - \frac{V(0)}{Z_w}\sinh \gamma x \tag{6-78}$$

If $V(0)$ and $I(0)$ are assumed known, then these equations permit us to compute the currents and voltages, and thus the real and reactive powers all along the line.

### 6-4.2 COMPUTATIONAL CONSIDERATIONS

In using the above equations we must realize that, generally, both $\gamma$ and $Z_w$ are complex numbers. For computational purposes it is helpful to express $Z_w$ and $\gamma$ in terms of the *real* line parameters, defined as follows:

$$Z_w \triangleq R_w + jX_w \tag{6-79}$$
$$\gamma \triangleq \alpha + j\beta \tag{6-80}$$

For a typical high-energy transmission line we usually have

$$G \approx 0 \tag{6-81}$$

and

$$R \ll \omega L \tag{6-82}$$

In view of Eq. (6-81), $Z_w$ and $\gamma$ take on the following values:

$$Z_w = \sqrt{\frac{R + j\omega L}{j\omega C}} = \sqrt{\frac{L}{C}}\left(1 - j\frac{R}{\omega L}\right)^{1/2} = \sqrt{\frac{L}{C}}\left(1 - j\frac{R}{2\omega L} \cdots\right)$$

$$\gamma = \sqrt{(R + j\omega L)\, j\omega C} = j\omega\sqrt{LC}\left(1 - j\frac{R}{\omega L}\right)^{1/2}$$

$$= j\omega\sqrt{LC}\left(1 - j\frac{R}{2\omega L} \cdots\right)$$



If we then make use of the inequality (6-82), we have

$$Z_w = R_w + jX_w \approx \sqrt{\frac{L}{C}}\left(1 - j\frac{R}{2\omega L}\right)$$
$$\gamma = \alpha + j\beta \approx j\omega\sqrt{LC}\left(1 - j\frac{R}{2\omega L}\right) \tag{6-83}$$

Thus

$$R_w \approx \sqrt{\frac{L}{C}}$$
$$X_w \approx -\frac{1}{2}\frac{R}{\omega\sqrt{LC}}$$
$$\alpha \approx \frac{R}{2\omega}\sqrt{\frac{C}{L}} \tag{6-84}$$
$$\beta \approx \omega\sqrt{LC}$$

The hyperbolic sines and cosines of the complex argument $\gamma x$ can be separated into real and imaginary parts by use of the formulas

$$\cosh \gamma x = \cosh(\alpha + j\beta)x = \cosh \alpha x \cos \beta x + j \sinh \alpha x \sin \beta x$$
$$\sinh \gamma x = \sinh(\alpha + j\beta)x = \sinh \alpha x \cos \beta x + j \cosh \alpha x \sin \beta x \tag{6-85}$$

As will be demonstrated in examples, the argument $\alpha x$ will, as a rule, be considerably less than unity (due to the relatively small resistance in high-power lines), and we can therefore, with sufficient accuracy, approximate the hyperbolic functions with the first two terms in the series:

$$\sinh \alpha x = \alpha x + \frac{(\alpha x)^3}{6} + \cdots$$
$$\cosh \alpha x = 1 + \frac{(\alpha x)^2}{2} + \cdots \tag{6-86}$$

**Example 6-7** We shall consider the transposed three-phase line for which we earlier computed the inductance and capacitance, in Examples 6-2 and 6-6. As we remember, the line consisted of 1-in. conductors per phase, with a spacing between the conductors of 20 ft. The line parameters were computed as follows:

$L = 1.33 \times 10^{-6}$ H/m and phase
$C = 8.86 \times 10^{-12}$ F/m and phase

From manufacturers' tables we also had found the resistance

$R = 0.93 \times 10^{-4}\Omega$/m and phase

We shall neglect the shunt conductance and therefore set $G = 0$.

The line is operated at a sending-end voltage of 220 kV and a sending-end power of $S(0) = 150 + j50$. We wish to find the voltage and power at the receiving end of the line, which is assumed 300 km (≈ 190 miles) long.

We first compute $Z_w$ and $\gamma$.

$$Z_w = \sqrt{\frac{0.93 \times 10^{-4} + j377 \times 1.33 \times 10^{-6}}{0 + j377 \times 8.86 \times 10^{-12}}} = 391e^{-j5°.3} = 389 - j36.1 \quad \Omega \tag{6-87}$$

$$\gamma = \sqrt{(0.93 \times 10^{-4} + j377 \times 1.33 \times 10^{-6})(0 + 377 \times 8.86 \times 10^{-12})}$$

$$= (0.118 + j1.30)10^{-6} \quad m^{-1} \tag{6-88}$$

For the given line length, $3 \times 10^5$ m, we then get

$$\gamma l = \alpha l + j\beta l = 3 \times 10^5(0.118 + j1.30)10^{-6} = 0.0354 + j0.390$$

We next compute the hyperbolic sines and cosines:

$$\sinh \gamma l = \sinh 0.0354 \cos 0.390 + j \cosh 0.0354 \sin 0.390 = 0.0327 + j0.380$$
$$\cosh \gamma l = \cosh 0.0354 \cos 0.390 + j \sinh 0.0354 \sin 0.390 = 0.925 + j0.0134$$

Before making use of Eqs. (6-78), we must first find $V(0)$ and $I(0)$ from given data. We choose $V(0)$ as our reference phasor, and since the sending-end voltage was given as 220 kV, we have

$$V(0) = \frac{220}{\sqrt{3}} = 127e^{j0} \quad \text{kV/phase}$$

Also, from the given power data,

$$\sqrt{3} \times 220 I^*(0) = 150 + j50$$

and hence

$$I(0) = \frac{150 - j50}{\sqrt{3} \times 220} = 0.394 - j0.132 = 0.415e^{-j18°.5} \quad \text{kA}$$

We now apply Eq. (6-78):

$$V(l) = 127(0.925 + j0.0134) - (389 - j36.1)(0.394 - j0.132)(0.0327 + j0.380)$$

$$I(l) = (0.394 - j0.132)(0.925 + j0.0134) - \frac{127}{389 - j36.1}(0.0327 + j0.380)$$

Upon performing the complex algebra called for in these equations, we obtain

$$V(l) = 87.5 - j52.4 = 102e^{-j30°.9} \quad \text{kV}$$

$$I(l) = 0.367 - j0.241 = 0.440e^{-j33°.3} \quad \text{kA}$$

We note that we have experienced a 20 percent voltage drop along the line. At the same time the current has actually *increased* about 6 percent. The student should contemplate the physical reason for this latter fact.

It is interesting to compute the complex power at the receiving end:

$$S(l) = 3V(l)I^*(l) = 3 \times 102 \times 0.440e^{j2°.4} = 135 + j5.7$$



Thus

$$P(l) = 135 \text{ MW}$$

and

$$Q(l) = 5.7 \text{ Mvar}$$

We have evidently lost 15 MW in real power and 44.3 Mvar in reactive power along the line. The transmission *efficiency* is therefore

$$\eta_{tr} = \frac{135}{150} \times 100 = 90\%$$

Note also that the loss of reactive power† would have been much greater if the line had not generated a considerable amount of reactive power in its shunt capacitance. The reader should estimate how much reactive power this line actually produces.

### 6-4.3 EQUIVALENT NETWORK OF LONG LINE

In Chaps. 4 and 5 we found that it is possible to represent generators and transformers by "equivalent" networks. This is also possible in the case of a transmission line. Consider the $\pi$ network in Fig. 6-17, consisting of one series branch $Z$ and two shunt branches $Y_1$ and $Y_2$. By inspection we write the relationships between the terminal voltages and currents for this network:

$$V(x) = V(0) - Z[I(0) - Y_1V(0)] \tag{6-89}$$

and for the currents:

$$I(x) = I(0) - Y_1V(0) - Y_2V(x) \tag{6-90}$$

Equation (6-89) can be written

$$V(x) = V(0)(1 + ZY_1) - ZI(0) \tag{6-91}$$

† In the line reactance.

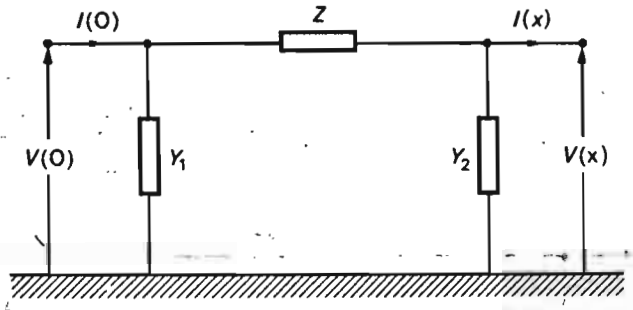


$$Z = Z_w \sinh \gamma x$$
$$Y_1 = Y_2 = \frac{1}{Z_w} \tanh \frac{\gamma x}{2}$$

**Fig. 6-17** Equivalent circuit of long line.

and Eq. (6-90), upon substitution of $V(x)$, changes to

$$I(x) = I(0)(1 + ZY_2) - V(0)(Y_1 + Y_2 + ZY_1Y_2) \tag{6-92}$$

If we compare this last pair of equations with Eqs. (6-78), we conclude that they can be made identical by setting

$$\begin{aligned} 1 + ZY_1 &= 1 + ZY_2 = \cosh \gamma x \\ Z &= Z_w \sinh \gamma x \\ Y_1 + Y_2 + ZY_1Y_2 &= \frac{1}{Z_w} \sinh \gamma x \end{aligned} \tag{6-93}$$

We readily confirm that these equations will be satisfied by choosing

$$\begin{aligned} Z &= Z_w \sinh \gamma x \\ Y_1 = Y_2 &= \frac{1}{Z_w} \frac{\cosh \gamma x - 1}{\sinh \gamma x} = \frac{1}{Z_w} \tanh \frac{\gamma x}{2} \end{aligned} \tag{6-94}$$

which parameter values therefore constitute the branch elements for the equivalent network.

**Example 6-8** Find the equivalent network for the 300-km line discussed in Example 6-7.

We had found $Z_w$ and the hyperbolic sines and cosines in our earlier computations. We repeat them here for easy reference:

$$Z_w = 389 - j36.1$$

$$\sinh \gamma l = 0.0327 + j0.380$$

$$\cosh \gamma l = 0.925 + j0.0134$$

From Eqs. (6-94) we thus get

$$\begin{aligned} Z &= (389 - j36.1)(0.0327 + j0.380) = 26.4 + j146.4 \quad \Omega \\ Y_1 = Y_2 &= \frac{0.925 + j0.0134 - 1}{(389 - j36.1)(0.0327 + j0.380)} \approx j5.11 \times 10^{-4} \quad \mho \end{aligned} \tag{6-95}$$

Clearly, the equivalent diagram, depicted in Fig. 6-18, will consist of a series branch containing a 26.4-Ω resistance and a 146.4-Ω reactance, and two shunt branches, each representing a 0.511-m℧ capacitor.

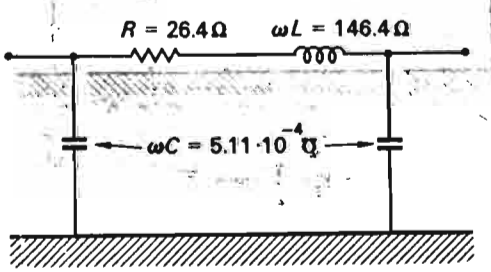


**Fig. 6-18** Equivalent circuit for line in Example 6-8.



### 6-4.4 THE LOSSLESS LINE

The reader will recall that it was possible in the case of synchronous machines and transformers to neglect the influence of the resistance and obtain network models which contain only *reactive* elements. As we have exemplified, high-energy transmission lines also have resistance values that are small compared with the line reactance. It is possible to expose some interesting features of the high-energy transmission line by considering the line *lossless:* i.e., we neglect the resistance altogether. By letting $R$ and $G$ approach zero, the wave impedance $Z_w$ takes on a purely real, and the propagation constant $\gamma$ a purely imaginary, value in accordance with

$$\begin{aligned} Z_w = R_w &= \sqrt{\frac{L}{C}} \\ \gamma = j\beta &= j\omega\sqrt{LC} \end{aligned} \tag{6-96}$$

For example, if we use these formulas to compute $Z_w$ and $\gamma$ in Example 6-7, we will obtain

$$Z_w = 387\ \Omega$$

and

$$\gamma = j1.29 \times 10^{-6}\ \text{m}^{-1}$$

By comparison with the exact values (6-87) and (6-88), we note how very good the approximations really are.

Since the argument $\gamma x$ is now purely imaginary, the hyperbolic functions in Eqs. (6-78) thus can be written

$$\begin{aligned} \cosh \gamma x &= \cos \beta x \\ \sinh \gamma x &= j \sin \beta x \end{aligned}$$

Equations (6-78) can therefore be put in the following form:

$$\begin{aligned} V(x) &= V(0) \cos \beta x - jR_w I(0) \sin \beta x \\ I(x) &= I(0) \cos \beta x - j \frac{V(0)}{R_w} \sin \beta x \end{aligned} \tag{6-97}$$

**Concept of wavelength** Equations (6-97) tell us a very interesting story:

*The voltage and current vary harmonically along the line with respect to the space coordinate $x$.*

A full voltage and current cycle along the line corresponds to a change in the angular argument, $\beta x$, of $2\pi$ rad. The length corresponding to one full cycle is referred to as the *wavelength* $\lambda$. The wavelength evidently is

obtained from the equality

$$\lambda = \frac{2\pi}{\beta} = \frac{2\pi}{\omega\sqrt{LC}} = \frac{1}{f\sqrt{LC}} \tag{6-98}$$

For example, at 60 Hz the line in Example 6-7 has a wavelength of

$$\lambda = \frac{1}{60\sqrt{1.33 \times 10^{-6} \times 8.86 \times 10^{-12}}} = 4.88 \times 10^{6} \text{ m}$$

(or 3000 miles, approx.)

**Equivalent network for lossless line** The equivalent network for the lossless line is readily obtained from the general network in Fig. 6-17. As seen in Fig. 6-19, all branch elements are purely reactive. The reader will note that in this diagram the argument $\beta x$ has been replaced with the expression

$$\beta x = \frac{x}{\lambda} 2\pi \tag{6-99}$$

which is obtained directly from Eq. (6-98).

Note that the shunt admittance is of the form

$$Y = jB$$

where $B$ is positive for $\tan (x\pi/\lambda) > 0$.

This means, in effect, that the admittance is *capacitive* for $x < \lambda/2$.

The series reactance is of the form

$$Z = jX$$

and is obviously *inductive* for

$$\sin \frac{x2\pi}{\lambda} > 0 \qquad \text{i.e., for } x < \frac{\lambda}{2}$$

When the line length exceeds half a wavelength (about 1500 miles at 60 Hz), the series reactance turns capacitive, and the shunt admittance

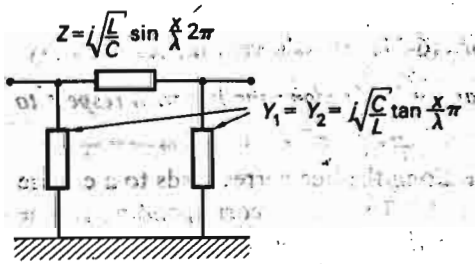


**Fig. 6-19** Equivalent circuit for lossless long line.



inductive. In reality, all our transmission lines in present use are actually shorter than a quarter wavelength ($\approx$ 750 miles).

**Concept of electrically short line** If the line is sufficiently short, the magnitude of the factor $x/\lambda$ is so small that we can set with good accuracy

$$\sin \frac{x}{\lambda} 2\pi \approx \frac{x}{\lambda} 2\pi$$

$$\tan \frac{x}{\lambda} \pi \approx \frac{x}{\lambda} \pi$$

The impedance and admittance elements of Fig. 6-19 can then be written

$$Z = j\sqrt{\frac{L}{C}} \sin \frac{x}{\lambda} 2\pi \approx j\sqrt{\frac{L}{C}} \frac{x}{\lambda} 2\pi = j\omega L x$$
$$Y_1 = Y_2 = j\sqrt{\frac{C}{L}} \tan \frac{x}{\lambda} \pi \approx j\sqrt{\frac{C}{L}} \frac{x}{\lambda} \pi = j \frac{\omega C x}{2} \tag{6-100}$$

We note that the series impedance is simply obtained by multiplying the reactance per meter by the length of the line. The shunt admittance is obtained in an analogous manner (and divided into two equal parts at each end). Typical lines have, at 60 Hz, wavelengths of about 3000 miles. For a line length of 100 miles we have $x/\lambda = 1/30$, and the foregoing approximations will be less than 1 percent. *We conclude therefore, that for line lengths below approximately* 100 *miles, we can neglect the distribution effect and actually "lump" the line parameters.* We refer to the line *in this case as "electrically short."*

**Example 6-9** In this last example we demonstrate the usage of the equivalent line network to solve a typical operational problem. Consider the simple network segment shown in Fig. 6-20*a*, consisting of a 30-mile 120-kV line connecting two buses 1 and 2. It is known that the receiving-end power equals

$$P_2 + jQ_2 = 30 + j15 \qquad \text{MVA}$$

It is also known that the voltage of bus 1 is kept at 120 kV exactly.

We wish to determine on the basis of these data what the receiving-end voltage level is, and also the sending-end powers.

We shall make the following assumptions regarding the line:

1. All real losses neglected
2. Wave impedance = 400 Ω
3. Wavelength = 3000 miles

Since the line is electrically short, that is, $x/\lambda = 0.01$, we can with confidence use the approximate equations (6-100) to obtain the series and shunt elements of

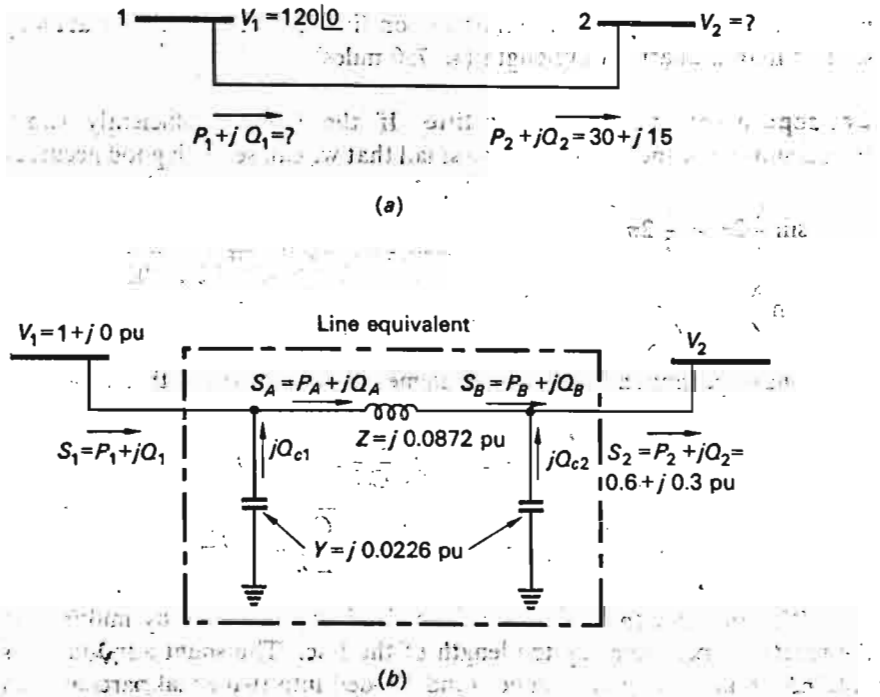


**Fig. 6-20** Equivalent circuit for line in Example 6-9.

the equivalent network. We get

$$Z = j400 \times \frac{1}{100} \times 2\pi = j25.1 \quad \Omega$$

$$Y_1 = Y_2 = j\frac{1}{400} \times \frac{1}{100} \times \pi = j0.785 \times 10^{-4} \quad \mho$$

We shall prefer to work in per-unit values, and choose for that purpose the following† power and voltage bases:

50 MVA = 1 pu power

120 kV = 1 pu voltage

Using Eq. (2-50), we obtain the following per-unit network elements:

$$Z_{pu} = j25.1 \frac{50}{(120)^2} = j0.0872 \quad \text{pu}$$

$$Y_{pu} = j0.785 \times 10^{-4} \frac{(120)^2}{50} = j0.0226 \quad \text{pu}$$

† The static transmission capacity of this line, assuming the voltage is kept at 120 kV at each end, is computed from Eq. (3-2) to equal $P_{max} = 574$ MW. Our chosen base power is therefore well below this limit.



We have indicated these values in Fig. 6-20*b*. In the same diagram we have identified the various power flows, also in per-unit values. Note that the powers $S_A$ and $S_B$ are "fictitious powers," since they cannot be measured anywhere in the actual line. The sum of the reactive powers $Q_{c1}$ and $Q_{c2}$ is the total generated reactive power in the line. Using Eq. (2-42), we can immediately obtain expressions for these:

$$Q_{c1} = 0.0226 \times |1|^2 = 0.0226 \quad \text{pu Mvar}$$

$$Q_{c2} = 0.0226 \times |V_2|^2 \quad \text{pu Mvar}$$

The way the problem is specified makes it difficult to compute directly the data sought. To obtain, for example, the receiving-end voltage $V_2$, we would like to know the *currents* in the various circuit branches. This would permit us to compute the voltage drop across $Z$, and since we know $V_1$, we would then know $V_2$.

However, we are given a priori knowledge about the *power* $S_2$, but since the voltage $V_2$ is unknown, we *cannot directly* find the current. This is a typical problem statement in EESE, and we shall discuss later, in Chap. 7, various computer methods for attacking this type of "load flow problem." We shall see that it is impossible to obtain analytical solutions in the general case.

Since we have neglected line losses and since our chosen network is simple, containing only one line, we shall attempt a solution. For this purpose, we make use of Eqs. (3-14), which, in terms of our variables, take on the form

$$P_A = P_B = \frac{|V_1||V_2|}{X} \sin \delta$$

$$Q_A = \frac{1}{X}(|V_1|^2 - |V_1||V_2| \cos \delta) \tag{6-101}$$

$$Q_B = \frac{1}{X}(|V_1||V_2| \cos \delta - |V_2|^2)$$

We remember that $\delta$ is the phase difference $\underline{/V_1} - \underline{/V_2}$. Note that, because we have no real losses, the two real power components $P_A$ and $P_B$ must be equal.

We now substitute the values that are known, and if we make use of the fact that

$$S_A = S_1 + jQ_{c1}$$

$$S_B = S_2 - jQ_{c2} \tag{6-102}$$

we get from Eq. (6-101)

$$0.6 = \frac{1\,|V_2|}{0.0872} \sin \delta$$

$$Q_1 + 0.0226 = \frac{1}{0.0872}(1 - |V_2| \cos \delta) \tag{6-103}$$

$$0.3 - 0.0226\,|V_2|^2 = \frac{1}{0.0872}(|V_2| \cos \delta - |V_2|^2)$$

We have three equations for three unknowns, $|V_2|$, $\delta$, and $Q_1$. The problem is therefore solved in principle. There are some numerical obstacles in our way, however. Equations (6-103) are *nonlinear*, and we cannot solve them *analytically*.

We can, of course, compute *numerical* solutions of any degree of accuracy we care to specify. For example, we may eliminate $|V_2|$ between the first and the third equations and obtain an equation for $\delta$. Possessing knowledge of $\delta$, we can then compute $|V_2|$ from the first equation, and finally $Q_1$ from the second one.

We will not perform the computations just outlined. In the next chapter we shall present more systematic numerical approaches to this type of problem.

## 6-5 SUMMARY

The most important design parameters of a transmission line from a systems analysis point of view are the series inductance and the shunt capacitance. Methods for computing these parameters have been developed in this chapter, first for a single-phase line, then for a three-phase line. We have confirmed under balanced operation that it is possible to define per-phase parameters. We earlier concluded that this could be done for generators and transformers, and therefore, we know at this stage that per-phase analysis is permissible for the overall system *under balanced load conditions.*

The advantages of bundle conductor design have been pointed out. It may be commented at this time that bundling of conductors is a "cheap" substitute for adding a parallel line to an existing one. One obviously saves the cost of a new right-of-way plus the construction cost of the line itself. However, whereas bundling reduces the reactance by about 25 percent (Example 6-3), and thus increases the power capacity of the line by about one-third, the new line would reduce the total reactance by 50 percent and thus double the power capacity.

For lines having a length in excess of about 100 miles, it becomes necessary to take the distribution effect of parameters into account. We have derived the so-called "long-line" equations and presented the corresponding equivalent network.

We emphasize that all analysis in this chapter was based upon the assumption of balanced load conditions and three-phase symmetry of voltages and currents. In Chap. 11 we shall investigate the effect of nonbalanced conditions.

## EXERCISES

**6-1.** The conductors of a three-phase line are placed in the corners of an equilateral triangle. The conductor spacing is 3 m, and each copper conductor has a diameter of 10 mm.

(*a*) Compute resistance and series and shunt reactance per meter and phase of the line. The frequency is 60 Hz, and you may neglect the influence of earth. Is there a need to transpose the phases in this line?

(*b*) Give an equivalent network for a 50-km section of this line. Consider it electrically short.



**6-2.** The line of Exercise 6-1 is fed from a 66-kV bus. Use the equivalent network derived in Exercise 6-1 to find:

(*a*) The receiving-end voltage and the sending-end current when the line is open-circuited.

(*b*) The reactive power generated by the line (as measured at the 66-kV bus) when operated as in part (*a*).

**6-3.** A telephone line runs parallel with an untransposed power line. Figure 6-21 gives the dimensions of the two. The power line carries a balanced three-phase current of 500 A (rms) per phase. Compute the 60-Hz voltage induced in the telephone line per meter.

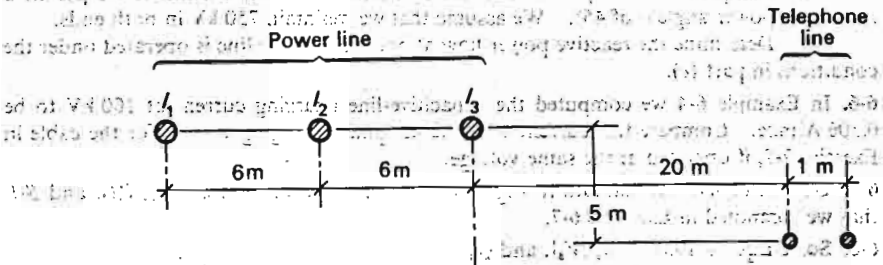


**Fig. 6-21** Telephone line running parallel with power line.

*Hint:* Use the apparent mutual inductances and compute the voltage induced in each telephone wire. The difference is your answer. Note that you will have to compute a *small* difference between relatively large terms; so you must be careful to obtain sufficient accuracy.

**6-4.** A 750-kV line utilizes a bundling arrangement of four conductors per phase, as shown in Fig. 6-22.

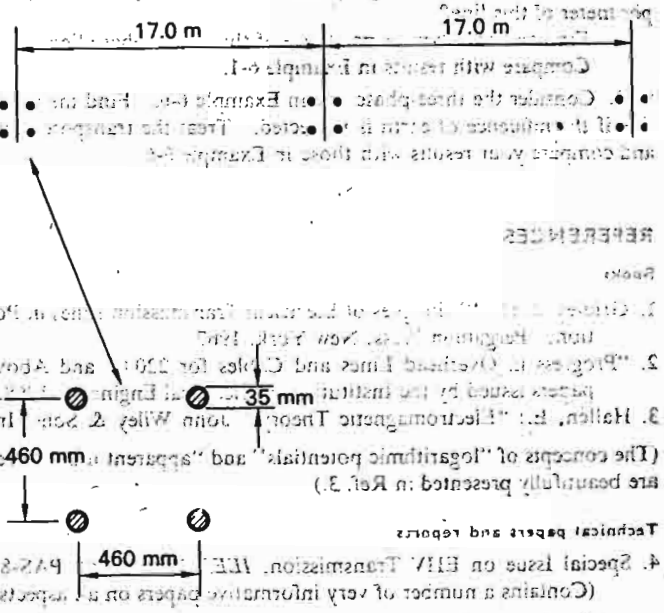


**Fig. 6-22** Physical dimensions of 750-kV line in Exercise 6-4.

(*a*) Compute the reactance per phase of this line at 60 Hz. Each conductor carries 25 percent of the phase current, and we assume transposition.

(*b*) Use Eq. (6-30) to find the cable dimensions of a hypothetical single-conductor line that would have the same inductance as the given line.

(*c*) Compute the shunt capacitance per phase of the given line. Assume that the line charge per phase divides equally between the four conductors.

**6-5.** Neglect the resistance of the line of Exercise 6-4.

(*a*) Find $R_w$ and $\gamma$.

(*b*) Find the equivalent network of a 900-km section of the line.

(*c*) Compute the real power that can be transmitted over the line if we permit a maximum power angle $\delta$ of 45°. We assume that we maintain 750 kV in both ends.

(*d*) Determine the reactive power flow at both ends if the line is operated under the conditions in part (*c*).

**6-6.** In Example 6-4 we computed the capacitive-line charging current at 100 kV to be 0.306 A/mile. Compare this current with the per-phase charging current for the cable in Exercise 2-7, if operated at the same voltage.

**6-7.** Use the equivalent diagram in Fig. 6-18 to obtain the values for $V(l)$, $I(l)$, and $S(l)$ that we computed in Example 6-7.

**6-8.** Solve Eqs. (6-103) for $\delta$, $|V_s|$, and $Q_1$.

**6-9.** Consider a lossless line of quarter-wave length. The wave impedance is 400 Ω.

(*a*) Find the $\pi$ equivalent of the line.

(*b*) If this line were operated with the receiving end open, what would be the ratio between the sending- and receiving-end voltages? Could the line actually be operated this way?

(*c*) Suppose the line were loaded with a 400-Ω resistor. Find the ratio between currents and voltages in both ends.

**6-10.** Consider the transmission line in Exercise 6-1. If two of the wires are paralleled and used as return lead in a single-phase transmission system, what will be the reactance per meter of this line?

Find also the shunt capacitance of this single-phase line.

Compare with results in Example 6-1.

**6-11.** Consider the three-phase line in Example 6-6. Find the capacitance matrix for this line if the influence of earth is neglected. Treat the transposed and untransposed cases, and compare your results with those in Example 6-6.

## REFERENCES


### Books

1. Gridley, J. H.: "Principles of Electrical Transmission Lines in Power and Communication," Pergamon Press, New York, 1967.
2. "Progress in Overhead Lines and Cables for 220 kv and Above," a compilation of papers issued by the Institution of Electrical Engineers, 1968.
3. Hallén, E.: "Electromagnetic Theory," John Wiley & Sons, Inc., New York, 1962.

(The concepts of "logarithmic potentials" and "apparent inductance" used in this chapter are beautifully presented in Ref. 3.)

### Technical papers and reports

4. Special Issue on EHV Transmission, *IEEE Trans.*, vol. PAS-85, no. 6, June, 1966. (Contains a number of very informative papers on all aspects of EHV.)





5. Chambers, F., et al.: Tennessee Valley Authority's 500-kv System, *IEEE Trans.*, vol. PAS-85, no. 1, pp. 22–53, January, 1966. A sequence of four papers.
6. Peterson, H. A.: An Analog Computer Study of a Parallel AC and DC Power System, *IEEE Trans.*, vol. PAS-85, no. 3, pp. 191–209, March, 1966.
7. Peterson, H. A., and P. C. Krause: A Direct- and Quadrature-axis Representation of a Parallel AC and DC Power System, *IEEE Trans.*, vol. PAS-85, no. 3, pp. 210–225, March, 1966.
8. Laboratory Evaluation of 345 kv Cable, *IEEE Trans.*, vol. PAS-85, no. 4, April, 1966. (A series of nine papers on underground cables.)
9. Anderson, J. G., et al.: Corona-loss Characteristics of EHV Transmission Lines, *IEEE Trans.*, vol. PAS-85, no. 12, pp. 1196–1212, December, 1966.
10. Coleman, D., et al.: Digital Calculation of Overhead Transmission-line Constants, *AIEE Trans.* (*PAS*), vol. 77, pp. 1266–1268, 1958.
11. Shipley, R. B., et al.: Power Circuit Representation for Digital Studies, *IEEE Trans.*, vol. PAS-83, pp. 376–380, April, 1964.
12. Holley, H., et al.: Untransposed EHV Line Computations, *IEEE Trans.*, vol. PAS-83, pp. 291–296, March, 1964.
13. Manuzio, C.: Forces on Bundle Conductors under Fault Conditions, *IEEE Trans.*, vol. PAS-86, no. 2, pp. 166–184, February, 1967.
14. Gross, E. T. B., and C. Wing: Electrostatic Unbalance of Untransposed Single Circuit Lines, *IEEE Trans.*, vol. PAS-87, no. 1, pp. 24–34, 1967.
15. Samuelson, A. J.: AEP's 765-kv Transmission Line Project, *IEEE Trans.*, vol. PAS-88, no. 5, pp. 703–709, May, 1969.

# 7

# The Energy System in Steady State—System Modeling and Load Flow Analysis

At this stage of our understanding of the basic characteristics of the individual components of the electric energy system, we are prepared to approach the central topic of our study: the operational features of the overall system. The most important mode of operation is the *symmetrical steady state*, and we devote this entire chapter and the next two to the problems associated with this, the *normal* state of operation.

We have already pointed out in Chap. 3 that the primary function of an energy system is to provide the real and reactive powers demanded by the various loads connected to the system. Simultaneously, the frequency and the various bus voltages must be kept within specified tolerances, in spite of the fact that the load demands may undergo large, and to a certain extent unpredictable, changes.

As we shall see, we may conveniently divide the overall steady-state systems operations problem into the following three subareas:

1. System modeling and load flow analysis
2. Development of optimum generating strategy
3. Systems control





This chapter covers the first area. The following two chapters are concerned with the second and third topics.

## 7-1 A DEMONSTRATION EXAMPLE

We can best introduce the reader to the essential features of the operations problem by discussing the simple two-bus system depicted in Fig. 7-1*a*. A

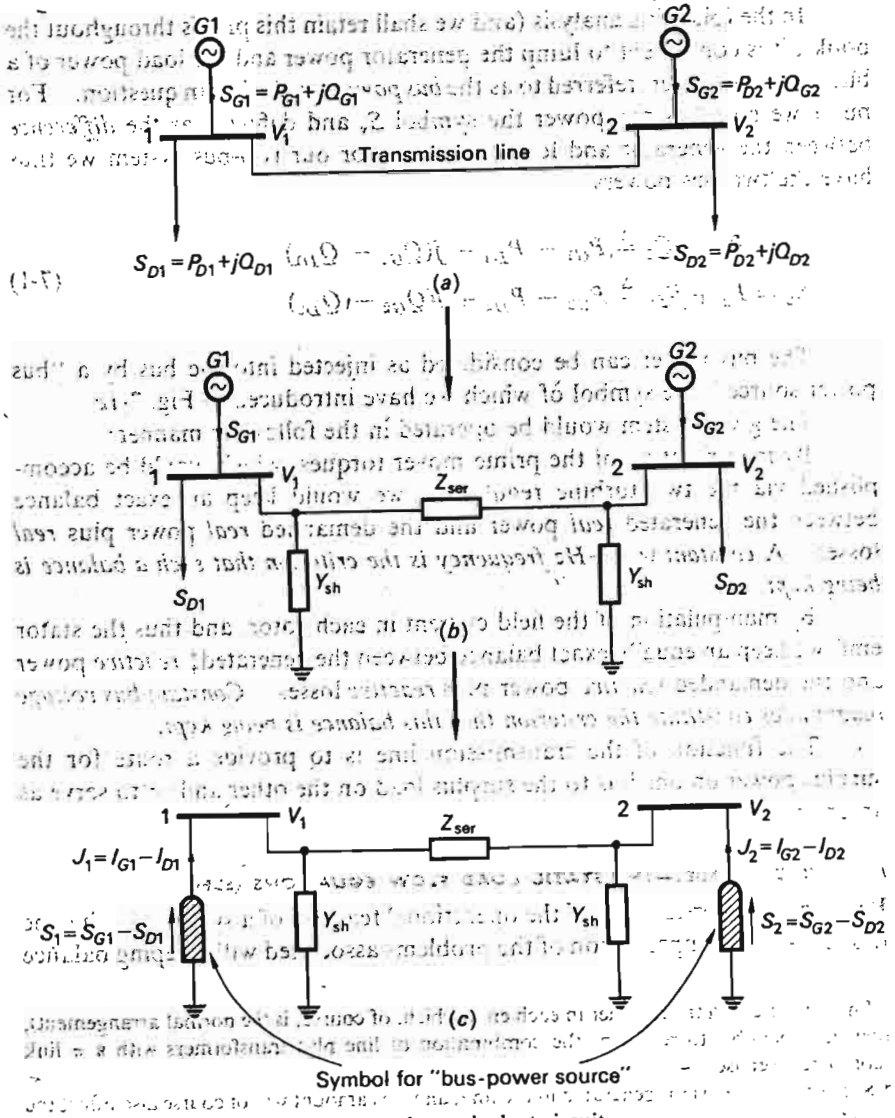


**Fig. 7-1** Two-bus example system—its equivalent circuit.

real power system never is this simple; nevertheless, it will serve the demonstration purpose well.

Each bus is being fed from generator units which inject the powers $S_{G1}$ and $S_{G2}$, respectively, into the buses. Loads are tapped from each bus in the amounts $S_{D1}$ and $S_{D2}$. The two buses are interconnected via a transmission line that is characterized (Fig. 7-1*b*) by a series impedance $Z_{ser}$ and two shunt admittances $Y_{sh}$.† The two bus voltages are symbolized $V_1$ and $V_2$, respectively.

In the following analysis (and we shall retain this praxis throughout the book), it is convenient to lump the generator power and the load power of a bus into a *net* power, referred to as the *bus power* for the bus in question. For bus $\nu$ we give this bus power the symbol $S_\nu$ and define it as the *difference* between the generator and load powers. For our two-bus system we thus have the two bus powers

$$\begin{aligned} S_1 &= P_1 + jQ_1 \triangleq P_{G1} - P_{D1} + j(Q_{G1} - Q_{D1}) \\ S_2 &= P_2 + jQ_2 \triangleq P_{G2} - P_{D2} + j(Q_{G2} - Q_{D2}) \end{aligned} \tag{7-1}$$

The bus power can be considered as injected into the bus by a "bus power source," the symbol of which we have introduced in Fig. 7-1*c*.

The given system would be operated in the following manner:

By manipulation of the prime mover torques, which would be accomplished via the two turbine regulators, we would keep an exact balance between the generated *real* power and the demanded *real* power plus *real* losses. A *constant* 60.00-*Hz frequency is the criterion that such a balance is being kept.*

By manipulation of the field current in each rotor, and thus the stator emf, we keep an equally exact balance between the generated‡ *reactive* power and the demanded *reactive* power plus *reactive* losses. *Constant bus voltage magnitudes constitute the criterion that this balance is being kept.*

The function of the transmission line is to provide a route for the surplus power on one bus to the surplus load on the other and/or to serve as an emergency link.

### 7-1.1 SYSTEM MODEL—THE STATIC LOAD FLOW EQUATIONS (SLFE)

Basic to an understanding of the operational features of a system like the one in Fig. 7-1 is an appreciation of the problems associated with keeping balance

† Should there be a transformer in each end (which, of course, is the normal arrangement), then it is possible to represent the combination of line plus transformers with a $\pi$ link (compare Exercise 7-4).

‡ Some reactive power is generated in the line, and this amount will of course also affect the balance.



between the powers, voltages, and frequency. We will presently introduce the reader to this matter, and will begin by finding an appropriate mathematical model for the demonstration example. Clearly, our system in Fig. 7-1*c* is an electric *network*, and by using well-known network formulas, we can readily construct our model. For example, consider the *currents* entering and leaving the buses. For bus 1, the current $S_1^*/V_1^*$, corresponding to the bus power and voltage of this bus, must equal the current entering the line. The latter current consists of two components,† one component, $V_1 Y_{sh}$, flowing into the shunt admittance, and one component, $(V_1 - V_2)/Z_{ser}$, flowing into the series impedance of the equivalent line network.

Thus, for current balance at bus 1, we have

$$\frac{S_1^*}{V_1^*} = V_1 Y_{sh} + \frac{V_1 - V_2}{Z_{ser}}$$

and similarly for bus 2,

$$\frac{S_2^*}{V_2^*} = V_2 Y_{sh} + \frac{V_2 - V_1}{Z_{ser}} \tag{7-2}$$

The shunt admittance is, as we decided in Chap. 6, for practical purposes, purely *capacitive*, and we therefore have

$$Y_{sh} = \frac{j}{X_c} \tag{7-3}$$

where $X_c$ is the capacitive reactance of *half* the line.

The series impedance can be written

$$Z_{ser} = R + jX_L$$

We define a loss factor

$$\alpha \triangleq \frac{R}{X_L}$$

and since the losses are always comparatively small, we usually have

$$\alpha \ll 1$$

On this assumption we can write

$$Z_{ser} \approx X_L e^{j(\pi/2 - \alpha)} \tag{7-4}$$

† These components cannot be individually measured. Why?

The bus voltages $V_1$ and $V_2$ are characterized by *magnitude* and *phase*, and can be written

$$V_1 = |V_1|\, e^{j\delta_1} \qquad V_2 = |V_2|\, e^{j\delta_2} \tag{7-5}$$

Upon substitution of Eqs. (7-1), (7-3), (7-4), and (7-5) into the two complex equations (7-2), and upon separating the real and imaginary parts, we obtain *four real* equations, which read

$$\begin{aligned}
P_{G1} - P_{D1} - \frac{|V_1|^2}{X_L}\sin\alpha + \frac{|V_1|\,|V_2|}{X_L}\sin[\alpha - (\delta_1 - \delta_2)] &= 0 \\
P_{G2} - P_{D2} - \frac{|V_2|^2}{X_L}\sin\alpha + \frac{|V_1|\,|V_2|}{X_L}\sin[\alpha + (\delta_1 - \delta_2)] &= 0 \\
Q_{G1} - Q_{D1} + \frac{|V_1|^2}{X_c} - \frac{|V_1|^2}{X_L}\cos\alpha + \frac{|V_1|\,|V_2|}{X_L}\cos[\alpha - (\delta_1 - \delta_2)] &= 0 \\
Q_{G2} - Q_{D2} + \frac{|V_2|^2}{X_c} - \frac{|V_2|^2}{X_L}\cos\alpha + \frac{|V_1|\,|V_2|}{X_L}\cos[\alpha + (\delta_1 - \delta_2)] &= 0
\end{aligned} \tag{7-6}$$

The reader should verify these equations.

Equations (7-6) are of great importance for our further discussions. We shall henceforth refer to them as the *static loadflow equations* (SLFE).

### 7-1.2 IMPORTANT CHARACTERISTICS OF SLFE

We make the following observations relating to Eqs. (7-6):

1. The equations are *algebraic* because they represent a model of a *static* system, or a system operating in steady state.
2. The equations are *nonlinear*. This may be initially disturbing to the reader, who knows that this fact signals great difficulties ahead in trying to obtain *analytical* solutions. However, we shall be content to obtain *numerical* solutions and shall have no difficulty doing so by digital computer.
3. Usually, in network analysis, the network equations relate voltages and *currents*. Our equations relate voltages and *powers*, because we are never explicitly interested in currents.
4. Nowhere in the formulas do we find *explicitly* the frequency variable $f$. (It does of course enter into the reactances $X_L = 2\pi fL$ and $X_c = 1/2\pi fC$.) In writing Eqs. (7-2), we tacitly assumed a *steady state:* i.e., we assumed *constant* frequency. We must, however, always remember, in working with these equations, that the frequency implicitly is always "in the background." A note of interest: the frequency constancy in today's network is $\pm 0.05$ Hz.
5. The "real power balance" discussed earlier can be demonstrated in mathematical terms by adding the first two of Eqs. (7-6):

$$P_{G1} + P_{G2} = P_{D1} + P_{D2} + \frac{\sin\alpha}{X_L}\left[|V_1|^2 + |V_2|^2 - 2\,|V_1|\,|V_2|\cos(\delta_1 - \delta_2)\right] \tag{7-7}$$

This equation states that the sum of the real generation equals the sum of the real demand plus the real losses $P_L$. Note that the loss term disappears for $\alpha = 0$. Usually, it is small, amounting to only a few percent of the total demand.

6. The "reactive power balance" can be similarly demonstrated by adding the last two of Eqs. (7-6):

$$Q_{G1} + Q_{G2} = Q_{D1} + Q_{D2} + \frac{\cos\alpha}{X_L}\left[|V_1|^2 + |V_2|^2 - 2\,|V_1|\,|V_2|\cos(\delta_1 - \delta_2)\right] - \frac{|V_1|^2 + |V_2|^2}{X_c} \tag{7-8}$$

The third term represents the reactive losses $Q_L$, and the fourth term, the reactive generation of the line (note the sign).

7. The loss terms are functions of the voltage variables *only*. We can in effect write

$$\begin{aligned}
P_L &= P_L(|V_1|, |V_2|, \delta_1, \delta_2) \\
Q_L &= Q_L(|V_1|, |V_2|, \delta_1, \delta_2)
\end{aligned} \tag{7-9}$$

8. Note that in all four of Eqs. (7-6) the phase angles $\delta_1$ and $\delta_2$ appear in difference form, $\delta_1 - \delta_2$. This fact will have great bearing on our following discussions.
9. In addition to the fixed network parameters $\alpha$, $X_L$, and $X_c$, Eqs. (7-6) contain 12 variables (excluding the implicit frequency variable $f$). Consequently, it is not possible to obtain a solution for any of the variables unless we reduce the number of "unknowns" by fixing the values for some of the variables. *We must, in fact, reduce the number of "unknowns" from twelve to four to match the number of equations.* Thus we must a priori specify eight of the variables. The remaining four can then, at least in principle, be solved† from Eqs. (7-6).

† Even in this case we have, of course, no guarantee that we obtain a *unique* solution, since it is possible that a nonlinear equation of this type has *several* solutions. (Recall, for example, that the nonlinear equation

$$\sin x = 0$$

has an infinite number of solutions.)

As a rule, however, there is only one solution that is of stable practical significance.

### 7-1.3 CLASSIFICATION OF SYSTEM VARIABLES

The last observation brings into focus one of the most important features of the problems to be discussed in this chapter. Since we wish to obtain a feel for the cause-effect relationship of the system, it is imperative that we bring some measure of order into the abundance of variables. For this purpose we divide them into the following natural groups.

**Uncontrollable or disturbance variables** Of the 12 variables we agree that the demand variables $P_{D1}$, $P_{D2}$, $Q_{D1}$, and $Q_{D2}$ are completely *beyond our control since they are determined by the customer.* We shall find it convenient to symbolize, for distinguishing purposes, these *uncontrollable*, or *disturbance*, variables by the symbols $p_1, \ldots, p_4$. The latter name refers to the fact that the unpredictable changes in these variables cause the system to deviate from its nominal state.

The disturbance variables thus defined constitute the components of a four-dimensional *disturbance vector* $\mathbf{p}$, defined as follows:

$$\mathbf{p} = \begin{bmatrix} p_1 \\ p_2 \\ p_3 \\ p_4 \end{bmatrix} \triangleq \begin{bmatrix} P_{D1} \\ Q_{D1} \\ P_{D2} \\ Q_{D2} \end{bmatrix} \tag{7-10}$$

**State and control variables** The eight variables that are left, $|V_1|$, $|V_2|$, $\delta_1$, $\delta_2$, $P_{G1}$, $P_{G2}$, $Q_{G1}$, and $Q_{G2}$, can easily be grouped into two categories, "independent" and "dependent" variables, which in control theory are given the names *control* and *state variables*, respectively. In the former category we include those variables that, physically, are used to manipulate, or "control," the latter. Clearly, then, the generator outputs $P_{G1}$, $P_{G2}$, $Q_{G1}$, and $Q_{G2}$ are our control variables.

As we later shall find, by manipulation of $Q_{G1}$ and $Q_{G2}$ we strongly affect the voltage magnitudes $|V_1|$ and $|V_2|$. $P_{G1}$ and $P_{G2}$ similarly affect $\delta_1$ and $\delta_2$.

To summarize, we define the variables $|V_1|$, $|V_2|$, $\delta_1$, and $\delta_2$ as state variables. To conform with accepted symbol practice, they will be represented by the symbols $x_1, \ldots, x_4$. The variables $P_{G1}$, $P_{G2}$, $Q_{G1}$, and $Q_{G2}$ are our control variables, for which we shall prefer to adopt the usual symbols $u_1, \ldots, u_4$.

We introduce, therefore, the *state vector* $\mathbf{x}$ and the *control vector* $\mathbf{u}$, defined as follows:

$$\mathbf{x} = \begin{bmatrix} x_1 \\ x_2 \\ x_3 \\ x_4 \end{bmatrix} \triangleq \begin{bmatrix} \delta_1 \\ |V_1| \\ \delta_2 \\ |V_2| \end{bmatrix} \qquad \mathbf{u} = \begin{bmatrix} u_1 \\ u_2 \\ u_3 \\ u_4 \end{bmatrix} \triangleq \begin{bmatrix} P_{G1} \\ Q_{G1} \\ P_{G2} \\ Q_{G2} \end{bmatrix} \tag{7-11}$$



### 7-1.4 SOLUTION OF SLFE—A BASIC DILEMMA

Having thus classified the 12 variables in Eqs. (7-6), the solution of these equations could seemingly proceed in the following steps:

*Step* 1 From an assumed knowledge of the customer demand, we possess an a priori knowledge of the four $p$ parameters.

*Step* 2 We make an a priori assumption about the four control variables; i.e., we specify the bus generations.

*Step* 3 The remaining four state variables constitute, then, our "unknowns." With exactly four equations, we should, in principle, be able to solve for these unknowns.

At a closer examination we find, however, that there are two basic roadblocks that prevent us from proceeding along the outlined steps:

1. *We cannot a priori specify all the four generation variables because the losses $P_L$ and $Q_L$ are not known.* In accordance with Eqs. (7-7) and (7-8), the sum of the control variables must equal the sum of the demands plus the losses. The latter, as shown by Eqs. (7-9), are functions of the *state* variables, which as yet are unknown. Consequently, we do not a priori know the *total* real and reactive generations $P_{G1} + P_{G2}$ and $Q_{G1} + Q_{G2}$, respectively. We can, of course, specify two of the individual generations, for example, $P_{G2}$ and $Q_{G2}$, which would then leave $P_{G1}$ and $Q_{G1}$ as unknowns.
2. *The SLFE will never permit us to solve for the individual phase angles $\delta_1$ and $\delta_2$, but only their difference, $\delta_1 - \delta_2$.* The truth of this statement becomes immediately obvious if it is realized that *any arbitrary* value added to both $\delta_1$ and $\delta_2$ in Eq. (7-6) will not affect the equations.

### 7-1.5 MODIFIED SPECIFICATIONS—SOLUTION OF OUR DILEMMA

We can bypass the above two problems in the following way. Since we realize that $\delta_1 - \delta_2$, rather than $\delta_1$ and $\delta_2$, must be treated as an unknown, we choose to fix either $\delta_1$ and $\delta_2$ at some arbitrary value.

*In this book we shall always choose $\delta_1 = 0$, thereby in effect designating the voltage of bus 1 as our reference phasor.* We thus have reduced the number of *unknown* state variables from four to three ($|V_1|$, $|V_2|$, and $\delta_2$).

We earlier had concluded that two control variables, $P_{G1}$ and $Q_{G1}$, also were a priori unknown. *As a result, we are left with a total of five unknowns, but have only four equations.*

Since it is always desirable to have the voltage level of the system under good control, we find now a good opportunity to do so. We simply reduce the number of unknowns from five to four by a priori specifying one of the two voltage states, $|V_1|$ or $|V_2|$. *In this book we shall always choose $|V_1|$, that is, the voltage magnitude of the reference bus.*

In view of the foregoing reasoning, we can now modify the SLFE solution procedure as follows:

*Step* 1 Assume demand variables as before.

*Step* 2 Specify one each of the real and reactive generation variables but leave the two others unspecified. For example, specify $P_{G2}$ and $Q_{G2}$ but leave $P_{G1}$ and $Q_{G1}$ open, since we do not yet know the losses. Set $\delta_1 = 0$.

*Step* 3 Specify $|V_1|$. For example, set $|V_1| = 1$ pu.

*Step* 4 Solve the SLFE for the four unknowns $|V_2|$, $\delta_2$, $P_{G1}$, and $Q_{G1}$.

This completely solves our problem. However, the solution procedure thus outlined has one big drawback: upon solution of $|V_2|$ we may find that this voltage is lower or higher than actually desired.

Before we suggest a more practical solution procedure to cope with this problem, it is necessary to state what the *practical* limitations are for *all* our variables. Let us simultaneously extrapolate our discussions to embrace a general $n$-bus system.

### 7-1.6 GENERALIZATION TO $n$-BUS SYSTEM

In terms of the three vectors $\mathbf{x}$, $\mathbf{u}$, and $\mathbf{p}$, we can evidently write the four Eqs. (7-6) in the form

$$f_i(\mathbf{x},\mathbf{u},\mathbf{p}) = 0 \qquad \text{for } i = 1, 2, 3, 4 \tag{7-12}$$

Upon introducing the function vector

$$\mathbf{f} \triangleq \begin{bmatrix} f_1 \\ f_2 \\ f_3 \\ f_4 \end{bmatrix} \tag{7-13}$$

we can write Eq. (7-6) in the very compact vector form

$$\mathbf{f}(\mathbf{x},\mathbf{u},\mathbf{p}) = 0 \tag{7-14}$$

*This is therefore the vector form of the SLFE.*

In our sample system the vector equation is four-dimensional, but realistic-size power systems may contain hundreds of buses and generators and thousands of lines. We wish now to extend the foregoing discussions valid for a two-bus system to the general case of an $n$-bus system. For such a system we have the following variables:

$n$ bus voltage magnitudes $|V_i|$
$n$ bus voltage phase angles $\delta_i$
$n$ real power generations $P_{Gi}$
$n$ reactive power generations $Q_{Gi}$
$n$ real power demands $P_{Di}$
$n$ reactive power demands $Q_{Di}$



This amounts to a total of $6n$ variables. (In the case of a two-bus system we had $6 \times 2 = 12$.)

Since we can write one complex current equation of the type of Eqs. (7-2) for each bus, we will in effect have a total of $2n$ real equations of the type of Eqs. (7-6); i.e., our vector form of SLFE will be $2n$-dimensional. In direct analogy with Eqs. (7-10) and (7-11), we now define the following $2n$-dimensional vectors:

$$\mathbf{p} = \begin{bmatrix} p_1 \\ p_2 \\ \cdot \\ \cdot \\ \cdot \\ p_{2n} \end{bmatrix} \triangleq \begin{bmatrix} P_{D1} \\ Q_{D1} \\ P_{D2} \\ Q_{D2} \\ \cdot \\ \cdot \\ \cdot \\ P_{Dn} \\ Q_{Dn} \end{bmatrix} \tag{7-15}$$

$$\mathbf{x} = \begin{bmatrix} x_1 \\ x_2 \\ \cdot \\ \cdot \\ \cdot \\ x_{2n} \end{bmatrix} \triangleq \begin{bmatrix} \delta_1 \\ |V_1| \\ \delta_2 \\ |V_2| \\ \cdot \\ \cdot \\ \cdot \\ \delta_n \\ |V_n| \end{bmatrix} \tag{7-16}$$

$$\mathbf{u} = \begin{bmatrix} u_1 \\ u_2 \\ \cdot \\ \cdot \\ \cdot \\ u_{2n} \end{bmatrix} \triangleq \begin{bmatrix} P_{G1} \\ Q_{G1} \\ P_{G2} \\ Q_{G2} \\ \cdot \\ \cdot \\ \cdot \\ P_{Gn} \\ Q_{Gn} \end{bmatrix} \tag{7-17}$$

### 7-1.7 PRACTICAL STATE-VARIABLE CONSTRAINTS

The solution of the SLFE will be of practical acceptance only if all $4n$ state and control variables lie within practical limits. What are these limits or constraints? We list, first, the state-variable constraints:

1. The state variables $|V_i|$ must satisfy the inequality relations

$$|V_i|_{\min} < |V_i| < |V_i|_{\max} \qquad \text{for } i = 1, 2, \ldots, n \tag{7-18}$$

   This constraint simply states that we do not accept that any bus voltage magnitude lies outside a certain tolerated "band." The bands usually are very narrow, for example, 5 to 10 percent around the nominal values.
2. Certain state variables $\delta_i$ must satisfy the inequality constraint

$$|\delta_i - \delta_j| < (\delta_i - \delta_j)_{\max} \tag{7-19}$$

   This inequality simply specifies a maximum power angle for a transmission line between buses $i$ and $j$. (See discussion of electrical stiffness in Chap. 3.)

### 7-1.8 PRACTICAL CONTROL-VARIABLE CONSTRAINTS

Due to practical limitations of our $P$ and $Q$ sources, the following limitations must be observed in regard to the control variables $P_{Gi}$ and $Q_{Gi}$:

$$\begin{aligned} P_{Gi,\min} &< P_{Gi} < P_{Gi,\max} \\ Q_{Gi,\min} &< Q_{Gi} < Q_{Gi,\max} \end{aligned} \tag{7-20}$$

If some particular buses do not have $P$ and/or $Q$ sources, then for these buses we obviously have

$$P_{Gi} = 0$$

and/or

$$Q_{Gi} = 0$$

Equations (7-7) and (7-8) tell us that the *total* production of real and reactive power must equal the total demand plus losses. *But the equations tell us nothing about how to share the generations among the P and Q sources.* For example, in our two-bus problem, should we share the load between the two generators in ratio 50:50 or 75:25 or some other ratio?

In Chap. 8 we shall see that, if we prescribe that the system must be operated in some *optimum* fashion in, for example, the economic sense, then the load sharing must be performed in a *unique* ratio. Should this be the case, then of course this imposes an *economic constraint* upon our control forces in addition to the above magnitude constraints.



### 7-1.9 PRACTICAL VARIABLE SPECIFICATION PROCEDURE

Since very tight practical limitations are thus put on the voltage magnitudes $|V_i|$, it may not be possible to use the earlier specification method introduced in Secs. 7-1.4 and 7-1.5.

In such a practical situation it is much better to make a priori specifications about those important voltage magnitudes, and let other *less restricted* variables assume the role of "unknowns."

Let us exemplify by actually performing some typical specifications on our two-bus system in Fig. 7-1.

Assume that the system is characterized by the following network data:

$$\begin{aligned} X_L &= 0.1 \quad \text{pu} \\ X_c &= 10 \quad \text{pu} \\ \alpha &= 0.01 \end{aligned}$$

Let us also assume that the bus loads are equal and of magnitudes

$$\begin{aligned} P_{D1} &= P_{D2} = 20 \text{ pu MW} \\ Q_{D1} &= Q_{D2} = 10 \text{ pu Mvar} \end{aligned}$$

We consider the following operating cases.

*Case 1* Let us set the following variable specifications: $|V_1| = |V_2| = 1.00$ pu; i.e., we have required a so-called "flat voltage profile."

In addition, we set

$$\delta_1 = 0 \qquad \text{(bus 1 is reference bus)}$$

and

$$P_{G2} = 15 \text{ pu MW}$$

The last specification may follow, for example, from the fact that the rating of unit 2 is only 15 pu, or it has been found that this setting will result in best economy.

Note also the following remarks:

1. The above specification results in a deficiency of 5 pu MW on bus 2, and this power will therefore have to be transported on the line. (Does the line have sufficient capacity for this?)
2. The generation of unit 1 will be 25 pu MW plus losses.

Clearly our unknown variables in this case are

$$P_{G1},\ \delta_2,\ Q_{G1}, \text{ and } Q_{G2}$$

Four unknowns and four equations! Thus, OK!

*Case 2* Clearly, the specifications in case 1 were based on the assumption that *we have Q sources at both buses.* Assume that we do not have any

$Q$ source at bus 2; i.e., we have the restriction

$$Q_{G2} = 0$$

We have now no means of controlling the voltage at bus 2, and we must therefore lift the specification on $|V_2|$.

Our new specifications are thus

$|V_1| = 1.00$ as before
$\delta_1 = 0$ as before
$P_{G2} = 15$ pu MW as before
$Q_{G2} = 0$

Solution of the SLFE will render $|V_2|$, $\delta_2$, $P_{G1}$, and $Q_{G1}$.

Should the value of $|V_2|$ turn out to be too low, we can go back and respecify $|V_1|$ at a somewhat higher value. This will then lift $|V_2|$ also.

#### 7-1.10 BUS CLASSIFICATION ON THE BASIS OF SPECIFICATION TYPE

The preceding cases tell us that, based on the type of a priori specification used, it is possible to classify the buses into three categories:

*Bus type* 1 For this type of bus we *know* a priori $P_{Di}$ and $Q_{Di}$ and *specify* $P_{Gi}$ and $Q_{Gi}$. In effect, we thus specify the bus powers $P_i$ and $Q_i$.

Solution of the load flow equations will *render* $|V_i|$ and $\delta_i$. A *load bus* which, due to its lack of generating equipment, is characterized by zero $P_{Gi}$ and $Q_{Gi}$ evidently falls in this category.

*Bus type* 2 For this type of bus we *know* a priori $P_{Di}$ and $Q_{Di}$ and *specify* $|V_i|$ and $P_{Gi}$. In effect, we thus specify the bus power $P_i$.

Solution of the load flow equations will *render* $Q_{Gi}$ (and thus $Q_i$) and $\delta_i$.

This is a *voltage control bus*, so called because its voltage can be controlled.

*Bus type* 3 For this type of bus we *know* a priori $P_{Di}$ and $Q_{Di}$ and *specify* $|V_i|$ and $\delta_i$, the latter usually being set equal to 0.

Solution of the load flow equations will *render* $P_{Gi}$ and $Q_{Gi}$ (and thus $P_i$ and $Q_i$).

This is the *reference bus*. Sometimes it is called *slack bus* because it takes up the slack in losses. The term *swing bus* is also used.

We shall have opportunities to work several examples on load flow analysis based upon these types of specifications. However, first we need to attend to another important matter.

Of great concern in system operation is the problem of *sensitivity*. When a certain control variable is changed, how are the state variables



affected? Specifically, does a particular control variable affect some state variables more strongly than others? Are some not affected at all? Sensitivity analysis helps us find answers to these questions.

### 7-2 SENSITIVITY ANALYSIS AND THE PROBLEM OF CONTROL

Let us assume that our system operates in a *nominal* steady state $\mathbf{x}^0$, corresponding to the nominal values $\mathbf{u}^0$ and $\mathbf{p}^0$ for the $\mathbf{u}$ and $\mathbf{p}$ vectors, respectively. In this state the system equation (7-14) thus reads

$$\mathbf{f}(\mathbf{x}^0,\mathbf{u}^0,\mathbf{p}^0) = \mathbf{0} \tag{7-21}$$

We wish to keep the system in this operating state, but due to fluctuations in the demands, the vector $\mathbf{p}$ experiences deviations $\Delta\mathbf{p}$ around the nominal value $\mathbf{p}^0$. If we leave the control vector constant, the result would be changes in the state vector $\mathbf{x}$. This cannot be tolerated; so, to offset the effects of $\Delta\mathbf{p}$, we must exert control on the system by changing the $\mathbf{u}$ vector with certain amounts $\Delta\mathbf{u}$. If these control actions are 100 percent successful, then the changes in the state, $\Delta\mathbf{x}$, will be reduced to zero.

Of paramount importance for the design of a control system is a full understanding of how changes in $\mathbf{p}$ and $\mathbf{u}$ affect the state $\mathbf{x}$, or differently stated, of the manner in which the state $\mathbf{x}$ is sensitive to changes in $\mathbf{p}$ and $\mathbf{u}$. Such knowledge can be had from a *perturbation*, or *sensitivity*, analysis, on which we now embark.

#### 7-2.1 PERTURBATION OR SENSITIVITY ANALYSIS

Assume that all three vectors $\mathbf{x}$, $\mathbf{u}$, and $\mathbf{p}$ are perturbed by the amounts $\Delta\mathbf{x}$, $\Delta\mathbf{u}$, and $\Delta\mathbf{p}$, respectively. Equation (7-21) therefore changes to

$$\mathbf{f}(\mathbf{x}^0 + \Delta\mathbf{x}, \mathbf{u}^0 + \Delta\mathbf{u}, \mathbf{p}^0 + \Delta\mathbf{p}) = \mathbf{0} \tag{7-22}$$

or in component form,†

$$f_\nu(x_1^0 + \Delta x_1, x_2^0 + \Delta x_2, \ldots ; u_1^0 + \Delta u_1, u_2^0 + \Delta u_2, \ldots ; p_1^0 + \Delta p_1, p_2^0 + \Delta p_2, \ldots) = 0 \qquad \text{for } \nu = 1, 2, \ldots, 2n \tag{7-23}$$

If we expand $f_\nu$ in a Taylor series around the nominal value $f_\nu(\mathbf{x}^0,\mathbf{u}^0,\mathbf{p}^0)$, and if we assume that the perturbations are so small that we can neglect terms

† It must be strongly emphasized that the changes we are talking about are *steady-state*, or *static*, changes. When $\mathbf{p}$ changes with the amount $\Delta\mathbf{p}$, the frequency will most surely experience a transient deviation (Chap. 9). The changes $\Delta\mathbf{x}$, $\Delta\mathbf{u}$, and $\Delta\mathbf{p}$ are those static changes that can be measured *after* the transients have died out, and the frequency due to the action of the load frequency controller (to be described in Chap. 9) is back to nominal value.

of order $\Delta^2$ and higher, then we get

$$f_\nu(\mathbf{x}^0,\mathbf{u}^0,\mathbf{p}^0) + \frac{\partial f_\nu}{\partial x_1}\Delta x_1 + \frac{\partial f_\nu}{\partial x_2}\Delta x_2 + \cdots + \frac{\partial f_\nu}{\partial u_1}\Delta u_1 + \frac{\partial f_\nu}{\partial u_2}\Delta u_2 + \cdots + \frac{\partial f_\nu}{\partial p_1}\Delta p_1 + \frac{\partial f_\nu}{\partial p_2}\Delta p_2 + \cdots \approx 0 \qquad \text{for } \nu = 1, 2, \ldots, 2n$$

or in view of Eq. (7-21),

$$\frac{\partial f_\nu}{\partial x_1}\Delta x_1 + \frac{\partial f_\nu}{\partial x_2}\Delta x_2 + \cdots + \frac{\partial f_\nu}{\partial u_1}\Delta u_1 + \frac{\partial f_\nu}{\partial u_2}\Delta u_2 + \cdots + \frac{\partial f_\nu}{\partial p_1}\Delta p_1 + \frac{\partial f_\nu}{\partial p_2}\Delta p_2 + \cdots = 0 \qquad \text{for } \nu = 1, 2, \ldots, 2n \tag{7-24}$$

All partial derivatives in Eq. (7-24) must be computed for the nominal variable values.

At this time we recall that the state variable $\delta_1$ had been arbitrarily set equal to zero, for reasons outlined earlier. This means that we must set $\Delta x_1 = 0$ in all the $2n$ Eqs. (7-24). With this restriction on $\Delta x_1$, the latter equations can be tabulated in the following matrix form:

$$\left[\begin{array}{c|ccc} \frac{\partial f_1}{\partial x_1} & \frac{\partial f_1}{\partial x_2} & \cdots & \frac{\partial f_1}{\partial x_{2n}} \\ \hline \frac{\partial f_2}{\partial x_1} & \frac{\partial f_2}{\partial x_2} & \cdots & \frac{\partial f_2}{\partial x_{2n}} \\ \vdots & \vdots & \mathbf{J}_x & \vdots \\ \frac{\partial f_{2n}}{\partial x_1} & \frac{\partial f_{2n}}{\partial x_2} & \cdots & \frac{\partial f_{2n}}{\partial x_{2n}} \end{array}\right]\left[\begin{array}{c} 0 \\ \hline \Delta x_2 \\ \vdots \\ \Delta x_{2n} \end{array}\right] + \left[\begin{array}{ccc} \frac{\partial f_1}{\partial u_1} & \cdots & \frac{\partial f_1}{\partial u_{2n}} \\ \hline \frac{\partial f_2}{\partial u_1} & \cdots & \frac{\partial f_2}{\partial u_{2n}} \\ \vdots & \mathbf{J}_u & \vdots \\ \frac{\partial f_{2n}}{\partial u_1} & \cdots & \frac{\partial f_{2n}}{\partial u_{2n}} \end{array}\right]\left[\begin{array}{c} \Delta u_1 \\ \Delta u_2 \\ \vdots \\ \Delta u_{2n} \end{array}\right]$$

$$+ \left[\begin{array}{ccc} \frac{\partial f_1}{\partial p_1} & \cdots & \frac{\partial f_1}{\partial p_{2n}} \\ \hline \frac{\partial f_2}{\partial p_1} & \cdots & \frac{\partial f_2}{\partial p_{2n}} \\ \vdots & \mathbf{J}_p & \vdots \\ \frac{\partial f_{2n}}{\partial p_1} & \cdots & \frac{\partial f_{2n}}{\partial p_{2n}} \end{array}\right]\left[\begin{array}{c} \Delta p_1 \\ \Delta p_2 \\ \vdots \\ \Delta p_{2n} \end{array}\right] = \left[\begin{array}{c} 0 \\ 0 \\ \vdots \\ 0 \end{array}\right] \tag{7-25}$$



### 7-2.2 JACOBIAN AND SENSITIVITY MATRICES

The matrices having as elements the partial derivatives are referred to as *jacobians*. Because of the zero value for $\Delta x_1$, we have partitioned the matrices as indicated, and in this process we have obtained the square matrix $\mathbf{J}_x$ of dimension $2n - 1$, and the rectangular matrices $\mathbf{J}_u$ and $\mathbf{J}_p$ of dimension $2n - 1$ by $2n$. In terms of these matrices we obviously have

$$\mathbf{J}_x\,\Delta\mathbf{x} + \mathbf{J}_u\,\Delta\mathbf{u} + \mathbf{J}_p\,\Delta\mathbf{p} = \mathbf{0} \tag{7-26}$$

Here we have introduced the *perturbation vectors*

$$\Delta\mathbf{x} \triangleq \left[\begin{array}{c} \Delta x_2 \\ \vdots \\ \Delta x_{2n} \end{array}\right] \qquad \Delta\mathbf{u} \triangleq \left[\begin{array}{c} \Delta u_1 \\ \vdots \\ \Delta u_{2n} \end{array}\right] \qquad \Delta\mathbf{p} \triangleq \left[\begin{array}{c} \Delta p_1 \\ \vdots \\ \Delta p_{2n} \end{array}\right] \tag{7-27}$$

From Eq. (7-26) we then solve for $\Delta\mathbf{x}$.

$$\Delta\mathbf{x} = -\mathbf{J}_x^{-1}\mathbf{J}_u\,\Delta\mathbf{u} - \mathbf{J}_x^{-1}\mathbf{J}_p\,\Delta\mathbf{p} \triangleq \mathbf{S}_u\,\Delta\mathbf{u} + \mathbf{S}_p\,\Delta\mathbf{p} \tag{7-28}$$

In this last step we have introduced the so-called *sensitivity matrices*

$$\mathbf{S}_u \triangleq -\mathbf{J}_x^{-1}\mathbf{J}_u \qquad \mathbf{S}_p \triangleq -\mathbf{J}_x^{-1}\mathbf{J}_p \tag{7-29}$$

which in effect inform us how sensitive $\mathbf{x}$ is to changes in $\mathbf{u}$ and $\mathbf{p}$.

**Example 7-1** Let us use sensitivity analysis to determine the effects of small changes around a nominal state for our two-bus system in Fig. 7-1.

For simplicity, let us assume that the system is lossless, and let us also neglect the capacitive generation of the line; i.e., we set

$$\alpha = 0$$

$$X_c = \infty$$

The line reactance $X_L$ is assumed to equal 0.1 pu. This corresponds to a static transmission capacity of 10 pu, at a nominal 1 pu voltage level.

For these parameter values, and upon introducing the $\mathbf{x}$, $\mathbf{u}$, and $\mathbf{p}$ vectors, Eqs. (7-6) take on the form

$$\begin{aligned} f_1(\cdots) &= u_1 - p_1 + \frac{x_2 x_4}{0.1}\sin(x_2 - x_1) = 0 \\ f_2(\cdots) &= u_2 - p_2 + \frac{x_2 x_4}{0.1}\sin(x_1 - x_2) = 0 \\ f_3(\cdots) &= u_2 - p_2 - \frac{x_2^2}{0.1} + \frac{x_2 x_4}{0.1}\cos(x_2 - x_1) = 0 \\ f_4(\cdots) &= u_4 - p_4 - \frac{x_4^2}{0.1} + \frac{x_2 x_4}{0.1}\cos(x_1 - x_2) = 0 \end{aligned} \tag{7-30}$$

Let us consider an operational case characterized by the nominal load configurations

$$\mathbf{p}^0 = \begin{bmatrix} p_1^0 \\ p_2^0 \\ p_3^0 \\ p_4^0 \end{bmatrix} = \begin{bmatrix} P_{G1}^0 \\ Q_{G1}^0 \\ P_{G2}^0 \\ Q_{G2}^0 \end{bmatrix} = \begin{bmatrix} 20 \\ 10 \\ 20 \\ 10 \end{bmatrix} \begin{matrix} \text{pu} \\ \text{pu} \\ \text{pu} \\ \text{pu} \end{matrix}$$

and a flat voltage profile

$|V_1^0| = x_2^0 = 1$ pu

$|V_2^0| = x_4^0 = 1$ pu

For simplicity, we shall assume that the two generators share the real load equally. In view of the assumed bus loads, this means that the line load equals zero. Due to the flat voltage profile, the line carries no reactive load either. Our nominal $\mathbf{x}$ and $\mathbf{u}$ vectors, therefore, are

$$\mathbf{x}^0 = \begin{bmatrix} \delta_1^0 \\ |V_1^0| \\ \delta_2^0 \\ |V_2^0| \end{bmatrix} = \begin{bmatrix} 0 \\ 1 \\ 0 \\ 1 \end{bmatrix} \begin{matrix} \text{rad} \\ \text{pu} \\ \text{rad} \\ \text{pu} \end{matrix} \qquad \mathbf{u}^0 = \begin{bmatrix} P_{G1}^0 \\ Q_{G1}^0 \\ P_{G2}^0 \\ Q_{G2}^0 \end{bmatrix} = \begin{bmatrix} 20 \\ 10 \\ 20 \\ 10 \end{bmatrix} \begin{matrix} \text{pu} \\ \text{pu} \\ \text{pu} \\ \text{pu} \end{matrix}$$

Since the nominal state and the equations $f_i(\cdots)$ are known, the stage is now set for the sensitivity analysis. However, one additional matter must be attended to before we are able to compute the jacobian matrices.

In computing the partial derivatives $\partial f_i/\partial x_j$, we note that we encounter terms of the type $\partial p_i/\partial x_j$. These terms physically represent the variation of the load demands with respect to the state variables.† The load $P_{D1} + jQ_{D1}$ will depend upon $|V_1|$, and the load $P_{D2} + jQ_{D2}$ upon $|V_2|$.

Let us assume that all loads are of "impedance" type (Chap. 3), in which case the voltage variations are quadratic. We therefore have

$$p_1 = 20x_2^2 \qquad p_2 = 10x_2^2 \qquad p_3 = 20x_4^2 \qquad p_4 = 10x_4^2$$

We demonstrate how to find the jacobians by computing the element $\partial f_3/\partial x_2$ of the matrix $\mathbf{J}_x$. We have

$$\frac{\partial f_3}{\partial x_2} = \frac{\partial}{\partial x_2}\left[u_2 - p_2 - \frac{x_2^2}{0.1} + \frac{x_2 x_4}{0.1}\cos(x_3 - x_1)\right]$$

$$= \frac{\partial u_2}{\partial x_2} - \frac{\partial p_2}{\partial x_2} - \frac{2x_2}{0.1} + \frac{x_4}{0.1}\cos(x_3 - x_1)$$

$$= 0 - 20 - 20 + 10\cos x_3^0 = -40 + 10 = -30$$

† A bus load $P_{Di} + jQ_{Di}$ changes for *two* different reasons:

1. The addition (or subtraction) of *extra* load. This change is represented by the terms $\Delta p_i$, and shall be referred to as a *primary* perturbation.
2. The change of the *existing* load with the voltage. This change is expressed by the terms $\partial p_i/\partial |V_i|$, and shall be called a *secondary* load perturbation.



Following this procedure, we compute all nine elements of the $\mathbf{J}_x$ matrix We obtain

$$\mathbf{J}_x = \begin{bmatrix} 0 & -10 & -40 \\ -30 & 0 & 10 \\ 10 & 0 & -30 \end{bmatrix}$$

The jacobians $\mathbf{J}_u$ and $\mathbf{J}_p$ have the simple values

$$\mathbf{J}_u = -\mathbf{J}_p = \begin{bmatrix} 0 & 0 & 1 & 0 \\ 0 & 1 & 0 & 0 \\ 0 & 0 & 0 & 1 \end{bmatrix}$$

We next compute (using digital computers) the inverse

$$\mathbf{J}_x^{-1} = \begin{bmatrix} 0 & -0.0375 & -0.0125 \\ -0.1 & 0.050 & 0.150 \\ 0 & -0.0125 & -0.0375 \end{bmatrix}$$

Finally, we obtain from Eqs. (7-29) the sensitivity matrices

$$\mathbf{S}_u = -\mathbf{S}_p = \begin{bmatrix} 0 & 0.0375 & 0 & 0.0125 \\ 0 & -0.050 & 0.1 & -0.150 \\ 0 & 0.0125 & 0 & 0.0375 \end{bmatrix}$$

Let us use the result to study the changes in $\mathbf{x}$ as a result of perturbations in $\mathbf{u}$. We assume the primary $p$ perturbations to be zero. (The secondary ones, however, will be very much in evidence.) From Eq. (7-28) we have

$$\begin{bmatrix} \Delta|V_1| \\ \Delta\delta_2 \\ \Delta|V_2| \end{bmatrix} = \begin{bmatrix} 0 & 0.0375 & 0 & 0.0125 \\ 0 & -0.050 & 0.1 & -0.150 \\ 0 & 0.0125 & 0 & 0.0375 \end{bmatrix} \begin{bmatrix} \Delta P_{G1} \\ \Delta Q_{G1} \\ \Delta P_{G2} \\ \Delta Q_{G2} \end{bmatrix} \tag{7-31}$$

or in component form,

$$\begin{aligned} \Delta|V_1| &= 0.0375\Delta Q_{G1} + 0.0125\Delta Q_{G2} \\ \Delta\delta_2 &= -0.050\Delta Q_{G1} + 0.1\Delta P_{G2} - 0.150\Delta Q_{G2} \\ \Delta|V_2| &= 0.0125\Delta Q_{G1} + 0.0375\Delta Q_{G2} \end{aligned} \tag{7-32}$$

We make the following important observations:

*Observation* 1 The bus voltage magnitudes are *completely insensitive* to changes in the *real* bus powers.

*Observation* 2 The magnitude of the voltage at a particular bus is three times (375/125) as sensitive to changes in the reactive bus powers at that same bus as to changes at the other bus.

It should be emphasized that these results are valid only under assumed conditions, i.e.,

1. Light (actually zero) line load
2. Impedance-type loads

Other nominal operating conditions and load characteristics must be judged on their own merits.

We also emphasize the following important fact. The above sensitivity analysis assumed only that the state variable $x_1 = \delta_1$ had to be constant. This resulted in a jacobian $\mathbf{J}_x$ of order $2n - 1$. If we had required that another state variable, say, $x_2 = |V_1|$, also be constant, then the jacobian would be of order $2n - 2$. This would be the case if a voltage regulator keeps the voltage $|V_1|$ at a constant value. For every state variable that we thus constrain, we lose a corresponding row and column in the matrix $\mathbf{J}_x$.

## 7-3 DEFINITION OF THE LOAD FLOW PROBLEM

It should have been made clear from preceding discussions that a given power system subject to a given set of power demands at its various buses can be operated in an infinite number of "states" and still satisfy the given demands. For the systems engineer the job becomes one of selecting the best possible state out of the myriad of possibilities. He selects this particular one after comparing a number of possible candidates, obtained from what we shall refer to as a *load flow study*.

We concluded in the preceding section that the "state" of the system could be represented by a vector, the *state vector*, made up of the bus voltage magnitudes and phase angles. *With all the bus voltages known to both magnitude and phase, we in effect also know the line flows. In other words, we know the total structure of the power flow in the system.* Equally important is the knowledge, also obtained from a properly conducted load flow study, *how* a particular state or load flow structure is attained. The key here is the *control force vector* $\mathbf{u}$, containing $2n$ components, consisting of the real and reactive power outputs from the $P$ and $Q$ sources.

In terms of our earlier introduced "nominal" variables $\mathbf{x}^0$, $\mathbf{u}^0$, and $\mathbf{p}^0$, we can define a load flow study as follows:

*Assume a certain nominal bus load configuration* $\mathbf{p}^0$. *Specify then exactly* $2n$ *components of the two vectors* $\mathbf{x}^0$ *and* $\mathbf{u}^0$. *Solve the remaining* $2n$ *unspecified components by using the* $2n$ *SLFE. Finally, with all bus voltages known, compute all line flows.*

Having obtained from such a study a selection of possible load flow configurations, how do we compare them in order finally to select *the one* configuration that we should use?



We summarize some of the considerations on which such a selection must be based:

1. The total amount of real power in the network emanates from the generator stations, the location and size of which are fixed. The generation must equal the demand at each moment, and since this power must be divided between the generators in a *unique* ratio (Chap. 8) in order to achieve optimum economic operation, we conclude that the individual generator outputs must be closely maintained at predetermined set points. It is important to remember (Chap. 3) that the demand undergoes *slow but wide changes* throughout the 24 h of the day. We must therefore slowly, either continuously or in discrete steps, change these set points as the hours wear on. This means that a load flow configuration that fits the demand of a certain hour of the day may look quite different the next hour.
2. Certain transmission links can carry only certain amounts of power (Chap. 3), and we must make sure that we do not operate these links too close to their stability limits.
3. It is necessary to keep the voltage levels of certain buses at rather close tolerances. This can be achieved by proper scheduling of reactive powers.
4. If the power system is part of a larger pool, it must fulfill certain contractural power-scheduling commitments via its "tie lines" to neighboring systems.
5. The disturbances following a massive network fault can cause system outages, the effects of which can be minimized by proper prefault load flow strategies.
6. Load flow analyses are very important in the planning stages of new networks or additions to existing ones.

The overall load flow problem can be divided into the following subproblems, each of which we shall discuss separately.

1. The formulation of a suitable mathematical network model. The model must describe adequately the relationships between voltages and powers in the interconnected system. As before, we shall refer to this model as the SLFE.
2. A specification of the power and voltage constraints that must apply to the various buses of the network. (Discussed in Sec. 7-1.)
3. Numerical computation of the load flow equations subject to the above constraints. These computations should give us, with sufficient accuracy, the values of all bus voltages.
4. When all bus voltages have thus been determined, we must, finally, compute the actual load flows in all transmission lines.

## 7-4 NETWORK MODEL FORMULATION

The first step in any analysis of an electric energy system must be the formulation of a suitable network model. Such a model, exemplified by Eqs. (7-6), should relate a selected set of network voltages to another selected set of network currents or powers. In this section we discuss methods for network model formulation.

The networks that we shall be concerned with in our work are *very large*, containing often many hundreds, perhaps thousands, of individual network elements, and when we combine these individual elements to form the overall system model, we are faced with the need of performing tens of thousands of elementary algebraic operations. Human beings are known to perform such computations with relatively poor accuracy (only *one* single error is enough to make the entire analysis worthless), and it is therefore imperative to prepare the data in such a manner that a computer can do a maximum part of the job. A digital computer can perform billions of operations without one single error.

Clearly, there is a need to develop network assembly methods that are *systematic* and *amenable to computer use*. The *tabular* nature of matrices makes them particularly well adapted to digital computer programming, and it is therefore natural that we should search for matrix network assembly techniques. Also, the methods should possess *flexibility* with regard to network changes. If we wish to perform investigations of the effects of certain localized network changes, we should be able to do so with a minimum of computational effort.

### 7-4.1 A DEMONSTRATION EXAMPLE

Throughout the remaining part of this chapter we shall make reference to the sample system depicted in Fig. 7-2*a*. The system contains three buses† and three transmission lines. Bus 1 is a *mixed bus*, featuring both generation and load. Bus 2 is a *generator bus*, having generation but no load. Bus 3 is a *load bus*, having load but no real generation. This bus has, however, a bank of variable capacitors that generates reactive power. This three-bus system contains, actually, the most essential ingredients found on a larger system. On representing the lines with their $\pi$ equivalents, and the generators and loads with their bus power sources, we obtain the network shown in Fig. 7-2*b*.‡

The network in Fig. 7-2*b* has been redrawn in Fig. 7-3. In the process we have done some self-explanatory "lumping" of admittances, resulting in

† We could have used the two-bus system in Fig. 7-1. However, it is too small to demonstrate some general features that a three-bus system permits.

‡ Should we have transformers in each line end, we can still represent the link by a $\pi$ equivalent. See Exercise 7-4.



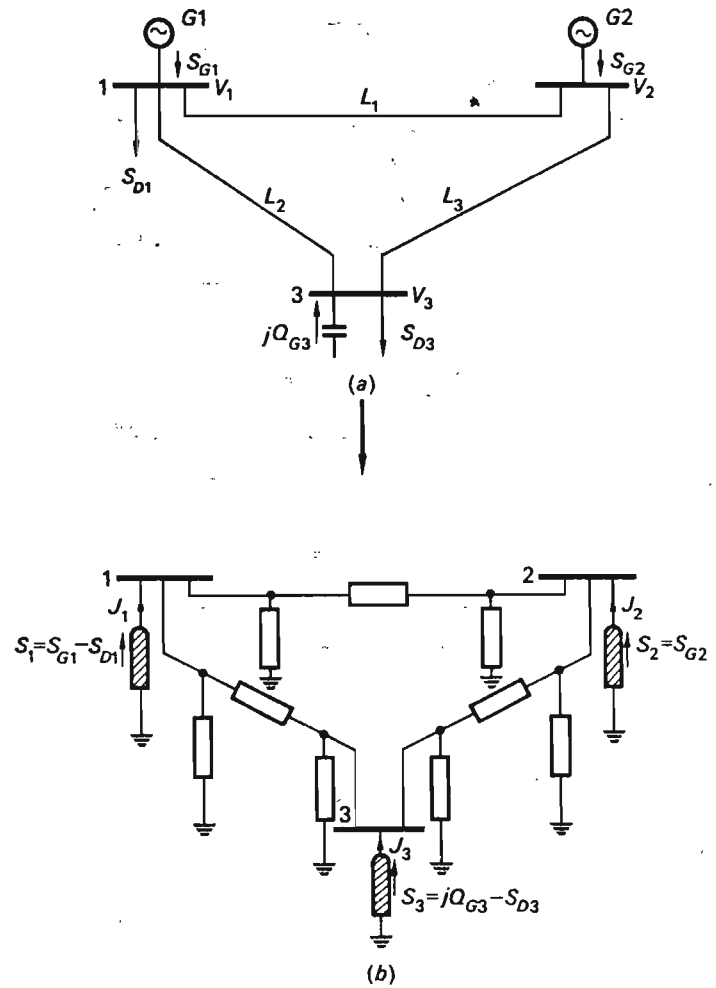


**Fig. 7-2** Three-bus sample system—its equivalent circuit.

the six branch admittances $Y_1, \ldots, Y_6$. Also, we have shown the buses as "nodes" to conform with usual network symbolism.

The source currents injected into the nodes by the three bus power sources are labeled $J_1$, $J_2$, and $J_3$. The bus voltages are called $V_1$, $V_2$, and $V_3$.

By requiring that the sum of all currents entering the three nodes be zero, we obtain the following three equations:

$$\begin{aligned} J_1 &= V_1 Y_1 + (V_1 - V_2) Y_5 + (V_1 - V_3) Y_4 \\ J_2 &= V_2 Y_2 + (V_2 - V_1) Y_5 + (V_2 - V_3) Y_6 \\ J_3 &= V_3 Y_3 + (V_3 - V_1) Y_4 + (V_3 - V_2) Y_6 \end{aligned} \tag{7-33}$$

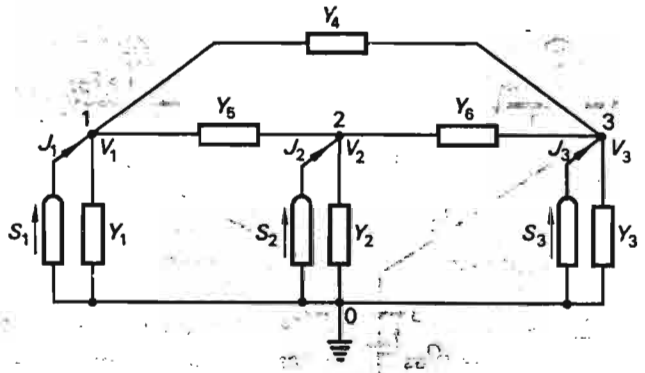


**Fig. 7-3** The network in Fig. 7-2 lumped and redrawn.

We introduce at this juncture the following admittances.

$$\begin{aligned} y_{11} &\triangleq Y_1 + Y_4 + Y_5 \quad & y_{23} &= y_{32} = -Y_6 \\ y_{22} &\triangleq Y_2 + Y_5 + Y_6 \quad & y_{13} &= y_{31} = -Y_4 \\ y_{33} &= Y_3 + Y_4 + Y_6 \quad & y_{12} &= y_{21} = -Y_5 \end{aligned} \tag{7-34}$$

Equations (7-33) can now be rewritten

$$\begin{aligned} J_1 &= y_{11}V_1 + y_{12}V_2 + y_{13}V_3 \\ J_2 &= y_{21}V_1 + y_{22}V_2 + y_{23}V_3 \\ J_3 &= y_{31}V_1 + y_{32}V_2 + y_{33}V_3 \end{aligned} \tag{7-35}$$

### 7-4.2 SLFE IN GENERAL FORM

Equations (7-35) obviously can be summarized in matrix form. In so doing we shall at the same time extend the equations to the general case of $n$ buses.

We introduce the following vectors and matrix:

$$\mathbf{J}_{\text{bus}} \triangleq \begin{bmatrix} J_1 \\ \cdot \\ \cdot \\ \cdot \\ J_n \end{bmatrix} \qquad \textit{bus current vector} \tag{7-36}$$

$$\mathbf{V}_{\text{bus}} \triangleq \begin{bmatrix} V_1 \\ \cdot \\ \cdot \\ \cdot \\ V_n \end{bmatrix} \qquad \textit{bus voltage vector} \tag{7-37}$$

$$\mathbf{Y}_{\text{bus}} \triangleq \begin{bmatrix} y_{11} & \cdots & y_{1n} \\ \cdots & \cdots & \cdots \\ y_{n1} & \cdots & y_{nn} \end{bmatrix} \qquad \textit{nodal bus admittance matrix} \tag{7-38}$$



We then have

$$\mathbf{J}_{\text{bus}} = \mathbf{Y}_{\text{bus}}\mathbf{V}_{\text{bus}} \tag{7-39}$$

This *nodal current equation* is a vector equation consisting of $n$ scalar equations. We remember that the bus *powers* $S_i$, rather than the bus *currents* $J_i$, are, in practice, specified, and if we replace $J_i$ by using the formula $J_i^* = S_i/V_i$, we can write Eq. (7-39) in the following *component form:*

$$\frac{P_i - jQ_i}{V_i^*} = y_{i1}V_1 + y_{i2}V_2 + \cdots + y_{in}V_n \qquad \text{for } i = 1, 2, \ldots, n \tag{7-40}$$

or

$$P_i - jQ_i - y_{i1}V_1V_i^* - y_{i2}V_2V_i^* - \cdots - y_{in}V_nV_i^* = 0 \qquad \text{for } i = 1, 2, \ldots, n \tag{7-41}$$

Eqs. (7-41) constitute the *general* form for the SLFE.

Sometimes it proves useful to write Eq. (7-39) in *inverted* form:

$$\mathbf{V}_{\text{bus}} = \mathbf{Z}_{\text{bus}}\mathbf{J}_{\text{bus}} \tag{7-42}$$

where the *nodal bus impedance matrix* $\mathbf{Z}_{\text{bus}}$ is obtained from $\mathbf{Y}_{\text{bus}}$ by matrix inversion; i.e.,

$$\mathbf{Z}_{\text{bus}} \triangleq \mathbf{Y}_{\text{bus}}^{-1} = \begin{bmatrix} z_{11} & \cdots & z_{1n} \\ \cdots & \cdots & \cdots \\ z_{n1} & \cdots & z_{nn} \end{bmatrix} \tag{7-43}$$

It should be noted that the $n$ load flow equations (7-41) are *complex*, and these $n$ equations therefore represent $2n$ *real* equations. The reader should note that in the special case $n = 2$, Eqs. (7-41) are identical with Eqs. (7-6).

The matrices $\mathbf{Y}_{\text{bus}}$ and/or $\mathbf{Z}_{\text{bus}}$ evidently constitute models of the passive portions of the $n$-bus networks, *in systematic form.* From Eqs. (7-34) we conclude the following simple rules for finding the elements of the $\mathbf{Y}_{\text{bus}}$ matrix:

*The diagonal element $y_{ii}$ is obtained as the algebraic sum of all admittances incident to node i.*

*The off-diagonal elements $y_{ij} = y_{ji}$ are obtained as the negative of the admittance connecting nodes i and j.*

The matrix pair $\mathbf{Y}_{\text{bus}}$ and $\mathbf{Z}_{\text{bus}}$ represent but one form of a network model. It is of great theoretical, pedagogical, and also practical value to dwell somewhat deeper on the topic of network matrix assembly, and for this reason we include the discussions that follow.

### 7-4.3 NETWORK TERMINOLOGY

In what follows we shall tacitly assume that voltages and currents are *sinusoidal*, which means that we can represent them as *phasors*, always

symbolized by capital-letter symbols. We shall, furthermore, assume that all *passive network elements* (resistors, inductors, capacitors) are *constants*, which fact, coupled with the first assumption, permits us to represent them in our analysis as *impedances* and/or *admittances*. We have seen how transformers and transmission lines can be represented in terms of such passive network elements. Voltages across and currents through *passive* network elements are symbolized by the letter symbols $V$ and $I$, respectively. Source currents are designated $J$.

By *branch* we shall understand a single impedance (admittance), or possibly a series or parallel combination of impedances (admittances). The exact meaning will always be clear from the context. A branch may or may not contain *active sources* (see below). For example, in our sample network (Fig. 7-3), we have grouped the network elements into six well-defined branches, three of which contain active sources. In general, a network will contain $b$ branches.

A *node* is a junction of two or more branches. In a power network, buses naturally constitute the network nodes, as was demonstrated in Fig. 7-3. Generally, our power networks will contain $m$ modes, one of which (always designated node 0) is at ground potential. A *path* is a specified train of branches. For example, in Fig. 7-3, one path starts at node 1 and continues via the branch $Y_5$ to node 2, and thence via branch $Y_6$ to node 3. This path is *open*. If we were to continue the path via the branch $Y_3$, the ground node, and branch $Y_1$ back to node 1, we would have a *closed* path. If each node in the closed path connects two, and only two, branches, the closed path is *simple*. A simple closed path is also referred to as a *loop*. The closed path we just exemplified constitutes a loop.

A passive network attains practical significance only if we insert *sources*, or *generators*, into it. This is particularly true in EESE. From courses in circuit theory, the student no doubt is already familiar with the concepts of *voltage* and *current sources*. These devices possess the assumed property of delivering at their terminals a specified voltage $E$ and current $J$, respectively, *independently of the state of the rest of the network. Physical* sources never behave in this idealized manner. Take a synchronous generator, for example. We know from our discussion in Chap. 4 that if its prime mover torque is kept constant, its real power output $P_G$ is also constant, *independent of fluctuations in its bus voltage.*† At the same time its reactive power output $Q_G$ will fluctuate with the bus voltage *even if we keep the field current constant*. Clearly, the synchronous generator has the properties of neither a voltage nor a current source.

A synchronous generator therefore represents a source the properties of which lie somewhere in between those of a current and a voltage source.

† We assume, of course, that the frequency is approximately constant.



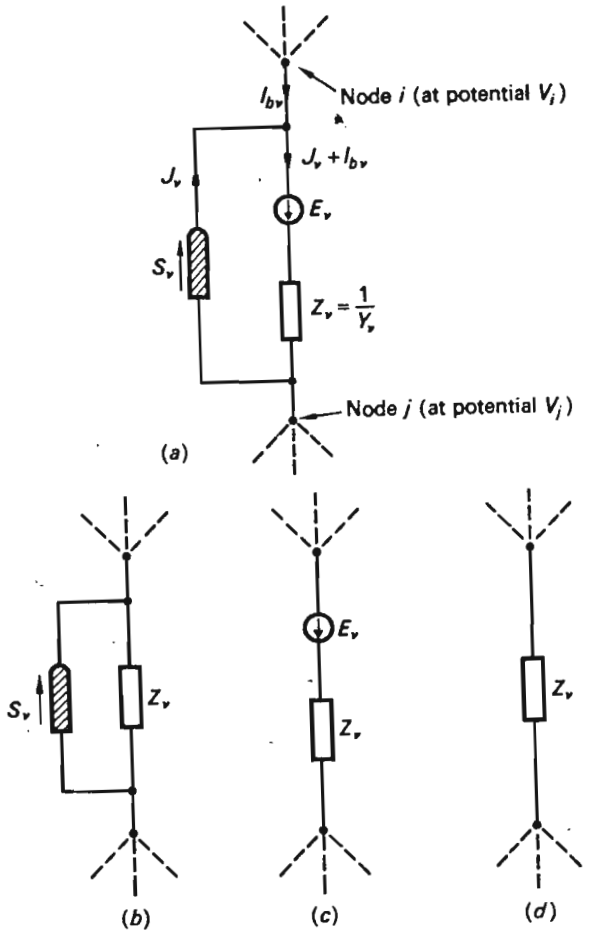


**Fig. 7-4** Primitive networks. (*a*) Passive and active elements in most general configuration. (*b*) Only bus power source included. (*c*) Only voltage source included. (*d*) No sources included.

We therefore give it a special symbol (Fig. 7-1*c*) and *agree also* to include in this symbol all "negative generation," i.e., "load" that is tapped from the bus in question. Since typical loads contain a high percentage of synchronous motor load, this is clearly a logical decision.

It must be added that although we find the *bus power source* just defined to be the obvious source representation for the synchronous machine in *steady state*, this does not necessarily apply to the machine under *transient* conditions. For example, we shall find in Chap. 10 that a voltage source is a much better representation for short-circuit analysis.

### 7-4.4 PRIMITIVE NETWORKS

A network, as exemplified in Fig. 7-3, is built by interconnection of individual branches, each of which, as we pointed out earlier, could consist of passive and/or active network elements.

Figure 7-4*a* shows a branch that contains active and passive elements in a most general combination. The reader should note that by setting $E_\nu$ or $S_\nu$ or both equal to zero, we obtain the three *primitive networks* depicted in Fig. 7-4*b* to *d*.

Assume that the branch in question (branch $\nu$) connects the nodes $i$ and $j$, having the potentials $V_i$ and $V_j$, respectively. If we define the *branch voltage* for branch $\nu$

$$V_{b\nu} \triangleq V_i - V_j \tag{7-44}$$

we can write the following voltage relation for this branch:

$$V_{b\nu} + E_\nu = Z_\nu(I_{b\nu} + J_\nu) \tag{7-45}$$

The *branch current* $I_{b\nu}$ is defined positive in the direction $i \rightarrow j$.

By systematically writing this equation for branches $1, 2, \ldots, b$, we get

$$\begin{aligned} V_{b1} + E_1 &= Z_1(I_{b1} + J_1) \\ V_{b2} + E_2 &= Z_2(I_{b2} + J_2) \\ &\cdots\cdots\cdots\cdots\cdots \\ V_{bb} + E_b &= Z_b(I_{bb} + J_b) \end{aligned} \tag{7-46}$$

We introduce at this juncture the vector and matrix quantities

$$\mathbf{V}_b \triangleq \begin{bmatrix} V_{b1} \\ \cdot \\ \cdot \\ \cdot \\ V_{bb} \end{bmatrix} \qquad \textit{branch voltage vector} \tag{7-47}$$

$$\mathbf{I}_b \triangleq \begin{bmatrix} I_{b1} \\ \cdot \\ \cdot \\ \cdot \\ I_{bb} \end{bmatrix} \qquad \textit{branch current vector} \tag{7-48}$$

$$\mathbf{J}_b \triangleq \begin{bmatrix} J_1 \\ \cdot \\ \cdot \\ \cdot \\ J_b \end{bmatrix} \quad \text{and} \quad \mathbf{E}_b \triangleq \begin{bmatrix} E_1 \\ \cdot \\ \cdot \\ \cdot \\ E_b \end{bmatrix} \qquad \textit{branch source vectors} \tag{7-49}$$



and

$$\mathbf{Z} \triangleq \begin{bmatrix} Z_1 & & 0 \\ & \cdot & \\ & & \cdot \\ 0 & & Z_b \end{bmatrix} \qquad \mathbf{Y} \triangleq \mathbf{Z}^{-1} = \begin{bmatrix} \frac{1}{Z_1} & & 0 \\ & \cdot & \\ & & \cdot \\ 0 & & \frac{1}{Z_b} \end{bmatrix} \tag{7-50}$$

$\mathbf{Z}$ and $\mathbf{Y}$ are referred to as the *primitive impedance* and *admittance matrices*, respectively.

In terms of the above vectors and matrices, we can write the system of Eqs. (7-46) in the following compact form:

$$\mathbf{V}_b + \mathbf{E}_b = \mathbf{Z}(\mathbf{I}_b + \mathbf{J}_b) \quad \text{or} \quad \mathbf{Y}(\mathbf{V}_b + \mathbf{E}_b) = \mathbf{I}_b + \mathbf{J}_b \tag{7-51}$$

Should no voltage sources be present, Eq. (7-51) reduces to

$$\mathbf{V}_b = \mathbf{Z}(\mathbf{I}_b + \mathbf{J}_b) \quad \text{or} \quad \mathbf{Y}\mathbf{V}_b = \mathbf{I}_b + \mathbf{J}_b \tag{7-52}$$

If only voltage sources are present Eq. (7-51) takes the form

$$\mathbf{V}_b + \mathbf{E}_b = \mathbf{Z}\mathbf{I}_b \quad \text{or} \quad \mathbf{Y}(\mathbf{V}_b + \mathbf{E}_b) = \mathbf{I}_b \tag{7-53}$$

And finally, if we have only passive branches

$$\mathbf{V}_b = \mathbf{Z}\mathbf{I}_b \quad \text{or} \quad \mathbf{Y}\mathbf{V}_b = \mathbf{I}_b \tag{7-54}$$

Note that the $\mathbf{Z}$ and $\mathbf{Y}$ matrices are of *diagonal* type. (Only if there were magnetic coupling between the branches would the matrices contain nonzero off-diagonal elements. This would, for instance, be the case if two lines in the circuit in Fig. 7-1 were running parallel for an appreciable distance.)

### 7-4.5 LINEAR NETWORK GRAPHS

If in a network we replace all branches by lines, we obtain what is called a *linear graph*, or simply *graph*, of the network. For example, Fig. 7-5 shows a graph of our network in Fig. 7-3. Such a graph depicts the *topological* structure of the network; i.e., it shows in simplest possible form the interconnection of the various branches.† The graph in Fig. 7-5 can be divided into *subgraphs*, a couple of which are shown in Fig. 7-6.

A graph is *connected* if and only if there exists a path between *every* node of the graph. If we assign a *direction*, or polarity, to a branch

† In linear graph theory the term *edge*, or *element*, is used for branch, and *vertex* for node. However, we shall not introduce more terms than necessary and shall therefore use the designations "branch" and "node."

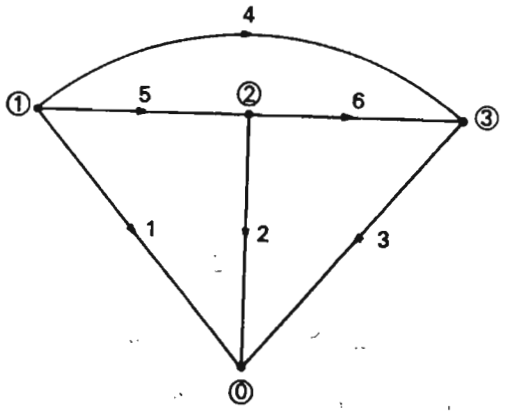


**Fig. 7-5** Linear graph of circuit in Fig. 7-3.

(Fig. 7-5), it is said to be *oriented. For convenience, we shall always use a direction that coincides with the assumed positive direction of the branch current.*

For our later discussions we shall find it useful to consider a particular type of connected subgraph, the so-called *tree. A tree is a connected subgraph that contains all nodes of the graph but no loops.* In Fig. 7-7*a* and *b*, we show two possible tree graphs for our example network. (Several more can be found, and the reader is encouraged to find them.) The branches belonging to a tree are referred to as *tree branches.* The branches *not* belonging to the tree are referred to as *links* (or link branches), and they constitute a subgraph (not necessarily connected) referred to as a *co-tree* (Fig. 7-7*c* and *d*).

### 7-4.6 CHOICE OF LINEARLY INDEPENDENT NETWORK VARIABLES

Linear network graphs provide us with a means for systematic network model assembly. A basic problem in deriving mathematical models for large and complex networks is to designate a set of voltage and current variables which *completely describe* the network; i.e., *the chosen variables must permit us to compute the currents and voltages in all branches of the network.* The most obvious choice of variables would be the branch

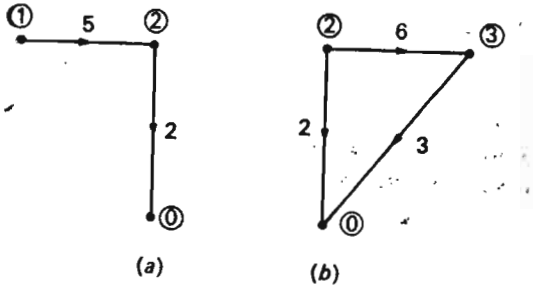


**Fig. 7-6** Subgraphs of linear graph in Figure 7-5.



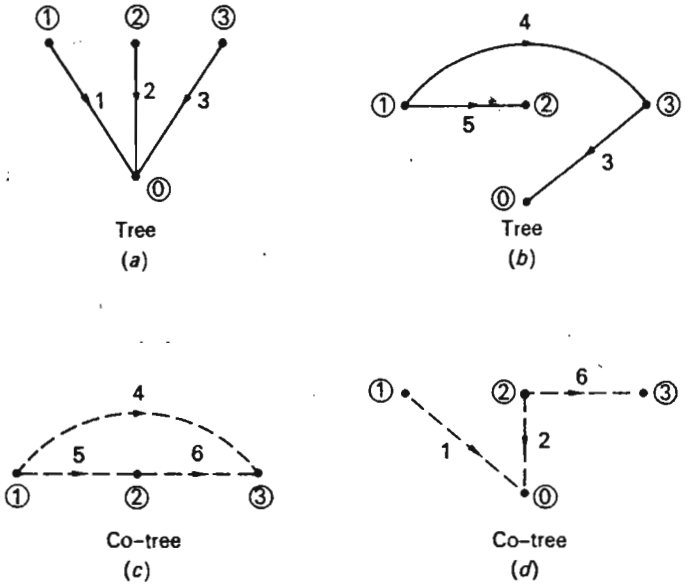


**Fig. 7-7** Trees and co-trees.

currents and branch voltages themselves. For example, our example system contains six branches, and we could therefore designate the six *branch voltages* $V_{b1}, \ldots, V_{b6}$ and the six *branch currents* $I_{b1}, \ldots, I_{b6}$, for a total of twelve variables.

This is not a practical choice, however, and it would lead us into analytical troubles, because this set of variables actually *overspecifies* the network. By application of Kirchhoff's voltage law (KVL) and current law (KCL) to the loops and nodes of the network, we can easily demonstrate this point. For example, by applying KVL to the loop formed by branches 4 to 6, we obtain

$$V_{b4} - V_{b6} - V_{b5} = 0 \tag{7-55}$$

and if we apply KCL to node 0, we get

$$I_{b1} + I_{b2} + I_{b3} = 0 \tag{7-56}$$

Equation (7-55) implies that if, say, $V_{b5}$ and $V_{b6}$ are known, then automatically $V_{b4}$ is known also. A similar statement can be made about the currents in branches 1 to 3.

Among the 12 chosen variables, we thus have a large number of *redundant* ones.

*The problem we are faced with is that of selecting a minimum, or zero-redundancy, set of current or voltage variables which suffice to give us information about all branch voltages and currents.*†

How should we go about finding such a set? And how many variables does it contain?

Answers to both these questions can be obtained by considering the concept of tree, defined above.

In the following discussion we shall refer to the specific graph in Fig. 7-5 and the specific tree graph in Fig. 7-7*a*.

We note first that if a network has $m$ nodes and $b$ branches ($m = 4$ and $b = 6$, in our case), the number of tree branches‡ $t$ and link branches $l$ are:

$$t = m - 1 \tag{7-57}$$

$$l = b - t = b - m + 1 \tag{7-58}$$

Thus, for the graph in Fig. 7-5, we have

$$t = 3$$

$$l = 3$$

(In general, we do not of course have an equal number of link and tree branches.)

### 7-4.7 NETWORK VARIABLES IN LOOP FRAME OF REFERENCE

When we add the link branches, one by one to the tree, as shown in Fig. 7-8, we note that we form, one by one, new loops, each of which is characterized by the fact that it contains one, and only one, link branch. We obtain $l$ such *basic loops*. Note that if we had chosen a different tree, the basic loops would have looked different.

**Loop currents** We associate now each basic loop with a circulating current, *a loop current*, having a direction coinciding with that of the associated link branch. In our example we obtain thus three loop currents $I_1$, $I_2$, and $I_3$ (Fig. 7-8). In the general case, we have $l$ loop currents, constituting a *loop-current vector* of dimension $l$.

$$\mathbf{I}_{\text{loop}} \triangleq \begin{bmatrix} I_1 \\ I_2 \\ \cdot \\ \cdot \\ \cdot \\ I_l \end{bmatrix} \tag{7-59}$$

† A mathematician talks about a "linearly independent" set.

‡ Note that $t$ equals $n$, that is, the number of buses in the network.



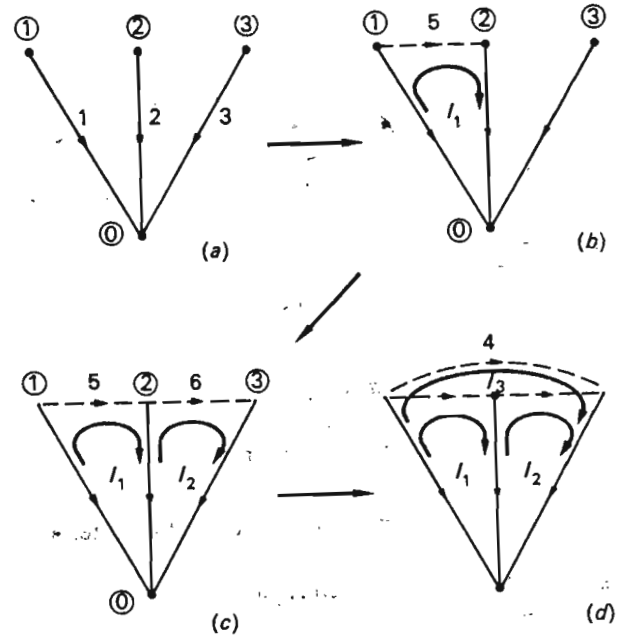


**Fig. 7-8** Formation of basic loops for circuit in Fig. 7-3.

*The $l$ loop currents thus defined constitute a zero-redundancy set of network variables.*

The truth in this statement is appreciated if we realize that:

1. Knowledge of the $l$ loop currents permits us to compute *all* branch currents (and therefore all branch voltages, the branch impedances being assumed known), since for topological reasons the $l$ loops must involve *all* branches.
2. Since for topological reasons each loop involves only one link and there are $l$ links, we realize that this must be the minimum number of variables.

**Loop incidence matrix** For our specific example system we obtain from Fig. 7-8*d* the following relations between branch and loop currents:

$$\begin{aligned} I_{b1} &= -I_1 - I_3 \\ I_{b2} &= I_1 - I_2 \\ I_{b3} &= I_2 + I_3 \\ I_{b4} &= I_3 \\ I_{b5} &= I_1 \\ I_{b6} &= I_2 \end{aligned} \tag{7-60}$$

or in matrix form,

$$\mathbf{I}_b = \mathbf{C}\mathbf{I}_{loop} \tag{7-61}$$

where the *loop incidence matrix* $\mathbf{C}$ has the value

$$\mathbf{C} = \begin{bmatrix} -1 & 0 & -1 \\ 1 & -1 & 0 \\ 0 & 1 & 1 \\ 0 & 0 & 1 \\ 1 & 0 & 0 \\ 0 & 1 & 0 \end{bmatrix} \tag{7-62}$$

*This $b \times l$ matrix gives the one-to-one correspondence between the branches and the basic loops of the network.* Its elements $c_{ij}$ are chosen in accordance with the following rules:

$c_{ij} = 1$ if the $i$th branch is part of and oriented in the same direction as the $j$th basic loop.
$c_{ij} = -1$ if the $i$th branch is part of and oriented in the opposite direction to the $j$th basic loop.
$c_{ij} = 0$ if the $i$th branch is not part of the $j$th basic loop.

**Finding $\mathbf{I}_{loop}$** Being thus convinced that the set of loop currents constitutes a suitable set of network variables, we must now find a way of computing them from available data about network parameters and sources. For that purpose we start with the vector equation (7-51), replacing $\mathbf{I}_b$ with $\mathbf{I}_{loop}$ in accordance with

$$\mathbf{V}_b + \mathbf{E}_b = \mathbf{Z}\mathbf{I}_b + \mathbf{Z}\mathbf{J}_b = \mathbf{Z}\mathbf{C}\mathbf{I}_{loop} + \mathbf{Z}\mathbf{J}_b \tag{7-63}$$

Each term in this vector equation is a $b$-dimensional vector, and we are therefore allowed to premultiply each term by the $l \times b$ matrix $\mathbf{C}^T$, that is, the *transpose* of $\mathbf{C}$:

$$\mathbf{C}^T\mathbf{V}_b + \mathbf{C}^T\mathbf{E}_b = \mathbf{C}^T\mathbf{Z}\mathbf{C}\mathbf{I}_{loop} + \mathbf{C}^T\mathbf{Z}\mathbf{J}_b \tag{7-64}$$

Each term in this new vector equation is an $l$-dimensional vector.

At this juncture we make a very important observation about the $l$-dimensional vector $\mathbf{C}^T\mathbf{V}_b$: *Each row of this vector represents the algebraic sum of branch voltages around a basic loop.* For example, the first row reads

$$-V_{b1} + V_{b2} + V_{b5}$$

In accordance with KVL, each such sum must add up to zero, and we thus get

$$\mathbf{C}^T\mathbf{V}_b = \mathbf{0} \tag{7-65}$$



Using identical reasoning, we conclude that each component of the vector $\mathbf{C}^T\mathbf{E}_b$ represents the algebraic sum of voltage sources around the basic loops. For brevity, we give this vector a new name, $\mathbf{E}_{loop}$, that is,

$$\mathbf{C}^T\mathbf{E}_b \triangleq \mathbf{E}_{loop} \tag{7-66}$$

Finally, let us, for simplicity, assume that only voltage type sources are present; i.e., we assume

$$\mathbf{J}_b = \mathbf{0} \tag{7-67}$$

If we substitute Eqs. (7-65) to (7-67) into Eq. (7-64), we get

$$\mathbf{E}_{loop} = \mathbf{C}^T\mathbf{Z}\mathbf{C}\mathbf{I}_{loop} \tag{7-68}$$

The triple product matrix $\mathbf{C}^T\mathbf{Z}\mathbf{C}$ is of dimension $l \times l$, and we shall name it the *loop impedance matrix* and give it the shorter name $\mathbf{Z}_{loop}$, that is,

$$\mathbf{Z}_{loop} \triangleq \mathbf{C}^T\mathbf{Z}\mathbf{C} \tag{7-69}$$

and obtain then the final expression

$$\mathbf{E}_{loop} = \mathbf{Z}_{loop}\mathbf{I}_{loop} \tag{7-70}$$

This equation will be referred to as the *loop voltage equation* and *constitutes our network model in the loop frame of reference.*

We sometimes find it more convenient to write it in inverted form. We define for that purpose the *loop admittance matrix*

$$\mathbf{Y}_{loop} \triangleq \mathbf{Z}_{loop}^{-1} \tag{7-71}$$

and obtain then directly from Eq. (7-70)

$$\mathbf{I}_{loop} = \mathbf{Y}_{loop}\mathbf{E}_{loop} \tag{7-72}$$

**Example 7-2** Let us find the loop impedance matrix for our three-bus example network in Fig. 7-2. Since we assume that we know the branch impedances $Z_1 \cdots Z_6$, we first form the square primitive impedance matrix

$$\mathbf{Z} = \begin{bmatrix} Z_1 & & & & & 0 \\ & Z_2 & & & & \\ & & Z_3 & & & \\ & & & Z_4 & & \\ & & & & Z_5 & \\ 0 & & & & & Z_6 \end{bmatrix}$$

We then have

$$\mathbf{ZC} = \begin{bmatrix} -Z_1 & 0 & -Z_1 \\ Z_2 & -Z_2 & 0 \\ 0 & Z_3 & Z_3 \\ 0 & 0 & Z_4 \\ Z_5 & 0 & 0 \\ 0 & Z_6 & 0 \end{bmatrix}$$

and finally,

$$\mathbf{Z}_{\text{loop}} = \mathbf{C}^T\mathbf{Z}\mathbf{C} = \begin{bmatrix} Z_1 + Z_2 + Z_5 & -Z_2 & Z_1 \\ -Z_2 & Z_2 + Z_3 + Z_6 & Z_3 \\ Z_1 & Z_3 & Z_1 + Z_3 + Z_4 \end{bmatrix}$$

Note the inherent simplicity in these operations. We first tabulate the diagonal **Z** matrix; whereupon we perform the matrix multiplications by the **C** and $\mathbf{C}^T$ matrices that contain only ones and zeros.

To find the loop currents, we must invert the $\mathbf{Z}_{\text{loop}}$ matrix to obtain $\mathbf{Y}_{\text{loop}}$, and then perform the matrix product called for in Eq. (7-72). Note that all these matrix operations are "routine" on digital computers. Subroutines are available for matrix transposition, multiplication, and inversion.

### 7-4.8 NETWORK VARIABLES IN BUS FRAME OF REFERENCE

In the loop of frame reference we utilize the $l$ basic loop currents as our network variables. Note that these variables are identical with the *l link-branch currents.*

Another useful set of network variables are the *t tree-branch voltages.* We may easily confirm, by using a topological reasoning similar to that we used in the case of loop currents, that from these variables we can deduce *all* other branch voltages (and currents) in the network, and also confirm that they constitute a "nonredundant" set.

We obtain a particularly important case if we limit attention to the tree graph, which we can construct by choosing one node (always the ground node, in our case) as reference node and making all the $t = m - 1$ tree branches incident to that node, as demonstrated in Fig. 7-7*a*. *We realize that the t tree branch voltages in this case are identical with our bus voltages defined earlier* [Eq. (7-37)].

**Bus incidence matrix** For our specific example system in Fig. 7-7*a* we obtain the following relations between the six branch voltages and the three bus voltages $V_1$, $V_2$, and $V_3$:

$$\begin{aligned} V_{b1} &= V_1 \\ V_{b2} &= V_2 \\ V_{b3} &= V_3 \\ V_{b4} &= V_1 - V_3 \\ V_{b5} &= V_1 - V_2 \\ V_{b6} &= V_2 - V_3 \end{aligned} \tag{7-73}$$

or in matrix form,

$$\mathbf{V}_b = \mathbf{A}\mathbf{V}_{\text{bus}} \tag{7-74}$$



where the *bus incidence matrix* **A** has the value

$$\mathbf{A} = \begin{bmatrix} 1 & 0 & 0 \\ 0 & 1 & 0 \\ 0 & 0 & 1 \\ 1 & 0 & -1 \\ 1 & -1 & 0 \\ 0 & 1 & -1 \end{bmatrix}$$

This $b \times t$ matrix gives the one-to-one correspondence between the branches and the buses of the network. Its elements $a_{ij}$ are chosen in accordance with the following rules:

$a_{ij} = 1$ if the $i$th branch is incident to and oriented away from the $j$th node (bus).
$a_{ij} = -1$ if the $i$th branch is incident to but oriented toward the $j$th node (bus).
$a_{ij} = 0$ if the $i$th branch is not incident to the $j$th node (bus).

**Finding $\mathbf{Y}_{\text{bus}}$** Let us now consider a network containing only bus power sources. Upon substitution of Eq. (7-74) into Eq. (7-52), we obtain:

$$\mathbf{Y}\mathbf{A}\mathbf{V}_{\text{bus}} = \mathbf{I}_b + \mathbf{J}_b \tag{7-75}$$

Each term in this equation is a $b$-dimensional vector, and we are therefore allowed to premultiply each term by the $t \times b$ matrix $\mathbf{A}^T$; that is,

$$\mathbf{A}^T\mathbf{Y}\mathbf{A}\mathbf{V}_{\text{bus}} = \mathbf{A}^T\mathbf{I}_b + \mathbf{A}^T\mathbf{J}_b \tag{7-76}$$

Each component of the $t$-dimensional vector $\mathbf{A}^T\mathbf{I}_b$ consists of the algebraic sum of the branch currents entering the nodes $1, 2, \ldots, n$, and in accordance with the KCL we must therefore have

$$\mathbf{A}^T\mathbf{I}_b = \mathbf{0} \tag{7-77}$$

Similarly, each component of the vector $\mathbf{A}^T\mathbf{J}_b$ is identified as the algebraic sum of all *source* currents injected into nodes $1, 2, \ldots, n$. These components are thus recognized as the *bus currents* defined in Eq. (7-36), and we therefore have

$$\mathbf{A}^T\mathbf{J}_b = \mathbf{J}_{\text{bus}} \tag{7-78}$$

Equation (7-76) therefore reduces to

$$\mathbf{A}^T\mathbf{Y}\mathbf{A}\mathbf{V}_{\text{bus}} = \mathbf{J}_{\text{bus}} \tag{7-79}$$

This last equation is immediately recognized as our old friend the *nodal current equation* (7-39). Following a different but more systematic approach, we have in effect arrived at a new expression for the nodal bus admittance matrix:

$$\mathbf{Y}_{bus} = \mathbf{A}^T\mathbf{Y}\mathbf{A} \tag{7-80}$$

The symmetry between Eqs. (7-69) and (7-80) is obvious. What we said about methods for computing $\mathbf{Z}_{loop}$ applies equally well to $\mathbf{Y}_{bus}$.

**Example 7-3** We shall find $\mathbf{Y}_{bus}$ for our three-bus example system and start by forming the primitive square admittance matrix

$$\mathbf{Y} = \begin{bmatrix} Y_1 & & & & & & 0 \\ & Y_2 & & & & & \\ & & Y_3 & & & & \\ & & & Y_4 & & & \\ & & & & Y_5 & & \\ 0 & & & & & & Y_6 \end{bmatrix}$$

Note that each of the diagonal elements is the inverse of the corresponding elements of the Z matrix in Example 7-2.

We get next

$$\mathbf{YA} = \begin{bmatrix} Y_1 & 0 & 0 \\ 0 & Y_2 & 0 \\ 0 & 0 & Y_3 \\ Y_4 & 0 & -Y_4 \\ Y_5 & -Y_5 & 0 \\ 0 & Y_6 & -Y_6 \end{bmatrix}$$

And finally,

$$\mathbf{Y}_{bus} = \mathbf{A}^T\mathbf{Y}\mathbf{A} = \begin{bmatrix} Y_1 + Y_4 + Y_5 & -Y_5 & -Y_4 \\ -Y_5 & Y_2 + Y_5 + Y_6 & -Y_6 \\ -Y_4 & -Y_6 & Y_0 + Y_4 + Y_6 \end{bmatrix}$$

The elements of this matrix agree with our previous results, Eq. (7-34).

## 7-5 A LOAD FLOW SAMPLE STUDY

Taking stock of our progress, we conclude that we have so far covered ground as follows:

1. We have developed systematic methods of assembling the network models and obtaining the SLFE for general-size networks.



2. We have discussed the general characteristics of the SLFE and, in particular, performed a logic classification of the large number of system variables.
3. We have discussed the important matter of a priori specification of control and state variables.
4. By means of sensitivity analysis we have also learned how changes in our control and disturbance variables affect the state variables.

The remaining portion of this chapter will be devoted to the problem of actually *solving* the SLFE. In a practical situation we would invariably make use of computer for this task, and we shall, in fact, devote considerable time to this special aspect of the problem.

Presently, we shall introduce the reader to the problem of solving the SLFE by means of an example, so simplified so as to eliminate the need for the computer.

The simplifications are of two kinds:

1. We shall neglect all line resistances, which will considerably reduce the complexity of the load flow equations.
2. The line loads are of low magnitude, resulting in small-magnitude power angles; so small, in fact, that we may set $\sin\delta \approx \delta$. This approximation will linearize our nonlinear SLFE and make them amenable to analytic solution.

**Network data** Consider the three-bus sample system in Fig. 7-2, previously discussed. Let each of the three transmission lines be characterized by the data as computed for the 30-mile 120-kV line in Example 6-9 and shown in Fig. 6-20, *with the following simplifying modifications:*

1. Neglect the shunt admittance.
2. Round off the value of the series impedance to $Z = j0.1$ pu.

Under these assumptions the $\mathbf{Y}_{bus}$ matrix† (Example 7-3) takes on the value

$$\mathbf{Y}_{bus} = \begin{bmatrix} -j20 & j10 & j10 \\ j10 & -j20 & j10 \\ j10 & j10 & -j20 \end{bmatrix} \tag{7-81}$$

† Although not evident from this simple example, the $\mathbf{Y}_{bus}$ matrix is, for systems of realistic size, *very sparse*, i.e., most of its elements are zeros. The element $y_{ij}$ equals zero when no line exists between buses $i$ and $j$. For a system containing 100 buses, the degree of sparsity may be in excess of 95 percent, i.e., more than 95 percent of the 10,000 elements are zeros. This sparsity feature facilitates to a great extent the numerical computation of the SLFE.

(We recall that the admittances are expressed in per units, based on 50 MVA and 120 kV.)

**Bus voltage specifications** It is specified that all three bus voltages be kept at a magnitude of 1.00 pu; i.e., we require that

$$|V_1| = |V_2| = |V_3| = 1.00 \text{ pu}$$

**Bus power specifications** The bus powers at the three buses are specified in Table 7-1 (compare also Fig. 7-9). All power data are in per-unit form, on 50-MVA base.

**Table 7-1**

| *Bus* | *Real demand* | *Reactive demand* | *Real generation* | *Reactive generation* |
|---|---|---|---|---|
| 1 | $P_{D1} = 1.0$ | $Q_{D1} = 0.5$ | $P_{G1} = 0.5$ | $Q_{G1}$ (unspecified) |
| 2 | $P_{D2} = 0$ | $Q_{D2} = 0$ | $P_{G2} = 1.5$ | $Q_{G2}$ (unspecified) |
| 3 | $P_{D3} = 1.0$ | $Q_{D3} = 1.0$ | $P_{G3} = 0$ | $Q_{G3}$ (unspecified) |

We make the following observations in regard to the tabulated voltage and power specification:

1. Having specified *all* bus voltage magnitudes, it is necessary that we have available at *each* bus *controllable* $Q$ sources. At buses 1 and 2, we designate this job to the generators. At bus 3 our $Q$ source is a switchable shunt capacitor.

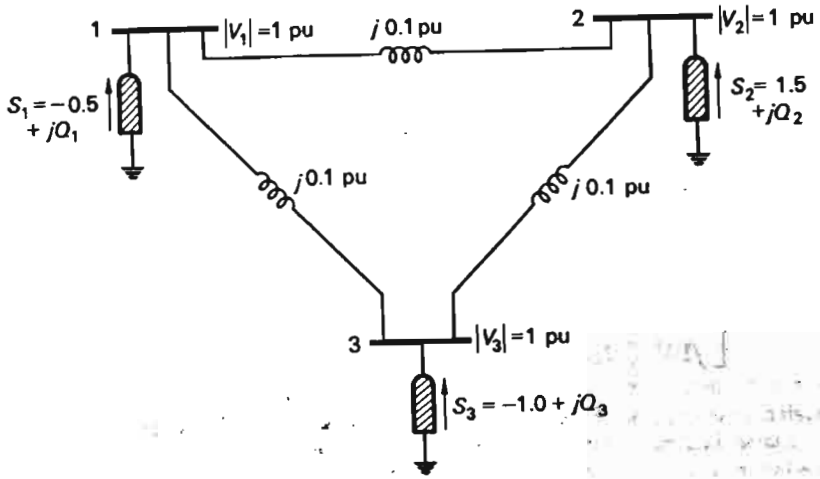


**Fig. 7-9** Lossless three-bus example system.



2. Since all network losses are assumed zero, the total real demand (= 2.0 pu) must equal the total real generation. Knowing thus a priori the value of $P_{G1}$, this means, in effect, that instead of $2n = 2 \times 3 = 6$ unknowns, we have in reality only 5. As a result, our six load flow equations will reduce to five. We shall later confirm this observation.
3. Due to the reactive losses in the line reactances, the total reactive demand (1.5 pu) will *not* equal the total reactive generation.
4. Our unknown state and control variables are in this case $\delta_2$, $\delta_3$, $Q_{G1}$, $Q_{G2}$, and $Q_{G3}$. In reference to observation 2 above, $P_{G1}$ is *not* an a priori unknown control variable.

For the bus powers we now have

$$\begin{aligned} S_1 &= P_1 + jQ_1 = -0.5 + j(Q_{G1} - 0.5) \\ S_2 &= P_2 + jQ_2 = 1.5 + jQ_{G2} \\ S_3 &= P_3 + jQ_3 = -1.0 + j(Q_{G3} - 1.0) \end{aligned} \tag{7-82}$$

**Load flow equations** By using the admittance data of Eq. (7-81) and the bus power data of Eqs. (7-82), we can write the static load flow equations (7-41), in this case:

$$\begin{aligned} -0.5 - jQ_1 &= -j20V_1V_1^* + j10V_2V_1^* + j10V_3V_1^* \\ 1.5 - jQ_2 &= j10V_1V_2^* - j20V_2V_2^* + j10V_3V_2^* \\ -1.0 - jQ_3 &= j10V_1V_3^* + j10V_2V_3^* - j20V_3V_3^* \end{aligned} \tag{7-83}$$

At this time we designate bus 1 as our reference bus, or slack bus;† i.e., we arbitrarily choose the phase angle $\delta_1 = \angle V_1 = 0$. We also introduce the phase angles $\delta_2$ and $\delta_3$ for $\angle V_2$ and $\angle V_3$, respectively, and for the bus voltages we thus can write

$$\begin{aligned} V_1 &= |V_1| = 1.00 \quad \text{pu} \\ V_2 &= |V_2|\, e^{j\delta_2} = e^{j\delta_2} = \cos\delta_2 + j\sin\delta_2 \quad \text{pu} \\ V_3 &= |V_3|\, e^{j\delta_3} = e^{j\delta_3} = \cos\delta_3 + j\sin\delta_3 \quad \text{pu} \end{aligned} \tag{7-84}$$

Equations (7-83) can therefore be written

$$\begin{aligned} -0.5 - jQ_1 &= -j20 + j10(\cos\delta_2 + j\sin\delta_2) + j10(\cos\delta_3 + j\sin\delta_3) \\ 1.5 - jQ_2 &= j10(\cos\delta_2 - j\sin\delta_2) - j20 \\ &\quad + j10[\cos(\delta_3 - \delta_2) + j\sin(\delta_3 - \delta_2)] \\ -1.0 - jQ_3 &= j10(\cos\delta_3 - j\sin\delta_3) + j10[\cos(\delta_2 - \delta_3) \\ &\quad + j\sin(\delta_2 - \delta_3)] - j20 \end{aligned} \tag{7-85}$$

† Since we have no real losses in this case, the term "slack bus" is less appropriate.

If we separate the real and imaginary parts of these last equations, we get the following six real equations:

$$\begin{aligned} -0.5 &= -10 \sin \delta_2 - 10 \sin \delta_3 \\ 1.5 &= 10 \sin \delta_2 - 10 \sin (\delta_3 - \delta_2) \\ -1.0 &= 10 \sin \delta_3 - 10 \sin (\delta_2 - \delta_3) \\ -Q_1 &= -20 + 10 \cos \delta_2 + 10 \cos \delta_3 \\ -Q_2 &= 10 \cos \delta_2 - 20 + 10 \cos (\delta_3 - \delta_2) \\ -Q_3 &= 10 \cos \delta_3 + 10 \cos (\delta_2 - \delta_3) - 20 \end{aligned} \tag{7-86}$$

We note that we have *six* equations for *five* unknowns ($\delta_2, \delta_3, Q_1, Q_2, Q_3$). This apparent inconsistency was explained earlier. Due to the lossless system, $P_{G1}$ is known a priori. Of the six equations, one must be superfluous. A check reveals that if we add the first and third equations, we obtain the second, which means in effect that, instead of six equations, we have only five independent ones.

**Solution of load flow equations** The solution of Eq. (7-86) offers no principal difficulties. We obtain $\delta_2$ and $\delta_3$ from the first three (actually two) equations, and knowledge of these phase angles then immediately yields $Q_1$, $Q_2$, and $Q_3$. If we realize that the angles $\delta_2$ and $\delta_3$ are relatively small (why?), we can linearize the first equations as follows:

$$\begin{aligned} -0.5 &\approx -10\delta_2 - 10\delta_3 \\ 1.5 &\approx 10\delta_2 - 10(\delta_3 - \delta_2) \end{aligned} \tag{7-87}$$

Thus

$$\delta_2 \approx 0.0667 \text{ rad}$$

$$\delta_3 \approx -0.0167 \text{ rad}$$

and then, upon substitution,

$$Q_1 = 0.023 \text{ pu}$$

$$Q_2 = 0.057 \text{ pu}$$

$$Q_3 = 0.036 \text{ pu}$$

Our analysis is now, in the main, completed, since we know all bus voltages (magnitudes *and* phases) and all bus powers (real *and* reactive parts). From a practical point of view it is of more interest to know the actual *generated* powers, and also the *line* powers.

From Eqs. (7-82) we get, for the reactive generations,

$$\begin{aligned} Q_{G1} &= Q_1 + 0.5 = 0.523 \text{ pu} \\ Q_{G2} &= Q_2 = 0.057 \text{ pu} \\ Q_{G3} &= 1.0 + Q_3 = 1.036 \text{ pu} \end{aligned} \tag{7-88}$$



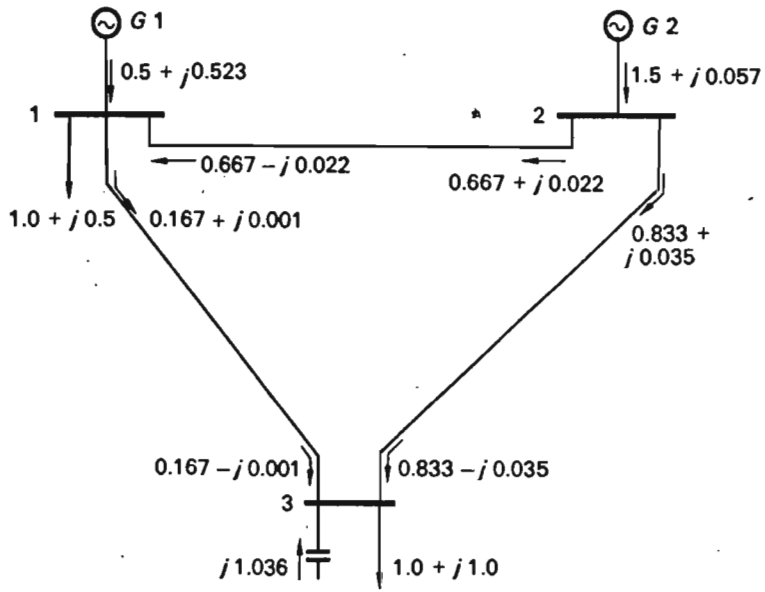


**Fig. 7-10** Load flow picture for example system.

(Since the sum of the generated reactive powers equals 1.616 pu Mvar, and since the total reactive demand is 1.5 pu, we conclude that the reactive losses on the three lines equal 0.116 pu Mvar.)

The power flowing in the three lines is readily obtained, since we know all bus voltages. Having neglected the real line losses, we can compute the real and reactive line flows from Eqs. (3-14).

We obtain

$$\begin{aligned} P_{13} &= \frac{1 \times 1}{0.1} \sin (\delta_1 - \delta_3) \approx 10(\delta_1 - \delta_3) = 0.167 \text{ pu} \\ P_{12} &\approx 10(\delta_1 - \delta_2) = -0.667 \text{ pu} \\ P_{23} &\approx 10(\delta_2 - \delta_3) = 0.833 \text{ pu} \\ Q_{13} = Q_{31} &= \frac{1^2 - 1 \times 1 \cos (\delta_1 - \delta_3)}{0.1} \approx 5(\delta_1 - \delta_3)^2 = 0.001 \text{ pu} \\ Q_{12} = Q_{21} &\approx 5(\delta_1 - \delta_2)^2 = 0.022 \text{ pu} \\ Q_{23} = Q_{32} &\approx 5(\delta_2 - \delta_3)^2 = 0.035 \text{ pu} \end{aligned} \tag{7-89}$$

We have summarized the result of our load flow study in the flow diagram of Fig. 7-10.

## 7-6 COMPUTATIONAL ASPECTS OF THE LOAD FLOW PROBLEM

We have given a general formulation of the load flow problem for the $n$-bus energy system, and we have also developed general methods for assembling the necessary mathematical models. We have, finally, outlined the bus power and voltage constraints that must be observed in a practical situation. We have not, however, tried to *solve* the load flow equations except in an unrealistically simple case where, in addition, we neglected the line losses. We must now attend to this important aspect of load flow analysis. Let us first enumerate the necessary requirements that must be met by any computational techniques that we propose:

1. They must be able to handle nonlinear algebraic equations.
2. They must be able to handle systems having, perhaps, hundreds of buses.
3. They should not be limited to loss-free systems.
4. They must have sufficient accuracy.
5. They should not be too time-consuming since we may wish, in a practical situation, to perform many series of computations for various combinations of bus power and voltage specifications in order to obtain the best possible flow picture.
6. The $n$ load flow equations (7-41) are complex equations. Our computer programs must take this fact into account.

It soon becomes obvious that, in order to meet all these requirements, we must look for *machine* computational methods.

Historically, the load flow problem was solved on special analog computers, referred to as "network analyzers." These were nothing but miniature replicas of the system to be studied, some of them operated on direct, some on alternating, current. There are still (1970) network analyzers in use both on campus and in industry. However, the vast majority of today's network computations are performed on *digital computers:* indeed, the trend toward digital methods is so overwhelming that we shall not even waste time on discussing the use of any other methods. With the knowledge that today's student, graduate or undergraduate, possesses of the versatility and accuracy of digital computers, we see no need for further motivations for our choice.

### 7-6.1 ITERATIVE COMPUTATION OF NONLINEAR ALGEBRAIC EQUATIONS

As we have hinted on several occasions, in preceding chapters, when we are faced with the problem of obtaining solutions for a system of simultaneous nonlinear algebraic equations, the method of "systematic guessing" becomes a practical necessity. A great many methods have been proposed in the vast literature on numerical techniques; we shall look closer at three specific



methods of numerical *iteration* that have proved useful in EESE. In order of simplicity these are

1. The Gauss iterative method
2. The Gauss-Seidel method.
3. The Newton-Raphson method.

Equations (7-41) are of the form

$$f_1(x_1, \ldots, x_n) = 0$$
$$\cdots\cdots\cdots\cdots$$
$$f_n(x_1, \ldots, x_n) = 0$$

or for short,

$$\mathbf{f(x)} = \mathbf{0} \tag{7-90}$$

and our problem is to solve for the unknown complex $x$ variables.†

Equations (7-90) are of such complexity that no exact *analytical* solution is obtainable. We must resort to some approximate technique that will render a sufficiently accurate *numerical* solution. The methods we shall now compare approach the problem of solution in the following manner:

1. An initial solution is guessed at.
2. This solution is used in conjunction with the original equation (7-90) to compute a new *and better* second estimate.
3. The second estimate is used for finding a third estimate, etc.

This repetitive process of converging on the solution is referred to as an *iterative method*. The different methods utilize somewhat different schemes in computing the new estimates. By the term *algorithm* we mean a list of computer instructions specifying the sequence of operations used. Clearly, the quality of the algorithm must be judged by the *speed of convergence*. The three methods we shall compare differ considerably in this respect. Generally, we obtain an increase in speed of convergence by paying a price in terms of complexity.

**Gauss iterative method** We introduce this method by finding iteratively the roots of the one-dimensional nonlinear equation

$$f(x) = x^2 - 5x + 4 = 0$$

The reader confirms easily that the roots of this equation are

$$x_1 = 1$$
$$x_2 = 4$$

† The present complex $x$ variables should not be confused with "state" variables introduced earlier.

We have plotted the function $f(x)$ versus $x$ in Fig. 7-11.
We next write the equation in the form

$$x = \tfrac{1}{5}x^2 + \tfrac{4}{5}$$

More generally, this last form is of the type

$$x = F(x) \tag{7-91}$$

It is *always* possible to find a function $F(x)$ for *any* function $f(x)$.†
The function $F(x)$ has also been plotted in Fig. 7-11.

† The function $F(x)$ is, of course, not unique. For example, in our case we could have written alternately

$$x = \frac{5x - 4}{x}$$

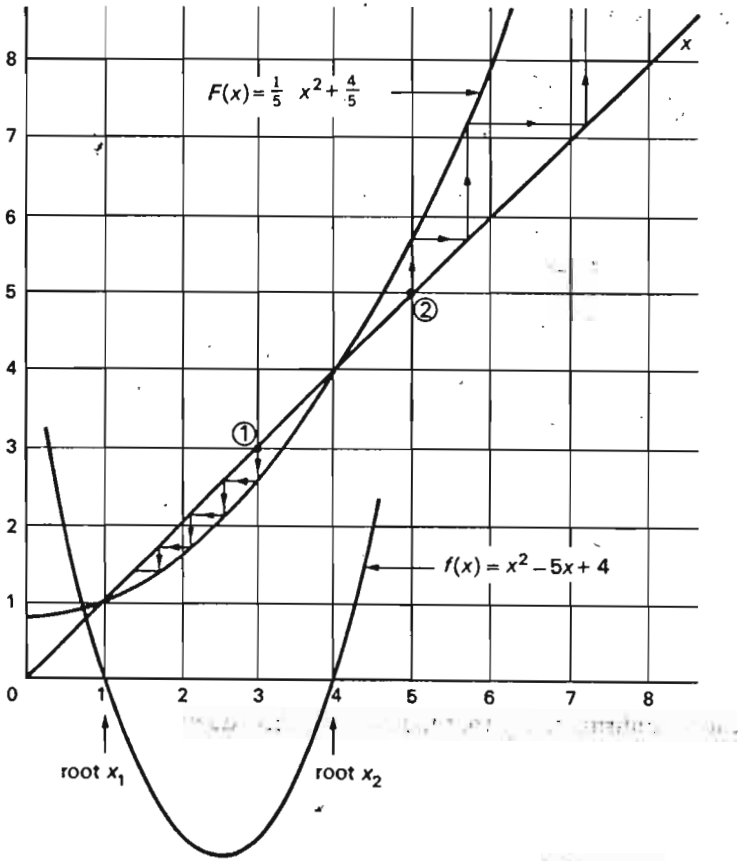


**Fig. 7-11** Plots of $f(x)$ and $F(x)$.



On basis of Eq. (7-91), we choose now the following algorithm for our iterative computational process:

$$x^{(\nu+1)} \triangleq F(x^{(\nu)}) \tag{7-92}$$

We demonstrate the procedure by presenting the first few steps of the process:

*Iteration* 0 Make the arbitrary initial guess for the sought root

$$x^{(0)} = 3$$

*Iteration* 1 From the iteration equation (7-92), we get

$$x^{(1)} = F(3) = \tfrac{1}{5} \times 3^2 + \tfrac{4}{5} = 2.60$$

*Iteration* 2

$$x^{(2)} = F(2.60) = \tfrac{1}{5} \times (2.60)^2 + \tfrac{4}{5} = 2.15$$

etc.

The process has been depicted graphically in Fig. 7-11. Starting at the point marked (1), we proceed in a zigzag pattern between the line $x$ and the curve $F(x)$ and approach the root $x_1 = 1$. The iterative process will be ended when the improvement between two consecutive iterations is less than a certain tolerance $\varepsilon$, that is, when

$$|x^{(\nu+1)}| - |x^{(\nu)}| < \varepsilon$$

We note from Fig. 7-11 that we probably will need quite a few iterations to reach sufficiently close to the root. The slow convergence is one disadvantage of this method.

*Another disadvantage is that the process may not converge at all.* This is demonstrated in Fig. 7-11 in an attempt to find the second root, $x_2 = 4$. Starting from $x^{(0)} = 5$, we actually diverge.

The above method can readily be extended to the $n$-dimensional equation (7-90). We write the equation first in the different form

$$\mathbf{x} = \mathbf{F}(\mathbf{x}) \tag{7-93}$$

corresponding to Eq. (7-91), and select then, in analogy with Eq. (7-92), the iteration formula

$$\mathbf{x}^{(\nu+1)} \triangleq \mathbf{F}(\mathbf{x}^{(\nu)}) \tag{7-94}$$

**Example 7-4** Consider the system of nonlinear equations

$$2x_1 + x_1x_2 - 1 = 0$$
$$2x_2 - x_1x_2 + 1 = 0$$

These equations are of the form of Eq. (7-90). We change them next into form of Eq. (7-93):

$$x_1 = 0.5 - \frac{x_1 x_2}{2}$$

$$x_2 = -0.5 + \frac{x_1 x_2}{2}$$

Before we start our iteractions, we note that the solutions of our given equations are

$$x_1 = 1$$
$$x_2 = -1$$

We wish now to demonstrate how, by means of the Gauss method, we can step by step approach this solution.

*Start* Make the initial arbitrary guess

$$x_1^{(0)} = 0$$
$$x_2^{(0)} = 0$$

*Iteration* 1 From Eq. (7-94) find $x_1^{(1)}$ and $x_2^{(1)}$.

$$x_1^{(1)} = 0.5 - 0 = 0.5$$
$$x_2^{(1)} = -0.5 + 0 = -0.5$$

*Iteration* 2 From Eq. (7-94) find $x_1^{(2)}$ and $x_2^{(2)}$.

$$x_1^{(2)} = 0.5 + \frac{0.5 \times 0.5}{2} = 0.625$$

$$x_2^{(2)} = -0.5 - \frac{0.5 \times 0.5}{2} = -0.625$$

*Iteration* 3 Find $x_1^{(3)}$ and $x_2^{(3)}$.

$$x_1^{(3)} = 0.5 + \frac{0.625 \times 0.625}{2} = 0.695$$

$$x_2^{(3)} = -0.5 - \frac{0.625 \times 0.625}{2} = -0.695$$

etc.

We note that we converge, *but slowly*, on the exact solutions. This is indeed generally true about this method, and it is the price we pay for simplicity. When employing this method for load flow solutions, we often need to use in excess of 100 iterations before we obtain sufficient accuracy.

**The Gauss-Seidel (GS) method** The GS iteration method achieves higher speed of convergence (compared with the Gauss method) by the very simple and obvious modification of making use of the upgraded iterates *as soon as they are available*. For example, in Example 7-4, in computing the new value for $x_2^{(\nu+1)}$, we make use *not* of $x_1^{(\nu)}$, but of $x_1^{(\nu+1)}$, because it is



already available. The iterations in Example 7-4 therefore change as follows:

*Iteration* 1 Unchanged.

*Iteration* 2

$$x_1^{(2)} = 0.5 + \frac{0.5 \times 0.5}{2} = 0.625$$

$$x_2^{(2)} = -0.5 - \frac{0.625 \times 0.5}{2} = -0.656$$

*Iteration* 3

$$x_1^{(3)} = 0.5 + \frac{0.625 \times 0.656}{2} = 0.705$$

$$x_2^{(3)} = -0.5 - \frac{0.656 \times 0.705}{2} = -0.731$$

etc. Clearly, the speed of convergence has been increased.

**Application of acceleration factor** Both of the preceding methods can be made to converge considerably faster by application of a so-called "acceleration factor" $\alpha$, the effect of which on the iterative process is closely analogous to that of the loop gain in a servo mechanism. Those readers familiar with the characteristics of closed-loop control systems know that by increasing the loop gain, we generally increase the speed of response of the servo, *but if we increase it too much, the servo may go unstable.*

Consider Example 7-4. Let us introduce the difference variables

$$\Delta x_1^{(\nu)} \triangleq x_1^{(\nu)} - x_1^{(\nu-1)}$$
$$\Delta x_2^{(\nu)} \triangleq x_2^{(\nu)} - x_2^{(\nu-1)}$$

$\Delta x_1^{(\nu)}$ and $\Delta x_2^{(\nu)}$ indicate the variable change in the iterative process between the $(\nu - 1)$st and the $\nu$th iteration. Let us now multiply this difference by a factor $\alpha$ *which is larger than unity*, and let us then compute the new *accelerated* iterates on the basis of these magnified difference variables in accordance with the algorithm

$$x_{1,\text{acc}}^{(\nu)} = x_{1,\text{acc}}^{(\nu-1)} + \alpha\, \Delta x_1^{(\nu)}$$
$$x_{2,\text{acc}}^{(\nu)} = x_{2,\text{acc}}^{(\nu-1)} + \alpha\, \Delta x_2^{(\nu)} \qquad (7\text{-}95)$$

The actual effect of the acceleration factor is shown graphically in Fig. 7-12*a*, showing how the process in Fig. 7-11 is speeded up by using an $\alpha$

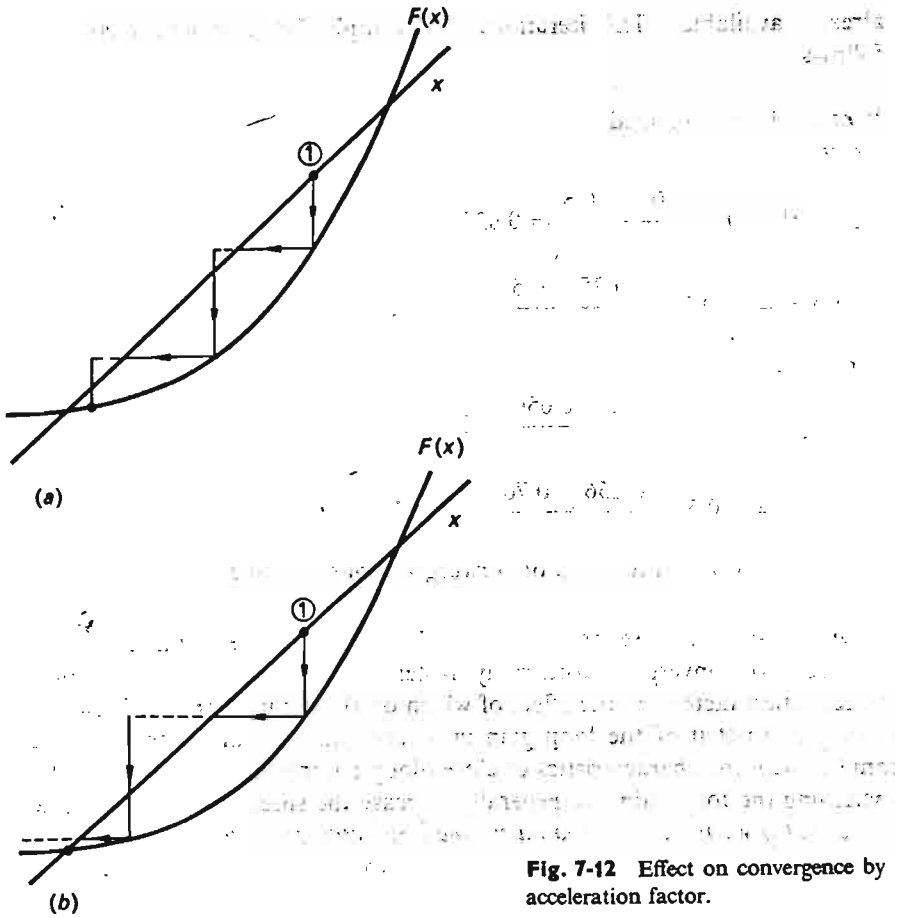


**Fig. 7-12** Effect on convergence by acceleration factor.

factor of 1.5. But the graph in Fig. 7-12*b* shows also how too large an $\alpha$ value actually will cause "overshoot."

**Example 7-5** Let us see what effect this will have on the iterative process demonstrated in Example 7-4. We shall use a factor $\alpha = 1.5$. We obtain:

$$x_1^{(1)} = 0.5 \quad \text{as before}$$

$$x_2^{(1)} = -0.5 \quad \text{as before}$$

$$\Delta x_1^{(1)} = 0.5 - 0 = 0.5$$

$$\Delta x_2^{(1)} = -0.5 - 0 = -0.5$$

$$x_{1,\text{acc}}^{(1)} = 0 + 1.5 \times 0.5 = 0.750$$

$$x_{2,\text{acc}}^{(1)} = 0 + 1.5 \times (-0.5) = -0.750$$



*Iteration* 2

$$x_1^{(2)} = 0.5 + \frac{0.75 \times 0.75}{2} = 0.781$$

$$x_2^{(2)} = -0.5 - \frac{0.75 \times 0.75}{2} = -0.781$$

$$\Delta x_1^{(2)} = 0.781 - 0.750 = 0.031$$

$$\Delta x_2^{(2)} = -0.781 - (-0.750) = -0.031$$

$$x_{1,\text{acc}}^{(2)} = 0.750 + 1.5 \times 0.031 = 0.797$$

$$x_{2,\text{acc}}^{(2)} = -0.750 - 1.5 \times 0.031 = -0.797$$

etc.

We note that the speed of convergence has been increased considerably. What specific value we should choose for $\alpha$ must be determined from case to case. For the solution of the load flow equations (7-41), an $\alpha$ value of about 1.5 to 1.7 has proved to offer the best convergence features.

**The Newton-Raphson (NR) method** This iteration method is by far the most sophisticated. Not only will it work in most cases without risk of divergence, but it will as a rule converge faster than the preceding methods.

We shall, for simplicity, present the method for a system of only two equations of the type of Eqs. (7-90):

$$\begin{aligned} f_1(x_1,x_2) &= 0 \\ f_2(x_1,x_2) &= 0 \end{aligned} \tag{7-96}$$

Our results can be extended with ease to the general case with $n$ unknowns.

Assume we have made an initial guess $x_1^{(0)}$ and $x_2^{(0)}$ for our unknowns. We now ask ourselves what difference variables $\Delta x_1^{(0)}$ and $\Delta x_2^{(0)}$ we should add to our initial guess in order to obtain the correct solutions. In other words, we assume that $x_1^{(0)} + \Delta x_1^{(0)}$ and $x_2^{(0)} + \Delta x_2^{(0)}$, respectively, represent the solutions sought. As such, they must most certainly satisfy the given Eqs. (7-96); i.e., we can write

$$\begin{aligned} f_1(x_1^{(0)} + \Delta x_1^{(0)},\, x_2^{(0)} + \Delta x_2^{(0)}) &= 0 \\ f_2(x_1^{(0)} + \Delta x_1^{(0)},\, x_2^{(0)} + \Delta x_2^{(0)}) &= 0 \end{aligned} \tag{7-97}$$

By expanding these equations in a Taylor series around the initial guess, we get

$$f_1(x_1^{(0)},x_2^{(0)}) + \Delta x_1^{(0)} \left(\frac{\partial f_1}{\partial x_1}\right)^{(0)} + \Delta x_2^{(0)} \left(\frac{\partial f_1}{\partial x_2}\right)^{(0)} + \cdots = 0$$

$$f_2(x_1^{(0)},x_2^{(0)}) + \Delta x_1^{(0)} \left(\frac{\partial f_2}{\partial x_1}\right)^{(0)} + \Delta x_2^{(0)} \left(\frac{\partial f_2}{\partial x_2}\right)^{(0)} + \cdots = 0$$

The symbols $(\ )^{(0)}$ mean that the partial derivatives must be computed for $x_1 = x_1^{(0)}$ and $x_2 = x_2^{(0)}$.

We neglect at this point the higher-order terms† and write the last equation in vector form.

$$\mathbf{f}^{(0)} + \mathbf{J}^{(0)}\,\Delta\mathbf{x}^{(0)} \approx 0 \tag{7-98}$$

We have here introduced the following matrix and vectors and extended in the same step our results to the general case:

$$\mathbf{J}^{(0)} \triangleq \begin{bmatrix} \left(\frac{\partial f_1}{\partial x_1}\right)^{(0)} & \cdots & \left(\frac{\partial f_1}{\partial x_n}\right)^{(0)} \\ \cdots\cdots\cdots\cdots\cdots\cdots \\ \left(\frac{\partial f_n}{\partial x_1}\right)^{(0)} & \cdots & \left(\frac{\partial f_n}{\partial x_n}\right)^{(0)} \end{bmatrix}$$

Compare this "jacobian" matrix with $\mathbf{J}_x$ in Eq. (7-25)

$$\mathbf{f}^{(0)} \triangleq \begin{bmatrix} f_1(\mathbf{x}^{(0)}) \\ \cdot \\ \cdot \\ \cdot \\ f_n(\mathbf{x}^{(0)}) \end{bmatrix} \qquad \Delta\mathbf{x}^{(0)} \triangleq \begin{bmatrix} \Delta x_1^{(0)} \\ \cdot \\ \cdot \\ \cdot \\ \Delta x_n^{(0)} \end{bmatrix}$$

From Eq. (7-98) we get directly

$$\Delta\mathbf{x}^{(0)} \approx -[\mathbf{J}^{(0)}]^{-1}\mathbf{f}^{(0)} \tag{7-99}$$

The differences $\Delta x_1^{(0)} \cdots \Delta x_n^{(0)}$ that, in accordance with our assumption, will take us from the initial guess to the exact solution are thus known, *but since we were forced to make an approximation in their computation, we will not quite get there.* We need to take our improved $x$ values, make renewed use of Eq. (7-99), and obtain a better estimate, etc.

**Example 7-6** We shall use the NR iteration method to solve the sample equations in Example 7-4.

*Iteration* 1

STEP 1 Make the initial guess as before

$$x_1^{(0)} = 0$$

$$x_2^{(0)} = 0$$

STEP 2 Find a general expression for the jacobian matrix.

$$\mathbf{J} = \begin{bmatrix} 2 + x_2 & x_1 \\ -x_2 & 2 - x_1 \end{bmatrix} \tag{7-100}$$

† This is tantamount to saying that $\Delta x_1$ and $\Delta x_2$ are assumed small.



STEP 3 Compute the jacobian for the initial $x$ values.

$$\mathbf{J}^{(0)} = \begin{bmatrix} 2 & 0 \\ 0 & 2 \end{bmatrix}$$

STEP 4 Compute the $\mathbf{f}^{(0)}$ vector.

$$\mathbf{f}^{(0)} = \begin{bmatrix} -1 \\ 1 \end{bmatrix}$$

STEP 5 Invert $\mathbf{J}^{(0)}$

$$[\mathbf{J}^{(0)}]^{-1} = \begin{bmatrix} 0.5 & 0 \\ 0 & 0.5 \end{bmatrix}$$

STEP 6 Find $\Delta\mathbf{x}^{(0)}$ from Eq. (7-99).

$$\Delta\mathbf{x}^{(0)} = -\begin{bmatrix} 0.5 & 0 \\ 0 & 0.5 \end{bmatrix}\begin{bmatrix} -1 \\ 1 \end{bmatrix} = \begin{bmatrix} 0.5 \\ -0.5 \end{bmatrix}$$

*Iteration* 2 Repeat steps 3 to 6 around the upgraded $\mathbf{x}$ value:

$$\mathbf{x}^{(1)} = \mathbf{x}^{(0)} + \Delta\mathbf{x}^{(0)} = \begin{bmatrix} 0.5 \\ -0.5 \end{bmatrix}$$

STEP 3

$$\mathbf{J}^{(1)} = \begin{bmatrix} 1.5 & 0.5 \\ 0.5 & 1.5 \end{bmatrix}$$

STEP 4

$$\mathbf{f}^{(1)} = \begin{bmatrix} -0.25 \\ 0.25 \end{bmatrix}$$

STEP 5

$$(\mathbf{J}^{(1)})^{-1} = \begin{bmatrix} 0.75 & -0.25 \\ -0.25 & 0.75 \end{bmatrix}$$

STEP 6

$$\Delta\mathbf{x}^{(1)} = -\begin{bmatrix} 0.75 & -0.25 \\ -0.25 & 0.75 \end{bmatrix}\begin{bmatrix} -0.25 \\ 0.25 \end{bmatrix} = \begin{bmatrix} 0.250 \\ -0.250 \end{bmatrix}$$

The second iteration has thus taken us to

$$\begin{bmatrix} x_1^{(2)} \\ x_2^{(2)} \end{bmatrix} = \begin{bmatrix} 0.5 + 0.250 \\ -0.5 - 0.250 \end{bmatrix} = \begin{bmatrix} 0.750 \\ -0.750 \end{bmatrix}$$

which, compared, for example, with the "accelerated" Gauss method, is not too impressive. However, if we care to make two more iterations, the convergence superiority of the NR method will become evident. Our first two iterations are slow because of our poor initial guess. When we are approaching the correct values, the NR method "zeros in" extremely fast. The greatest disadvantage of the method is the need for finding and inverting the jacobian matrix. However, subroutines are available for this operation in most cases.

It should be added that the matrix inversion is made easier by the fact that the jacobian matrix, like $\mathbf{Y}_{bus}$, is *very sparse*. Tinney[45] and others have seized upon this feature and developed very fast and ingenious inversion techniques.

### 7-6.2 ITERATIVE COMPUTATION OF THE LOAD FLOW EQUATIONS

After this brief introduction to iterative computation techniques, we now turn to the computation of the load flow equations (7-41). Because of space limitation, we can discuss the use of only one of the iterative methods we have presented. We choose the Gauss method because of its inherent simplicity. However, since we shall treat the *general* case with $n$ buses, and since we shall explain all computations in *detail*, the reader should not have any difficulty in applying any method of his own choice.

**No type 2 buses present** The simplest computational case is the one where we have no "voltage control buses" present. This means that all $n$ buses minus one are of type 1, the remaining one being a slack bus of type 3. We shall by proper bus coding *always* assign the slack job to bus 1; i.e., the buses 2, 3, . . . , $n$ are the type 1 buses.

Of our $n$ complex unknowns, $n-1$ consist of the voltages $V_2, \ldots, V_n$. The remaining one is the complex generator power, $P_{G1} + jQ_{G1}$ (or the bus power, $P_1 + jQ_1$), of the slack bus.

The slack bus voltage $V_1$ is a priori specified, and so are all the bus powers $S_2, S_3, \ldots, S_n$. Our computations therefore will proceed in the following steps:

*Step* 1 Assembly of $\mathbf{Y}_{bus}$.

*Step* 2 Solve iteratively Eqs. (7-41) for $i = 2, 3, \ldots, n$. We have, obviously, $n-1$ complex equations for the $n-1$ complex unknowns $V_2, V_3, \ldots, V_n$.

*Step* 3 After the bus voltages $V_2, \ldots, V_n$ are thus solved, and since $V_1$ is a priori specified, we can now, from the remaining one (i.e., the first one), of Eqs. (7-41) solve for the bus power at the slack bus.

*Step* 4 All $n$ bus voltages now being known, we can compute the power flows in all transmission lines, and our load flow analysis is completed. Let us look now at the computational details in each of these four steps.

*Step* 1. *Assembly of* $\mathbf{Y}_{bus}$ *matrix* Upon providing the computer with the input data in the form of the primitive admittance matrix $\mathbf{Y}$ [Eq. (7-50)] and the bus incidence matrix $\mathbf{A}$ [Eq. (7-74)], we compute $\mathbf{Y}_{bus}$ directly from Eq. (7-80), or by using the simple rules on page 223.

*Step* 2. *The iterative computation of* $V_2, V_3, \ldots, V_n$ Since we wish to use the Gauss method, we must first put the load flow equations in the form



of Eqs. (7-93). From the $i$th of Eqs. (7-41), we obtain upon solving for $V_i$

$$V_i = \frac{1}{y_{ii}}\left(\frac{P_i - jQ_i}{V_i^*} - \sum_{\substack{\mu=1 \\ \mu \neq i}}^{n} y_{i\mu} V_\mu\right) \qquad \text{for } i = 2, \ldots, n \tag{7-101}$$

($\mu$ is a summation variable. Note that the summation must exclude $\mu = i$.)

The Gauss iterative algorithm (7-94) therefore reads

$$V_i^{(\nu+1)} = \frac{1}{y_{ii}}\left[\frac{P_i - jQ_i}{(V_i^{(\nu)})^*} - \sum_{\substack{\mu=1 \\ \mu \neq i}}^{n} y_{i\mu} V_\mu^{(\nu)}\right]$$

$$\text{for } i = 2, 3, \ldots, n \tag{7-102}$$

and $\nu$ being the iteration count.

It is necessary to begin the iterations with an initial guess, and since we know that in a real system the voltage spread will not be too great, it is customary to use a "flat voltage start," meaning that we set initially all voltages equal to the specified slack bus voltage $V_1$, for example, $1 + j0$ pu.

It is important to realize that the $n-1$ equations (7-101) are *complex*, each voltage having a real and an imaginary part, or a magnitude and phase angle, so that we then, in effect, have $2(n-1)$ *real* unknowns to solve for. We can write the bus voltage

$$V_i = V_{pi} + jV_{qi} = |V_i| e^{j\delta_i} \tag{7-103}$$

Upon completion of the solution of the $n-1$ Eqs. (7-102), we possess, in effect, knowledge of the $2(n-1)$ components $V_{pi}$ and $V_{qi}$ *or*, if we so instruct the computer, the value pairs $|V_i|$ and $\delta_i$.

Modern computer languages invariably accept complex variables; so there is no need to separate here the real and imaginary portions of Eqs. (7-102). This is automatically being done by the computer. However, should our computer not "understand" complex variables, we must go to the extra effort to separate Eq. (7-102) and all other complex equations that follow into two real equations.

A considerable saving in computer time can be achieved if we perform in advance, once and for all, those arithmetic operations *that do not change with the iterations.* In Eqs. (7-102), the quantities $y_{ii}$, $P_i$, $Q_i$, and $y_{i\mu}$ do not change throughout the iteration process, and we therefore compute separately the following quantities:

$$\frac{P_i - jQ_i}{y_{ii}} \triangleq A_i \qquad \text{for } i = 2, 3, \ldots, n \tag{7-104}$$

$$\frac{y_{i\mu}}{y_{ii}} \triangleq B_{i\mu} \tag{7-105}$$

$$\text{for } i = 2, 3, \ldots, n;\ \mu = 1, 2, \ldots, n \text{ (except } \mu = i)$$

Note that $A_i$ and $B_{i\mu}$ both are complex parameters.

In terms of these new parameters, the voltage equations (7-102) take on the form

$$V_i^{(\nu+1)} = \frac{A_i}{(V_i^{(\nu)})^*} - \sum_{\substack{\mu=1 \\ \mu\neq i}}^{n} B_{i\mu} V_\mu^{(\nu)} \qquad \text{for } i = 2, 3, \ldots, n \tag{7-106}$$

The iterative process must continue until the magnitude of the change of the bus voltage, $|\Delta V_i^{(\nu+1)}|$, between two consecutive iterations is less than a certain tolerance level $\varepsilon$ for *all* bus voltages. We express this in mathematical form as follows:

$$|\Delta V_i^{(\nu+1)}| \triangleq |V_i^{(\nu+1)} - V_i^{(\nu)}| < \varepsilon \qquad \text{for } i = 2, 3, \ldots, n \tag{7-107}$$

*Step* 3. *Computation of slack bus power* This step is simple. After the iterations have converged, we substitute our computed voltages (plus $V_1$) into the first one of Eqs. (7-40) and obtain directly $S_1 = P_1 + jQ_1$.

*Step* 4. *Computation of line flows* The final step in the load flow analysis is the computation of the load flows on the various transmission lines of the network. Consider the line connecting the two buses $i$ and $j$ in Fig. 7-13. The line plus transformers can be represented by the series admittance $Y_{ij}$ and the two shunt admittances $Y_{sh}$, as described in Chap. 6.†

The line current $I_{ij}$, measured at bus $i$ and defined positive in the direction $i \to j$, equals

$$I_{ij} = I_{ser} + I_{sh,i} = (V_i - V_j)Y_{ij} + V_i Y_{sh,i} \tag{7-108}$$

(For definition of $I_{ser}$ and $I_{sh,i}$ see Fig. 7-13.) The line power $S_{ij}$, measured at bus $i$ and defined positive in the direction $i \to j$, therefore equals

$$S_{ij} = P_{ij} + jQ_{ij} = V_i I_{ij}^* = V_i(V_i^* - V_j^*)Y_{ij}^* + V_i V_i^* Y_{sh,i} \tag{7-109}$$

This completes the load flow study.

† $Y_{ij}$ should not be confused with the elements $y_{ij}$ of the $\mathbf{Y}_{bus}$ matrix.

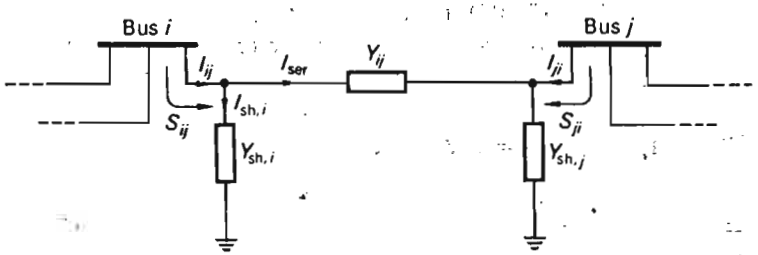


**Fig. 7-13** Line parameters used in line flow calculation.



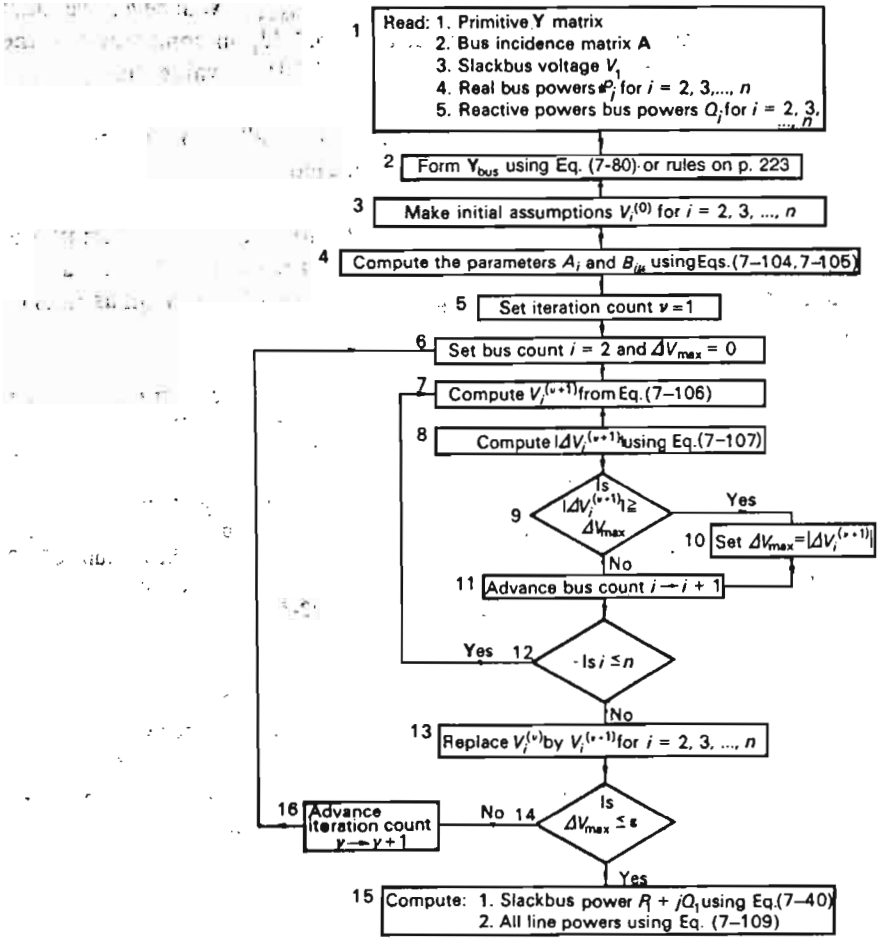


**Fig. 7-14** Flow diagram for computation of the SLFE and line powers. No type 2 buses present.

We summarize now all the computational steps in the detailed flow diagram of Fig. 7-14. This flow diagram serves as a basis for the computer program.

Let us point out a few features of this flow diagram:

1. There are two iterative loops in the diagram. The inner ("bus count") loop is circled exactly $n - 1$ times for every step in the outer ("iteration count") loop. We are thus assured that all bus voltages (except the slack bus voltage) are computed in each iterative cycle.

2. We have introduced a "dummy variable" $\Delta V_{\max}$. Whenever we start the bus count, this variable is reset to zero. Upon completion of the bus count, this variable tells us the largest $|\Delta V_i^{(\nu+1)}|$ value that has been recorded for *any* bus.
3. At the end of the bus count, should $\Delta V_{\max}$ not fall below the tolerance value $\varepsilon$, then a new iteration cycle is initiated.

The flow diagram of Fig. 7-14 is sufficiently detailed to permit the reader to write his own computer program. We recommend that he do so, because it provides him an excellent opportunity to *really* learn all aspects of load flow studies.

**Example 7-7** We shall again consider the three-bus system for which we made a load flow study in Sec. 7-5. Since we now are going to delegate all the computational drudgery to the computer, we shall make the study in total disregard of the numerical complexities. In consequence, we shall use for the three transmission lines the equivalent network in Fig. 6-20, without neglecting the shunt admittances or without using any rounded-off, or "beautified," numerical values. In addition, to make the problem still more realistic, we shall add losses to the lines in the amount of 0.2 Ω/mile, for a total of 6.0 Ω for the overall 30-mile line. We must, of course, express this resistance in per-unit values, and by using Eq. (2-50), we get

$$R = 6.0 \times \frac{50}{(120)^2} = 0.021 \text{ pu}$$

In our analysis each transmission line will therefore be represented by the equivalent diagram shown in Fig. 7-15.

*Network data* The linear graph for our three-bus system is shown in Fig. 7-5. The primitive admittance matrix for this system can now be written down directly:

$$\mathbf{Y} = \begin{bmatrix} j0.0452 & & 0 \\ & j0.0452 & \\ & & j0.0452 \\ & & & 2.61 - j10.8 \\ & & & & 2.61 - j10.8 \\ 0 & & & & & 2.61 - j10.8 \end{bmatrix} \tag{7-110}$$

$Z_{ser} = 0.021 + j\,0.0872$ pu

(or $Y_{ser} = 2.61 - j\,10.8$ pu)

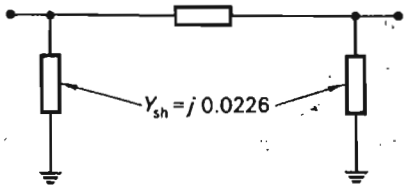


**Fig. 7-15** Line data used in load flow study in Example 7-7.



The bus incidence matrix was found earlier (page 235). We restate it here:

$$\mathbf{A} = \begin{bmatrix} 1 & 0 & 0 \\ 0 & 1 & 0 \\ 0 & 0 & 1 \\ 1 & 0 & -1 \\ 1 & -1 & 0 \\ 0 & 1 & -1 \end{bmatrix} \tag{7-111}$$

The Y and A matrices are read into the computer memory.

*Bus power and voltage specifications* We shall perform the load flow analysis based on the bus power and voltage specifications given in Table 7-2.

**Table 7-2**

| Bus | *Real load demand* | *Reactive load demand* | *Real power generation* | *Reactive power generation* | *Voltage specification* |
|---|---|---|---|---|---|
| 1 | $P_{D1} = 2.0$ | $Q_{D1} = 1.0$ | Unspecified | Unspecified | $V_1 = 1.05 + j0$ (slack bus) |
| 2 | Zero | Zero | 0.6 | 1.0 | Unspecified (type 1) |
| 3 | $P_{D3} = 1.2$ | $Q_{D3} = 0.6$ | Zero | Zero | Unspecified (type 1) |

In terms of these tabulated specifications, we therefore have for the bus powers

$S_1 =$ unspecified
$S_2 = 0.6 + j1.0$
$S_3 = -1.2 - j0.6$

$V_1$, $S_2$, and $S_3$ are read into the computer memory.

*Computer results* Using the computer program in Appendix B (which is based upon the more general flow diagram of Fig. 7-18), we obtain:

1. Bus power (and thus generation) for the slack bus
2. Voltage magnitudes for buses 2 and 3
3. Load flows in the three lines

The results are summarized in the load flow diagram of Fig. 7-16. A voltage tolerance of $\varepsilon = 0.0001$ was used. Initially, all voltages were set equal to the slack bus voltage. It is interesting to note how the iterative computations converge, and for that reason we have plotted in Fig. 7-17 the bus voltage $|V_3|$ versus iteration cycle $\nu$. A total of ten iterations were needed in this case.

**Type 2 ("voltage control") buses present** Should we wish to specify the voltage at $m$ of the buses† (and in most practical situations this is normally

† Including the slack bus.

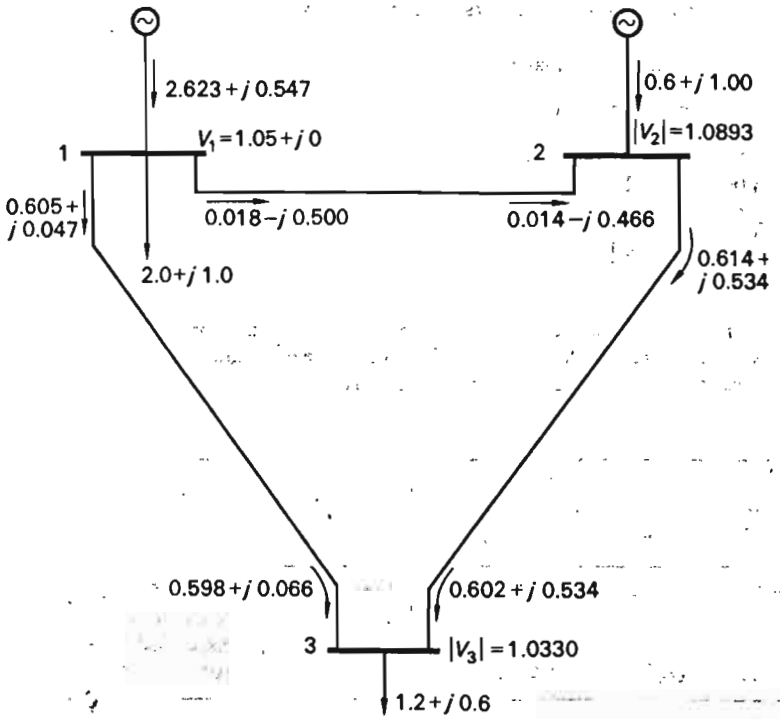


**Fig. 7-16** Result of load flow study in Example 7-7.

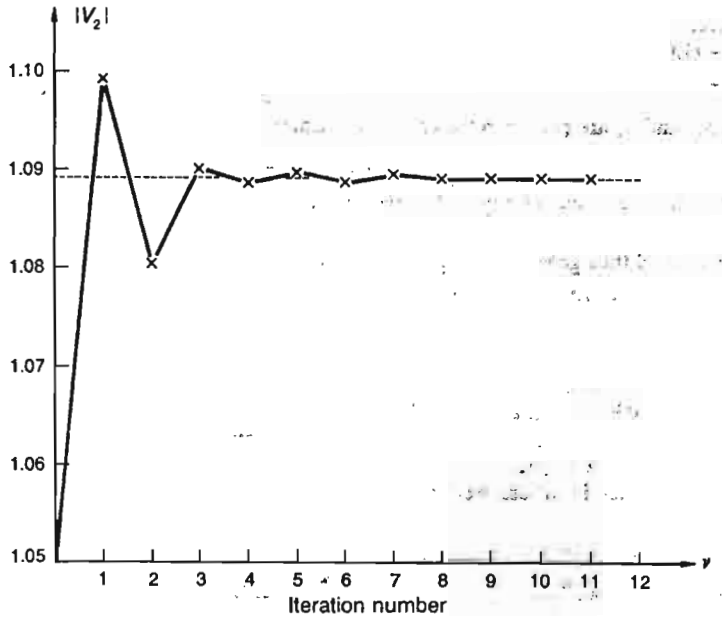


**Fig. 7-17** Convergence characteristics of the computational process.





the case), we must change the computational procedure in accordance with the flow diagram of Fig. 7-18. This diagram is based on the following coding of buses:

$i = 1$: type 3 slack bus (as before)
$i = 2, 3, \ldots, m$: type 2 voltage control buses
$i = m + 1, \ldots, n$: type 1 buses (as before)

Our first difference between the diagrams of Figs. 7-14 and 7-18 is noticed in block 1. The reactive bus powers $Q_i$ are specified only for the type 1 buses. For the type 2 buses we specify, instead, the voltage magnitudes $|V_i|_{\text{spec}}$. We must also read in the reactive power limits for each type 2 bus since we must not violate the reactive power limits (7-20) for the various generators.

Our next difference comes in block 3. We need to make initial assumptions $V_i^{(0)}$, not only about the voltages $V_i$ at *all*† buses (except the slack bus), but also about the reactive bus powers $Q_i$ at all the voltage control buses as well. This will make possible *tentative* (for type 2 buses) computation of the parameters $A_i$ in the next block, 4. For type 1 buses the $A_i$ values computed in this block will be final.

The presence of type 2 buses makes necessary a major change in the inner loop of our flow diagram. This change is indicated by the added blocks labeled $a, b, \ldots, k$ in Fig. 7-18. In the first ($a$) of these blocks, we make the computer distinguish between type 1 and type 2 buses. For type 1 buses we go directly to block 7, and the computations are then identical with the preceding case. For type 2 buses we must check that the following conditions are satisfied:

*Condition* 1 The voltages $V_i$ must satisfy, *if possible*, the specified requirements

$$|V_i| = |V_i|_{\text{spec}} \qquad \text{for } i = 2, \ldots, m \tag{7-112}$$

*Condition* 2. We must *under no circumstances* violate the requirement

$$Q_{i,\min} < Q_i < Q_{i,\max} \qquad \text{for } i = 2, \ldots, m \tag{7-113}$$

† Note that, although initially the voltage *magnitudes* have been specified for the type 2 buses, we do *not* know the real and reactive components of those voltages. It is *not* necessary to make sure at this stage that the initially guessed voltage components of the type 2 buses satisfy

$$|V_i^{(0)}| = |V_i|_{\text{spec}} \tag{7-114}$$

Our computation routine (see below) will make sure that this requirement is met at the end of the computation.

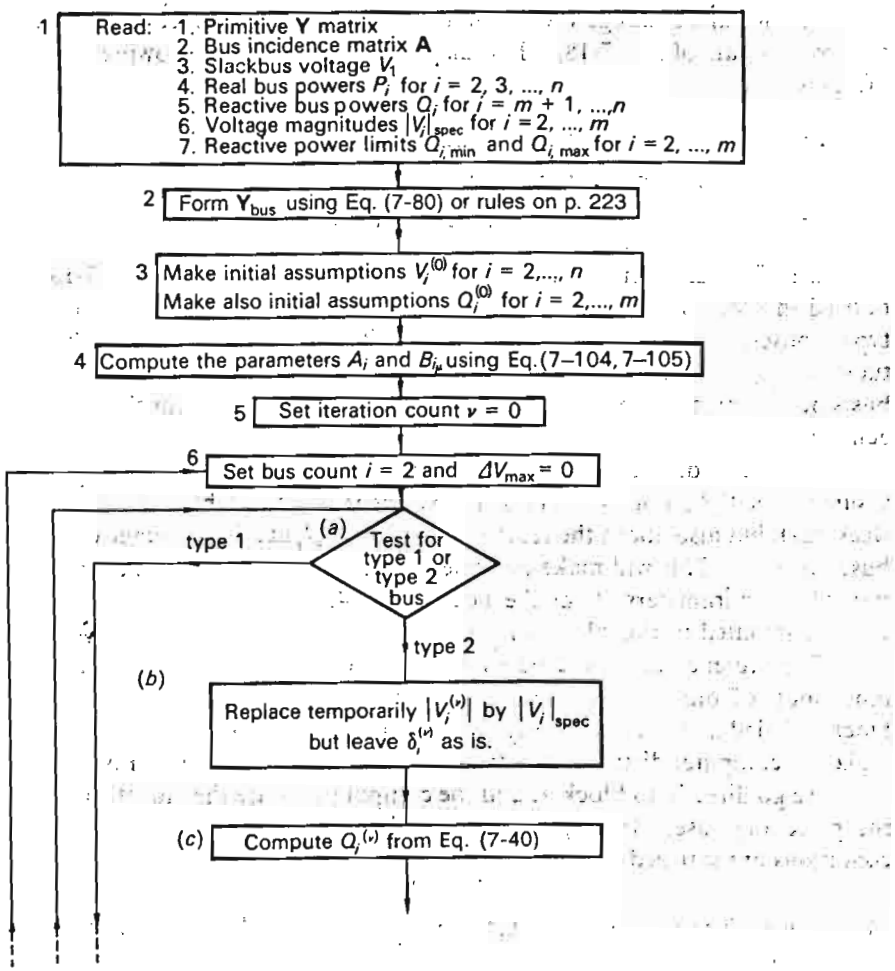


**Fig. 7-18** Flow diagram for computation of the SLFE and line powers. Voltage control (type 2) buses present.

The second requirement may be violated if the specified voltage magnitude $|V_i|_{spec}$ is either *too* low or *too* high. We remember that the only means of controlling $|V_i|$ at our disposal is the reactive power $Q_i$, and since we a priori do not know exactly how much reactive power is needed to reach the specified voltage, it may conceivably happen that we have specified a $|V_i|$ value beyond the capability of the $Q_i$ source. Our control strategy will therefore be the following one.

If it is possible to obtain $|V_i|_{spec}$ without going outside the permissible $Q_i$ range, then we should do so. If, during the iteration process, we find that we hit the $Q_i$ limits, then we must stop there and let the voltage take on



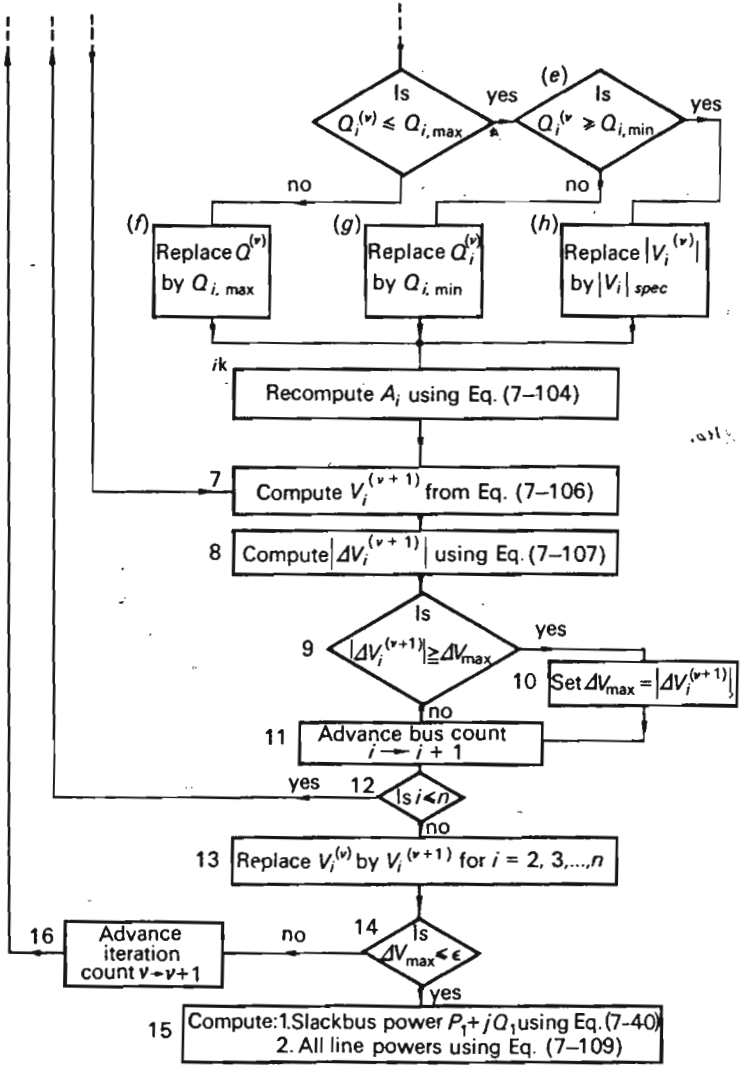


**Fig. 7-18** (*continued*)

whatever value the following iterations render. *Note that if this happens, our bus in effect changes from type 2 to type 1.*

Conditions 1 and 2 [Eqs. (7-112) and (7-113)] are being tested during each iterative cycle by the computational operations in blocks *b* to *k*. We detail these operations step by step.

*Step* 1 Having identified in block *a* the bus as being of type 2, we immediately make the *temporary* voltage *magnitude* substitution called for in block *b*. Voltage *phase* $\delta_i$ is kept as is.

*Step* 2 In block *c* we compute, then, the amount of reactive bus power needed at bus $i$ to maintain the voltage magnitude specified. *Note that this computation is based upon specified voltage magnitude.* (This is the reason why we included block *b*.)

*Step* 3 In the "logic" blocks *d* and *e* we test the magnitude of the computed $Q_i^{(\nu)}$ in relation to the nonequality (7-113). Three alternatives present themselves.

*Alternative* 1 $Q_i^{(\nu)} > Q_{i\,\max}$. We must now, in accordance with our previously stated strategy, set $Q_i^{(\nu)}$ equal to $Q_{i,\max}$, which is done in block *f*. Thereupon we simply enter the type 1 route (after first updating the value for $A_i$ in block *i*).

*Alternative* 2 $Q_i^{(\nu)} < Q_{i,\min}$. Now we set $Q_i^{(\nu)}$ equal to $Q_{i,\min}$ and again enter the type 1 route.

*Alternative* 3 $Q_{i,\min} < Q_i^{(\nu)} < Q_{i,\max}$. We are now inside the permissible $Q$ range. We therefore will proceed on the assumption that we can maintain the specified voltage magnitude $|V_i|_{\text{spec}}$ of the bus in question. This means that in all computations to follow we shall make sure that $|V_i^{(\nu)}| = |V_i|_{\text{spec}}$. This is accomplished in block *h* by simply replacing $|V_i^{(\nu)}|$ by $|V_i|_{\text{spec}}$. From then on we enter the regular iterative loop (after first updating $A_i$ in block *k*).

**Example 7-8** Our last load flow problem relates to the three-bus system used in the Example 7-7. The bus power and voltage specifications that we shall use are summarized in Table 7-3.

**Table 7-3**

| Bus | *Real load demand* | *Reactive load demand* | *Real power generation* | *Reactive power generation* | *Voltage specification* |
|---|---|---|---|---|---|
| 1 | $P_{D1} = 2.0$ | $Q_{D1} = 1.0$ | Unspecified | Unspecified | $V_1 = 1.05 + j0$ (slack bus) |
| 2 | Zero | Zero | 0.6 | 1.0 | Unspecified (type 1) |
| 3 | $P_{D3} = 1.2$ | $Q_{D3} = 0.6$ | Zero | $Q_{G3} = ?$ | $\|V_3\| = 1.05$ (type 2) |

We note that those specifications are the same as in Example 7-7, except for bus 3 where we now are told to hold the voltage at $|V_3| = 1.05$ pu. For this purpose we assume that a controllable reactive power source is available at this bus. The source consists of a switched bank of capacitors. When the whole bank is fully switched on, the maximum generation is 70 Mvar (= 1.4 pu). The reactive part $Q_3$ of the bus power $S_3$ thus can be varied throughout the range

$$-0.6 < Q_3 < 1.4 - 0.6$$



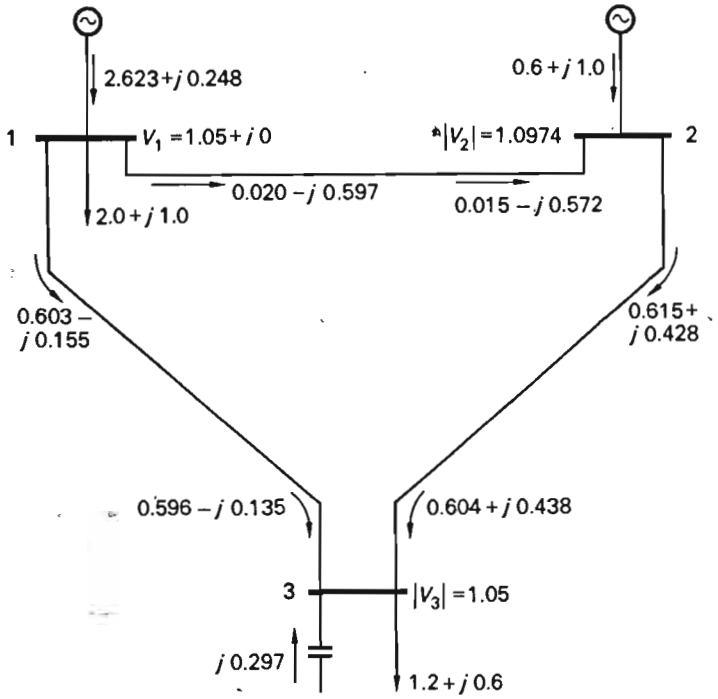


**Fig. 7-19** Result of load flow study in Example 7-8.

The limits for $Q_3$ are therefore

$$Q_{3,\max} = 0.8$$

$$Q_{3,\min} = -0.6$$

A computer program was written based upon the flow graph in Fig. 7-18 (App. B). The results of the computer run are shown in Fig. 7-19.

It is interesting to note the difference in the line flows between this case and the one computed in Example 7-7 (Fig. 7-16). The injected reactive power of bus 3 has resulted in a considerable change in the *reactive* line flows, but left the *real* powers almost unchanged. (Compare our earlier discussions of sensitivity measures.)

## 7-7 EFFECTS OF REGULATING TRANSFORMERS

In all our preceding discussions, lines and transformers could be adequately represented by series and shunt impedances. If the network contains

regulating transformers with controllable tap settings, then it becomes necessary to modify the approach somewhat.

Consider as an example the two-bus system in Fig. 7-1, previously discussed. Assume that a regulator, RT, having a controllable voltage ratio $V_1/V_2 = a$, is connected between bus 1 and the line, as indicated in Fig. 7-20*a*. In Fig. 7-20*b* we give the equivalent network representation under the somewhat simplifying assumption that the regulator impedances can be neglected.

Neglecting the magnetizing and leakage impedances of the RT is tantamount to saying that it is loss-free. The bus power $S_1$ entering its primaries must thus exit at its secondaries, as indicated in Fig. 7-20*b*.

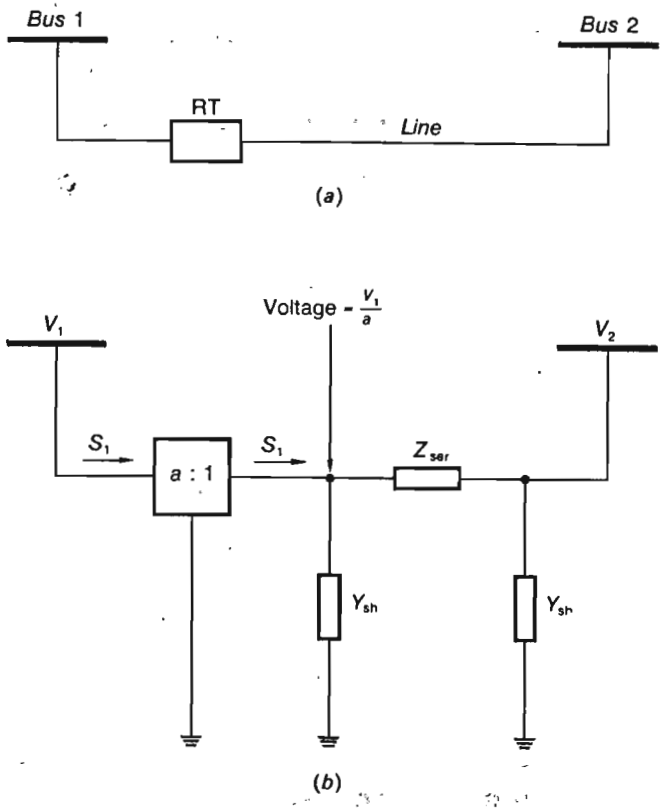


**Fig. 7-20** The presence of a regulating transformer, RT, changes the network representation as given in Fig. 7-1.



The static load flow equations (7-2) will now be modified as follows:

$$\frac{S_1^*}{(V_1/a)^*} = \frac{V_1}{a} Y_{sh} + \frac{V_1/a - V_2}{Z_{ser}}$$
$$\frac{S_2^*}{V_2^*} = V_2 Y_{sh} + \frac{V_2 - V_1/a}{Z_{ser}} \qquad (7\text{-}115)$$

Clearly, we have added one additional variable, $a$, to the earlier 12 state, control, and disturbance variables. This new variable is definitely a control variable, and it must thus be included in the control vector $\mathbf{u}$, which will now be amended, as follows:

$$\mathbf{u} \triangleq \begin{bmatrix} P_{G1} \\ Q_{G1} \\ P_{G2} \\ Q_{G2} \\ a \end{bmatrix} \qquad (7\text{-}116)$$

Generally, if $r$ regulating transformers are included in the network, the control vector must be amended by the addition of the $r$ control variables $a_1, a_2, \ldots, a_r$.

The change in the SLFE† as caused by the RT will of course affect the function vector $\mathbf{f}$ defined by Eq. (7-13). This change can, as a rule, be accounted for by an appropriate adjustment of the bus admittance matrix $\mathbf{Y}_{bus}$. The reader has an opportunity to study this situation by working Exercise 7-10.

In Sec. 8-4.1 we will present an additional example on analysis procedures involving regulating transformers.

## 7-8 SUMMARY

An understanding of the laws that govern and factors that control the steady-state operation of a power system is of basic importance for the systems engineer. In this chapter we have attempted to put some order into the complexities of large interconnected systems and thereby provide some insight into their functioning.

The complexity of a system is directly proportional to the number of nodes, or "buses," which it contains. At these nodes we inject and extract

† Compare Eqs. (7-2) and (7-115).

power, and we have concluded that the overall steady-state functioning of the system can be described in terms of six variables per node:

Extracted power components $P_{Di}$ and $Q_{Di}$
Injected power components $P_{Gi}$ and $Q_{Gi}$
Bus voltage magnitude and phase $|V_i|$ and $\delta_i$

We have divided these variables into three groups:

1. Uncontrolled, or disturbance, variables
2. Independent, or control, variables
3. Dependent, or state, variables

The variables of the first group, made up of the demand powers, are beyond the influence of the systems operator. The control variables, however, can be chosen within certain practical limits by the operator, and this choice will then determine the third group, i.e., the state of the system. This state of the system is characterized by a certain frequency, voltage profile, and load flow structure.

The mathematical model that describes the interrelationship between the above three groups of variables is referred to as the static load flow equations. We have developed systematic computer-oriented methods for assembling this model and also solving it. Although we have demonstrated these methods for a three-bus example system only, they can be used successfully for systems containing hundreds of buses.

Since the control variables can be chosen in an infinite number of combinations, we can, obviously, operate our system in an infinite number of states. We have not yet discussed to any depth the problem of how to select the "best" state of operation. In the next chapter we return to these questions. We have likewise avoided the question of how to maintain the system in a chosen operating state. This important problem of systems control must wait until Chap. 9.

## EXERCISES

(Exercises 7-8 and 7-9 require usage of the digital computer.)

**7-1.** Work the load flow problem in Sec. 7-5 with the same bus power specifications as given in Table 7-1, but with the voltage specifications changed as follows:

$$|V_1| = 1.00 \text{ pu}$$
$$|V_2| = 1.05 \text{ pu}$$
$$|V_3| = 0.95 \text{ pu}$$

Your results should demonstrate that no essential change will take place in the *real* power flow, but the *reactive* flow will change radically.



**7-2.** As in Exercise 7-1, work the load flow problem assuming that the real generation is divided between the generators as follows:

$$P_{G1} = 1.0 \text{ pu}$$
$$P_{G2} = 1.0 \text{ pu}$$
$$P_{G3} = 0 \text{ pu}$$

The real demand is unchanged, and the desired voltage profile is still $|V_1| = |V_2| = |V_3| = 1$.

Your results should now demonstrate that the *reactive* flow is essentially unchanged but the real flow is different.

**7-3.** Consider the two-bus example system discussed in the text. The line parameters were defined in Eqs. (7-3) and (7-4). Set $X_c = 10.0$ pu, $X_L = 0.20$ pu, and $\alpha = 0$.

Assemble $\mathbf{Y}_{bus}$ and compute $\mathbf{Z}_{bus}$ for the system.

**7-4.** In the text the gaussian iterative method was applied to the equation $x^2 - 5x + 4 = 0$. Will the method succeed if we redefine the $F(x)$ function as indicated in footnote on p. 244?

**7-5.** In Example 7-6 we made use of the NR algorithm

$$\mathbf{x}^{(\nu+1)} = \mathbf{x}^{(\nu)} - [\mathbf{J}^{(\nu)}]^{-1}\mathbf{f}^{(\nu)}$$

For a *scalar* function $f(x)$ this algorithm can be written:

$$x^{(\nu+1)} = x^{(\nu)} - \left[\left(\frac{\partial f}{\partial x}\right)^{(\nu)}\right]^{-1} f^{(\nu)} = x^{(\nu)} - \frac{f^{(\nu)}}{(\partial f/\partial x)^{(\nu)}}$$

Give a *graphical* interpretation of the convergence by plotting $f(x)$ versus $x$, and show how $x^{(0)}, x^{(1)}, \ldots$, approach the exact solution of the equation $f(x) = 0$.

**7-6.** Consider Example 7-1. Assume that we increase $Q_{G1}$ by 5 percent, i.e., $0.05 \times 10 = 0.5$ pu Mvar. From the sensitivity coefficients that we derived, this means an increase in bus voltages by the amounts

$$\Delta|V_1| = 0.0375 \times 0.5 = 0.01875 \text{ pu}$$

$$\Delta|V_2| = 0.0125 \times 0.5 = 0.00625 \text{ pu}$$

The phase angle $\delta_2$ will experience a change of the amount

$$\Delta\delta_2 = -0.050 \times 0.5 = -0.025 \text{ rad}$$

The change in $\delta_2$ signifies a change in real line flow.

(*a*) Compute the change in $P_{D2}$ due to the change in $|V_2|$ and confirm that this change exactly equals the change in line flow. Why must it be so?

(*b*) Vector equation (7-26) contains in compact format the last $2n - 1$ components of the linear system (7-25). The remaining first component of system (7-25) reads

$$\frac{\partial f_1}{\partial x_2}\Delta x_2 + \cdots + \frac{\partial f_1}{\partial x_{2n}}\Delta x_{2n} + \frac{\partial f_1}{\partial u_1}\Delta u_1 + \cdots + \frac{\partial f_1}{\partial u_{2n}}\Delta u_{2n} + \frac{\partial f_1}{\partial p_1}\Delta p_1 + \cdots + \frac{\partial f_1}{\partial p_{2n}}\Delta p_{2n} = 0$$

Use this equation to compute the change $\Delta P_{G1} = \Delta u_1$ in our case.

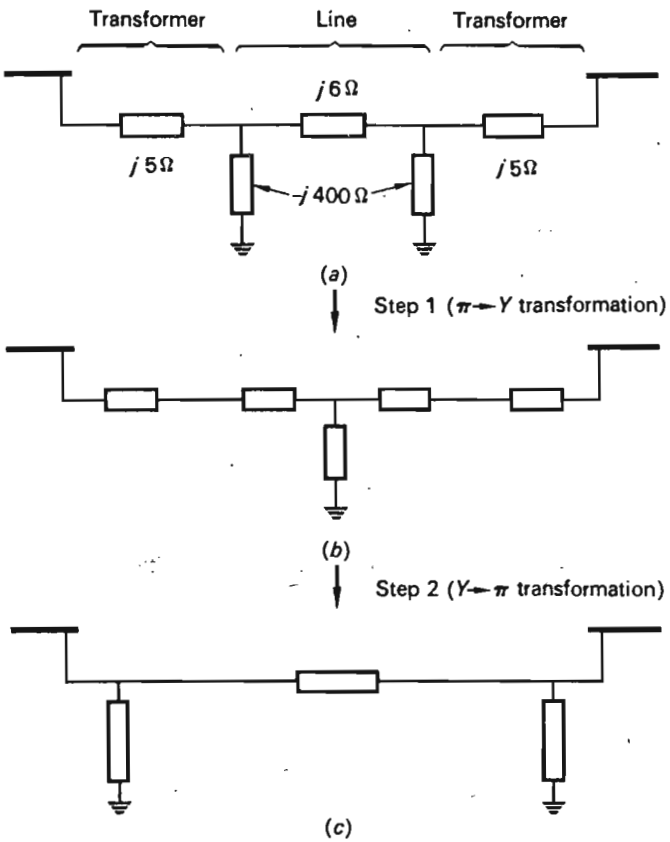


**Fig. 7-21** Transmission line, including terminal transformers, can be represented by $\pi$ equivalent.

**7-7.** In all examples in the text we developed the bus admittance matrices on the assumption that the connecting links between the buses could be represented by a $\pi$ link. (See, for examples, Figs. 7-2 and 7-15.)

If the link consists of a line plus transformers, then it is not immediately evident that this assumption is correct. The equivalent diagram would now look as depicted in Fig. 7-21*a*. This network can, however, in two simple self-explanatory steps, be transformed into an equivalent $\pi$ link, as demonstrated in the figure.

(*a*) Perform the transformations called for, assuming the numerical impedance values given in Fig. 7-21*a*.

(*b*) If you were simply to move the 400-Ω capacitors outside of the transformer impedances, you could obtain your $\pi$ link in one *approximate* step. What percent error would this entail?

**7-8.** (*a*) Find the bus incidence matrix **A** for the five-bus system in Fig. 7-22.

(*b*) Find the primitive admittance matrix for the system, assuming that all the lines are characterized by a series impedance of $0.111 + j0.851$ Ω/mile and a shunt admittance



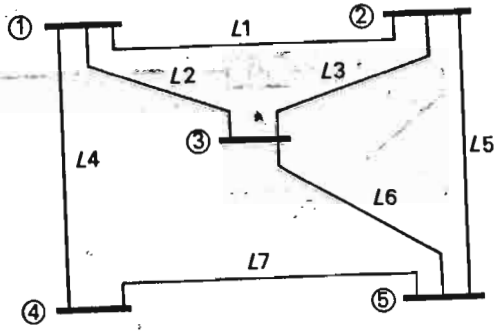


**Fig. 7-22** A five-bus seven-line example system.

of $j0.522 \times 10^{-5}$ Ω/mile. All seven lines are rated at 138 kV and have the following lengths:

*L*1 — 70.4 miles
*L*2 — 53.1 miles
*L*3 — 40.8 miles
*L*4 — 71.9 miles
*L*5 — 62.8 miles
*L*6 — 30.6 miles
*L*7 — 98.4 miles

You can consider them all as "electrically short."

(*c*) Find the bus admittance matrix for the system. Use the base values 138 kV and 100 MVA. Express all impedances and admittances in per units.

**7-9.** Perform a load flow study for the system in Fig. 7-22. The bus power and voltage specifications are given in Table 7-4.

**Table 7-4**

| Bus | Bus power, pu | | Voltage magnitude, pu | Bus type |
|---|---|---|---|---|
| | *Real* | *Reactive* | | |
| 1 | Unspecified | Unspecified | 1.000 | 3 |
| 2 | 0.931 | Unspecified | 1.000 | 2 |
| 3 | −2.202 | −1.031 | Unspecified | 1 |
| 4 | 0.900 | Unspecified | 1.000 | 2 |
| 5 | −0.911 | −0.212 | Unspecified | 1 |

You should compute the unspecified bus voltages, all bus powers, and all line powers (in both ends). Make a power flow chart. Assume unlimited *Q* sources.

**7-10.** In this final exercise the student is invited to examine how a load flow analysis may be performed if a regulating transformer (RT) is employed in the system. To emphasize the

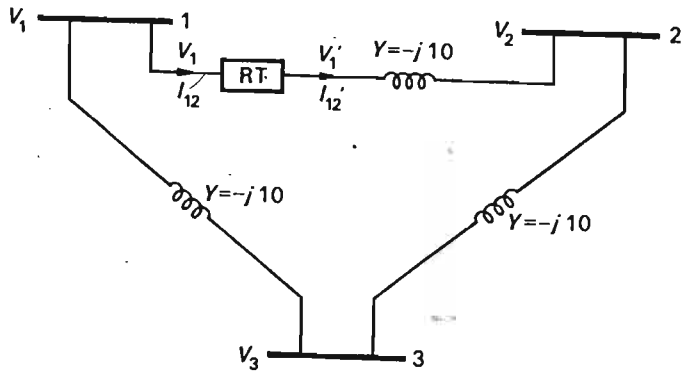


**Fig. 7-23** Three-bus example system containing a regulating transformer.

nature of the load flow changes that the RT introduces, we choose to study the same system as in Sec. 7-5, *subject to the same bus power and voltage specifications.* The RT is introduced in $L1$ at bus 1, as shown in Fig. 7-23.

The student should investigate the following two cases:

*Case* 1. The RT is a magnitude regulator of the type depicted in Fig. 5-18, with a ratio

$$a \triangleq \frac{V_1}{V_1'} = 0.98$$

(For symbols see Fig. 7-23.)

*Case* 2. The RT is a phase angle regulator of the type depicted in Fig. 5-19, having a ratio

$$a \triangleq \frac{V_1}{V_1'} = e^{j2^\circ}$$

To be able to work with the same branch admittances as in the text, we shall neglect the impedance introduced by the RT. Since no power is therefore lost in the device, we have the following relation between the input and output variables:

$$V_1 I_{12}^* = V_1'(I_{12}')^* \tag{7-117}$$

We therefore have the current relation

$$I_{12}' = I_{12}\left(\frac{V_1}{V_1'}\right)^* = I_{12}a^* \tag{7-118}$$

(*a*) Prove that the bus admittance matrix for the circuit in Fig. 7-23 takes on the value

$$\mathbf{Y}_{\text{bus}} = \begin{bmatrix} -j10\left(1+\dfrac{1}{|a^2|}\right) & \dfrac{j10}{a^*} & j10 \\ \dfrac{j10}{a} & -j20 & j10 \\ j10 & j10 & -j20 \end{bmatrix}$$

[Note that $\mathbf{Y}_{\text{bus}}$ reduces to Eq. (7-81) for $a = 1$.]



(*b*) Solve the load flow equations in cases 1 and 2, using techniques similar to those we employed in solving Eqs. (7-83). Compare the load flow picture with the one in Fig. 7-10. Prove, in particular, that in case 1, only the reactive flow will change, whereas in case 2, the changes will occur in the real power flow. Explain.

## REFERENCES

**Books**

1. Mortlock, J. R., and M. W. Humphrey Davies: "Power System Analysis," Chapman and Hall, Ltd., London, 1952.
2. Stevenson, W. D.: "Elements of Power System Analysis," 2d ed., McGraw-Hill Book Company, New York, 1962.
3. Stagg, G. W., and A. H. El-Abiad: "Computer Methods in Power Systems Analysis," McGraw-Hill Book Company, New York, 1968.
4. Ostrowski, A. M.: "Solution of Equations and Systems of Equations," Academic Press Inc., New York, 1966.
5. Traub, J. F.: "Iterative Methods for the Solution of Equations," Prentice-Hall, Inc., Englewood Cliffs, N.J., 1964.
6. Guillemin, E.: "Introductory Circuit Theory," John Wiley & Sons, Inc., New York, 1953.
7. Seshu, S., and M. B. Reed: "Linear Graphs and Electric Networks," Addison-Wesley Publishing Company, Inc., Reading, Mass., 1961.

(References 1 and 2 give brief coverage of network modeling and load flow analysis. Reference 3 gives detailed and excellent presentation of both these topics. References 4 and 5 are recommended for those readers who want a deeper insight into the techniques of iterative computation. References 6 and 7 give an excellent account of the use of linear graphs in network theory.)

**Technical papers and reports**

8. Dunstan, L. A.: Digital Load Flow Studies, *Trans. AIEE*, vol. 73, pt. IIIA, pp. 825–832, 1954.
9. Bennett, J. M.: Digital Computers and the Load Flow Problem, paper 1957M, *Proc. IEE*, vol. 103B, suppl. 1, p. 16, December, 1955.
10. Ward, J. B., and H. W. Hale: Digital Computer Solution of Power Flow Problems, paper 56–164, *Trans. AIEE*, vol. 75, pt. III, pp. 398–404, June, 1956.
11. Glimn, A. F., and G. W. Stagg: Automatic Calculation of Load Flows, *Trans. AIEE*, vol. 76, pt. III, pp. 817–828, 1957.
12. Brown, R. J., and W. F. Tinney: Digital Solutions for Large Power Networks, paper 57–147, *Trans. AIEE*, vol. 76, pt. III, pp. 347–355, 1957.
13. Jordan, R. H.: Rapidly Converging Digital Load Flows, *Trans. AIEE*, vol. 76, pt. III, pp. 1433–1438, 1957.
14. Hale, H. W., and R. W. Goodrich: Digital Computation of Power Flow—Some New Aspects, paper 59-224, *Trans. AIEE*, vol. 78, pt. III, pp. 919–924, 1959.
15. Van Ness, J. E.: Iteration Methods for Digital Load Flow Studies, *Trans. AIEE*, vol. 78, pt. III, pp. 583–588, 1959.

(The above papers are the classical contributions to the art of digital load flow analysis.)

16. Sato, N., and W. F. Tinney: Techniques for Exploiting the Sparsity of the Network Admittance Matrix, *IEEE Trans.*, vol. 82, pt. III, pp. 944–949, December, 1963.
17. El-Abiad, A. H., G. W. Stagg, and M. Watson: The Load Flow Problem: Its Formulation and Solution, *Power Systems Computation Conf.*, Queen Mary College, London, September, 1963.

18. Dineley, J. L. (ed.): The Use of Digital Computers in Electric Power Systems, Oriel Press, Newcastle upon Tyne, England, 1967.
19. Brown, H. E., O. K. Carter, H. H. Happ, and C. E. Person: Power Flow Solution by Impedance Matrix Iterative Method, paper 62-214, *Trans. AIEE*, vol. 82, pt. III, p. 1, 1963.
20. Brameller, A., and J. K. Denmead: Some Improved Methods for Digital Network Analysis, paper 3778S, *Proc. IEE*, vol. 109, pt. A, no. 43, pp. 109–116, February, 1962.
21. Baumann, R., G. Boll, W. Schneider, and Vorbach: Experience with Use of Electronic Computers in the Planning and Optimal Operation of Electric Power Systems, paper 309, CIGRE, Paris, 1962.
22. Carpentier, J.: Application of Newton's Method to the Load Flow Problem, *Proc. Power Systems Computations Conf.*, Queen Mary College, September, 1963.
23. Cronin, J. H., and M. B. Newman: Digital Load Flow Program for 1000 Bus Systems, *Trans. IEEE Power Apparatus Systems*, vol. 83, no. 7, pp. 718–720, July, 1964.
24. Laughton, M. A., and M. W. Humphrey Davies: Numerical Techniques in the Solution of the Power System Load Flow Problem, paper 4511P, *Proc. IEE*, vol. III, no. 9, pp. 1575–1588, September, 1964.
25. Baumann, R.: Some New Aspects on Load Flow Calculation, pt. I, Impedance Matrix Generation Controlled by Network Topology, *Proc. Power Ind. Computer Appl. Conf.*, May, 1965.
26. Aubin, J. P., and P. A. Raviart: On the Resolution of Equations Arising in Load Flow Problems, *Proc. Power Ind. Computer Appl. Conf.*, pp. 119–132.
27. Norimatsu, T. A. T.: Theory of Convergence of Digital Load Flow Solutions by Ward and Hale Method, *Proc. Power Ind. Computer Appl. Conf.*, pp. 133–143.
28. Brown, H. E., et al.: Investigation of Z-matrix Algorithms in Load Flow Programs, *Proc. Power Ind. Computer Appl. Conf.*, pp. 144–158.
29. Feingold, D., and D. Spohn: Direct Methods for Linear Networks of Load Flow Computation, *Proc. Power Systems Computation Conf.*, pt. II, rept. 4.4, Stockholm, 1966.
30. Brameller, A.: The Application of Diacoptics to Network Analysis, *Proc. Power Systems Computation Conf.*, rept. 4.6, Stockholm, 1966.
31. Edelmann, H.: Ordered Triangular Factorization of Matrices: A Multipurpose Approach for Treating Problems in Large Electric Networks, *Proc. Power Systems Computation Conf.*, rept. 4.12, Stockholm, 1966.
32. Baumann, R., and H. Rub: Load Flow Iterative Techniques Using Sparse Hybrid Matrices, *Proc. Power Systems Computation Conf.*, rept. 4.14, Stockholm, 1966.
33. Bonaparte, J. E., and W. W. Maslin: Simplified Load Flow, *Proc. Power Ind. Computer Appl. Conf.*, Pittsburgh, Pa., 1967, pp. 385–394.
34. Peschon, J., et al.: Sensitivity in Power Systems, *Proc. Power Ind. Computer Appl. Conf.*, Pittsburgh, Pa., 1967, pp. 209–220.
35. Adibi, M. M., et al.: Power System Computer Feasibility Study, vol. I, IBM Research Division, San Jose, Calif.
36. Specifications for Tomorrow's Power Flow and Dynamic Stability Programs, Western Systems Coordinating Council Committee Report, *Proc. Power Ind. Computer Appl. Conf.*, Denver, Colo., 1969.
37. Klos, A.: Algebraic Model of Electrical Network, *Proc. Power Ind. Computer Appl. Conf.*, Denver, Colo., 1969.
38. Schweppe, F. C., et al.: Power System Static State Estimation, *Proc. Power Ind. Computer Appl. Conf.*, Denver, Colo., 1969.
39. Oqbuobiri, E. C., et al.: Sparsity-directed Decomposition for Gaussian Elimination on Matrices, *Proc. Power Ind. Computer Appl. Conf.*, Denver, Colo., 1969.



40. Sasson, A. M.: Decomposition Techniques Applied to the Nonlinear Programming Load Flow Method, *Proc. Power Ind. Computer Appl. Conf.*, Denver, Colo., 1969.
41. Meisel J., and R. D. Barnard: Application of Fixed-point Techniques to Load-flow Studies, *Proc. Power Ind. Computer Appl. Conf.*, Denver, Colo., 1969.
42. Wallach, Y.: Gradient Method for Load-flow Problems, *IEEE Trans.*, vol. PAS-86, no. 5, May, 1968.
43. Happ, H. H.: Orthogonal Networks, *IEEE Trans.*, vol. PAS-85, no. 3, pp. 281–291, March, 1966.
44. Sasson, A. M., and F. J. Jaimes: Digital Methods Applied to Power Flow Studies, *IEEE Trans.*, vol. PAS-86, pp. 860–867, no. 7, July, 1967.
45. Tinney, W. F., and J. W. Walker: Direct Solutions of Sparse Network Equations by Optimally Ordered Triangular Factorizations, *Proc. IEEE*, vol. 55, pp. 1801–1809, November, 1967.

# 8

# The Energy System in Steady State—Optimum Operating Strategies

From our discussions in the preceding chapter, we have learned that it is possible to supply a given load demand in an infinite number of operating configurations. It is necessary to choose one particular configuration; i.e., the systems operator must specify exactly two variables per bus and, in addition, decide on appropriate tap settings on all regulating transformers. For a type 1 bus he must specify $P_G$ and $Q_G$, for a type 2 bus, $P_G$ and $|V|$, and for the slack bus, he must select $|V|$.

On what basis are these specifications made? The simplest method is to use an "intelligent guess." Many systems are today operated on that basis. In this chapter we discuss more sophisticated methods for selecting a "best" or "optimum" operating strategy. It must be remembered, however, that in the final analysis someone must make the decision as to what shall be understood by best or optimum in each particular instance. The choice of an *optimum criterion* is therefore always a subjective one.





## 8-1 THE GENERAL PROGRAMMING PROBLEM

In engineering systems analysis we are faced on many occasions with the problem of optimizing† a scalar *cost criterion*, or *objective function*, $C$, which is a function of the state, control, and/or disturbance variables of the system in question, simultaneously observing certain *equality* and/or *inequality constraints* for these same variables. Expressed mathematically, the problem amounts to optimizing the scalar function

$$C = C(\mathbf{x},\mathbf{u},\mathbf{p}) \tag{8-1}$$

and simultaneously satisfying the equations

$$\mathbf{h}(\mathbf{x},\mathbf{u},\mathbf{p}) = \mathbf{0} \tag{8-2}$$

and/or the inequalities

$$\mathbf{g}(\mathbf{x},\mathbf{u},\mathbf{p}) \leq \mathbf{0} \tag{8-3}$$

The number of constraints, i.e., the dimensions of the $\mathbf{h}$ and $\mathbf{g}$ vectors, need not be related to the number of state or control variables.

The problem thus posed is referred to as a *general programming problem*. If the $C$ function and Eqs. (8-2) and inequalities (8-3) are *linear* in the $\mathbf{x}$, $\mathbf{u}$, and $\mathbf{p}$ variables, then we talk about *linear programming*. In our case we shall find that some or all of the expressions (8-1) to (8-3) are *nonlinear*, and we have then a *nonlinear programming problem* on our hands. Such a programming problem is by no means trivial. Rarely are we led to an *analytical* solution. The best we can hope for is to develop computational algorithms that will render *numerical* solutions.

In our presentation we choose to start with the simplest possible programming formulation, and then successively lead up to the most advanced methods in use today. In order of complexity, we divide our problem into the following three categories:

1. Optimum economic dispatch, neglecting line losses (Sec. 8-2)
2. Optimum economic dispatch, considering line losses (Sec. 8-3)
3. The general optimum operating problem (Sec. 8-4)

In the first two categories we discuss the classical problem of finding the *economically best* operating configuration. Our criterion function $C$ is thus chosen to mean dollars per hour. The overall operating cost is strongly influenced by the allocation of the real power generations $P_{Gi}$ between the system generators. Other variables, such as voltage magnitudes $|V_i|$,

† By "optimize" we mean either *minimize* or *maximize*, depending upon the problem at hand. In this book we always mean the former.

affect the cost only slightly. We therefore commit only a negligible error by assuming that $C$ is an explicit function of the $P_{Gi}$'s only.

In the third category we shall consider the optimization problem where the cost function $C$ is of a more general, not necessarily economical, nature.

## 8-2 OPTIMUM GENERATOR ALLOCATION—LINE LOSSES NEGLECTED

### 8-2.1 COST CRITERION

As mentioned above, we choose as our criterion the dollar cost of operation. We do this for the simple reason that it is generally a meaningful, unambiguous, and reasonably easy to measure cost function.

Since we are going to consider a system *already in existence*, we do not concern ourselves with those cost components that are *fixed*, like salaries, plant installation costs, etc. We consider only those costs that, by proper strategy, we can *control*, i.e., the fuel costs in the various generator stations.

Let $c_i$ mean the cost, expressed, for example, in dollars per hour, of producing energy in the generator units at bus $i$. The overall system production cost therefore will be

$$C = \sum_{i=1}^{n} c_i \quad \text{dollars/h} \tag{8-4}$$

How do the various state and control variables affect this cost?

The generated real power $P_{Gi}$ certainly accounts for the major influence on $c_i$. The individual real generations are raised by increasing the prime mover torques, and this requires an increased expenditure of fuel. The reactive generations $Q_{Gi}$ do not have any measurable influence on $c_i$ because they are controlled by varying the field current.

The individual production cost $c_i$ of generator unit $i$ is therefore for all practical purposes a function only of $P_{Gi}$, and we can write

$$c_i = c_i(P_{Gi}) \quad \text{dollars/h} \tag{8-5}$$

For the overall production cost, we therefore have

$$C = \sum_{i=1}^{n} c_i(P_{Gi}) = c_1(P_{G1}) + \cdots + c_n(P_{Gn}) \tag{8-6}$$

When the cost function $C$ can be written as a sum of terms where each term depends only upon one independent variable, we say that $C$ is *separable*.

The cost functions $c_i$ are always determined empirically. The fuel costs, of course, constitute the major portions, but operation and maintenance, etc., also enter in. Figure 8-1 depicts a typical cost-versus-megawatt

The general nature of the cost functions (but of course not the magni-

e the same for coal, oil, or gas-fired stations. Nuclear stations can



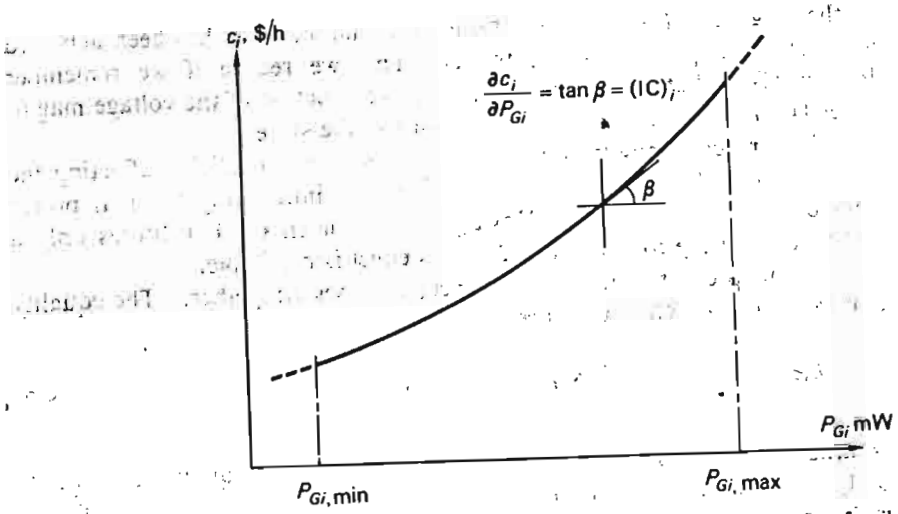


**Fig. 8-1** Typical production cost–versus–megawatt chart for fossil-fueled generator unit.

also be included. Hydrostations, for obvious reasons, are not, and the following analysis therefore applies only to thermal and nuclear generation.

### 8-2.2 CONSTRAINT RELATIONS

A set of real generation variables $P_{Gi}$ must now be selected that will minimize the cost function (8-6). The selection cannot be arbitrary as it is necessary to observe simultaneously certain equality and inequality constraints.

**Equality constraints** As the choice of the $P_{Gi}$'s must be consistent with the static balance of the system *it is clear that the SLFE constitute our equality constraints.*

Searching an optimum set of $P_{Gi}$'s and simultaneously making sure that the $2n$ SLFE are satisfied is a rather formidable mathematical problem. We can achieve considerable simplification by making use of our earlier observation that the reactive powers do not *explicitly* affect $C$. By thus freeing ourselves from the need for monitoring the reactive power balance and associated voltage profile, we turn our full attention to the *real power balance* in the system. In accordance with Eq. (7-7) the latter can be stated:

$$h(P_{G1}, \ldots, P_{Gn}) \triangleq \sum_{i=1}^{n} P_{Gi} - P_D - P_L \doteq 0 \tag{8-7}$$

where the total demand $P_D$ is obtained from

$$P_D \triangleq \sum_{i=1}^{n} P_{Di} \tag{8-8}$$

Having divorced the reactive powers from our optimization problem has thus permitted us to reduce the number of equality constraints from $2n$

to the single Eq. (8-7). This considerable simplification has been achieved at a slight approximation, however. This we realize if we remember [cf. Eq. (7-9)] that the real power loss $P_L$ is a function of the voltage magnitudes $|V_i|$ *and thus the reactive power flows* in the system.

The reactive power components, although not explicitly affecting the cost function (8-6), will affect it *implicitly* by influencing the real power balance via the real losses. However, as $P_L$ normally constitutes only a few percent of the total demand $P_D$, this effect is negligible.

In the present section we shall neglect losses altogether. The equality constraint (8-7) therefore reduces to

$$h(P_{G1}, \ldots, P_{Gn}) \triangleq \sum_{i=1}^{n} P_{Gi} - P_D = 0 \tag{8-9}$$

**Inequality constraints** Having thus disposed of the equality constraints of type (8-2) we now proceed to state the inequality constraints of type (8-3) that apply.

Since each generator must not be operated above its rating or below some minimum power (zero, for example), the generator powers $P_{Gi}$ cannot lie outside the range stated by the inequality (7-20), which we restate for easy reference:

$$P_{Gi,\min} \leq P_{Gi} \leq P_{Gi,\max} \qquad \text{for } i = 1, 2, \ldots, n \tag{8-10}$$

In addition, although these variables do not directly affect our cost we must not violate the limit conditions imposed on $Q_{Gi}$ and $|V_i|$ as stated by the inequalities (7-18) and (7-20).

These three inequalities represent thus the constraints (8-3).

Having thus stated our problem, it is reasonable to question whether the problem has a solution, and also if the solution is unique. Consider, for example, the simplest† case, $n = 2$, and assume that $P_D = 100$ MW.

The power balance equation (8-9) could be satisfied in an infinite number of ways. For example, we may let the two generators generate 50 MW each, or one of them could generate 75 MW and the other one 25 MW. *Intuitively*, we feel that there must be *one* combination that is better, in an economic sense, than all the others. Clearly, the nature of the cost functions $c_i$ determines the optimum power settings.

### 8-2.3 OPTIMUM DISPATCH STRATEGY FOR A TWO-BUS SYSTEM

We shall develop the optimum dispatch strategy first for a two-generator system, because in this case we can give it a simple geometrical interpretation not possible in the general $n$-generator case. It is easy later to extend our results to the general case.

† Why do we not consider the still simpler case $n = 1$?



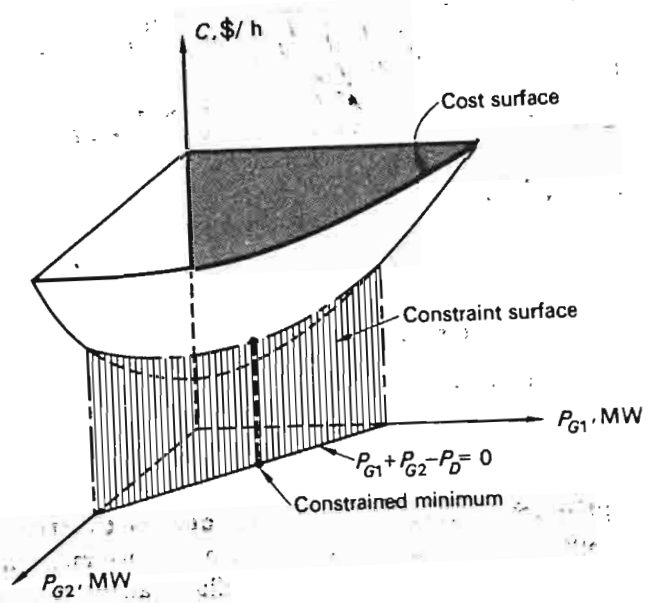


**Fig. 8-2** Cost surface.

For $n = 2$ Eqs. (8-6) and (8-9) reduce to

$$C = c_1 + c_2 = c_1(P_{G1}) + c_2(P_{G2}) \tag{8-11}$$

$$h(P_{G1}, P_{G2}) = P_{G1} + P_{G2} - P_D = 0 \tag{8-12}$$

The individual cost functions $c_1$ and $c_2$ are functions of $P_{G1}$ and $P_{G2}$, respectively, and therefore the total cost function $C$ must be a function of both generator outputs, and we can plot it versus $P_{G1}$ and $P_{G2}$ in a three-dimensional coordinate system, as has been done in Fig. 8-2. We obtain a bowl-shaped "cost surface."†

The surface indicates clearly that minimum generation cost is obtained for $P_{G1} = P_{G2} = 0$—not a surprising observation. We cannot, of course, operate at this point, since we must satisfy the constraint equation (8-12), which represents another surface, "the constraint surface" (a plane in this case), in our chosen coordinate system. Our problem can thus be summarized as follows: *For minimum cost, we must operate so that we stay as far down as possible on our cost surface but still remain on the constraint plane.* This evidently puts us at the point marked "constrained minimum" in Fig. 8-2.

† Note that the surface does not necessarily have rotational symmetry around the $C$ axis.

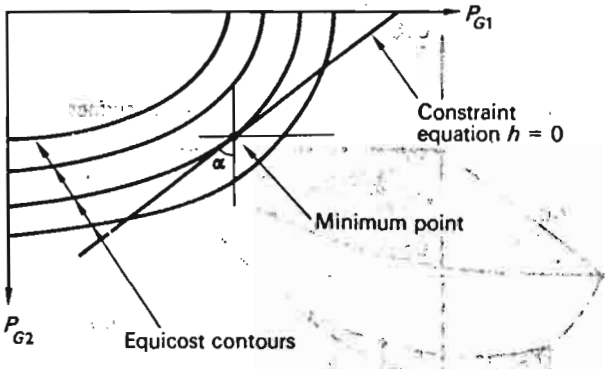


**Fig. 8-3** Equicost contours.

**Optimum dispatch formula—inequality constraints neglected** The question we now must answer is: How do we mathematically identify this optimum point? The situation is illuminated in Fig. 8-3, where we have shown the cost surface of Fig. 8-2 in a different way. We have actually "sliced" the cost surface horizontally. The intersections we thus obtain with the cost surface are *equicost contours*, along each of which the cost $C$ is constant. *We make now the important observation that in our minimum point the constraint line* $h(P_{G1}, P_{G2}) = 0$ *is tangential to the cost contours.* We make use of this "tangency requirement" in the following way.

We find, first, the slope of the cost contour by differentiating

$$C(P_{G1},P_{G2}) = \text{const}$$

We get

$$dC = \frac{\partial C}{\partial P_{G1}}\,dP_{G1} + \frac{\partial C}{\partial P_{G2}}\,dP_{G2} = 0 \tag{8-13}$$

For the slope we thus get

$$\frac{dP_{G2}}{dP_{G1}} = -\frac{\partial C/\partial P_{G1}}{\partial C/\partial P_{G2}} \tag{8-14}$$

Differentiation of the constraint equation

$$h(P_{G1},P_{G2}) = 0$$

similarly gives its slope,

$$\frac{dP_{G2}}{dP_{G1}} = -\frac{\partial h/\partial P_{G1}}{\partial h/\partial P_{G2}} \tag{8-15}$$



The tangency requirement thus results in the equation

$$\frac{\partial C/\partial P_{G2}}{\partial C/\partial P_{G1}} = \frac{\partial h/\partial P_{G2}}{\partial h/\partial P_{G1}} = -\tan\alpha \tag{8-16}$$

(see Fig. 8-3 for the definition of $\alpha$).

We may write Eq. (8-16) in the form

$$\frac{\partial C/\partial P_{G2}}{\partial h/\partial P_{G2}} = \frac{\partial C/\partial P_{G1}}{\partial h/\partial P_{G1}} = \text{const} \triangleq \lambda \tag{8-17}$$

The constant $\lambda$ is referred to as a *Lagrange multiplier.*

Equations (8-17) can be written

$$\frac{\partial C}{\partial P_{G1}} - \lambda\frac{\partial h}{\partial P_{G1}} = 0$$

$$\frac{\partial C}{\partial P_{G2}} - \lambda\frac{\partial h}{\partial P_{G2}} = 0 \tag{8-18}$$

and if we at this juncture define an *augmented* (or *constrained*) *cost function*

$$C^* \triangleq C - \lambda h = c_1 + c_2 - \lambda(P_{G1} + P_{G2} - P_D) \tag{8-19}$$

we thus have concluded that the constrained minimum is characterized by

$$\frac{\partial C^*}{\partial P_{G1}} = 0$$

$$\frac{\partial C^*}{\partial P_{G2}} = 0 \tag{8-20}$$

The optimum dispatch problem is now mathematically solved. Let us look at the results from a physical point of view. Before making use of Eqs. (8-18), we first compute from Eqs. (8-11) and (8-12) the partial derivatives

$$\frac{\partial h}{\partial P_{G1}} = \frac{\partial h}{\partial P_{G2}} = 1$$

and

$$\frac{\partial C}{\partial P_{G1}} = \frac{\partial c_1}{\partial P_{G1}}$$

$$\frac{\partial C}{\partial P_{G2}} = \frac{\partial c_2}{\partial P_{G2}}$$

These partial derivatives are substituted into Eqs. (8-18), which then tell us that we should operate our system so that the following *optimum dispatch equations* are satisfied:

$$\frac{\partial c_1}{\partial P_{G1}} = \frac{\partial c_2}{\partial P_{G2}} = \lambda \tag{8-21}$$

Note that the two Eqs. (8-21) and the constraint equation (8-12) exactly suffice for finding the three unknowns $P_{G1}$, $P_{G2}$, and $\lambda$.

What is the physical significance of our findings?

The partial derivatives $\partial c_i/\partial P_{Gi}$ are referred to as *incremental costs* (IC) of generation. They represent the slope of the cost curve, as shown in Fig. 8-1. As the unit for $c_i$ is dollars per hour, the incremental cost unit must be dollars per hour per kilowatt, or dollars per kilowatthour. For large generator units, a better unit is dollars per megawatthour.

Stating our findings in words:

*For optimum dispatch we should make sure that our individual generators operate at equal incremental production costs.*

**Example 8-1** Consider the case of a two-generator system where we have found that the cost curves (Fig. 8-1) may be approximated ("curve fitting") by second-order polynomials of the form

$$\begin{aligned} c_1 &= \alpha_1 + \beta_1 P_{G1} + \gamma_1 P_{G1}^2 \quad \text{dollars/h} \\ c_2 &= \alpha_2 + \beta_2 P_{G2} + \gamma_2 P_{G2}^2 \quad \text{dollars/h} \end{aligned} \tag{8-22}$$

where the $\alpha$, $\beta$, and $\gamma$ are constants. The incremental costs are obtained by differentiation and are in this case straight lines,

$$(\text{IC})_1 = \frac{\partial c_1}{\partial P_{G1}} = \beta_1 + 2\gamma_1 P_{G1} \quad \text{dollars/MWh}$$

$$(\text{IC})_2 = \frac{\partial c_2}{\partial P_{G2}} = \beta_2 + 2\gamma_2 P_{G2} \quad \text{dollars/MWh}$$

depicted in Fig. 8-4.

By application of the optimum dispatch rule (8-21) and the equality constraint equation (8-12), we get

$$\begin{aligned} \beta_1 + 2\gamma_1 P_{G1} &= \beta_2 + 2\gamma_2 P_{G2} \\ P_{G1} + P_{G2} &= P_D \end{aligned} \tag{8-23}$$

We solve these equations for $P_{G1}$ and $P_{G2}$:

$$\begin{aligned} P_{G1} &= \frac{\gamma_2}{\gamma_1 + \gamma_2} P_D + \frac{\beta_2 - \beta_1}{2(\gamma_1 + \gamma_2)} \\ P_{G2} &= \frac{\gamma_1}{\gamma_1 + \gamma_2} P_D + \frac{\beta_1 - \beta_2}{2(\gamma_1 + \gamma_2)} \end{aligned} \tag{8-24}$$



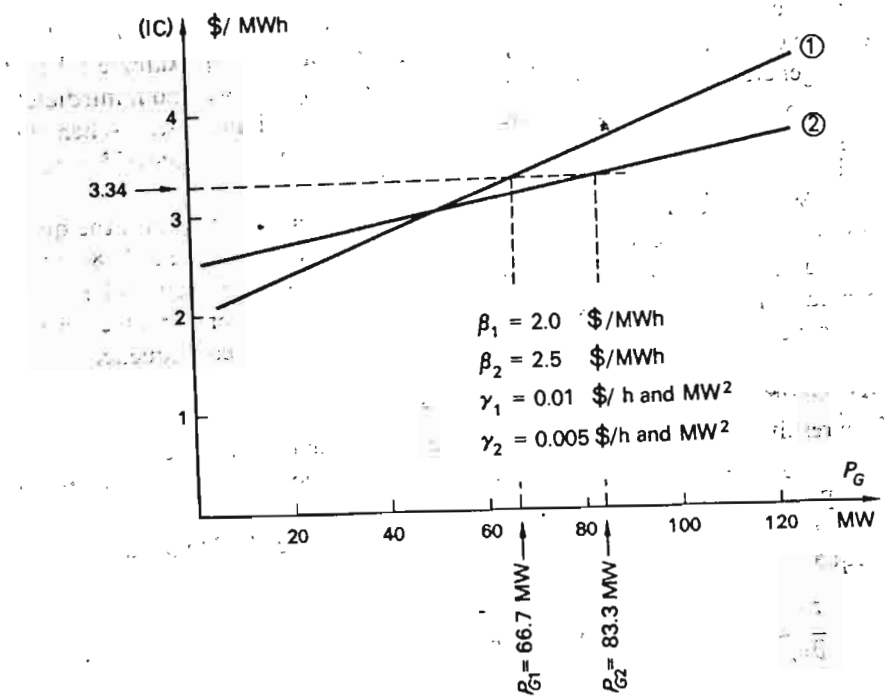


**Fig. 8-4** Linear incremental cost curves.

If we use the specific numerical values for the $\beta$ and $\gamma$ parameters given in Fig. 8-4 and a $P_D$ value of 150 MW, we obtain the optimum generator settings

$$P_{G1} = 66.7 \text{ MW}$$
$$P_{G2} = 83.3 \text{ MW}$$

The incremental cost (see dotted lines in Fig. 8-4) will be \$3.34/MWh. The total minimum cost of operation at this load equals

$$C = c_1 + c_2 = \alpha_1 + \alpha_2 + 2.0 \times 66.7 + 2.5 \times 83.3 + 0.01 \times (66.7)^2 + 0.005 \times (83.3)^2 = \alpha_1 + \alpha_2 + 421 \quad \text{dollars/h}$$

No lower production cost is possible. The reader may easily check that if we use a different load division between the generator units, for example, $P_{G1} = 90$ and $P_{G2} = 60$, the production cost will be higher.

**Optimum dispatch formula—inequality constraints considered** In deriving the optimum dispatch formula (8-21), we tacitly assumed that each generator output remained within permissible limits; i.e., the inequalities (8-10) were observed. As the total load demand increases, it may happen, as

we move upward on the graphs in Fig. 8-4, that we reach the rated power limit on one or both of the generators. For example, assume in Example 8-1 that each generator has a rating of 100 MW. From Fig. 8-4 we find immediately that, as the load increases, generator 2 reaches this limit first. When this happens, the load on unit 1 will be about 75 MW; i.e., it is only 75 percent full-loaded.

When one or several generators thus reach their limit values, the question is: How should we operate the remaining units? In Example 8-1 this, of course, poses no problem, since there is only one unit left and it *must* generate the difference $P_D - P_{G2,\max}$. We conclude, therefore, that in the two-generator case, the inequality constraint is of trivial consequence.

### 8-2.4 OPTIMUM DISPATCH OF *n*-BUS SYSTEM

The results discussed above may be readily extended to the *n*-generator case. In this general case we no longer can obtain such a simple geometrical interpretation as was possible in Figs. 8-2 and 8-3.

For the general case we must require that, instead of two Eqs. (8-20), *n* equations

$$\frac{\partial C^*}{\partial P_{Gi}} = 0 \qquad i = 1, 2, \ldots, n \tag{8-25}$$

must be satisfied.

The constrained cost function $C^*$ is now defined by

$$C^* \triangleq c_1 + c_2 + \cdots + c_n - \lambda\left(\sum_{i=1}^{n} P_{Gi} - P_D\right) \tag{8-26}$$

By substitution of Eq. (8-26) into Eq. (8-25), we obtain the *optimum dispatch strategy*

$$\frac{\partial c_i}{\partial P_{Gi}} = (\mathrm{IC})_i = \lambda \qquad \text{for } i = 1, 2, \ldots, n \tag{8-27}$$

We note that the *n* Eq. (8-27) plus the constraint equation (8-9) are exactly sufficient to solve for the $n + 1$ unknowns $P_{G1}, P_{G2}, \ldots, P_{Gn}$ and $\lambda$.

We give a graphical interpretation of the optimum dispatch strategy in Fig. 8-5. Each of the individual (IC) curves is terminated at the various $P_{Gi,\max}$ values.

Equations (8-27) apply if no inequality constraints are violated, i.e., if we range within rated generator outputs. How shall we adjust our optimum strategy if the load increases to a point where one of the generators becomes full-loaded? In Fig. 8-5 this happens first for generator 2.

We state without proof the following intuitively sound, amended optimum policy:



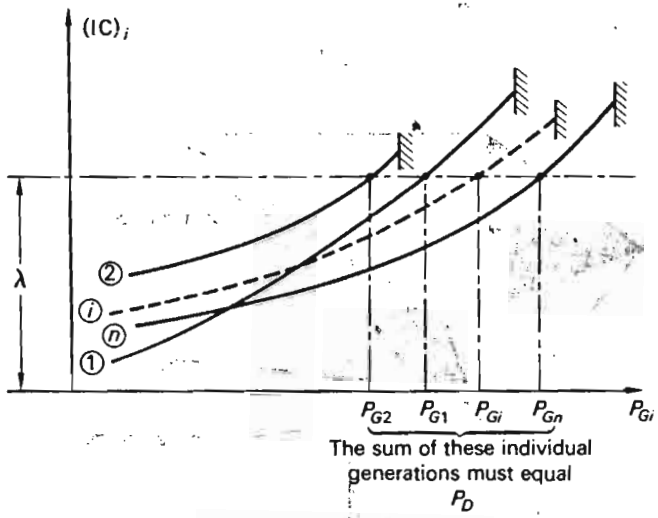


**Fig. 8-5** Graphical depiction of Eq. (8-27).

*If one or several generators reach their limit values, the optimum strategy calls for the remaining ones to operate so as to satisfy the equal-IC-rule.*

We make at this time the following observations:

1. The power demand $P_D$ has been tacitly assumed constant in our analysis. In reality, it will slowly change from hour to hour. It is therefore necessary to reset the generator outputs as the hours wear on.
2. The Lagrange multiplier $\lambda$ in this case simply equals the IC. It is usually possible, in constrained optimization problems of this type, to attach physical significance to $\lambda$.
3. In a simple "textbook" problem (Example 8-1) we have shown how, in a two-generator system and with *linear* IC curves, it is possible to obtain by *analytical* means the optimum generator settings. Clearly, in a general *n*-generator system with nonlinear IC curves (and they usually are), we must resort to iterative computational techniques. We shall discuss such techniques in the next section.
4. We presented the Lagrange multiplier method in a heuristic manner. We did not even hint at the possibility that it may fail under certain conditions. It is easy to construct cases where the method is useless. Assume, for example, that the cost surface would be "hopper-shaped," as indicated in Fig. 8-6. The reader will agree that the basic "tangency" equation (8-16) now would be meaningless. The minimum must be sought in different ways.

Our only defense for using the method is that the cost surfaces

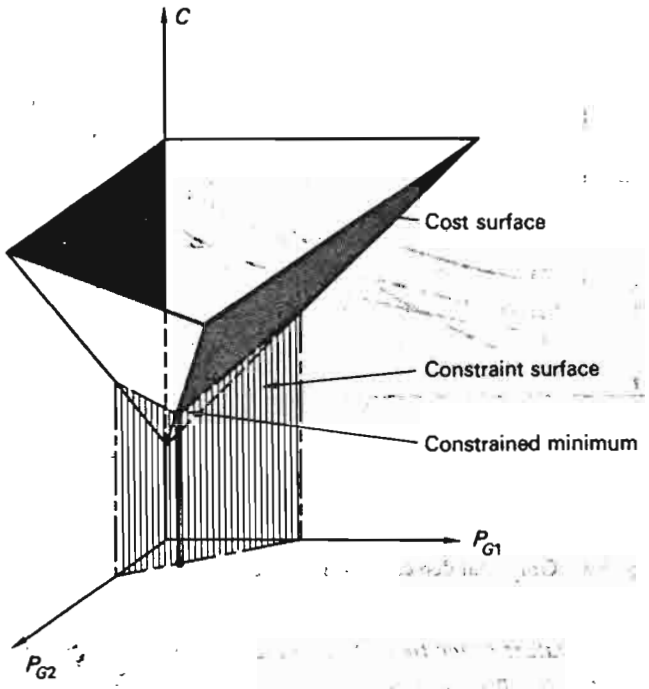


**Fig. 8-6** Example of cost surface where analytical method presented will not work.

that we use are well behaved, in a mathematical sense, and possess the partial derivatives upon which the whole technique hinges.

### 8-2.5 COMPUTATIONAL CONSIDERATIONS

In a practical situation the IC curves depicted in Fig. 8-5 are obtained empirically. Not only are they always nonlinear, but they may also show discontinuities, or "jumps." A simple analytical procedure for finding the optimum strategy is not possible in such a case.

Before we suggest a numerical computer approach, let us, with reference to Fig. 8-5, see how we may obtain a solution *graphically*. Since we know that the optimum strategy calls for equal IC values at all generators (except those which are full-loaded), the individual generator settings must be found on the horizontal line shown in the figure. We can therefore, in trial fashion, guess a reasonable $\lambda$ value and read off the corresponding values for $P_{Gi}$. They must together add up to the total demand $P_D$. If they do not, we must make a second better guess for $\lambda$, and again check whether the power balance constraint is satisfied. We converge thus on the optimum value in an iterative fashion.



Utilizing a computer, we would obtain the optimum generator allocations in the following steps:

*Step* 1 Make an initial guess $\lambda^{(0)}$ for the Lagrange multiplier.

*Step* 2 Compute the individual generations $P_{G1}^{(0)}, P_{G2}^{(0)}, \ldots, P_{Gn}^{(0)}$, corresponding to $(\text{IC})^{(0)} = \lambda^{(0)}$.

This computation can be performed in the following manner:

The $(\text{IC})_i$ curves in Fig. 8-5 are stored in the computer memory in the form of polynomials:

$$P_{Gi} = \alpha_i + \beta_i(\text{IC})_i + \gamma_i(\text{IC})_i^2 + \cdots \qquad i = 1, 2, \ldots, n \tag{8-28}$$

How many terms to include in such a curve fitting depends upon the required accuracy. We need, of course, only store the parameters $\alpha_i, \beta_i, \gamma_i, \ldots$ and simply command the computer to use Eq. (8-28) to compute the values $P_{Gi}^{(0)}$.

*Step* 3 Check if the relationship

$$\sum_{i=1}^{n} P_{Gi}^{(0)} = P_D \tag{8-29}$$

is satisfied.

*Step* 4 If not, make a second guess, $\lambda^{(1)}$, and repeat the above steps. This guess must, of course, be guided by the results in step 3. For example, if we find that the total generation exceeds $P_D$, then we know that

$$\lambda_{\text{correct}} < \lambda^{(0)}$$

How to perform such a $\lambda$ iteration is exemplified for a three-bus system in Fig. 8-7. (This figure relates to Exercise 8-2.)

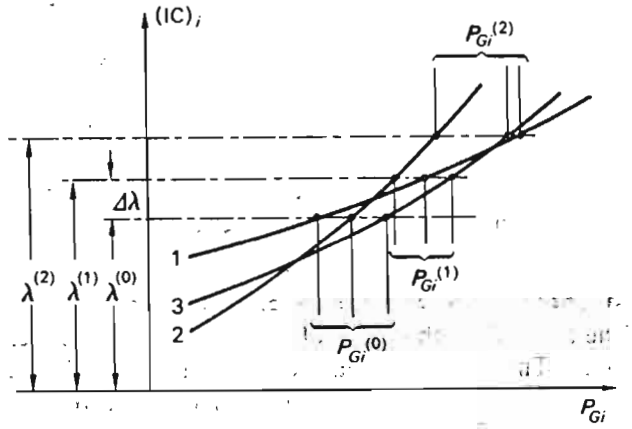


**Fig. 8-7** Graphic depiction of $\lambda$ iteration.

Upon making our first $\lambda$ guess, $\lambda^{(0)}$, we find from the IC curves the three corresponding generator settings $P_{G1}^{(0)}$, $P_{G2}^{(0)}$, and $P_{G3}^{(0)}$. Assume that the sum of these is less than $P_D$. We add now an increment, $\Delta\lambda$, to $\lambda^{(0)}$. For this $\lambda^{(1)}$ value we find the increased generations $P_{Gi}^{(1)}$.

We proceed in this manner, increasing $\lambda$ in constant steps, until eventually $\sum P_{Gi}^{(\nu)} > P_D$. We now select a smaller $\lambda$ increment and iterate in opposite $\lambda$ direction until our total generation falls below $P_D$. In a zigzag fashion we converge on the correct $\lambda$ value, using increasingly smaller $\Delta\lambda$.

## 8-3 OPTIMUM GENERATOR ALLOCATION, INCLUDING THE EFFECT OF TRANSMISSION LOSSES

A system serving an urban area characterized by high load density will as a rule have relatively small transmission losses, of the order of a few percent of the total load $P_D$. In such a case the simplified optimum dispatch strategy just developed may render sufficient accuracy.

When it is necessary to transmit energy over large distances, or when in general we serve a vast area of relatively low load density, the transmission losses may in extreme cases amount to 20 to 30 percent of the total load $P_D$, and it now becomes necessary to take them into account when developing a dispatch strategy.

It is obvious that the presence of losses means that we no longer can make use of the simple "equal incremental loss" formula. For example, consider, for simplicity, a two-bus system where the generators at both buses are identical (including identical IC curves). Assume that the load is concentrated close to generator 2, and the generator 1 must deliver its energy via a long lossy line. The "equal-IC" equation (8-27) tells us that we should let each generator carry half of the total load. However, common sense tells us that it must be more economical to let generator 2 supply most of the local demand, thus reducing the transmission losses. In this section we investigate how the best load division is found in a case like the one just mentioned.

Before we proceed with the analysis, we must warn the student that we will, of necessity, encounter some equations and formulas that look quite cumbersome and formidable. This fact should not, however, discourage us since, in the end, we will numerically process these formulas by digital computer.

### 8-3.1 DERIVATION OF OPTIMUM DISPATCH FORMULA

The analysis in this case follows closely the approach taken in the lossless case. Thus we shall again optimize the overall cost of generation as expressed by Eq. (8-6), but we shall now use the more general constraint equation (8-7).



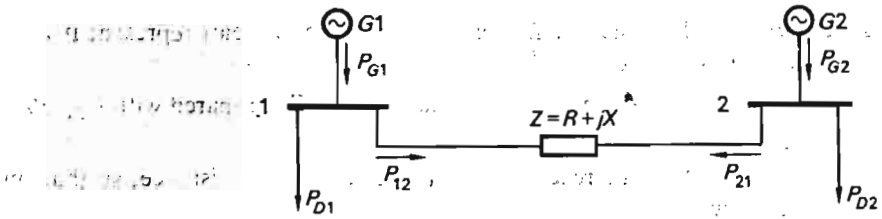


**Fig. 8-8** Example two-bus system.

In making use of the Lagrange multiplier method introduced in the preceding section, we first form the augmented cost function

$$C^* \triangleq \sum_{i=1}^{n} c_i - \lambda \left( \sum_{i=1}^{n} P_{Gi} - P_D - P_L \right) \tag{8-30}$$

For reasons stated in the previous section we shall disregard the effect on $P_L$ by the reactive power flows (or the voltages $|V_i|$). This is tantamount to setting all voltage magnitudes constant in our following analysis. Our only variables open for manipulation are thus the $P_{Gi}$'s.

By partial differentiation of Eq. (8-30), we obtain on the above assumption the following equations that must be satisfied for optimum real-power dispatch:

$$\frac{\partial C^*}{\partial P_{Gi}} = (\mathrm{IC})_i - \lambda + \lambda \frac{\partial P_L}{\partial P_{Gi}} = 0 \quad \text{for } i = 1, 2, \ldots, n \tag{8-31}$$

(Note that $P_D$ must be considered a constant when performing the operation $\partial/\partial P_{Gi}$.)

The *n optimum dispatch equations* (8-31), together with the power balance equation (8-7), suffice for finding the $n + 1$ unknowns $P_{G1}, \ldots, P_{Gn}$ plus $\lambda$. The partial derivative $\partial P_L/\partial P_{Gi}$ is referred to as the "incremental transmission loss $(\mathrm{ITL})_i$, associated with generating unit $i$." In terms of this new symbol, we can write the optimum dispatch equations (8-31) as follows:

$$(\mathrm{IC})_i = \lambda[1 - (\mathrm{ITL})_i] \qquad \text{for } i = 1, 2, \ldots, n \tag{8-32}$$

### 8-3.2 OPTIMUM DISPATCH STRATEGY FOR TWO-BUS SYSTEM

In the lossless case we started our analysis by considering the practically unimportant but tutorially significant two-bus system. We shall follow the same pattern now and start, therefore, by finding the optimum load division between the two generators in Fig. 8-8.

In order not to obscure the important aspects of the problem with unnecessary algebra, we shall work the problem under the following simplifying but reasonable assumptions:

*Assumption* 1 The line is relatively short, so that we can represent it by a series impedance $Z = R + jX$ only.

*Assumption* 2 The loss power $P_L$ is relatively small compared with $P_{G1}$, $P_{G2}$, $P_{D1}$, and $P_{D2}$.

*Assumption* 3 The line reactance dominates over the resistance, so that, in effect, we can set

$$X^2 \gg R^2$$

*Assumption* 4 We shall operate the system with a "flat voltage profile"; i.e., we shall assume

$$|V_1| = |V_2| = |V|$$

*Assumption* 5 We shall operate the line relatively far below the static stability limit. Specifically, we shall assume that the real line power is so small that the power angle

$$\delta = \angle V_1 - \angle V_2$$

attains values for which we can approximately set

$$\begin{aligned} \sin \delta &\approx \delta \\ \cos \delta &\approx 1 - \tfrac{1}{2}\delta^2 \end{aligned} \tag{8-33}$$

*Assumption* 6 The two generators are identical and have also identical IC curves. We assume that those curves are of the linear form

$$\begin{aligned} (\mathrm{IC})_1 &= \alpha + \beta P_{G1} \\ (\mathrm{IC})_2 &= \alpha + \beta P_{G2} \end{aligned} \tag{8-34}$$

Let us, specifically, work with the following numerical values:

$R = 0.02$ pu
$X = 0.10$ pu
$|V_1| = |V_2| = |V| = 1.00$ pu
$\alpha = 2.00$ dollars/h and pu MW
$\beta = 1.00$ dollars/h and (pu MW)$^2$
$P_{D1} = 1.00$ pu MW
$P_{D2} = 3.00$ pu MW

If the losses could be neglected, the two generators, because of their identical IC curves, would share the total load 4.00 pu equally. The line would therefore carry a load of 1.00 pu MW in the direction $1 \rightarrow 2$.

The presence of losses will cause generator 2 to carry more than 2 pu MW, and as a result the line load will be less than 1 pu. Since the capacity of the line is about 10 pu MW, it follows that assumption 5 is satisfied.



From the first and third of Eqs. (2-47), we have for the real line powers in both ends of the line

$$\begin{aligned} P_{12} = P_{G1} - P_{D1} &= \frac{R}{R^2 + X^2}(1 - \cos\delta) + \frac{X}{R^2 + X^2}\sin\delta \\ P_{21} = P_{G2} - P_{D2} &= \frac{R}{R^2 + X^2}(1 - \cos\delta) - \frac{X}{R^2 + X^2}\sin\delta \end{aligned} \tag{8-35}$$

The total line losses $P_L$ are obtained as the sum

$$P_L = P_{12} + P_{21} = \frac{2R}{R^2 + X^2}(1 - \cos\delta) \tag{8-36}$$

The stage is now set for finding the ITL's. From Eq. (8-36) we get

$$\begin{aligned} (\mathrm{ITL})_1 &\triangleq \frac{\partial P_L}{\partial P_{G1}} = \frac{dP_L}{d\delta}\frac{\partial\delta}{\partial P_{G1}} = \frac{2R}{R^2 + X^2}\sin\delta\frac{\partial\delta}{\partial P_{G1}} \\ (\mathrm{ITL})_2 &\triangleq \frac{\partial P_L}{\partial P_{G2}} = \frac{dP_L}{d\delta}\frac{\partial\delta}{\partial P_{G2}} = \frac{2R}{R^2 + X^2}\sin\delta\frac{\partial\delta}{\partial P_{G2}} \end{aligned} \tag{8-37}$$

The partial derivatives $\partial\delta/\partial P_{Gi}$ in these equations are readily obtained upon differentiating partially Eqs. (8-35).

$$\begin{aligned} 1 &= \frac{R}{R^2 + X^2}\sin\delta\frac{\partial\delta}{\partial P_{G1}} + \frac{X}{R^2 + X^2}\cos\delta\frac{\partial\delta}{\partial P_{G1}} \\ 1 &= \frac{R}{R^2 + X^2}\sin\delta\frac{\partial\delta}{\partial P_{G2}} - \frac{X}{R^2 + X^2}\cos\delta\frac{\partial\delta}{\partial P_{G2}} \end{aligned} \tag{8-38}$$

From these equations we solve for the partials.

$$\begin{aligned} \frac{\partial\delta}{\partial P_{G1}} &= \frac{R^2 + X^2}{R\sin\delta + X\cos\delta} \\ \frac{\partial\delta}{\partial P_{G2}} &= \frac{R^2 + X^2}{R\sin\delta - X\cos\delta} \end{aligned} \tag{8-39}$$

Upon substitution into Eqs. (8-37), we thus have

$$\begin{aligned} (\mathrm{ITL})_1 &= 2R\frac{\sin\delta}{R\sin\delta + X\cos\delta} \\ (\mathrm{ITL})_2 &= 2R\frac{\sin\delta}{R\sin\delta - X\cos\delta} \end{aligned} \tag{8-40}$$

The reader should note that these equations are *exact*. If we now make use of assumptions 3 and 5, we can readily obtain the simpler but approximate formulas

$$(\text{ITL})_1 \approx 2\frac{R}{X}\delta$$
$$(\text{ITL})_2 \approx -2\frac{R}{X}\delta \tag{8-41}$$

The student should stop and contemplate why the two ITL's are equal and of opposite sign.

By using the assumptions 2, 3, and 5, we conclude that the "line power," computed as the average of $P_{12}$ and $-P_{21}$, equals

$$P_{\text{line}} \approx P_{G1} - P_{D1} \approx P_{D2} - P_{G2} \approx \frac{\sin\delta}{X} \approx \frac{\delta}{X} \tag{8-42}$$

We therefore get the alternative expressions for the ITLs.

$$(\text{ITL})_1 \approx -(\text{ITL})_2 \approx 2R(P_{G1} - P_{D1}) = 0.04(P_{G1} - 1) \tag{8-43}$$

Our optimum dispatch equations (8-32) thus finally take on the form

$$(\text{IC})_1 = \alpha + \beta P_{G1} = \lambda[1 - 0.04(P_{G1} - 1)]$$
$$(\text{IC})_2 = \alpha + \beta P_{G2} = \lambda[1 + 0.04(P_{G1} - 1)] \tag{8-44}$$

We have two equations for three unknowns. We need one more. This is, of course, the power balance equation (8-7). Since the losses $P_L$ can be written

$$P_L = \frac{2R}{R^2 + X^2}(1 - \cos\delta) \approx \frac{R}{X^2}\delta^2 \approx RP_{\text{line}}^2 \approx 0.02(P_{G1} - 1)^2$$

the power balance equation takes on the form

$$P_{G1} + P_{G2} = 4.00 + 0.02(P_{G1} - 1)^2 \tag{8-45}$$

Equations (8-44) plus the power balance equation (8-45) are sufficient for finding the three unknowns $P_{G1}$, $P_{G2}$, and $\lambda$. There is one hitch, however. If we, for example, try to eliminate $\lambda$ and obtain two equations for the two unknowns $P_{G1}$ and $P_{G2}$, we shall find to our dismay that these equations turn out *nonlinear*. We can circumvent these difficulties by the following solution technique.

Since the total demand is 4.00 pu, and since the physics of the problem intuitively tells us that generator 1, due to the line losses, should contribute *less* than 50 percent and generator 2 consequently *more* than 50 percent, we can therefore set

$$P_{G1} = 2 - \varepsilon_1 \quad \text{pu MW}$$
$$P_{G2} = 2 + \varepsilon_2 \quad \text{pu MW}$$



where $\varepsilon_1$ and $\varepsilon_2$ should be relatively small positive quantities. By substituting these values into Eqs. (8-44) and dividing the two equations, we get

$$\frac{4 - \varepsilon_1}{4 + \varepsilon_2} = \frac{1 - 0.04(1 - \varepsilon_1)}{1 + 0.04(1 + \varepsilon_1)}$$

From Eq. (8-45) we obtain

$$\varepsilon_2 - \varepsilon_1 = 0.02(1 - \varepsilon_1)^2$$

These two last equations contain the two unknowns $\varepsilon_1$ and $\varepsilon_2$. By neglecting second-order terms (we remember that $\varepsilon_1$ and $\varepsilon_2$ should turn out to be small), we readily solve them and obtain

$$\varepsilon_1 = 0.153$$
$$\varepsilon_2 = 0.167$$

For optimum operation we should therefore share the load as follows:

$$P_{G1} = 2 - \varepsilon_1 = 1.847 \text{ pu MW}$$
$$P_{G2} = 2 + \varepsilon_2 = 2.167 \text{ pu MW}$$

Note that the losses equal

$$P_L = \varepsilon_2 - \varepsilon_1 = 0.014 \text{ pu MW}$$

This concludes the analysis. We make the following pertinent observations.

1. Even for an exceedingly simple system for which we, in addition, have made many further simplifying assumptions, we still end up with nonlinear equations. This certainly lends credence to our emphasis on computer methods.
2. In spite of relatively small losses (less than 1 percent of $P_D$), the generator load division will be considerably off the 50:50 ratio.

### 8-3.3 OPTIMUM DISPATCH STRATEGY FOR *n*-BUS SYSTEM

The simple two-bus system treated above taught us several important lessons:

1. The individual generators will operate at different incremental costs.
2. Those individual generators that are characterized with a high positive ITL value will operate at the lowest IC.
3. Whereas the IC values are always positive, the ITL values can take on both positive and negative values.

These characteristics apply equally to the general *n*-bus case. Just as the graphs in Fig. 8-5 give us a good graphical interpretation of the optimum

dispatch strategy in the lossless case, so do the graphs in Fig. 8-9 tell us graphically the story in the lossy case.

It is obvious from Fig. 8-9 that in order to obtain the individual real generator outputs $P_{Gi}$, we must know the individual incremental transmission losses $(\mathrm{ITL})_i$. To find the latter, we must first investigate how the losses $P_L$ vary with respect to the generations $P_{Gi}$. We proceed, therefore, to find a suitable formula for the real losses in a general $n$-bus case.

**Derivation of general transmission loss formula** We can obtain a compact matrix formula for the network losses by simply adding the bus powers at the $n$ buses of the network. We remember [compare Eq. (7-1)] that the bus power $S_i$ injected into bus $i$ represented the generated power minus the bus load. By adding all $n$ bus powers, we therefore obtain the total generated power minus the total load; i.e., we obtain the *total* network losses

$$P_L + jQ_L = \sum_{i=1}^{n} S_i = \sum_{i=1}^{n} V_i J_i^* \tag{8-46}$$

In accordance with Eq. (A-5), the last sum can be written as the vector product $\mathbf{V}_{\text{bus}}^T \mathbf{J}_{\text{bus}}^*$, and we thus have

$$P_L + jQ_L = \mathbf{V}_{\text{bus}}^T \mathbf{J}_{\text{bus}}^* \tag{8-47}$$

By making use of Eqs. (7-42) and (A-30), this equation can be written

$$P_L + jQ_L = \mathbf{J}_{\text{bus}}^T \mathbf{Z}_{\text{bus}}^T \mathbf{J}_{\text{bus}}^* = \mathbf{J}_{\text{bus}}^T \mathbf{Z}_{\text{bus}} \mathbf{J}_{\text{bus}}^* \tag{8-48}$$

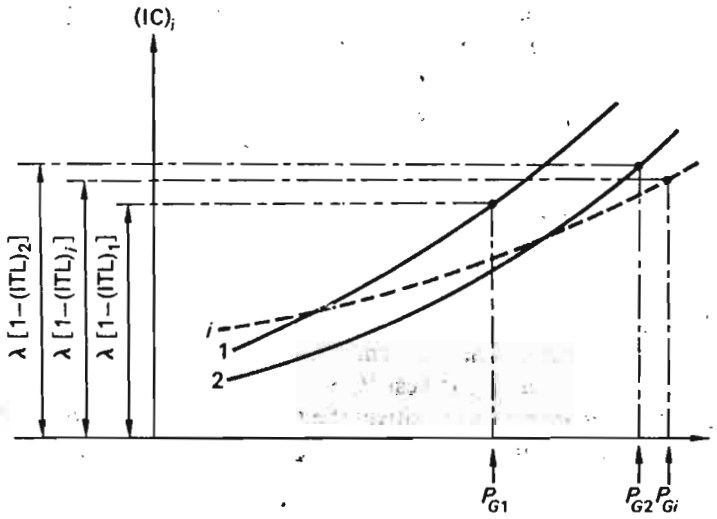


**Fig. 8-9** Graphic depiction of Eq. (8-32).



The last step follows because $\mathbf{Z}_{\text{bus}}$ is a symmetric matrix.

We can write the bus impedance matrix as a sum of a bus resistance and a bus reactance matrix.

$$\mathbf{Z}_{\text{bus}} \triangleq \mathbf{R} + j\mathbf{X} = \begin{bmatrix} r_{11} & \cdots & r_{1n} \\ \cdots & \cdots & \cdots \\ r_{n1} & \cdots & r_{nn} \end{bmatrix} + j \begin{bmatrix} x_{11} & \cdots & x_{1n} \\ \cdots & \cdots & \cdots \\ x_{n1} & \cdots & x_{nn} \end{bmatrix} \tag{8-49}$$

Similarly, we write the bus current vector as a sum of a real and a reactive component vector as follows:

$$\mathbf{J}_{\text{bus}} \triangleq \mathbf{J}_p + j\mathbf{J}_q = \begin{bmatrix} J_{p1} \\ \cdot \\ \cdot \\ \cdot \\ J_{pn} \end{bmatrix} + j \begin{bmatrix} J_{q1} \\ \cdot \\ \cdot \\ \cdot \\ J_{qn} \end{bmatrix} \tag{8-50}$$

Equation (8-48) can therefore be written

$$P_L + jQ_L = (\mathbf{J}_p + j\mathbf{J}_q)^T (\mathbf{R} + j\mathbf{X})(\mathbf{J}_p - j\mathbf{J}_q) \tag{8-51}$$

By taking the real part of this triple matrix product we get

$$P_L = \mathbf{J}_p{}^T \mathbf{R} \mathbf{J}_p + \mathbf{J}_p{}^T \mathbf{X} \mathbf{J}_q + \mathbf{J}_q{}^T \mathbf{R} \mathbf{J}_q - \mathbf{J}_q{}^T \mathbf{X} \mathbf{J}_p \tag{8-52}$$

Because $\mathbf{X}$ is a symmetric matrix, it is easy to confirm that the second and fourth terms are identical, and we thus obtain the following simpler formula for $P_L$:

$$P_L = \mathbf{J}_p{}^T \mathbf{R} \mathbf{J}_p + \mathbf{J}_q{}^T \mathbf{R} \mathbf{J}_q \tag{8-53}$$

or by using index notation,

$$P_L = \sum_{\substack{j=1 \\ k=1}}^{n} r_{jk} (J_{pj} J_{pk} + J_{qj} J_{qk}) \tag{8-54}$$

This equation expresses the total loss power in terms of bus *currents*. Since we usually know the bus *powers* and the bus *voltages*, we find it more practical to express $P_L$ in terms of these quantities.

We have for the bus powers at bus $i$

$$\begin{aligned} P_i + jQ_i = V_i J_i^* &= V_i (J_{pi} - jJ_{qi}) \\ &= |V_i| (\cos \delta_i + j \sin \delta_i)(J_{pi} - jJ_{qi}) \end{aligned} \tag{8-55}$$

where $\delta_i$ is the phase angle of $V_i$ with respect to the reference bus voltage (i.e., slack bus voltage). By separating the real and imaginary parts of Eq. (8-55), we get

$$J_{pi} = \frac{1}{|V_i|}(P_i \cos \delta_i + Q_i \sin \delta_i)$$
$$J_{qi} = \frac{1}{|V_i|}(P_i \sin \delta_i - Q_i \cos \delta_i) \tag{8-56}$$

If we substitute these expressions for the currents into the loss equation (8-54), we get $P_L$, after some algebraic operations, in the following alternative form:

$$P_L = \sum_{\substack{j=1 \\ k=1}}^{n} [\alpha_{jk}(P_jP_k + Q_jQ_k) + \beta_{jk}(Q_jP_k - P_jQ_k)] \tag{8-57}$$

where, for brevity in notation, we have introduced the new parameters $\alpha_{jk}$ and $\beta_{jk}$, defined as follows:

$$\alpha_{jk} \triangleq \frac{r_{jk}}{|V_j|\,|V_k|} \cos(\delta_j - \delta_k)$$
$$\beta_{jk} \triangleq \frac{r_{jk}}{|V_j|\,|V_k|} \sin(\delta_j - \delta_k) \tag{8-58}$$

**Derivation of general expression for** $(\text{ITL})_i$ The incremental transmission loss $(\text{ITL})_i$ is obtained by partial differentiation of $P_L$ with respect to $P_{Gi}$; that is,

$$(\text{ITL})_i \triangleq \frac{\partial P_L}{\partial P_{Gi}} = \sum_{\substack{j=1 \\ k=1}}^{n} \frac{\partial}{\partial P_i} [\alpha_{jk}(P_jP_k + Q_jQ_k) + \beta_{jk}(Q_jP_k - P_jQ_k)] \tag{8-59}$$

Note that we have replaced $\partial P_{Gi}$ by $\partial P_i$, which can be done as a consequence of the relationship

$$P_i \triangleq P_{Gi} - P_{Di}$$

Equation (8-59) tells us that we must perform the operation $\partial/\partial P_i$ on four different terms for eaeh index pair $j, k$. The results turn out different, depending upon the values of the summation indices $j$ and $k$. In Table 8-1 we summarize the results.



**Table 8-1**

| *Index* | | *Term* | | | |
|---|---|---|---|---|---|
| $j$ | $k$ | $\frac{\partial}{\partial P_i}(\alpha_{jk}P_jP_k)$ | $\frac{\partial}{\partial P_i}(\alpha_{jk}Q_jQ_k)$ | $\frac{\partial}{\partial P_i}(\beta_{jk}Q_jP_k)$ | $\frac{\partial}{\partial P_i}(-\beta_{jk}P_jQ_k)$ |
| $j=i$ | $k=i$ | $2P_i\alpha_{ii}$ | 0 | 0 | 0 |
| $j=i$ | $k\neq i$ | $P_k\left(\alpha_{ik}+P_i\frac{\partial\alpha_{ik}}{\partial P_i}\right)$ | $Q_iQ_k\frac{\partial\alpha_{ik}}{\partial P_i}$ | $Q_iP_k\frac{\partial\beta_{ik}}{\partial P_i}$ | $-Q_k\left(\beta_{ik}+P_i\frac{\partial\beta_{ik}}{\partial P_i}\right)$ |
| $j\neq i$ | $k=i$ | $P_j\left(\alpha_{ji}+P_i\frac{\partial\alpha_{ji}}{\partial P_i}\right)$ | $Q_jQ_i\frac{\partial\alpha_{ji}}{\partial P_i}$ | $Q_j\left(\beta_{ji}+P_i\frac{\partial\beta_{ji}}{\partial P_i}\right)$ | $-P_jQ_i\frac{\partial\beta_{ji}}{\partial P_i}$ |
| $j\neq i$ | $k\neq i$ | $P_jP_k\frac{\partial\alpha_{jk}}{\partial P_i}$ | $Q_jQ_k\frac{\partial\alpha_{jk}}{\partial P_i}$ | $Q_jP_k\frac{\partial\beta_{jk}}{\partial P_i}$ | $-P_jQ_k\frac{\partial\beta_{jk}}{\partial P_i}$ |

In view of the differentiation results, we can write $(\text{ITL})_i$ in the following rather cumbersome form:

$$\begin{aligned}(\text{ITL})_i &= 2\alpha_{ii}P_i \\ &+ \sum_{\substack{k=1 \\ k\neq i}}^{n}\left[\alpha_{ik}P_k - \beta_{ik}Q_k + (P_iP_k + Q_iQ_k)\frac{\partial\alpha_{ik}}{\partial P_i} + (Q_iP_k - P_iQ_k)\frac{\partial\beta_{ik}}{\partial P_i}\right] \\ &+ \sum_{\substack{j=1 \\ j\neq i}}^{n}\left[\alpha_{ji}P_j + \beta_{ji}Q_j + (P_iP_j + Q_iQ_j)\frac{\partial\alpha_{ji}}{\partial P_i} + (Q_jP_i - P_jQ_i)\frac{\partial\beta_{ji}}{\partial P_i}\right] \\ &+ \sum_{\substack{j=1 \\ j\neq i}}^{n}\sum_{\substack{k=1 \\ k\neq i}}^{n}\left[(P_jP_k + Q_jQ_k)\frac{\partial\alpha_{jk}}{\partial P_i} + (Q_jP_k - P_jQ_k)\frac{\partial\beta_{jk}}{\partial P_i}\right]\end{aligned} \tag{8-60}$$

We can reduce this expression considerably if we realize that $\alpha_{jk} = \alpha_{kj}$ and $\beta_{jk} = -\beta_{kj}$. If at the same time we introduce the shorter symbols

$$\frac{\partial\alpha_{jk}}{\partial P_i} \triangleq \alpha'_{jk}$$
$$\frac{\partial\beta_{jk}}{\partial P_i} \triangleq \beta'_{jk} \tag{8-61}$$

then Eq. (8-60) reduces to

$$\begin{aligned}(\text{ITL})_i &= 2\sum_{k=1}^{n}(P_k\alpha_{ik} - Q_k\beta_{ik}) \\ &+ \sum_{\substack{j=1 \\ k=1}}^{n}[(P_jP_k + Q_jQ_k)\alpha'_{jk} - (P_jQ_k - Q_jP_k)\beta'_{jk}]\end{aligned} \tag{8-62}$$

This equation is not directly useful for computation of the ITLs. We must first derive explicit expressions for the partial derivatives $\alpha'_{jk}$ and $\beta'_{jk}$.

This work is not too difficult, considering what already we have undertaken.

Upon differentiating the expressions for $\alpha_{jk}$ and $\beta_{jk}$ given by Eqs. (8-58), we get

$$\begin{aligned}\frac{\partial \alpha_{jk}}{\partial P_i} &\triangleq \alpha'_{jk} = -\frac{r_{jk}}{|V_j|\,|V_k|}\sin(\delta_j-\delta_k)\left(\frac{\partial \delta_j}{\partial P_i}-\frac{\partial \delta_k}{\partial P_i}\right)\\ \frac{\partial \beta_{jk}}{\partial P_i} &\triangleq \beta'_{jk} = \frac{r_{jk}}{|V_j|\,|V_k|}\cos(\delta_j-\delta_k)\left(\frac{\partial \delta_j}{\partial P_i}-\frac{\partial \delta_k}{\partial P_i}\right)\end{aligned} \tag{8-63}$$

We then borrow the expression for $P_i$ from Eq. (7-40).

$$P_i = \mathrm{Re}\left\{\sum_{v=1}^{n} y_{iv}V_vV_i^*\right\} \tag{8-64}$$

Since

$$V_i^* = |V_i|\,e^{-j\delta_i}$$

and

$$V_v = |V_v|\,e^{j\delta_v}$$

and if we write the elements of $\mathbf{Y}_{\text{bus}}$ in polar form,

$$y_{iv} = |y_{iv}|\,e^{j\psi_{iv}} \tag{8-65}$$

then Eq. (8-64) transforms into

$$P_i = \mathrm{Re}\left\{\sum_{v=1}^{n} |y_{iv}V_vV_i|\,e^{j(\delta_v-\delta_i+\psi_{iv})}\right\} \tag{8-66}$$

By separating the real part of Eq. (8-66), we get

$$P_i = \sum_{v=1}^{n} |y_{iv}V_vV_i|\cos(\delta_v-\delta_i+\psi_{iv}) \tag{8-67}$$

From Eq. (8-67) we have, upon differentiation,

$$\frac{\partial P_i}{\partial \delta_j} = -|y_{ij}V_jV_i|\sin(\delta_j-\delta_i+\psi_{ij}) \tag{8-68}$$

or

$$\frac{\partial \delta_j}{\partial P_i} = -\frac{1}{|y_{ij}V_iV_j|\sin(\delta_j-\delta_i+\psi_{ij})}$$

We substitute this partial derivative into Eqs. (8-63) and obtain the



following final formulas for computation of $\alpha'_{jk}$ and $\beta'_{jk}$:

$$\begin{aligned}\alpha'_{jk} &= \frac{r_{jk}\sin(\delta_j-\delta_k)}{|V_i|\,|V_j|\,|V_k|}\left[\frac{1}{|y_{ij}|\,|V_j|\sin(\delta_j-\delta_i+\psi_{ij})}\right.\\ &\qquad\left.-\frac{1}{|y_{ik}|\,|V_k|\sin(\delta_k-\delta_i+\psi_{ik})}\right]\\ \beta'_{jk} &= \frac{r_{jk}\cos(\delta_j-\delta_k)}{|V_i|\,|V_j|\,|V_k|}\left[\frac{1}{|y_{ik}|\,|V_k|\sin(\delta_k-\delta_i+\psi_{ik})}\right.\\ &\qquad\left.-\frac{1}{|y_{ij}|\,|V_j|\sin(\delta_j-\delta_i+\psi_{ij})}\right]\end{aligned} \tag{8-69}$$

Equations (8-69), combined with Eq. (8-62), permit us to compute the ITLs from a knowledge of bus voltages and bus powers. Due to the presence of the double sum in Eq. (8-62), the computations demand considerable computer time. For typical system parameters the double sum contributes only an insignificant part of ITL, and for most situations we should therefore be able to use the following approximate but timesaving formula for $(\text{ITL})_i$:

$$(\text{ITL})_i \approx 2\sum_{k=1}^{n}(P_k\alpha_{ik}-Q_k\beta_{ik}) \tag{8-70}$$

### 8-3.4 COMPUTATIONAL CONSIDERATIONS

The $n$ Eqs. (8-32), together with the power balance equation (8-7), tell us how to set the $n$ individual generator settings in order to achieve overall cost minimization. It is *in principle* as simple to solve the equations in this case as it was in the lossless case. We recall (see page 287 and Fig. 8-7) that the procedure involved an initial guess of $\lambda$ and a subsequent iterative computation converging on the optimum settings. We must expect in this case a somewhat more complicated computation procedure since both the "optimum dispatch equations" and the "power balance equation" contain loss terms *which themselves are functions of all the individual generator outputs.* We remember that the lossless dispatch equations (8-27) were *uncoupled:* i.e., the $i$th equation depended only upon $P_{Gi}$. Now each equation is a function of *all* $P_{Gi}$'s; that is, the equations are *coupled.*

Figure 8-10 shows a flow chart for a proposed digital computation of the equations.

The basic ideas underlying the proposed computational scheme are as follows:

1. An initial guess is made in regard to the individual generator outputs $P_{Gi}$. *We have no assurance that these are optimal in any sense.*
2. Based upon this initial guess, and assuming a knowledge of all load demands $S_{Di}$ and voltage specifications $|V_i|$ for the type 2 buses, we

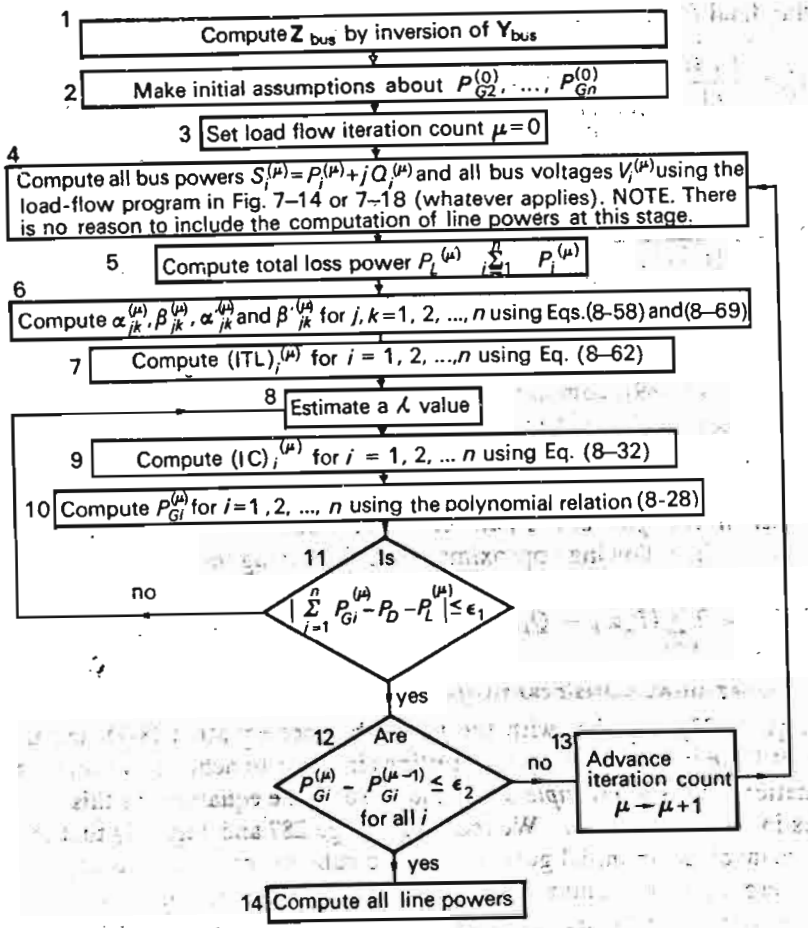


**Fig. 8-10** Flow diagram for computation of optimum dispatch strategy with consideration of losses.

perform a load flow study of the type discussed in Chap. 7. This study renders *all* bus and generator powers, including that of the slack bus plus *all* bus voltages.

3. Having this knowledge available, we can compute all the $(ITL)_i$. This permits us to solve by means of a $\lambda$ iteration the optimum dispatch equations, and thus obtain a *first* set of optimum generator values $P_{Gi,opt}$.
4. If we readjust the generator settings in accordance with these computed optimum settings, then we change all the bus powers, and thus the whole basis for our original load flow study. We must therefore make a new load flow study based upon these *upgraded* $P_{Gi}$ values and then repeat the optimization process in 3.



Clearly, we have here an iterative computational process that involves a full load flow analysis per iteration cycle. We will proceed now to comment on some of the individual blocks in the flow chart. Note that the superscript $\mu$ refers to the load flow iteration count.

**Comment on flow diagram in Fig. 8-10** (The numbering of the following comments coincides with the block numbering in Fig. 8-10.)

1. In the load flow analysis as we presented it in Chap. 7, we obtain the system model in the form of the matrix $\mathbf{Y}_{bus}$. We must invert this matrix since we need elements of $\mathbf{Z}_{bus}$ in the computations of block 6.

4. The load flow study need not be complete in the sense that we compute line flows. These will be computed in block 14 only after our load flow iterations have converged.

8–11. This inner "$\lambda$ loop" checks that the constraint equation (8-7) is satisfied. This is accomplished by an iterative search of $\lambda$ as described on page 287. We can exit from this loop only when Eq. (8-7) is satisfied within a tolerance of $\varepsilon_1$.

12. This logic block checks how much the generator settings $P_{Gi}^{(\mu)}$, computed in block 10, have changed since previous load flow iteration.

The load flow iteration will continue until the changes

$$P_{Gi}^{(\mu)} - P_{Gi}^{(\mu-1)}$$

are less than a given tolerance $\varepsilon_2$.

**Example 8-2** We shall digitally compute the optimum generator settings for the three-bus system depicted in Fig. 8-11. All three transmission lines are assumed identical and can be electrically described by the $\pi$ representation in Fig. 8-12. (The reader should note that these line data correspond approximately with the 300-km 220-kV line treated in Examples 6-7 and 6-8.)

Table 8-2 contains the load data and the bus voltage specifications.

**Table 8-2**

| *Bus* | *Real load demand, MW* | *Reactive load demand, Mvar* | *Real generation, MW* | *Reactive generation, Mvar* | *Voltage magnitude specification, kV* |
|---|---|---|---|---|---|
| 1 | 150 | 50 | Optimum | Unspecified | 220 |
| 2 | 50 | 25 | Optimum | Unspecified | 220 |
| 3 | 150 | 60 | Zero | Unspecified | 220 |

The cost curves for the two generators are determined by the following IC data:

$$(IC)_1 = 2.00 + 0.03P_{G1} \quad \text{dollars/MWh}$$
$$(IC)_2 = 3.00 + 0.02P_{G2} \quad \text{dollars/MWh} \qquad (8\text{-}71)$$

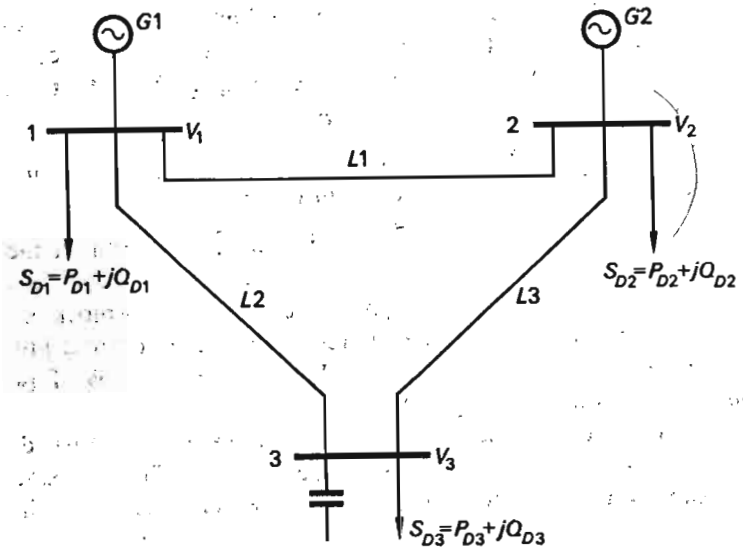


**Fig. 8-11** Example three-bus system.

(In these formulas $P_{G1}$ and $P_{G2}$ must be measured in megawatts.)

A computer program was written based upon the computational flow diagram of Fig. 8-10. We make the following comments about some of the details in this program:

1. The total demand $P_D = 350$ MW will be kept constant throughout the analysis.
2. Since we need to make an initial guess as to the generator loading, it would probably be best to assume that the two generators share the load equally. This, then, would mean that we would guess $P_{G2}^{(0)}$ at about 175 MW ($P_{G1}$ need not be guessed, since this is the slack generator).

   However, we shall willfully make a poor initial guess by assuming that generator 1 carries all the load; i.e., we set

   $$P_{G2}^{(0)} = 0$$

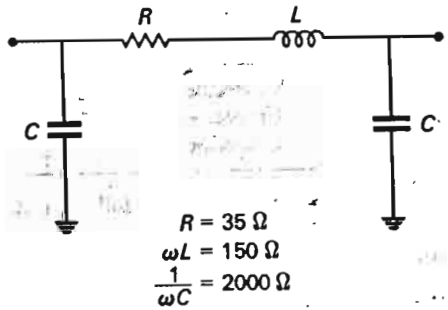


**Fig. 8-12** Line representation for system in Fig. 8-11.



With this large initial "error," we will have an excellent opportunity to study the convergence features of our program.

3. In block 8 (Fig. 8-10) we must estimate a $\lambda$ value. We know that in the lossless case the $\lambda$ value equals the (IC) value at which we will operate. In the lossy case [Eq. (8-32)] this statement is not exactly true. However, having thus identified the physical meaning of $\lambda$ as the approximate incremental cost of operation expressed in dollars per megawatthour, we also know the range within which its numerical value must of necessity lie. A reasonable first guess might be to take the lowest possible (IC) value from the (IC) curves given by Eqs. (8-71). In the given case we therefore try $\lambda = \$2.0$/MWh.
4. Finding $P_{Gi}$ from a knowledge of $(IC)_i$ as required in block 10 is simple when the relationship is linear, as in our example. We have from Eqs. (8-71)

$$P_{G1} = \frac{(IC)_1 - 2.00}{0.03} \quad \text{MW}$$
$$P_{G2} = \frac{(IC)_2 - 3.00}{0.02} \quad \text{MW} \tag{8-72}$$

Figures 8-13 and 8-14 depict the result of the computer study. Figure 8-13 shows how the generator outputs converge toward the optimum settings. The load

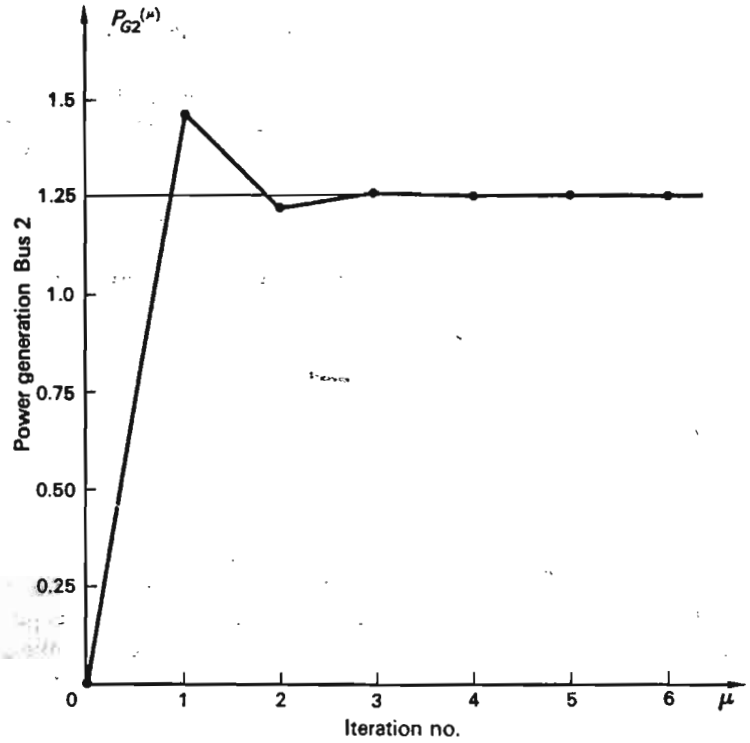


**Fig. 8-13** Convergence speed for computer program of Fig. 8-10. Generator power in per unit of base = 150 MW.

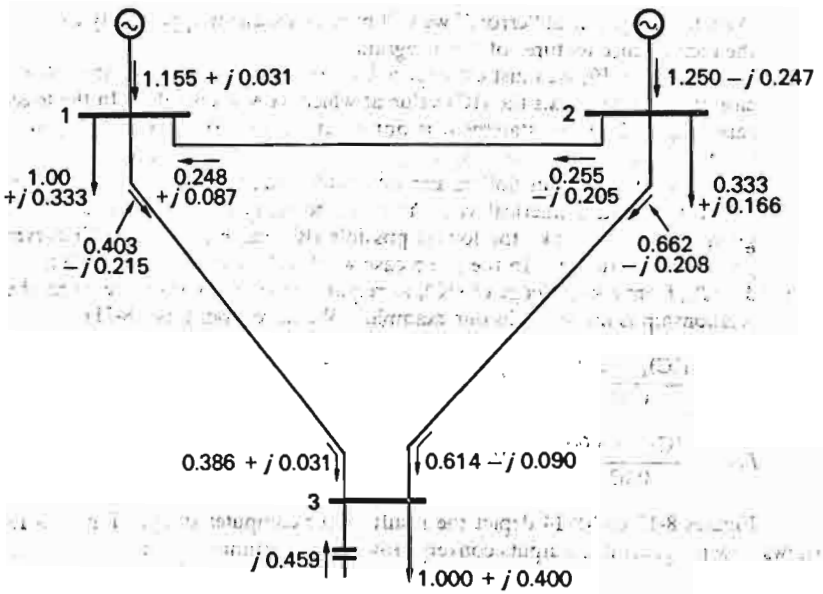


**Fig. 8-14** Optimum load flow picture for Example 8-2. Base power = 150 MW.

flow iterations are terminated when the change in any of the two generator outputs is less than $\varepsilon_2 = 1$ MW. In this case six iterations were needed to bring us within this tolerance. After the load flow iterations thus have converged, we compute the corresponding line powers (block 14). The final load flow picture is shown in Fig. 8-14.

## 8-4 THE GENERAL OPTIMUM OPERATIONAL PROBLEM

In this final section we develop methods that enable us to obtain, within practical computational limits, the optimum operating strategies under very general conditions. Since the methods are characterized by a fair degree of mathematical complexity, we present the theory in parallel with a practical example.

### 8-4.1 A DEMONSTRATION EXAMPLE

Consider the three-bus system depicted in Fig. 8-15. It is similar to our earlier three-bus example systems, except that we have explicitly pointed out that the two step-up transformers at bus 1 are of the TCUL type, having the controllable transformation ratios $a_1$ and $a_2$, respectively.† We assume that the three high-voltage lines traverse densely populated areas, and thus are designed as underground cables, which have very high shunt capacitance. Herein lies our problem. As the load drops off during the night hours,

† Only voltage *magnitude* control is assumed.



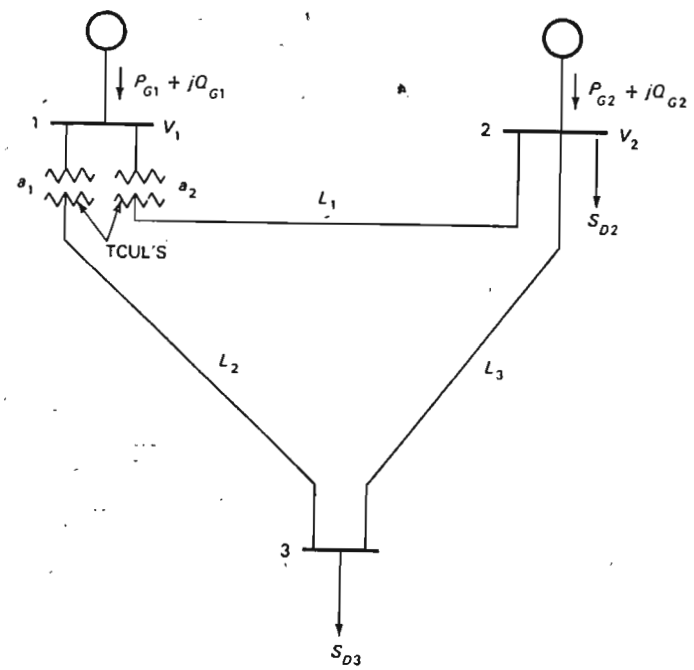


**Fig. 8-15** Three-bus example system. Transformation ratios of the two TCUL's can be varied throughout the range $a_{\min} < a < a_{\max}$.

the reactive line generation, which during the day hours is consumed by the inductive loads, must now be routed elsewhere. The generators are the obvious "sinks" for this surplus reactive power. By running them underexcited, they will consume reactive power, as we noted in Chap. 4. This, however, is really not a desirable way to operate the generators, since it requires that their internal emfs be of low magnitude, thus reducing their stability margins.

An alternative means of eliminating some of the surplus reactive power is to cause a high circulating reactive current to flow in the loop formed by the three lines. Reactive power will now be consumed in the line and transformer reactances, thus permitting us to run the generators at a lesser degree of underexcitation. The circulating current can be produced by proper manipulation of the TCUL taps. We wish to do so in an "optimum" way.

### 8-4.2 MATHEMATICAL PROBLEM FORMULATION

We now formulate the above problem as a "general programming problem." Due to space limitation, the presentation must of necessity be sketchy. For a more detailed coverage the reader is referred to a paper by Elgerd and Sullivan;[19] a paper by Dommel and Tinney[15] is also recommended.

**Cost criterion** The first step in our analysis is to define a suitable cost criterion. We propose

$$C \triangleq Q_{G1}^2 + Q_{G2}^2 + k(Q_{G1} - Q_{G2})^2 \tag{8-73}$$

where $k$ is a positive weight factor. Note that $C$, thus defined, will always be positive.

The two first terms penalize the individual reactive absorption in each generator. The third term penalizes a reactive unbalance between the two generators. By minimizing the chosen $C$, we minimize the total reactive power absorbed by the generators and simultaneously force the generators to absorb these powers proportionately.

**Equality constraints** In the previous sections of this chapter we developed optimum operating strategies in the case when the cost criterion $C$ is an explicit function of the *real* power variables of the system.

Now our cost function depends explicitly upon *reactive* power variables. We could therefore employ an analysis technique similar to the one we used before. Thus, we would turn our attention to the reactive-power-balance Eq. (7-8), which would now be our equality constraint. We would then divorce all those system variables from our problem which affect the real power balance and only consider those that have a strong influence on the reactive power balance. They are primarily the reactive generator outputs $Q_{G1}$ and $Q_{G2}$, and also the controllable transformer ratios $a_1$ and $a_2$.

We shall take a more generally useful approach, one that would be applicable in a case when the cost function were dependent upon both real and reactive system variables. The SLFE represent a most general set of equality constraints and we shall therefore choose, for our constraints of type (8-2), Eqs. (7-14), which we restate:

$$f(\mathbf{x},\mathbf{u},\mathbf{p}) = 0 \tag{8-74}$$

**Nonequality constraints** Let us now look closer at some of the inequality constraints we must impose upon our $\mathbf{x}$ and $\mathbf{u}$ variables. The constraints can be classified as either "hard" or "soft." For an example of the former, consider the tap settings $a_1$ and $a_2$. When the mechanical limits are reached on the tap changer, we can go no further. The tap settings can thus be chosen only within the *hard* limits

$$a_{i,\min} < a_i < a_{i,\max} \tag{8-75}$$

The limits set on a bus voltage represent a *soft* nonequality constant. If, for example, we prescribed that a voltage must be kept within 0.95 to 1.05 pu, we would, in reality, accept a value of 0.94, perhaps even 0.91.



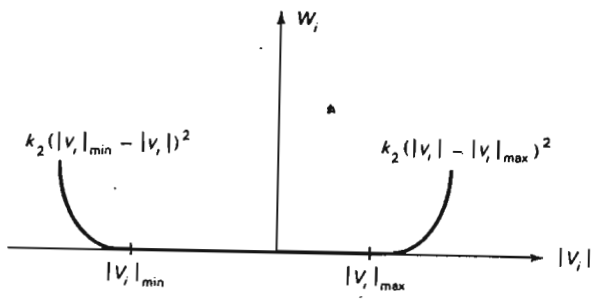


**Fig. 8-16** Soft penalty function add to overall cost if voltage magnitudes fall outside permissible range. The positive constant $k_2$ controls degree of penalty.

In our analysis we handle these two types of constraints in the following manner:

If, during the course of our computational iterations, one of the $a$ variables reaches a hard limit, we let it remain there for the next iteration.

For the soft variables we assign a penalty function $W$, defined in Fig. 8-16. The function is zero if the voltages lie within prescribed limits. Outside these limits the function increases monotonously. The penalty function thus defined is added to the $C$ function and penalizes "softly" any voltage excursions outside the permitted range.

### 8-4.3 NECESSARY CONDITIONS FOR OPTIMUM $C$

Upon adding the "soft" penalty function $W$ to our chosen $C$ function, we define in analogy with Eq. (8-19) the following augmented cost function:

$$C^* \triangleq C + W - \lambda_1 f_1 - \lambda_2 f_2 \cdots - \tag{8-76}$$

We must introduce one Lagrange $\lambda$ multiplier for each one of the SLFE. If we now define the $\boldsymbol{\lambda}$ vector

$$\boldsymbol{\lambda} \triangleq \begin{bmatrix} \lambda_1 \\ \lambda_2 \\ \cdot \\ \cdot \\ \cdot \end{bmatrix} \tag{8-77}$$

then we can write Eq. (8-76) more compactly.

$$C^* = C + W - \boldsymbol{\lambda}^T \mathbf{f} \tag{8-78}$$

(The superscript $T$ stands for transposition.)

We now must seek the necessary conditions for an optimum for $C^*$. Since $C^*$ is a function of the variables $\mathbf{x}$ and $\mathbf{u}$, we form first its total differential, i.e.,

$$dC^* = \frac{\partial C^*}{\partial x_1} dx_1 + \frac{\partial C^*}{\partial x_2} dx_2 + \cdots + \frac{\partial C^*}{\partial u_1} du_1 + \frac{\partial C^*}{\partial u_2} du_2 + \cdots \tag{8-79}$$

or in compact vector form,

$$dC^* = \mathbf{dx}^T \frac{\partial C^*}{\partial \mathbf{x}} + \mathbf{du}^T \frac{\partial C^*}{\partial \mathbf{u}} \tag{8-80}$$

Here we have defined the new vectors

$$\mathbf{dx} \triangleq \begin{bmatrix} dx_1 \\ dx_2 \\ \cdot \\ \cdot \\ \cdot \end{bmatrix} \qquad \mathbf{du} \triangleq \begin{bmatrix} du_1 \\ du_2 \\ \cdot \\ \cdot \\ \cdot \end{bmatrix} \tag{8-81}$$

and also

$$\frac{\partial C^*}{\partial \mathbf{x}} \triangleq \begin{bmatrix} \dfrac{\partial C^*}{\partial x_1} \\ \dfrac{\partial C^*}{\partial x_2} \\ \cdot \\ \cdot \\ \cdot \end{bmatrix} \qquad \frac{\partial C^*}{\partial \mathbf{u}} \triangleq \begin{bmatrix} \dfrac{\partial C^*}{\partial u_1} \\ \dfrac{\partial C^*}{\partial u_2} \\ \cdot \\ \cdot \\ \cdot \end{bmatrix} \tag{8-82}$$

If the system were operating at its optimum state, characterized by $\mathbf{u} = \mathbf{u}_{\text{opt}}$ and $\mathbf{x} = \mathbf{x}_{\text{opt}}$, then an *arbitrary* differential change in any of the $\mathbf{u}$ or $\mathbf{x}$ variables would not change $C^*$. By thus requiring that $dC^*$ be zero, following an excursion of *any one* of these variables, we conclude from Eq. (8-80) that the necessary conditions for optimum are

$$\frac{\partial C^*}{\partial \mathbf{x}} = \mathbf{0} \qquad \frac{\partial C^*}{\partial \mathbf{u}} = \mathbf{0} \tag{8-83}$$



If Eq. (8-78) is substituted into Eqs. (8-83), we get upon differentiation

$$\frac{\partial C^*}{\partial \mathbf{x}} = \frac{\partial C}{\partial \mathbf{x}} + \frac{\partial W}{\partial \mathbf{x}} - \left(\frac{\partial \mathbf{f}}{\partial \mathbf{x}}\right)^T \boldsymbol{\lambda} = \mathbf{0} \tag{8-84}$$

$$\frac{\partial C^*}{\partial \mathbf{u}} = \frac{\partial C}{\partial \mathbf{u}} + \frac{\partial W}{\partial \mathbf{u}} - \left(\frac{\partial \mathbf{f}}{\partial \mathbf{u}}\right)^T \boldsymbol{\lambda} = \mathbf{0} \tag{8-85}$$

Here we have introduced the jacobian matrices

$$\frac{\partial \mathbf{f}}{\partial \mathbf{x}} \triangleq \begin{bmatrix} \dfrac{\partial f_1}{\partial x_1} & \dfrac{\partial f_1}{\partial x_2} & \cdots \\ \dfrac{\partial f_2}{\partial x_1} & \dfrac{\partial f_2}{\partial x_2} & \cdots \\ \cdots\cdots\cdots\cdots \end{bmatrix}$$

$$\frac{\partial \mathbf{f}}{\partial \mathbf{u}} \triangleq \begin{bmatrix} \dfrac{\partial f_1}{\partial u_1} & \dfrac{\partial f_1}{\partial u_2} & \cdots \\ \dfrac{\partial f_2}{\partial u_1} & \dfrac{\partial f_2}{\partial u_2} & \cdots \\ \cdots\cdots\cdots\cdots \end{bmatrix} \tag{8-86}$$

(It should be noted that in our specific example $W$ is a function of *state* variables only. Therefore $\partial W/\partial \mathbf{u} = \mathbf{0}$. Also, for similar reasons, $\partial C/\partial \mathbf{x} = \mathbf{0}$.)

### 8-4.4 COMPUTATIONAL PROCEDURE

The stage is now set for developing an iterative computational algorithm that will converge on an optimum solution $\mathbf{x} = \mathbf{x}_{\text{opt}}$ and $\mathbf{u} = \mathbf{u}_{\text{opt}}$. This optimum solution, if substituted back into Eqs. (8-84) and (8-85), will satisfy both these vector equations within a certain tolerance. This will thus be our convergence criterion.

We perform the computations in the following steps:

*Step* 1 Make an initial assumption $\mathbf{u}^{(0)}$ for the control force vector.

*Step* 2 Substitute $\mathbf{u}^{(0)}$ into the SLFE (8-74) and solve these iteratively by methods outlined in Chap. 7. Upon convergence we are left with a solution $\mathbf{x}^{(0)}$.

*Step* 3 Evaluate the partial derivatives in Eqs. (8-84) and (8-85) for $\mathbf{x} = \mathbf{x}^{(0)}$ and $\mathbf{u} = \mathbf{u}^{(0)}$.

*Step* 4 Vector equation (8-84), upon completion of step 3, is a linear system of equations in the unknowns $\boldsymbol{\lambda}^{(0)}$. Solve this system for $\boldsymbol{\lambda}^{(0)}$. The most straightforward way to do this is first to invert the matrix

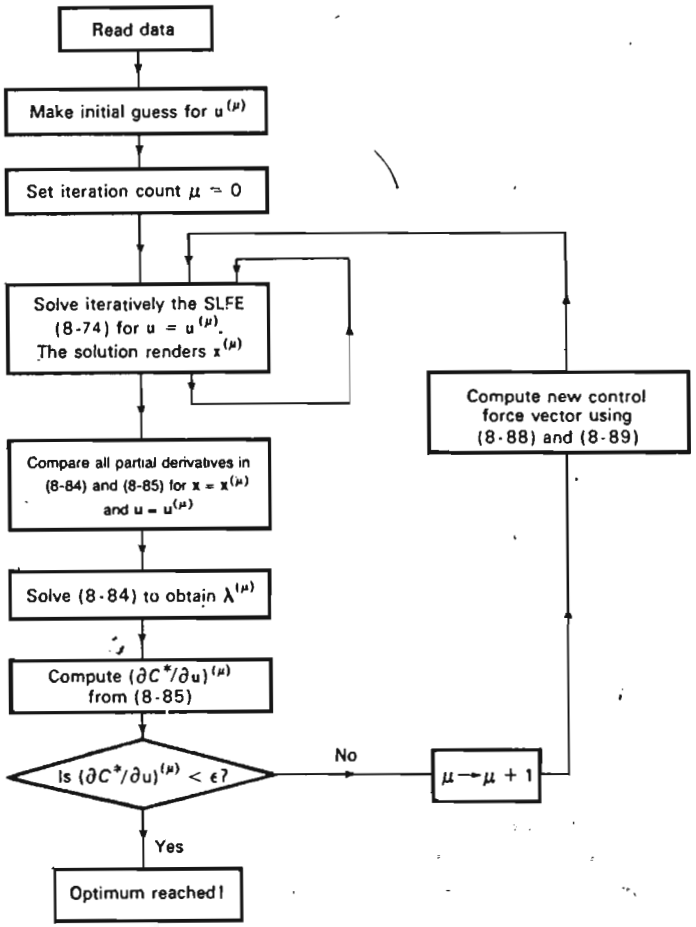


**Fig. 8-17** Algorithm for obtaining the optimum operational strategy by means of the method of steepest descent.

$(\partial \mathbf{f}/\partial \mathbf{x})^T$. The $\boldsymbol{\lambda}$ solution is then obtained from the formula

$$\boldsymbol{\lambda}^{(0)} = \left[\left(\frac{\partial \mathbf{f}}{\partial \mathbf{x}^{(0)}}\right)^T\right]^{-1}\left(\frac{\partial C}{\partial \mathbf{x}^{(0)}} + \frac{\partial W}{\partial \mathbf{x}^{(0)}}\right) \tag{8-87}$$

*Step 5* Substitute the value for $\boldsymbol{\lambda}^{(0)}$ into Eq. (8-85) and obtain a first value for the partial derivatives $(\partial C^*/\partial \mathbf{u})^{(0)}$. If this value equals **0** within given tolerances, then our first guess for **u** will be the optimum control force, since both Eqs. (8-83) are satisfied.



Most probably this will not occur, and we must thus try a better value $\mathbf{u}^{(1)}$ for **u**, and repeat steps 2 to 5.

The question that arises now is how to select a better $\mathbf{u}^{(1)}$. We shall add an increment $\Delta\mathbf{u}^{(1)}$ to our present value in accordance with

$$\mathbf{u}^{(1)} = \mathbf{u}^{(0)} + \Delta\mathbf{u}^{(1)} \tag{8-88}$$

*The added increment must, however, be so chosen that the resulting decrease $\Delta C^*$ in the objective function $C^*$ will be as large as possible.* The second term in Eq. (8-80) gives us the clue as to how this can be achieved. In Sec. A-1.3 is shown how the scalar product of two vectors is being optimized if the two vectors are *collinear*. By applying this rule to the two vectors $\Delta\mathbf{u}$ and $\partial C^*/\partial\mathbf{u}$, we thus conclude:

*The vector increment $\Delta\mathbf{u}^{(1)}$ must be chosen collinear with the vector $\partial C^*/\partial\mathbf{u}$ and of opposite sign*, i.e.,

$$\Delta\mathbf{u}^{(1)} = -\alpha\left(\frac{\partial C^*}{\partial \mathbf{u}}\right)^{(0)} \tag{8-89}$$

The vector $\partial C^*/\partial\mathbf{u}$ is referred to as the *gradient*, and by moving in its negative direction, we move in the "direction of steepest descent." The positive scalar factor $\alpha$ in Eq. (8-89) determines the length of the step.

We summarize the above computational method in the flow diagram of Fig. 8-17.

Figure 8-18 shows how the minimum value for the cost function is obtained in 10 iterations in our three-bus example system.

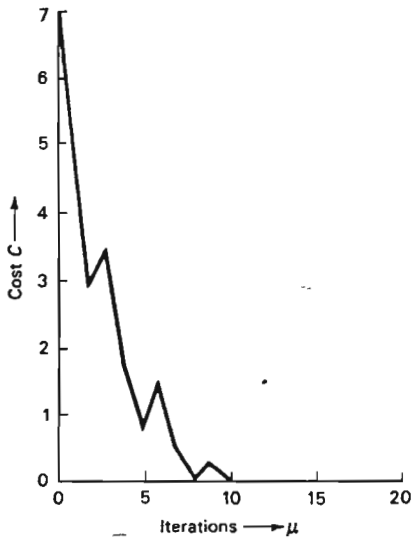


**Fig. 8-18** Reduction of cost function $C$ to its minimum value takes place in 10 iteration cycles.

## 8-5 SUMMARY

A given load demand can be met by an infinite number of configurations of generator outputs and bus voltage profiles. It is necessary to decide upon a "best" configuration, or in different terminology, an "optimum operating strategy." In this chapter we have developed methods for finding this strategy.

First, we have presented the classical methods of optimum dispatch, i.e., the combination of generator power settings that result in minimum economic operating cost. The strategy was simple: all generators must be operated at equal incremental cost. If the transmission losses had to be considered, this strategy had to be slightly adjusted.

We have finally presented the method of steepest descent to find the optimum operating strategy under more general conditions and for cost criteria that are not necessarily of the economical variety. It is to be expected that such advanced criteria will be used in increasing frequency to handle the great variety of operating conditions that characterize EESE.

We have *not*, in this chapter, discussed the equally important problem of designing a control system that automatically adjusts the generator power and bus voltage settings to their optimal values. Since such a *dispatch controller* is but part of the overall *load frequency control system*, we find it necessary to postpone a discussion of it until, in the next chapter, we have covered the problem areas of system dynamics and pool operations, both of which are fundamental to an understanding of these matters.

## EXERCISES

**8-1.** Consider Example 8-1. How many dollars per hour would we lose if we were operating about 20 percent off the optimum settings, that is, $P_{G1} = 50$ MW and $P_{G2} = 100$ MW?

**8-2.** Consider the three IC curves in Fig. 8-7. They have been curve-fitted with polynomials in accordance with

$$P_{G1} = -103 + 53(\text{IC})_1 - 2.10(\text{IC})_1^2$$
$$P_{G2} = -130 + 56(\text{IC})_2 - 2.16(\text{IC})_2^2$$
$$P_{G3} = -92 + 47(\text{IC})_3 - 1.95(\text{IC})_3^2$$

If IC is inserted in dollars per megawatthour, the formulas render the powers in megawatts. (The formulas are valid only for positive $P_{Gi}$'s.)

The total load demand at a certain hour of the day equals 362 MW. Neglect real losses and develop a computer program that will render a solution for the optimum generator settings within an accuracy of $\pm 0.1$ MW.

**8-3.** The network data for the five-bus system of Fig. 7-22 were given in Exercise 7-8. Develop a computer program from the flow diagram in Fig. 8-10 and find the optimum power dispatch if the following power and voltage specifications are assumed. Base values are 100 MVA, 138 kV.



**Table 8-3**

| Bus | Bus type | Load demand, pu $P_{Di}$ | Load demand, pu $Q_{Di}$ | Bus voltage magnitude, pu | Generation |
|---|---|---|---|---|---|
| 1 | 3 | 2.31 | 0.86 | 1.05 | Yes |
| 2 | 1 | 2.01 | 1.28 | Unspecified | No |
| 3 | 2 | 1.61 | 0.42 | 1.02 | Yes |
| 4 | 1 | 1.71 | 1.28 | Unspecified | No |
| 5 | 2 | 2.11 | 0.76 | 1.02 | Yes |

Generators are installed at buses 1, 3, and 5. We assume for simplicity that all three generator stations are characterized by equal cost curves:

$$P_{Gi} = -3.00 + 1.50(\text{IC})_i - 0.050(\text{IC})_i^2 \qquad (\text{IC in dollars/pu MWh})$$

**8-4.** Recompute the two-bus example in the text without making *any* approximations; i.e., use the *exact* equation (8-40) and the *exact* equations (8-35), (8-36), and (8-7).

*Hint:* Note that $(\text{ITL})_1$, $(\text{ITL})_2$, $P_L$, $P_{G1}$, and $P_{G2}$ are functions of the power angle $\delta$ *only*. Therefore guess an initial $\delta$ value and then develop a digital computer program that in an iterative fashion converges on the correct $\delta$ value.

**8-5.** (This is a tough one.) In Example 8-2 in the text we found the optimum operating strategy under the assumption that the bus voltages were a priori fixed. Assume now that we can tolerate all three bus voltages to vary within the range

$$200 \text{ kV} < |V_i| < 250 \text{ kV}$$

We have now, in effect, "released" the *reactive* generator powers $Q_{Gi}$, and added them to the list of true manipulative control variables.

(*a*) Find the optimum generator settings, real *and* reactive powers, for minimum operating cost. Formulate the problem so that you can make use of the "gradient method."

(*b*) How does your new cost minimum compare with the one we obtained when the voltages were held fixed.

(*c*) Make your problem still harder by adding additional constraints. For example, specify that the power angle on a particular line must be kept at a predetermined value.

## REFERENCES

### Books

1. Steinberg, M. J., and T. H. Smith: "Economy Loading of Power Plants and Electric Systems," John Wiley & Sons, Inc., New York, 1943.
2. Kirchmayer, L. K.: "Economic Operation of Power Systems," John Wiley & Sons, Inc., New York, 1958.
3. Stevenson, W. D.: "Elements of Power System Analysis," McGraw-Hill Book Company, New York, 1962.
4. Zaborszky, L., and J. W. Rittenhouse: "Electric Power Transmission," The Ronald Press Company, New York, 1954.
5. Hadley: "Nonlinear and Dynamic Programming," Addison-Wesley Publishing Company, Inc., Reading Mass., 1964.

(References 1 and 2 give a classical treatment of the optimum dispatch problem. Abbreviated discussions are presented in Refs. 3 and 4. Reference 5 gives a very good presentation of the general programming problem.)

**Technical papers and reports**

6. Kuhn, H. W., and A. W. Tucker: Nonlinear Programming, *Proc. Second Berkeley Symp. Math. Stat. Prob.*, University of California Press, Berkeley, Calif., 1951.
7. Lowery, P. G.: Generating Unit Commitment by Dynamic Programming, *Proc. Power Ind. Computer Appl. Conf.*, 1965, pp. 523–530.
8. Hano, I., et al.: An Application of the Maximum Principle to the Most Economical Operation of Power Systems, *Proc. Power Ind. Computer Appl. Conf.*, 1965, pp. 482–496.
9. Kerr, R. H., et al.: Unit Commitment, *Proc. Power Ind. Computer Appl. Conf.*, 1965, pp. 531–538.
10. Roth, J. E., et al.: Economic Dispatch of Penna–New Jersey–Maryland Interconnection System Generation on a Multi-area Basis, *Proc. Ind. Computer Appl. Conf.*, 1967, pp. 117–126.
11. Dauphin, G., et al.: Methods of Optimizing the Production of Generating Stations of a Power Network, *Proc. Power Ind. Computer Appl. Conf.*, 1967, pp. 133–140.
12. Dopazo, J. F., et al.: An Optimization Technique for Real and Reactive Power Allocation, *Proc. Power Ind. Computer Appl. Conf.*, 1967, pp. 141–154.
13. Hill, E. F., and W. D. Stevenson: An Improved Method for Determining Incremental Loss Factors, *Proc. Power Ind. Computer Appl. Conf.*, 1967, pp. 155–166.
14. Aitchison, A., et al.: Optimum Loading of Hydro Plant Units, *Proc. Power Ind. Computer Appl. Conf.*, 1967, pp. 177–188.
15. Dommel, H. W., and W. F. Tinney: Optimal Power Flow Solutions, *IEEE Trans.*, vol. PAS-87, no. 10, pp. 1866–1876, October, 1968.
16. Peschon, J., et al.: Optimum Control of Reactive Power Flow, *IEEE Trans.*, vol. PAS-87, no. 1, pp. 40–48, January, 1968.
17. Balet, W. J., and R. L. Webb: Reactive Power and Its Control in a Large Metropolitan Supply System, *IEEE Trans.*, vol. PAS-87, no. 1, pp. 49–52, January, 1968.
18. Kennedy, T., and A. G. Hoffman: On-line Digital Computer Application Techniques for Complex Electric System Dispatch, *IEEE Trans.*, vol. PAS-87, no. 1, pp. 67–73, January, 1968.
19. Elgerd, O. I., and R. L. Sullivan: Minimally Proportioned Reactive Generation Control via Automatic Tap-changing Transformers, *Proc. Power Ind. Computer Appl. Conf.*, Denver, Colo., 1969.
20. Peterson, H.: An Example of the Use of Dynamic Programming for Economic Operation of a Hydro-thermal System, rept. 6.4, *Proc. Power Systems Computation Conf.*, Stockholm, 1966.
21. Dahlin, E. B., and D. W. C. Shen: Optimal Solution to the Hydrosteam Dispatch Problem for Certain Practical Systems, *IEEE Trans.*, vol. PAS-85, no. 5, pp. 437–458, May, 1966.
22. Sasson, A. M.: Nonlinear Programming Solutions for Load-flow, Minimum-loss, and Economic Dispatching Problems, *IEEE Trans.*, vol. PAS-88, no. 4, pp. 399–409, April, 1969.
23. El-Abiad, A. H., and F. J. Jaimes: A Method for Optimum Scheduling of Power and Voltage Magnitude, *IEEE Trans.*, vol. PAS-88, no. 4, pp. 413–422, April, 1969.

# 9

# The Energy System in Steady State—The Control Problem

The two preceding chapters were devoted to the problems associated with the selection of a nominal operating state for our system. In this chapter we concern ourselves with the problem of *keeping* the system in this state by means of *continuous closed-loop control.*

As the demand vector deviates from its nominal value $\mathbf{p}^0$ with the unpredictable small amount $\Delta\mathbf{p}$, the state of the system will change with the amount $\Delta\mathbf{x}$. The control system must detect these changes, and initiate in "real time" a set of "counter" control force changes $\Delta\mathbf{u}$, which will eliminate as quickly and effectively as possible the state deviation $\Delta\mathbf{x}$.

## 9-1 CONTROL SYSTEMS STRUCTURE

Figure 9-1 depicts the general structure of the control system that we shall investigate. The state variables of the system are continuously monitored via *sensors*, the outputs of which we shall refer to as the *controlled variables* $c_1, c_2, \ldots$. Some state variables, such as the bus voltage magnitudes $|V_i|$, can be measured directly, and are thus easily monitored. Others, such as

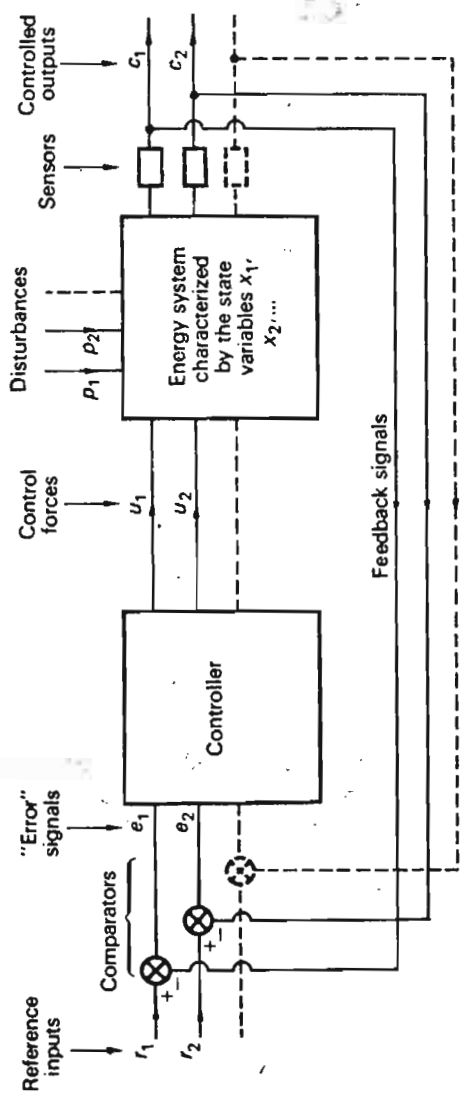


Fig. 9-1 Multiple-input–multiple-output control system.





the bus voltage phase angles $\delta_i$, are more difficult to measure, and can in effect be obtained only *indirectly* by measuring, for example, the real line powers, which, as we know, are functions of these phase angles.

The controlled variables are compared with *reference inputs* $r_1, r_2, \ldots,$ in *comparators* which provide *error signals* $e_1, e_2, \ldots$. When, as in our case, the reference inputs are constant, we refer to the system as a *regulator*.

The error signals, usually of very low power level, constitute the inputs to the *controller* which processes these signals, i.e., amplifies, mixes, and transforms them, and finally, in transducers, changes them into the control forces $u_1, u_2, \ldots,$ which directly affect the state of the plant. Since we have

$$e_i \triangleq r_i - c_i = r_i^0 - (c_i^0 + \Delta c_i) = -\Delta c_i \tag{9-1}$$

we recognize that the operation of the control system is based on signals which represent deviations from the nominal settings. We are therefore concerned below exclusively with *incremental analysis*.

A system of the type just discussed is referred to as a multiple-input–multiple-output (MIMO) control system. The reader who has taken a course in control system theory has probably acquired a healthy respect for the complexity associated with the design of such a system. The most difficult problem, as a rule, is the design of the controller, which constitutes both the brain and the brute-force portion of the system. The difficulty of design is closely related to the *degree of coupling* between the various inputs, the stringency of the control requirements and the complexity of the system model.

At first glance it would seem that the MIMO regulator for a power system would represent a particularly complex design problem, inasmuch as we are requiring control of voltage levels at, perhaps, hundreds of buses, in addition to keeping the frequency constant within close tolerances. We furthermore may wish to keep the individual generator outputs at levels corresponding to optimum economy (Chap. 8) and also keep the power flows in certain lines (*tie lines*) at specified levels.

It must also be understood that since we are concerned with the *dynamic* performance of the control system, our models will consist of *differential*† equations rather than algebraic ones, as was the case in our earlier static analysis. Furthermore, whereas the *static* state of a bus could be represented by only two state variables, it takes about ten state variables (see next section) to describe adequately the *dynamic* state of a bus (including the control system itself). For a 100-bus system our incremental dynamic model would thus consist of about 1000 coupled differential equations.

The synthesis of a closed-loop control system is based to a considerable degree on intuitive reasoning. Intuition grows from an understanding of the

† Because the perturbations are *small*, the differential equations will be *linear*, just as our *static* algebraic perturbation equations in Chap. 7 were linear.

physical processes involved, and it is therefore essential, indeed imperative, that we penetrate the seemingly overwhelming complexity of our system and lay bare its elementary functions. Three important characteristics permit us to simplify to a considerable extent the mathematical model of our system:

1. The degree of decoupling between the so-called "load frequency" and "voltage" control channels.
2. The degree of decoupling between the voltage control channels for the individual buses.
3. The coherency of the phase angle dynamics that exists among groups of system buses.

### 9-1.1 DYNAMIC INCREMENTAL STATE VARIABLES

In static operation the angular nominal frequency

$$\omega^0 = 2\pi f^0$$

is constant throughout the system, and the individual bus voltages have the form

$$v_i = \sqrt{2}\,|V_i^0| \sin(\omega^0 t + \delta_i^0) \tag{9-2}$$

In Chap. 7 we identified $|V_i|$ and $\delta_i$ as our static state variables. When the system is subject to small dynamic perturbations, these state variables will undergo small changes; i.e., we can write

$$\begin{aligned} \delta_i &= \delta_i^0 + \Delta\delta_i \\ |V_i| &= |V_i^0| + \Delta\,|V_i| \end{aligned} \tag{9-3}$$

and the bus voltages will therefore be of the form

$$v_i = \sqrt{2}\,(|V_i^0| + \Delta\,|V_i|) \sin(\omega^0 t + \delta_i^0 + \Delta\delta_i) \tag{9-4}$$

The angular velocity $\omega_i$ of the $i$th bus equals

$$\omega_i = \frac{d}{dt}(\omega^0 t + \delta_i^0 + \Delta\delta_i) = \omega^0 + \frac{d}{dt}\Delta\delta_i \tag{9-5}$$

and is no longer constant, since it evidently is characterized by a nonzero perturbation

$$\Delta\omega_i \triangleq \frac{d}{dt}\Delta\delta_i \quad \text{r/s}$$

or, if expressed in cycles per second,

$$\Delta f_i = \frac{1}{2\pi}\frac{d}{dt}\Delta\delta_i \quad \text{Hz} \tag{9-6}$$



Due to the high inertia of the synchronous generators, it is generally true that

$$|\Delta f_i| \ll f^0 = 60 \text{ Hz} \tag{9-7}$$

The stored kinetic energy of the synchronous machines connected to a bus varies as the square of the speed or frequency. As a bus at two different instants of time may be characterized by identical phase angle perturbations $\Delta\delta_i$, but *different* speeds, it is obvious that the variable $\Delta\delta_i$ alone cannot carry all state information. *We must add the velocity $\Delta f_i$ to the list of dynamic state variables for a total of three: $|\Delta V_i|$, $\Delta\delta_i$, and $\Delta f_i$.*

In addition to these "primary" state variables, we have "secondary" state variables associated with the control equipment for those control systems that we are about to describe. Even the most coarse modeling of these devices involves the introduction of six to seven additional state variables per bus. This means that in dynamic analysis of power systems we involve state variables of the order of ten per bus in toto.

### 9-1.2 COHERENCY

Generally, the $n$ bus frequency perturbations $\Delta f_i$ are all of different magnitudes. If, however, two or several buses are characterized by equal $\Delta f_i$, then they swing in unison, or *coherently*.

Consider an assembly of $n$ masses (compare Fig. 9-17) interconnected via springs of different stiffness. If two masses are connected via a relatively stiff spring, these two masses will perform almost identical oscillations. An analogous situation usually exists in a power system. Groups of buses (usually those belonging to one power system) are interconnected via relatively "stiff" (term to be defined later) lines. The tielines which interconnect such groups into power pools are relatively "weak." In a first approximation, we may therefore consider the buses belonging to one power system to swing coherently. Such a lumping of buses into "control areas" simplifies considerably our system analysis.

### 9-1.3 *Pf* VERSUS *QV* CONTROL

From a number of load flow studies and from our static sensitivity investigations, we made the following important observations in Chap. 7 in regard to the static sensitivity properties of a typical network:

1. *Static* changes $\Delta P_i$ in the *real* bus power affect, essentially, only the bus voltage *phase angles* (and thus the *real* line flows) but leave the bus voltage magnitudes (and thus the reactive line flows) almost unchanged.
2. *Static* changes $\Delta Q_i$ in the *reactive* bus power affect, essentially, only the bus voltage *magnitudes* (and thus the *reactive* line flows) but leave the bus voltage phase angles (and thus the real line flows) almost unchanged.

3. *Static* changes in the reactive bus power at a particular bus affects most strongly the magnitude of the bus voltage of the same bus, but in less degree the magnitudes of the bus voltages at remote buses.

We emphasize that these observations apply only to *static* bus power changes.

It is also important to stress that these properties apply only when the line loads, as is normally the case, are well below the static stability limits of the lines, and the deviations from the nominal settings are small, or "first-order," in a mathematical sense. For major disturbances, where the deviations are large, the above conditions do not apply (Chap. 12).

Based upon the above sensitivity properties, we propose to divide the overall control job into the following two separate control channels. Compare with Fig. 9-2.

**Megawatt frequency, or *Pf*, control channel** The objective of this control channel is to exert control of frequency and *simultaneously* of the real power exchange via outgoing lines. We sense the frequency "error" $\Delta f_i$ and the increments in real tie line powers, which will indirectly provide

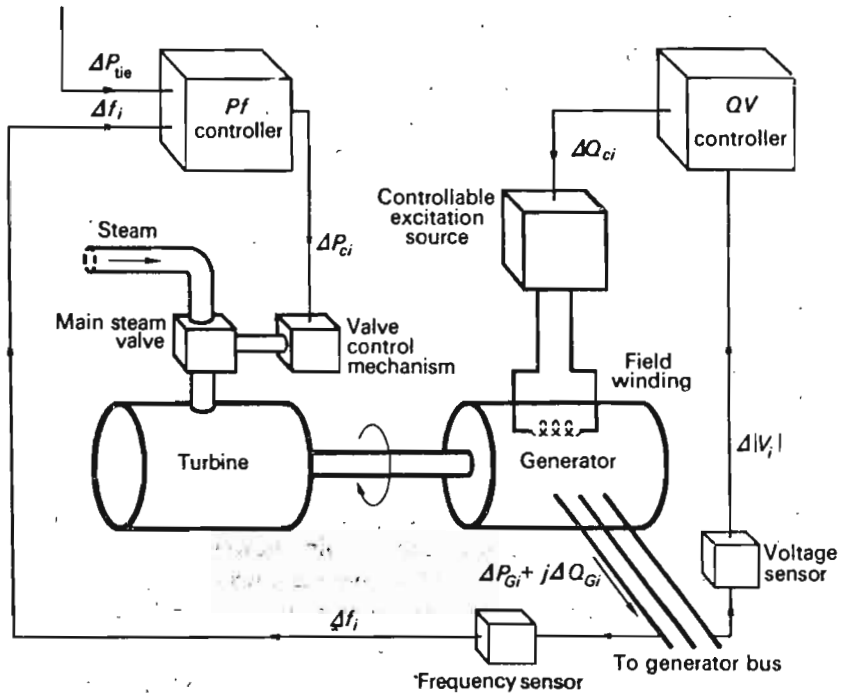


**Fig. 9-2** Generator controllers.



information about the incremental state error $\Delta\delta_i$. These sensor signals are amplified, mixed, and transformed into a real-power command signal $\Delta P_{ci}$, which is sent to the prime mover to call for an increment in the torque. As a result, we get a change, $\Delta P_{Gi}$, in the real generation, which will then change the state increments we originally sensed.

**Megavar voltage, or *QV*, control channel** The objective of this channel is to exert control of the voltage state $|V_i|$. The voltage error $\Delta|V_i|$ is sensed, and this signal is transformed into a reactive-power command signal $\Delta Q_{ci}$, which is fed to the excitation source. The result is a change in the rotor field current, and thus in the generator emf, which finally adds up to an incremental change in the reactive generation $\Delta Q_{Gi}$.

### 9-1.4 DYNAMIC INTERACTION BETWEEN *Pf* AND *QV* LOOPS

In a *static* sense, and for small deviations, there is little interaction between the *Pf* and *QV* control loops.

During *dynamic* perturbations we encounter considerable coupling between the two control channels, for two different reasons:

1. As the voltage magnitude fluctuates at a bus, the real load of that bus will likewise change as a result of the voltage load characteristics ($\partial P_D / \partial |V|$), discussed in Chap. 3.
2. As the voltage magnitude fluctuates at a bus, the synchronizing coefficients (or "electric spring constants") of all outgoing transmission lines will change.

A dynamic perturbation in the *QV* loop thus will affect the real-power balance in the system.† *In general, the QV loop is much faster than the Pf loop, due to the mechanical inertia constants (see next section) in the latter.* If it can be assumed that the transients in the *QV* loop are essentially over before the *Pf* loop reacts, then the coupling between loops can be neglected.

This is a reasonable assumption, and we shall adopt it in the following analysis, due to the resulting simplicity. In Sec. 9-4.6 we show that the coupling between the two control loops can be advantageously used to introduce damping into the *Pf* loop.

## 9-2 THE MEGAWATT FREQUENCY CONTROL PROBLEM

We shall first consider the problem of controlling the real power output of electric generators within a prescribed area in response to changes in system

† On the contrary, a dynamic change in the *Pf* loop will have little influence on the *QV* loops. Why?

frequency and tie line loading or the relation of these to each other, so as to maintain the scheduled system frequency and the established interchange with other areas within predetermined limits. The term *automatic load frequency control* (ALFC) is also often used to identify this problem area.

### 9-2.1 FUNDAMENTAL CHARACTERISTICS OF THE POWER CONTROL MECHANISM OF AN INDIVIDUAL GENERATOR

The real power in a power system is being controlled by controlling the driving torques of the individual turbines (steam or hydro) of the system. It is important for the further discussions of *Pf* control to understand the workings of the individual power regulators. Figure 9-3 shows in a highly schematical fashion the operating features of such a *speed-governing system.*†

† The terminology used agrees with the standards accepted by the industry. All systems are, of course, not identical. We chose a representative example for demonstration.

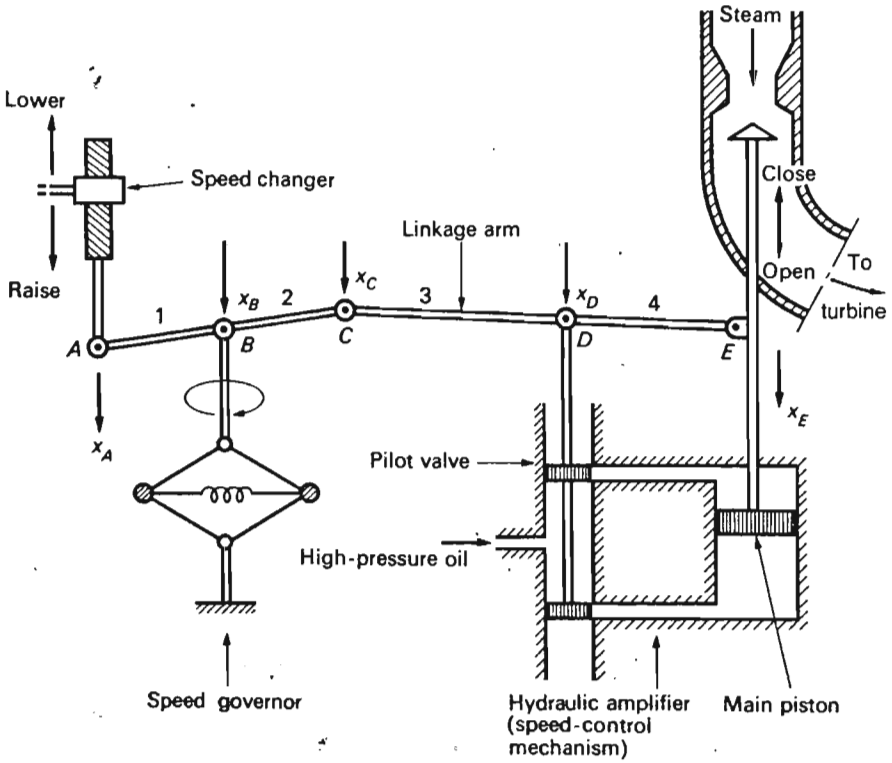


**Fig. 9-3** Typical real-power control mechanism. Linkage arms 1 and 2 are stiffly coupled, and so are arms 3 and 4. All five linkage points are free.



By controlling the position, measured by the coordinate $x_E$, of the *governor-controlled valves* (or *gates*, in the case of a hydroturbine), we can exert control over the flow of high-pressure steam (or water) through the turbine, and thus the turbine torque, which, via the electromechanical mechanism discussed in Chap. 4, determines the generator real power output $P_G$.

Very large mechanical forces are needed to position the main valve (or gate) against the high steam (or hydro) pressure, and these forces are obtained via several stages of *hydraulic amplifiers*. In our simplified version we show only one stage. The input to this amplifier is the position $x_D$ of the pilot valve. The output is the position $x_E$ of the main piston. Because the high-pressure hydraulic fluid exerts only a slight differential force on the pilot valve, the force amplification is very great.

The position of the pilot valve can be affected via the linkage system in three ways:

1. *Directly*, by moving the linkage point $A$ by "raise" or "lower" commands of the *speed changer*.
2. *Indirectly*, via *feedback*, due to position changes of the main piston.
3. *Indirectly*, via *feedback*, due to position changes of linkage point $B$ resulting from speed changes.

It should prove a useful exercise for the reader to find, *qualitatively*, the workings of the mechanism. For example, give a "raise" command to the speed changer and prove that this indeed results in an increase in generator output. Prove also by simple reasoning that a speed drop will give the same effect.

Presently we shall give a *quantitative* description of the mechanism.

**Mathematical model of speed-governing system** The model that we develop applies to *small* deviations around a nominal steady state. We consequently assume the following chain of events.

1. The system is initially in a constant steady state, characterized by a *constant* nominal speed or frequency $f^0$, a *constant* prime mover valve setting $x_E{}^0$, and a *constant* generator output power $P_G{}^0$.
2. By means of the speed changer, we command a power increase $\Delta P_c$. As a result of this command, the linkage point $A$ moves downward a *small* distance $\Delta x_A$ proportional to $\Delta P_c$.
3. The movement of linkage point $A$ causes *small* position changes $\Delta x_C$ and $\Delta x_D$ of the linkage points $C$ and $D$.† As oil flows into the hydraulic

† At this time no speed changes have taken place, which means that point $B$ is fixed. Points $C$ and $D$ therefore move upward.

motor, the steam valve will move the *small* distance $\Delta x_E$, resulting in increased turbine torque and, consequently, a power increase $\Delta P_G$.

4. The increased power output causes a momentary surplus, or *accelerating*, power in the system. If the system is very large ("infinite"), the increased generator power will not noticeably affect the speed or frequency. However, if the system is of finite size, the speed and frequency will experience a slight increase $\Delta f$ that will cause the linkage point $B$ to move downward a *small* distance $\Delta x_B$ *proportional* to $\Delta f$. The speed governor being fast, we neglect any time delay in it. Consequently, we set $\Delta x_B$ proportional to $\Delta f$.

All incremental movements $\Delta x_A, \ldots, \Delta x_E$ are assumed positive in directions indicated.

Since all linkage movements are small, we have the linear relationships

$$\begin{aligned} \Delta x_C &= k_1 \Delta f - k_2 \Delta P_c \\ \Delta x_D &= k_3 \Delta x_C + k_4 \Delta x_E \end{aligned} \tag{9-8}$$

The positive constants $k_1$ and $k_2$ depend upon the lengths of the linkage arms 1 and 2 and upon the proportional constants of the speed changer and the speed governor. The positive constants $k_3$ and $k_4$ depend upon the lengths of the linkage arms 3 and 4.

If we assume that the oil flow into the hydraulic motor is proportional to position $\Delta x_D$ of the pilot valve, we obtain the following relationship for the position of the main piston:

$$\Delta x_E = k_5 \int (-\Delta x_D)\, dt \tag{9-9}$$

The positive constant $k_5$ depends upon orifice and cylinder geometries and fluid pressure.

By taking the Laplace transform of Eqs. (9-8) and (9-9), and eliminating the variables $\Delta x_C$ and $\Delta x_D$, we obtain the following equation:

$$\Delta X_E(s) = \frac{k_2 k_3 \Delta P_c(s) - k_1 k_3 \Delta F(s)}{k_4 + s/k_5} \tag{9-10}$$

We have introduced the Laplace transforms

$$\begin{aligned} \Delta F(s) &\triangleq \mathcal{L}[\Delta f] \\ \Delta X_E(s) &\triangleq \mathcal{L}[\Delta x_E] \\ \Delta P_c(s) &\triangleq \mathcal{L}[\Delta P_c] \end{aligned}$$

We rewrite Eq. (9-10) as follows:

$$\Delta X_E(s) = \frac{K_G}{1 + sT_G}\left[\Delta P_c(s) - \frac{1}{R}\Delta F(s)\right] \triangleq G_G(s)\left[\Delta P_c(s) - \frac{1}{R}\Delta F(s)\right] \tag{9-11}$$



where

$$R \triangleq \frac{k_2}{k_1} = \text{speed "regulation" due to governor action}$$

$$K_G \triangleq \frac{k_2 k_3}{k_4} = \text{static gain of speed-governing mechanism}$$

$$T_G \triangleq \frac{1}{k_4 k_5} = \text{time constant of speed-governing mechanism}$$

$$G_G(s) \triangleq \frac{K_G}{1 + sT_G} = \text{transfer function of speed-governing mechanism}$$

$T_G$ is a measure of the reaction speed of the mechanism. Normal values are less than 100 ms. (As to numerical values for $K_G$ and $R$, see Example 9-1 below.)

**Turbine models** We are not primarily interested in turbine valve position per se, but rather the resulting generator power increase $\Delta P_G$. The change in valve position, $\Delta x_E$, causes an incremental increase in turbine power, $\Delta P_T$, which, via the electromechanical interactions within the generator, will result in an increased generator power $\Delta P_G$.

This overall mechanism is relatively complicated, particularly if the generator voltage simultaneously undergoes wild swings due to major network disturbances. These matters are discussed in detail in Chap. 12.

If, as in the present case, we can assume that the voltage level is constant and the torque variations are of small size, then an incremental analysis of the type we performed for the speed governor, above, will give a relatively simple dynamic relationship between $\Delta x_E$ and $\Delta P_G$. Such an analysis reveals considerable differences, not only between steam turbines and hydroturbines, but also between various types (reheat and nonreheat) of steam turbines. In the crudest model representation we can characterize a *nonreheat* turbine generator with a single gain factor $K_T$ and a single time constant $T_T$, and thus write

$$G_T(s) \triangleq \frac{\Delta P_G(s)}{\Delta X_E(s)} = \frac{K_T}{1 + sT_T} \tag{9-12}$$

Typically, the time constant $T_T$ lies in the range 0.2 to 2 s. (As to the gain constant $K_T$, see Example 9-1 below.)

In standard block-diagram symbols we can represent Eqs. (9-11) and (9-12), as shown in Fig. 9-4*a*, which diagram therefore represents the linearized model of a nonreheat turbine controller, including the speed governor mechanism.

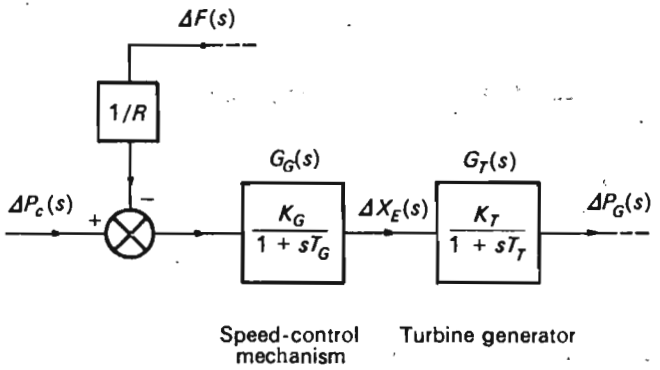


(*a*)

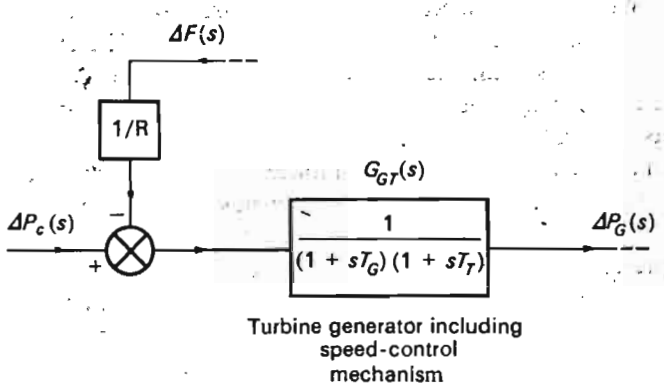


(*b*)

**Fig. 9-4** Transfer function representation of power control mechanism of generator. Nonreheat turbine assumed.

A reheat turbine can quite adequately be represented by the transfer block

$$G_T(s) \triangleq \frac{\Delta P_G(s)}{\Delta X_E(s)} = \frac{K_T(1 + sK_rT_r)}{(1 + sT_T)(1 + sT_r)} \tag{9-13}$$

The time constant $T_r$ has a value in the range of 10 s, and approximates the time delay for charging the reheat section of the boiler. $K_r$ is a reheat coefficient, equal to the proportion of torque developed in the high-pressure section of the turbine, which is approximately equal to 1 minus the fraction



of steam reheated. Thus, when there is no reheat, $K_r = 0$, and the transfer function reduces to a single time constant [as expressed by Eq. (9-12)].

The transfer functions (9-12) and (9-13) give good representation within, perhaps, the first 20 s following the incremental disturbance. They do *not* account for the slower boiler dynamics.

**Example 9-1** We shall use the block diagram in Fig. 9-4*a* to analyze the performance of a governor-controlled turbine generator unit. We shall consider two cases:

*Case A* The generator is synchronized to a network of very large size, so large in fact, that the speed or frequency will be essentially independent of any changes in the power output of this individual generator.

Since we thus have

$$\Delta F(s) = 0$$

we obtain from Fig. 9-4*a*

$$\Delta P_G(s) = \frac{K_G}{1 + sT_G}\frac{K_T}{1 + sT_T}\Delta P_c(s)$$

Let us assume that we make a step change of magnitude $\Delta P_c$ of the speed changer. We wish to find the resulting static, or steady-state, change in the generator output.

We have for a step input

$$\Delta P_c(s) = \frac{\Delta P_c}{s}$$

Thus

$$\Delta P_G(s) = \frac{K_G}{1 + sT_G}\frac{K_T}{1 + sT_T}\frac{\Delta P_c}{s}$$

The static, or "final," value $\Delta P_{G,\text{stat}}$ is now readily obtained by the *final-value theorem*

$$\Delta P_{G,\text{stat}} = \lim_{s \to 0} [s\,\Delta P_G(s)] = K_GK_T\,\Delta P_c$$

*For a generator operated at a (forced) constant speed, we thus have a direct proportionality between the power command and resulting static power output.*

It is, of course, very practical to arrange so that the proportionality constant is unity, and we then have

$$K_GK_T \triangleq 1$$

In view of this simple gain relationship, and due to the fact that we always are interested in the *combined* response of governor plus turbine generator, we have lumped the transfer functions $G_G$ and $G_T$ into one, $G_{GT}$, as shown in Fig. 9-4*b*.

*Case B* In case *A* we considered the extreme case where the speed is held fixed by a network of "infinite size."

Presently we shall consider the other extreme case, where we have no external network at all. The generator is now delivering power to a single load, which we may, for simplicity, assume to be of simple resistive type. We shall study the response of the generator unit, assuming that the load suddenly increases by a

small amount $\Delta P_D$. The speed changer position will not be changed; i.e., we assume $\Delta P_c = 0$.

Since there is no immediate change in the turbine power, upon the onset of the load increase the generator finds itself momentarily in a power-deficiency situation, delivering more power than it receives. It can do this only by "borrowing" energy from somewhere, and the lending source is the stored kinetic energy of the rotating masses. Since we thus start to consume this energy at the rate $\Delta P_D$ MW, *the speed will drop*. As time passes and the speed decreases, the speed control mechanism of Fig. 9-3 goes into effect. The linkage point $B$ moves upward, and so does the pilot valve, resulting in an opening of the steam valve, and thus an *increase* in generation.

Since more power is thus being generated, less energy will need to be "borrowed" from the kinetic storage, and the speed will drop at a decreasing rate. Eventually, we will level off at a new *static* steady state characterized by lower speed and a new generation that has increased with the *exact* amount to offset the original load increase.

Let us use our mathematical model to find this new *static* equilibrium.

Since $\Delta P_c = 0$, we obtain from the diagram in Fig. 9-4*b*

$$\Delta P_G(s) = \frac{\mathrm{I}}{(1 + sT_G)(1 + sT_T)} \left( -\frac{\Delta F(s)}{R} \right)$$

By again making use of the final-value theorem, we find that, for *static* signals,

$$\frac{\Delta f_{\text{stat}}}{\Delta P_{G,\text{stat}}} = -R \qquad \text{Hz/MW} \tag{9-14}$$

This result points out the physical significance of the feedback parameter $R$, the so-called "speed regulation." The physical unit for $R$ is, obviously, hertz per megawatt. In practice, the power is measured in per units, and in this case the unit for $R$ will be cycles per second per unit megawatt.

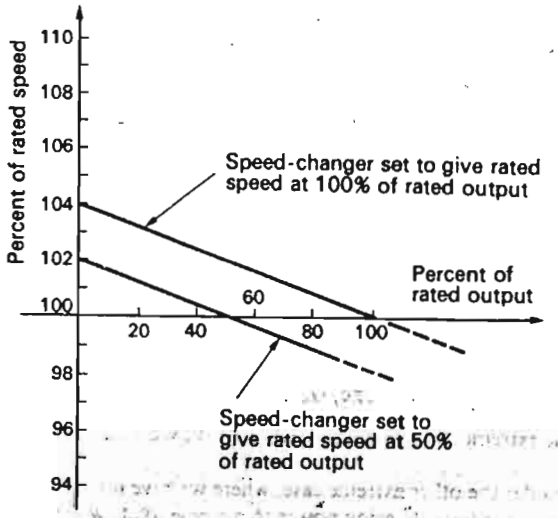


**Fig. 9-5** Static speed-load characteristics of power control mechanism in Fig. 9-3.



If the frequency drop is measured in per units of nominal frequency (= 60 Hz), and if the power is measured in per unit megawatts, then the unit for $R$ will be in per units also.

Figure 9-5 depicts a typical drooping speed-load graph of a turbine generator unit which experiences a 4 percent drop in speed between no load and full load. For this particular station the regulation is therefore

$$R = \frac{0.04 \times 60}{1.0} = 2.4 \text{ Hz/pu MW}$$

A static load increase of, for example, 0.05 pu MW would give a static frequency drop of

$$2.4 \times 0.05 = 0.12 \text{ Hz}$$

In a later section we shall find that the $R$ parameter also fills an important *damping* function in interconnected systems [compare Eq. (9-58)].

### 9-2.2 DIVISION OF POWER SYSTEM INTO CONTROL AREAS

The conceptual block diagram in Fig. 9-2 depicts individual control of each generator bus in the system. This is normally the case as far as the $QV$ loop is concerned, since the voltage of each generator bus is being regulated by field control of the local generators.

**Definition of control area** The load frequency control, in contrast to the above, is handled collectively by a unison effort by all generator units within a so-called *control area*. Usually, the boundaries of the control areas coincide with those of the individual power systems belonging to the pool. In the strictest sense, all the generators in a control area should constitute a coherent group. In the analysis to follow, coherency is tacitly assumed.

The concept of "control area" is really a relative one. For example, the eastern and western power blocks in the United States each contain many individual control areas. These two blocks are interconnected via relatively weak midwestern tie lines, and in the study of power swings in these lines, it is possible to consider both areas as two huge coherent machine groups swinging against each other.

**Incremental power balance of control area** We shall proceed now to develop a dynamic model describing the incremental $Pf$ dynamics of a control area, $i$, connected via tie lines to neighboring areas, as depicted in Fig. 9-6. We shall assume that the area experiences a real load change of magnitude $\Delta P_{Di}$ MW. Due to the actions of the turbine controllers, the area increases its output by the amount $\Delta P_{Gi}$ MW. The net power surplus in the area therefore equals $\Delta P_{Gi} - \Delta P_{Di}$ MW, and this power will be absorbed by the system in three ways:

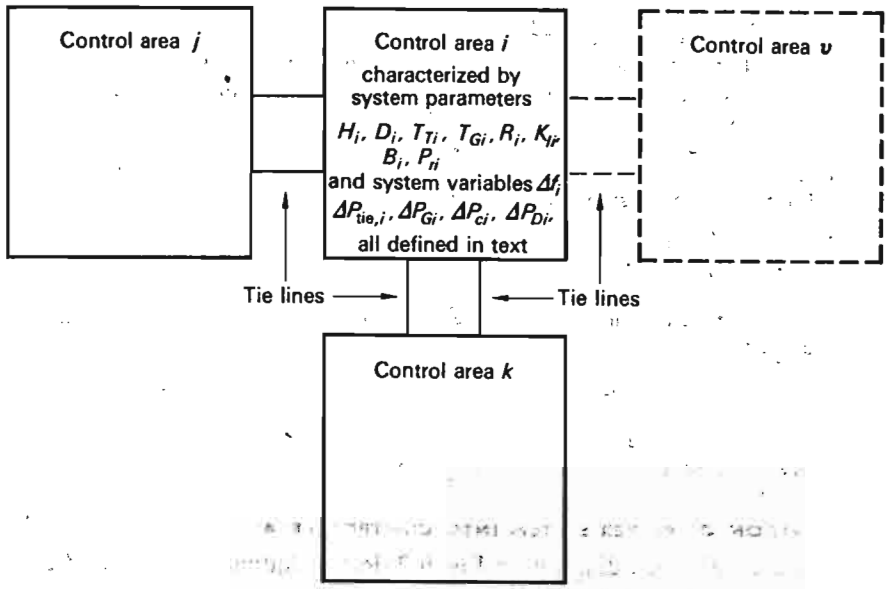


**Fig. 9-6** Interconnected "control areas."

1. By increasing the area kinetic energy $W_{kin,i}$ at the rate $(d/dt)W_{kin,i}$.
2. By an increased load consumption. All typical loads (because of the dominance of motor load) experience an increase, $D = \partial P_D/\partial f$ MW/Hz, with speed or frequency. This $D$ parameter can be found empirically (Chap. 3).
3. By increasing the export of power via tie lines, with the total amount $\Delta P_{tie,i}$ MW defined positive out from the area.

We can express this situation mathematically by

$$\Delta P_{Gi} - \Delta P_{Di} = \frac{d}{dt} W_{kin,i} + D_i \Delta f_i + \Delta P_{tie,i} \tag{9-15}$$

The second term on the right side has already been discussed in Chap. 3. Let us comment on the first and third terms.

*The kinetic energy $W_{kin,i}$* The total kinetic energy $W_{kin,i}$, of the control area varies as the square of the speed or frequency, and we can therefore write

$$W_{kin,i} = \left(\frac{f_i}{f^0}\right)^2 W^0_{kin,i} \tag{9-16}$$

where $W^0_{kin,i}$ is the area kinetic energy, MW or MJ, measured at nominal



frequency. $f_i$ is the instantaneous frequency of the control area. Since we have

$$f_i = f^0 + \Delta f_i \tag{9-17}$$

and $\Delta f_i$ is *small*, we can write Eq. (9-16) as follows:

$$W_{kin,i} = \left(\frac{f^0 + \Delta f_i}{f^0}\right)^2 W^0_{kin,i} \approx \left(1 + 2\frac{\Delta f_i}{f^0}\right) W^0_{kin,i} \tag{9-18}$$

The first term in Eq. (9-15) therefore takes on the form

$$\frac{d}{dt} W_{kin,i} = \frac{2W^0_{kin,i}}{f^0} \frac{d}{dt} \Delta f_i \qquad \text{MW} \tag{9-19}$$

*The incremental tie line power $\Delta P_{tie,i}$* The total incremental real power exported from area $i$, $\Delta P_{tie,i}$, equals the sum of all outflowing incremental line powers, $\Delta P_{tie,iv}$, in the lines connecting area $i$ with neighboring areas; i.e.,

$$\Delta P_{tie,i} = \sum_v \Delta P_{tie,iv} \qquad \text{MW} \tag{9-20}$$

The summation will be extended over all tie lines $v$ that terminate in area $i$.

If the line losses are neglected, the individual incremental line powers can be written in the form

$$\Delta P_{tie,iv} = T_{iv}{}^0(\Delta\delta_i - \Delta\delta_v) \qquad \text{MW} \tag{9-21}$$

In this equation $T_{iv}{}^0$ is the "synchronizing coefficient" defined by Eq. (3-6), having the value

$$T_{iv}{}^0 = P_{max,iv} \cos(\delta_i{}^0 - \delta_v{}^0) \qquad \text{MW/rad} \tag{9-22}$$

$P_{max,iv}$ is the static transmission capacity of the tie line in question.† $\delta_i{}^0$ and $\delta_v{}^0$ are the nominal phase angles of the voltages in both ends, and $\Delta\delta_i$ and $\Delta\delta_v$ are the incremental changes in these angles. Since our incremental frequency variable $\Delta f_i$ is related to the phase angle deviation through Eq. (9-6), we can, obviously, write Eq. (9-21) in the following way:

$$\Delta P_{tie,iv} = 2\pi T_{iv}{}^0 \left(\int \Delta f_i \, dt - \int \Delta f_v \, dt\right)$$

The total incremental tie line power out of area $i$ thus takes on the final form

$$\Delta P_{tie,i} = 2\pi \sum_v T_{iv}{}^0 \left(\int \Delta f_i \, dt - \int \Delta f_v \, dt\right) \tag{9-23}$$

† If $P_{max,iv}$ is small compared with $P_{ri}$ (the total megawatt rating of area $i$,) then we term the tie line "weak."

**Block-diagram representation of control area** Consider Eq. (9-15). If we divide all terms by $P_{ri}$, that is, the *total* megawatt rating of area $i$, the equation, in view of Eq. (9-19), takes on the form

$$\Delta P_{Gi} - \Delta P_{Di} = \frac{2H_i}{f^0}\frac{d}{dt}(\Delta f_i) + D_i\,\Delta f_i + \Delta P_{\text{tie},i} \tag{9-24}$$

The variables $\Delta P$ and $D$ are now measured *in per units* of $P_{ri}$. The quantity

$$H_i \triangleq \frac{W^0_{\text{kin},i}}{P_{ri}} \tag{9-25}$$

having the dimension seconds, is a *per-unit inertia constant* with the desirable property that it is practically independent of system size. Typical $H$ values lie in the range 2 to 8 s.

Let us now Laplace-transform Eqs. (9-23) and (9-24). We get

$$\Delta P_{\text{tie},i}(s) = \frac{2\pi}{s}\sum_{\nu} T_{i\nu}{}^0\,[\Delta F_i(s) - \Delta F_\nu(s)] \tag{9-26}$$

and

$$[\Delta P_{Gi}(s) - \Delta P_{Di}(s) - \Delta P_{\text{tie},i}(s)]G_{pi}(s) = \Delta F_i(s) \tag{9-27}$$

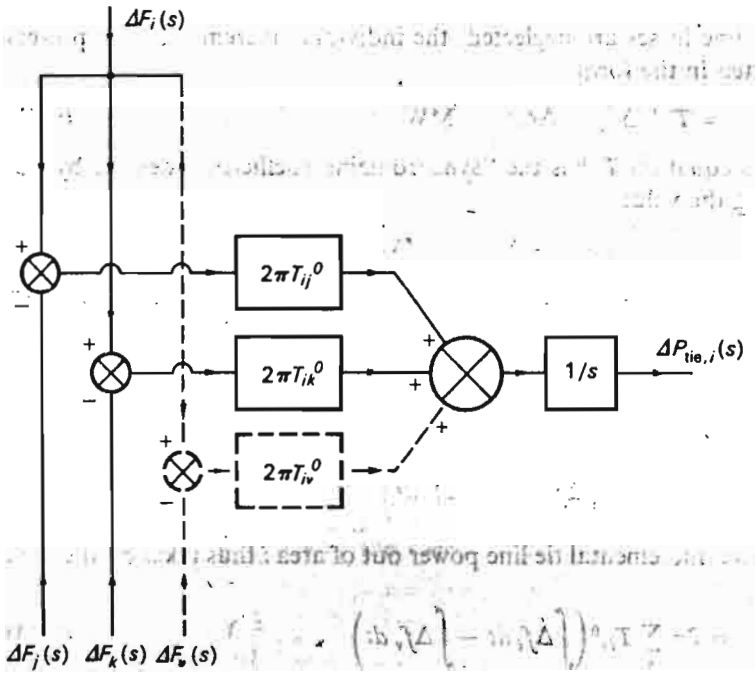


**Fig. 9-7** Block-diagram representation of Laplace-transformed equation (9-26).



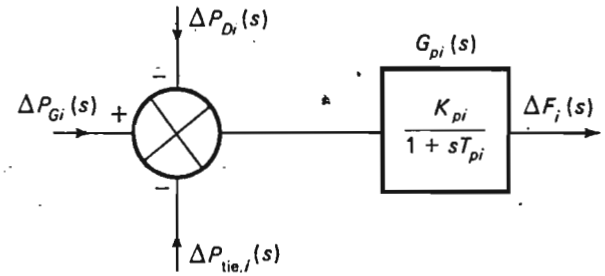


**Fig. 9-8** Block-diagram representation of Laplace-transformed equation (9-27).

where, for brevity, the following new parameters have been introduced:

$$T_{pi} \triangleq \frac{2H_i}{f^0 D_i} \quad \text{s} \tag{9-28}$$

$$K_{pi} \triangleq \frac{1}{D_i} \quad \text{Hz/pu MW} \tag{9-29}$$

$$G_{pi}(s) \triangleq \frac{K_{pi}}{1 + sT_{pi}} \tag{9-30}$$

Equations (9-26) and (9-27) can be represented by the block diagrams in Figs. 9-7 and 9-8, respectively. By combining these two block diagrams with the one in Fig. 9-4*b*, we finally arrive at the complete block diagram representation of a control area, shown in Fig. 9-9.

### 9-2.3 *Pf* CONTROL OF SINGLE CONTROL AREA

To get a feel for the dynamics of *Pf* control systems, we begin by investigating the simplest possible case consisting of a single control area. The block diagram for a single-area system (Fig. 9-10) is obtained by simply deleting the tie lines from Fig. 9-9.

**The uncontrolled case** We consider, first, the *uncontrolled* case, with $\Delta P_c = 0$. This means that we do not change the speed changer position.

*System data* To make our study as realistic as possible, we shall work with the following typical numerical values:

Total rated area capacity $P_r = 2000$ MW
Nominal operating load $P_D{}^0 = 1000$ MW
Inertia constant $H = 5.0$ s
Regulation $R = 2.40$ Hz/pu MW (Example 9-1)

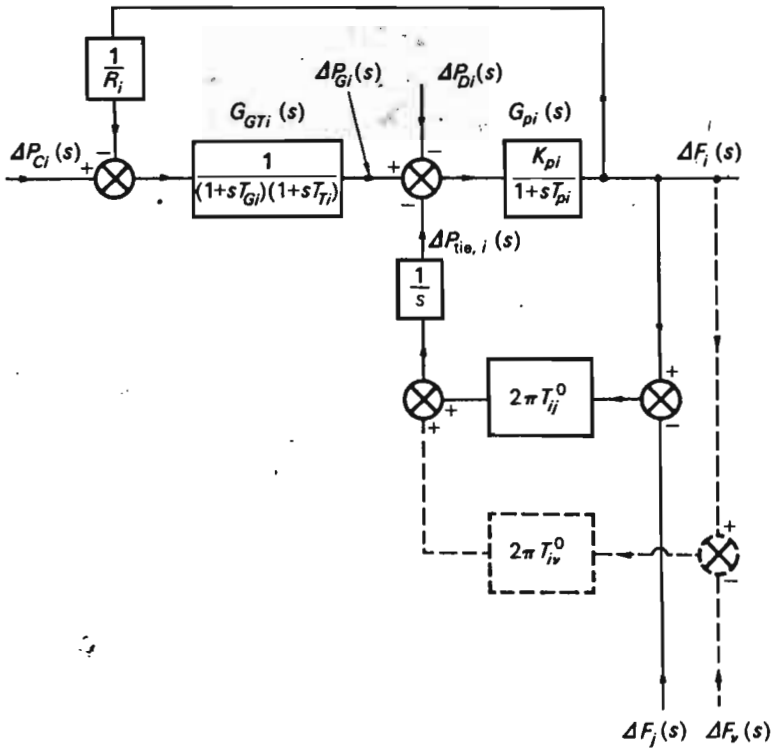


**Fig. 9-9** Complete block-diagram representation of control area *i*.

We shall assume that the load frequency characteristic is *linear*, meaning that the load would increase 1 percent for 1 percent frequency increase.

Thus

$$D = \frac{\partial P_D{}^0}{\partial f} = \frac{1000}{60} \qquad \text{MW/Hz}$$

or in per units of area capacity,

$$D = \frac{1000}{60 \times 2000} = 8.33 \times 10^{-3} \text{ pu MW/Hz}$$

We then get, from Eqs. (9-28) and (9-29),

$$T_p = \frac{2 \times 5.0}{60 \times 8.33 \times 10^{-3}} = 20 \text{ s}$$

$$K_p = \frac{1}{D} = 120 \text{ Hz/pu MW}$$



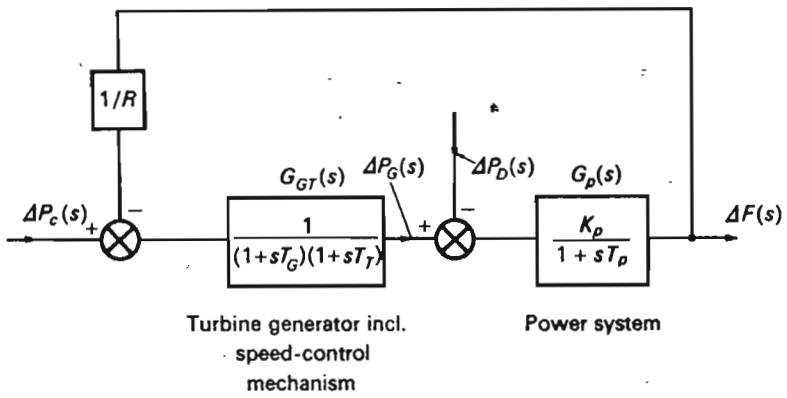


**Fig. 9-10** Block-diagram representation of single control area.

*Static frequency drop following step load change* From the block diagram in Fig. 9-10, we obtain for $\Delta P_c = 0$

$$\Delta F(s) = -\frac{G_p(s)}{1 + (1/R)G_p(s)G_{GT}(s)} \Delta P_D(s) \tag{9-31}$$

We shall find the response for a step load change of magnitude $\Delta P_D$. We have in this case

$$\Delta P_D(s) = \frac{\Delta P_D}{s} \tag{9-32}$$

Using the final-value theorem, we readily obtain from Eq. (9-31) the static frequency drop

$$\Delta f_{\text{stat}} = \lim_{s \to 0} [s\, \Delta F(s)] = -\frac{K_p}{1 + K_p/R} \Delta P_D = -\frac{\Delta P_D}{D + 1/R}$$

We introduce here the so-called *area frequency response characteristic* (AFRC) $\beta$, defined as

$$\beta \triangleq D + \frac{1}{R} \qquad \text{pu MW/Hz} \tag{9-33}$$

and obtain, then,

$$\Delta f_{\text{stat}} = -\frac{\Delta P_D}{\beta} \qquad \text{Hz} \tag{9-34}$$

For the above numerical data we get

$$\beta = 8.33 \times 10^{-3} + \frac{1}{2.40} = 0.425 \qquad \text{pu MW/Hz}$$

For example, a load increase of

$$\Delta P_D = 20 \text{ MW} = 20/2000 = 0.01 \text{ pu MW}$$

results in a static frequency change of

$$\Delta f_{\text{stat}} = -\frac{0.01}{0.425} = -0.0235 \text{ Hz}$$

*Time response* The *dynamic* frequency behavior $\Delta f(t)$ can be obtained by taking the inverse Laplace transform of Eq. (9-31). This is a straightforward procedure, in principle, but can get numerically involved if the transfer functions $G_{GT}$ and $G_p$ are complex. We have concluded in our preceding analysis that they together will contain at least three time constants, which will have the result that the denominator of Eq. (9-31) will be of third order.

We can simplify the analysis considerably by making the reasonable assumption that the action of the speed governor plus the turbine generator is "instantaneous" compared with the rest of the power system. The latter, as demonstrated in our present example, has a time constant of 20 s, and since the other two time constants are of the order of 1 s, we will perform an approximate analysis by setting $T_G = T_T = 0$.

From Eq. (9-31) we then get

$$\Delta F(s) \approx -\frac{\dfrac{K_p}{1+sT_p}}{1+\dfrac{1}{R}\dfrac{K_p}{1+sT_p}}\frac{\Delta P_D}{s}$$

$$= -\Delta P_D \frac{RK_p}{R+K_p}\left(\frac{1}{s} - \frac{1}{s+\dfrac{R+K_p}{RT_p}}\right) \tag{9-35}$$

If we make use of the previous numerical values, we obtain

$$\Delta F(s) \approx -0.0235\left(\frac{1}{s} - \frac{1}{s+2.55}\right) \tag{9-36}$$

The approximate time response is therefore purely exponential.

$$\Delta f(t) \approx -0.0235(1 - e^{-2.55t}) \quad \text{Hz} \tag{9-37}$$

Figure 9-11 shows an analog computer recording† of this response. For comparison, we also simulated the loop response with the inclusion of

† The author gratefully acknowledges the assistance of Charles E. Fosha, a graduate assistant at the University of Florida, in obtaining all computer recordings in this chapter.



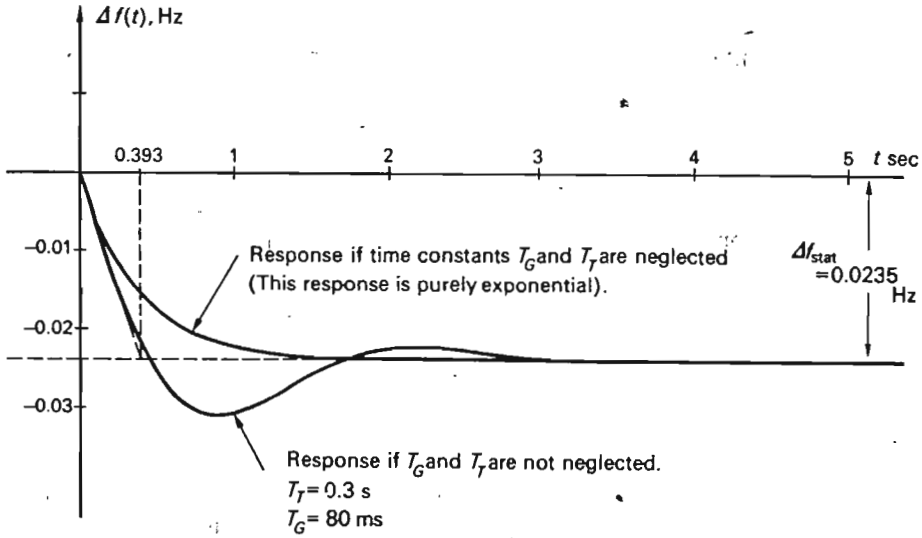


**Fig. 9-11** Dynamic frequency deviation following a step load change. Speed changer position fixed.

the time constants $T_G$ and $T_T$. We make the following observations in regard to our results:

1. The overall *closed loop* system time constant equals only $1/2.55 = 0.393$ s, which is a considerable reduction from the value $T_p = 20$ s, characterizing the plant itself. This speedup is a result of the feedback arrangement of the speed governor. Note that the system can be made still faster by reducing $R$, that is, by increasing the static loop gain.
2. Reduction of $R$ also reduces the static frequency error.
3. If we performed the above analysis by *not* disregarding the time constants $T_T$ and $T_G$, then the response would not be purely exponential as above. In Fig. 9-11 we show the difference. Note that the added delays cause a larger transient frequency dip. Why?
4. The speed governor operated in the above *noncontrolled mode* (i.e., without manipulation of the speed changer) gives a reasonable performance with a static frequency drop of only 2.4 Hz between zero and full load and settling times of the order of 5 s (as depicted in Fig. 9-11). However, with the extremely severe restrictions we in reality impose on frequency constancy (see next section), the results are, in fact, entirely unacceptable. We must do much better.
5. The foregoing analysis may not have given the reader a full *physical* understanding of the load frequency mechanism of the *uncontrolled* single-area system. Since such an understanding is invaluable to

appreciate fully so-called bias control in multiarea systems (see next section), we shall attempt now to shed some light on the physical mechanism.

*Physical interpretation of results* When the load suddenly increased by 1 percent (= 20 MW), where did this power come from? Certainly, it must have come from somewhere, as can be certified by the customer who threw the switch and expected *and got instantaneously* his demanded 20 MW.

In the milliseconds following the closure of the switch, the frequency has not changed a measurable amount, and therefore no power increase has had time to develop in the turbine (where the steam valve has not yet moved).

*In those first instants the total additional load demand* 20 MW *is obtained from the stored kinetic energy, which therefore will decrease at an initial rate of* 20 MW. The kinetic energy is released by speed reduction.

Since the speed is dropping (and from Fig. 9-11 we note that the *initial* deceleration is 0.0235/0.393 = 0.06 Hz/s), the generator valve is opened up, due to the mechanism described earlier, and this means increased generator output. Also, *and this is important to realize*, since the speed is now dropping, the initial "old" load (1000 MW in this case) decreases at the rate of $D = 1000/60 = 16.67$ MW/Hz.

*Since the appearance on the scene of this "released" power means that less power needs to be generated, we can in effect consider it to be a direct contribution to the new load demand.*

In conclusion, as the speed is dropping, the demand increase of 20 MW is thus made up of three components:

1. "Borrowed" kinetic energy from the rotating system machines
2. Increased generation
3. "Released" customer load

Initially, the last two components are zero, but as the speed is dropping, they will account for an increased contribution. Consequently, the kinetic energy will be consumed at a decreased rate, and this is confirmed in Fig. 9-11, which shows that the deceleration decreases as time goes on.

Eventually (theoretically, after infinite time), the speed will level off at a new constant lower value. At this time the kinetic energy is constant (at a lower value), and the 20-MW load increase is therefore made up of the last two components only. It is interesting to see in what ratio the last two components contribute.

The static speed drop being 0.0235 Hz, we can compute these contributions as follows:



1. The generator regulation is 4.00 percent, or 2.40 Hz/pu MW, and the increase in generation after the new steady state is reached will be

$$\frac{0.0235}{2.40} = 0.0098 \text{ pu MW}$$

$$= 0.0098 \times 2000 = 19.6 \text{ MW}$$

2. Since the "old" load decreases at the rate of 16.67 MW/Hz, the speed drop of 0.0235 Hz will "release"

$$0.0235 \times 16.67 = 0.4 \text{ MW}$$

These two components evidently add up to 20 MW. Note that the largest contribution, by far, is from new generation.

**The controlled case** It is necessary to achieve much better frequency constancy than is obtained by the speed governor system itself, as demonstrated above. To accomplish this we must manipulate the speed changer in accordance with some suitable *control strategy*. Before we do so, it is necessary to settle for a set of *control specifications* the stringency of which will in the end determine the sophistication of the proposed control method.

*Suggested control system specifications* We are presently discussing a single-area system, and the control specifications for such a system are considerably simpler than those imposed upon a multiple-area system (*power pool*).

Here follow some realistic specifications:

1. The control loop must be characterized by a sufficient degree of stability.
2. Following a step load change, the frequency error should return to *zero*. This is referred to as *isochronous control*. The magnitude of the transient frequency deviation should be minimized. (This magnitude depends, of course, upon the magnitude of the load change.)
3. The *integral* of the frequency error (this integral has dimension of cycles) should not exceed a certain maximum value. The North American Power Systems Interconnection Committee proposes 180 Hz as a minimum.
4. The individual generators of the control area should divide the total load for optimum economy (Chap. 8).

Let us comment on each of these requirements:

1. Stability is *always* a problem in closed-loop control. The tighter the error specifications, the greater the risk that the proposed loop will turn unstable.

2. The need for frequency constancy was discussed in Chap. 3. Isochronous (*iso* = equal, *chronos* = time) control gives assurance that the synchronous clocks run on time, *but not without error* (see point 3).
3. Isochronous control guarantees that the *static* frequency error following a *step* load change will vanish. No control system can, however, eliminate the *transient* frequency error (see Fig. 9-13 for a demonstration of this point). The time error of synchronous clocks is proportional to the *integral of the frequency error*. It is therefore necessary to put limits on this integral.

   The particular control strategy we shall propose below does not have the ability to reduce the error integral automatically to arbitrarily small values. During the periods of heavy load, the system frequency will have a tendency to be below 60.00 Hz, during periods of the light load above.

   For example, assume that the frequency averages 59.99 Hz during a prolonged heavy-load period. We would now accumulate a time error of $-0.01 \times 3600 = -36$ Hz/h. This corresponds to a time error of $-36/60 = -0.6$ s/h.

   The customary way to handle such a slowly accumulating time error (in the United States) is as follows:

   The error is measured by comparing the "system time" with that of the National Bureau of Standards. When an error of $\pm 3$ s has accumulated (and, as exemplified, this will normally take many hours), the speed changer is offset intentionally an amount of, say, 0.02 Hz for a sufficiently long time for the time error to reduce to zero.

   In the case of a power pool, one usually designates a pool member to keep track of the time error and inform the other pool members regularly of the need to reduce the error by a *unison* effort.
4. The first three specifications are taken care of by a control system (see below) with a response time of the order of a few seconds or half a minute. When these *primary* control requirements are met, one attends to the *secondary* economic requirement. This is usually being done by a slower economic dispatch control scheme, having response times of the order of a minute or longer.

*Integral control* By using the control strategy shown in Fig. 9-12, we obtain an overall system that will meet performance specifications 1 and 2 above. We have added to the uncontrolled system in Fig. 9-10 so-called *integral control:* i.e., we let the speed changer be commanded by a signal obtained by first amplifying and then integrating the frequency error.

$$\Delta P_c \triangleq -K_I \int \Delta f \, dt \tag{9-38}$$



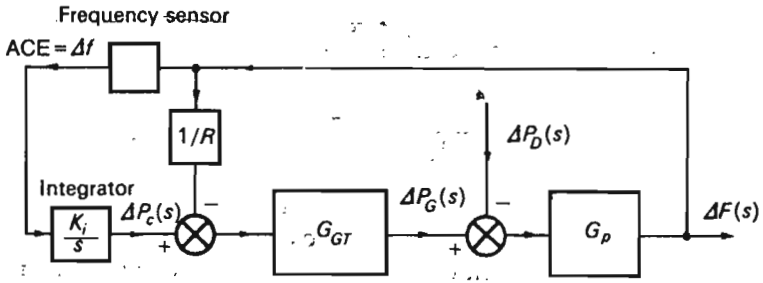


**Fig. 9-12** Integral control of single-area system.

Note the negative polarity of the integral controller. This polarity must be chosen so as to cause a positive frequency error to give rise to a negative, or "decrease," command. The signal fed into the integrator is referred to as *area control error* (ACE), i.e.,

$$\text{ACE} \triangleq \Delta f \tag{9-39}$$

Integral control will give rise to zero static frequency error following a *step* load change, for the following physical reason:

As long as an error remains, the integrator output will increase, causing the speed changer to move. *The integrator output, and thus the speed changer position, attains a constant value only when the frequency error has been reduced to zero.*

The gain constant $K_I$ controls the rate of integration, and thus the speed of response of the loop. The integration is actually performed in electronic integrators of the same type as found in analog computers.

Here follows an analysis of the proposed system, subject to a step load change. To avoid cumbersome numerical analysis, we shall as before neglect the time constants $T_T$ and $T_G$. In addition, we also make the assumption that the speed changer action is instantaneous. This is not perfectly correct, since the device is electromechanical and will therefore have a nonzero response time. These approximations will make possible relatively simple analysis without distorting the essential features of the response. It is also worth mentioning that the errors we thus introduce into our analysis affect only the transient, *not the static*, response. (This was clearly demonstrated in Fig. 9-11.)

From Eq. (9-38) we get, upon Laplace transformation,

$$\Delta P_c(s) = -\frac{K_I}{s} \Delta F(s) \tag{9-40}$$

After making use of the block diagram in Fig. 9-12 and Eqs. (9-32) and (9-40), we get, after some algebra,

$$\Delta F(s) = -\frac{K_p}{T_p}\frac{\Delta P_D}{s^2 + s[(1 + K_p/R)/T_p] + K_I K_p/T_p} \tag{9-41}$$

We obtain the time response $\Delta f(t)$ upon inverse transformation of this expression. Since the response depends upon the poles† of Eq. (9-41), we must first turn our attention to the second-order-denominator polynomial, which can be written

$$s^2 + s\frac{1 + K_p/R}{T_p} + \frac{K_I K_p}{T_p} = \left(s + \frac{1 + K_p/R}{2T_p}\right)^2 + \frac{K_I K_p}{T_p} - \left(\frac{1 + K_p/R}{2T_p}\right)^2 \tag{9-42}$$

Clearly, the nature of the poles depends upon the magnitude of the integral gain $K_I$. If

$$\frac{K_I K_p}{T_p} > \left(\frac{1 + K_p/R}{2T_p}\right)^2$$

i.e., if

$$K_I > \frac{1}{4T_p K_p}\left(1 + \frac{K_p}{R}\right)^2 \triangleq K_{I,\text{crit}} \tag{9-43}$$

then we can write the denominator polynomial in the form

$$(s + \alpha)^2 + \omega^2$$

where $\alpha$ and $\omega^2$ are both positive and real. This is the *supercritical case.*

The expression for $\Delta F(s)$ now has a conjugate-complex pole pair in the stable $s$ plane, and the time response $\Delta f(t)$ therefore contains damped *oscillatory* terms of the types

$$e^{-\alpha t}\sin \omega t \quad \text{and} \quad e^{-\alpha t}\cos \omega t$$

If, on the contrary,

$$K_I < K_{I,\text{crit}} \tag{9-44}$$

(*subcritical* integral control),

† These *closed-loop poles* obtained from a solution of the *characteristic equation* (i.e., the denominator expression set equal to zero) are also referred to as *closed-loop eigenvalues.*



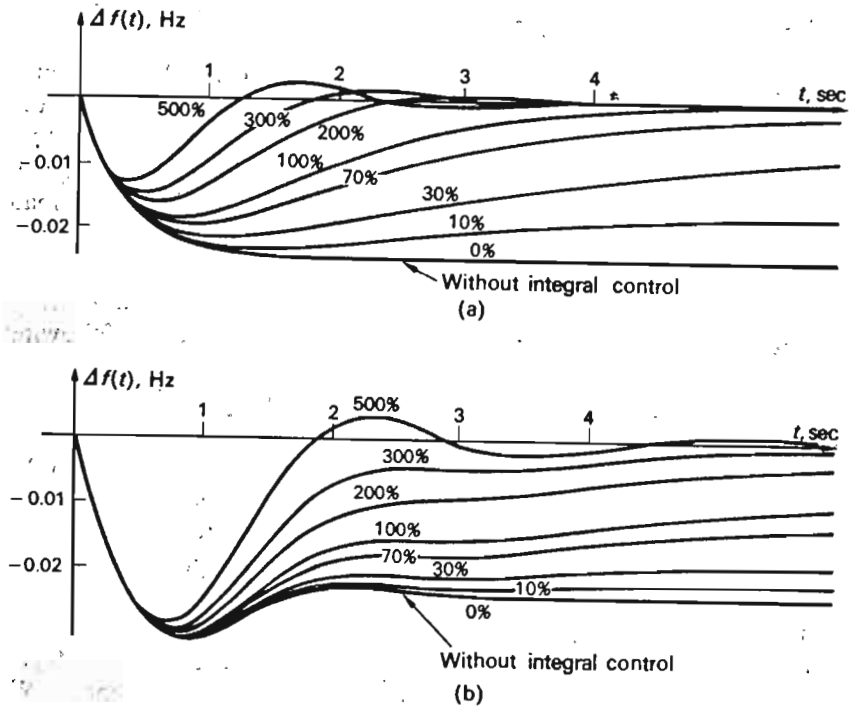


**Fig. 9-13** Dynamic frequency swings following step load disturbance for system in Fig. 9-12. The response is shown for different gain settings $K_I$. 100 percent gain is defined as the critical gain introduced in the text. (*a*) $T_G = T_T = 0$; (*b*) $T_G = 0.080$ s, $T_T = 0.30$ s. (Note that for $K_I = 0$, we obtain the "noncontrolled" curves in Fig. 9-11.)

then we can write the polynomial in the form

$$(s + \beta_1)(s + \beta_2)$$

where $\beta_1$ and $\beta_2$ are both positive.

Equation (9-41) now has a real pole pair in the stable $s$ plane, and the corresponding *nonoscillatory* time response $\Delta f(t)$ contains terms of the types

$$e^{-\beta_1 t} \quad \text{and} \quad e^{-\beta_2 t}$$

In either of the above two cases, $\Delta f(t)$ will thus approach zero, proving that we indeed have both *stable* and *isochronous* frequency control. Our first and second system requirements are thus met. In Fig. 9-13 we depict the actual simulated time responses for different values of the gain setting $K_I$. The family of curves in Fig. 9-13*a* correspond to $T_T = T_G = 0$, i.e., the case we just analyzed. Figure 9-13*b* includes the effect of these time constants.

We make the following general comments about integral type control:

1. If we use subcritical gain settings ($K_I < 100$ percent), we obtain sluggish nonoscillatory response of the control loop. This means that the integral of $\Delta f(t)$, and thus the time error, will be relatively large. In a practical situation this setting is most often used. The advantage is that the generator now will not unnecessarily "chase" rapid load fluctuations, causing equipment wear.
2. If we want to speed up the response by increasing the gain $K_I$, the *response turns oscillatory*. This is the price we pay for reducing the time error.
3. A careful study of the response graphs in Fig. 9-13 reveals the following features:

   As the sudden load increase sets in, the frequency starts falling off *at the same exponential rate as for the uncontrolled system* (compare Fig. 9-11). During these first instants the integral controller has not yet had time to go into action, and the system responds in its uncontrolled manner, which we discussed previously in great detail. After a certain time (the shorter the time, the higher integral gain $K_I$), the integral controller comes into action and eventually lifts the frequency back to its original value.
4. The reader must realize that in order to keep the analysis of the integral controller simple, we have made several simplifying assumptions. We shall summarize these:
   *a*. The time constants $T_T$ and $T_G$ were neglected (but they were included in the simulated graphs in Fig. 9-13*b*).
   *b*. The speed changer response was assumed instantaneous.
   *c*. All nonlinearities in the equipment, such as dead zone, etc., have been neglected.
   *d*. It has been tacitly assumed that the generator can change its generation $\Delta P_G$ as fast as it is commanded by the speed changer to do so. In reality, there is a practical limit to the *rate*, expressed as megawatts per second, at which a steam generator can pick up load. We have neglected this rate limitation during the few seconds we are considering.
   *e*. We have assumed that the ACE is available as a *continuous* signal. In reality, the measurement of the frequency deviation $\Delta f$ takes place discontinuously in *sampled-data* fashion. If the sampling rate is relatively high (compared with the fastest changes in the response of Fig. 9-13), then the above analysis gives good results.

### 9-2.4 ECONOMIC DISPATCH CONTROLLER

The integral controller just described results in a system that meets the first three of the specified control requirements. The fourth requirement, i.e.,



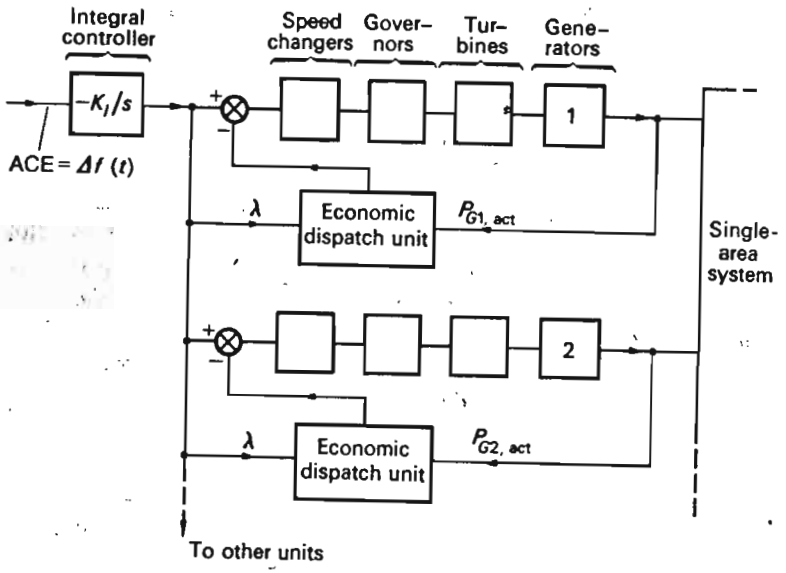


**Fig. 9-14** Automatic load frequency control with optimum economic dispatch added.

that pertaining to economic dispatch, can be met if we provide for additional "economic dispatch control equipment" to be added to the system in Fig. 9-12.

We now describe one possible solution of instrumentation for economic control.

We first remind the reader (Chap. 8) that the basis for economic dispatch is the so-called incremental transmission losses and generation costs, ITL and IC, respectively. The incremental cost of generation, IC, is by far the most important parameter. The incremental transmission loss ITL becomes important only when the transmission losses reach appreciable magnitudes. We shall limit the following discussion to an economic dispatch controller which bases its generation upon the IC's only; i.e., we neglect the influence of transmission losses. This assumption will simplify our discussion, and is furthermore justified by the fact that many economic dispatch installations actually disregard the losses. If we wish to take them into consideration, only a slight modification is needed to the instrumentation we are about to discuss.

Consider the single-area system depicted in Fig. 9-14. It contains $n$ generating units, which we wish to control so as to meet the requirement for optimum economic dispatch. As we recall from Chap. 8, the economic optimum is reached (in the loss-free case) when all generators are operated

at equal incremental costs; i.e., we must see to it that

$$\lambda = (\text{IC})_1 = (\text{IC})_2 = \cdots = (\text{IC})_n \qquad (9\text{-}45)$$

Consider the operation of the system by first disregarding the blocks which we have labeled "economic dispatch unit." All the $n$ generators are now operated in unison under the parallel command from the integral controller. The performance of the system will be identical with that which we derived for the system in Fig. 9-12; i.e., the *total* generation is being controlled so as to meet the specified frequency-error requirements. *However, we have little or no control over the division of the total load among the n individual generators.* As a matter of fact, it is quite conceivable that some of the generators might be commanded to generate more than their rating would permit. A certain degree of load division control could, of course, be achieved by feeding the integrated signal to each generator speed changer via individual gains (not indicated in Fig. 9-14).

It is the job of the economic dispatch unit to readjust the individual generations so that the "equal incremental cost" requirement is satisfied. This is being accomplished in the following manner:

Assume that the system, initially, is in a static nominal state, characterized by zero frequency error and a set of generator outputs that actually meet the requirement [Eq. (9-45)]. Assume, then, a sudden load increase of, say, 1 percent of area capacity. In a manner discussed in the preceding section, this load increase sets into operation the mechanism that, in a few seconds, has increased the total generation so as to account for the increase. All $n$ generators take part in this primary readjustment. Since all the IC curves for the $n$ individual generators supposedly look different, the generators after the initial readjustment will *not* operate with equal IC's. There will, in effect, be an "economic error" for each unit, this error being defined as the difference between the desired generator output $P_{Gv,\text{des}}$ and the actual output, $P_{Gv,\text{act}}$.

The economic dispatch unit is designed to detect this error and, then, in a slower mode of operation, command a *secondary* readjustment of the individual speed changers. The system thus, basically, contains two superimposed control loops. The *primary* integral loop provides for fast (a few seconds) frequency control. The *secondary* economic loop provides for slower (half a minute) adjustment to economic optimum settings.

Figure 9-15 shows how, in principle, the economic dispatch unit works. From a hardware point of view, it may be built by analog computer elements, or the entire control function for each of the $n$ units can be performed by a central digital computer. The central feature of the economic dispatch unit is a $P_G$-IC "function generator" that relates the power output to the incremental cost of each unit. If the equipment is built by analog elements, this function generator is built by diodes and resistors, like any other



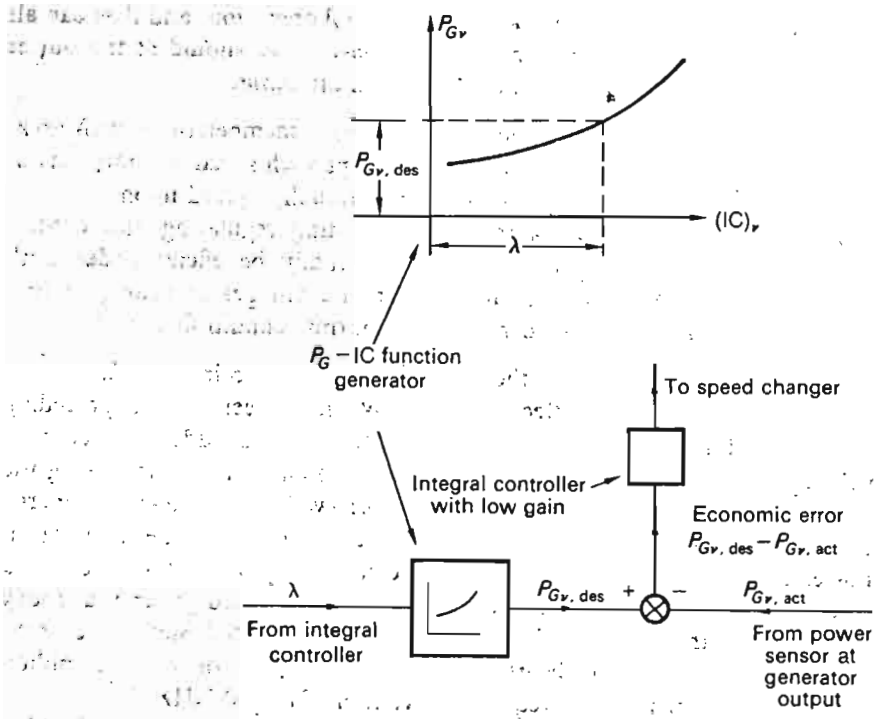


**Fig. 9-15** Detailed operation of the economic dispatch unit.

nonlinear function generator. If the control is instrumented digitally, the function is stored as a polynomial in the computer memory.

All units are receiving as inputs the signal from the common integral controller. We have labeled this signal $\lambda$, because it in fact takes on the physical significance of the Lagrange multiplier introduced in Chap. 8. The $\lambda$ signal is fed into the $P_G$-IC generator, and the output from this block is therefore the "desired economic" generation for the $\lambda$ in question. Upon comparison with the actual generation an "economic error signal" is formed, which, via an integrator of *low* gain, is fed to the speed changer. The low gain guarantees slow secondary adjustment operation.

### 9-2.5 *Pf* CONTROL OF MULTI-CONTROL-AREA SYSTEMS (POOL OPERATION)

From a practical point of view, the problems of frequency control of interconnected areas, or *power pools*, are more important than those of isolated areas. Practically, all power systems today are tied together with neighboring areas, and the problem of load frequency control becomes a joint undertaking. Closely associated is the problem of controlling the power flows on the interties.

Many advantages can be derived from pool operation, and they can all be summarized in two words, *mutual assistance*. We should at the outset state the following operating principles, which are basic:

1. Under normal operating conditions each pool member or control area, should strive to carry its own load, except such scheduled portions of the other members' load as have been mutually agreed upon.
2. Each control area must agree upon adopting regulating and control strategies and equipment that are mutually beneficial under both normal and abnormal situations. The advantages of belonging to a pool are particularly evident under abnormal conditions.

Let us consider some of the advantages referred to in point 2.

First, consider the effect of *size*. We have seen in the preceding examples in this chapter how the frequency, following a sudden load change, will sag as a result of the fact that, during the first moments following the load increase, the needed energy is being "borrowed" from the kinetic energy of the system. Clearly, the larger the system, the more kinetic energy it possesses, and therefore the more energy can be temporarily borrowed for a given speed drop. For example, the large interconnected group that today (1970) covers the central and eastern parts of the United States and some Canadian provinces can absorb a sudden load change of about 3 million kilowatts and experience a frequency deviation of only 0.1 Hz.

A small system of, say, 1000-MW capacity, if it suddenly loses 300-MW capacity (which represents 30 percent), *and if operating alone*, will be in dire trouble. Its frequency will undergo an extensive drop, and chances are that the transient power angle swings that would ensue (Chap. 12) would tear the whole system apart, resulting in a complete blackout.

If the same system were part of a pool of, say, 100,000 MW capacity, the same 300-MW generation failure would represent only a 0.3 percent loss. The frequency would be "saved," and support power to the extent that 300 MW would instantaneously flow into the crippled area via the tie lines to carry its load until normal generation is restored.

System size also reduces the need for reserve power among the pool members. A system that operates alone as a "single area" must provide power to handle not only the anticipated peaks, but also the sudden requirements due to equipment failures. The reserves are classified on the basis of their readiness. "Spinning" reserves can be called upon for *instantaneous* (at least as fast as the controllers can react) assistance. They are made up of fully operating but only partially loaded units. Hydroelectric-, diesel-, and gas-turbine-operated units can be called upon at a few minutes' notice. Steam reserves range all the way from "low bank" (i.e., idling at pressure and heat levels below that required for service) to "cold reserves" (operative, but not in operation).



Since peak demands occur† at various hours of the day in various areas, the ratio between peak and average load for a large pool is smaller than that of the individual systems. It is obvious, therefore, that all pool members can benefit from a reduced need of reserve capacity by a scheduled arrangement of energy interchange.

**The two-area system** It was possible in Chap. 7 to introduce the reader to the fundamental problems associated with the *static* operation of an $n$-bus system by discussing, first, the simplest of all multibus systems, the two-bus system. We shall find it equally instructive to introduce the reader to the load frequency dynamics of the $n$-area system by studying first the dynamics of the two-area system.

Let us therefore turn our attention to a system consisting of two control areas of the type indicated in Fig. 9-6, interconnected via a relatively weak tie line. The areas are generally of different size and characteristics.

**Block diagram of two-area system** Each area is characterized by the block diagram shown in Fig. 9-9 in terms of its incremental $Pf$ dynamics. By connecting two of these block diagrams together, we therefore obtain the two-area model shown in Fig. 9-16. (Disregard, for the time being, the dotted portions of this diagram.)

An explanation must be given about the block having the transfer function $a_{12}$. We remember that in Eq. (9-24) the term $\Delta P_{\text{tie},i}$ represented the tie line power *out* from area $i$, expressed in *per-unit megawatts* of the area capacity $P_{ri}$. For the two-area system the tie line power $\Delta P_{\text{tie},1}$ must equal the negative of $P_{\text{tie},2}$ if *both* are expressed in *megawatts*. Expressed mathematically, this means that

$$P_{r1}\,\Delta P_{\text{tie},1} = -P_{r2}\,\Delta P_{\text{tie},2}$$

or

$$\Delta P_{\text{tie},2} = a_{12}\,\Delta P_{\text{tie},1} \tag{9-46}$$

where

$$a_{12} \triangleq -\frac{P_{r1}}{P_{r2}} \tag{9-47}$$

**Mechanical analog of two-area system** Before we proceed with an analysis of the two-area system, we shall present, without proof, a mechanical system that is a perfect analog of our electrical two-area system. Consider

† For example, New York is 2 h ahead of Denver. Florida has a summer peak, whereas Michigan has a winter peak.

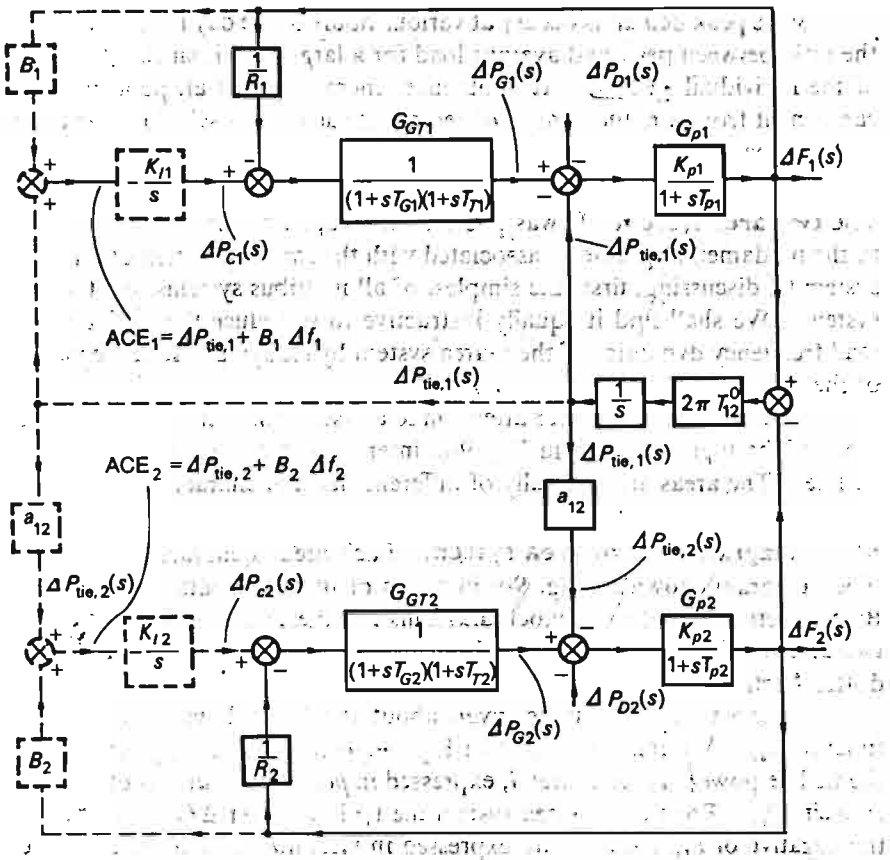


**Fig. 9-16** Load frequency control of two-area system. (Dotted portions refer to "controlled" case).

the train in Fig. 9-17. If this train is traveling at a nominal constant speed $v^0$ and "tie spring" power and suddenly is subject to incremental load changes, the velocity will change. The two-car assemblies will experience the velocity perturbations $\Delta v_1$ and $\Delta v_2$, respectively, and the tie spring power will change with the amount $\Delta P_{\text{tie}}$. By writing† the incremental dynamic equations for this system, one can readily confirm that they are of the identical form as our system equations (9-23) and (9-24). This means that the systems are analogs of each other. The following variables correspond to each other:

$$\Delta v_1 \leftrightarrow \Delta f_1$$

$$\Delta v_2 \leftrightarrow \Delta f_2$$

† The reader should not take the author's word for this, but actually prove it to his own satisfaction.



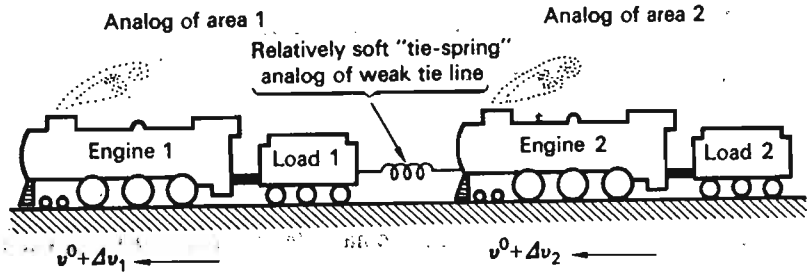


**Fig. 9-17** Mechanical analog of two-area system.

Tie spring power ↔ tie line power

The train analog can thus be used as an aid in achieving a better feel for the behavior of the electric system.

**Static response of uncontrolled two-area system** We shall first investigate the response of the two-area system under uncontrolled conditions, i.e., fixed speed changer positions:

$$\Delta P_{c1} = \Delta P_{c2} = 0$$

We assume that the loads in each area are suddenly increased by the incremental *steps* $\Delta P_{D1}$ and $\Delta P_{D2}$. We shall limit our analysis to finding the *static* changes that result in frequency and tie line power. Let us call those changes† $\Delta f_{\text{stat}}$ and $\Delta P_{\text{tie 1,stat}}$.

Since the incremental increase in generation in this static case is determined by the static loop gains only, we obtain from Fig. 9-16

$$\Delta P_{G1,\text{stat}} = -\frac{1}{R_1}\Delta f_{\text{stat}}$$

$$\Delta P_{G2,\text{stat}} = -\frac{1}{R_2}\Delta f_{\text{stat}} \tag{9-48}$$

From Eq. (9-24) we get, upon setting $d(\Delta f_i)/dt = 0$ and making use of Eqs. (9-46) and (9-48),

$$-\frac{1}{R_1}\Delta f_{\text{stat}} - \Delta P_{D1} = D_1 \Delta f_{\text{stat}} + \Delta P_{\text{tie 1,stat}}$$

$$-\frac{1}{R_2}\Delta f_{\text{stat}} - \Delta P_{D2} = D_2 \Delta f_{\text{stat}} + a_{12}\Delta P_{\text{tie 1,stat}} \tag{9-49}$$

† In steady state the frequency drops in the two areas will be equal (compare graphs in Fig 9-18).

We solve for $\Delta f_{stat}$ and $\Delta P_{tie\ 1,stat}$ and obtain

$$\Delta f_{stat} = -\frac{\Delta P_{D2} - a_{12}\Delta P_{D1}}{\beta_2 - a_{12}\beta_1} \quad \text{Hz}$$

$$\Delta P_{tie\ 1,stat} = \frac{\beta_1 \Delta P_{D2} - \beta_2 \Delta P_{D1}}{\beta_2 - a_{12}\beta_1} \quad \text{pu MW} \tag{9-50}$$

where, in analogy with Eq. (9-33), we have defined the AFRCs of each area:

$$\beta_1 \triangleq D_1 + \frac{1}{R_1}$$

$$\beta_2 \triangleq D_2 + \frac{1}{R_2} \tag{9-51}$$

Equations (9-50) become particularly simple if we assume *identical* area parameters; i.e.,

$$D_1 = D_2 = D$$
$$R_1 = R_2 = R$$
$$\beta_1 = \beta_2 = \beta$$

and

$$a_{12} = -1$$

We then get

$$\Delta f_{stat} = -\frac{\Delta P_{D2} + \Delta P_{D1}}{2\beta} \quad \text{Hz}$$

$$\Delta P_{tie\ 1,stat} = -\Delta P_{tie\ 2,stat} = \frac{\Delta P_{D2} - \Delta P_{D1}}{2} \quad \text{pu MW} \tag{9-52}$$

For example, if a step load change occurs in area 2, we get

$$\Delta f_{stat} = -\frac{\Delta P_{D2}}{2\beta} \quad \text{Hz} \tag{9-53}$$

$$\Delta P_{tie\ 1,stat} = \frac{\Delta P_{D2}}{2} \quad \text{pu MW} \tag{9-54}$$

These two last equations tell us, in a nutshell, the advantages of pool operation:

1. Fifty percent of the added load in area 2 will be supplied by area 1 via the tie line.
2. The frequency drop will be only half that which would be experienced if the areas were operating alone [compare Eq. (9-34)].



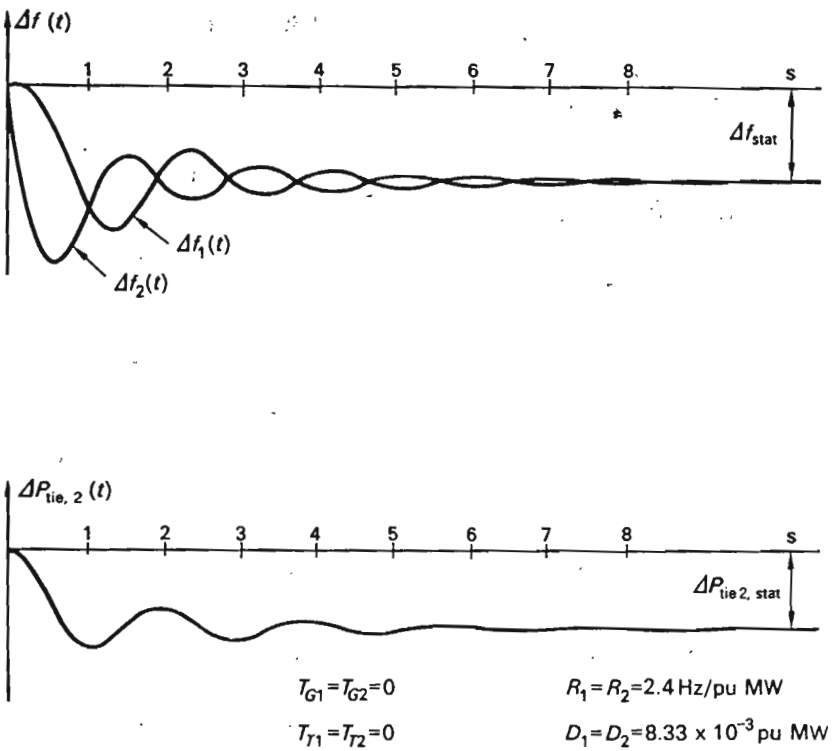


**Fig. 9-18** Frequency deviations in each area and the tie line power swings following a step load increase in area 2. Both area speed changers are fixed. Two areas identical.

**Dynamic response of uncontrolled two-area system** The system in Fig. 9-16 is of seventh order, even if we use the very simple turbine model in Eq. (9-12), and it would be entirely meaningless in an introductory text to attempt an analysis directly. It would be considerably more practical to put it on the analog computer. This we actually did, and obtained the results shown in Fig. 9-18.

It is possible, however, to expose some important characteristics by *analysis* by first making some reasonable and not too restrictive assumptions. We first state these:

*Assumption* 1 Consider the case of two *equal* areas.

*Assumption* 2 Consider the turbine controller *fast* relative to the rest of system, so that we can set $T_G = T_T = 0$, and therefore use $G_{GT1} = G_{GT2} = 1$.

*Assumption* 3 Neglect the system damping. This means that we assume the loads not to vary with frequency; i.e., we set $D_1 = D_2 = 0$. This

means, in accordance with Eqs. (9-28) to (9-30), that

$$G_{p1}(s) = G_{p2}(s) \rightarrow \frac{f^0}{s2H}$$

Based upon these assumptions, we can now obtain the following equations directly from the block diagram:

$$\Delta P_{G1}(s) = -\frac{1}{R}\Delta F_1(s)$$
$$\Delta P_{G2}(s) = -\frac{1}{R}\Delta F_2(s) \tag{9-55}$$

$$\Delta P_{\text{tie 1}}(s) = \frac{2\pi T_{12}^0}{s}[\Delta F_1(s) - \Delta F_2(s)]$$
$$\Delta P_{\text{tie 2}}(s) = -\Delta P_{\text{tie 1}}(s) \tag{9-56}$$

$$\Delta F_1(s) = \frac{f^0}{s2H}[\Delta P_{G1}(s) - \Delta P_{D1}(s) - \Delta P_{\text{tie 1}}(s)]$$
$$\Delta F_2(s) = \frac{f^0}{s2H}[\Delta P_{G2}(s) - \Delta P_{D2}(s) - \Delta P_{\text{tie 2}}(s)] \tag{9-57}$$

By substitution of Eqs. (9-55) and (9-56) into Eqs. (9-57), we can readily derive the following expression for the tie line power:

$$\Delta P_{\text{tie 1}}(s) = \frac{\Delta P_{D2}(s) - \Delta P_{D1}(s)}{s^2 + (f^0/2RH)s + 2\pi f^0 T_{12}^0/H}\frac{\pi f^0 T_{12}^0}{H} \tag{9-58}$$

This expression tells us several important facts:

1. The denominator being of the form

   $$s^2 + 2\alpha s + \omega^2 = (s + \alpha)^2 + \omega^2 - \alpha^2$$

   where $\alpha$ and $\omega^2$ are both positive, we know that the system is *stable* and *damped*.
2. Following a disturbance, the system will oscillate at the damped angular frequency

   $$\omega_0 = \sqrt{\omega^2 - \alpha^2} = \sqrt{\frac{2\pi f^0 T_{12}^0}{H} - \left(\frac{f^0}{4RH}\right)^2} \tag{9-59}$$

3. The system damping is strongly dependent upon the $\alpha$ parameter. Since $f^0$ and $H$ are essentially constants, *the damping will be a function of the R parameters.* Low $R$ values will give strong damping; high $R$ values, weak damping. The system will perform *undamped* oscillations of frequency $\omega_0 = \omega$ if $R = \infty$, that is, if the speed governor is nonexistent.
4. The fact that the system is *inherently* oscillatory could have been immediately predicted from the mechanical analog in Fig. 9-17.



**Example 9-2** Consider two equal areas, each having the parameters

$R = 3.0$ Hz/pu MW
$H = 5$ s
$f^0 = 60$ Hz

From Eq. (9-59) we thus get

$$\omega_0 = \sqrt{75.3T_{12}^0 - 1.0} \quad \text{r/s}$$

Assume the tie line has a capacity of 0.1 pu (10 percent of area capacity) and is operating at a power angle of 45°. From Eq. (3-6) we thus have

$$T_{12}^0 = 0.1 \cos 45° = 0.0707$$

The oscillating frequency is thus

$$\omega_0 = \sqrt{75.3 \times 0.0707 - 1.0} = 2.1 \text{ r/s} \quad \text{(or 0.33 Hz approx)}$$

The above *approximate* analysis confirmed stability. A more detailed analysis (see Refs. 12–14), taking all turbine and governor lags into account, reveals that with certain parameter combinations the system may actually turn *unstable*, a fact often confirmed by observations.

**The controlled two-area systems** The response curves in Fig. 9-18 indicate that, as in the single-area case, we must add integral control to our system. Let us state, first, the minimum requirements the system should meet.

*Suggested control-system specifications* We shall require that our system meet the four-point specifications that we stipulated for the single-area system in Sec. 9-2.3 In addition, we shall require that the steady-state tie line power variation, following a step load change, must be zero. This requirement guarantees that each area, in steady state, absorbs its own load—the guiding principle in pool operation.

*The tie line bias control strategy* Since we must now use a strategy that will cause *both* the frequency and tie line deviations to vanish, we shall, as in the single-area case, adopt integral control, but with the tie line deviation added to our area control error; i.e., we attempt

$$\text{ACE}_1 = \Delta P_{\text{tie 1}} + B_1 \Delta f_1$$
$$\text{ACE}_2 = \Delta P_{\text{tie 2}} + B_2 \Delta f_2 \tag{9-60}$$

The speed changer commands will thus be of the form

$$\Delta P_{c1} \triangleq -K_{I1} \int (\Delta P_{\text{tie }1} + B_1 \Delta f_1)\, dt \tag{9-61}$$

$$\Delta P_{c2} \triangleq -K_{I2} \int (\Delta P_{\text{tie }2} + B_2 \Delta f_2)\, dt \tag{9-62}$$

The constants $K_{I1}$ and $K_{I2}$ are integrator gains, and the constants $B_1$ and $B_2$ are the *frequency bias* parameters. This strategy has been indicated by the dotted portions in Fig. 9-16. The minus signs must be included since each area should *increase* its generation if *either* its frequency error $\Delta f_i$ *or* its tie line power increment $\Delta P_{\text{tie }i}$ is negative.

*Static system response* The chosen strategy will eliminate the steady-state frequency *and* tie line deviations for the following reason:

Following a step load change in either area, a new static equilibrium, *if such an equilibrium exists*, can be achieved only after the speed changer commands $\Delta P_{c1}$ and $\Delta P_{c2}$ have reached *constant* values. But this evidently requires that both integrands in Eq. (9-61) be zero; i.e.,

$$\Delta P_{\text{tie }1,\text{stat}} + B_1 \Delta f_{\text{stat}} = 0 \tag{9-63}$$

$$\Delta P_{\text{tie }2,\text{stat}} + B_2 \Delta f_{\text{stat}} = 0 \tag{9-64}$$

In view of Eq. (9-46), these conditions can be met *only* if

$$\Delta f_{\text{stat}} = \Delta P_{\text{tie }1,\text{stat}} = \Delta P_{\text{tie }2,\text{stat}} = 0 \tag{9-65}$$

*Note that this result is independent of the $B_1$ and $B_2$ values. In fact, one of the bias parameters (but not both) can be zero, and we still have a guarantee that Eq.* (9-65) *is satisfied.*

*Dynamic system response* The dynamic characteristics of the closed loop are as important as the static ones, if not more so. *From all we know at this stage, the proposed system may not even be stable.* To find the dynamic performance is still more difficult than in the uncontrolled case. The two added integrators have raised the system order to 9.

Without proof we give the following information pertaining to the stability properties of the "controlled" two-area system:

An approximate analysis based upon the same three simplifying assumptions as were used in arriving at Eq. (9-58) reveals that stability is *not* guaranteed as was the case for the "uncontrolled" system. For certain values of the integrator gains the oscillations will *grow*.



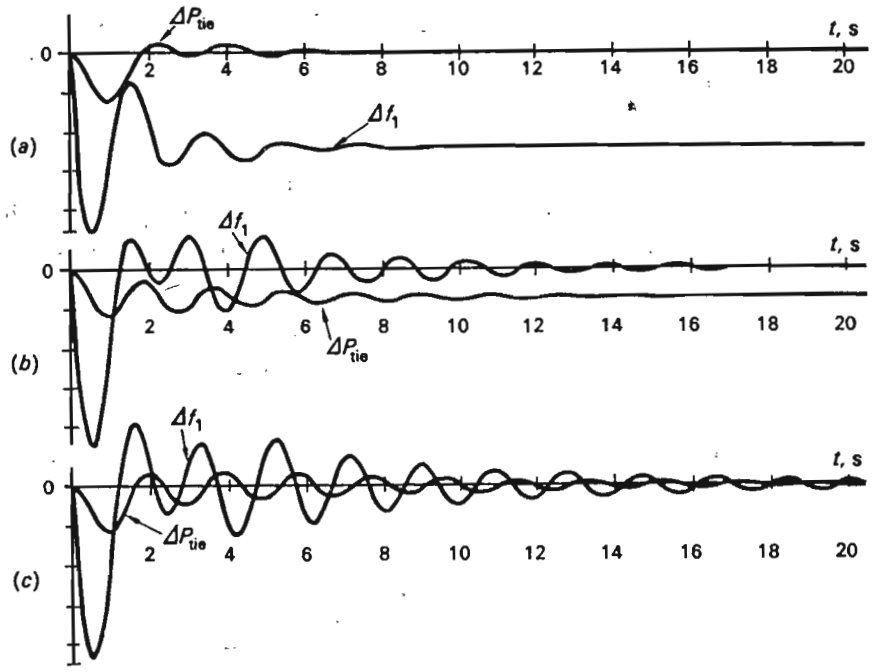


**Fig. 9-19** Frequency and tie line power deviations in a controlled two-area system following a step load disturbance. (Only area 1 frequency is shown.) The three cases correspond to the following widely different bias settings: (*a*) $B = 0$, $K_I = 1.0$; (*b*) $B = \infty$, $K_I B = 0.425$; (*c*) $B = 0.425$, $K_I = 1.0$. Remaining system parameters are the same as those used in Fig. 9-18.

The added integrators have contributed to the oscillatory nature of the system.

The situation is depicted in the simulated response graphs in Fig. 9-19. These recordings were obtained for the same system data as in Fig. 9-18.

The graphs of Fig. 9-19 depict the transient response for a step load change (in area 1). All graphs correspond to *stable* parameter combinations, but we have demonstrated the effect of varying the bias parameter $B$. Both areas are characterized by identical parameters. The graphs of Fig. 9-19*a* correspond to $B = 0$. The system now properly controls the tie line power, but the frequency will have a static error.

The graphs of Fig. 9-19*b* relate to the other extreme case, with $B = \infty$. (Note that the product $K_I B$ is finite, which means that $K_I = 0$.) The control actions are now insensitive to tie line power errors, and as a result we are left with a static power error, but the frequency is properly controlled.

The graphs of Fig. 9-19*c* show an intermediate case. Neither the frequency nor the tie line power will have any static error. *This is the practically important case!*

**Optimum parameter adjustment**† The graphs in Fig. 9-19*c* indicate clearly the great importance of proper parameter settings. The first and overriding requirement is the selection of a set of parameters which will result in a *stable* system. Having secured a stable system, our next objective must be to adjust the parameters until we have a "best" or optimum response.

*Control criterion* In developing strategies for optimum dispatch in the preceding chapter, we chose certain scalar cost functions on the basis of which we compared our strategies. We similarly need some meaningful measure for transient response. *Scalar integral error criteria*, or cost functions, have proved to be the most meaningful and convenient measures of dynamic performance.[1,2] Such a cost function is usually of the form

$$C \triangleq \int_0^\infty F(e_1, e_2, \ldots, e_n)\, dt \tag{9-66}$$

where $e_1, e_2, \ldots, e_n$ are the different "errors" that our control system is designed to eliminate. For example, in our system under discussion, the errors are represented by the frequency deviations $\Delta f_1$ and $\Delta f_2$ and the tie line power deviation $\Delta P_{\text{tie}}$. The function $F(\cdots)$ is a *penalty function* that determines the "cost" of the magnitude of the errors. The practical value of the error criterion depends upon the selection of a meaningful penalty function.

The effect of the integral in Eq. (9-66) is to add to the cost for as long as the errors persist. In summary, therefore, the effect of the function $F$ is to penalize the *magnitude* of the errors, and of the integral to penalize their *duration*.‡

A popular error criterion is the so-called *integral of the squared errors* (ISE) criterion,

$$C \triangleq \int_0^\infty (\alpha_1 e_1^2 + \alpha_2 e_2^2 + \cdots + \alpha_n e_n^2)\, dt \tag{9-67}$$

The constants $\alpha_\nu$ are weight factors the values of which determine the relative importance attached to the various errors $e_\nu$.

The quadratic functions $e_\nu^2$ attain relatively small magnitudes for small $e_\nu$ and relatively large magnitudes for large $e_\nu$, and the functions are always positive. It is clear, therefore, that the ISE criterion penalizes large errors of *any* signs, but is relatively lenient toward small errors. We shall choose the ISE criterion for the judgment of the two-area controller and shall specifically employ the criterion function

$$C \triangleq \int_0^\infty (\Delta P_{\text{tie}}^2 + \alpha\, \Delta f_1^2)\, dt \tag{9-68}$$

It is noted that we have not included $\Delta f_2$. The reason is that $\Delta f_1$ and $\Delta f_2$ behave in about the same manner, which means that inclusion of $\Delta f_2$ simply has the effect of increasing the weight factor $\alpha$.

Note also that the weight factor for $\Delta P_{\text{tie}}$ has been chosen unity. The reader should remember that, since we are interested in the *relative* magnitude of $C$ for various parameter settings, we can always set $\alpha_1$ in Eq. (9-67) equal to unity.

*Optimum-parameter search procedure* We shall exemplify the usage of the above cost criterion by finding the optimum parameters for a two-area system where, for simplicity, we shall assume that the two areas have identical parameters.

$$K_{I1} = K_{I2} = K_I$$

$$B_1 = B_2 = B$$

We proceed in the following steps:

1. Settle for a weight factor $\alpha$.
2. Investigate how the $C$ function depends upon the various parameters that are open for our choice. When we have tried all combinations, we choose those parameters which render $C$ a *minimum*.

The second step in the outlined procedure is, in practice, most cumbersome, should we attempt to use analysis. In principle, we would solve for $\Delta P_{\text{tie}}$ and $\Delta f_1$, substitute these solutions into Eq. (9-68), and evaluate the integral. This integral would, evidently, be a function of our two parameters; i.e.,

$$C = C(B, K_I)$$

If we were to plot the $C$ function versus the two parameters $B$ and $K_I$ in a three-dimensional coordinate system, we would obtain a bowl-shaped "cost surface," as depicted in Fig. 9-20 (compare also Fig. 8-2). The minimum point of this surface corresponds to the optimum parameter settings.

An analog computer is particularly useful in finding the optimum. It renders directly the functions $\Delta P_{\text{tie}}$ and $\Delta f_1$, and the only additional equipment needed is two multipliers to perform the squaring operations $\Delta P_{\text{tie}}^2$ and $\Delta f_1^2$. The summing and integrating operations called for in Eq. (9-68) are performed in regular summing and integrating amplifiers.

† The parameter-adjustment method presented here was suggested by Fosha and Elgerd.[13]

‡ The integration never needs to be extended over infinite time, of course. As noted in the graphs of Fig. 9-19, the errors will be negligible after finite time, and the integrations can be stopped without any appreciable effect on accuracy.

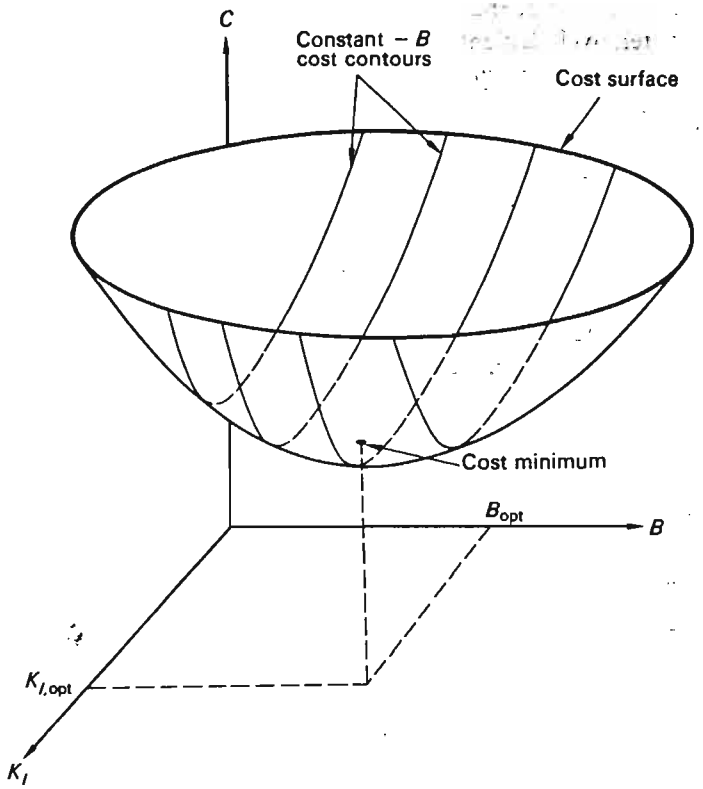


**Fig. 9-20** Cost surface for evaluation of transient response.

The most practical computer procedure is to fix one of the parameters, say, $B$, and then vary the other parameter in steps. In this way we obtain the "constant-$B$ cost contours" shown in Fig. 9-20.

**Example 9-3** We performed an optimum study of a two-area system characterized by the following realistic parameter values:

$P_{r1} = P_{r2} = 2000$ MW
$H_1 = H_2 = 5$ s
$D_1 = D_2 = 8.33 \times 10^{-3}$ pu MW/Hz
$R_1 = R_2 = 2.4$ Hz/pu MW
$T_{G1} = T_{G2} = 0.08$ s
$T_{T1} = T_{T2} = 0.3$ s
$P_{\max,12} = 200$ MW (tie line capacity)
$\delta_1^0 - \delta_2^0 = 30°$ (nominal tie line power angle)
$\beta_1 = \beta_2 = 0.425$ pu MW/Hz (AFRC)



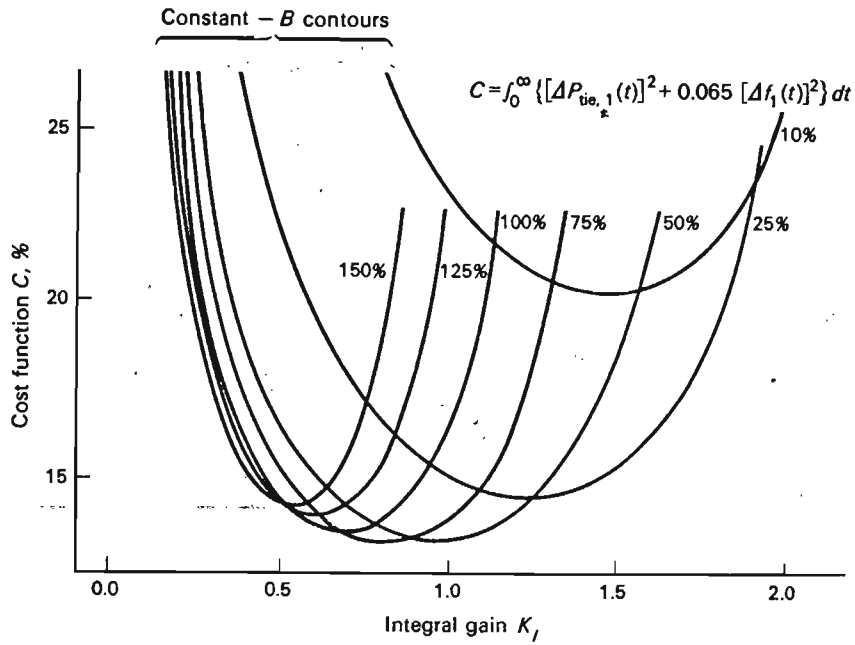


**Fig. 9-21** Constant-$B$ contours. These curves correspond to a weight factor $\alpha = 0.065$.

The system was simulated on an analog computer, the gain parameters $B$ and $K_I$ were adjusted, and the cost criterion $C$ was measured for each value pair. The results of the study are summarized in Figs. 9-21 and 9-22.

The cost contours in Fig. 9-21 correspond to a weight factor $\alpha = 0.065$. This value, obtained by trial and error, represents the particular case where the two terms in the integrand of Eq. (9-68) contribute equally to the integral as measured at the optimum point. In other words, we attach equal significance to tie line power and frequency errors.

The cost contours in Fig. 9-22 correspond to $\alpha = 0$; i.e., we attach all importance to the tie line power swings. In both figures we have plotted $C$ versus $K_1$, with the $B$ parameter varied in steps throughout the range

$$0.1\beta < B < 1.50\beta$$

In both cases we obtain an optimum setting that corresponds to the value pair

$$K_I \approx 1$$
$$B \approx 0.5\beta = 0.21 \text{ pu MW/Hz}$$

We conclude, from Eqs. (9-61) and (9-62), that the optimum control strategy is

$$\Delta P_{c1} = -\int (\Delta P_{\text{tie }1} + 0.21\,\Delta f_1)\,dt$$
$$\Delta P_{c2} = -\int (\Delta P_{\text{tie }2} + 0.21\,\Delta f_2)\,dt \qquad (9\text{-}69)$$

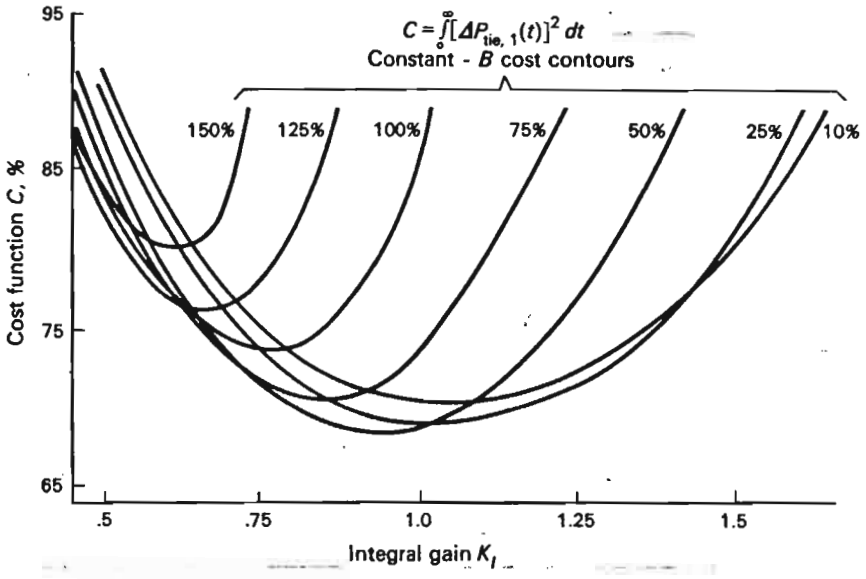


**Fig. 9-22** Constant-$B$ contours. Weight factor is now $\alpha = 0$.

The response curves in Fig. 9-19*c* correspond to these optimum parameter settings.

We make the following observations in regard to our results:

1. The above results apply, of course, only if the system parameters are those earlier assumed. For example, we had assumed a nonreheat turbine. We have no guarantee that our results apply for a reheat type.
2. The U.S. utility industry presently uses the recommended bias setting

   $$B = \beta$$

   which is twice the optimum value we have found. The industry does not make any specific recommendations concerning $K_I$. It does use a very low integrator gain, resulting in a very slow secondary adjustment. The motivation, as in the single-area case, is that the turbine controller should not attempt to "chase" the fast load swings.
3. Even with optimum-parameter choice, the oscillatory response curves in Fig. 9-19*c* certainly indicate a *poor stability margin*. This fact casts a doubt upon the control strategy presently used, and should serve as a motivation to seek better strategies. This we will do in Sec. 9-4.

We assumed in our analysis and simulations that the measurements of frequency and tie line power errors are performed *continuously*. In practice these variables are measured at fixed intervals in a *sampled-data* system. However, if the sampling rate is sufficiently high and the signals properly filtered, the results deviate very little from those we have presented.



***Pf* control of *n*-area system** The method of load frequency control discussed above for a two-area system can be *intuitively* extended to an $n$-area system. Let us consider a power pool consisting of $n$ individual areas. The $\nu$th area is connected to one or several of the other areas via tie lines over which it is exporting a total scheduled power which must be kept constant, in keeping with our fundamental pool-operation principle. We propose now, in analogy with Eqs. (9-60), an ACE of the form

$$\text{ACE}_\nu = \Delta P_{\text{tie},\nu} + B_\nu \Delta f_\nu \tag{9-70}$$

where $\Delta P_{\text{tie},\nu}$ represents the change of the total area power export *measured positive out from the area.*

As in the case of the two-area system, the area control errors must be integrated in order to eliminate the static errors; i.e., we form a speed-changer command signal of the form

$$\Delta P_{c\nu} = -K_{I\nu} \int \text{ACE}_\nu\, dt \tag{9-71}$$

We have now, in effect, $2n$ gain parameters, $K_{I\nu}$ and $B_{I\nu}$, to be selected. Beyond the recommendation that each area should set its bias parameter equal to its own AFRC, there seems to be no penetrating study that considers the *overall* problem. The author feels that much additional research needs to be done in this field. Here are some suggested research objectives:

1. Finding of more definite rules for optimum-parameter settings than those presently used. This could take the form of an extension of the above two-area analysis, based on the ISE criterion.
2. Investigation of the approximation involved in treating the $n$-area problem as a two-area problem (with one area much larger than the other).
3. Analysis of the effect of tie line strength and speed regulation.
4. A sensitivity analysis of the effects of turbine, generator, and other system parameters on the $C$ criterion.
5. Development of more advanced optimum control strategies (Sec. 9-4).

## 9-3 THE MEGAVAR VOLTAGE CONTROL PROBLEM

We have studied in considerable detail the megawatt frequency control problem for both single- and multiple-area systems. Basically, the problem was defined as one of keeping a delicate balance between the generated and consumed *real* power in the system, the frequency being the indicator that this balance is maintained. In the multiple-area system, we also had to

balance the real power within each individual area by sensing the changes in the tie line flow.

We now turn our attention to the second part of our systems control problem, that of controlling the *reactive* power balance within the system.

As pointed out earlier, an imbalance between the generated and demanded reactive power results in a bus voltage deviation. Sensitivity analysis has shown that the deviation will be largest at the bus where the reactive imbalance occurs.

### 9-3.1 CONTROL STRATEGY

There are, obviously, great similarities between the megawatt frequency and megavar voltage control problems. It is tempting, therefore, in selecting a suitable control strategy, in the latter case, to draw from our knowledge of the former. For example, we may define a *reactive control error*, RCE, and then, *intuitively*, by replacing frequency by voltage and megawatts by megavars, obtain, in the single-area case, in analogy with Eqs. (9-38) and (9-39),

$$\text{RCE} \triangleq \Delta |V|_{\text{av}} \tag{9-72}$$

$$\Delta Q_c = -K_I \int \text{RCE}\, dt$$

$\Delta |V|_{\text{av}}$ is a measure of the voltage level error of the buses in the control area and could, for example, be the average value of the errors of all bus voltages or a representative sample set.

$\Delta Q_c$ is the command signal to the $Q$ generator (or generators) of the area.

In the multiple-area case the control strategy, in analogy with Eqs. (9-70) and (9-71), should be

$$\text{RCE}_\nu \triangleq \Delta Q_{\text{tie},\nu} + C_\nu \Delta |V|_{\text{av},\nu} \tag{9-73}$$

$$\Delta Q_{c\nu} = -K_{I\nu} \int \text{RCE}_\nu\, dt$$

$\Delta Q_{\text{tie},\nu}$ is here the deviation in tie line reactive power (measured positive away from the area), and $C_\nu$ is an "area voltage bias" parameter measured in megavar per volt.

It should be noted that $\Delta Q_c$ in the above equations represents the *total* area reactive control command (compare the same meaning of $\Delta P_c$ in the preceding section).

Although the proposed strategy [Eq. (9-73)] is very attractive from a symmetry point of view, the author knows of no case where it has been



actually adopted. There are several reasons for this, of which the three most important are:

1. Generation of reactive power does not involve monetary costs to the same extent as generation of real power. For example, we do not have any equivalent of fuel costs. There is, of course, the installation and maintenance cost of $Q$ sources (capacitor banks and condensers) and $Q$ sinks (shunt reactors). In the case of real-power generation, we based our optimum $P$ dispatch entirely on economic criteria. Optimum $Q$ dispatch is based in part on economic consideration (it was pointed out in Chap. 8 that the $Q$ flow does affect the real-power losses, and thus the transmission costs) and in part on other considerations. Our mathematical criterion for optimum $Q$ dispatch will therefore have to be more complicated than that which governed our $P$ dispatch. (See also point 3 below.)
2. There is no practical need for controlling the voltage level to the same accuracy as the frequency. For example, whereas the frequency is controlled to within $\pm 0.03$ percent, the accuracy limits for bus voltages are of the order $\pm 1$ percent. Also, we required the steady-state frequency error to vanish, following a step load change. Static voltage errors can be tolerated, and this then eliminates the need for integral control.
3. In a typical power system the normal daily fluctuations in the reactive demand pose entirely different problems during the day hours as compared with the night hours.

   During the hours of heavy real-power demand we also find the largest demand for reactive power. The concern now is to dispatch the reactive power in such a manner as to minimize the real line losses.

   During the hours of light real load the $Q$ demand decreases to a minimum. If our system contains long transmission lines and/or extensive cables, we may find that the capacitive $Q$ generation is of such large magnitude that we have a *surplus* of reactive power. Our concern is now to get rid of this surplus. The chances are that our operating neighbors have the same problem; so we cannot export the surplus power. We may route it to our various generators, and by underexciting these, we may force them to absorb the reactive power. However, in so doing we are decreasing the machine emfs, and thus weakening the machines electrically, resulting in reduced stability margins. We may, actually, be forced to install shunt reactors that will consume the surplus reactive power. Our criterion for optimum $Q$ dispatch, which during peak load should be based upon loss minimization, should evidently, during night hours, be based upon best elimination of the reactive surplus power.

The control strategy most often used is characterized by the following main features:

1. Each generator bus is voltage-controlled individually.
2. The voltage profile of the system is preselected on the basis of a load flow study.
3. The voltage profile is changed periodically to account for the changing load patterns.

### 9-3.2 FUNDAMENTAL CHARACTERISTICS OF TYPICAL EXCITATION SYSTEM

Excitation control systems come in many shapes and varieties, just as was the case with turbine control systems. Figure 9-23 depicts a typical species. The main generator field is fed from a dc generator (*exciter*), which usually is driven from the same turbine shaft as the generator itself. The exciter field is controlled via an amplifier. Due to the exciter size, this amplifier usually consists of several stages. We have indicated only one.

**Transfer function model of exciter system** We present now a transfer function model for this system. The variables used in the following analysis are defined in Fig. 9-23. We treat the various components in the following order:

*Voltage comparator* This device compares the terminal voltage $|V|$ of the generator with a reference voltage which is set equal to the nominal

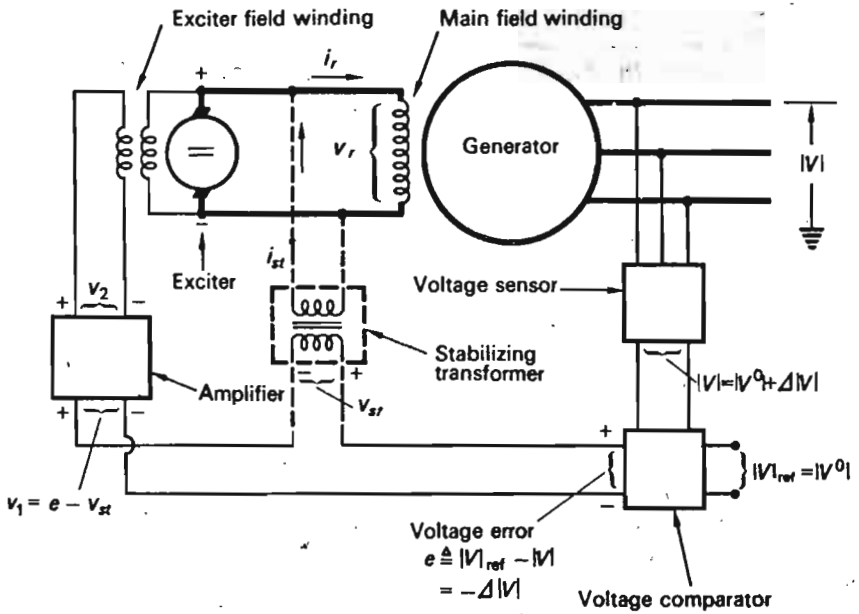


**Fig. 9-23** Typical voltage regulator.



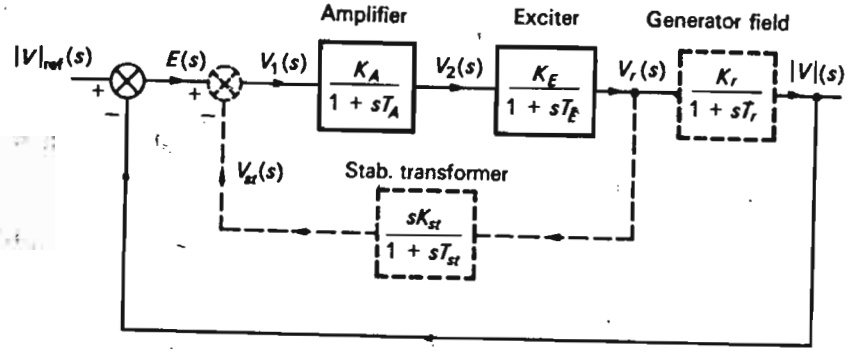


**Fig. 9-24** Block-diagram representation of voltage regulator in Fig. 9-23.

voltage $|V^0|$. The voltage error therefore equals

$$e \triangleq |V|_{ref} - |V| = |V^0| - (|V^0| + \Delta|V|) = -\Delta|V| \tag{9-74}$$

*Amplifier* This device can be characterized by a gain factor $K_A$ and a time constant $T_A$, the latter parameter typically having a magnitude of less than 100 ms. The transfer function of the amplifier is thus

$$\frac{V_2(s)}{V_1(s)} = \frac{K_A}{1 + sT_A} \tag{9-75}$$

*Exciter* This device, basically also an amplifier, has a similar transfer function.

$$\frac{V_f(s)}{V_2(s)} = \frac{K_E}{1 + sT_E} \tag{9-76}$$

$T_E$, the time constant of the exciter field winding, has typically a value of about 1 s.

**Generator representation** The model developed so far takes us up to the terminals of the generator field. It is necessary, of course, in order to be able to "close the loop" in Fig. 9-24, to derive the transfer characteristics of the generator itself, i.e., to find the transfer function which relates the rotor field voltage $v_f$ to the terminal voltage $|V|$.

*This transfer function depends to a certain extent upon the nominal operating state of the generator*, and we shall here derive it under the simplest of operating conditions. We shall assume that the generator is running open-circuited or operating into a network which is so lightly loaded that the impedance as viewed from the generator terminals is comparatively large. Under this assumption we can neglect the stator currents. As a consequence, the direct-axis current component $i_d$ will be of negligible magnitude, and the

last of Eqs. (4-36) takes on the simple form

$$v_r = r_r i_r + L_4 \frac{di_r}{dt} \tag{9-77}$$

Under no-load conditions the terminal voltage equals the generator emf, and from Eq. (4-46), we thus get

$$|V| = |E| = \frac{\omega L_5 i_r}{\sqrt{2}} \tag{9-78}$$

From Eqs. (9-77) and (9-78), we get

$$\frac{|V|(s)}{V_r(s)} = \frac{\omega L_5}{\sqrt{2}(r_r + sL_4)} = \frac{\omega L_5}{\sqrt{2} r_r} \frac{1}{1 + s(L_4/r_r)} \triangleq \frac{K_r}{1 + sT_r} \tag{9-79}$$

which is our sought transfer ratio. The time constant $T_r \triangleq L_4/r_r$ of the rotor field winding typically has a magnitude of several seconds.

If the generator carries stator currents, then we cannot, in general, neglect the derivative term $di_d/dt$ in Eq. (4-36). The resulting magnetic coupling between the stator and rotor introduces considerable complexity into our model.† The *essential* behavior of the generator can still be described in terms of a transfer function of the type of Eq. (9-79). The presence of stator currents reduces the time constant $T_r$ (see also the discussion on transient reactance, in the next chapter).

**Stabilizing circuit** We have concluded that the voltage control loop contains at least three time constants; i.e., its open-loop transfer function contains three negative real poles. The stability of this loop, as demonstrated by the root-locus plot in Fig. 9-25, would be impaired for high loop gains. Since the time constant $T_r$ is very large, we need very high loop gain in order to reduce the response time of the loop. This would inevitably render the system unstable.

The system can be stabilized in many ways. We have suggested one arrangement in Fig. 9-23, consisting simply of a transformer, which provides us with "derivative feedback"—the universal cure for unstable control systems. The device supplies a voltage, $v_{st}$, which is proportional to the derivative of $i_{st}$ and thus essentially also to $v_r$. This voltage, which therefore exists *before* $v_r$ has changed, is subtracted from the error voltage, and therefore in effect tells the amplifier to "go easy."

Mathematically, we can state this as follows:

First we have, for the transformer output,

$$v_{st} = M \frac{di_{st}}{dt}$$

† A more accurate model is presented in Sec. 12-5.2.



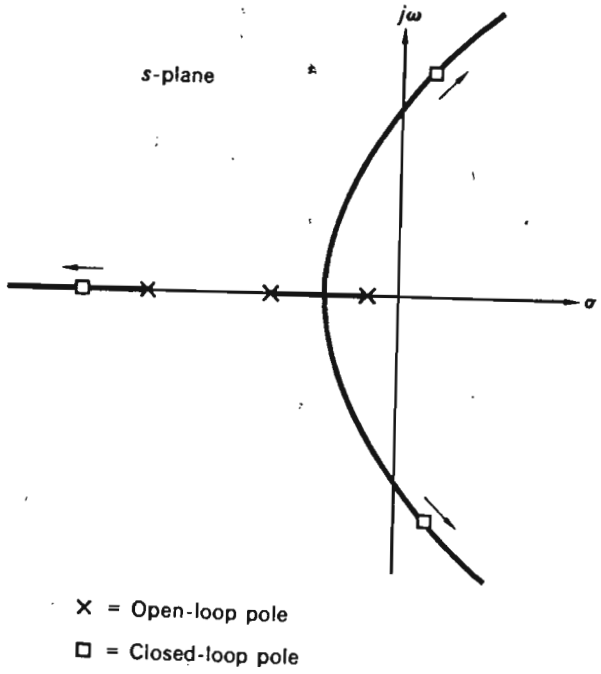


**Fig. 9-25** Root loci for unstabilized regulator. Instability indicated for high loop gain.

For the primary current we have the relation

$$v_r = Ri_{st} + L \frac{di_{st}}{dt}$$

Thus

$$\frac{V_{st}(s)}{V_r(s)} = \frac{sM}{R + sL} \triangleq \frac{sK_{st}}{1 + sT_{st}} \approx sK_{st} \tag{9-80}$$

The last approximation follows if we intentionally make

$$R \gg L$$

The reader should verify that the effect of the transformer is to add a zero to the three existing poles of the open-loop transfer function. This zero "bends" the unstable root loci of the uncompensated system into the stable $s$ plane, as shown in Fig. 9-26.

### 9-3.3 NEWER ASPECTS OF THE MEGAVAR VOLTAGE CONTROL PROBLEM

The megavar voltage control method discussed above aims at keeping a preselected bus voltage profile constant, in spite of the changing reactive

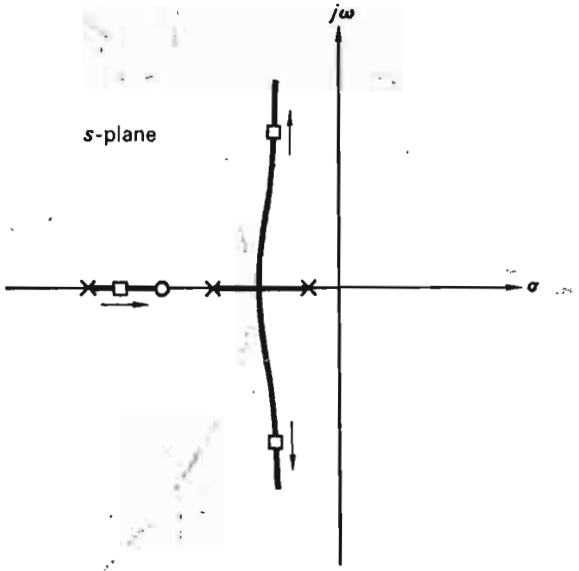


**Fig. 9-26** Root loci for stabilized regulator. Loop stable for high gains.

demand. The voltage profile is usually selected from a load flow study, and the choice is based (when a logical base is indeed used) upon transmission loss minimization.

We pointed out in Chap. 8 that the transmission losses are relatively small in most systems, and what we in fact are doing, therefore, is to minimize a scalar quantity the magnitude of which may be negligible even under the worst of operating conditions.

Clearly, it is fair to question whether other criteria exist which could equally well serve as a basis for our selection of an "optimum" $Q$ flow and which have at least equal or better value than the loss minimization criterion.

As of this writing the industry is taking a new critical look at the overall problem of reactive power control. Several questions are being asked, most of them presently lacking answers:

1. To what extent can the overall system operation be improved by controlling the interpool $Q$ flow?
2. Is it possible to increase the stability margin of a system by using $Q$ flow control strategies different from the present one?
3. Should the $Q$ flow criteria be different during high- and low-load periods? Specifically, what criteria should be used?



4. It was pointed out earlier that there is coupling between the $QV$ and $Pf$ control channels. Can this coupling be used to advantage?

In Sec. 8-4 we presented an example where a novel control criterion for reactive power was suggested. In the next section we shall see how, by the methods of modern optimum control, we can utilize the existing coupling between $QV$ and $Pf$ channels to improve the damping of the latter.

## 9-4 OPTIMUM SYSTEMS CONTROL

The control methods discussed in the preceding sections of this chapter could be referred to as "classical," since they represent (with some minor modifications) the present standard in the U.S. power industry.

A critical appraisal of presently employed control methods reveals several shortcomings:

1. The control strategies used [Eqs. (9-60), for example] are based entirely upon intuitive reasoning. Even if optimum-parameter-adjustment methods are used, the system response is very oscillatory. This is confirmed by the graphs of Fig. 9-19*c*, which apply to an optimally parameter-adjusted case.
2. Indeed, it can be shown analytically[14] that presently existing control loops may easily go unstable. Such occurrences have, in fact, been recorded. For example, recent attempts to synchronize the eastern and western power blocks in the United States have been only partially successful. Under certain operating conditions the tie lines have experienced power swings of increasing amplitudes, necessitating severance of the interconnection. This is, of course, a classical symptom of an unstable control system. Other parts of the U.S. grid have on occasion experienced similar instabilities.
3. No consideration is given to the coupling between the $Pf$ and $QV$ control channels.

### 9-4.1 "STATIC" VERSUS "DYNAMIC" STABILITY

We must also remember that we are discussing system stability in regard to *small perturbations*, sometimes referred to as "static" stability. The real test of the strength of the system "fabric" is the ability of a system to survive the shocks of *major* disturbances. This so-called "dynamic," or "transient," stability will be discussed in Chap. 12.

At this time we shall point out only that there is an important correlation between these two stability concepts. Consider the two situations depicted in Fig. 9-27. Both systems are "statically" stable, since both balls will return to the stable equilibrium positions following *small* disturbances.

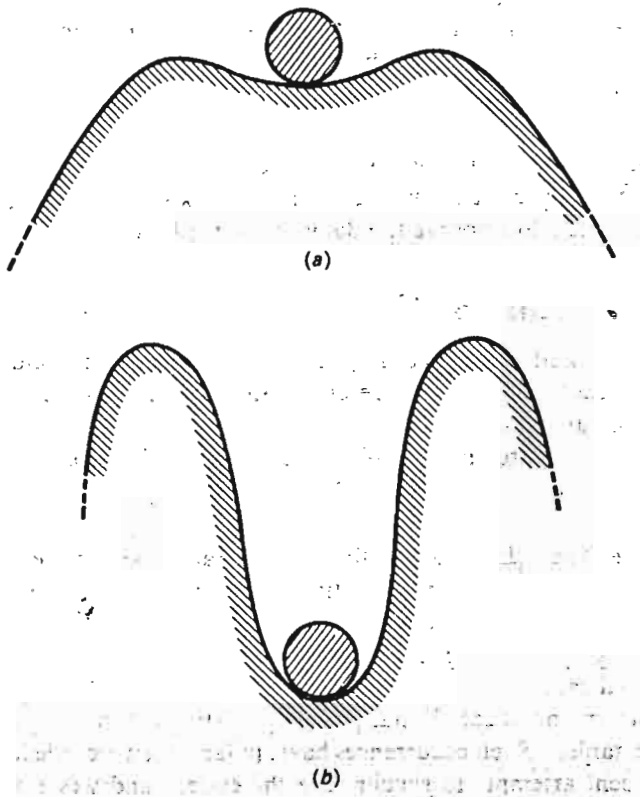


**Fig. 9-27** Both these systems are stable. System *b* has a better margin of stability.

It is obvious, however, that system *b* has a higher "dynamic" stability margin than system *a*. The lesson that this simple example teaches us is that we must strive to provide a system with the widest possible "static" stability margin in order to obtain at the same time the best possible "dynamic" margin. Presently employed control methods are certainly not optimal in this respect.

### 9-4.2 NEED FOR A NEW APPROACH

In two recent technical reports Fosha and Elgerd[13,14] have presented a novel approach to the power system control problem.† It can be said with confidence at this early stage that the suggested control methods offer considerable improvements over present methods in regard to their "static" stability properties. We shall give a brief exposé of the methods, but must refer the reader to the original reports and to other sources[1,2] for a more detailed coverage.

† As this is being written, additional contributions[39] are being published that closely relate to this problem.



The new control strategy is based on the design methods of modern control theory. We summarize the basic features of this theory:

1. No a priori assumption need be made about the structure of the control system or the control strategy.
2. It is necessary, in order to make use of the theory, to put the system models in so-called *state-variable form.*
3. An optimum control criterion must be preselected.
4. The theory can be applied (by use of digital computer) to systems of any order. This means, in our case, that we can find with ease the optimum controllers for general *n*-area systems.

Let us examine how to go about finding the optimum controller in our case.

### 9-4.3 DEVELOPMENT OF DYNAMIC STATE-VARIABLE MODEL FOR TWO-AREA SYSTEM

A prerequisite for making use of the optimum control theory is the availability of a dynamic system model in *state-variable* form. All our earlier system models have been in block-diagram (or "input-output") form.

Let us exemplify now how one may go about assembling a state model by considering the "uncontrolled" two-area system in Fig. 9-16. From this block diagram (the dotted portion not included), we have by inspection

$$\Delta F_1 = \frac{K_{p1}}{1 + sT_{p1}} (\Delta P_{G1} - \Delta P_{D1} - \Delta P_{\text{tie }1})$$

$$\Delta F_2 = \frac{K_{p2}}{1 + sT_{p2}} (\Delta P_{G2} - \Delta P_{D2} - a_{12}\,\Delta P_{\text{tie }1})$$

$$\Delta X_{E1} = \frac{1}{1 + sT_{G1}} \left(\Delta P_{c1} - \frac{1}{R_1}\,\Delta F_1\right)$$

$$\Delta X_{E2} = \frac{1}{1 + sT_{G2}} \left(\Delta P_{c2} - \frac{1}{R_2}\,\Delta F_2\right) \tag{9-81}$$

$$\Delta P_{G1} = \frac{1}{1 + sT_{T1}}\,\Delta X_{E1}$$

$$\Delta P_{G2} = \frac{1}{1 + sT_{T2}}\,\Delta X_{E2}$$

$$\Delta P_{\text{tie }1} = \frac{2\pi T_{12}{}^{0}}{s} (\Delta F_1 - \Delta F_2)$$

By inverse Laplace transformation of the above seven equations, we obtain the following set of seven differential equations:

$$\frac{d}{dt}\Delta f_1 = \frac{1}{T_{p1}}(-\Delta f_1 + K_{p1}\Delta P_{G1} - K_{p1}\Delta P_{D1} - K_{p1}\Delta P_{\text{tie }1})$$

$$\frac{d}{dt}\Delta f_2 = \frac{1}{T_{p2}}(-\Delta f_2 + K_{p2}\Delta P_{G2} - K_{p2}\Delta P_{D2} - K_{p2}a_{12}\Delta P_{\text{tie }1})$$

$$\frac{d}{dt}(\Delta x_{E1}) = \frac{1}{T_{G1}}\left(-\Delta x_{E1} + \Delta P_{c1} - \frac{1}{R_1}\Delta f_1\right)$$

$$\frac{d}{dt}(\Delta x_{E2}) = \frac{1}{T_{G2}}\left(-\Delta x_{E2} + \Delta P_{c2} - \frac{1}{R_2}\Delta f_2\right) \tag{9-82}$$

$$\frac{d}{dt}(\Delta P_{G1}) = \frac{1}{T_{T1}}(-\Delta P_{G1} + \Delta x_{E1})$$

$$\frac{d}{dt}(\Delta P_{G2}) = \frac{1}{T_{T2}}(-\Delta P_{G2} + \Delta x_{E2})$$

$$\frac{d}{dt}(\Delta P_{\text{tie }1}) = 2\pi T_{12}^0(\Delta f_1 - \Delta f_2)$$

At this time we define the *state vector* $\mathbf{x}$, consisting of the seven *state variables*:

$$\mathbf{x} = \begin{bmatrix} x_1 \\ x_2 \\ x_3 \\ x_4 \\ x_5 \\ x_6 \\ x_7 \end{bmatrix} \triangleq \begin{bmatrix} \Delta f_1 \\ \Delta f_2 \\ \Delta x_{E1} \\ \Delta x_{E2} \\ \Delta P_{G1} \\ \Delta P_{G2} \\ \Delta P_{\text{tie }1} \end{bmatrix} \tag{9-83}$$

and also the *control force vector* $\mathbf{u}$ and the *disturbance vector* $\mathbf{p}$:

$$\mathbf{u} = \begin{bmatrix} u_1 \\ u_2 \end{bmatrix} \triangleq \begin{bmatrix} \Delta P_{c1} \\ \Delta P_{c2} \end{bmatrix} \qquad \mathbf{p} = \begin{bmatrix} p_1 \\ p_2 \end{bmatrix} \triangleq \begin{bmatrix} \Delta P_{D1} \\ \Delta P_{D2} \end{bmatrix} \tag{9-84}$$

In terms of these vectors we can write Eqs. (9-82) more compactly:

$$\dot{\mathbf{x}} = \mathbf{A}\mathbf{x} + \mathbf{B}\mathbf{u} + \mathbf{\Gamma}\mathbf{p} \tag{9-85}$$



The *system matrix* $\mathbf{A}$, the *input distribution matrix* $\mathbf{B}$, and the *disturbance distribution matrix* $\mathbf{\Gamma}$ are defined as follows:

$$\mathbf{A} \triangleq \begin{bmatrix} -\frac{1}{T_{p1}} & 0 & 0 & 0 & \frac{K_{p1}}{T_{p1}} & 0 & -\frac{K_{p1}}{T_{p1}} \\ 0 & -\frac{1}{T_{p2}} & 0 & 0 & 0 & \frac{K_{p2}}{T_{p2}} & -a_{12}\frac{K_{p2}}{T_{p2}} \\ -\frac{1}{R_1 T_{G1}} & 0 & -\frac{1}{T_{G1}} & 0 & 0 & 0 & 0 \\ 0 & -\frac{1}{R_2 T_{G2}} & 0 & -\frac{1}{T_{G2}} & 0 & 0 & 0 \\ 0 & 0 & \frac{1}{T_{T1}} & 0 & -\frac{1}{T_{T1}} & 0 & 0 \\ 0 & 0 & 0 & \frac{1}{T_{T2}} & 0 & -\frac{1}{T_{T2}} & 0 \\ 2\pi T_{12}^0 & -2\pi T_{12}^0 & 0 & 0 & 0 & 0 & 0 \end{bmatrix} \tag{9-86}$$

$$\mathbf{B} \triangleq \begin{bmatrix} 0 & 0 \\ 0 & 0 \\ \frac{1}{T_{G1}} & 0 \\ 0 & \frac{1}{T_{G2}} \\ 0 & 0 \\ 0 & 0 \\ 0 & 0 \end{bmatrix} \qquad \mathbf{\Gamma} \triangleq \begin{bmatrix} -\frac{K_{p1}}{T_{p1}} & 0 \\ 0 & -\frac{K_{p2}}{T_{p2}} \\ 0 & 0 \\ 0 & 0 \\ 0 & 0 \\ 0 & 0 \\ 0 & 0 \end{bmatrix} \tag{9-87}$$

The reader should perform the matrix vector products called for in Eq. (9-85) and verify that he indeed obtains Eqs. (9-82).

The systematically written system of differential equations (9-85) represents our sought dynamic "state-variable model."

For the benefit of those readers who persist in seeing everything in block form, we present in Fig. 9-28 a symbolic representation of Eq. (9-85).

It must be emphasized that the dynamic state model can be put into the vector form of Eq. (9.85) only if the differential equations are *linear*. Should the differential equations be *nonlinear*, we can write them in the more general form (the symbol $\dot{(\cdot)}$ is shorthand for $d(\ )/dt$).

$$\dot{\mathbf{x}} = \mathbf{f}(\mathbf{x},\mathbf{u},\mathbf{p}) \tag{9-88}$$

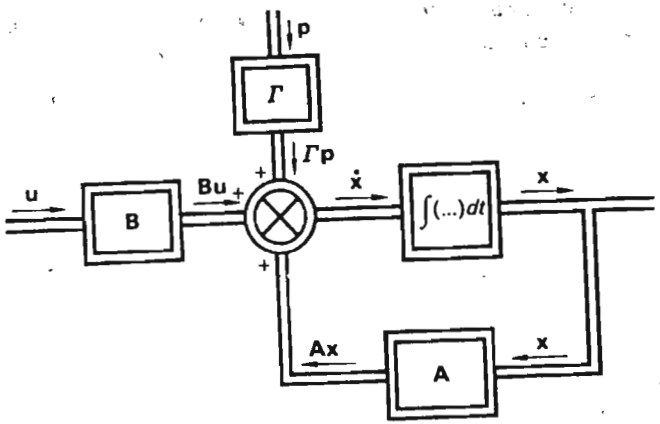


**Fig. 9-28** Block representation of state model.

We shall have an opportunity to use this form in Chap. 12. Note that if all state variables are *constant*, then the derivative vector $\dot{\mathbf{x}}$ vanishes, and the vector differential equation (9-88) reduces to the *algebraic* form

$$\mathbf{0} = \mathbf{f}(\mathbf{x},\mathbf{u},\mathbf{p})$$

(The *static* load flow equations in Chap. 7 appeared in this form, as the reader may recall.)

The advantages of having our dynamic system model put into the form of Eq. (9-85) can be summarized as follows:

1. Modern control theory is based upon this "standard" form.
2. By arranging the system parameters into matrices **A**, **B**, and **Γ**, we have set the stage for a very "organized" methodology of solving the system equations either analytically or by computer. This becomes important for huge systems, where a lack of organization easily results in errors.

As was evidenced by the preceding example, the state variables always have physical meaning, and are mostly measurable quantities. In defining the set of state variables, or *state*, for a particular physical system, one should keep the following general rule in mind:

*The state of a system is the minimum set of variables that contain sufficient information about the past history of the system to permit computation of all future states, assuming, of course, that all future control inputs are known and also the equations describing the system.*

The model derived above referred to a two-area system containing nonreheat turbines. (Reheat turbines have more complicated models and would require the introduction of additional state variables.) For every additional control area we would need to add three more state variables $\Delta f_i$, $\Delta P_{Gi}$, and $\Delta x_{Ei}$, plus one for each added tie line.



### 9-4.4 OPTIMUM CONTROL CRITERION

Having obtained a dynamic system state model, our next concern should be to select a dynamic optimum control criterion.

We shall again make use of the ISE criterion, but modified in one important respect. In addition to penalizing the "errors," we shall also penalize the control forces, the reason being that if we did *not* penalize them, they might take on infinite values (impulses) in our analysis.† This would not be consistent with physics.

For example, in our two-area system above, we may wish to penalize the frequency errors $\Delta f_1$ and $\Delta f_2$ and the control efforts $\Delta P_{c1}$ and $\Delta P_{c2}$, and should then use the criterion function

$$C \triangleq \int_0^\infty (\alpha_1 \Delta f_1^2 + \alpha_2 \Delta f_2^2 + \beta_1 \Delta P_{c1}^2 + \beta_2 \Delta P_{c2}^2)\, dt \tag{9-89}$$

which in view of matrices (9-83) and (9-84) will take on the form

$$C \triangleq \int_0^\infty (\alpha_1 x_1^2 + \alpha_2 x_2^2 + \beta_1 u_1^2 + \beta_2 u_2^2)\, dt \tag{9-90}$$

The $\alpha$'s and $\beta$'s are weight factors.

More generally, if *all* the $n$ state variables and *all* the $m$ control forces are penalized, the criterion function will have the form

$$C \triangleq \int_0^\infty (\alpha_1 x_1^2 + \cdots + \alpha_n x_n^2 + \beta_1 u_1^2 + \cdots + \beta_m u_m^2)\, dt \tag{9-91}$$

If a controller can be found that will minimize the $C$ function, the resulting control loop will be "optimally" stable.

### 9-4.5 OPTIMUM CONTROL STRATEGY

Having assembled a state model that adequately describes the incremental dynamic behavior of the system, and having settled for an optimum control criterion, we seek next an "optimum controller." Let us first state more precisely the job this controller must perform. The "optimum control problem" can be stated in many alternative ways. We shall choose the following one, which nicely fits our specific problem type.

*A system rests initially in a constant steady state, when it is suddenly disturbed by a set of step-type disturbances. Following an unavoidable transitory period, the system is required to reach a new prescribed steady state*

† The reader should contemplate why we did not penalize the control forces in our earlier "optimum parameter adjustment" technique.

*(for example, the original one). We seek a set of control forces* $\mathbf{u} = \mathbf{u}_{opt}$ *which not only will take the system to this new prescribed state, but will do so by simultaneously minimizing the chosen control criterion C.*

As an example, consider the curves in Fig. 9-18. As the reader will recall, they represented an uncontrolled (that is, $\mathbf{u} = \mathbf{0}$) two-area system subject to a step load increase in area 2. The system evidently changed from an initial constant zero state to another constant, but nonzero, final state in a very oscillatory manner. If we were to control this system optimally by adding control forces $\Delta P_{c1}$ and $\Delta P_{c2}$, we could specify, for example, the following two alternative control requirements:

*Alternative* 1 The control strategy $\mathbf{u} = \mathbf{u}_{opt}$ must steer the system from the original zero state *back to the same zero state*, simultaneously suppressing the transient oscillations by minimizing the ISE criterion function (9-91).

*Alternative* 2 The control strategy $\mathbf{u} = \mathbf{u}_{opt}$ must steer the system from the original zero state *to the same nonzero final state, as in Fig.* 9-18, but must suppress the transient oscillations optimally, as expressed by Eq. (9-91).†

The control strategy $\mathbf{u}_{opt}$ will of course *not* be the same in the above two cases, but is nevertheless *optimum* in the sense defined.

Modern control theory has developed methods for finding the *optimum control strategy* $\mathbf{u}_{opt}$ in a case like this. It is beyond the scope of this text to present the details of the type of analysis that will lead to a solution. These matters have been adequately treated elsewhere.[1,2,13,14] We shall summarize, however, the important features of the *optimum controller* that can be found by these synthesis methods:

1. If the system model is of the *linear* type of Eq. (9-85), and if the integrand in the cost integral is *quadratic* in $\mathbf{x}$ and $\mathbf{u}$ as is shown in Eq. (9-91), then the optimum control strategy will be of the *linear* type

$$\mathbf{u}_{opt} = \mathbf{K}\mathbf{x} \tag{9-92}$$

where the *gain matrix* $\mathbf{K}$ is an $m \times n$ *constant* matrix.

2. Equation (9-92) implies that *every* control force is a linear function of *every* state variable. For example, we have for $u_1$

$$u_1 = k_{11}x_1 + k_{12}x_2 + \cdots + k_{1n}x_n \tag{9-93}$$

† In this case we must be careful to define the "errors" in the integral (9-91) as the difference values between the actual $\mathbf{x}$ and $\mathbf{u}$ values and the final nonzero values, or the integral will not converge. This simply amounts to a coordinate "shift" for the $\mathbf{x}$ and $\mathbf{u}$.



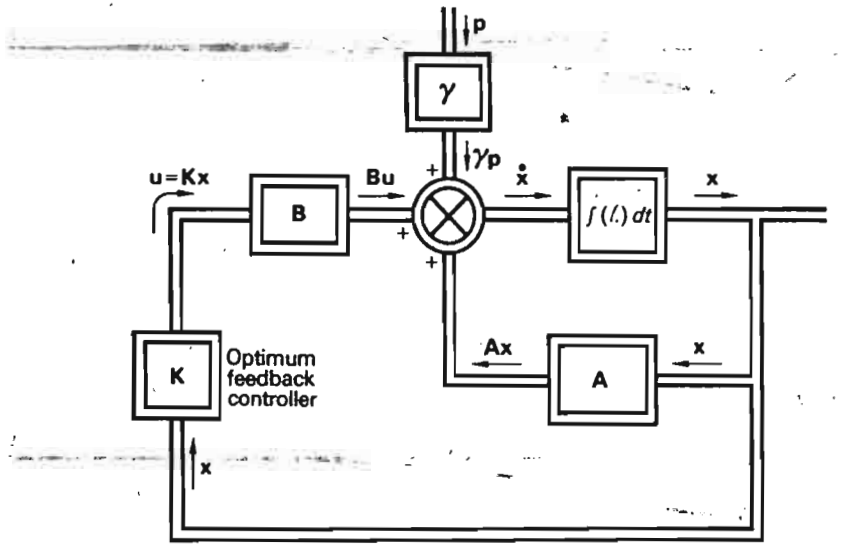


**Fig. 9-29** Optimum control system.

To implement the optimum control strategy, we therefore must measure all state variables, and then arrange for the summation as indicated by Eq. (9-93).

3. The various coefficients $k_{ij}$ of $\mathbf{K}$ evidently represent "weight factors," the relative magnitudes of which measure the importance of including the corresponding state variables in the control force. If, for example, $k_{12}$ in Eq. (9-93) were very small compared with all other $k_{1j}$'s, then we might drop $k_{12}x_2$ from the sum, and we would obtain a *suboptimal* strategy.
4. In view of Eq. (9-92), the optimum control loop takes on the structure shown in Fig. 9-29.

**Example 9-4** The foregoing theory was applied to the same two-area system for which we designed an optimally adjusted "classical" control system in Example 9-3. The reader will find a detailed discussion in Ref. 13. Here we will only summarize the important results:

1. Upon substitution of the numerical values assumed in Example 9-3 into our model (9-85), and upon selection of appropriate weight factors $\alpha$ and $\beta$ in our criterion function (9-91), we derived a gain matrix $\mathbf{K}$.
2. We specified that a step disturbance input in any area must result in zero steady-state change in both frequency and tie line power deviations.
3. Upon inclusion of the gain matrix $\mathbf{K}$ in our control loop, we simulated the response on an analog computer. The result is shown in Fig. 9-30. These graphs should be compared with those of Fig. 9-19*c*. Clearly, we have achieved a spectacular stability improvement over present control methods.

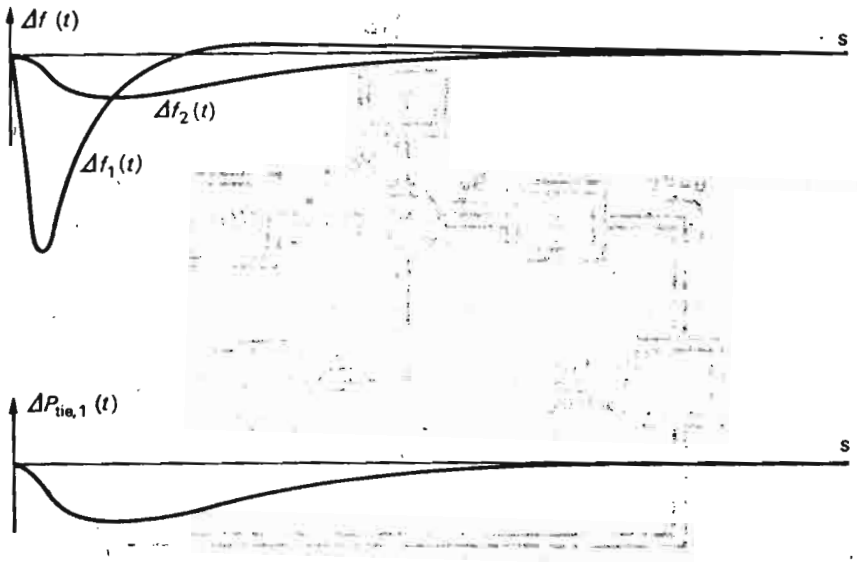


**Fig. 9-30** Dynamic response of optimum regulator to a step load change (compare with Fig. 9-19*c*).

4. The gain matrix **K** revealed an important property. It was found that the control forces needed to control each area could be synthesized from state variables available in that area only. The state variables from the other areas contribute insignificantly. As a matter of fact, the suboptimal response has no detectable difference from the one in Fig. 9-30.
5. The computer program developed to find the **K** matrix is described elsewhere.[37] It accepts a general $n$-dimensional model† of the type of Eqs. (9-85), and can therefore be used for an $n$-area system and/or with more detailed turbine models than those used above. The program, in addition, computes the eigenvalues for the system before and after inclusion of the **K**-matrix feedback loop. The program is also very fast. The total time for obtaining **K** for the above two-area system was only 3 s on an IBM 360. This speed feature permits the designer to experiment with many combinations of weight factors $\alpha$ and $\beta$, so as to obtain a system with desired response characteristics.

### 9-4.6 INTRODUCTION OF DAMPING INTO THE *Pf* LOOP THROUGH VOLTAGE CONTROL

In all our previous analysis of this chapter we assumed noninteraction between the *Pf* and *QV* control channels. This assumption is permissible when the speed of the voltage control loops is considerably greater than that of the ALFC loops.

In this section we show that it is possible by introduction of slow *deliberate* control actions in the *QV* loops to obtain positive damping effects in the *Pf* channel. Several investigators have verified this interesting

† It is, of course, limited by the core-memory size of the computer used.



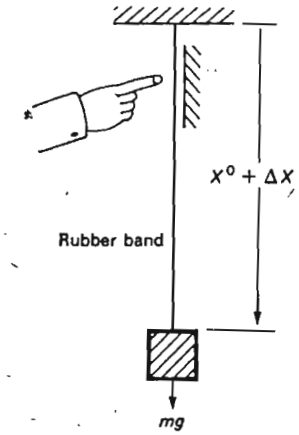


**Fig. 9-31** A simple oscillatory system used to demonstrate effects of manipulation of spring constant.

phenomenon experimentally.[17,21] We give a physical explanation of these effects and also suggest how the damping effects may be optimized by the use of optimal control strategies.

**A simple analog** It was suggested earlier that the oscillatory nature of two interconnected control areas could be explained in terms of the mechanical analog of Fig. 9-17. We shall now make further use of this analog.

We recall that the connecting spring represents the analog of the electric tie line. If we now were deliberately to change the terminal voltages of this line, we would in effect change its synchronizing coefficient [compare Eq. (3-6)] or its "electric spring constant." *The effects of these changes upon the two-area Pf dynamics can be simulated in the mechanical system in Fig.* 9-17 *if similar changes in the mechanical spring constant can be introduced.* Following this hint, we therefore turn our attention to the somewhat simpler analog in Fig. 9-31. When the two masses in Fig. 9-17 oscillate against each other, one point of the spring will always be stationary, and we can therefore limit our attention to a single-mass system.

We assume that the mass is initially in steady state, with the spring elongation $x^0$ and the initial spring tension $k^0x^0$, where $k^0$ is the spring constant. If the mass is now perturbed the distance $\Delta x$, and if simultaneously the spring constant is changed by the amount $\Delta k$, then we can write the following newtonian equation for the mass dynamics:

$$m\frac{d^2}{dt^2}(x^0 + \Delta x) = mg - (k^0 + \Delta k)(x^0 + \Delta x) \tag{9-94}$$

Since

$$mg = k^0x^0$$

and if we neglect the second-order term $\Delta k\,\Delta x$, we obtain from Eq. (9-94) the following differential perturbation equation:

$$m\frac{d^2}{dt^2}\Delta x + k^0\,\Delta x + x^0\,\Delta k = 0 \tag{9-95}$$

For zero spring constant perturbation, that is, $\Delta k = 0$, this equation reduces to

$$m\frac{d^2}{dt^2}\Delta x + k^0\,\Delta x = 0 \tag{9-96}$$

which is the well-known differential equation for a second-order *undamped* harmonic oscillator.

Let us now introduce a perturbation into the spring constant. *Intuitively*, we shall arrange it so that the spring increases its stiffness in proportion to the mass velocity; i.e., we *try*

$$\Delta k \triangleq a\frac{d}{dt}\Delta x \tag{9-97}$$

where $a$ is a *positive* constant.

Upon substitution of Eq. (9-97) into Eq. (9-95), we get

$$m\frac{d^2}{dt^2}\Delta x + ax^0\frac{d}{dt}\Delta x + k^0\,\Delta x = 0 \tag{9-98}$$

We recognize this to be the differential equation for a *damped* harmonic oscillator. The degree of damping is controlled by the constant $a$.

(By periodically fixing a point of the rubber band by pressing it against the wall, as indicated in Fig. 9-31, the above damping effect can be readily demonstrated.)

*By manipulating the spring constant in accordance with the strategy* (9-97) *we have been able to introduce positive damping into our undamped system.*

How do we now interpret these results in terms of our two-area system?

We first take note of the fact [compare Eq. (3-6)] that the increment in the electric tie line stiffness $\Delta T_{12}$ is directly proportional to increments $\Delta\,|V_1|$ and $\Delta\,|V_2|$ in the terminal line voltages. Second, we recall that speed perturbations in the train analog correspond to frequency perturbations in the electric system.



We thus conclude:

*To obtain positive damping we must change the tie line terminal voltages in proportion to the frequency deviations*, i.e.,

$$\Delta\,|V_1| \triangleq a\,\Delta f_1$$

or (9-99)

$$\Delta\,|V_2| = -a\,\Delta f_2$$

(How do you explain the minus sign in the second case?)

**Optimally voltage-damped two-area system** By approximating the two-area system by a second-order oscillator, we arrived at a tutorially attractive analog. If we wish to optimally damp the two-area system by voltage control, then we need to develop more exact models, which then can be used in the computer program developed earlier. We proceed now to develop such a model, and use as a starting point the following well-known expression for the tie line power $P_{\text{tie }1}$, assumed positive in direction $1 \to 2$.

$$P_{\text{tie }1} = \frac{|V_1|\,|V_2|}{X_{12}}\sin(\delta_1 - \delta_2) \tag{9-100}$$

The formula developed earlier for the tie line power deviation $\Delta P_{\text{tie }1}$ [Eqs. (9-20) and (9-21)] was derived on the assumption that only $\delta_1$ and $\delta_2$ were undergoing changes. If we now assume that $|V_1|$ and $|V_2|$ are also changing with the amounts $\Delta\,|V_1|$ and $\Delta\,|V_2|$, we get the more general formula

$$\Delta P_{\text{tie }1} = \frac{\partial P_{\text{tie }1}}{\partial\,|V_1|}\Delta\,|V_1| + \frac{\partial P_{\text{tie }1}}{\partial\,|V_2|}\Delta\,|V_2| + \frac{\partial P_{\text{tie }1}}{\partial(\delta_1 - \delta_2)}\Delta(\delta_1 - \delta_2) \tag{9-101}$$

Upon performing the partial differentiations called for, we write the formula more compactly:

$$\Delta P_{\text{tie }1} = T_1^0\,\Delta\,|V_1| + T_2^0\,\Delta\,|V_2| + T_{12}^0\,\Delta(\delta_1 - \delta_2) \tag{9-102}$$

where $T_{12}^0$ is the synchronizing coefficient earlier defined in Eq. (3-6). The new $T$ coefficients are defined as follows:

$$\begin{aligned} T_1^0 &\triangleq \frac{|V_2^0|}{X_{12}}\sin(\delta_1^0 - \delta_2^0) \qquad \text{pu MW/pu volt} \\ T_2^0 &\triangleq \frac{|V_1^0|}{X_{12}}\sin(\delta_1^0 - \delta_2^0) \qquad \text{pu MW/pu volt} \end{aligned} \tag{9-103}$$

Equation (9-102) tells us how the voltage perturbations result in added

increments to the tie line power. The added terms must therefore be injected at the $\Delta P_{tie}$ inputs in Fig. 9-16.

The voltage perturbations have one additional effect: they increase the loads in respective areas with the amounts $(\partial P_{D1}/\partial |V_1|)\,\Delta |V_1|$ and $(\partial P_{D2}/\partial |V_2|)\,\Delta |V_2|$, respectively. These terms must of course be added at the same input places as $\Delta P_{D1}$ and $\Delta P_{D2}$. Upon amending the block diagram in Fig. 9-16 in accordance with the above observations, we obtain the new one in Fig. 9-32.

If we develop a state model for this system, we find that the **A** and **Γ**

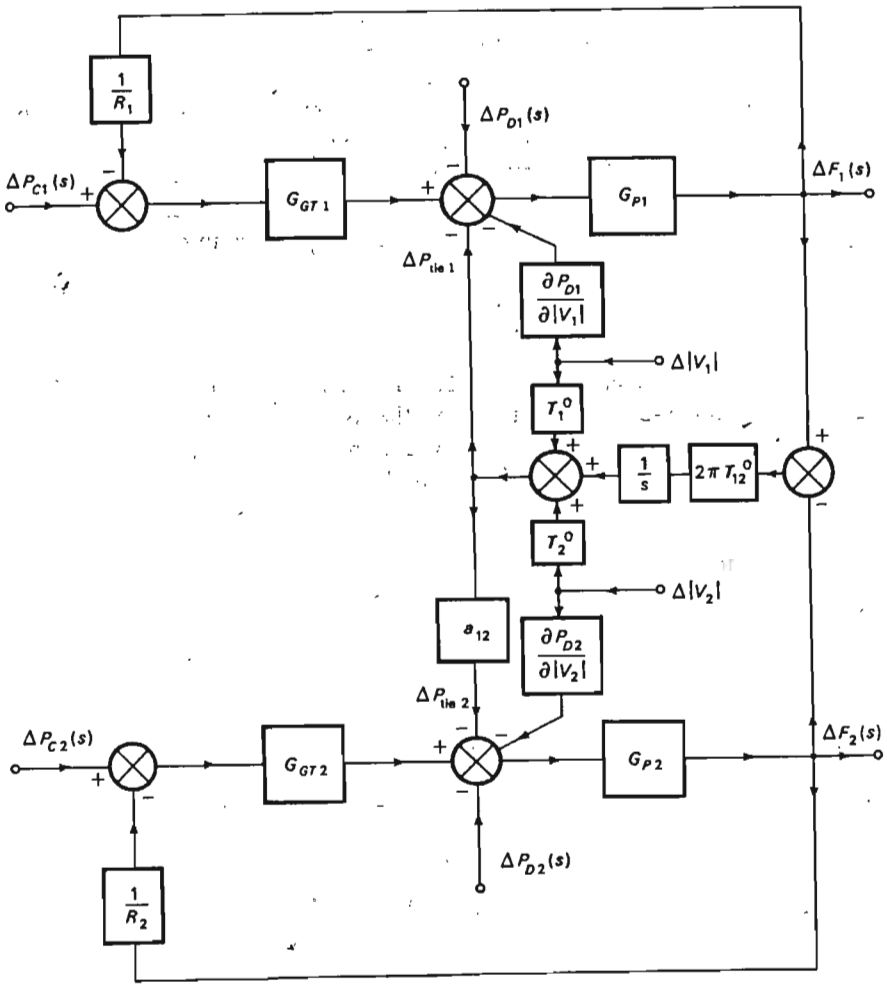


**Fig. 9-32** Block model of two-area system with voltage perturbations added as extra inputs.



matrices will be the same as before, but the **B** matrix will now have four columns, since our control vector now is four-dimensional.

$$\mathbf{u} = \begin{bmatrix} u_1 \\ u_2 \\ u_3 \\ u_4 \end{bmatrix} \triangleq \begin{bmatrix} \Delta P_{c1} \\ \Delta P_{c2} \\ \Delta |V_1| \\ \Delta |V_2| \end{bmatrix} \tag{9-104}$$

**Example 9-5** For the system discussed in Examples 9-3 and 9-4, we wish to develop an optimal controller for manipulation of the voltage inputs $\Delta |V_1|$ and $\Delta |V_2|$ so as to optimize the damping. To demonstrate what effect the voltage manipulation *alone* will have, we shall keep the two control forces $\Delta P_{c1}$ and $\Delta P_{c2}$ equal to zero. The details of our optimal controller design are given in Ref. 38. Here we give only the following summarizing comments:

1. We make direct use of the computer program described on page 380.
2. Since we wish to suppress the influence of the two control forces $u_1$ and $u_2$ to zero, we simply have to penalize these two u components heavily. In our computer program this is done by choosing very large values for the penalty factors $\beta_1$ and $\beta_2$.
3. The resulting response with the optimum controller added to our system is shown in Fig. 9-33.† These graphs should be compared with those of Fig. 9-18 to get an appreciation of the effectiveness of this control method.

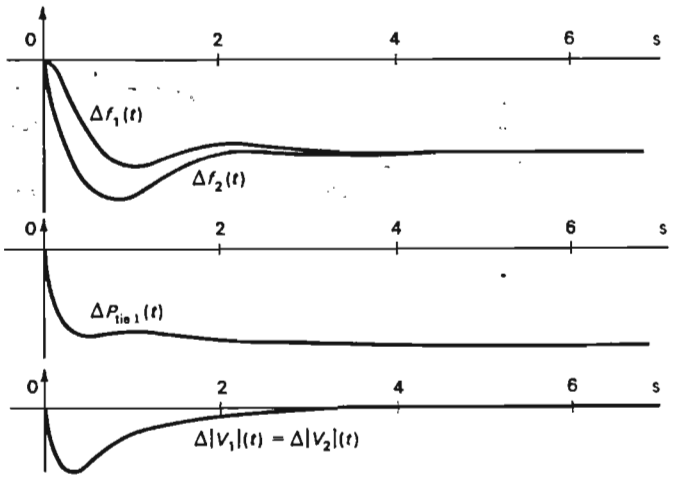


**Fig. 9-33** Effect on two-area system response of optimal voltage manipulation. (Optimal control strategy is also shown.)

4. We have assumed in the above analysis that the voltage perturbations are directly at our disposal for manipulative purposes. This is, of course, not exactly true. The voltages are manipulated via the exciter control loop discussed

† The author is indebted to C. Durick, a graduate assistant, for the computer simulations.

earlier in this chapter. Since the $Pf$ dynamics are much slower than the $QV$ loop, we may consider the latter as being instantaneous. If we wish to consider the delay of the $QV$ loop, we may do this by adding additional state variables to our model. Our computer program will easily handle this added "load."

## 9-5 SUMMARY

This chapter has been devoted to the problem of keeping, by means of closed-loop control, the system state at a desired nominal value. We have divided the overall control problem into two subproblems:

1. The megawatt frequency control problem
2. The megavar voltage control problem

System perturbation models have been derived, and due to the small-scale signal assumption, these have turned out to be of the linear time-invariant variety.

Because of the overall complexity of these models, we have of necessity been forced to perform the analysis under certain simplifying assumptions:

1. We have considered the megawatt frequency control loops completely decoupled from the megavar voltage control loops, but we have also discussed the effects of coupling between loops.
2. We have made use of the coherency feature and assumed that all buses within each "control area" are characterized by equal frequency.
3. We have assumed each generator bus individually voltage-controlled, and have neglected the coupling between the $QV$ loops of the various buses.

The control strategies currently used in the industry have been presented, and their advantages and shortcomings have been pointed out. Optimum-parameter-adjustment methods have been suggested.

Finally, we have introduced briefly the methods of modern control theory, and presented the results of a detailed design of an optimum $Pf$ controller for a two-area system. It is felt strongly that great improvements in stability margins can be achieved by means of these new techniques. Further research should be pursued in these matters.

## EXERCISES

(Exercise 9-6 presupposes a thorough knowledge of the design procedures of modern optimum control. See Refs. 1 and 2.)

**9-1.** The total installed generator capacity in the United States is, in 1970, about 300,000 MW. Assume that the average inertia constant is $H = 5$ s.



To get a feel for the amount of rotating inertia that the total U.S. system represents, find the diameter of a flywheel having the same kinetic energy. Make the following assumptions:

1. The wheel is made of solid steel.
2. It runs at 1800 r/min.
3. It has the shape of a cylinder, with a thickness equal to one-fifth of its diameter.

**9-2.** Consider the $Pf$ control system of a single-area treated in Sec. 9-2.3. Compute the time error caused by a step disturbance of magnitude $\Delta P_D$. Prove, in particular, that the error is reduced by increased gain $K_I$. Express the error in seconds and cycles (of 60 Hz).

**9-3.** Simulate on an analog computer the single-area system in Fig. 9-12 and two-area system in Fig. 9-16 and confirm the response curves (following a step load change) presented in the text. Use the same system parameters as were used in the text.

Demonstrate, in the two-area system, that too large $B$ and/or $K_I$ values render the control loop unstable.

**9-4.** Perform an analysis of the single-area $Pf$ control system under the assumption that $D = 0$. Set also for simplicity $T_T = T_G = 0$. Investigate the response following a step load increase. Study the "uncontrolled" and "controlled" cases, assuming integral control in the latter.

**9-5.** Equation (9-58) was derived based upon the three assumptions on page 353. Derive a similar expression for the "controlled" two-area system, adding the additional assumptions:

$$K_{I1} = K_{I2} = K_I$$

$$B_1 = B_2 = B$$

(*a*) Consider the following numerical case:

$$H_1 = H_2 = 5 \text{ s}$$

$$R_1 = R_2 = 3 \text{ Hz/pu MW}$$

$$T_{12}^0 = 0.1 \text{ pu MW/rad}$$

Investigate if certain values for the gain parameters $B$ and $K_I$ will render the system unstable. (Use Routh stability criterion.)

(*b*) Simulate the system on an analog computer. Confirm your results in (*a*).

(*c*) Assisted by the analog computer, perform an optimum parameter adjustment of the type discussed in the text.

**9-6.** Consider the "uncontrolled" two-area system having the numerical parameters given in Exercise 9-5. Design an optimum controller for the system. You should choose an optimum criterion of type (9-91), put the system equations in state form, and finally find the **K** matrix defined in Eq. (9-92).

Simulate the system upon completion and compare the response with the best you could obtain in 9-5(*c*).

## REFERENCES

**Books**

1. Elgerd, Olle I.: "Control Systems Theory," McGraw-Hill Book Company, New York, 1967.
2. Athans, M., and P. L. Falb: "Optimal Control," McGraw-Hill Book Company, New York, 1966.

3. Kirchmayer, L. K.: "Economic Control of Interconnected Systems," John Wiley & Sons, Inc., New York, 1959.
4. Zaborszky, L., and J. W. Rittenhouse: "Electric Power Transmission," The Ronald Press Company, New York, 1954.
5. Cohn, N.: Control of Interconnected Power Systems, chap. 17, "Handbook of Automation, Computation and Control," vol. 3, John Wiley & Sons, Inc., New York, 1961.
6. Gardner, M. F., J. L. Barnes: "Transients in Linear Systems," John Wiley & Sons, Inc., New York, 1942.

(Reference 1 gives a basic presentation of the general control problem and its modern formulation; it also introduces the reader to the state-variable method. Reference 2 is entirely devoted to the optimum control problem. References 3 to 5 discuss the ALFC problem from widely different viewpoints. Reference 6 gives an excellent presentation of the Laplace transform method, used extensively in this chapter.)

**Technical papers and reports**

7. Benson, A. R., et al.: Analysis of Dynamic Response of Electric Power Systems to Small Disturbances, *Proc. Power Ind. Computer Appl.*, Clearwater, Fla., 1965, pp. 247–259.
8. Van Ness, J. E.: PALS: A Program for Analyzing Linear Systems, report, Northwestern University, Evanston, Ill., March, 1969.
9. Stanton, K. N.: Use of Normal Operating Data from a Power System to Estimate Turbo Alternator Transfer Functions, *Proc. Power Ind. Computer Appl. Conf.*, 1967, pp. 69–82.
10. Concordia, C., and L. K. Kirchmayer: Tie-line Power and Frequency Control of Electric Power Systems, *AIEE Trans. Power Apparatus Systems*, pt. IIIA, vol. 72, pp. 562–572, 1953.
11. Fiedler, H. J., and L. K. Kirchmayer: Automation Developments in the Control of Interconnected Electric Utility Systems, *Proc. IEEE*, May, 1969, pp. 744–750.
12. Elgerd, O. I., and C. E. Fosha: Optimum Megawatt-frequency Control of Multi-area Electric Energy Systems, *Asilomar Conf. Proc.*, 1968.
13. Elgerd, O. I., and C. E. Fosha: The Megawatt-Frequency Control Problem: A New Approach via Optimal Control Theory, *Proc. Power Ind. Computer Appl. Conf.*, 1969.
14. Elgerd, O. I., and C. E. Fosha: Load-frequency Control of Power Systems: A Reassessment, *Proc. SEEE*, October, 1969, Washington, D.C.
15. Ross, C. W.: Error Adaptive Control Computer for Interconnected Power Systems, *IEEE Trans. Power Apparatus Systems*, vol. PAS-85, no. 7, July, 1966.
16. Ross, C. W.: A Comprehensive Direct Digital Load-frequency Controller, *Proc. Power Ind. Computer Appl. Conf.*, 1967.
17. Schleif, F. R., et al.: Control of Rotating Exciters for Power System Damping: Pilot Applications and Experience, IEEE Winter Power Meeting, January, 1969.
18. Ellis, H. M., J. E. Hardy, A. L. Blythe, and J. W. Skooglund: Dynamic Stability of the Peace River Transmission System, *IEEE Trans. Power Apparatus Systems*, vol. 85, pp. 586–600, June, 1966.
19. McClymont, K. R., G. Manchur, R. J. Ross, and R. J. Wilson: Experience with High-speed Rectifier Excitation Systems, *IEEE Trans. Power Apparatus Systems*, vol. 87, pp. 1464–1470, June, 1968.
20. Dandeno, P. L., A. N. Karas, K. R. McClymont, and W. Watson: Effect of High-speed Rectifier Excitation Systems on Generator Stability Limits, *IEEE Trans. Power Apparatus Systems*, vol. 87, pp. 190–201, January, 1968.
21. DeMello, F. P., and C. Concordia: Concepts of Synchronous Machine Stability as Affected by Excitation Control, paper 68-TP-129-PWR, IEEE Winter Power Conference, 1968.



22. Schleif, F. R., H. D. Hunkins, G. E. Martin, and E. E. Hattan: Excitation Control to Improve Power-line Stability, *IEEE Trans. Power Apparatus Systems*, vol. 87, pp. 1426–1434, June, 1968.
23. Byerly, R. T., J. W. Skooglund, and F. W. Keay: Control of Generator Excitation for Improved Power System Stability, *Proc. Am. Power Conf.*, vol. 29, 1967.
24. Schleif, F. R., G. E. Martin, and R. R. Angell: Damping of System Oscillations with a Hydrogenerating Unit, *IEEE Trans. Power Apparatus Systems*, vol. 86, pp. 438–442, April, 1967.
25. Computer Representation of Excitation Systems, IEEE Committee Report, *IEEE Trans. Power Apparatus Systems*, vol. 87, pp. 1460–1464, June, 1968.
26. Dineley, J. L., et al.: Optimized Transient Stability from Excitation Control of Synchronous Generators, *Proc. Power Ind. Computer Appl. Conf.*, 1967.
27. Sullivan, R. L., and O. I. Elgerd: Minimally Proportioned Reactive Generation via Automatic Tap-changing Transformers, *Proc. Power Ind. Computer Appl. Conf.*, 1969.
28. Preminger, J., and G. L. Park: Analysis of Dynamic Stability of a Power System under Deterministic Load Changes, *Proc. IFAC.*, 1969.
29. Quazza, G.: Regolazioni non interagenti di reti interconnesse, *Energia Elettricia*, August, 1963; see also (for the case of stiff interconnections) Non-interacting Controls of Interconnected Power Systems, *IEEE Trans. Power Apparatus Systems*, vol. PAS-85, no. 7, July, 1966.
30. Critères de qualité du réglage dans les réseaux équipés de dispositifs de réglage fréquence-puissance, rapport du Comité 13 CIGRE, Groupe de Travail A1, 1966.
31. Quazza, G.: Criteria for Equitable Participation of Areas in Tie-line Power and Frequency Control of an Interconnected Power System, *Automazione Strumentazione*, March, 1966.
32. Leum, M.: Electric Governors for Hydro Turbines, *Mech. Eng.*, vol. 85, pp. 55–58, April, 1963.
33. Leum, M.: The Development and Field Experience of a Transistor Electric Governor for Hydro Turbines, *IEEE Trans.*, vol. PAS-85, no. 4, pp. 393–402, April, 1966.
34. Usry, R.: Inadvertent Energy Interchange: Causes, Remedies and Balancing, *IEEE Trans.*, vol. PAS-87, no. 2, pp. 513–520, February, 1968.
35. Aggarval, R. P., and F. R. Bergseth: Dynamics of Load-frequency Control Systems, pts. I and II, *IEEE Trans.*, vol. PAS-87, no. 2, February, 1968.
36. Nicholson, H.: Hierarchical Control of a Multi-machine Power System Model, *IEEE Trans.*, vol. PAS-87, no. 7, pp. 1537–1548, July, 1968.
37. Elgerd, O. I., C. E. Fosha, Optimal Linear Control of Multivariate *Pf* Control Problem, *Proc. JACC*, 1969, Boulder, Colo.
38. Durick, C., Optimum Damping via Voltage Regulator Action, Proc. 2d Winter Institute on Electric Energy Eng., Dec. 9–11, 1969, Gainesville, Fla.
39. Wedman, N. L., and Y. N. Yu, Computation Techniques for the Stabilization and Optimization of High-order Power Systems, *Proc. PICA*, May, 1969, Denver, Colo.

# 10

# Energy System Transients—Surge Phenomena and Symmetrical Fault Analysis

The material contained in the last three chapters may, for purposes of classification, be grouped in the following two categories:

1. The theory of the energy system operated in *static* equilibrium. The system models turned out to be nonlinear algebraic equations.
2. The theory of *small-scale dynamic* perturbations around the static equilibrium point. The system models in this case were found to be linear differential equations with constant parameters.

In this and the following two chapters we shall discuss the energy system subject to major faults or disturbances resulting in dynamic-state fluctuations which must be classified as "large scale." System dynamics in this category will collectively be referred to as "transients."

## 10-1 CLASSIFICATION OF SYSTEM TRANSIENTS

Depending upon the *speed* of these transients, we can group them in the following three classifications.





### 10-1.1 CLASS A. ULTRAFAST TRANSIENTS—SURGE PHENOMENA

This type of transient is caused by atmospheric discharges on the exposed transmission lines and by the abrupt but normal network changes resulting from regular switching operations. These transients are entirely electric in nature and involve, essentially, only the transmission lines themselves. Physically, a disturbance of this type causes an electromagnetic wave that travels with almost the speed of light along the lines, giving rise to reflected waves at the line terminations.

In the case of a 90-mile line, a disturbance wave traveling at 180,000 miles/s will complete a round trip in 1 ms. *The phenomena associated with these waves take place, therefore, during the first few milliseconds after their initiation.* Due to the always present line losses, the waves attenuate fast and die out.

The high inductances of the transformers in most instances effectively "fence out" these disturbances from the generator windings, but in the reflection process high surge voltages will be built up that can destroy the insulation of the high-voltage equipment. The traveling charges can be discharged to ground via "lightning arresters" that serve (when they function properly) as fast-acting "safety valves." However, should the insulation be destroyed at some point, either in a transformer or between the phases of the lines, then this type of transient can lead to a *short circuit*, which is an abrupt and abnormal structural change of the network which will give rise to a new, slower type of transient that belongs to our next classification.

Our major reason for studying class A transients is to provide a basis for selection of the insulation level of the line equipment.

### 10-1.2 CLASS B. MEDIUM-FAST TRANSIENTS—SHORT-CIRCUIT PHENOMENA

Under this classification we list those system transients that are caused by abrupt abnormal structural changes—short circuits—in the system.

The vast majority of the short circuits occur on the exposed transmission lines due to insulation breakdowns following surge voltages described above: salt sprays on insulators, birds, and other mechanical causes. In order of severity, the short circuits can be divided into the following types:

1. *Metallic*, or *solid*, *symmetric* short circuit of all three phases. A "symmetric" (or "balanced") short circuit is caused by the applications of three equal *fault impedances* $Z'$ between the three phases and ground. The short circuit is said to be "solid" or "metallic" if $Z' = 0$.
2. Short circuit of two phases, with the third phase remaining healthy. The shorted phases may or may not be simultaneously grounded.
3. Short circuit between one phase and ground, with the two remaining phases healthy.

The power transmission capacity of a line subjected to the first type of short circuit will be instantaneously reduced to zero; short circuits of types 2 and 3 will partially cripple the line. As in the case of class A transients, the class B transients are also entirely *electric* in nature, and are determined basically by the magnetic interplay between the generator windings. The time constants of these windings range from a few cycles of the 60-Hz wave for the "damper" windings to, perhaps, 5 s for the field winding. These transients therefore will be considerably slower than the class A variety. *Since, usually, the first* 10 *cycles of the short-circuit currents are of greatest practical importance, we will be studying a time range of from* 10 *to* 100 *ms following the fault.*

A short circuit is always accompanied by an instantaneous collapse, total or partial, of the bus voltages throughout the system. With the generator voltages thus suddenly decreasing, we find an equally sudden reduction of the generator power output. Since the power *input* to the generator stays constant during those first instants before the mechanical turbine controllers come into play, each generator will be subject to a surplus accelerating torque, which, if sustained, will give rise to mechanical oscillations, to be discussed under class C transients, below.

In addition to destroying or reducing the energy-transmitting ability of parts of the system, the short-circuit currents may reach magnitudes far beyond the rated values for generators and transformers. Such high currents, if permitted to persist, may cause thermal damage to the equipment.† It is important, therefore, to *isolate* a faulty section as soon as possible so as to minimize overheating of equipment and/or the buildup of uncontrollable mechanical oscillations of the generators. Usually, we should not disconnect a larger portion of the system than necessary, and we should not keep it disconnected for longer periods than necessary. A large percentage of short circuits are "self-healing"; i.e., upon extinguishing the fault current, the short-circuit path will be deionized, and the insulation is restored. In practice, therefore, one utilizes "reclosure" breakers that automatically close once, twice, or several times, to test whether the line has recovered. Only if the fault persists does the breaker open permanently. Such a closing-opening-closing cycle may take of the order of 1 s or longer.

There are several reasons why we wish to have as accurate data as possible about short-circuit currents and voltages in a system:

1. The interrupting capacity of each circuit breaker in every switching locality must be based upon the most severe short-circuit case.
2. The protective relaying system which is intended to sense the fault and initiate selective switching bases its operation upon the magnitude and directions of fault currents.

† In rare instances, extremely severe short-circuit currents result in forces which may tear apart machine windings.



### 10-1.3 CLASS C. SLOW TRANSIENTS—TRANSIENT STABILITY

A class A transient may give rise to an insulation breakdown that initiates a class B transient. If the short circuit occurs on a very vital power link and/or if the damaged portion is not successfully disconnected, the fault sequence can develop into the most dangerous type of transient situation to which a power system can be subjected—mechanical oscillations of the synchronous machine rotors. These *electromechanical* transients may, under unfortunate circumstances, pull some or all of the machines out of synchronism. Such an occurrence constitutes a partial or complete breakdown of the energy system. The system is said to have reached its *transient-stability limit.* It may take hours to resynchronize a fully "blacked-out" system, and a systems engineer will go to almost any length to avoid such a nightmare. It is therefore extremely important that we be able to simulate such occurrences on computers and learn how to develop switching and load-shedding strategies that will minimize the effects of faults.

These rotor swings, being mechanical in nature, are relatively slow. The actual speed depends upon the *mode* of oscillations. For example, if one machine swings against another in the same power station, the rotors may complete three to four swing cycles per second. If all the machines in the Eastern United States swing as a coherent *block* against the western block, we may measure only three to four swing cycles per minute. A transient-stability study thus may concern itself with time periods that last for a fraction of a second to one minute or longer. In the latter case the thermal processes in the nuclear core or the boiler will change, and it now becomes necessary to take even these portions of the system into account in the simulation.

In this chapter we shall discuss class A transients, and also those class B transients which result from *symmetrical three-phase* short circuits.

In Chap. 11 we shall discuss class B transients following *unbalanced* faults. Finally, in Chap. 12, we shall discuss the transient-stability problems belonging to our class C category.

## 10-2 CLASS A. TRANSMISSION LINE TRANSIENTS

Overvoltages caused by atmospheric discharges and switching operations are of primary importance as a basis for selection of insulation level and surge protection. A systems engineer also needs to estimate their effect on the protective relaying.

We give a *brief* exposé of these phenomena, with the objective of conveying a general understanding of their nature. Our mathematical models are based on the following simplifying assumptions:

1. Line resistance is neglected. This is a reasonable assumption, and moreover, it gives results that are on the safe side.

2. We develop our model on a per-phase basis. This assumption leads, under certain conditions, to rather large errors, but on the whole is quite reliable in systems that have solidly grounded neutral. Certainly, in view of our limited objective and the considerable model simplification that it will entail, this is a logical assumption to make in an introductory text.

### 10-2.1 TRAVELING WAVES

Consider the per-phase representation of a differential element $dx$ of the transmission line depicted in Fig. 6-16 on page 183. The voltage $v(x,t)$, measured at the coordinate $x$, changes with the amount

$$\frac{\partial v(x,t)}{\partial x}\,dx$$

along the element. If the line resistance is neglected, the voltage drop along the element will be

$$L\frac{\partial i(x,t)}{\partial t}\,dx$$

For voltage equilibrium we thus must require

$$\frac{\partial v(x,t)}{\partial x} = -L\frac{\partial i(x,t)}{\partial t} \tag{10-1}$$

We similarly derive an expression for the current equilibrium:†

$$\frac{\partial i(x,t)}{\partial x} = -C\frac{\partial v(x,t)}{\partial t} \tag{10-2}$$

**The wave equation and its solution** Upon differentiating Eq. (10-1) with respect to $x$ and Eq. (10-2) with respect to $t$ and then combining the two, we get

$$\frac{\partial^2 v(x,t)}{\partial x^2} = \frac{1}{\kappa^2}\frac{\partial^2 v(x,t)}{\partial t^2} \tag{10-3}$$

where, for brevity, we have introduced

$$\kappa \triangleq \frac{1}{\sqrt{LC}} \tag{10-4}$$

Note that the new parameter $\kappa$ has the physical dimension of meters per second, i.e., velocity.

† Compare Eqs. (10-1) and (10-2) with Eqs. (6-70) and contemplate the difference between them.



Equation (10-3) is the famous *wave equation*. We can readily prove by substitution that it has the general solution

$$v(x,t) = v_1(x - \kappa t) + v_2(x + \kappa t) \tag{10-5}$$

In this solution $v_1(\cdots)$ and $v_2(\cdots)$ are *arbitrary* functions of the arguments $x - \kappa t$ and $x + \kappa t$, respectively. The actual shape of these functions is, as we shall see, determined by the *initial voltage and current distributions* along the line.

Equation (10-5) represents the *voltage* solution. The *current* solution is obtained from Eq. (10-1) in the following manner.

From our voltage solution we first compute the partial derivative

$$\frac{\partial v(x,t)}{\partial x} = \frac{dv_1(x - \kappa t)}{d(x - \kappa t)}\cdot 1 + \frac{dv_2(x + \kappa t)}{d(x + \kappa t)}\cdot 1$$

We thereupon substitute this derivative into Eq. (10-1):

$$\frac{dv_1(x - \kappa t)}{d(x - \kappa t)} + \frac{dv_2(x + \kappa t)}{d(x + \kappa t)} = -L\frac{\partial i(x,t)}{\partial t} \tag{10-6}$$

Integration with respect to $t$ gives

$$\int^t \frac{dv_1(x - \kappa t)}{d(x - \kappa t)}\,dt + \int^t \frac{dv_2(x + \kappa t)}{d(x + \kappa t)}\,dt = -Li(x,t)$$

Evaluation of the integrals gives the result

$$-\frac{1}{\kappa}v_1(x - \kappa t) + \frac{1}{\kappa}v_2(x + \kappa t) = -Li(x,t)$$

Since $L\kappa = \sqrt{L/C} = R_w$, that is, the wave impedance defined by Eq. (6-84), we finally have the current solution

$$i(x,t) = \frac{1}{R_w}v_1(x - \kappa t) - \frac{1}{R_w}v_2(x + \kappa t) \tag{10-7}$$

**Physical interpretation of results** Consider the first component, $v_1$, of solution equation (10-5). Since the argument $x - \kappa t$ will not change if we increase $t$ and $x$ by the amounts $\Delta t$ and $\kappa\,\Delta t$, respectively, it is clear that the function $v_1(x - \kappa t)$ represents a wave traveling in positive $x$ direction with the velocity

$$\frac{\Delta x}{\Delta t} = \kappa \quad \text{m/s}$$

We have demonstrated the situation in Fig. 10-1. The component $v_2$ similarly can be shown to represent a wave traveling in the negative $x$ direction with the same velocity.

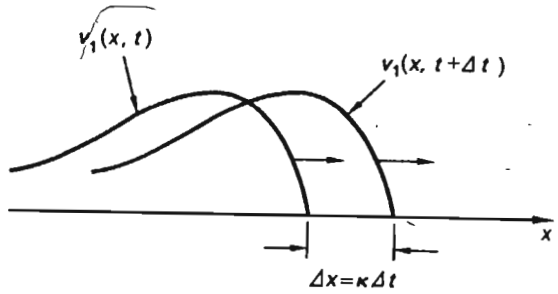


**Fig. 10-1** The function $v_1(x - \kappa t)$ represents a wavefront traveling with the speed $\kappa$ m/s in positive $x$ direction.

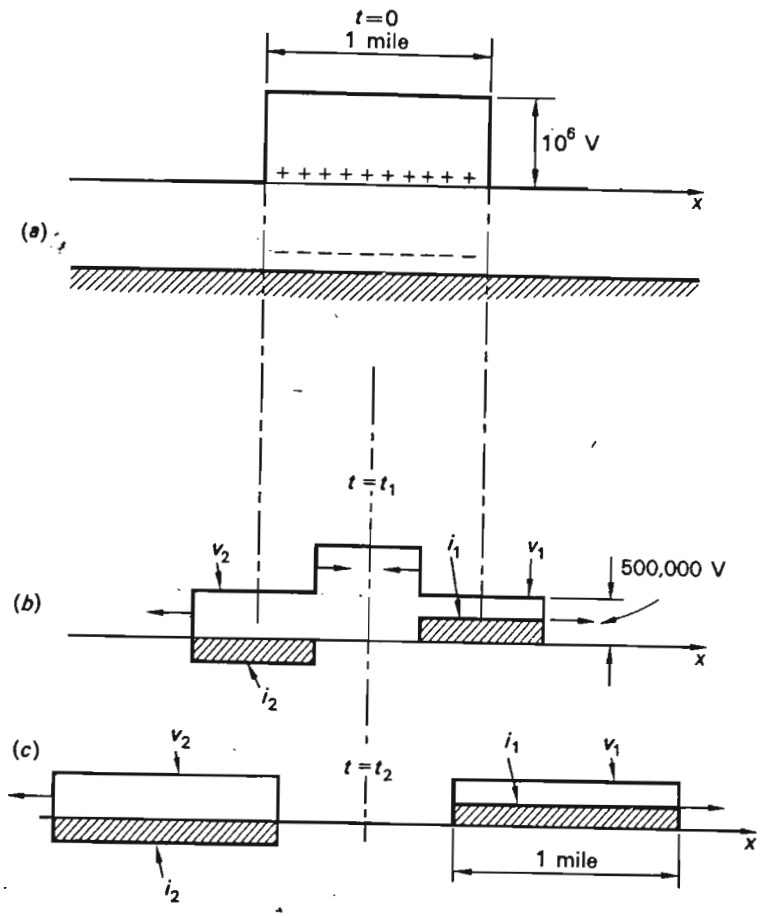


**Fig. 10-2** An initial uniform charge distribution of finite length causes two oppositely traveling rectangular wave systems.



**Example 10-1** Take, for example, the transmission line in Example 6-7. It was characterized by the parameters

$L = 1.33 \times 10^{-6}$ H/m and phase

$C = 8.86 \times 10^{-12}$ F/m and phase

The wave velocity is thus

$$\kappa = \frac{1}{\sqrt{LC}} = 2.91 \times 10^8 \text{ m/s (or 180,000 miles/s, approx)}$$

The wave impedance is

$$R_w = \sqrt{\frac{L}{C}} = 387\ \Omega$$

Assume that a lightning bolt discharges a uniform positive charge along a 1-mile stretch of the line, as shown in Fig. 10-2*a*. Initially, at $t = 0$, we thus find a constant voltage along the 1-mile stretch. Let us assume, for simplicity, that the magnitude is $10^6$ V.

The wave equation tells us that the voltage just cannot "sit there"; it must travel at the speed $\kappa$. For symmetry reason, half the charge travels to the left and half to the right, and at two different moments later, the voltage picture will be as shown in Fig. 10-2*b* and *c*.

Each voltage wave is accompanied by a current wave of magnitude 500,000/387 = 1300 A. Note that the $i_1$ wave is positive, corresponding to a positive charge traveling in the assumed positive current direction. A positive charge traveling in the negative $x$ direction represents a negative current.

**Wave reflections** When a wave like those in Fig. 10-2 hits a line discontinuity, it will give rise to reflected waves. The total voltage and current at the discontinuity are obtained by superposition of the two wave systems. Assume, for demonstration purposes, that the 500,000-V wave in Example 10-1 arrives at the end point of the line and hits the high-voltage terminal of a transformer. We shall assume that the impedance looking into the transformer is very large, so that for practical purposes the wave sees an open circuit. This means, in effect, that a reflected wave will develop, having a current of equal magnitude but opposite sign to the incident wave. When the two waves are superimposed, the result will be zero current, but the voltage will *double*.

Figure 10-3 shows how the reflection process unfolds in five easy to-follow steps.

Due to the ever-present resistance the waves will attenuate as they travel. Their profile will also change.

Note that we have not shown in Figs. 10-2 and 10-3 the regular 60-Hz voltage and currents upon which the waves are superimposed. Due to the extreme speed of the wave phenomena (as we said earlier, they will complete five round trips in 5 ms on a 90-mile line and will then, for all practical purposes, be dissipated), the regular 60 Hz is essentially constant.

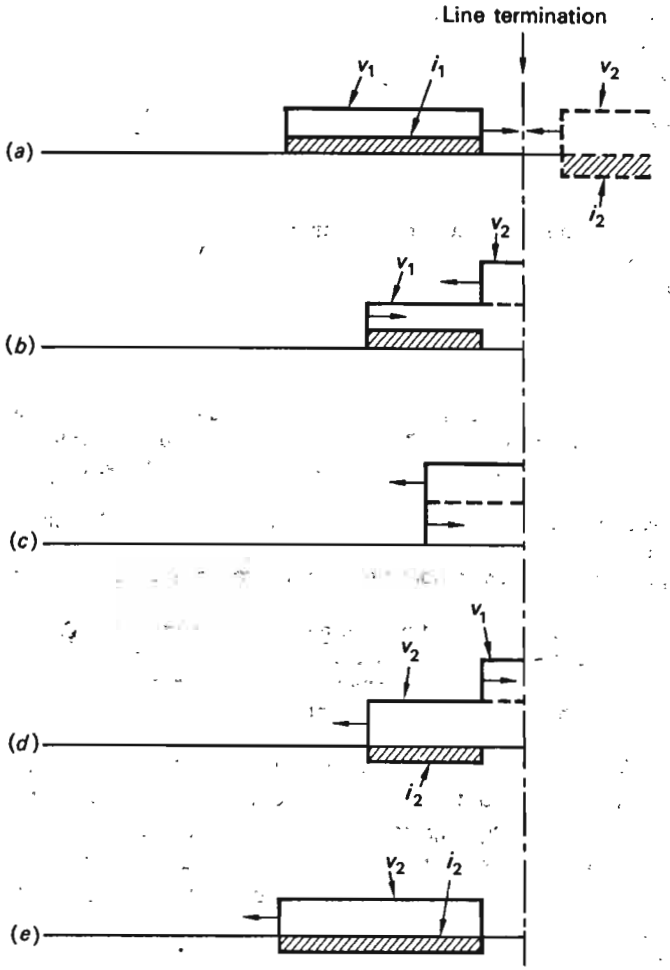


**Fig. 10-3** Reflection of rectangular wave system at open-circuited end of a transmission line, shown at five different instants of the reflection process.

**Parameter lumping** The wave-carrying ability of the transmission line is a consequence of its *continuous-parameter* character. Other physical *continua* (air, water, etc.) also have this capacity.

When simulating line transients on an analog computer, or when performing digital solution of the wave equation, "lumping" of the line parameters becomes a very useful concept. In Fig. 10-4 we indicate how such a lumping is performed in decreasing degree of coarseness. The *LC* representation of the line certainly emphasizes its oscillatory character.



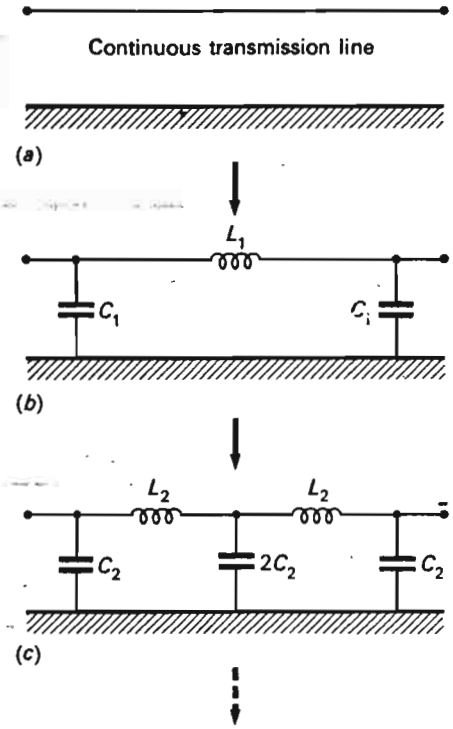


**Fig. 10-4** Lumping of transmission line parameters.

**Example 10-2** Consider a 90-mile stretch of the line discussed in Example 10-1. If we represented it in the coarsest possible fashion, as shown in Fig. 10.4*b*, we would get

$$L_1 = 90 \times 1609 \times 1.33 \times 10^{-6} = 1.92 \times 10^{-1}\ \text{H}$$
$$C_1 = \tfrac{1}{2} \times 90 \times 1609 \times 8.86 \times 10^{-12} = 6.43 \times 10^{-7}\ \text{F}$$

The resonant frequency of the corresponding *LC* circuit would be $f = 650$ Hz. The "actual" frequency would be $f = 1000$ Hz (since it takes 1 ms for a wave to complete one round trip).

(Compare also Exercise 10-3.)

### 10-2.2 SWITCHING TRANSIENTS

Rapidly appearing and fast disappearing waves, caused by atmospheric disturbances like those just discussed, represent one type of transmission line transients. Another type of fast transients of considerable practical significance is generated during normal switching operations. Collectively, we refer to these as *switching transients*. The simplest type of switching transient is generated by *switch-closing* operations, when a transmission line is being energized. This situation is depicted in Fig. 10-5. As the circuit breaker is closed, a wave is initiated that will travel down the line in the manner described above. The amplitude of the wavefront depends upon at

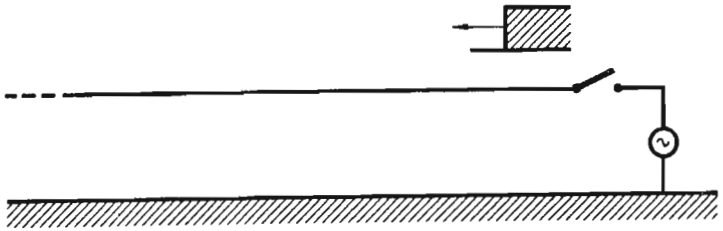

**Fig. 10-5** Switching transient caused by switch-closing maneuver.

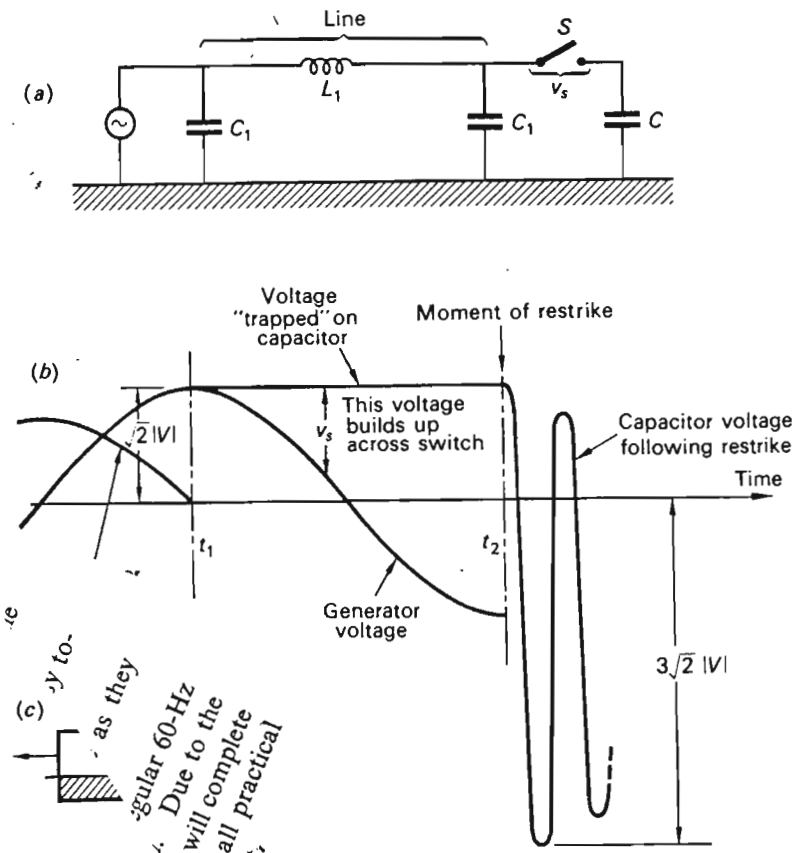


**Fig. 10-2** An initi... oppositely traveling ... shunt capacitor caused by switch opening



what instant of the 60-Hz cycle the breaker is closing. The worst case occurs if it closes at the maximum point. If the 60-Hz voltage has an rms value $|V|$, the wave amplitude will then be $\sqrt{2}\,|V|$. Upon reflection, this wave evidently can cause a voltage of magnitude $2\sqrt{2}\,|V|$.

"Restrike-type" switching transients occurring during *switch-opening* maneuvers can give rise to dangerous overvoltages. For purposes of illustration, consider the case shown in Fig. 10-6*a*. A shunt capacitor $C$ is connected to the end of a transmission line which we have lumped into a single $\pi$ link, in accordance with Fig. 10-4. Let us consider the following switching situation.

The capacitor is to be disconnected from the network, and for that purpose we send an "opening" command to the switch, the switching poles of which start to move apart. At the moment $t_1$, when the current wave is going through a zero, the arc is deionized and the current ceases. At this moment, however, the capacitor is charged to full peak voltage $\sqrt{2}\,|V|$. As the network voltage reverses, we therefore build up a voltage $v_s$ across the switch. If the switch can build up its recovery strength faster than the oncoming voltage $v_s$, the switching operation will be successful. If not, we will obtain a restrike, which simply means that the insulation gap collapses and the switch is essentially short-circuited.

In Fig. 10-6*b* we assume that such a restrike occurs at the most dangerous moment $t_2$, when the voltage $v_s$ is at its maximum value. The restrike causes a fast oscillatory voltage in the $LC$ circuit. The frequency of this transient will, typically, be in the kilocycles range. (Note that we have assumed zero generator impedance; i.e., we have assumed an "infinite" network.)

As we show in Fig. 10-6*b*, the voltage overshoot will amount to $3\sqrt{2}\,|V|$ volts.

## 10-3 SYMMETRICAL SHORT CIRCUITS

We now turn our attention to the next classification of system transients, the short-circuit phenomena. Consider the portion of a transmission system depicted in Fig. 10-7. Assume that a *symmetrical* short circuit occurs

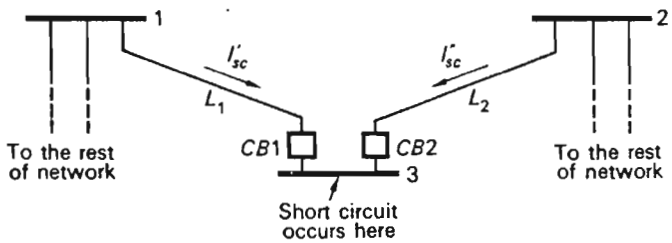


**Fig. 10-7** Short-circuit currents flow towards faulted bus.

at the load bus 3. The prefault bus voltage $V_3$, measuring about 100 percent, will instantaneously drop to zero. The network parts to the left and right which are assumed to contain active sources will immediately start feeding fault currents $I'_{sc}$ and $I''_{sc}$ into the fault via buses 1 and 2.† The magnitude of these currents will be determined by the "strength" of these buses and by the impedance of the lines $L_1$ and $L_2$. Usually, the short-circuit currents will reach magnitudes many times the normal current in the lines, and the circuit breakers $CB1$ and $CB2$, via fault sensors (relays), will be commanded to open, in order to isolate the faulty bus.

### 10-3.1 CONCEPT OF SHORT-CIRCUIT CAPACITY (SCC)

The voltages of buses 1 and 2 and all other network buses will sag during the duration of the short circuit. The magnitude of the voltage drop that the buses will experience is an indication of the "strength" of the network. We need a measure of this strength, and we also need a measure of the severity of the short-circuit stresses. Both of these objectives are met by a quantity referred to as the *short-circuit capacity* (sometimes also called the *fault level*) of the bus in question.

The short-circuit capacity, SCC, of a network bus is defined as the product of the magnitudes of *prefault voltage* and *postfault current*. Defined in this manner, the SCC will come out in per-unit voltamperes if the voltage and current are expressed in per unit.

$$|\text{SCC}| \triangleq |V_{\text{prefault}}|\,|I_{\text{postfault}}| \qquad \text{pu MVA} \tag{10-8}$$

If the voltage is measured in line-to-line kilovolts and the current in per-phase kiloamperes, the SCC will be obtained in three-phase megavoltamperes.

$$|\text{SCC}| \triangleq \sqrt{3}\,|V_{\text{prefault}}|\,|I_{\text{postfault}}| \qquad \text{MVA} \tag{10-9}$$

The prefault voltage is usually about 1.0 pu, and we therefore obtain from Eq. (10-8) the following approximate formula for short-circuit mega-

[illegible] pu MVA (10-10)

where with

[illegible] AND THEVENIN'S THEOREM

[illegible] takes on a much clearer significance [illegible] the very important *Thévenin's circuit* [illegible] om courses in elementary circuit theory,

$\kappa \doteq$ [illegible] component $v_2$ [illegible] negative $x$

Note that th[illegible] oad connected to bus $C$ is of impedance type and second, i.e., v[illegible] of motor load. Motors, synchronous and induc-

† Compare Eqs. (10[illegible] nts into the fault just like the rest of the synchronous them.



this theorem is useful in determining the changes that take place in currents and voltages of a *linear* network when an additional impedance is added between two nodes of the network. This situation clearly applies to a short circuit.

The Thévenin's theorem specifically states:

*The changes that take place in the network voltages and currents due to the addition of an impedance between two network nodes are identical with those voltages and currents that would be caused by an emf placed in series with the impedance and having a magnitude and polarity equal to the prefault voltage that existed between the nodes in question and all other active sources being zeroed.*†

To obtain the postfault currents and voltages in the network, we must superimpose these changes on the prefault currents and voltages.

We shall find the theorem extremely useful in this chapter and the next in determining the system-wide effects of short circuits. Presently, we shall use the theorem to compute in our example system in Fig. 10-7 the fault current $I^f$ in the branch itself.‡ By direct application of the theorem, we conclude that the current simply equals

$$I^f = \frac{V_3^0}{Z^f + Z_{in}} \tag{10-11}$$

or in the case of a *solid* short circuit,

$$I^f = \frac{V_3^0}{Z_{in}} \tag{10-12}$$

where $V_3^0$ is the prefault voltage of bus 3, and $Z_{in}$ is the impedance measured *into* the network from bus 3, with all active sources zeroed.

It should be noted that the same current would be obtained by connecting the impedance $Z^f$ to a voltage source having an emf $E = V_3^0$ and an internal impedance $Z_{in}$. If we apply this observation to our example system in Fig. 10-7, we may therefore, from bus 3, view the rest of the system as a voltage source $E = V_3^0$ behind an impedance $Z_{in}$, which, in accordance with Eq. (10-12), equals

$$Z_{in} = \frac{V_3^0}{I^f} \tag{10-13}$$

† By this term we mean that all active sources are removed and the remaining open terminals shorted, in the case of *voltage* sources, and left open, in the case of *current* sources.
‡ Throughout this chapter and the next we shall indicate all *prefault* variables with the superscript 0. All *postfault* or fault variables will be indicated by the superscript $f$. Note that the "prefault" variables are identical to the "nominal" variables discussed in Chap. 7.

If we express all quantities in per units and make use of the approximations

$$V_3^0 \approx 1.0 \text{ pu}$$

and

$$|\text{SCC}| \approx |I'|$$

then, from Eq. (10-13), we have

$$|Z_{in}| \approx \frac{1}{|\text{SCC}|} \tag{10-14}$$

The corresponding equivalent network is shown in Fig. 10-8.

We make at this time the following observations:

1. The equivalent impedance $Z_{in}$ is for all practical purposes *reactive*. We will prove this in subsequent sections.
2. It follows from this observation that the short-circuit megavoltamperes in the case of a *solid* short circuit for all practical purposes consists entirely of reactive power.
3. The short-circuit current as measured immediately following the short circuit is of larger magnitude than, say, the current measured half a second later. This means that the magnitude of $Z_{in}$ will have a minimum value immediately following the fault and then grow. This change of the short-circuit current with time is due to the characteristics of the synchronous generators and will be explained in the next section.
4. The strength of a bus, which we referred to earlier, is directly proportional to its short-circuit megavoltamperes. Note from Eq. (10-14) that as the SCC increases, the impedance as viewed into the network from the bus in question decreases. The ability of the bus to maintain its voltage when short circuits occur at *other* buses therefore increases (Example 10-3). Note, however, that if a short circuit occurs at the bus, the high SCC results in high currents. This taxes the circuit breakers. Actually, we sometimes find reason to reduce artificially the short-circuit megavoltamperes in a network point by inserting reactors in the network. (Compare Example 5-7.)

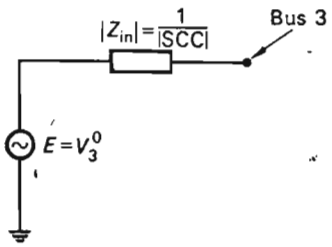


**Fig. 10-8** From the faulted bus the rest of the network appears as an emf behind an impedance.



5. Note that the short-circuit *megavoltamperes* as a measure of the stresses to which a breaker is subject is better than the short-circuit *current*, for the following reason. The first job of the circuit breaker is to extinguish the current. A fast breaker (air-blast type) will usually accomplish this after a couple of cycles. Once the current is zero, the breaker contacts must maintain sufficient insulation strength to withstand the voltage (*recovery voltage*) that will subsequently build up across each breaker pole. Upon completion of the interruption process, full network voltage, i.e., 1.0 pu, will be measured across the breaker. It is logical to rate a breaker for *both* the current it must extinguish and the voltage against which it must open. The product of those two quantities is by definition the short-circuit megavoltamperes at the breaker location in question.
6. Sometimes, in order to simplify our analysis, we assume that a bus is "infinitely strong." This means that we assume that the bus has an infinite SCC. Since this would imply a zero equivalent impedance, we conclude that such a bus would always be strong enough to maintain a constant voltage (except, of course, for a short circuit on the bus itself).

   We may add that in modern EHV systems the SCC may amount to 50,000 MVA. At 500 kV this corresponds to a short-circuit current of about 60 kA.

**Example 10-3** Consider the network depicted in Fig. 10-7. We are given the following data for it.

With the circuit breakers *CB*1 and *CB*2 open, the network is in effect divided into two portions. In this configuration buses 1 and 2 have the following measured short-circuit megavoltamperes:

$$|\text{SCC}_1| = 8.0 \text{ pu MVA}$$
$$|\text{SCC}_2| = 5.0 \text{ pu MVA}$$

The impedances of the lines $L_1$ and $L_2$ are 0.30 pu each.

If we now close the two circuit breakers, how will this affect the short-circuit megavoltamperes of buses 1 and 2, and also, what will be the strength of bus 3? We assume all impedances purely reactive.

*Solution* By making use of the equivalent network in Fig. 10-8, we obtain directly the equivalent network shown in Fig. 10-9*a*. In this network we have identified the three buses. By three consecutive and self-explanatory circuit transformations we obtain the simple network shown in Fig. 10-9*d*. From this we obtain directly the short-circuit megavoltamperes of bus 3:

$$|\text{SCC}_3| = \frac{1}{0.230} = 4.35 \text{ pu}$$

In the above transformation process we eliminated the identities of buses 1 and 2. If we wish to obtain information about, say, bus 1, then it is necessary to

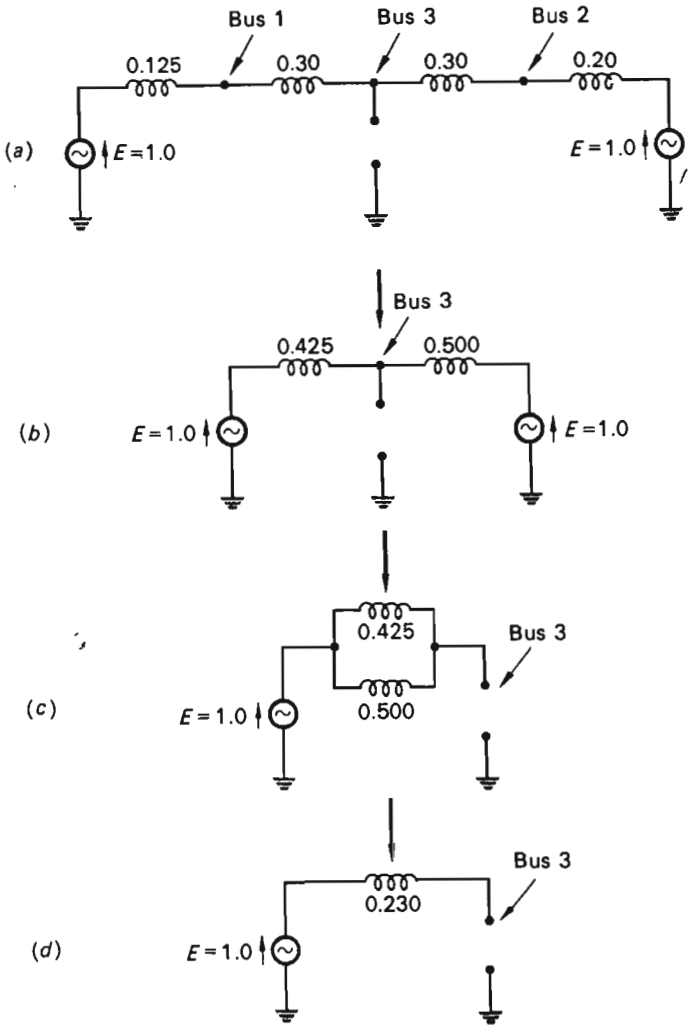


**Fig. 10-9** Equivalent short-circuit network and its step-by-step reduction.

retain the identity of this bus throughout the network reductions. This has been done in Fig. 10-10. From this figure we compute the new short-circuit megavolt-amperes for bus 1:

$$|\mathrm{SCC}_1| = \frac{1}{0.108} = 9.25 \text{ pu MVA}$$

The closing of the link $L_1L_2$ has thus resulted in a 16 percent increase in the strength of bus 1. The reader is encouraged to investigate the effects on bus 2.



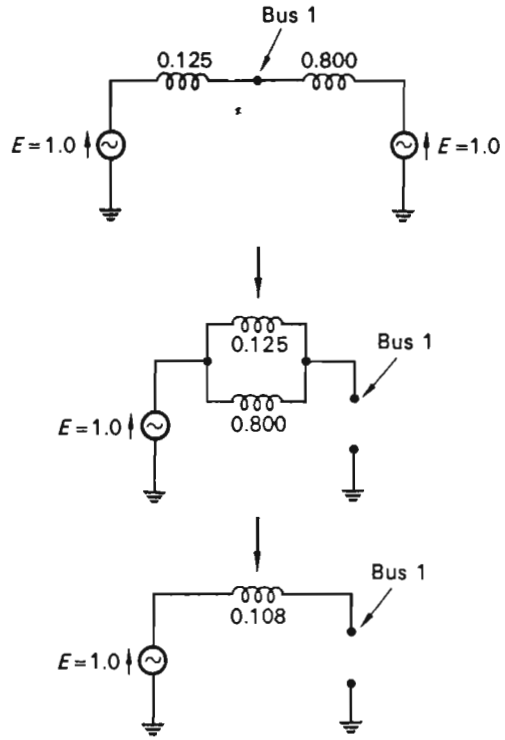


**Fig. 10-10** Network reduction proceeds differently if identity of a particular bus must be preserved.

## 10-4 BEHAVIOR OF THE SYNCHRONOUS MACHINE DURING A BALANCED SHORT CIRCUIT

It should have become obvious from the discussions in the preceding section that the magnitudes of the short-circuit currents and megavoltamperes in a system are directly related to the amount of current fed from the individual synchronous machines (generators or motors) during the short circuit. In this section we investigate these matters further.

### 10-4.1 ANALYSIS OF A BALANCED TERMINAL SHORT CIRCUIT—WINDING RESISTANCES NEGLECTED

Let us consider a synchronous machine running at constant speed, stator windings open-circuited, and excited with the constant rotor field current $i_r^0$. The machine is subjected at $t = 0$ to a symmetrical three-phase short circuit, and we wish to study the subsequent behavior of the stator currents. For our analysis we make use of the general set of performance equations (4-36).

We neglect all winding resistances in our analysis. This assumption will result in considerable numerical simplification, at a very modest price in

lost accuracy. Also, this assumption gives results which are on the "safe side."

The prefault terminal generator voltage equals the induced emf and has, in accordance with Eq. (4-46), the rms value

$$|V_a| = |V_b| = |V_c| = |E| = \frac{\omega L_5 i_r^0}{\sqrt{2}} \tag{10-15}$$

Upon application of the solid short, the stator voltages collapse to zero, and for $t > 0$, we therefore have

$$v_a = v_b = v_c = 0 \tag{10-16}$$

From Eq. (4-32) we thus conclude that, for $t > 0$,

$$v_d = v_q = v_0 = 0 \tag{10-17}$$

We shall also set $v_r = 0$ for $t > 0$; i.e., we short-circuit the field winding at the same instant as we short-circuit the stator. The reason for this is our assumption of zero field winding resistance. If we let the field emf source continue to feed into the resistanceless winding, the rotor current $i_r$ would eventually be boundless, and we wish to avoid this physical ambiguity. In view of Eq. (10-17) and our assumptions about $v_r$, $r_r$, and $r_s$, Eqs. (4-36) take on the form

$$\begin{aligned} 0 &= -L_d \frac{di_d}{dt} + L_5 \frac{di_r}{dt} + L_q \omega i_q \\ 0 &= -L_q \frac{di_q}{dt} + (L_5 i_r - L_d i_d)\omega \\ 0 &= -L_0 \frac{di_0}{dt} \\ 0 &= L_4 \frac{di_r}{dt} - \tfrac{3}{2} L_5 \frac{di_d}{dt} \end{aligned} \tag{10-18}$$

These four linear differential equations are sufficient for solution of the four unknown currents $i_d$, $i_q$, $i_0$, and $i_r$. Initially, the stator currents $i_a$, $i_b$, and $i_c$ are all zero, and in view of Eq. (4-26), we therefore have

$$i_d(0) = i_q(0) = i_0(0) = 0 \tag{10-19}$$

For the rotor current we had earlier assumed

$$i_r(0) = i_r^0$$



In solving for the currents we choose to start with the zero-sequence current $i_0$, since this current happens to have a simple solution. From the third of Eqs. (10-18) we get, upon integration,

$$i_0(t) = \text{const} = i_0(0) = 0 \tag{10-20}$$

We therefore need not worry further about this component.

**Transient inductance and reactance** We Laplace-transform the remaining three Eqs. (10-18). Capital letter symbols are used for the Laplace-transformed currents:

$$\begin{aligned} 0 &= -L_d s I_d + L_5(s I_r - i_r^0) + \omega L_q I_q \\ 0 &= -L_q s I_q + (L_5 I_r - L_d I_d)\omega \\ 0 &= L_4(s I_r - i_r^0) - \tfrac{3}{2} L_5 s I_d \end{aligned} \tag{10-21}$$

Without difficulty we then solve for $I_d$.

$$I_d = \frac{\omega^2 L_5 i_r^0}{L_d'} \frac{1}{s(s^2 + \omega^2)} \tag{10-22}$$

In this equation we have introduced, for the sake of brevity, the new inductance parameter

$$L_d' \triangleq L_d - \frac{3}{2}\frac{L_5^2}{L_4} \tag{10-23}$$

The parameter thus defined is referred to as the *d-axis transient inductance.*

From a Laplace transform table we obtain directly the inverse transform of Eq. (10-22).

$$i_d(t) = \frac{L_5 i_r^0}{L_d'}(1 - \cos \omega t) \tag{10-24}$$

or in view of Eq. (10-15),

$$i_d(t) = \sqrt{2}\frac{|E|}{\omega L_d'}(1 - \cos \omega t) = \sqrt{2}\frac{|E|}{X_d'}(1 - \cos \omega t) \tag{10-25}$$

The new parameter

$$X_d' \triangleq \omega L_d' \tag{10-26}$$

is referred to as the *d-axis transient reactance.*†

† For typical values of the transient reactance, see Table 4-1.

With equal ease we now solve for the currents $i_q$ and $i_r$. The details are left as an exercise for the reader. The results are

$$i_q(t) = \sqrt{2}\,\frac{|E|}{X_q}\sin \omega t \tag{10-27}$$

$$i_r(t) = i_r^0 + \frac{3}{2}\frac{L_5}{L_4}\frac{|E|}{X'_d}(1 - \cos \omega t) \tag{10-28}$$

**General Stator current expressions** At this stage in our analysis, we have the solution for the Blondel currents. We obtain the actual stator currents directly from Eq. (4-30). For the current in phase $a$ we get

$$i_a = i_d \cos \alpha - i_q \sin \alpha \tag{10-29}$$

The rotor angle $\alpha$ can be written

$$\alpha = \omega t + \alpha_0 \tag{10-30}$$

where $\alpha_0$ is the rotor position at the moment of short circuit. Upon substitution of Eqs. (10-25), (10-27), and (10-30) into Eq. (10-29), we get

$$i_a = \sqrt{2}\,\frac{|E|}{X'_d}\cos(\omega t + \alpha_0) - \frac{|E|}{\sqrt{2}}\left(\frac{1}{X'_d} + \frac{1}{X_q}\right)\cos \alpha_0 - \frac{|E|}{\sqrt{2}}\left(\frac{1}{X'_d} - \frac{1}{X_q}\right)\cos(2\omega t + \alpha_0) \tag{10-31}$$

Similar and symmetric expressions are obtained for the stator currents in the remaining two phases.

We make the following observations about the result:

1. The total stator current is made up of three components, which are, in order of importance: (*a*) A fundamental-frequency component; (*b*) a dc component; and (*c*) a double-frequency component.
2. The magnitude of the dc component varies with $\alpha_0$. For $\alpha_0 = 0$, its magnitude in $a$ phase is of the same order of magnitude as the fundamental-frequency term.
3. The magnitude of the double-frequency component is relatively insignificant, and its presence can usually be completely ignored.
4. Since we have neglected resistances, none of the three components contains any decaying factors.
5. The rms value of the fundamental-frequency component equals $|E|/X'_d$. In *steady state* (Chap. 4) the short-circuit stator current will have an rms value of $|E|/X_d$.



Since

$$X'_d < X_d$$

we conclude that the *transient* short-circuit current of frequency $\omega$ is of higher magnitude, usually three to ten times, than the steady-state current. (As will be pointed out in the next section, the "steady state" will be reached in about 5 to 10 s in a typical generator.)

6. The field current, constant up to the moment of short circuit, will in the postfault period contain a large 60-Hz component, which of course, if resistance is considered, will eventually die out.

   (It is the effect of this induced rotor current that results in the temporary reductions of the inductance as felt on the stator side. The student may compare the situation with a transformer having the primary and secondary winding inductances $L_p$ and $L_s$. If the secondary is open, we measure the inductance $L_p$ from the primary side. If we short-circuit the secondary, we measure a smaller "effective" inductance from the primary due to the coupling. The reduction in this effective inductance is the more pronounced, the better magnetic coupling we have between the windings.)

### 10-4.2 EFFECTS OF WINDING RESISTANCES AND DAMPER WINDINGS

In principle, the foregoing analysis would not be more difficult if we wished to include the effects of winding resistances. However, by adding the resistive terms to Eq. (10-18), we would run into some numerical complications. The inverse transformation of Eq. (10-22) was made easy by the fact that the third-order denominator appears in *factored* form. If the resistances are included, the denominator in the expression for $I_d$ will be a complete unfactored third-order polynomial in $s$, resulting in added difficulty in finding the poles of $I_d$.

We will not devote time to a complete study of this case here. Instead, we will summarize the results of such a study by pointing out how the actual stator currents will differ from the lossless ones in Eq. (10-31). Our comments apply to a typical synchronous machine with typical (i.e., small) stator resistance values.

1. The magnitudes of the three current components as measured immediately following the short circuit (i.e., during the first cycles of the fundamental wave) will be approximately equal to those given by Eq. (10-31).
2. The magnitude of the fundamental-frequency component will decay exponentially from its initial amplitude of rms $= |E|/X'_d$ to its

steady-state amplitude of rms $= |E|/X_d$, with a time constant

$$T'_d \approx \frac{X'_d}{X_d} T_r \quad \text{s} \tag{10-32}$$

where $T_r$ is the time constant of the rotor winding, i.e.,

$$T_r = \frac{L_4}{r_r} \tag{10-33}$$

The *transient time constant* $T'_d$ has numerical values of about 1 to 2 s for large machines, which means that the steady-state value is reached in about 5 to 10 s.

3. The dc component dies out very fast, usually in 8 to 10 cycles.
4. Usually, generators are equipped with so-called damper windings, consisting of a solidly short-circuited set of copper bars located in the pole faces of the rotor. In steady-state operation these windings carry no currents,† but when the machine is subject to power angle oscillations (Chap. 12), stabilizing currents will be induced in the windings.

During a short circuit, transient currents will likewise be induced in these windings. They are of short duration, lasting only a couple of periods of the fundamental frequency, but in this short period they have a significant effect upon the stator currents, which may have their first two or three peaks substantially increased.‡ It is customary to define a *subtransient*§ *reactance* $X''_d$, which permits us to compute the rms value of the first cycle as the ratio $|E|/X''_d$. Figure 10-11 shows a typical oscillogram of the stator short-circuit current in one phase.

### 10-4.3 PRACTICAL COMPUTATIONAL CONSIDERATIONS

The foregoing analysis has convinced us that the study of short-circuit transients in a singly operated synchronous machine is not a trivial undertaking, particularly if we wish to consider the effects of winding resistances and damper windings. In a practical situation many machines are interconnected, and an *exact* study would require that we solve a large set of *coupled* differential equations.

With modern computers this is not an impossible task, but seldom, if ever, is there a need to perform such an accurate short-circuit analysis. The data obtained from such a study are being used to size up the need for circuit breaker performance and/or to select proper relay settings. The fact is that considerable error margins can be accepted in most cases.

† Because the flux which is linked with the winding does not change.
‡ The reason for this is that the damper winding is tighter magnetically coupled with the stator winding than is the field winding.
§ For typical values for $X''_d$, see Table 4-1.



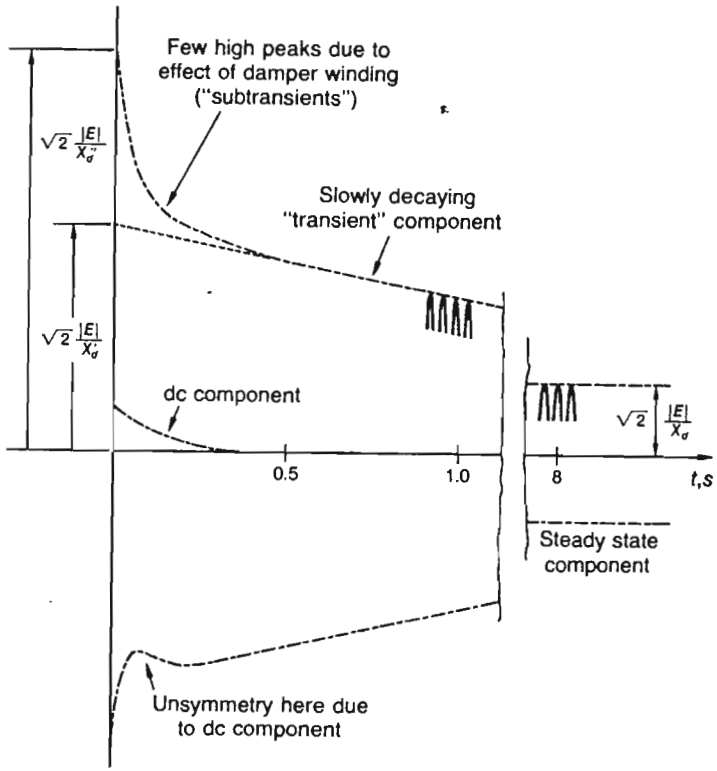


**Fig. 10-11** Transient short-circuit current of synchronous machine. Only the envelope of one phase shown.

In view of these circumstances, it is customary to perform the short-circuit analysis under the following simplifying assumptions:

1. All short-circuit current components but the dominating 60 Hz are neglected.
2. In spite of the fact that the 60-Hz component is decreasing exponentially from an initial maximum to an eventual steady-state minimum, the network analysis is performed as a regular ac problem; i.e., we make use of impedances for the machine representation.†
3. All network impedances are assumed purely reactive. For transformers and transmission lines we use the reactances presented in Chaps. 5 and 6. Synchronous machines are represented with an emf $E$ behind either

† The concept of impedance makes strict mathematical sense only when the network is in sinusoidal steady state. Since the 60-Hz component decays relatively slowly, this approximation is a very good one.

the subtransient or the transient reactance (depending upon whether we wish to know the short-circuit current immediately after the short circuit or after about 3 to 4 cycles).

4. The effect of the dc component is added in some empiric fashion. For example, in determining the megavoltampere interrupting rating for a breaker, we use the SCC, computed on the basis of the ac component and the transient machine reactances, multiplied by a factor that depends upon the speed of the breaker. The following recommendations are common:

| | |
|---|---|
| Two-cycle breaker: | 1.4 |
| Three-cycle breaker: | 1.2 |
| Eight-cycle breaker (or slower): | 1.0 |

## 10-5 SYMMETRICAL SHORT-CIRCUIT ANALYSIS—A SIMPLE DEMONSTRATION EXAMPLE

We are now ready to tackle a representative short-circuit analysis problem. We shall choose the simple three-bus system that we used in Chap. 7 to introduce the reader to load flow analysis. The system is depicted in Fig. 7-2. We make no attempt at the present to develop general computer methods, but instead focus our attention on useful approaches and approximation techniques.

### 10-5.1 STATEMENT OF THE PROBLEM

The system is initially (prefault) operating in steady state under assumed known generating and loading conditions. Load flows and bus voltages are assumed known.

A balanced solid three-phase short circuit occurs on bus 3. To determine circuit-breaker interrupting requirements and to procure data for proper relay settings, the following postfault data are sought:

1. Fault current at bus 3, measured as the 60-Hz rms at about three to four cycles following the short circuit
2. SCC at bus 3
3. The distribution of the postfault currents throughout the whole network
4. The postfault voltages of buses 1 and 2, also measured after about three to four cycles

### 10-5.2 SOLUTION PROCEDURE

We outline the analysis procedures:

*Step* 1 Assemble the equivalent *prefault* network diagram.
*Step* 2 From a regular load flow analysis (Chap. 7) determine the *prefault* current and voltage distribution throughout the network.



*Step* 3 Determine the *change* of the currents and voltages throughout the network as caused by the short circuit.
*Step* 4 Superimpose the changes in voltages and currents as computed in step 3 upon the *original* currents and voltages as computed in step 2 to obtain the *total postfault* current and voltage picture.

These four steps result in the mathematically correct postfault picture. Note that step 4 is simply an application of the superposition principle. In reality, we shall *not* perform each of the steps in blind obedience to all rules. We shall take several shortcuts that result in considerable savings in computational work but render results that are satisfactory from an engineering viewpoint. Whenever we make such approximations we shall motivate them.

**Step 1. Network assembly** The per-phase representation of our example system is shown in Fig. 10-12. All impedance and admittance elements have numerical values. We make the following comments about this network.

*Line representations* All the three transmission lines are assumed identical. The line data have been borrowed from Fig. 6-20, and represent, in round figures, a 30-mile 120-kV transmission line. The impedances are given in per units, referred to a 50-MVA 120-kV base.

*Generator and transformer representation* In accordance with our earlier discussion, each generator is represented by an emf behind a reactance. Since we are interested in the current values after about three to four cycles (i.e., when the subtransients have died out), we shall in our analysis use the transient reactance $X'_d$. For the transformers we use the leakage reactances. The generators and transformers have the following data:

$G1$: 100 MVA, transient reactance 20%
$G2$: 200 MVA, transient reactance 20%
$T1$: 100 MVA, leakage reactance 10%
$T2$: 200 MVA, leakage reactance 10%
(All reactances are based upon respective megavoltampere ratings.)

The total reactance of $G1 + T1$ is thus 30 percent, based upon 100 MVA, or 0.15 pu, based upon 50 MVA [using conversion formula (2-52)]. Similarly, we determine the reactance of $G2 + T2$ to 0.075 pu.

The reader should note that our simple generator model, which we have motivated earlier, is indeed a simplification of the real-life picture as discussed in the preceding section. This, then, is our *first* approximation in the overall short-circuit analysis.

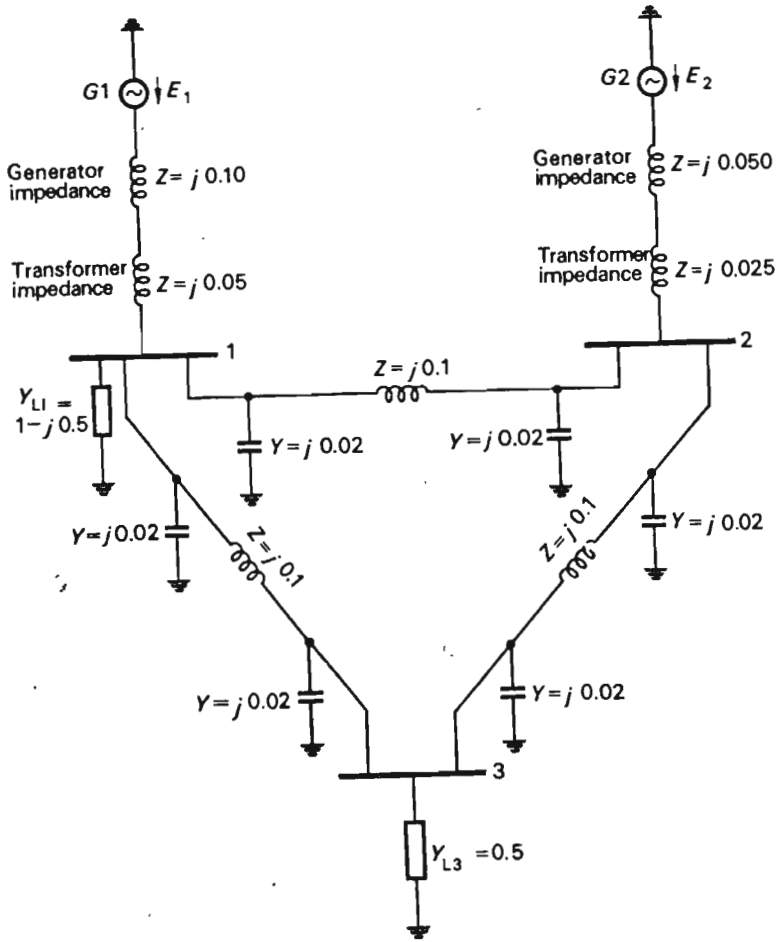


**Fig. 10-12** Sample network circuit parameters.

*Load representation* The prefault load demands at buses 1 and 3 are given:

$$S_{D1} = 1 + j0.5 \quad \text{pu}$$
$$S_{D3} = 0.5 + j0 \quad \text{pu}$$

If we assume that the prefault voltages of these two buses are to be kept at 1.0 pu, then, using Eq. (2-42), we can represent these loads by the load admittances $Y_{L1}$ and $Y_{L3}$, computed as follows:

$$1 + j0.5 = |1.0|^2\, Y_{L1}^*$$
$$0.5 + j0 = |1.0|^2\, Y_{L3}^*$$



that is,

$$Y_{L1} = 1 - j0.5$$
$$Y_{L3} = 0.5$$

Since we wish to preserve the *linearity* features of the network in order to have the right to apply Thévenin's theorem in step 3, we will assume the load admittances to be voltage-independent. We have thus introduced into the analysis our *second* approximation.

**Step 2. Prefault current and voltage picture** Once bus power and voltage specifications are assumed, a load flow analysis of the type discussed in Chap. 7 will render all voltage and current data prior to the short circuit. The prefault bus voltages can be expressed in our case as the three-vector

$$\mathbf{V}_{\text{bus}}^0 \triangleq \begin{bmatrix} V_1^0 \\ V_2^0 \\ V_3^0 \end{bmatrix} \tag{10-34}$$

Often we do not have the accurate prefault picture available, and instead of going to the extra trouble of computing it, we make the following assumptions:

1. All prefault bus voltages have unity magnitude (approximation 3)
2. All prefault currents are zero (approximation 4)

The voltage assumption is certainly accepted as reasonable since, in normal operation, all bus voltages are kept close to unity.

The reader may find it harder to accept the second assumption about the currents. The implication of this assumption is that all shunt admittances in Fig. 10-12 have been set equal to zero. There is no question that the line shunt capacitances that have an admittance of only 0.02 pu can be neglected. But what about the load admittances that have a magnitude of about 1 pu, thus carrying currents of about 1 pu magnitude?

The fact is that those changes in currents caused by the short circuit that we shall compute in our next step are limited only by the *series* impedance elements which are of the order of only 0.1 pu, resulting in currents that are of the order of 10 pu. Furthermore, these latter currents are almost purely reactive, whereas the prefault load currents are almost purely real.

The total postfault current (step 4) is therefore obtained as the vectorial sum of two currents having a phase difference of almost 90°. The reader will easily agree that the magnitude of this *total* current with good approximation equals the magnitude of the largest component. This is tantamount to saying that we might as well neglect the prefault current.

Figure 10-13 depicts the simplified version of our network representation after we have made these last approximations. This, then, is the diagram that we shall use in our further analysis.

**Step 3. Computation of changes in currents and voltages due to short circuit on bus 3** We shall now compute the changes that will occur in the network due to the structural change which the short circuit represents. The effect of the short circuit is equivalent to that of connecting the branch of impedance $Z'$ between bus 3 and ground, as indicated in Fig. 10-13. (If the short circuit is *solid*, as we will assume in our example, the fault impedance $Z'$ equals zero.)

Thévenin's theorem states that the *changes* in the network currents and voltages caused by the added branch are equivalent to those caused by the added emf† $E = V_3^0 \approx 1.0$ with all other sources short-circuited as shown in Fig. 10-14. (Note the polarity of the emf.) In this figure we have given symbols to all current changes. To compute these currents we have reduced

† The prefault voltage between bus 3 and ground is set equal to 1.0 pu in accordance with our earlier assumption 3. If we had known the exact prefault voltage of bus 3 from step 2, then of course we should use that value for better accuracy.

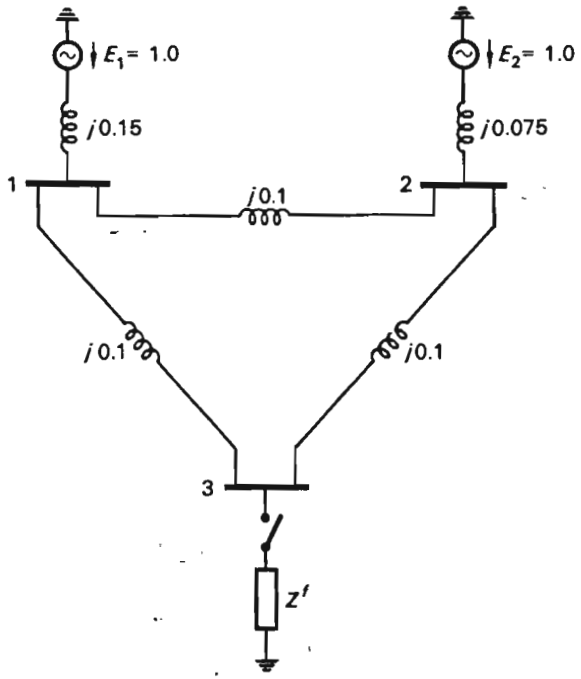


**Fig. 10-13** Simplified version of diagram in Fig. 10-12.



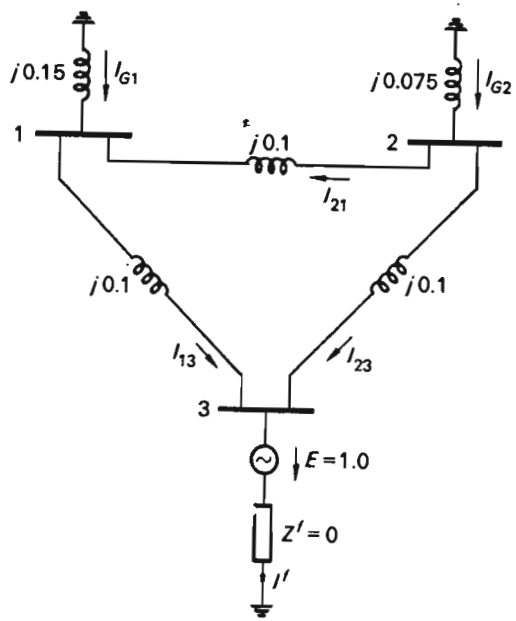


**Fig. 10-14** Thévenin equivalent network.

the network in four self-explanatory steps to the simple end product shown in Fig. 10-15*e*, from which we get directly for the fault current†

$$I' = \frac{1.0}{j0.1015} = -j9.85 \quad \text{pu}$$

($E$ is chosen as reference phasor.)

Figure 10-15*c* gives the clue as to how this fault current is divided between the two generators. We have

$$I_{G1} = \frac{j0.1083}{j0.1083 + j0.1833} I_f = -j3.67 \quad \text{pu}$$

$$I_{G2} = I' - I_{G1} = -j6.18 \quad \text{pu}$$

We next compute the voltage changes for buses 1 and 2. From Fig. 10-15*a* we get

$$V_1 = 0 - (j0.15)(-j3.67) = -0.550 \text{ pu}$$

$$V_2 = 0 - (j0.075)(-j6.18) = -0.463 \text{ pu}$$

† This is not a very *systematic* approach, but we use it here in this *simple* case in order to obtain results painlessly.

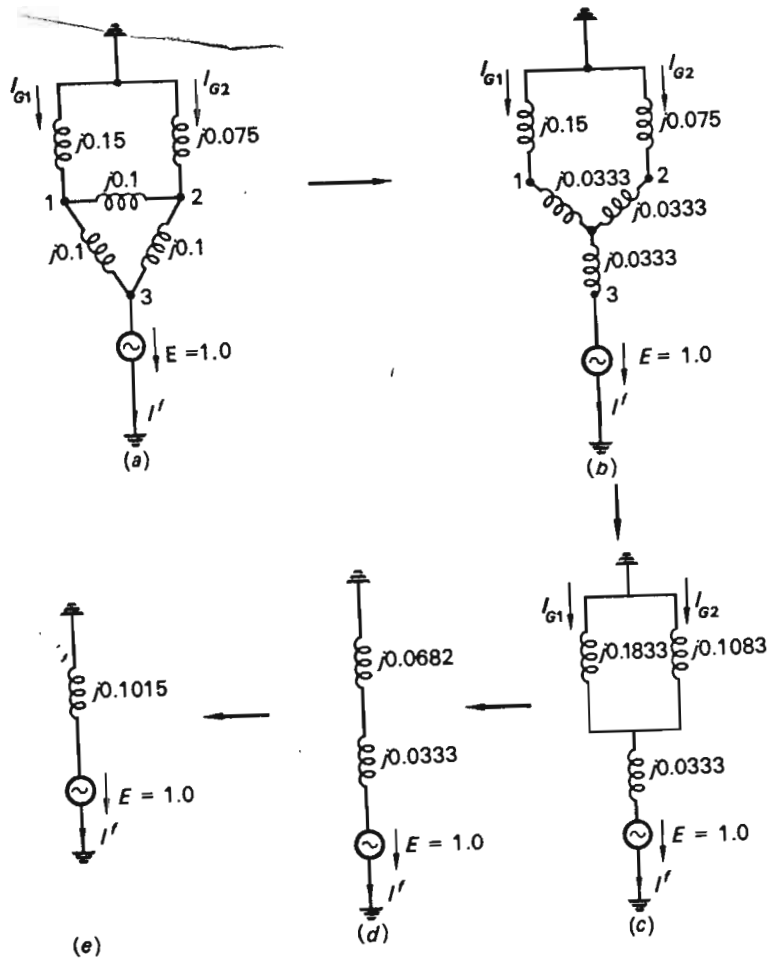


**Fig. 10-15** Step-by-step reduction of Thévenin equivalent network.

The voltage change of bus 3 is, of course,

$$V_3 = -1.0 \text{ pu}$$

These changes in the three bus voltages constitute a three-vector

$$\mathbf{V}_T \triangleq \begin{bmatrix} \text{change in voltage of bus 1} \\ \text{change in voltage of bus 2} \\ \text{change in voltage of bus 3} \end{bmatrix} = \begin{bmatrix} -0.550 \\ -0.463 \\ -1.000 \end{bmatrix} \tag{10-35}$$

which, for lack of a better name, we shall refer to as the "Thevenin's bus voltage vector."



All bus voltage changes being thus known, we can find the current changes in the three lines, as follows:

$$I_{21} = \frac{V_2 - V_1}{j0.1} = \frac{0.087}{j0.1} = -j0.87 \quad \text{pu}$$

$$I_{13} = \frac{V_1 - V_3}{j0.1} = \frac{0.450}{j0.1} = -j4.50 \quad \text{pu}$$

$$I_{23} = \frac{V_2 - V_3}{j0.1} = \frac{0.537}{j0.1} = -j5.37 \quad \text{pu}$$

This concludes step 3.

**Step 4. Postfault currents and voltages** In our last step we simply need to superimpose the results obtained in the previous step 3 upon the prefault conditions computed in step 2. In all cases we compute the magnitudes (or rms values). We get, first, for the bus voltages:

$$\begin{aligned} |V_1'| &= |V_1^0 + V_1| = |1.0 - 0.550| = 0.450 \text{ pu} \\ |V_2'| &= |V_2^0 + V_2| = |1.0 - 0.463| = 0.537 \text{ pu} \\ |V_3'| &= 0 \end{aligned} \tag{10-36}$$

For the currents we have

$$\begin{aligned} |I'| &= 9.85 \text{ pu (exact)} \\ |I_1'| &= |I_1^0 + I_1| \approx |0 - j3.67| \approx 3.67 \text{ pu} \\ |I_2'| &= |I_2^0 + I_2| \approx |0 - j6.18| \approx 6.18 \text{ pu} \\ |I_{21}'| &= |I_{21}^0 + I_{21}| = |? - j0.87| = ? \\ |I_{13}'| &= |I_{13}^0 + I_{13}| \approx |0 - j4.50| \approx 4.50 \text{ pu} \\ |I_{23}'| &= |I_{23}^0 + I_{23}| \approx |0 - j5.37| \approx 5.37 \text{ pu} \end{aligned}$$

In computing the above postfault quantities we have made use of approximations 3 and 4, except in the case of the current in line $L1$. In this latter case the current change $I_{21}$ is of the same magnitude as the prefault current, and we cannot therefore give the final value until we have computed the prefault value $I_{21}^0$. This task we pass on to the reader.

We complete our short-circuit study by computing the SCC of bus 3. From Eq. (10-10) we get directly

$$|\text{SCC}|_3 = 9.85 \text{ pu} = 9.85 \times 50 = 490 \text{ MVA}$$

In a real-life situation we would most probably also wish to perform studies of short circuits at buses 1 and 2, and possibly at other points of the network. In addition, we would most likely also investigate the effects of *unbalanced* short circuits (see the next chapter). Clearly, an exhaustive

short-circuit study leaves us with a vast amount of data. This fact, combined with the practical impossibility of using the above network reduction methods for large systems containing many buses, strengthens the case for digital computer application. We discuss this matter next.

## 10-6 SYSTEMATIC SHORT-CIRCUIT COMPUTATIONS

To involve the digital computer in short-circuit computations it is necessary to develop *systematic*, *general* computational procedures. The network reduction technique used in the preceding example can be used only in "textbook" examples of low dimensionality. We shall presently develop a technique that possesses full generality; i.e., it is directly applicable to an $n$-bus system.

The formulas we shall develop will permit us to compute the postfault bus voltages. If we possess knowledge of all bus voltages, we can of course immediately compute all postfault currents as well.

In presenting the method, we shall use the previous three-bus example as reference. Thévenin's theorem gave us the postfault bus voltages by superposition of the prefault bus voltages and the changes in the bus voltages caused by the equivalent emf connected to the faulted bus, as shown in Fig. 10-14. We can express this fact in the following vector equation:

$$\mathbf{V}'_{\text{bus}} = \mathbf{V}^0_{\text{bus}} + \mathbf{V}_T \tag{10-37}$$

The prefault bus voltage vector $\mathbf{V}^0_{\text{bus}}$ has already been defined by Eq. (10-34). The postfault bus voltage vector is defined by

$$\mathbf{V}'_{\text{bus}} \triangleq \begin{bmatrix} V_1' \\ V_2' \\ V_3' \end{bmatrix} \tag{10-38}$$

Finally, the third vector, $\mathbf{V}_T$, is the Thévenin's bus voltage vector defined in Eq. (10-35).

Let us consider the vector $\mathbf{V}_T$ for the moment. *It should be understood from Fig.* 10-14 *that we may consider the changes in the three bus voltages as resulting from the fault current $I'$ being drawn from bus* 3, *or differently stated, from the current $-I'$ being injected into bus* 3. If we therefore define a *fault-current vector*

$$\mathbf{I}_f \triangleq \begin{bmatrix} 0 \\ 0 \\ -I' \end{bmatrix} \tag{10-39}$$



it follows that we may obtain $\mathbf{V}_T$ directly by use of Eq. (7-42), which in terms of our new vectors reads

$$\mathbf{V}_T = \mathbf{Z}_{\text{bus}}\mathbf{I}' \tag{10-40}$$

where $\mathbf{Z}_{\text{bus}}$ is the $3 \times 3$ *bus impedance matrix* for the network in Fig. 10-14. By substituting this expression for $\mathbf{V}_T$ into Eq. (10-37), we get

$$\mathbf{V}'_{\text{bus}} = \mathbf{V}^0_{\text{bus}} + \mathbf{Z}_{\text{bus}}\mathbf{I}' \tag{10-41}$$

Before we take the next step in our analysis, we make the observation that, although we have derived this last vector equation with reference to a three-bus system, *it applies equally well to a general n-bus system.* From now on we shall therefore consider a *general* case. In making this extension of the validity of the equation, we need also to move the short circuit from bus 3 to the *general bus q*. In this more general case our fault-current vector therefore equals

$$\mathbf{I}' \triangleq \begin{bmatrix} 0 \\ \cdot \\ \cdot \\ \cdot \\ -I' \\ \cdot \\ \cdot \\ \cdot \\ 0 \end{bmatrix} \leftarrow q\text{th component} \tag{10-42}$$

As we proceed with our analysis we shall write the vector equation (10-41) in component form:

$$\begin{aligned} V_1' &= V_1^0 - z_{1q}I' \\ &\cdots\cdots\cdots\cdots \\ V_q' &= V_q^0 - z_{qq}I' \\ &\cdots\cdots\cdots\cdots \\ V_n' &= V_n^0 - z_{nq}I' \end{aligned} \tag{10-43}$$

At this stage the fault current $I'$ is as yet unknown. However, we know that the postfault voltage of the faulted bus, $V_q'$, is related to the fault current in the following way:

$$V_q' = Z'I' \tag{10-44}$$

where $Z'$ is the fault impedance.

If this expression for $V_q'$ is substituted into the $q$th equation (10-43), we obtain directly the following simple expression for the fault current:

$$I' = \frac{V_q^0}{Z' + z_{qq}} \tag{10-45}$$

Since $V_q^0$ is assumed known, so is the fault current. We therefore substitute $I^f$ into Eq. (10-43) and obtain the following final formulas for the postfault bus voltages:

$$V_i^f = V_i^0 - \frac{z_{iq}}{Z^f + z_{qq}} V_q^0 \qquad i \neq q$$
$$V_q^f = \frac{Z^f}{Z^f + z_{qq}} V_q^0 \tag{10-46}$$

If the short circuit is *solid* (that is, $Z^f = 0$), these formulas simplify to

$$I^f = \frac{V_q^0}{z_{qq}}$$
$$V_q^f = 0 \tag{10-47}$$
$$V_i^f = V_i^0 - \frac{z_{iq}}{z_{qq}} V_q^0 \qquad i \neq q$$

*Note:* The above formulas are *exact*. We assume that the prefault bus voltages $V_i^0$ are available from a load flow study. The $\mathbf{Z}_{\text{bus}}$ matrix is obtained by inversion of the bus admittance matrix $\mathbf{Y}_{\text{bus}}$. In assembling this latter matrix, using the formulas outlined in Chap. 7 *and making use of a*

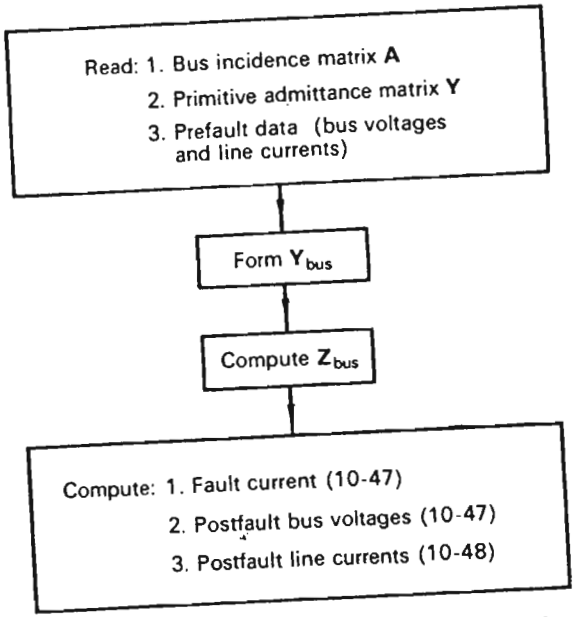


**Fig. 10-16** Computational flow diagram for short-circuit analysis of bus system.



*digital computer*, there is really no need for using *approximate* diagrams such as Fig. 10-13 in preference to *exact* diagrams such as Fig. 10-12.

Our analysis has rendered the values for the fault current $I^f$ and the postfault bus voltage $V_i^f$. We need also to know the postfault currents in all branches of the network. Let us consider the transmission line connecting buses $\nu$ and $\mu$. The impedance of this line is $Z_{\nu\mu}$, and the postfault current $I_{\nu\mu}{}^f$ in the line (defined positive in direction $\nu \rightarrow \mu$) therefore equals

$$I_{\nu\mu}{}^f = \frac{V_\mu^f - V_\mu^f}{Z_{\nu\mu}} \tag{10-48}$$

This, then, completes our analysis. The short-circuit analysis method presented above is by no means the only one existing. For example, instead of working in the bus frame of reference as we did, we could have used the loop frame of reference. Figure 10-16 shows a flow diagram for a short-circuit analysis program to be performed on a digital computer.

**Example 10-4** We shall recompute in this example the short-circuit problem that we worked with elementary techniques in Sec. 10-5.

We first form the bus admittance matrix for the approximate network in Fig. 10-13. Using Eqs. (7-34), we get

$$y_{11} = \frac{1}{j0.15} + \frac{1}{j0.1} + \frac{1}{j1.0} = -j26.67$$

$$y_{22} = \frac{1}{j0.075} + \frac{1}{j0.1} + \frac{1}{j0.1} = -j33.33$$

$$y_{33} = \frac{1}{j0.1} + \frac{1}{j0.1} = -j20.0$$

$$y_{12} = y_{21} = -\frac{1}{j0.1} = j10$$

$$y_{13} = y_{31} = -\frac{1}{j0.1} = j10$$

$$y_{23} = y_{32} = -\frac{1}{j0.1} = j10$$

We can now assemble the bus admittance matrix:

$$\mathbf{Y}_{\text{bus}} = \begin{bmatrix} -j26.67 & j10 & j10 \\ j10 & -j33.33 & j10 \\ j10 & j10 & -j20 \end{bmatrix} \tag{10-49}$$

By inversion of $\mathbf{Y}_{bus}$ we get

$$\mathbf{Z}_{bus} = \begin{bmatrix} j0.073 & j0.0386 & j0.0558 \\ j0.0386 & j0.0558 & j0.0472 \\ j0.0558 & j0.0472 & j0.1014 \end{bmatrix} \tag{10-50}$$

We obtain now the postfault bus voltages and the fault current by direct application of Eqs. (10-47).

$$V_1' = 1.00 - \frac{j0.0558}{j0.1014} \times 1.00 = 0.450 \quad \text{pu}$$

$$V_2' = 1.00 - \frac{j0.0472}{j0.1014} \times 1.00 = 0.535 \quad \text{pu}$$

$$V_3' = 0$$

$$I' = \frac{1.00}{j0.1014} = -j9.86 \quad \text{pu}$$

These values agree, within slide-rule accuracy, with those computed earlier (see pages 419 and 421).

At this juncture the critical reader (after having spent an hour checking the entries in $\mathbf{Y}_{bus}$ and $\mathbf{Z}_{bus}$) will question the advantage of the general method over the simple one used in the first runaround. It is always true that general methods represent "sledge-hammer" approaches to problems of simple objectives and low dimensionality. But we must not forget that the general method is intended for the digital computer, which would perform the algebraic operations (including assembly and inversion of $\mathbf{Y}_{bus}$) of the three-bus problem of Example 10-4 in a fraction of a second.

Furthermore, and this is extremely important, once we have computed $\mathbf{Z}_{bus}$, we can *immediately obtain all necessary short-circuit data for faults on any bus*. For example, in Example 10-4, the fault current for a fault on bus 1 will be

$$I' = \frac{1.00}{z_{11}} = \frac{1.00}{j0.073} = -j13.7 \quad \text{pu}$$

and for a fault on bus 2,

$$I' = \frac{1.00}{z_{22}} = \frac{1.00}{j0.0558} = -j17.9 \quad \text{pu}$$

(Give the physical reason why the last type of fault evidently is the most severe.)

## 10-7 SUMMARY

After classification of system transients into the categories "ultrafast," "medium fast," and "slow," we have taken a closer look at the two first



classes. The ultrafast transients, usually caused by atmospheric disturbances and switching operations, give rise to overvoltages, which usually disappear within milliseconds but may cause insulation breakdown. We studied methods of estimating the overvoltage magnitudes.

It should be understood that because atmospheric disturbances are difficult to measure, and even estimate, it does not make much sense to employ too sophisticated mathematical techniques in the solution of the wave equation. We made several simplifying assumptions which permitted us to obtain solutions relatively simply.

Of the "medium-fast" transients or "short-circuit" phenomena, we have considered in this chapter only the *balanced* case, i.e., when the short circuit involves *symmetrically* all three phases. Of all the short circuits that do occur, this is by far the rarest occurrence—but the most dangerous one. For this reason the balanced short-circuit computations are the most important.

Systematic, computerized methods for solving this type of short circuit on a general $n$-bus system have been presented. Reasonable model simplifications have been utilized, of which the most useful one is to represent the generator with an emf behind either the transient or the subtransient reactance.

## EXERCISES

**10-1.** In Example 10-4 we concluded that a solid symmetrical short circuit on bus 2 results in a current of 17.9 pu, or differently stated, bus 2 has a SCC of $17.9 \times 50 = 895$ MVA. To reduce the stresses on the circuit breaker, we wish to reduce the SCC to 500 MVA by adding reactors in series with $G2 + T2$. How much reactance per phase must be added? Express your answer

1. In per units
2. In ohms, assuming the reactors are placed on the low-voltage side of $T2$
3. In ohms, assuming the reactors are placed on the high-voltage side of $T2$
   (Where would *you* place them?)

The transformer has a nominal voltage rating of 120/20 kV.

**10-2.** Use the value of $\mathbf{Z}_{bus}$ computed in Example 10-4 and find in the simplest manner possible the postfault voltages on buses 1 and 3 if the *solid* short circuit occurs on bus 2.

**10-3.** Consider the 90-mile transmission line discussed in Example 10-1. Assume that the line is open-circuited in both ends and deenergized. Assume that one end of the line is applied to a dc battery of emf $E$ for 0.1 ms. This will initiate an 18-mile-long pulse wave of amplitude $E$.

Study the progress of the wave by analog computer. For example, lump the line into 10 $\pi$ segments, as demonstrated in Fig. 10-4. Choose the currents in each coil element and the voltage across each capacitor as state variables for a total of 20 state variables. Write the differential equation for each element, and you will obtain a linear coupled system of order 20. This system can easily be simulated on an analog computer having at

least 20 integrators. (If you do not have 20 integrators, choose a coarser lumping.) Note that you must *time-scale* your problem to match it to the slow computer.

Display the voltage of the capacitors representing midline and end of line and see how closely the voltages resemble the actual ones shown in Fig. 10-3.

**10-4.** Using an analog computer, simulate the restrike phenomenon depicted in Fig. 10-6. Assume that the capacitor bank $C$ is rated at 50 Mvar three-phase at 120 kV. Represent the 90-mile line by one $\pi$ link and assume that the generator bus has SCC $= \infty$.

**10-5.** Consider the five-bus system in Exercise 7-9. Write a computer program for finding the SCC of all five buses.

Assume that only buses 1, 2, and 4 have generators (plus step-up transformers). The generators and transformers have the following data, based upon 50 MVA.

| *Bus* | *Generator transient reactance* | *Transformer reactance* |
|---|---|---|
| 1 | 0.102 pu | 0.050 |
| 2 | 0.081 pu | 0.040 |
| 4 | 0.220 pu | 0.110 |

If you have already computed the voltage profile in Exercise 7-10, use these values for prefault values. If not, assume that all prefault voltages are 1.00 pu.

*Warning:* The $\mathbf{Y}_{bus}$ matrix you developed for your load flow study is not the $\mathbf{Y}_{bus}$ matrix you should use for the short-circuit study. Why not?

## REFERENCES


**Books**

1. Rüdenberg, R.: "Transient Performance of Electric Power Systems," McGraw-Hill Book Company, New York, 1950.
2. Bewley, L. V.: "Traveling Waves on Transmission Systems," John Wiley & Sons, Inc., New York, 1951.
3. Peterson, H. A.: "Transients in Power Systems," Dover Publications, Inc., New York, 1951.
4. Lewis, W. W.: "The Protection of Transmission Systems against Lightning," John Wiley & Sons, Inc., New York, 1950.
5. Mason, C. R.: "The Art and Science of Protective Relaying," John Wiley & Sons, Inc., New York, 1956.
6. Lyon, W. V.: "Transient Analysis of AC Machinery," Chapman and Hall, Ltd., London, 1954.
7. Fitzgerald, A. E., and C. Kingsley, Jr.: "Electric Machinery," McGraw Hill Book Company, New York, 1961.
8. Stagg, G. W., and A. H. El-Abiad: "Computer Methods in Power Systems Analysis," McGraw Hill Book Company, New York, 1968.

(References 1 to 3 give the classic treatment of power system transients of the "fast" and "medium-fast" classification. References 4 and 5 treat protective system relaying, which topic we have skipped altogether. References 6 and 7 discuss the behavior of the synchronous machine under transient conditions. Reference 8 treats the fault analysis by computer methods.)





**Technical papers and reports**

9. Laughton, M. A., and M. W. Humphrey Davies: Short-circuit Analysis for Large Systems, *Proc. Ind. Computer Appl.*, Clearwater, Fla., 1965, pp. 48–58.
10. Silva, R. F.: Short-circuit Equivalent Networks from Ordinary Fault Data, *Proc. Ind. Computer Appl.*, Clearwater, Fla., 1965, pp. 40–47.
11. Baba, J., et al.: New Method of Calculating Simultaneous Faults by Means of Digital Computer, *Proc. Ind. Computer Appl.*, Clearwater, Fla., 1965, pp. 59–73.
12. Brown, H. E., and C. E. Person: Short-circuit Studies of Large Systems, rept. 4.11, *Proc. Power Systems Computation Conf.*, Stockholm, Sweden, 1966.
13. Holmdahl, G., and R. Lundin: Digital Solution of Travelling Wave Problems in 3-phase systems, rept. 5.12, *Proc. Power Systems Computation Conf.*, Stockholm, Sweden, 1966.
14. Dommel, H. W.: A Method for Solving Transient Phenomena in Multiphase systems, rept. 5.8, *Proc. Power Systems Computation Conf.*, Stockholm, Sweden, 1966.
15. Brown, H. E., and C. E. Person: Short Circuit Studies of Large Systems by the Impedance Matrix Method, *Proc. Power Ind. Computer Appl.*, Pittsburgh, Pa., 1967, pp. 335–342.
16. Trihus, A. T., and R. Zimering: A Digital Computer Program for an Exhaustive Fault Study of a Large Power System Network, *Proc. Power Ind. Computer Appl.*, Pittsburgh, Pa., 1967, pp. 343–350.
17. Shipley, R. B., et al.: Digital Analysis of Single Pole Switching on EHV Lines, *Proc. Power Ind. Computer Appl.*, Pittsburgh, Pa., 1967, pp. 351–358.
18. Thoren, H. B., and K. L. Carlsson: A Digital Computer Program for the Calculation of Switching and Lightning Surges on Power Systems, *Proc. Power Ind. Computer Appl.*, 1969.
19. Sabath, J., et al.: Analog Computer Study of Switching Surge Transients for a 500 kv System, *IEEE Trans.*, vol. PAS-85, no. 1, pp. 1–9, January, 1966.
20. Catenacci, G., et al.: Transient Recovery Voltages in European Networks, *IEEE Trans.*, vol. PAS-86, no. 11, pp. 1420–1431, November, 1967.
21. EHV Line Outages, IEEE-EEI Committee Report, *IEEE Trans.*, vol. PAS-86, no. 5, May, 1967.
22. Lauber, T. S.: Maximum Overvoltages Produced by EHV Circuit Breaker Closure, *IEEE Trans.*, vol. PAS-87, no. 4, pp. 1026–1032, April, 1968.
23. Colombo, A., et al.: Determination of Transient Recovery Voltages by Means of Transient Network Analyzers, *IEEE Trans.*, vol. PAS-87, no. 6, pp. 1371–1380, June, 1968.
24. Dommel, H. W.: Digital Computer Solution of Electromagnetic Transients in Single- and Multiphase Systems, *IEEE Trans.*, vol. PAS-88, no. 4, pp. 388–399, April, 1969.
25. Rockefeller, G. D.: Fault Protection with a Digital Computer, *IEEE Trans.*, vol. PAS-88, no. 4, pp. 438–464, April, 1969.
26. Thomas, C. H.: Switching Surges on Transmission Lines Studied by Differential Analyzer Simulation, *IEEE Trans.*, vol. PAS-88, no. 5, pp. 636–645, May, 1969.

# 11

# Unbalanced System Analysis

In all our previous work we have based our analysis on the assumption that complete phase symmetry, or balance, is maintained. Thus the load (or fault) impedances are the same on all three phases, and the voltages, emfs, and currents are characterized by complete three-phase symmetry; i.e., they are of equal magnitude in each phase and displaced 120 and 240° in time. Under this assumption we have then studied the system on a per-phase basis; i.e., we have focused attention on the above quantities in one of the phases. Knowledge of the current or the voltage in this phase implies knowledge of the corresponding variables in the other two phases. The total power, real or reactive, is obtained by multiplying the phase power by three.

Differently expressed, the impedance matrices of symmetrically operated three-phase generators, transformers, and (transposed) transmission lines are *diagonal, with all diagonal elements equal.* This fact results in *decoupling* between phases.

In an unsymmetrically faulted or loaded system, neither the currents nor the voltages will possess three-phase symmetry. The impedance





matrices of generators, transformers, and lines will all be nondiagonal. It is no longer possible to limit the analysis to one phase, because coupling exists between the three phases. It is necessary to treat the different phases individually.

## 11-1 THE SYMM. COMP. TRANSF. (SCT)

The resulting increase in analysis complexity can be offset to a considerable extent by the systematizing features of the so-called *symmetrical components.*

### 11-1.1 DEFINITIONS

The basic feature of this method, as the name implies, is the resolution of the unsymmetrical phase currents and voltages into a set of components that possess certain symmetry features. If $I_a$, $I_b$, and $I_c$ represent the three *unbalanced* phase currents in some point of the network, then, by definition, we resolve these three currents into the following nine components:†

$$\begin{aligned} I_a &\triangleq I_{a+} + I_{a-} + I_{a0} \\ I_b &\triangleq I_{b+} + I_{b-} + I_{b0} \\ I_c &\triangleq I_{c+} + I_{c-} + I_{c0} \end{aligned} \tag{11-1}$$

We may, of course, resolve three phasors into nine components in an infinite number of ways. To make the three Eqs. (11-1) render unique solutions, it is necessary for us to impose six additional restrictions on the nine new variables. We choose to impose the following conditions upon them:

$$\begin{aligned} I_{b+} &= I_{a+}e^{-j120^\circ} \qquad I_{b-} = I_{a-}e^{j120^\circ} \\ I_{c+} &= I_{a+}e^{j120^\circ} \qquad I_{c-} = I_{a-}e^{-j120^\circ} \\ I_{a0} &= I_{b0} = I_{c0} \end{aligned} \tag{11-2}$$

The actual meaning of these restrictions should be clear from Fig. 11-1. We note that we have, in effect, required that the components $I_{a+}$, $I_{b+}$, and $I_{c+}$ constitute a set of phasors *possessing three-phase symmetry* and having the phase sequence *abca* . . . . They will henceforth be referred to as the *positive-sequence* current components.

The *negative-sequence* components $I_{a-}$, $I_{b-}$, and $I_{c-}$ likewise possess three-phase symmetry, but with the *reversed phase sequence acba* . . . . Finally, the *zero-sequence* current components $I_{a0}$, $I_{b0}$, and $I_{c0}$ are of both *equal magnitude and phase.*

† We will throughout assume sinusoidal variables, which entitles us to work with phasor quantities.

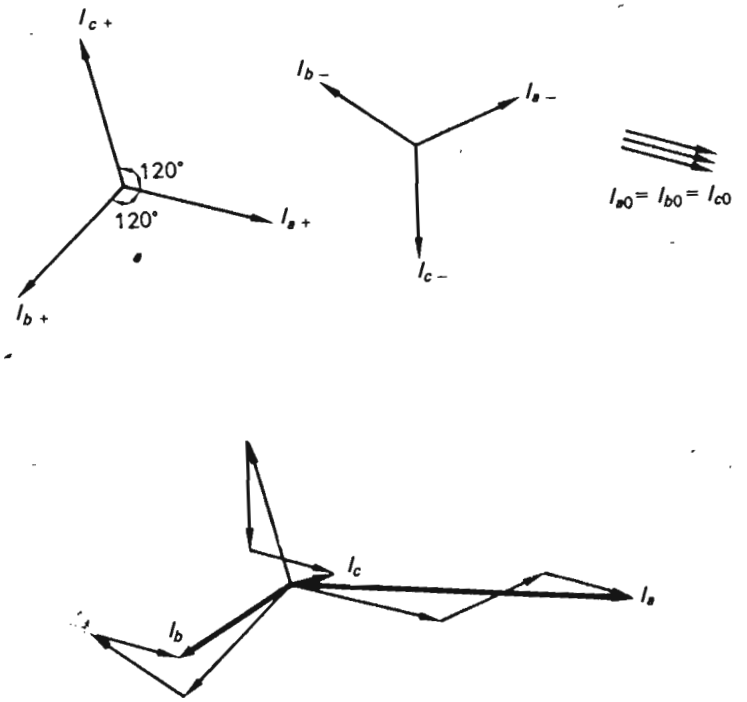


**Fig. 11-1** Resolution of unbalanced phasor system $(I_a, I_b, I_c)$ into symmetrical components.

Substitution of conditions (11-2) into Eqs. (11-1) gives

$$\begin{aligned} I_a &= I_{a+} + I_{a-} + I_{a0} \\ I_b &= \alpha^2 I_{a+} + \alpha I_{a-} + I_{a0} \\ I_c &= \alpha I_{a+} + \alpha^2 I_{a-} + I_{a0} \end{aligned} \tag{11-3}$$

For shorter notations we have here introduced the brevity symbol

$$\alpha \triangleq e^{j120^\circ} = \cos 120^\circ + j \sin 120^\circ = -0.500 + j0.866 \tag{11-4}$$

We may easily confirm that the following identities apply for $\alpha$:

$$\begin{aligned} &\alpha^2 = e^{j240^\circ} = e^{-j120^\circ} = -0.500 - j0.866 \\ &\alpha^3 = 1 \\ &1 + \alpha + \alpha^2 = 0 \\ &\alpha^* = \alpha^2 \\ &(\alpha^2)^* = \alpha \end{aligned} \tag{11-5}$$



Equations (11-3) can be written in compact matrix form:

$$\mathbf{I}_p = \mathbf{T}\mathbf{I}_s \tag{11-6}$$

where the matrix

$$\mathbf{T} \triangleq \begin{bmatrix} 1 & 1 & 1 \\ \alpha^2 & \alpha & 1 \\ \alpha & \alpha^2 & 1 \end{bmatrix} \tag{11-7}$$

is referred to as the *symmetrical component transformation matrix*.

The current vectors

$$\mathbf{I}_p \triangleq \begin{bmatrix} I_a \\ I_b \\ I_c \end{bmatrix}$$

and (11-8)

$$\mathbf{I}_s \triangleq \begin{bmatrix} I_{a+} \\ I_{a-} \\ I_{a0} \end{bmatrix} \quad \text{or for brevity†} \quad \mathbf{I}_s \triangleq \begin{bmatrix} I_+ \\ I_- \\ I_0 \end{bmatrix}$$

represent the actual phase currents and the symmetrical current components, respectively.

From Eq. (11-6) we obtain upon inversion

$$\mathbf{I}_s = \mathbf{T}^{-1}\mathbf{I}_p \tag{11-9}$$

where

$$\mathbf{T}^{-1} = \frac{1}{3}\begin{bmatrix} 1 & \alpha & \alpha^2 \\ 1 & \alpha^2 & \alpha \\ 1 & 1 & 1 \end{bmatrix} \tag{11-10}$$

Equations (11-9) and (11-6) define, respectively, the *direct* and *indirect* SC transforms.

We may, of course, apply the SCT to voltage phasors as well. If the vectors

$$\mathbf{V}_p \triangleq \begin{bmatrix} V_a \\ V_b \\ V_c \end{bmatrix} \quad \text{and} \quad \mathbf{V}_s \triangleq \begin{bmatrix} V_{a+} \\ V_{a-} \\ V_{a0} \end{bmatrix} \quad \text{or in shorter form} \quad \begin{bmatrix} V_+ \\ V_- \\ V_0 \end{bmatrix} \tag{11-11}$$

† In using the abbreviated symbols we must always remember that the components $I_+$, $I_-$, and $I_0$ refer to phase $a$.

represent the actual phase voltages and the symmetrical voltage components, respectively, we have the SC transform pair for voltages:

$$\begin{aligned} \mathbf{V}_p &= \mathbf{T}\mathbf{V}_s \\ \mathbf{V}_s &= \mathbf{T}^{-1}\mathbf{V}_p \end{aligned} \tag{11-12}$$

### 11-1.2 USEFUL PROPERTIES OF SCT

We have not so far given any motivations for having introduced the SCT. At a first glance it would seem that the involvement of three new variables would actually represent a complication of matters. However, the SCT is characterized by many properties that, taken together, render it a practical tool in unsymmetrical system study. We shall now expose the more important of these properties.

**Effect of SCT on the power formulas** Our basic concern on most occasions will be the power flow in the system. In terms of the actual phase voltages and currents, the total power flow equals

$$S = P + jQ = V_a I_a^* + V_b I_b^* + V_c I_c^* = \mathbf{V}_p^T \mathbf{I}_p^* \tag{11-13}$$

By substitution of Eqs. (11-6) and (11-12) into Eq. (11-13), we get

$$S = P + jQ = (\mathbf{T}\mathbf{V}_s)^T (\mathbf{T}\mathbf{I}_s)^* = \mathbf{V}_s^T \mathbf{T}^T \mathbf{T}^* \mathbf{I}_s^* \tag{11-14}$$

The last step follows from Eq. (A-30). The matrix product $\mathbf{T}^T\mathbf{T}^*$ is then evaluated.

$$\mathbf{T}^T\mathbf{T}^* = \begin{bmatrix} 1 & \alpha^2 & \alpha \\ 1 & \alpha & \alpha^2 \\ 1 & 1 & 1 \end{bmatrix} \begin{bmatrix} 1 & 1 & 1 \\ \alpha & \alpha^2 & 1 \\ \alpha^2 & \alpha & 1 \end{bmatrix} = 3 \begin{bmatrix} 1 & 0 & 0 \\ 0 & 1 & 0 \\ 0 & 0 & 1 \end{bmatrix} = 3\mathbf{I} \tag{11-15}$$

In view of the result (11-15), we may write the power formula (11-14) as follows:

$$S = P + jQ = 3\mathbf{V}_s^T \mathbf{I}_s^* = 3V_+ I_+^* + 3V_- I_-^* + 3V_0 I_0^* \tag{11-16}$$

*In words*, the total power in the unbalanced system can be computed as the sum of the symmetrical component powers. We also note that each component power equals 3 times its per-phase value, a consequence of the fact that each component system is symmetric.

**Effect of SCT on the performance equations of passive network element** A passive network element (transformers and transmission lines) operated under unbalanced conditions can be described (see below)



by a vector equation of the alternative forms

$$\mathbf{V}_p = \mathbf{Z}\mathbf{I}_p \tag{11-17}$$

$$\mathbf{I}_p = \mathbf{Y}\mathbf{V}_p \tag{11-18}$$

where $\mathbf{Z}$ and $\mathbf{Y}$ are $3 \times 3$ matrices.

By substitution of Eqs. (11-6) and (11-12) into Eqs. (11-17) and (11-18), we obtain the following transformed relations:

$$\mathbf{V}_s = \mathbf{T}^{-1}\mathbf{Z}\mathbf{T}\mathbf{I}_s \triangleq \mathbf{Z}_s\mathbf{I}_s \tag{11-19}$$

and

$$\mathbf{I}_s = \mathbf{T}^{-1}\mathbf{Y}\mathbf{T}\mathbf{V}_s \triangleq \mathbf{Y}_s\mathbf{V}_s \tag{11-20}$$

**SC-transformed impedance and admittance matrices** The new impedance and admittance matrices

$$\mathbf{Z}_s \triangleq \mathbf{T}^{-1}\mathbf{Z}\mathbf{T} \tag{11-21}$$

$$\mathbf{Y}_s \triangleq \mathbf{T}^{-1}\mathbf{Y}\mathbf{T} \tag{11-22}$$

are referred to as *SC-transformed*. They give the relationships between the SC-transformed voltages $\mathbf{V}_s$ and $\mathbf{I}_s$ for the element in question.

*The greatest inherent value of the SCT as an analysis tool is associated with the fact that these matrices turn out to be diagonal for the elements most widely used in EESE.*

As a consequence, *no coupling* exists between the plus-, minus-, and zero-sequence systems, *and they can be treated separately*. It is this "decoupling feature" that has made the SCT such a popular and widely used analysis tool. Let us demonstrate.

**Performance equations for unbalanced passive element** Consider the case of an unsymmetrically operated *static* network element, i.e., a transformer or transmission line or a combination of the two. In Fig. 11-2 we have depicted a transmission link connecting two buses 1 and 2. The link may represent a line with its transformers.

Under *balanced* operating conditions the currents and the voltages in both ends possess three-phase symmetry. Since the sum of the three phase currents equals zero, there is no "neutral," or return, current $I_n$, and there can therefore be no potential difference between the two "local neutral" points; i.e.,

$$V_{n1} = V_{n2} = 0$$

Under *unbalanced* loading conditions neither the voltages nor the currents possess three-phase symmetry. The sum of the phase currents is

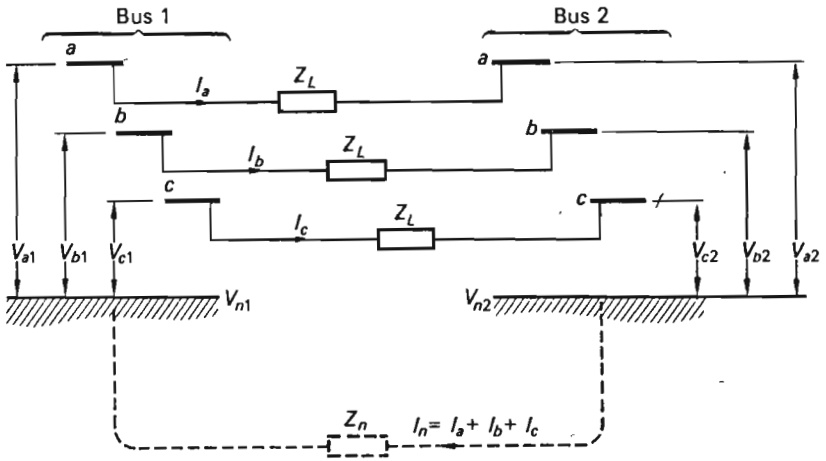


**Fig. 11-2** Unsymmetrically loaded transmission line.

not zero, and we therefore have a nonzero neutral current

$$I_n = I_a + I_b + I_c$$

which causes a voltage drop across the neutral impedance $Z_n$. The result is that the local "grounds" are not at equal potential. We can write the following voltage equations for the link:

$$\begin{aligned} V_{a1} - V_{a2} &= I_a Z_L + (I_a + I_b + I_c)Z_n \\ V_{b1} - V_{b2} &= I_b Z_L + (I_a + I_b + I_c)Z_n \\ V_{c1} - V_{c2} &= I_c Z_L + (I_a + I_b + I_c)Z_n \end{aligned} \tag{11-23}$$

or in vector form,

$$\begin{bmatrix} V_{a1} \\ V_{b1} \\ V_{c1} \end{bmatrix} - \begin{bmatrix} V_{a2} \\ V_{b2} \\ V_{c2} \end{bmatrix} = \begin{bmatrix} Z_L + Z_n & Z_n & Z_n \\ Z_n & Z_L + Z_n & Z_n \\ Z_n & Z_n & Z_L + Z_n \end{bmatrix} \begin{bmatrix} I_a \\ I_b \\ I_c \end{bmatrix} \tag{11-24}$$

or in shorter form,

$$\Delta \mathbf{V}_p = \mathbf{Z}\mathbf{I}_p \tag{11-25}$$

where

$$\Delta \mathbf{V}_p \triangleq \mathbf{V}_{p1} - \mathbf{V}_{p2} = \begin{bmatrix} \Delta V_a \\ \Delta V_b \\ \Delta V_c \end{bmatrix} \tag{11-26}$$

represents the voltage drop along the link. *Note that the phase voltages* $\mathbf{V}_{p1}$ *and* $\mathbf{V}_{p2}$ *are measured with respect to their respective neutrals.*



Equation (11-25) is of the form of Eq. (11-17), and we therefore make use of Eq. (11-21) to obtain the SC-transformed impedance. We get

$$\begin{aligned} \mathbf{Z}_s &= \mathbf{T}^{-1} \begin{bmatrix} Z_L + Z_n & Z_n & Z_n \\ Z_n & Z_L + Z_n & Z_n \\ Z_n & Z_n & Z_L + Z_n \end{bmatrix} \mathbf{T} \\ &= \begin{bmatrix} Z_L & 0 & 0 \\ 0 & Z_L & 0 \\ 0 & 0 & Z_L + 3Z_n \end{bmatrix} \end{aligned} \tag{11-27}$$

**Sequence impedances** We define at this juncture the following *sequence impedances*:

$$\begin{aligned} z_+ &\triangleq Z_L && \textit{positive-sequence impedance} \\ z_- &\triangleq Z_L && \textit{negative-sequence impedance} \\ z_0 &\triangleq Z_L + 3Z_n && \textit{zero-sequence impedance} \end{aligned} \tag{11-28}$$

In accordance with Eq. (11-19), the SC-transformed version of Eq. (11-24) therefore reads†

$$\begin{aligned} V_{+1} - V_{+2} &= z_+ I_+ \\ V_{-1} - V_{-2} &= z_- I_- \\ V_{01} - V_{02} &= z_0 I_0 \end{aligned} \tag{11-29}$$

We note that, the $\mathbf{Z}_s$ matrix (11-27) being diagonal, *there is complete decoupling between the sequence component systems.*

**Effect of SCT on the performance equations of an unsymmetrically loaded synchronous machine** A synchronous machine under balanced loading conditions is characterized by complete decoupling between the three

† As to the symbols used, we make the following agreements:

1. The phase voltages at bus $i$ are represented by the vector

$$\mathbf{V}_{pi} \triangleq \begin{bmatrix} V_{ai} \\ V_{bi} \\ V_{ci} \end{bmatrix}$$

The voltages $V_{ai}$, $V_{bi}$, and $V_{ci}$ are measured relative to "*local ground.*"

2. The symmetrical voltage components at bus $i$ are symbolized by the vector

$$\mathbf{V}_{si} \triangleq \begin{bmatrix} V_{+i} \\ V_{-i} \\ V_{0i} \end{bmatrix}$$

(As usual, we refer to phase $a$.)

phases, as expressed by Eqs. (4-77) and (4-78). The behavior of a synchronous machine under unbalanced loading conditions presents a more complicated picture. We can readily analyze the situation following the procedure in Sec. 4-4.2, but starting with an unbalanced set of armature currents instead of the balanced set (4-47).

The results of such an analysis reveal that the performance equations are still of the form† of Eq. (4-77):

$$\mathbf{V}_p = \mathbf{E}_p - \mathbf{Z}\mathbf{I}_p \tag{11-30}$$

The impedance matrix $\mathbf{Z}$ is no longer diagonal, but of the form

$$\mathbf{Z} = \begin{bmatrix} z_1 & z_2 & z_3 \\ z_3 & z_1 & z_2 \\ z_2 & z_3 & z_1 \end{bmatrix} \tag{11-31}$$

where the impedance elements $z_1$, $z_2$, and $z_3$ are functions of the inductance parameters $L_1, \ldots, L_5$ defined in Sec. 4-3.1.

If we make use of Eqs. (11-6) and (11-12), the vector equation (11-30) attains the form

$$\mathbf{T}\mathbf{V}_s = \mathbf{E}_p - \mathbf{Z}\mathbf{T}\mathbf{I}_s$$

We premultiply this equation by $\mathbf{T}^{-1}$ and obtain

$$\mathbf{V}_s = \mathbf{T}^{-1}\mathbf{E}_p - \mathbf{T}^{-1}\mathbf{Z}\mathbf{T}\mathbf{I}_s = \mathbf{T}^{-1}\mathbf{E}_p - \mathbf{Z}_s\mathbf{I}_s \tag{11-32}$$

The last step follows from Eq. (11-21).

We perform the multiplications called for and obtain

$$\mathbf{T}^{-1}\mathbf{E}_p = \frac{1}{3}\begin{bmatrix} 1 & \alpha & \alpha^2 \\ 1 & \alpha^2 & \alpha \\ 1 & 1 & 1 \end{bmatrix}\begin{bmatrix} E_a \\ \alpha^2 E_a \\ \alpha E_a \end{bmatrix} = \frac{1}{3}\begin{bmatrix} E_a(1+\alpha^3+\alpha^3) \\ E_a(1+\alpha^4+\alpha^2) \\ E_a(1+\alpha^2+\alpha) \end{bmatrix} = \begin{bmatrix} E_a \\ 0 \\ 0 \end{bmatrix} \tag{11-33}$$

and

$$\mathbf{Z}_s = \mathbf{T}^{-1}\begin{bmatrix} z_1 & z_2 & z_3 \\ z_3 & z_1 & z_2 \\ z_2 & z_3 & z_1 \end{bmatrix}\mathbf{T} = \begin{bmatrix} z_1 + \alpha^2 z_2 + \alpha z_3 & 0 & 0 \\ 0 & z_1 + \alpha z_2 + \alpha^2 z_3 & 0 \\ 0 & 0 & z_1 + z_2 + z_3 \end{bmatrix} \tag{11-34}$$

† This statement is slightly approximate since it turns out that the terminal voltage will contain higher harmonics. Their magnitudes are relatively insignificant, and we neglect them (compare Exercise 11-12).



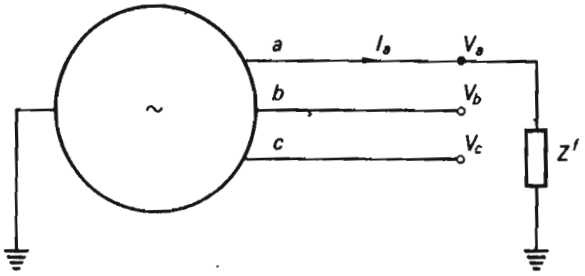


**Fig. 11-3** Synchronous generator subject to a line-to-ground short-circuit.

Again, the $\mathbf{Z}_s$ matrix turned out *diagonal*, indicating decoupling. We introduce the generator sequence impedances

$$\begin{aligned} z_+ &\triangleq z_1 + \alpha^2 z_2 + \alpha z_3 && \text{positive-sequence impedance} \\ z_- &\triangleq z_1 + \alpha z_2 + \alpha^2 z_3 && \text{negative-sequence impedance} \\ z_0 &\triangleq z_1 + z_2 + z_3 && \text{zero-sequence impedance} \end{aligned} \tag{11-35}$$

and can then, in view of the results (11-33) and (11-34), write Eq. (11-32) in component form:

$$\begin{aligned} V_+ &= E_a - z_+ I_+ \\ V_- &= 0 - z_- I_- \\ V_0 &= 0 - z_0 I_0 \end{aligned} \tag{11-36}$$

We note again the decoupling between the sequence component systems. We note also the obvious fact that no negative- or zero-sequence emf is generated in a symmetrically designed generator.

**A demonstration example** We have probably saturated the reader with theory at this point, and it may be wise to exemplify the use of it all. For this purpose we shall consider the single-phase-to-ground short-circuited generator in Fig. 11-3. We shall compute, using the symmetrical component method, the short-circuit current $I_a$ in phase $a$, and the voltages $V_b$ and $V_c$ of the healthy phases. We shall assume that the generator neutral is solidly grounded.

The problem is artificially simple, and the analysis procedure that we shall use does not claim any degree of generality. A general and systematic method suited for solution of large-scale-network problems will be offered later in this chapter. For the present, we wish only to acquaint the reader with the use of a new tool.

Since $I_b = I_c = 0$ for the type of fault that we have assumed, we obtain

$$\mathbf{I}_p = \begin{bmatrix} I_a \\ 0 \\ 0 \end{bmatrix}$$

From Eq. (11-9) we therefore get

$$I_+ = I_- = I_0 = \tfrac{1}{3} I_a \tag{11-37}$$

The single-phase-to-ground fault is thus characterized by *equal* symmetrical current components. By substitution of Eq. (11-37) into Eq. (11-36), we thus have

$$\begin{aligned} V_+ &= E_a - z_+ \frac{I_a}{3} \\ V_- &= 0 - z_- \frac{I_a}{3} \\ V_0 &= 0 - z_0 \frac{I_a}{3} \end{aligned} \tag{11-38}$$

The voltage $V_a = I_a Z^f$ is the sum of its symmetrical components:

$$V_a = I_a Z^f = V_+ + V_- + V_0 \tag{11-39}$$

Upon summation of Eqs. (11-38), we thus have

$$I_a Z^f = E_a - \frac{I_a}{3}(z_+ + z_- + z_0)$$

or

$$I_a = \frac{E_a}{Z^f + \frac{1}{3}(z_+ + z_- + z_0)} \tag{11-40}$$

Since $E_a$ and all impedances are assumed known, this settles the value for the fault current. The voltages $V_b$ and $V_c$ are also readily obtained. Like $V_a$ they are the sum of their components. For $V_b$ we get from Eq. (11-12):

$$V_b = \alpha^2 V_+ + \alpha V_- + V_0$$

By making use of Eq. (11-38), we thus get

$$V_b = \alpha^2\left(E_a - z_+ \frac{I_a}{3}\right) - \alpha z_- \frac{I_a}{3} - z_0 \frac{I_a}{3}$$

By substitution of the value for $I_a$ from Eq. (11-40), we obtain, finally,

$$V_b = E_a \frac{3\alpha^2 Z^f + z_-(\alpha^2 - \alpha) + z_0(\alpha^2 - 1)}{3Z^f + (z_+ + z_- + z_0)} \tag{11-41}$$



A similar expression can be obtained for $V_c$. The expression for $V_b$ takes on a very simple value in the case when all sequence impedances for the generator are equal, i.e., in the hypothetical case†

$$z_+ = z_- = z_0$$

In this case Eq. (11-41) reduces to

$$V_b = \alpha^2 E_a = E_b$$

We can similarly prove that in this case

$$V_c = E_c$$

## 11-2 SEQUENCE IMPEDANCES OF NETWORK COMPONENTS

As illustrated in the preceding example, it is necessary to possess knowledge of the sequence impedances for all system components. We shall now attend to the problem of how to determine these parameters.

The procedure for finding these impedances will be the same in all cases. Whether we wish to determine them by test or by analytical means, we must subject the component in question to a set of currents and voltages satisfying the description for the respective sequence system in question. With the machine operating under those conditions, we then either measure or compute the sought impedances, depending upon whether we seek the parameters by test or analysis.

### 11-2.1 SEQUENCE IMPEDANCES OF SYNCHRONOUS MACHINES

All sequence impedances for a synchronous machine are essentially purely reactive. The words "impedance" and "reactance" will therefore be used interchangeably.

**Positive-sequence impedance** This is the simplest parameter to determine. A system component operating under balanced conditions of voltages and currents (of phase sequence *abca*. . .) is in effect in a "positive-sequence mode." In Chaps. 4 and 10 we have penetratingly discussed the impedance situation for a synchronous machine under balanced load and fault conditions. We summarize our earlier findings:

For *steady state*, use

$$z_+ = jX_d \tag{11-42}$$

For *fault*, if the 1 cycle transient is of interest, use

$$z_+ = jX_d'' \tag{11-43}$$

† This equality is approximately true (Sec. 11-2.1) in the case when we are looking at conditions immediately (= first cycle) after the fault.

If the 3–4 cycle transient is of interest, use

$$z_+ = jX'_d \tag{11-44}$$

If we wish to obtain $z_+$ by test, the simplest procedure will be to short-circuit the machine from no load, having excited the machine to a 100 percent emf. If from an oscillogram† we measure the per-unit rms values of the 60-Hz current component at $|I''|$, $|I'|$, and $|I_{ss}|$ at 1 cycle, 3–4 cycles, and in steady state, respectively, then we obtain the reactances

$$\begin{aligned} X_d &= \frac{1}{|I_{ss}|} \quad \text{pu} \\ X'_d &= \frac{1}{|I'|} \quad \text{pu} \\ X''_d &= \frac{1}{|I''|} \quad \text{pu} \end{aligned} \tag{11-45}$$

Typical numerical values for these reactances are found in Table 4-1.

**Negative-sequence impedance obtained by test** Figure 11-4 depicts the setup for obtaining the negative-sequence impedance of a synchronous machine from *test*. With the machine *running* (driven by a prime mover) at 100 percent speed and the emfs reduced to zero by short-circuiting‡ the field supply, a negative-sequence voltage is applied from an external source (for example, another synchronous machine). The resulting currents that are fed into the test machine are measured. The negative-sequence impedance is obtained as

$$z_- = \frac{V_a}{I_a} \tag{11-46}$$

*Caution:* $z_-$ usually is of quite small magnitude (Table 4-1); care should be taken not to overload the armature windings.

† One should take the average in the three phases. By measuring peak to peak, the influence of the dc component is avoided.

‡ Note that you may *not* zero the emfs by *opening* the field winding. Negative-sequence stator currents will induce considerable rotor currents [see Eq. (11-50)], which will affect the impedance as felt from the stator side (i.e., the impedance we are measuring). Opening the rotor circuit would prevent those currents from forming, thus making the test useless.

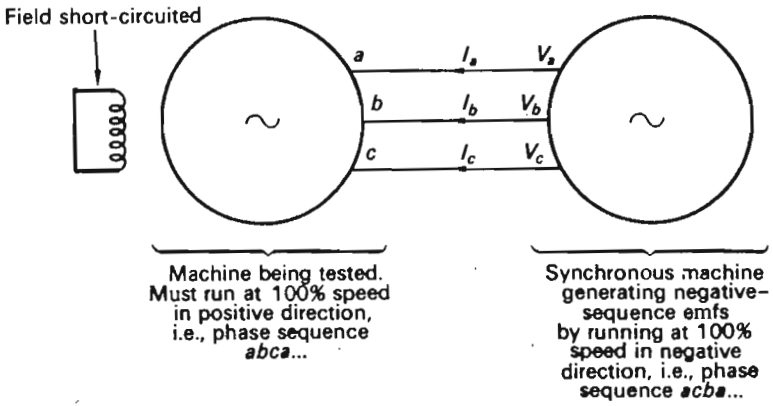


**Fig. 11-4** Measurement of negative-sequence impedance of synchronous machine.



**Negative-sequence impedance obtained analytically** If we want to obtain $z_-$ *analytically*, we proceed by injecting stator currents of negative phase sequence:

$$\begin{aligned} i_a &= i_{\max} \cos \omega t \\ i_b &= i_{\max} \cos (\omega t + 120°) \\ i_c &= i_{\max} \cos (\omega t - 120°) \end{aligned} \tag{11-47}$$

Upon Blondel-transforming these currents [using Eq. (4-26)], we get

$$\begin{aligned} i_d &= i_{\max} \cos 2\omega t \\ i_q &= -i_{\max} \sin 2\omega t \\ i_0 &= 0 \end{aligned} \tag{11-48}$$

The physical meaning of Eqs. (11-48) is that the stator mmf *measured relative to the rotor* pulsates at 120 Hz, inducing 120-Hz currents in the field winding. (The mmf wave travels, actually, with full synchronous speed in opposite direction to the rotor.)

By substitution of Eqs. (11-48) into the general performance equations (4-36), we get (upon neglecting the armature resistance)

$$\begin{aligned} v_d &= 2\omega L_d i_{\max} \sin 2\omega t + L_5 \frac{di_r}{dt} - \omega L_q i_{\max} \sin 2\omega t \\ v_q &= 2\omega L_q i_{\max} \cos 2\omega t + \omega(L_5 i_r - L_d i_{\max} \cos 2\omega t) \\ 0 &= L_4 \frac{di_r}{dt} - \tfrac{3}{2} L_5 \frac{di_d}{dt} \end{aligned} \tag{11-49}$$

The last equation tells us that the current induced in the rotor winding equals

$$i_r = \frac{3}{2}\frac{L_5}{L_4} i_d = \frac{3}{2}\frac{L_5}{L_4} i_{\max} \cos 2\omega t \tag{11-50}$$

and upon substitution of this value for $i_r$ in the first two of Eqs. (11-49), these can be reduced to

$$v_d = \left[ i_{\max} 2\omega \left( L_d - \frac{3}{2} \frac{L_5^2}{L_4} \right) - \omega L_q i_{\max} \right] \sin 2\omega t$$
$$v_q = \left[ 2\omega L_q i_{\max} - \omega \left( L_d - \frac{3}{2} \frac{L_5^2}{L_4} \right) i_{\max} \right] \cos 2\omega t \tag{11-51}$$

In Eqs. (11-51) we recognize the expressions for $X_q$ and $X'_d$, and we can thus simplify them as follows:

$$v_d = -(X_q - 2X'_d) i_{\max} \sin 2\omega t$$
$$v_q = -(X'_d - 2X_q) i_{\max} \cos 2\omega t \tag{11-52}$$

By an inverse Blondel transformation we now obtain the stator voltages:

$$v_a = v_d \cos \omega t - v_q \sin \omega t = -(X_q - 2X'_d) i_{\max} \sin 2\omega t \cos \omega t + (X'_d - 2X_q) i_{\max} \cos 2\omega t \sin \omega t$$
$$= -\frac{X_q + X'_d}{2} i_{\max} \cos (\omega t + 90) - \tfrac{3}{2}(X_q - X'_d) i_{\max} \sin 3\omega t \tag{11-53}$$

We pause at this point and make the following observations:

1. If *sinusoidal* currents of frequency $\omega$ and negative phase sequence are injected into the stator winding, the resulting stator *voltages* will contain one component of frequency $\omega$ and another of frequency $3\omega$.
2. If attention is directed toward the $\omega$ component of voltage, and if the $3\omega$ component is neglected, the impedance of the machine must equal

$$z_- = j \frac{X_q + X'_d}{2} \tag{11-54}$$

3. Actually, Eqs. (11-53) and (11-54) *are not very accurate* because our general performance equations (4-36) were derived under the assumption of *no damper windings*. Since in this case the stator mmf sweeps by the rotor at a speed of $2\omega$, the damper windings *that are present* in an *actual* machine will be very much in evidence.

   Instead of "feeling the *transient* reactance $X'_d$" from the stator, we will "feel the *subtransient* reactance $X''_d$," since the currents induced (of frequency $2\omega$) in the *fast* damper winding will dominate over those in the *rotor field* winding. Likewise, instead of feeling $X_q$ in the $q$ direction, we will feel a smaller "effective" reactance $X''_q$ due to the damper windings in the $q$ direction. The *real* negative-sequence reactance, with consideration given to the damper windings, will therefore be

$$z_{-\text{real}} = j \frac{X''_q + X''_d}{2} \tag{11-55}$$

4. If we take the effect of the damper windings into account, the $3\omega$ component of the voltage will have a magnitude of

   $\tfrac{3}{2}(X''_q - X''_d) i_{\max}$

   This component is very small, numerically, compared with the $\omega$ component of magnitude

   $$\frac{X''_q + X''_d}{2} i_{\max}$$

   and supports our approximation of neglecting the $3\omega$ component besides the dominating $\omega$ component.



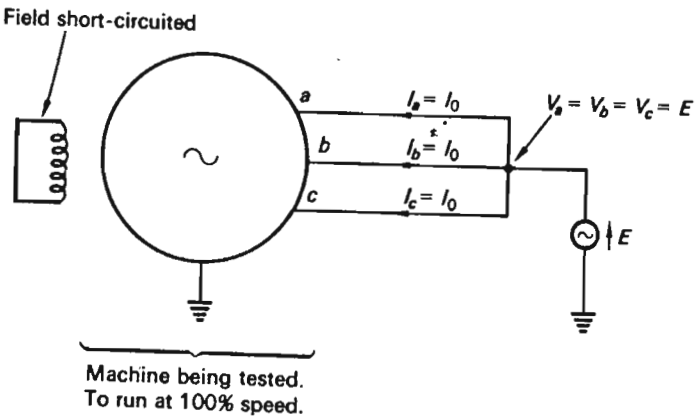


**Fig. 11-5** Measurement of zero-sequence impedance of synchronous machine.

**Zero-sequence impedance** Figure 11-5 depicts a setup by which the zero-sequence impedance of a synchronous machine can be obtained by *test*. The machine is being run at synchronous speed, and its field is shorted. A single-phase source impresses zero-sequence potentials upon the three stator windings.

The zero-sequence impedance is obtained from

$$z_0 = \frac{E}{I_0} \tag{11-56}$$

*Analytic* determination of $z_0$ follows lines similar to those we used for $z_-$. We now inject zero-sequence currents into the stator, and can thus write

$$i_a = i_b = i_c = i_{\max} \cos \omega t \tag{11-57}$$

From Eqs. (4-26) we then find

$$\begin{aligned} i_d &= 0 \\ i_q &= 0 \\ i_0 &= i_{\max} \cos \omega t \end{aligned} \tag{11-58}$$

By substitution into the general performance equations (4-36), we get, if resistances are neglected,

$$\begin{aligned} v_d &= 0 \\ v_q &= 0 \\ v_0 &= -L_0 \frac{di_0}{dt} = \omega L_0 i_{\max} \sin \omega t \end{aligned} \tag{11-59}$$

By an inverse Blondel transformation we obtain the stator voltages

$$v_a = v_0 = \omega L_0 i_{\max} \sin \omega t = \omega L_0 i_{\max} \cos (\omega t + 90°) \tag{11-60}$$

Clearly, the zero-sequence impedance equals

$$z_0 = j\omega L_0 = jx_0 \tag{11-61}$$

Table 4-1 gives some representative numerical values for sequence impedances (= reactances) for various types of synchronous machines.

### 11-2.2 SEQUENCE IMPEDANCES OF TRANSFORMERS

**Positive- and negative-sequence impedances** The positive-sequence impedance of a transformer equals, of course, the leakage impedance. It may be obtained by a *short-circuit test* in a manner detailed in Example 5-1. Since the transformer is a *static* device, the leakage impedance will *not* change if the phase sequence is altered from *abca* . . . to *acba* . . . . As a result, we can conclude that the positive- and negative-sequence impedances are identical; i.e.,

$$z_+ = z_- = Z_{\text{leakage}} \tag{11-62}$$

**Zero-sequence impedance** The zero-sequence impedance of a transformer depends greatly on the winding type ($\Delta$ or $Y$) and also upon whether or not the neutrals are grounded.

Whereas the positive- and negative-sequence per-unit impedances are independent of whether the sequence currents are injected into the primaries or secondaries, the zero-sequence impedance will in general have widely different values, depending upon what terminals we view.

Figure 11-6 depicts the test setup for finding the impedance experimentally. The zero-sequence impedance $z_0 = E/I_0$ may or may not have



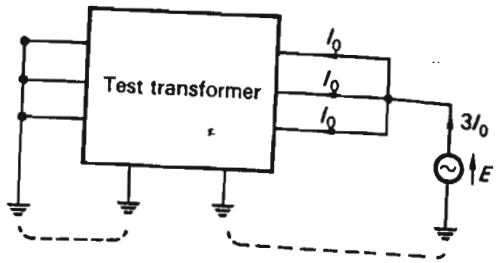


**Fig. 11-6** Measurement of zero-sequence impedance of transformer.

different values as measured from one side or the other. Let us demonstrate with three important cases.

*Case A. Transformer YY-connected; both neutrals solidly grounded* This case is depicted in Fig. 11-7*a*. The solid grounding of both neutrals guarantees that the ground currents $3I_0$ and $3I_0/a$ have free circulating paths. Clearly, the current is impeded only by the leakage impedance per phase,

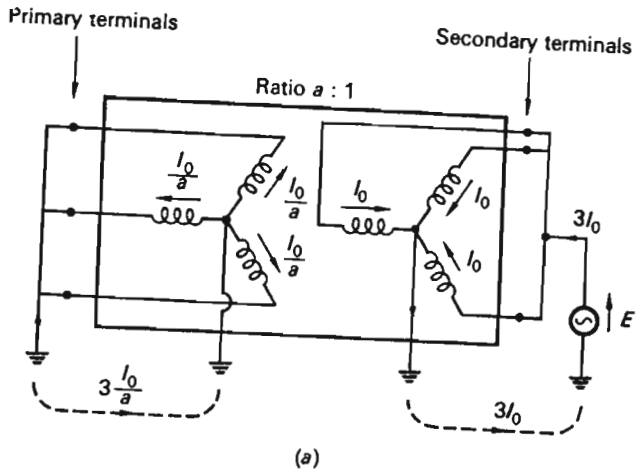


(*a*)

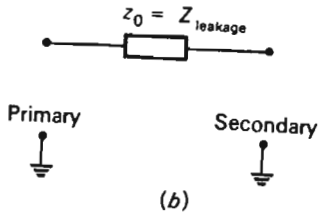


(*b*)

**Fig. 11-7** Zero-sequence network for YY-connected transformer. Both neutrals solidly grounded.

and the zero-sequence impedance therefore equals the leakage impedance. Obviously, we measure the same impedance from *both sides* (if expressed in *per unit*, of course; the *ohmic* values would be in the ratio $a^2$). We may represent the zero-sequence impedance characteristics as has been done in Fig. 11-7*b* (referred to as a *sequence network*).

*Case B. Transformer Y$\Delta$-connected; neutral solidly grounded* This case, depicted in Fig. 11-8*a*, indicates that the zero-sequence impedance measured from the Y side equals the leakage impedance. Note also that as the secondary currents *circulate* in the $\Delta$, *no zero-sequence currents will leave these terminals*. This explains the short circuit to ground in the sequence network in Fig. 11-8*b*. No zero-sequence currents can be injected into the $\Delta$ terminals. Thus, in the sequence network, we have an interrupt in the corresponding terminals.

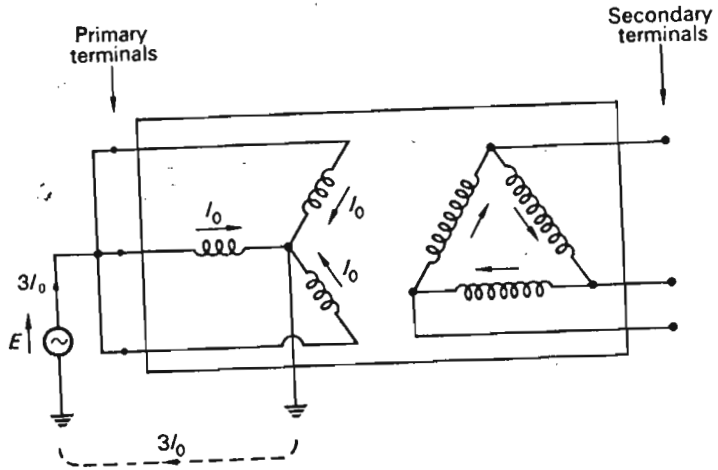


(*a*)

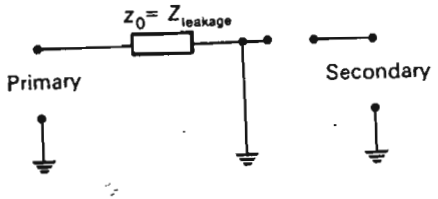


(*b*)

**Fig. 11-8** Zero-sequence network for Y$\Delta$-connected transformer. Neutral solidly grounded.



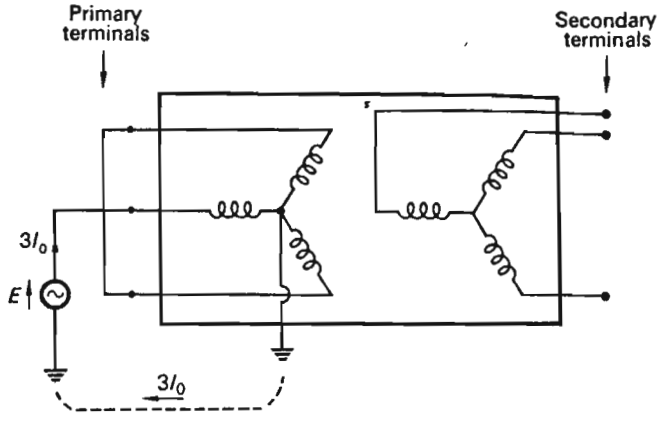


(*a*)

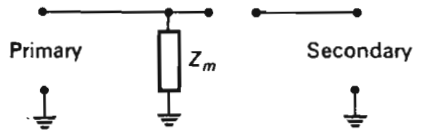


(*b*)

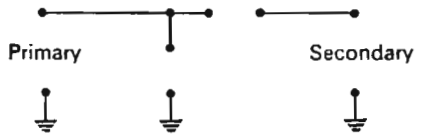


(*c*)

**Fig. 11-9** Zero-sequence network for YY-connected transformer. Only one neutral grounded.

*Case C. Transformer YY-connected; one neutral grounded* This case is shown in Fig. 11-9.

It should be noted that although a path is provided to ground for the zero-sequence currents in the primaries, no such path exists in the secondaries. Consequently, from a zero-sequence point of view, the secondaries will act as if *open-circuited;* i.e., from the primary side we will measure the open-circuit, or *magnetizing, impedance.* From the secondary side the zero-sequence currents will meet a total interruption. The zero-sequence network will thus appear as shown in Fig. 11-9*b*. It should be noted that, since the magnetizing impedance is very large ($\approx$ 10,000 percent), we can in practice

assume infinite impedance from *both* terminals, as was indicated in Fig. 11-9*c*.

The above three cases are the most important from a practical point of view. In determining the zero-sequence networks for *any* three-phase transformer, the following simple rules should be followed:

1. Does the winding type permit zero-sequence currents a path to ground? If not, the sequence network will contain an interruption for the winding in question.
2. Are the zero-sequence currents confined to circulation in a specific winding? If so, provide a short circuit to ground in the sequence network.
3. Does the absence of a path to ground mean that the transformer is effectively open-circuited for zero-sequence currents? If so, the zero-sequence network must contain the magnetizing impedance in the branch in question.
4. Do the zero-sequence currents injected into a set of terminals flow *freely*? If so, add only the leakage impedance to this branch in question.

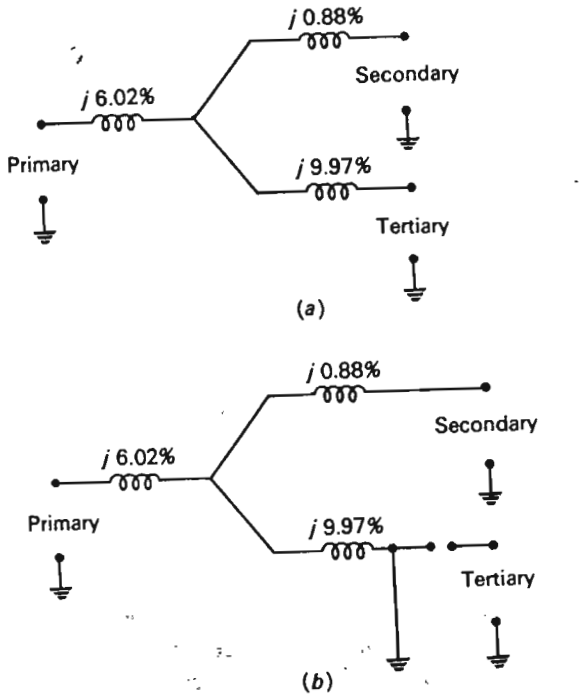


**Fig. 11-10** Sequence networks for three-winding transformer in Example 5-5. (*a*) Positive- and negative-sequence networks; (*b*) zero-sequence network.



**Example 11-1** Find the zero-sequence network for the three-winding transformer treated in Example 5-5, assuming that both the primary and secondary neutrals are solidly grounded. The analysis performed in Example 5-5 rendered the equivalent (positive- and negative-sequence) network that we have shown in Fig. 11-10*a* for easy reference.

By direct application of the set of rules given above we obtain the zero-sequence network shown in Fig. 11-10*b*. Note that all leakage impedances are the same as those computed for the positive-sequence network.

### 11-2.3 SEQUENCE IMPEDANCES FOR TRANSMISSION LINES

**Positive- and negative-sequence impedances** The transmission line, like a transformer, is a *static* component. Its positive- and negative-sequence impedances are therefore identical, and the reader is referred to Chap. 6 for a detailed exposition of these parameters.

**Zero-sequence impedance** Positive- and negative-sequence currents flowing in a transmission line require no return path because their algebraic sum equals zero.

When zero-sequence currents flow in a transmission line, they may choose any available return path. Some of the current may return through ground, some via the overhead ground wires. These latter wires are usually grounded at each transmission tower, and therefore the return current in them may not be uniform throughout the line.

The zero-sequence impedance will have different values, depending upon the actual return path. Since the ground impedance depends greatly upon soil, humidity, and other empiric factors, it is customary to make certain simplifying assumptions regarding the actual current distributions.

**Example 11-2** Compute the zero-sequence reactance for the transmission line, the positive-sequence reactance of which we determined, in Example 6-2, to be about

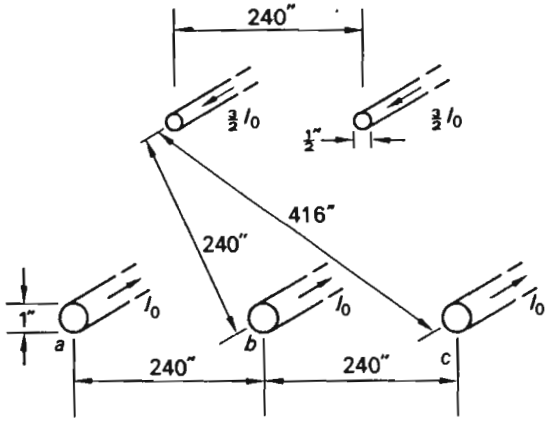


**Fig. 11-11** Transmission line with two ground wires.

0.80 Ω/mile and phase. The line configuration is shown in Fig. 11-11. The line is equipped with two ½-in. ground wires, which will be assumed to carry the total return zero-sequence current of $1.5I_0$ each.

We assume the line to be transposed and therefore the phase conductors will carry equal zero-sequence currents.

By application of Eq. (6-22) we obtain for the inductive voltage drop in one of the outer phase conductors:

$$\Delta V_a = j\omega \frac{\mu_0}{2\pi}\left[I_a\left(\tfrac{1}{4} + \ln\frac{1}{0.5}\right) + I_b \ln\tfrac{1}{240} + I_c \ln\tfrac{1}{480} - 2 \times \tfrac{3}{2} I_0 \ln\tfrac{1}{416}\right]$$

$$= j4.93 \times 10^{-4} I_0 \quad V/m \quad \text{or} \quad j0.793 I_0 \quad V/\text{mile}$$

For the center phase conductor we similarly get:

$$\Delta V_b = j0.780 I_0 \quad V/\text{mile}$$

The average voltage drop is therefore $j0.790I_0$ volts per phase conductor. We compute, finally, the voltage drop for one of the ground wires and obtain $\Delta V_g = j1.36I_0$ V/mile (assumed positive in the return direction). The total loop-drop thus equals $j2.15I_0$ V/mile corresponding to a zero-sequence reactance of $x_0 = 2.15\ \Omega$/mile and phase.

Because of the uncertainty as to the actual distribution of the return current, the computed values for $z_0$ of transmission lines are our most approximate parameters in system studies. It is recommendable to obtain this parameter by actual field tests.

## 11-3 DIGITAL COMPUTATION OF UNBALANCED FAULTS

We presented in Chap. 10 a *general* and *systematic* computational approach for the case of a balanced-fault situation. We shall now attempt to do the same for the unbalanced case. In effect, we shall merge the SCT method outlined in this chapter with Thévenin's method as used in Chap. 10. With certain modifications we can actually follow the analysis procedure in Chap. 10 step by step. As we encounter dissimilarities, we shall attempt to explain them. To make the comparison with Chap. 10 still more illustrative, we shall apply our analysis methods to the same three-bus example that we used in Chap. 10.

Since we must distinguish between prefault and postfault variables, phase values of currents and voltages, and their symmetrical components, in addition to keeping track of our regular vectors and matrices, with their respective subscripts, there is a possibility that we may end up in symbol confusion. To avoid this, and also to alert the reader, we shall agree from the outset on certain symbol rules:

*Rule* 1 Prefault conditions are indicated by the superscript 0.
*Rule* 2 Postfault or fault conditions are indicated by the superscript *f*.



*Rule* 3 Phase values of currents and voltages are indicated collectively by the subscript *p*, and individually by the subscripts *a*, *b*, and *c*.
*Rule* 4 Symmetrical components are indicated either collectively by the subscript *s* or individually by the subscripts +, −, or 0.
*Rule* 5 A number subscript always refers to the bus coding.

### 11-3.1 SEQUENCE NETWORK ASSEMBLY

Our first chore is to assemble a suitable network model. In preceding chapters we preferred to use the bus, rather than the loop, frame of reference, and we shall stick to this choice in this chapter also.

For a *balanced* network study the end result of the network model construction is the $n \times n$ bus admittance matrix $\mathbf{Y}_{\text{bus}}$, or its inverse, the $n \times n$ bus impedance matrix $\mathbf{Z}_{\text{bus}}$. For an *unbalanced* network study the model gets slightly more complex, since we now must build separately the network models for the three separate component systems and, as we have seen in preceding sections, *they are in general all different.*

**Sequence networks** Consider, for example, the network model associated with the positive-sequence component system. From a knowledge of the positive-sequence impedances for all generators, transformers, and lines, we can assemble a *positive-sequence network* for the overall *n*-bus system. For this network we find the $n \times n$ diagonal primitive admittance matrix $\mathbf{Y}_+$, and from a knowledge of the bus incidence matrix $\mathbf{A}$, we can then, using Eq. (7-80), or the rules on page 223, obtain our *positive-sequence bus admittance matrix*

$$\mathbf{Y}_{+\text{bus}} = \mathbf{A}^T\mathbf{Y}_+\mathbf{A} = \begin{bmatrix} y_{+11} & \cdots & y_{+1n} \\ \cdots & \cdots & \cdots \\ y_{+n1} & \cdots & y_{+nn} \end{bmatrix} \tag{11-64}$$

This matrix and its inverse $\mathbf{Z}_{+\text{bus}}$ relate the positive-sequence components $V_{+i}$ of the bus voltages with the positive-sequence components $J_{+i}$ of the injected bus currents in the following manner:

$$\mathbf{J}_{+\text{bus}} = \mathbf{Y}_{+\text{bus}}\mathbf{V}_{+\text{bus}} \tag{11-65}$$

or

$$\mathbf{V}_{+\text{bus}} = \mathbf{Z}_{+\text{bus}}\mathbf{J}_{+\text{bus}} \tag{11-66}$$

where the vectors $\mathbf{J}_{+\text{bus}}$ and $\mathbf{V}_{+\text{bus}}$ are defined as follows:

$$\mathbf{V}_{+\text{bus}} \triangleq \begin{bmatrix} V_{+1} \\ V_{+2} \\ \cdot \\ \cdot \\ \cdot \\ V_{+n} \end{bmatrix} \quad \text{and} \quad \mathbf{J}_{+\text{bus}} \triangleq \begin{bmatrix} J_{+1} \\ J_{+2} \\ \cdot \\ \cdot \\ \cdot \\ J_{+n} \end{bmatrix} \tag{11-67}$$

Similar procedures render the *negative-* and *zero-sequence bus admittance* matrices $\mathbf{Y}_{-\text{bus}}$ and $\mathbf{Y}_{0,\text{bus}}$ and their respective inverse matrices $\mathbf{Z}_{-\text{bus}}$ and $\mathbf{Z}_{0,\text{bus}}$. (It should be noted that the bus incidence matrix $\mathbf{A}$ is identical in the three cases but the primitive admittance matrices will, of course, be different.) These matrices relate the negative-sequence components $V_{-i}$ of the bus voltages with the negative-sequence bus current components $J_{-i}$, in accordance with

$$\mathbf{J}_{-\text{bus}} = \mathbf{Y}_{-\text{bus}}\mathbf{V}_{-\text{bus}} \tag{11-68}$$

or

$$\mathbf{V}_{-\text{bus}} = \mathbf{Z}_{-\text{bus}}\mathbf{J}_{-\text{bus}} \tag{11-69}$$

and similarly for the zero-sequence components $V_{0i}$ and $J_{0i}$:

$$\mathbf{J}_{0,\text{bus}} = \mathbf{Y}_{0,\text{bus}}\mathbf{V}_{0,\text{bus}} \tag{11-70}$$

or

$$\mathbf{V}_{0,\text{bus}} = \mathbf{Z}_{0,\text{bus}}\mathbf{J}_{0,\text{bus}} \tag{11-71}$$

where the vectors $\mathbf{J}_{-\text{bus}}$, $\mathbf{V}_{-\text{bus}}$ and $\mathbf{J}_{0,\text{bus}}$, $\mathbf{V}_{0,\text{bus}}$ are defined as follows:

$$\mathbf{V}_{-\text{bus}} \triangleq \begin{bmatrix} V_{-1} \\ V_{-2} \\ \cdot \\ \cdot \\ \cdot \\ V_{-n} \end{bmatrix} \quad \text{and} \quad \mathbf{J}_{-\text{bus}} \triangleq \begin{bmatrix} J_{-1} \\ J_{-2} \\ \cdot \\ \cdot \\ \cdot \\ J_{-n} \end{bmatrix} \tag{11-72}$$

$$\mathbf{V}_{0,\text{bus}} \triangleq \begin{bmatrix} V_{01} \\ V_{02} \\ \cdot \\ \cdot \\ \cdot \\ V_{0n} \end{bmatrix} \quad \text{and} \quad \mathbf{J}_{0,\text{bus}} \triangleq \begin{bmatrix} J_{01} \\ J_{02} \\ \cdot \\ \cdot \\ \cdot \\ J_{0n} \end{bmatrix} \tag{11-73}$$

**The SC bus voltage and current vectors** All the foregoing vector equations are $n$-dimensional. For analysis purposes it proves useful to condense them into *one* $3n$-dimensional equation by arranging the components of the *six* $n$-dimensional voltage and current vectors into *two* new



$3n$-dimensional vectors as follows:

$$\mathbf{V}_{s,\text{bus}} \triangleq \begin{bmatrix} V_{+1} \\ V_{-1} \\ V_{01} \\ \hdashline \cdot \\ \cdot \\ \cdot \\ \hdashline V_{+i} \\ V_{-i} \\ V_{0i} \\ \hdashline \cdot \\ \cdot \\ \cdot \\ \hdashline V_{+n} \\ V_{-n} \\ V_{0n} \end{bmatrix} = \begin{bmatrix} \mathbf{V}_{s1} \\ \cdot \\ \cdot \\ \cdot \\ \mathbf{V}_{si} \\ \cdot \\ \cdot \\ \cdot \\ \mathbf{V}_{sn} \end{bmatrix} \quad \text{and} \quad \mathbf{J}_{s,\text{bus}} \triangleq \begin{bmatrix} J_{+1} \\ J_{-1} \\ J_{01} \\ \hdashline \cdot \\ \cdot \\ \cdot \\ \hdashline J_{+i} \\ J_{-i} \\ J_{0i} \\ \hdashline \cdot \\ \cdot \\ \cdot \\ \hdashline J_{+n} \\ J_{-n} \\ J_{0n} \end{bmatrix} = \begin{bmatrix} \mathbf{J}_{s1} \\ \cdot \\ \cdot \\ \cdot \\ \mathbf{J}_{si} \\ \cdot \\ \cdot \\ \cdot \\ \mathbf{J}_{sn} \end{bmatrix} \tag{11-74}$$

We refer to these new vectors as the *SC bus voltage* and *bus current vectors*, respectively.

In terms of these new vectors we can summarize the three $n$-dimensional vector equations (11-65), (11-68), and (11-70) into the *single* $3n$-dimensional equation

$$\mathbf{J}_{s,\text{bus}} = \mathbf{Y}_{s,\text{bus}}\mathbf{V}_{s,\text{bus}} \tag{11-75}$$

The $3n \times 3n$ matrix $\mathbf{Y}_{s,\text{bus}}$ is made up of the elements $y_{+ij}$, $y_{-ij}$, and $y_{0ij}$ of the matrices $\mathbf{Y}_{+\text{bus}}$, $\mathbf{Y}_{-\text{bus}}$, and $\mathbf{Y}_{0,\text{bus}}$, arranged in the following systematic pattern:

$$\mathbf{Y}_{s,\text{bus}} \triangleq \begin{bmatrix} y_{+11} & 0 & 0 & \cdots & y_{+1n} & 0 & 0 \\ 0 & y_{-11} & 0 & & 0 & y_{-1n} & 0 \\ 0 & 0 & y_{011} & & 0 & 0 & y_{01n} \\ \hdashline & \cdot & & & & \cdot & \\ & \cdot & & & & \cdot & \\ & \cdot & & & & \cdot & \\ \hdashline y_{+n1} & 0 & 0 & \cdots & y_{+nn} & 0 & 0 \\ 0 & y_{-n1} & 0 & & 0 & y_{-nn} & 0 \\ 0 & 0 & y_{0n1} & & 0 & 0 & y_{0nn} \end{bmatrix} \triangleq \begin{bmatrix} \mathbf{Y}_{s11} & \cdots & \mathbf{Y}_{s1n} \\ \cdots & \cdots & \cdots \\ \mathbf{Y}_{sn1} & \cdots & \mathbf{Y}_{snn} \end{bmatrix} \tag{11-76}$$

*The student should write Eq.* (11-75) *in component form and convince himself that this new vector equation is indeed identical with the three Eqs.* (11-65), (11-68), *and* (11-70).

We can also write the equations in the following alternative way:

$$\mathbf{V}_{s,\text{bus}} = \mathbf{Z}_{s,\text{bus}}\mathbf{J}_{s,\text{bus}} \tag{11-77}$$

The $3n \times 3n$ matrix $\mathbf{Z}_{s,\text{bus}}$ is made up of the elements $z_{+ij}$, $z_{-ij}$, and $z_{0ij}$ arranged in a pattern similar to that of the elements of $\mathbf{Y}_{s,\text{bus}}$.

The matrices $\mathbf{Y}_{s,\text{bus}}$ and $\mathbf{Z}_{s,\text{bus}}$ are referred to as the *SC bus admittance* and *bus impedance matrix*, respectively.

**Example 11-3** Let us exemplify the construction of the SC admittance and impedance matrices by considering the same three-bus system that we investigated in Example 10-4. The system is depicted in Fig. 10-12, where also the positive-sequence impedances are identified. Let us find, separately, the positive-, negative-, and zero-sequence networks.

*The positive-sequence network* The positive-sequence network is identical with the network (Figs. 10-12 and 10-13) upon which we based our symmetrical short-circuit study in Example 10-4. We had already computed the bus admittance and bus impedance matrices for this network [Eqs. (10-49) and (10-50)]. We repeat them here for easy reference:

$$\mathbf{Y}_{+\text{bus}} = \begin{bmatrix} -j26.67 & j10 & j10 \\ j10 & -j33.33 & j10 \\ j10 & j10 & -j20 \end{bmatrix} \tag{11-78}$$

$$\mathbf{Z}_{+\text{bus}} = \begin{bmatrix} j0.073 & j0.0386 & j0.0558 \\ j0.0386 & j0.0558 & j0.0472 \\ j0.0558 & j0.0472 & j0.1014 \end{bmatrix} \tag{11-79}$$

*The negative-sequence network* The only changes from the positive-sequence network are found in the generator representations. There are no negative-sequence emfs generated, and the impedance will change from $jX'_d$ to $jx_-$. Since in most cases $x_-$ and $X'_d$ will have almost equal numerical values, we will for simplicity assume them equal.† (This assumption is very common in practice.)

The resulting negative-sequence network is shown in Fig. 11-12. The corresponding bus admittance and impedance matrices will be identical with those computed for the positive-sequence network; i.e.,

$$\left.\begin{aligned} \mathbf{Y}_{-\text{bus}} &= \mathbf{Y}_{+\text{bus}} \\ \mathbf{Z}_{-\text{bus}} &= \mathbf{Z}_{+\text{bus}} \end{aligned}\right\} \text{ see Eqs. (11-78) and (11-79)}$$

† Compare also Table 4-1 on page 96.



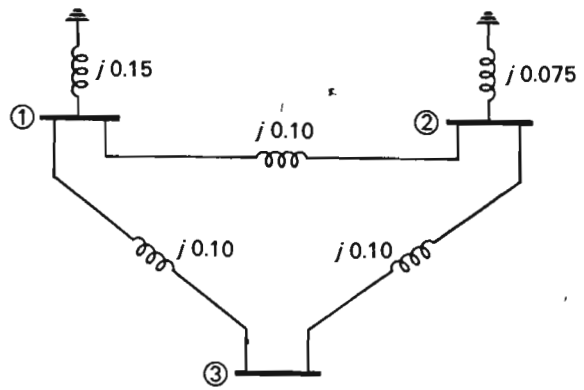


**Fig. 11-12** Negative-sequence network of example system.

*The zero-sequence network* Whereas the positive- and negative-sequence networks are approximately equal from an impedance point of view, the zero-sequence network will be vastly different from both. To obtain this network we must make the following assumptions about the system components:

*Generators* Neutrals solidly grounded. The zero-sequence reactance is 10 percent (based upon ratings).

*Transformers* Connected $\Delta Y$ (the generator side is $\Delta$). The neutrals solidly grounded.

*Transmission lines* The zero-sequence impedance is measured to be $j20$ percent (50-MVA basis) in all three lines.

We can now assemble the zero-sequence network (see Fig. 11-13).

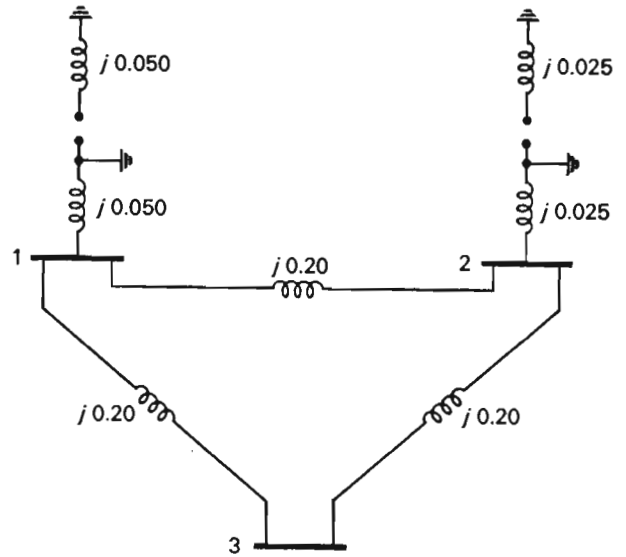


**Fig. 11-13** Zero-sequence network of example system.

For this network we write down the bus admittance matrix by inspection:†

$$\mathbf{Y}_{0,\text{bus}} = \begin{bmatrix} -j30 & j5 & j5 \\ j5 & -j50 & j5 \\ j5 & j5 & -j10 \end{bmatrix} \tag{11-80}$$

We then obtain by inversion

$$\mathbf{Z}_{0,\text{bus}} = \begin{bmatrix} j0.0380 & j0.0060 & j0.0220 \\ j0.0060 & j0.0220 & j0.0140 \\ j0.0220 & j0.0140 & j0.1180 \end{bmatrix} \tag{11-81}$$

We construct, finally, the $9 \times 9$ SC bus impedance matrix:

$$\mathbf{Z}_{s,\text{bus}} = j\left[\begin{array}{ccc:ccc:ccc} 0.0730 & 0 & 0 & 0.0386 & 0 & 0 & 0.0558 & 0 & 0 \\ 0 & 0.0730 & 0 & 0 & 0.0386 & 0 & 0 & 0.0558 & 0 \\ 0 & 0 & 0.0380 & 0 & 0 & 0.0060 & 0 & 0 & 0.0220 \\ \hdashline 0.0386 & 0 & 0 & 0.0558 & 0 & 0 & 0.0472 & 0 & 0 \\ 0 & 0.0386 & 0 & 0 & 0.0558 & 0 & 0 & 0.0472 & 0 \\ 0 & 0 & 0.0060 & 0 & 0 & 0.0220 & 0 & 0 & 0.0140 \\ \hdashline 0.0558 & 0 & 0 & 0.0472 & 0 & 0 & 0.1014 & 0 & 0 \\ 0 & 0.0558 & 0 & 0 & 0.0472 & 0 & 0 & 0.1014 & 0 \\ 0 & 0 & 0.0220 & 0 & 0 & 0.0140 & 0 & 0 & 0.1180 \end{array}\right] \tag{11-82}$$

### 11-3.2 GENERAL FORMULAS FOR POSTFAULT CURRENTS AND VOLTAGES

It should be noted that the $3n$-dimensional vectors $\mathbf{V}_{s,\text{bus}}$ and $\mathbf{J}_{s,\text{bus}}$ each are made up of $n$ three-dimensional *subvectors* $\mathbf{V}_{si}$ and $\mathbf{J}_{si}$, respectively. These subvectors, the components of which are

$$\mathbf{V}_{si} = \begin{bmatrix} V_{+i} \\ V_{-i} \\ V_{0i} \end{bmatrix} \qquad i = 1, 2, \ldots, n \tag{11-83}$$

and

$$\mathbf{J}_{si} = \begin{bmatrix} J_{+i} \\ J_{-i} \\ J_{0i} \end{bmatrix} \qquad i = 1, 2, \ldots, n \tag{11-84}$$

evidently represent the symmetrical components of the bus voltages and bus currents, respectively, at bus $i$.

† Note that the generator impedances do not even enter the picture, the reason being that any zero-sequence currents originating from a short circuit of any bus or line will never reach farther than the $\Delta$ windings of the transformers.



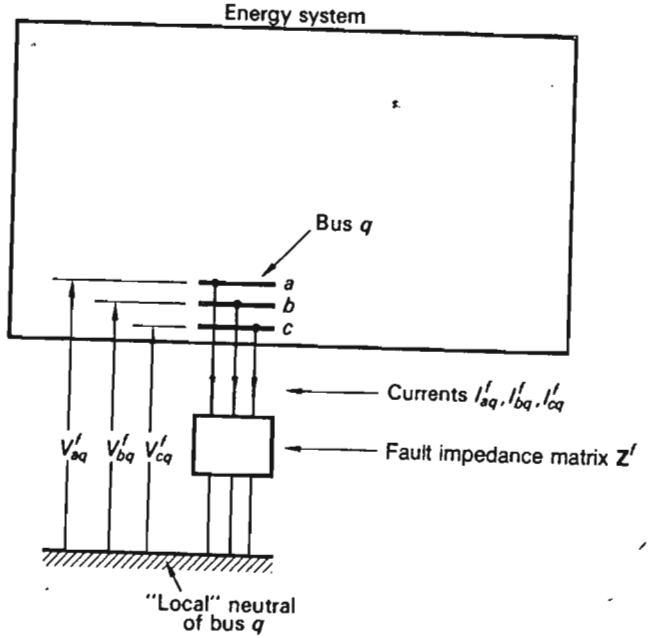


**Fig. 11-14** Unbalanced fault (or loading) on bus $q$ of energy system.

We likewise note that the $3n \times 3n$ matrices $\mathbf{Y}_{s,\text{bus}}$ and $\mathbf{Z}_{s,\text{bus}}$ are each composed of the $n^2$ *submatrices* $\mathbf{Y}_{sij}$ and $\mathbf{Z}_{sij}$, respectively, each of dimension $3 \times 3$. These submatrices are actually all diagonal.

We can therefore write Eq. (11-77) as follows:

$$\begin{bmatrix} \mathbf{V}_{s1} \\ \mathbf{V}_{s2} \\ \vdots \\ \mathbf{V}_{sn} \end{bmatrix} = \begin{bmatrix} \mathbf{Z}_{s11} & \mathbf{Z}_{s12} & \cdots & \mathbf{Z}_{s1n} \\ \mathbf{Z}_{s21} & \mathbf{Z}_{s22} & \cdots & \mathbf{Z}_{s2n} \\ \cdots & \cdots & \cdots & \cdots \\ \cdots & \cdots & \cdots & \cdots \\ \cdots & \cdots & \cdots & \cdots \\ \mathbf{Z}_{sn1} & \cdots & \cdots & \mathbf{Z}_{snn} \end{bmatrix} \begin{bmatrix} \mathbf{J}_{s1} \\ \mathbf{J}_{s2} \\ \vdots \\ \mathbf{J}_{sn} \end{bmatrix} \tag{11-85}$$

Consider now the case where an unbalanced fault occurs on bus $q$. The fault (Fig. 11-14) results in the fault currents $I_{aq}'$, $I_{bq}'$, and $I_{cq}'$ in phases $a$, $b$, and $c$, respectively; i.e., we can express the fault currents of bus $q$ as a three-vector:

$$\mathbf{I}_{pq}' \triangleq \begin{bmatrix} I_{aq}' \\ I_{bq}' \\ I_{cq}' \end{bmatrix} \tag{11-86}$$

The phase voltages of the faulted bus (measured relative to the "local" ground) take on the postfault values $V_{aq}{}^f$, $V_{bq}{}^f$, and $V_{cq}{}^f$, and we can likewise summarize these in a three-vector,

$$\mathbf{V}_{pq}{}^f \triangleq \begin{bmatrix} V_{aq}{}^f \\ V_{bq}{}^f \\ V_{cq}{}^f \end{bmatrix} \tag{11-87}$$

The three-vectors $\mathbf{I}_{pq}{}^f$ and $\mathbf{V}_{pq}{}^f$ can be related, as we will demonstrate through either an *impedance* relationship,

$$\mathbf{V}_{pq}{}^f \triangleq \mathbf{Z}^f \mathbf{I}_{pq}{}^f \tag{11-88}$$

or an *admittance relationship*,

$$\mathbf{I}_{pq}{}^f = \mathbf{Y}^f \mathbf{V}_{pq}{}^f \tag{11-89}$$

where the *fault impedance matrix* $\mathbf{Z}^f$, or *the fault admittance matrix* $\mathbf{Y}^f$, has values that depend upon the type of fault in question. In Sec. 11-3.3 we shall determine the actual values for these matrices for the most common types of unbalanced faults.

It should be noted that the vectors $\mathbf{I}_{pq}{}^f$ and $\mathbf{V}_{pq}{}^f$ represent the actual *phase values* of bus current and bus voltage at the faulted bus. Since our equations for the rest of the network are expressed in symmetrical component values, it is necessary to SC-transform Eqs. (11-88) and (11-89) to obtain a match. By making use of Eqs. (11-19) and (11-20), Eqs. (11-88) and (11-89) take on the transformed appearance

$$\mathbf{V}_{sq}{}^f = \mathbf{Z}_s{}^f \mathbf{I}_{sq}{}^f \tag{11-90}$$

and

$$\mathbf{I}_{sq}{}^f = \mathbf{Y}_s{}^f \mathbf{V}_{sq}{}^f \tag{11-91}$$

The *SC-transformed fault impedance and admittance matrices* $\mathbf{Z}_s{}^f$ and $\mathbf{Y}_s{}^f$ are related to the untransformed fault matrices through the equations

$$\mathbf{Z}_s{}^f = \mathbf{T}^{-1}\mathbf{Z}^f\mathbf{T} \tag{11-92}$$

$$\mathbf{Y}_s{}^f = \mathbf{T}^{-1}\mathbf{Y}^f\mathbf{T} \tag{11-93}$$

At this point we invoke the Thévenin's theorem that gives us [compare Eq. (10-41)] the postfault bus voltages from the formula

$$\mathbf{V}_{s,\text{bus}}^f = \mathbf{V}_{s,\text{bus}}^0 + \mathbf{Z}_{s,\text{bus}}\mathbf{I}_{s,\text{bus}}^f \tag{11-94}$$

In this equation the fault current vector $\mathbf{I}_{s,\text{bus}}^f$ has as its components the fault currents injected at the various buses. Since fault current is being pumped into the system only at bus $q$ in the amount $-\mathbf{I}_{sq}{}^f$, we can write the fault current vector in the form



$$\mathbf{I}_{s,\text{bus}}^f = \begin{bmatrix} \mathbf{0} \\ \mathbf{0} \\ \cdot \\ \cdot \\ \cdot \\ -\mathbf{I}_{sq}{}^f \\ \cdot \\ \cdot \\ \cdot \\ \mathbf{0} \end{bmatrix} \leftarrow q\text{th component} \tag{11-95}$$

The vector equations (11-94) and (11-95) correspond to Eqs. (10-41) and (10-42) in the balanced case. The basic difference between our present vector equations and those in Chap. 10 is the dimensionality. The present vector equations have $3n$ components. We can group them, as we have done, into $n$ "components" of three scalars each, each such "three-group" representing the three symmetrical components of voltage or current at each bus. For example, in Eq. (11-95), the $q$th component refers to the three-group at bus $q$.

It should be noted that at this stage we do *not* know the fault current $\mathbf{I}_{sq}{}^f$, and consequently, Eq. (11-94) cannot provide *directly* the postfault bus voltages, although $\mathbf{V}_{s,\text{bus}}^0$ and $\mathbf{Z}_{s,\text{bus}}$ *both are known*. We can, however, find $\mathbf{I}_{sq}{}^f$ in the following manner.

Write Eq. (11-94) in component form. We do *not* write out the $3n$ scalar components, but rather the $n$ vector "components," i.e.,

$$\begin{aligned} &\mathbf{V}_{s1}{}^f = \mathbf{V}_{s1}{}^0 - \mathbf{Z}_{s1_q}\mathbf{I}_{sq}{}^f \\ &\cdots\cdots\cdots\cdots\cdots \\ &\mathbf{V}_{sq}{}^f = \mathbf{V}_{sq}{}^0 - \mathbf{Z}_{sqq}\mathbf{I}_{sq}{}^f \\ &\cdots\cdots\cdots\cdots\cdots \\ &\mathbf{V}_{sn}{}^f = \mathbf{V}_{sn}{}^0 - \mathbf{Z}_{snq}\mathbf{I}_{sq}{}^f \end{aligned} \tag{11-96}$$

This set of $n$ *vector* equations corresponds to the set of $n$ *scalar* equations (10-43). Between the $q$th equation (11-96) and Eq. (11-90), we can now eliminate the postfault bus voltage $\mathbf{V}_{sq}{}^f$. We get

$$\mathbf{Z}_s{}^f\mathbf{I}_{sq}{}^f = \mathbf{V}_{sq}{}^0 - \mathbf{Z}_{sqq}\mathbf{I}_{sq}{}^f \tag{11-97}$$

In this three-dimensional vector equation *everything* is known except $\mathbf{I}_{sq}{}^f$, and we therefore solve for this unknown.

We obtain

$$\mathbf{I}_{sq}{}^f = (\mathbf{Z}_s{}^f + \mathbf{Z}_{sqq})^{-1}\mathbf{V}_{sq}{}^0 \tag{11-98}$$

This three-dimensional vector equation corresponds to the scalar equation (10-45).

Since now the fault currents *are* known, we can substitute $\mathbf{I}_{sq}^{f}$ back into Eq. (11-96) and obtain the postfault bus voltages. Substitution renders

$$\mathbf{V}_{si}^{f} = \mathbf{V}_{si}^{0} - \mathbf{Z}_{siq}(\mathbf{Z}_{s}^{f} + \mathbf{Z}_{sqq})^{-1}\mathbf{V}_{sq}^{0} \qquad \text{for } i \neq q \tag{11-99}$$

For the faulted bus itself, we get

$$\mathbf{V}_{sq}^{f} = \mathbf{Z}_{s}^{f}(\mathbf{Z}_{s}^{f} + \mathbf{Z}_{sqq})^{-1}\mathbf{V}_{sq}^{0} \tag{11-100}$$

The vector equations (11-99) and (11-100) correspond to the scalar equations (10-46).

This, in principle, completes our analysis. With the fault current and all postfault bus voltages known, we can compute the short-circuit currents in all lines. Consider the short-circuit current in the transmission line connecting the buses $\nu$ and $\mu$. Assume that the line is characterized by the admittance matrix

$$\mathbf{Y}_{s\nu\to\mu} = \begin{bmatrix} y_{+} & 0 & 0 \\ 0 & y_{-} & 0 \\ 0 & 0 & y_{0} \end{bmatrix} \tag{11-101}$$

The postfault current $\mathbf{I}_{s\nu\to\mu}^{f}$ (defined positive in the direction $\nu \to \mu$) flowing in the line can be computed from

$$\mathbf{I}_{s\nu\to\mu}^{f} = \mathbf{Y}_{s\nu\to\mu}(\mathbf{V}_{s\nu}^{f} - \mathbf{V}_{s\mu}^{f}) \tag{11-102}$$

The following comments are in order concerning the use of the above set of formulas:

1. The formulas are completely general and can be used therefore for an $n$-bus system. Note also that the fault has been placed at the likewise general bus $q$.
2. As a result of the above generality, once the SC bus admittance and bus impedance matrices $\mathbf{Y}_{s,\text{bus}}$ and $\mathbf{Z}_{s,\text{bus}}$ have been assembled and computed and placed in computer memory, we can with equal ease extend our short-circuit analysis to *any* faulted bus and *any* unbalanced type of fault.
3. All formulas involve three-dimensional vectors and $3 \times 3$ matrices. The matrices $\mathbf{Z}_{sij}$ are diagonal, but the matrix $\mathbf{Z}_{s}^{f}$ is not. In any case, all the involved matrix operations are easily programmed on a digital computer.
4. Although the matrix $\mathbf{Y}_{s,\text{bus}}$ is of dimension $3n \times 3n$, we need only invert at the most $n \times n$ matrices to obtain $\mathbf{Z}_{s,\text{bus}}$. This was demonstrated in Example 11-3. The reason is the complete decoupling between the three-sequence component systems.



5. All formulas give us the postfault currents and voltages *in terms of symmetrical components*. Since, of course, the actual phase currents and voltages are of interest in the final analysis, we must complete each short-circuit analysis with an *indirect* SC transformation, converting all SC components into phase values, using Eqs. (11-6) and (11-12).
6. The prefault voltages are, of course, *balanced*, and $\mathbf{V}_{si}^{0}$ contains, thus, no negative- and zero-sequence components; i.e., we have

$$\mathbf{V}_{si}^{0} = \begin{bmatrix} V_{+i}^{0} \\ 0 \\ 0 \end{bmatrix} = \begin{bmatrix} V_{i}^{0} \\ 0 \\ 0 \end{bmatrix} \qquad i = 1, 2, \ldots, n \tag{11-103}$$

The prefault bus voltages $V_{i}^{0}$ are either obtained from a load flow analysis or, as we pointed out in Chap. 10, are usually set equal to 1.0 pu; i.e.,

$$\mathbf{V}_{si}^{0} \approx \begin{bmatrix} 1 \\ 0 \\ 0 \end{bmatrix} \qquad \text{for } i = 1, 2, \ldots, n \tag{11-104}$$

7. All the foregoing equations were derived, based on the existence of the fault impedance matrix $\mathbf{Z}_{s}^{f}$. We have hinted at the possibility, and shall confirm this in the next section, that in some cases $\mathbf{Z}_{s}^{f}$ *is not defined*, but the admittance matrix $\mathbf{Y}_{s}^{f}$ is. In such a case we must develop a new set of equations, making use of $\mathbf{Y}_{s}^{f}$ instead of $\mathbf{Z}_{s}^{f}$. This is simply done by eliminating $\mathbf{I}_{sq}^{f}$ instead of $\mathbf{V}_{sq}^{f}$ in deriving Eq. (11-97). The above analysis thus changes as follows: Instead of Eq. (11-97), we get

$$\mathbf{V}_{sq}^{f} = \mathbf{V}_{sq}^{0} - \mathbf{Z}_{sqq}\mathbf{Y}_{s}^{f}\mathbf{V}_{sq}^{f} \tag{11-105}$$

From this equation we can solve for the unknown postfault voltage vector at bus $q$,

$$\mathbf{V}_{sq}^{f} = (\mathbf{I} + \mathbf{Z}_{sqq}\mathbf{Y}_{s}^{f})^{-1}\mathbf{V}_{sq}^{0} \tag{11-106}$$

where $\mathbf{I}$ is the identity matrix.

Equation (11-91) will next give us the fault current.

$$\mathbf{I}_{sq}^{f} = \mathbf{Y}_{s}^{f}\mathbf{V}_{sq}^{f} = \mathbf{Y}_{s}^{f}(\mathbf{I} + \mathbf{Z}_{sqq}\mathbf{Y}_{s}^{f})^{-1}\mathbf{V}_{sq}^{0} \tag{11-107}$$

The postfault voltages at the buses, other than the faulted one, are obtained upon substitution of Eq. (11-107) into Eq. (11-96). We get

$$\mathbf{V}_{si}^{f} = \mathbf{V}_{si}^{0} - \mathbf{Z}_{siq}\mathbf{I}_{sq}^{f} = \mathbf{V}_{si}^{0} - \mathbf{Z}_{siq}\mathbf{Y}_{s}^{f}(\mathbf{I} + \mathbf{Z}_{sqq}\mathbf{Y}_{s}^{f})^{-1}\mathbf{V}_{sq}^{0} \qquad i \neq q \tag{11-108}$$

For the case of *nondefined* $\mathbf{Z}_s{}^f$, the general equations (11-98) to (11-100) must therefore be replaced by Eqs. (11-106) to (11-108).

### 11-3.3 DETERMINATION OF THE FAULT MATRICES $\mathbf{Z}_s{}^f$ AND $\mathbf{Y}_s{}^f$

From the preceding discussions it should have become clear that a key feature of the overall analysis is the availability of the fault impedance or admittance matrices $\mathbf{Z}_s{}^f$ and $\mathbf{Y}_s{}^f$. In this regard the unbalanced short-circuit analysis is very different from, and much more complicated than, the balanced analysis of Chap. 10. The reader may remember that in Chap. 10 we introduced a *scalar* fault impedance $Z^f$, and it was never doubted that this parameter would not suffice to handle *all* possible cases. In the one *extreme* case where the short circuit was *solid*, we encountered no analytical difficulty because we simply set $Z^f = 0$ in our formulas. In the other extreme case, i.e., where $Z^f = \infty$, we have, of course, no problems either, since we now have *no fault*.

The situation is quite different in the present unbalanced case. Whenever we have the *extreme* cases of zero or infinite fault impedance on *one* phase, the fault admittance or impedance matrix, respectively, will be *undefined*, and thus *useless*, in our general formulas. Such extreme cases are, however, more the rule than the exception, and it is necessary, therefore, that we learn how to handle them in our analysis.

Consider the *general* unbalanced case depicted in Fig. 11-15. By assigning proper values to the impedances $Z_a$, $Z_b$, $Z_c$, and $Z_g$, we can obtain

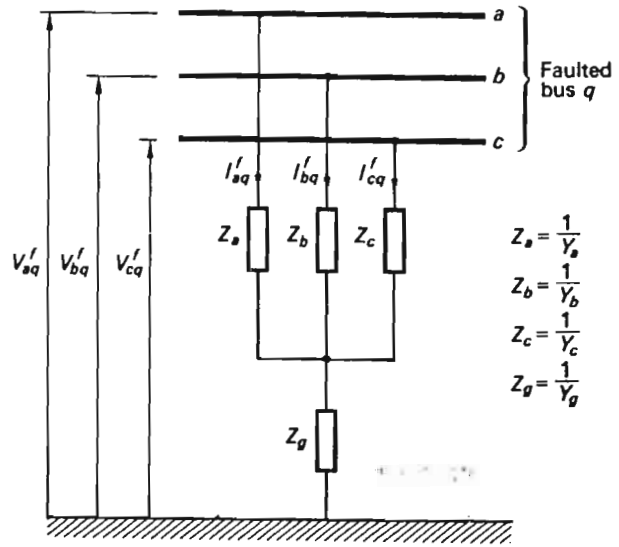


**Fig. 11-15** A general unbalanced fault (or loading) case. $Z_a \neq Z_b \neq Z_c \neq Z_g$.



any practically important fault case that we wish. For example, by setting

$$Z_a = Z_g = 0$$

and

$$Z_b = Z_c = \infty$$

we have, in effect, created a solid single-phase-to-ground short circuit on phase *a*. By setting

$$Z_a = \infty$$

and

$$Z_b = Z_c = Z_g = 0$$

we have obtained a solid phase-to-phase short circuit with simultaneous ground contact. Other practically important fault configurations can likewise be created.

If we therefore find the *general* expressions for $\mathbf{Z}_s{}^f$ and $\mathbf{Y}_s{}^f$ for this general case, we can obtain the simpler, special (but important) cases by assigning appropriate values to the four impedance elements.

For the circuit in Fig. 11-15 we have the following relationships between voltages and currents:

$$\begin{aligned} V_{aq}{}^f &= I_{aq}{}^f Z_a + (I_{aq}{}^f + I_{bq}{}^f + I_{cq}{}^f)Z_g \\ V_{bq}{}^f &= I_{bq}{}^f Z_b + (I_{aq}{}^f + I_{bq}{}^f + I_{cq}{}^f)Z_g \\ V_{cq}{}^f &= I_{cq}{}^f Z_c + (I_{aq}{}^f + I_{bq}{}^f + I_{cq}{}^f)Z_g \end{aligned} \tag{11-109}$$

or in vector form,

$$\begin{bmatrix} V_{aq}{}^f \\ V_{bq}{}^f \\ V_{cq}{}^f \end{bmatrix} = \begin{bmatrix} Z_a + Z_g & Z_g & Z_g \\ Z_g & Z_b + Z_g & Z_g \\ Z_g & Z_g & Z_c + Z_g \end{bmatrix} \begin{bmatrix} I_{aq}{}^f \\ I_{bq}{}^f \\ I_{cq}{}^f \end{bmatrix} \tag{11-110}$$

Identification with Eq. (11-88) gives us the fault impedance matrix

$$\mathbf{Z}^f = \begin{bmatrix} Z_a + Z_g & Z_g & Z_g \\ Z_g & Z_b + Z_g & Z_g \\ Z_g & Z_g & Z_c + Z_g \end{bmatrix} \tag{11-111}$$

If we SC-transform this impedance matrix, using Eq. (11-92), we get

$$\mathbf{Z}_s{}^f = \tfrac{1}{3} \begin{bmatrix} Z_a + Z_b + Z_c & Z_a + \alpha^2 Z_b + \alpha Z_c & Z_a + \alpha Z_b + \alpha^2 Z_c \\ Z_a + \alpha Z_b + \alpha^2 Z_c & Z_a + Z_b + Z_c & Z_a + \alpha^2 Z_b + \alpha Z_c \\ Z_a + \alpha^2 Z_b + \alpha Z_c & Z_a + \alpha Z_b + \alpha^2 Z_c & Z_a + Z_b + Z_c + 9Z_g \end{bmatrix} \tag{11-112}$$

If, instead, we express the relations between the currents and voltages in Fig. 11-15 in admittance form, we get, after some algebra,

$$\begin{bmatrix} I_{aq}{}^f \\ I_{bq}{}^f \\ I_{cq}{}^f \end{bmatrix} = \frac{1}{Y_a + Y_b + Y_c + Y_g} \times \begin{bmatrix} Y_a(Y_g + Y_b + Y_c) & -Y_aY_b & -Y_aY_c \\ -Y_aY_b & Y_b(Y_g + Y_a + Y_c) & -Y_bY_c \\ -Y_aY_c & -Y_bY_c & Y_c(Y_g + Y_a + Y_b) \end{bmatrix} \begin{bmatrix} V_{aq}{}^f \\ V_{bq}{}^f \\ V_{cq}{}^f \end{bmatrix} \tag{11-113}$$

If we SC-transform the admittance matrix $\mathbf{Y}^f$ in this last equation, using Eq. (11-93), we get the following rather cumbersome expression for $\mathbf{Y}_s{}^f$:

$$\mathbf{Y}_s{}^f = \frac{1}{Y_a + Y_b + Y_c + Y_g} \times \begin{bmatrix} \frac{1}{3}Y_g(Y_a + Y_b + Y_c) + (Y_aY_b + Y_bY_c + Y_cY_a) & \frac{1}{3}Y_g(Y_a + \alpha^2 Y_b + \alpha Y_c) - (Y_bY_c + \alpha Y_aY_b + \alpha^2 Y_aY_c) & \frac{1}{3}Y_g(Y_a + \alpha Y_b + \alpha^2 Y_c) \\ \frac{1}{3}Y_g(Y_a + \alpha Y_b + \alpha^2 Y_c) - (Y_bY_c + \alpha^2 Y_aY_b + \alpha Y_aY_c) & \frac{1}{3}Y_g(Y_a + Y_b + Y_c) + (Y_aY_b + Y_bY_c + Y_cY_a) & \frac{1}{3}Y_g(Y_a + \alpha^2 Y_b + \alpha Y_c) \\ \frac{1}{3}Y_g(Y_a + \alpha^2 Y_b + \alpha Y_c) & \frac{1}{3}Y_g(Y_a + \alpha Y_b + \alpha^2 Y_c) & \frac{1}{3}Y_g(Y_a + Y_b + Y_c) \end{bmatrix} \tag{11-114}$$

We note that neither $\mathbf{Z}_s{}^f$ nor $\mathbf{Y}_s{}^f$ is necessarily diagonal.

Let us now look at some important special cases.

**Case 1. Equal phase impedances** This case, shown in Fig. 11-16, is characterized by

$$Z_a = Z_b = Z_c = Z = \frac{1}{Y}$$

From Eqs. (11-112) and (11-114) we get the following simple expressions for the fault matrices:

$$\mathbf{Z}_s{}^f = \begin{bmatrix} Z & 0 & 0 \\ 0 & Z & 0 \\ 0 & 0 & Z + 3Z_g \end{bmatrix} \tag{11-115}$$

$$\mathbf{Y}_s{}^f = \begin{bmatrix} Y & 0 & 0 \\ 0 & Y & 0 \\ 0 & 0 & \dfrac{YY_g}{Y_g + 3Y} \end{bmatrix} \tag{11-116}$$

We make the important observation that in this case the fault matrices are *diagonal*. Let us point out the consequences of this fact. Consider, for



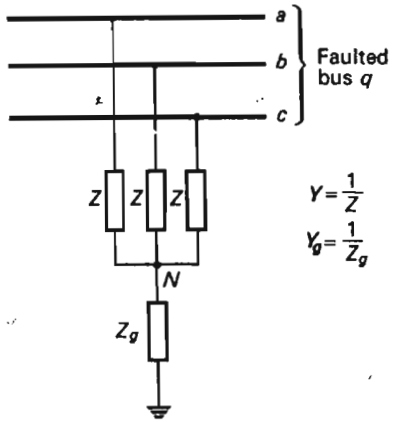


**Fig. 11-16** The case of equal phase impedances.

example, the fault current $\mathbf{I}_{sq}{}^f$ in Eq. (11-98). Since $\mathbf{Z}_s{}^f$ is diagonal and the same is true about $\mathbf{Z}_{sqq}$, it follows that the inverse matrix $(\mathbf{Z}_s{}^f + \mathbf{Z}_{sqq})^{-1}$ is also diagonal. Since the vector $\mathbf{V}_{sq}{}^0$ contains only a positive-sequence component [Eq. (11-103)], it follows that *the fault current contains only a positive-sequence component also; i.e., it possesses three-phase symmetry.* In fact, all postfault currents and voltages will contain no negative- and zero-sequence components, as the reader may easily find from Eqs. (11-99) and (11-100). Since no zero-sequence current exists, the neutral point $N$ in Fig. 11-16 will thus be at zero potential, and since no current flows through $Z_g$, the ground impedance does in no way enter the picture. The reader may find that this case is indeed identical with the one discussed in Chap. 10.

**Case 2. Single-phase-to-ground short circuit** This important case (Fig. 11-17) is obtained by setting

$$Z_b = Z_c = \infty$$

$$Z_g = 0 \quad \text{(that is, } Y_g = \infty\text{)} \qquad Z_a = Z^f = \frac{1}{Y^f}$$

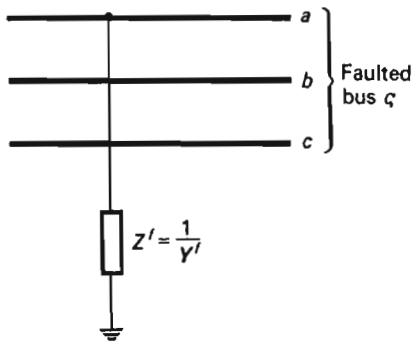


**Fig. 11-17** The single-phase-to-ground fault case.

We obtain from Eqs. (11-112) and (11-114)

$$\mathbf{Z}_s' = \begin{bmatrix} \infty & \infty & \infty \\ \infty & \infty & \infty \\ \infty & \infty & \infty \end{bmatrix} \tag{11-117}$$

$$\mathbf{Y}_s' = \frac{Y'}{3}\begin{bmatrix} 1 & 1 & 1 \\ 1 & 1 & 1 \\ 1 & 1 & 1 \end{bmatrix} \tag{11-118}$$

We conclude that $\mathbf{Z}_s'$ will be *undefined* in this case; so we must use $\mathbf{Y}_s'$ and make use of Eqs. (11-106) to (11-108) in our short-circuit analysis. Note that if we make the short circuit *solid* by setting $Y' = \infty$, then also the $\mathbf{Y}_s'$ matrix will be undefined. In such a case we can still perform the analysis by means of a *limit study*. We shall exemplify later.

**Case 3. Phase-to-phase short circuit** This case, depicted in Fig. 11-18, is obtained by setting

$$Z_a = \infty \qquad \text{(that is, } Y_a = 0\text{)}$$
$$Z_g = \infty \qquad \text{(that is, } Y_g = 0\text{)}$$
$$Y_b = Y_c = 2Y_f$$

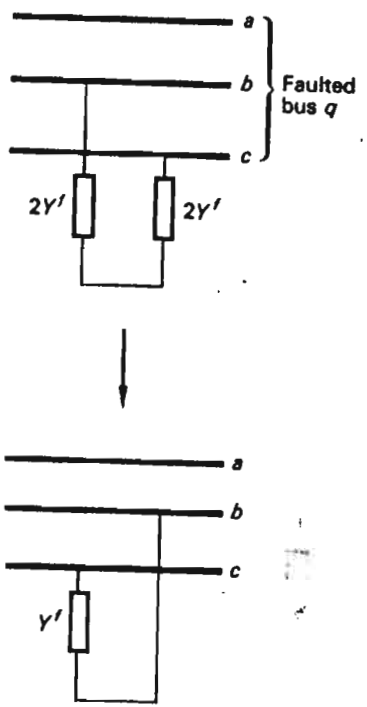


**Fig. 11-18** The phase-to-phase short-circuit case. No ground contact.



For the fault matrices we have

$$\mathbf{Z}_s' = \begin{bmatrix} \infty & \infty & \infty \\ \infty & \infty & \infty \\ \infty & \infty & \infty \end{bmatrix} \tag{11-119}$$

$$\mathbf{Y}_s' = Y'\begin{bmatrix} 1 & -1 & 0 \\ -1 & 1 & 0 \\ 0 & 0 & 0 \end{bmatrix} \tag{11-120}$$

Again, the impedance matrix is undefined, and we must work with the admittance matrix.

The above three cases will have to suffice. On occasion it may be necessary to study other unbalanced short-circuit types than those in Figs. 11-17 and 11-18, and the reader should find it no problem to derive the appropriate fault matrices from the general case.

**Example 11-3 (cont.)** We now make use of our analysis results to finish the three-bus example that we started earlier. We had assembled the $\mathbf{Z}_{s,\text{bus}}$ matrix for the system in question. It is given in Eq. (11-82).

We shall find the postfault voltages and currents throughout the system caused by a single-phase-to-ground short circuit on bus 3. We identify this as case 2 above, and we conclude that, since the $\mathbf{Z}_s'$ matrix is undefined, we must make use of the $\mathbf{Y}_s'$ matrix given by Eq. (11-118).

We start our computations by first computing the voltage of the faulted bus, using Eq. (11-106).

By substitution of the various matrices and the vector $\mathbf{V}_{sq}^0$, we get

$$\mathbf{V}_{sq}' = \left\{ \begin{bmatrix} 1 & 0 & 0 \\ 0 & 1 & 0 \\ 0 & 0 & 1 \end{bmatrix} + \begin{bmatrix} z_{+qq} & 0 & 0 \\ 0 & z_{-qq} & 0 \\ 0 & 0 & z_{0qq} \end{bmatrix} \frac{Y'}{3} \begin{bmatrix} 1 & 1 & 1 \\ 1 & 1 & 1 \\ 1 & 1 & 1 \end{bmatrix} \right\}^{-1} \begin{bmatrix} V_q^0 \\ 0 \\ 0 \end{bmatrix} \tag{11-121}$$

By performing the matrix operations called for, this vector equation simplifies to

$$\mathbf{V}_{sq}' = \frac{V_q^0}{1 + (Y'/3)(z_{+qq} + z_{-qq} + z_{0qq})} \begin{bmatrix} 1 + \dfrac{Y'}{3}(z_{-qq} + z_{0qq}) \\ -z_{-qq}\dfrac{Y'}{3} \\ -z_{0qq}\dfrac{Y'}{3} \end{bmatrix} \tag{11-122}$$

For the short-circuit current at the faulted bus, we use Eq. (11-107).

$$\mathbf{I}_{sq}' = \mathbf{Y}_s'\mathbf{V}_{sq}' = V_q^0 \frac{Y'/3}{1 + (Y'/3)(z_{+qq} + z_{-qq} + z_{0qq})} \begin{bmatrix} 1 \\ 1 \\ 1 \end{bmatrix} \tag{11-123}$$

Finally, the postfault voltages at the buses other than the faulted one are obtained from Eq. (11-108).

$$\mathbf{V}_{si}{}' = \mathbf{V}_{si}{}^0 - \mathbf{Z}_{siq}\mathbf{I}_{sq}{}'$$

$$= \begin{bmatrix} V_i{}^0 \\ 0 \\ 0 \end{bmatrix} - \begin{bmatrix} z_{+iq} & 0 & 0 \\ 0 & z_{-iq} & 0 \\ 0 & 0 & z_{0iq} \end{bmatrix} \mathbf{I}_{sq}{}'$$

Upon substitution of the expression for $\mathbf{I}_{sq}{}'$, we obtain

$$\mathbf{V}_{si}{}' = \begin{bmatrix} V_i{}^0 \\ 0 \\ 0 \end{bmatrix} - V_q{}^0 \frac{Y'/3}{1 + (Y'/3)(z_{+qq} + z_{-qq} + z_{0qq})} \begin{bmatrix} z_{+iq} \\ z_{-iq} \\ z_{0iq} \end{bmatrix} \tag{11-124}$$

Equations (11-122) to (11-124) simplify considerably if we assume that the short circuit is *solid*, that is, $Y' = \infty$. A further simplification is obtained if we make the reasonable assumption that all prefault voltages, $V_i{}^0$, equal 1 pu. Upon making use of these two assumptions, the above formulas reduce to the following simple forms:

$$\mathbf{V}_{sq}{}' = \frac{1}{z_{+qq} + z_{-qq} + z_{0qq}} \begin{bmatrix} z_{-qq} + z_{0qq} \\ -z_{-qq} \\ -z_{0qq} \end{bmatrix} \tag{11-125}$$

$$\mathbf{I}_{sq}{}' = \frac{1}{z_{+qq} + z_{-qq} + z_{0qq}} \begin{bmatrix} 1 \\ 1 \\ 1 \end{bmatrix} \tag{11-126}$$

$$\mathbf{V}_{si}{}' = \begin{bmatrix} 1 \\ 0 \\ 0 \end{bmatrix} - \frac{1}{z_{+qq} + z_{-qq} + z_{0qq}} \begin{bmatrix} z_{+iq} \\ z_{-iq} \\ z_{0iq} \end{bmatrix} \qquad \text{for } i \neq q \tag{11-127}$$

It should be noted that these formulas are very general, in the sense that they are applicable for a short circuit (of the single-phase-to-ground variety) on *any* bus. If a digital computer is used for the numerical computations, Eqs. (11-125) to (11-127) are preferred over Eqs. (11-106) to (11-108) for the following reasons:

1. The former equations involve no matrix inversions (the inversion having been performed once and for all in deriving the formulas). This means reduced computer time.
2. Should the fault admittance $Y'$ be infinite, as we assumed, the former equations could not be used at all, because the computer cannot handle infinite numbers.

We will now finish our problem by using the numerical values that apply to our three-bus system. Since the short circuit occurs on bus 3, we have $q = 3$.



From Eq. (11-82), we then get

$$\mathbf{Z}_{sqq} = \mathbf{Z}_{s33} = \begin{bmatrix} z_{+33} & 0 & 0 \\ 0 & z_{-33} & 0 \\ 0 & 0 & z_{033} \end{bmatrix} = j \begin{bmatrix} 0.1014 & 0 & 0 \\ 0 & 0.1014 & 0 \\ 0 & 0 & 0.1180 \end{bmatrix}$$

From Eqs. (11-125) and (11-126) we therefore get

$$\mathbf{V}_{s3}{}' = \frac{1}{j(0.1014 + 0.1014 + 0.1180)} \begin{bmatrix} j(0.1014 + 0.1180) \\ -j0.1014 \\ -j0.1180 \end{bmatrix} = \begin{bmatrix} 0.685 \\ -0.317 \\ -0.369 \end{bmatrix} \text{ pu}$$

and

$$\mathbf{I}_{sq}{}' = \mathbf{I}_{s3}{}' = \frac{1}{j(0.1014 + 0.1014 + 0.1180)} \begin{bmatrix} 1 \\ 1 \\ 1 \end{bmatrix} = -j \begin{bmatrix} 3.12 \\ 3.12 \\ 3.12 \end{bmatrix} \text{ pu} \tag{11-128}$$

To compute the postfault voltages on buses 1 and 2, we need to know the impedance matrices $\mathbf{Z}_{s13}$ and $\mathbf{Z}_{s23}$. From Eq. (11-82), we have

$$\mathbf{Z}_{s13} = \begin{bmatrix} z_{+13} & 0 & 0 \\ 0 & z_{-13} & 0 \\ 0 & 0 & z_{013} \end{bmatrix} = j \begin{bmatrix} 0.0558 & 0 & 0 \\ 0 & 0.0558 & 0 \\ 0 & 0 & 0.0220 \end{bmatrix}$$

$$\mathbf{Z}_{s23} = \begin{bmatrix} z_{+23} & 0 & 0 \\ 0 & z_{-23} & 0 \\ 0 & 0 & z_{023} \end{bmatrix} = j \begin{bmatrix} 0.0472 & 0 & 0 \\ 0 & 0.0472 & 0 \\ 0 & 0 & 0.0140 \end{bmatrix}$$

From Eq. (11-127) we now get

$$\mathbf{V}_{s1}{}' = \begin{bmatrix} 1 \\ 0 \\ 0 \end{bmatrix} - \frac{1}{j(0.1014 + 0.1014 + 0.1180)} \begin{bmatrix} j0.0558 \\ j0.0558 \\ j0.0220 \end{bmatrix} = \begin{bmatrix} 0.826 \\ -0.174 \\ -0.069 \end{bmatrix} \text{ pu} \tag{11-129}$$

$$\mathbf{V}_{s2}{}' = \begin{bmatrix} 1 \\ 0 \\ 0 \end{bmatrix} - \frac{1}{j(0.1014 + 0.1014 + 0.1180)} \begin{bmatrix} j0.0472 \\ j0.0472 \\ j0.0140 \end{bmatrix} = \begin{bmatrix} 0.853 \\ -0.147 \\ -0.044 \end{bmatrix} \text{ pu} \tag{11-130}$$

We note the following facts about these numerical values:

1. The fault current contains the three sequence components in equal proportions.
2. The bus voltages contain more of the positive-sequence and less of the negative- and zero-sequence components the farther from the fault the buses are located.

Since we now know all postfault bus voltages, we can readily compute all postfault line currents. As an example, let us compute the current in the line

connecting buses 1 and 3. We remember that the line had the sequence impedances

$$\mathbf{Z}_{s1\to3} = \begin{bmatrix} j0.10 & 0 & 0 \\ 0 & j0.10 & 0 \\ 0 & 0 & j0.20 \end{bmatrix} \text{ pu}$$

or in admittance form,

$$\mathbf{Y}_{s1\to3} = \begin{bmatrix} -j10 & 0 & 0 \\ 0 & -j10 & 0 \\ 0 & 0 & -j5 \end{bmatrix} \text{ pu}$$

From Eq. (11-102) we then compute the line currents:

$$\mathbf{I}'_{s1\to3} = \begin{bmatrix} -j10 & 0 & 0 \\ 0 & -j10 & 0 \\ 0 & 0 & -j5 \end{bmatrix} \left\{ \begin{bmatrix} 0.826 \\ -0.174 \\ -0.069 \end{bmatrix} - \begin{bmatrix} 0.685 \\ -0.317 \\ -0.369 \end{bmatrix} \right\} = -j \begin{bmatrix} 1.42 \\ 1.42 \\ 1.50 \end{bmatrix} \quad (11\text{-}131)$$

It must be noted that all the above voltages and currents are obtained in SC form. We are probably more interested in knowing them in actual phase values. If this is the case, we must make them all subject to an *indirect* SC transformation by the matrix **T**. We get for the phase voltages of bus 3

$$\mathbf{V}_{p3}' = \begin{bmatrix} V_{a3}' \\ V_{b3}' \\ V_{c3}' \end{bmatrix} = \mathbf{T}\mathbf{V}_{s3}' = \begin{bmatrix} 0 \\ -0.553 - j0.868 \\ -0.553 + j0.868 \end{bmatrix}$$

or, in RMS values,

$$\begin{bmatrix} |V_{a3}'| \\ |V_{b3}'| \\ |V_{c3}'| \end{bmatrix} = \begin{bmatrix} 0 \\ 1.03 \\ 1.03 \end{bmatrix} \text{ pu}$$

For the phase currents in the fault,

$$\mathbf{I}_{p3}' = \begin{bmatrix} I_{a3}' \\ I_{b3}' \\ I_{c3}' \end{bmatrix} = \mathbf{T}\mathbf{I}_{s3}' = -j \begin{bmatrix} 9.36 \\ 0 \\ 0 \end{bmatrix} \text{ pu}$$

For the phase voltages of buses 1 and 2,

$$\mathbf{V}_{p1}' = \begin{bmatrix} V_{a1}' \\ V_{b1}' \\ V_{c1}' \end{bmatrix} = \mathbf{T}\mathbf{V}_{s1}' = \begin{bmatrix} 0.583 \\ -0.395 - j0.866 \\ -0.395 + j0.866 \end{bmatrix}$$

$$\mathbf{V}_{p2}' = \begin{bmatrix} V_{a2}' \\ V_{b2}' \\ V_{c2}' \end{bmatrix} = \mathbf{T}\mathbf{V}_{s2}' = \begin{bmatrix} 0.662 \\ -0.400 - j0.865 \\ -0.400 + j0.865 \end{bmatrix}$$



or, in RMS values,

$$\begin{bmatrix} |V_{a1}'| \\ |V_{b1}'| \\ |V_{c1}'| \end{bmatrix} = \begin{bmatrix} 0.583 \\ 0.952 \\ 0.952 \end{bmatrix} \text{ pu} \quad \text{and} \quad \begin{bmatrix} |V_{a2}'| \\ |V_{b2}'| \\ |V_{c2}'| \end{bmatrix} = \begin{bmatrix} 0.662 \\ 0.955 \\ 0.955 \end{bmatrix} \text{ pu}$$

For the line currents,

$$\mathbf{I}'_{p1\to3} = \mathbf{T}\mathbf{I}_{s1\to3} = -j \begin{bmatrix} 4.34 \\ 0.08 \\ 0.08 \end{bmatrix}$$

We make these observations in regard to the above numerical values:

1. The fault current 9.36 pu in the short-circuited phase almost equals the value obtained for a solid symmetrical fault on the same bus, 9.87 pu (Chap. 10).
2. As the voltage on the faulted phase drops to zero, the voltages of the two healthy phases jump to 103 percent.
3. Although zero currents flow in phases *b* and *c* at the fault, the same phases of the lines leading to the faulted bus carry a slight current.

In the three-bus demonstration example just completed, all numerical computations were performed on a slide rule. It is obvious that in the general *n*-bus case we should delegate the entire numerical job, including the assembly of $\mathbf{Y}_{s,\text{bus}}$, to the digital computer.

Although the general formulas for the fault current $\mathbf{I}_{sq}'$, and the post-fault bus voltages $\mathbf{V}_{si}'$ can be directly programmed on the computer, it is better, as we pointed out in the foregoing example, first to perform "manually" the matrix inversions called for in the general formulas, once we have settled upon fault type. These inversions are either

$$(\mathbf{Z}_s' + \mathbf{Z}_{sqq})^{-1}$$

or

$$(\mathbf{I} + \mathbf{Z}_{sqq}\mathbf{Y}_s')^{-1}$$

depending upon whether we use the fault impedance or admittance matrix, and they need only to be performed *once*.

## 11-4 SUMMARY

In this chapter we have outlined analysis procedures which have proved useful in handling unbalanced fault calculations. The symmetrical component transformation (SCT) occupies a central position. The basic idea behind this transformation is the decomposition of the unbalanced network into three symmetrical component systems. The characteristics of generators, transformers, and transmission lines are such that the three component systems are decoupled from each other. We therefore are permitted to treat them separately.

A sequence network is assembled for each component system. These networks are generally of different structure. The computer assembly methods developed in Chap. 7 may be applied to each sequence network, and the entire network data can be concentrated in a single matrix, the SC admittance matrix.

General formulas have been derived by means of which we can compute the currents and voltages in a general $n$-bus system, subject to a completely general unbalanced load or fault situation. We demonstrated their use by finding the short-circuit currents, following a single-phase-to-ground fault in a three-bus system.

## EXERCISES

**11-1.** Figure 11-1 reveals how the phase currents may be obtained *graphically* by vectorial addition of the sequence components.

Show how the sequence components may be obtained graphically from the phase currents.

**11-2.** Whereas the *phase* voltages in a three-phase system may, in general, contain all three sequence components, prove that the *line* voltages can never contain zero-sequence voltages.

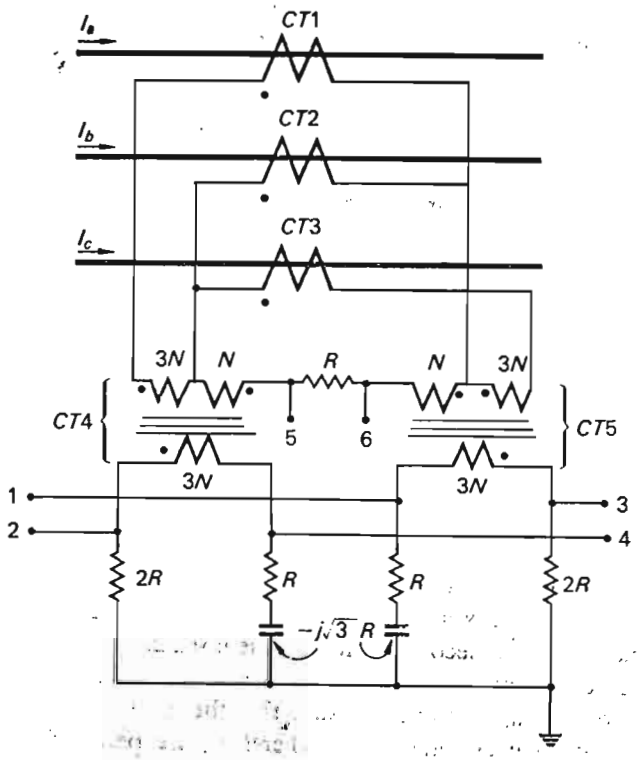


**Fig. 11-19** Sequence current component filter.



**11-3.** For relaying purposes it is often necessary to sense the sequence components of currents and voltages. Figure 11-19 depicts a sequence component filter which has the ability to "filter" out the positive- and negative-sequence components from the line currents $I_a$, $I_b$, and $I_c$. The filter consists of the three identical current transformers $CT1$, $CT2$, and $CT3$, the two three-winding current transformers $CT4$ and $CT5$, and an $RC$ network. The three windings of the latter transformers have the turns ratios 3:3:1 and a polarity as indicated.

It is assumed that the line currents contain all three sequence components. Prove that the voltage across terminals 1-2 is proportional to the positive-sequence component only; i.e., the negative- and zero-sequence components are filtered out. Prove that, similarly, the voltage across terminals 3-4 contains only the negative-sequence component, and finally, that, the voltage across terminals 5-6 contains only the zero-sequence component.

**11-4.** Design a filter which will separate the three sequence components from the phase *voltages* of the system in Fig. 11-19.

**11-5.** Find the fault admittance matrix $\mathbf{Y}_f'$ for a phase-to-phase short circuit with simultaneous solid ground contact.

**11-6.** Consider the three-bus example system treated in the text. Assume that a solid phase-to-phase short circuit (without ground contact) occurs on bus 3. Determine the short-circuit current in the fault and the voltage (to ground) of the healthy phase. Use the transient generator reactance in your analysis; i.e., your answers will be valid 3-4 cycles following the fault.

**11-7.** Consider the system portion depicted in Fig. 5-14. Assume that the 15- and 66-kV buses have infinite SSC. A solid phase-to-phase short circuit occurs on the 4.8-kV bus. Compute the fault current. Use the sequence networks given in Fig. 11-10.

**11-8.** Assume that the fault in Example 11-7 had been of the single-phase-to-ground variety. What would the fault current be now? What would be the voltages of the healthy phases?

**11-9.** Write a computer program to be used in studying solid single-phase-to-ground fault effects on the five-bus system in Fig. 7-22. We are interested in finding the fault currents and all bus voltages and line currents following a short circuit on *any one* of the five buses. Use the impedance data given in Exercises 7-8 and 10-5. Assume that all transformers are of the Y$\Delta$ type, with their neutrals (always on the high-voltage side) solidly grounded.

Assume that the negative- and positive-sequence impedances of the generators are equal. The zero-sequence reactances for the lines are assumed to have values of three times the positive-sequence reactances. Set all prefault voltages = 1 pu, and make the computer assemble the sequence networks by use of Eq. (7-80).

**11-10.** An unbalanced three-phase load consists of a 10-$\Omega$ resistor connected between phase $a$ and ground, and a 10-$\Omega$ reactor between phases $b$ and $c$. The voltage is balanced and of magnitude 4.8 kV (line-to-line).

(*a*) Find the sequence components of the load currents.
(*b*) Find the real and reactive powers consumed by the load using Eq. (2-42).
(*c*) Find the powers using Eq. (11-16) and compare results.

**11-11.** Analysis of the previous exercise was relatively simple because the voltage was assumed balanced. Assume now that the same unbalanced load is connected across the terminals of a 4.8-kV generator having the following internal sequence impedances (measured in steady state):

$z_+ = j8$ $\Omega$/phase
$z_- = j2$ $\Omega$/phase
$z_0 = j1$ $\Omega$/phase

Find the steady-state load powers, assuming that the generator terminal voltage was a balanced 4.8-kV *before* the application of the load. Generator neutral is solidly grounded.

**11-12.** Derive Eq. (11-30) using the general performance equations for the synchronous machine.

## REFERENCES


**Books**

1. Clarke, E.: "Circuit Analysis of A-C Power Systems," vols. I and II, John Wiley & Sons, Inc., New York, 1943.
2. Calabrese, G. O.: "Symmetrical Components," The Ronald Press Company, New York, 1959.
3. Stagg, G. W., and A. H. El-Abiad: "Computer Methods in Power Systems Analysis," McGraw-Hill Book Company, New York, 1968.
4. Lyle, A. G.: "Major Faults on Power Systems," Chapman and Hall, Ltd., London, 1952.

(References 1 and 2 give a detailed presentation of the analysis of unbalanced systems, including the SC method. Reference 3 discusses the digital computational techniques.)

**Technical papers and reports**

5. El-Abiad, A. H., et al.: 3-phase Analysis of Unbalanced Distribution Circuits, *Proc. Power Ind. Computer Appl. Conf.*, 1967, pp. 411–420.
6. Storry, J. O., and H. E. Brown: Improved Method of Incorporating Mutual Couplings in Single-phase Short-circuit Calculations, *Proc. Power Ind. Computer Appl.*, 1969.
7. Przyluski, A.: Vector Theory of Symmetrical Components, *Proc. Power Systems Computation Conf.*, rept. 4.7, Stockholm, Sweden, 1966.
8. Smith, D. C., and E. C. Stokes: Effect of Out of Balance of Transmission Line Impedances on the Design of a 500 kv Network, *Proc. Power Systems Computation Conf.*, rept. 4.15, Stockholm, Sweden, 1966.
9. Hwang, H. H.: Unbalanced Operations of AC Machines, *IEEE Trans.*, vol. PAS-84, pp. 1054–1066, November, 1965.


# 12
# Transient Stability Analysis

## 12-1 INTRODUCTION

In this final chapter we shall concern ourselves with the slowest but most important type of transients, the electromechanical generator rotor swings following a major network disturbance. We can obtain a good feel for the general nature of the problem by considering the simple mechanical analog in Fig. 12-1.

A number of masses (representing the generators in the electric system) are suspended from a "network" consisting of elastic strings, the latter representing the electric transmission lines. The system is in a static steady state, with each string loaded below its break point (corresponding to the fact that each transmission line is operated below its static stability limit).

At this point one of the strings is suddenly cut (corresponding to a sudden loss of an electric line). As a result the masses will experience transient coupled motions, and the forces in the strings will fluctuate. The

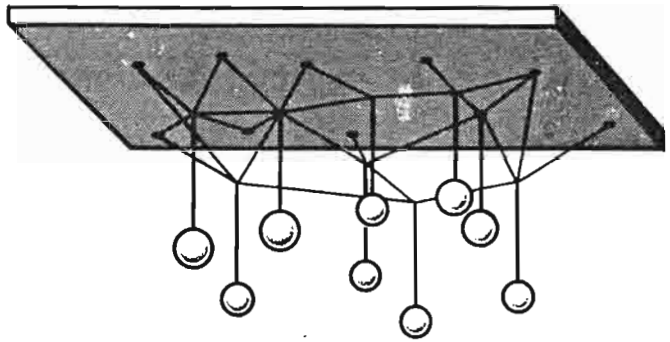

**Fig. 12-1** Mechanical analog for demonstration of transient stability.

sudden disturbance may cause one of two end effects:

1. The system will settle down to a new equilibrium state, characterized by a new set of string forces (i.e., line powers in the electric case).
2. Due to the transient forces, one additional string will break, causing a still weaker network, resulting in an ensuing chain reaction of broken strings and eventual total system collapse.

If the system has the inherent strength to survive the disturbance and settle in a new steady state, we refer to it as "transient stable for the fault in question." *It should be noted, of course, that the system may be transient stable following the loss of one particular link but unstable following another or others.*

The events that follow upon the loss of a transmission line in a power system are quite similar in nature to the transients in the above system. In detail, the analog has, of course, many discrepancies.

Depending upon the nature and *duration* of the fault, the ensuing mechanical rotor transients may be over in a second, or they may continue and grow in severity over the next seconds, or even minutes, ending, eventually, in total system collapse or recovery. For the following analysis we shall find it fruitful to divide the transient period into the following three distinct time intervals:

1. *The "initial" interval*, extending approximately throughout the first second following the fault. This interval includes the onset and possible removal of initial fault. The rotor dynamics in this interval are completely *uncontrolled* in the sense that the behavior of the generators is essentially beyond the influence of both the *Pf* and *QV* controllers. The only "control" we have in this interval is that associated with *switching operations*, including removal and reclosure of faulty line sections, insertion of supporting capacitors, disconnection of faulty generators, etc.
2. *The "intermediate" interval*, following the initial interval and lasting for approximately another 5 s. In this period the effects of the *Pf* and *QV* controllers are being felt.
3. *The "final" interval*, lasting, perhaps, several minutes after onset of fault. In this period we experience the "long-term" effects, including the thermal time constants of steam and nuclear-core systems and permanent loss of generating equipment, load shedding, etc.



The events during the first two intervals are of importance in that order as they determine whether the system will survive the initial "shock," i.e., whether the system integrity is preserved or if it is going to pieces.

If the system survives this shock, the danger is not over. Due to permanent loss of equipment, we may be "losing frequency" at a slow or fast rate, and we must now resort to "secondary control," aiming at recovery of frequency. Our "major control force" is now *load shedding*. By disconnecting low-priority load we may be able to reverse the downward frequency trend.

The following analogy may illuminate the situation.

A jet liner flying at 35,000 ft suddenly loses its two right engines. In the next few seconds the overshadowing problem is to prevent the violent motions from shaking the plane apart.

If the pilot can regain control, he finds that he loses altitude at a frightening rate, and he must now decide which passenger section to dump to save the rest.

In this chapter we shall pay particular attention to the events in intervals 1 and 2. It would go beyond the scope of our introductory text to attempt a deep discussion of all aspects of long-term effects in a system.

## 12-2 TRANSIENT SYSTEM MODELS

If we were to investigate the system in Fig. 12-1 as to its transient stability, we would proceed as follows:

1. Determine the initial prefault state.
2. Initiate the fault.
3. Compute the postfault transient motion of the masses and resulting forces in the strings.
4. If these forces do not exceed the break points of the strings, the system would be judged stable for the fault in question.

A transient stability study of an electric energy system proceeds along similar lines. Following the disturbance, the rotor angular positions will experience transient deviations. Since the fault is assumed to be of *major* proportions, these swings will be of *large-scale* magnitude, not the small-scale perturbations that we discussed in Chap. 9. If it can be ascertained by analysis that *all* the individual rotor angles will settle down to new postfault steady-state values, corresponding to a new stable synchronous equilibrium state, then we will conclude that the system is indeed transient stable.

The key issue is, obviously, the accuracy with which we can predict the postfault rotor swings. This accuracy is intimately connected with the accuracy of the dynamic models that we use. Deriving a useful mathematical model is therefore of primary importance, and shall be our immediate concern.

### 12-2.1 BASIC ASSUMPTIONS

It is important that we agree on some basic assumptions upon which our subsequent models will be built. We summarize them here:

1. In our earlier study of the load frequency dynamics, we made the assumption that all generators belonging to a specific "control area" were controlled in unison and also performed their dynamics in unison. This coherency assumption does not apply in the present case. We must now treat the generators *individually*. Only if it can be ascertained with great certainty that some groups of generators (for example, those in some relatively remote power station) are coherent, should we attempt "lumping."
2. As a consequence of this "individuality" of generator dynamics, we will expect to find certain generators which perform fast swings and others that swing slowly. When, in our earlier analysis, we found that entire control areas swung coherently and in a relatively slow mode against other areas, it proved practical to use the various area *frequency* deviations as our dependent variables. Presently we shall find it more practical to use the rotor angular *positions* $\delta_i$ which better convey the stability states of the various machines than do their respective velocities $\dot{\delta}_i$. For example, the two terminal bus voltages of a particular line may be momentarily separated by 90 electrical degrees, but be characterized by equal velocities. Based upon velocity information alone, we would therefore be ignorant of the extremely dangerous situation of this line, in reality.
3. Due to the high machine inertias, the individual rotor velocity deviations (as measured relative to a 60-Hz synchronous reference) are *very small* compared with the synchronous velocity $\omega = 377$ rad/s. For all practical purposes we can therefore consider the static portion (lines and transformers) of the electric network to be in a 60-Hz steady state.



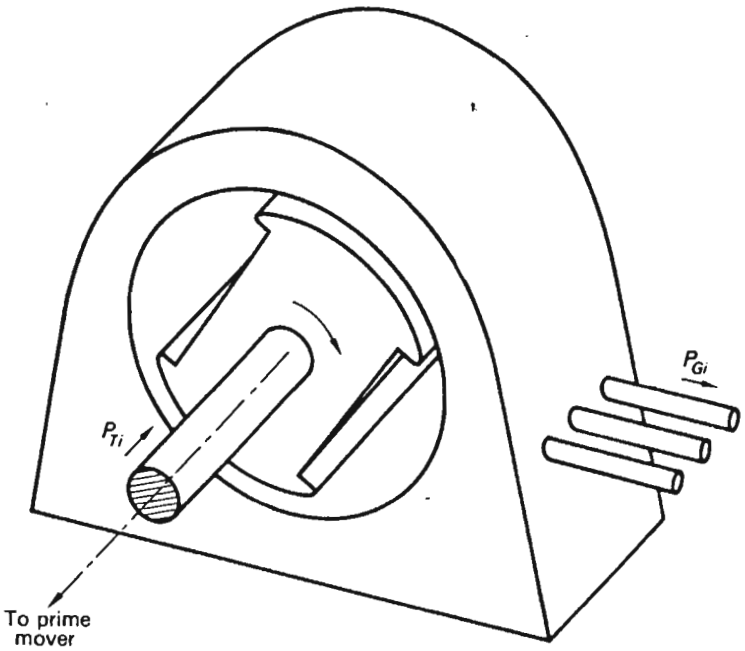


**Fig. 12-2** Definition of $P_G$ and $P_T$.

All voltages, currents, and powers will therefore be computed from the *algebraic* equations we derived in Chap. 7. This important assumption has the following consequence: The individual generators will be described by *differential* equations, the so-called "swing equations," which are mutually *coupled* via *algebraic* equations describing the lines and transformers.

4. In the case of a *balanced* disturbance, the algebraic coupling equations just referred to are the equations relating currents or voltages at the various network buses, i.e., the SLFE.
5. In the case of an *unbalanced* disturbance, we must use those equations that relate the *positive-sequence* currents or voltage at the various buses. This follows from the fact that only the positive-sequence components result in synchronizing forces within the machines.

These, then, are the major assumptions upon which our subsequent analysis will be based. There are also some minor additional assumptions to be made, but these will be pointed out as the analysis proceeds.

### 12-2.2 THE SWING EQUATION

Consider the $i$th generator unit of an $n$-unit system. The generator (Fig. 12-2) receives via the shaft from the turbine the mechanical input, or *turbine*

*power*, $P_{Ti}$. It delivers the electrical output, or *generator power*, $P_{Gi}$, via the bus bars to the network. If these two powers are equal (neglecting the relatively insignificant machine losses), the generator will run at its constant synchronous speed.

If, on the contrary, a difference exists between these two powers, this difference will be used:

1. To change the kinetic energy, or speed, of the unit
2. To overcome the damping torque that develops mainly in the damper windings

We express this mathematically thus:

$$P_{Ti} - P_{Gi} = \frac{d}{dt}(W_{kin,i}) + P_{\text{damper}} \tag{12-1}$$

**The kinetic energy term** $W_{\text{kin},i}$ represents the total kinetic energy of the generator plus turbine, expressed in megawatt·seconds or megajoules. In view of Eqs. (9-19) and (9-6), we can write the first term on the right side of Eq. (12-1) in the form

$$\frac{d}{dt} W_{\text{kin},i} = \frac{W^0_{\text{kin},i}}{\pi f^0} \frac{d^2\delta_i}{dt^2} \qquad \text{MW} \tag{12-2}$$

In this equation $W^0_{\text{kin},i}$ represents the kinetic energy of unit $i$ measured in megajoules at *rated* frequency. $\delta_i$ represents the angular rotor position, measured in *electrical radians* of the rotor relative to a synchronously rotating reference.† [Note that we have discarded the prefix $\Delta$ which appears in Eqs. (9-6) and (9-19). The reason is that the angular perturbations are not incremental, as was the case in Chap. 9.]

**The damping term** As the speed of the rotor deviates from the synchronous speed, currents will be induced in the damper windings on the rotor. It is well known that the effect of such induced currents is to cause forces (and torques) that tend to impede the motions.‡ The magnitude of the torque

† This synchronous reference will be chosen as the *prefault* bus voltage of the slack, or reference, generator. (Following the fault, the reference generator will of course also participate in the transient swings, and the angles $\delta_i$ will therefore, in the postfault state, have to be measured relative to a *hypothetical* generator running at an unperturbed constant synchronous speed and having a phase coinciding with that of the reference generator prior to the fault.)

‡ The basic job of the damper windings is to provide this extra stabilizing torque. If we disregard their presence in our analysis, we obtain results which are on the "safe side." This is often done.



increases with the relative speed $d\delta_i/dt$, and it is customary, although not quite correct, to assume proportionality between torque (or power) and velocity; i.e.,

$$P_{\text{damper}} \approx D_i \frac{d\delta_i}{dt} \qquad \text{MW} \tag{12-3}$$

where $D_i$ is a positive machine parameter measured in megawatts per electrical radians per second. [This parameter should not be confused with the "load damping" $D_i$ in Eq. (9-15).]

In view of the results, Eqs. (12-2) and (12-3), we can write Eq. (12-1) thus:

$$P_{Ti} - P_{Gi} = \frac{W^0_{\text{kin},i}}{\pi f^0} \frac{d^2\delta_i}{dt^2} + D_i \frac{d\delta_i}{dt} \qquad \text{MW} \tag{12-4}$$

**The swing equation in per-unit form** All terms in Eq. (12-4) are measured in megawatts. Dividing by the base megavolt amperes, we have each term expressed in per units:

$$P_{Ti} - P_{Gi} = \frac{H_i}{\pi f^0} \frac{d^2\delta_i}{dt^2} + D_i \frac{d\delta_i}{dt} \qquad \text{per unit MW} \tag{12-5}$$

The constant $H_i$ is our old friend the per-unit inertia constant, defined in Eq. (9-25).

*Note:* There is an important difference in meaning of $H_i$ in Eqs. (9-25) and (12-5). In Chap. 9, $H_i$ represented the kinetic inertia of the *entire* control area expressed in per unit of the rated power of that same area. Here, $H_i$ is a measure of the inertia of unit $i$ in per unit of that base power used in our analysis. (Compare also the statement in Exercise 12-1.)

### 12-2.3 THE TRANSIENT TURBINE POWER $P_T$

The rotor dynamics of the $i$th generator depends, in accordance with Eq. (12-5), entirely upon the power difference, $P_{Ti} - P_{Gi}$. When this difference power is positive, the rotor will accelerate; when negative, it will decelerate. We now investigate more closely the nature of this difference power, and do so by studying independently the individual terms $P_{Ti}$ and $P_{Gi}$. In this section we turn our attention to the first term, the turbine power $P_{Ti}$.

We make, first, the following all-important observation:

*The changes in the turbine power are entirely dependent upon the control actions initiated by the load frequency (Pf) controller discussed in Chap.* 9.

In the first second ("initial" interval) the turbine power will stay essentially constant, and for this initial transient period we therefore set the postfault power equal to the *constant* prefault value, i.e.,

$$P_T \approx P_T{}^0 = \text{const} \tag{12-6}$$

In Sec. 12-5.1 we discuss how to obtain the turbine power in the subsequent interval.

### 12-2.4 THE TRANSIENT GENERATOR POWER $P_G$

We next turn our attention to the generated electric power $P_G$. It should be noted that we *cannot* use Eqs. (4-65) and (4-66) since they were derived on the assumption of *static* operation. We must develop formulas that give us the electric generator output as a function of the angular position $\delta$ during the *transient* swings.

A typical situation is as follows: A generator is operating in nominal steady state onto a large network. A short circuit occurs somewhere out in this network, and as a result, the voltages on all its buses will experience sudden changes, as demonstrated in Chaps. 10 and 11. The bus voltage at our particular generator will change from the prefault value $V^0$ to the postfault value $V^I$, as shown in Fig. 12-3. For our subsequent discussion we shall make the following assumptions about these voltages:

1. $V^0$ and $V^I$ are both sinusoidal and possess three-phase symmetry. The postfault voltage $V^I$ may not necessarily be in phase with the prefault voltage $V^0$.
2. The change in voltage will be assumed *instantaneous*. Compared with the relatively slow mechanical rotor transients, this is a good assumption.

As a result of the sudden change in terminal voltage, there will be a corresponding change in the armature currents, and thus in the real (and reactive) generator output. Let us investigate the nature of these changes.

**The prefault current picture** In Fig. 12-3 we show in phasor diagram form the voltage and current situations before (solid lines) and immediately after the fault (dotted lines). We show the currents and voltages separately in order not to clutter up the diagram.

The prefault steady-state voltage phasor diagram is obtained directly from Fig. 4-11. The prefault voltage has the $d$-axis and $q$-axis components $V_d^0$ and $V_q^0$, respectively.

The prefault steady-state generator current $I_G^0$ has the $d$ and $q$ components $I_d^0$ and $I_q^0$, respectively. From Fig. 12-3 we obtain directly the following expressions for these steady-state current components:

$$|I_q^0| = \frac{|V_d^0|}{X_q} \tag{12-7}$$

$$|I_d^0| = \frac{|E^0| - |V_q^0|}{X_d} \tag{12-8}$$



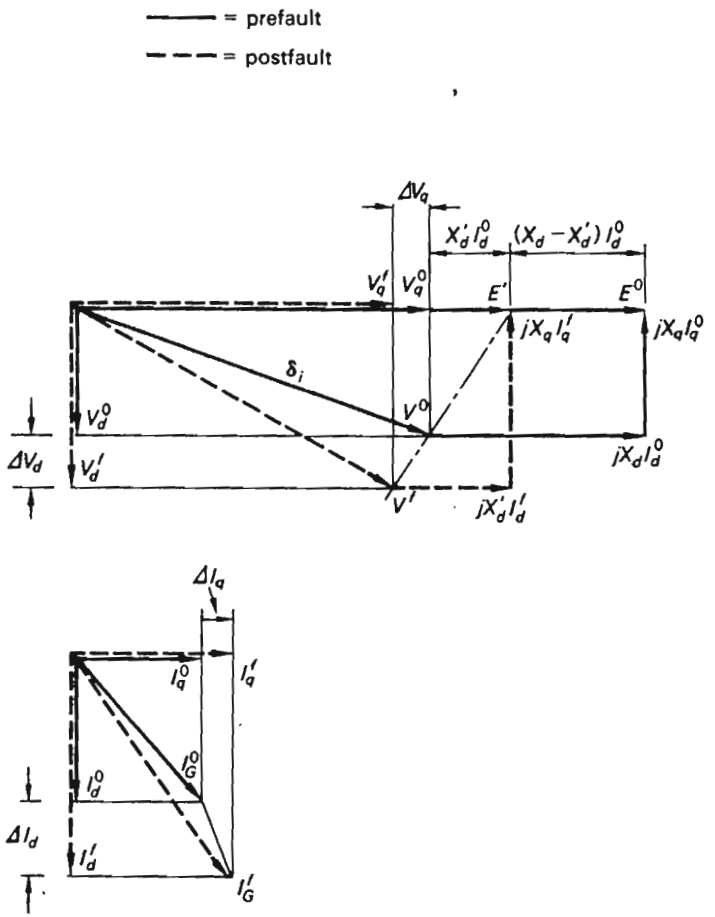


**Fig. 12-3** Phasor diagram showing the relationships between prefault and postfault voltages and currents.

The real part of the product $V^0(I_G^0)^*$ renders the prefault generator power $P_G^0$, and if we care to compute this product, we obtain the earlier Eq. (4-65).

**The postfault current picture** As a result of the fault, the $d$ and $q$ components of the bus voltage change instantaneously with the amounts $\Delta V_d$ and $\Delta V_q$, respectively. These changes tend to bring about corresponding changes in the $q$ and $d$ components of the stator current. Let us study the nature of these changes.

**Current changes in $d$ direction** In Chap. 10 we analyzed the behavior of the synchronous machine under transient conditions. We are reminded that any changes in the current component $i_d$ brings about proportional changes in the rotor current $i_r$ [compare the last of Eqs. (10-18)].

The effect of this *magnetic coupling* is a *reduction* of the *effective reactance* from the "steady-state" value $X_d$ to the "transient" value $X_d'$.

A *very gradual* change in the voltage difference $|E| - |V_q|$ would, in accord with Eq. (12-8), bring about a current change that would be determined by the reactance $X_d$. A *very sudden* change, $|\Delta V_q|$, will, on the contrary, give cause to a much larger current change, which will be computed from

$$|\Delta I_d| = \frac{|\Delta V_q|}{X_d'} \tag{12-9}$$

**Current changes in $q$ direction** Things are much simpler in $q$ direction. The armature flux associated with the $i_q$ current component is *not* linked with the rotor field winding and is thus free to change "inertialess." Almost, that is. We must remember the damper winding. But this winding is very fast and its transients are over in a couple of cycles.

If we disregard the very short "subtransient bip" due to the damper winding, we conclude that changes in $I_q$ can be computed from the static relationship (12-7), i.e.,

$$|\Delta I_q| = \frac{|\Delta V_d|}{X_q} \tag{12-10}$$

Let us return for a moment to the prefault voltage and current state. Assume that we were to change, suddenly, the armature current to zero by disconnecting the generator from the network. Since the $d$ and $q$ current components would now change suddenly with the amounts $I_d^0$ and $I_q^0$, the corresponding change in the terminal voltage components in $q$ and $d$ direction would, in accordance with Eqs. (12-9) and (12-10), be $X_d' I_d^0$ and $X_q I_q^0$. The generator terminal voltage would thus instantaneously change to the new value marked $E'$ in Fig. 12-3. (Note that the tips of the three phasors, $V^0$, $V^I$, and $E'$, must lie on a straight line. Why?)

We note from Fig. 12-3 that the voltage $E'$ has the magnitude

$$|E'| = |E^0| - (X_d - X_d')\,|I_d^0| \tag{12-11}$$

If we substitute $|I_d^0|$ from Eq. (12-8), we can express $|E'|$ in terms of the prefault voltages thus:

$$|E'| = \frac{X_d'\,|E^0| + (X_d - X_d')\,|V_q^0|}{X_d} \tag{12-12}$$



**Transient power formula** The phasor diagram in Fig. 12-3 clearly indicates that the *transient postfault* voltage phasors $V^I$, $jX_d' I_d^I$, $jX_q I_q^I$, and $E'$ are related to each other in a similar manner as are the *static prefault* voltage phasors $V^0$, $jX_d I_d^0$, $jX_q I_q^0$, and $E^0$. *In fact, the static and transient phasor diagrams become of identical form if we make the substitutions*

$$E^0 \to E'$$

$$X_d \to X_d'$$

This observation is important since it permits us to derive very simply an expression for the generator power valid under transient conditions. We remember that the *static* power equation (4-65) was derived from the phasor diagram of Fig. 4-11. Due to the above identity, the transient power must therefore be obtained from the same formula, with the above substitutions.

We therefore have for the *transient* power

$$P_G = \frac{|V^I|\,|E'|}{X_d'} \sin\delta + \frac{|V^I|^2}{2}\left(\frac{1}{X_q} - \frac{1}{X_d'}\right)\sin 2\delta \tag{12-13}$$

where $\delta \triangleq \angle E' - \angle V^I$ and must not be confused with $\delta_i$ in Eq. (12-2).

**Example 12-1** Consider a synchronous turbogenerator characterized by the following parameters:

$$X_d = X_q = 1.00 \text{ pu} \qquad X_d' = 0.20 \text{ pu}$$

Let us assume that the static dc excitation corresponds to an emf $|E^0| = 1.50$ pu. Let us also assume that the generator operates onto a strong infinite bus having $|V^0| = |V^I| = 1.0$ pu.

The *static* power output of this generator follows from Eq. (4-65):

$$P_{G,\text{stat}} = \frac{1.5 \times 1.0}{1.00} \sin\delta = 1.50 \sin\delta \qquad \text{pu MW}$$

The static power is plotted versus $\delta$ in Fig. 12-4 (curve A).

For the transient power we must know the emf $E'$, which can be determined only from a knowledge of the static prefault operating point. We shall assume that the generator delivers statically 0.75 pu MW to the network. This corresponds

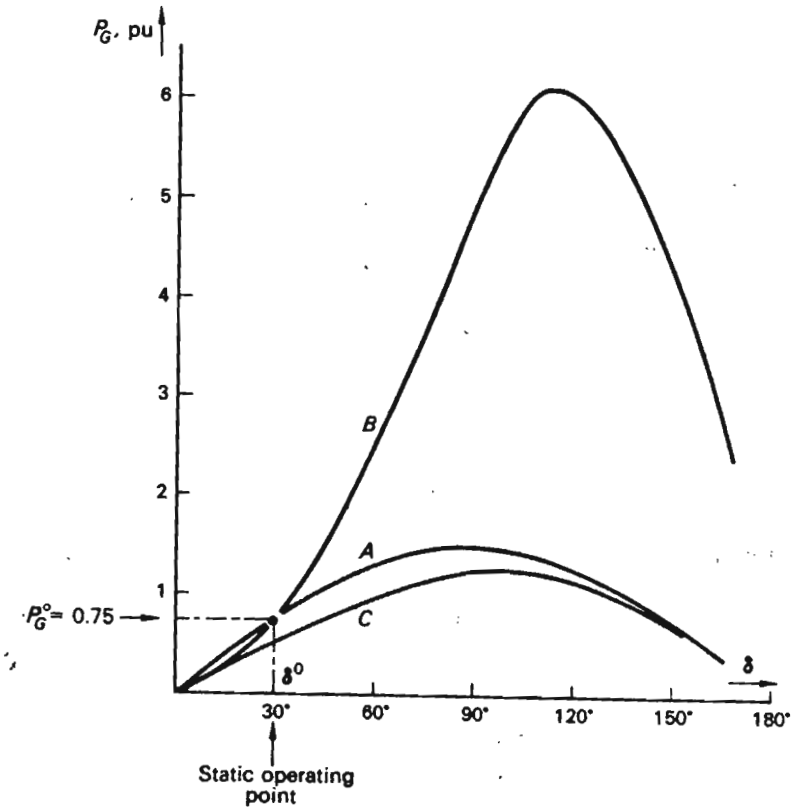


**Fig. 12-4** Static and transient generator powers for turbogenerator in text. (*A*) Static power; (*B*) transient power if terminal voltage remains fixed at 1.00 pu; (*C*) Transient power if terminal voltage drops to 0.25 pu.

to an initial power angle $\delta^0$ of 30°. The static operating point is identified in Fig. 12-4. From a knowledge of $\delta^0$, we now get

$$|V_q^0| = |V^0| \cos \delta^0 = 1.00 \cos 30° = 0.866 \text{ pu}$$

Equation (12-12) then renders

$$|E'| = \frac{0.20 \times 1.50 + (1.00 - 0.20)0.866}{1.00} = 0.993 \text{ pu}$$

From Eq. (12-13) we get directly the transient generator power

$$P_{G,\text{transient}} = 4.96 \sin \delta - 2.00 \sin 2\delta \quad \text{pu MW} \tag{12-14}$$

This power is plotted versus $\delta$ (curve *B*) in Fig. 12-4.



**Example 12-2** The transient power equation (12-14) was derived on the assumption that $|V'| = 1$, i.e., the terminal voltage is fixed. Let us now obtain a formula based upon the assumption that the terminal voltage drops instantaneously to $|V'| = 0.25$.

By using Eq. (12-13), we get for $|V'| = 0.25$ and $|E'| = 0.993$

$$P_{G,\text{transient}} = 1.24 \sin \delta - 0.13 \sin 2\delta \quad \text{pu MW} \tag{12-15}$$

This is curve *C* in Fig. 12-4.

We make the following observations in regard to the above results:

1. For very slow (quasi-static) changes, curve *A* tells us the relationship between power output and rotor position.
2. For sudden changes (for example, loss of turbine torque) *but constant terminal voltage*, curve *B* applies.
3. For a sudden 75 percent drop in terminal voltage, curve *C* applies.
4. The static-torque curve does not have a "saliency" term because we assumed $X_d = X_q$.
5. The transient torque contains a saliency term (i.e., the one proportional to sin $2\delta$), the magnitude of which is of second order.
6. The transient power may attain very large peaks compared with the static power.

**Transient power formula, neglecting saliency** The preceding examples [compare Eq. (12-15)] indicate that the sin $2\delta$ term is of comparably insignificant magnitude in many cases.† We find it convenient on occasion to neglect it altogether. This means, in effect in Eq. (12-13) that we set

$$X_q = X_d' \tag{12-16}$$

The transient power equation (12-13) simplifies now to

$$P_G \approx \frac{|V'|\,|E'|}{X_d'} \sin \delta \tag{12-17}$$

† The sin $2\delta$ term, in addition to being relatively small, also has the property of subtracting from the total power in the region

$$0° < \delta < 90°$$

but adding to it in the region

$$90° < \delta < 180°$$

When our angular swings range throughout these regions, the overall effect of this term therefore has a tendency to average out to zero.

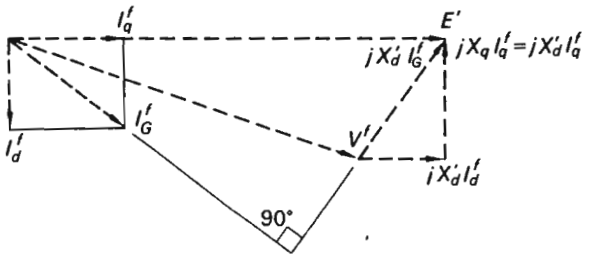


**Fig. 12-5** If saliency is neglected, i.e., if $X_q = X_d'$, the postfault portion of Fig. 12-3 looks like this.

If Eq. (12-16) applies, the postfault portion of the phasor diagram of Fig. 12-3 will look as depicted in Fig. 12-5. The important feature is that the difference voltage $E' - V'$ is 90° ahead of the generator current $I_G'$. This is tantamount to saying that, from a postfault transient point of view, the following relation applies:

$$V' = E' - jI_G' X_d' \tag{12-18}$$

[Compare also Eq. (4-76) and Fig. 4-14.]

In this case the generator can be represented by an emf $E'$ in series with the transient reactance $X_d'$, as shown in Fig. 12-6. For this reason the voltage, or emf $E'$, is often referred to as the "voltage behind the transient reactance."

Concluding our present discussion of transient modeling of the generator, we wish to stress that the emf $E'$ in our preceding equations can be treated as a constant only if the field winding time constant is infinite. As the rotor transient dies out, Eq. (12-18) gradually, over a period of several seconds, changes to Eq. (4-76). Also, we must remember that, superimposed upon this change, we have the effect caused by the voltage regulator. In Sec. 12-5 we discuss the latter. In most instances we will not introduce too much error in assuming that $|E'|$ is a constant during the "initial" portion of our transient period [compare Eq. (12-77)].

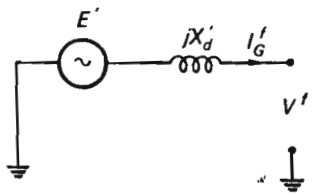


**Fig. 12-6** Equivalent network representation of synchronous generator for the nonsalient case.



## 12-3 SOLUTION OF SWING EQUATION—THE SINGLE-GENERATOR CASE

Having thus established the mathematical models for the individual generators, we are now faced with the next problem, the solution of the swing equations. Having concluded that the transient generator power $P_{Gi}$ is a *nonlinear* function of the dependent variable $\delta_i$, we are faced with the prospect of solving a system of coupled *nonlinear* differential equations. In general, no analytical solutions exist, and we must therefore resort to numerical computational techniques.

As a matter of fact, even the simplest conceivable case of a single generator operating onto an infinite network does not, in general, possess an elementary solution. Nevertheless, this simple case will afford us an opportunity to expose some important features of large-scale system dynamics. The system is depicted in Fig. 12-7. The generator is connected to the infinite bus via a line (or lines) and transformer. We shall study the dynamics of the generator rotor following certain disturbances. Throughout

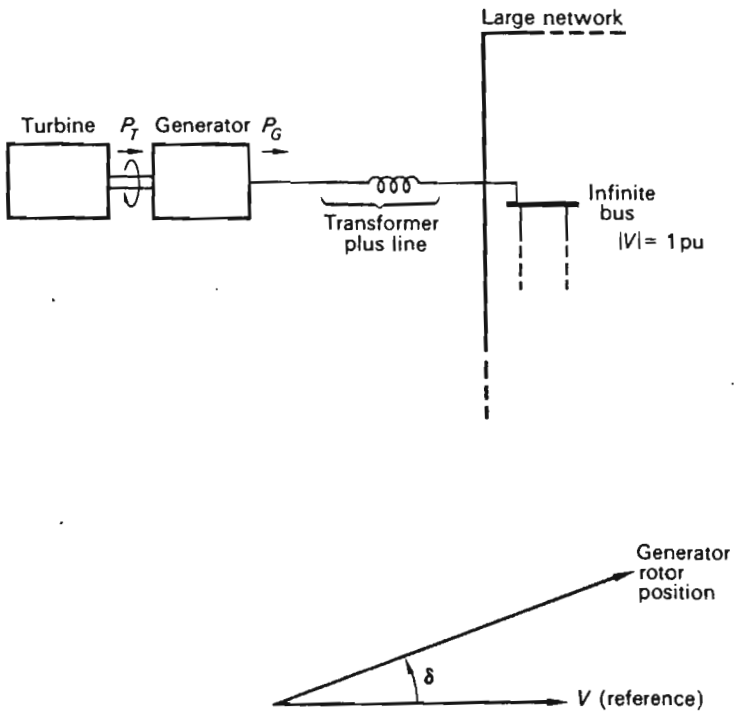


**Fig. 12-7** Single generator operating onto an infinite bus.

this section we shall base our analysis on the following assumptions:

1. The bus voltage $V$ has a magnitude of 1.00 pu, which will remain constant during the transients.
2. The network frequency is assumed constant under all conditions. We will actually use $V$ as our reference voltage.
3. The turbine power is constant $= P_T^0$.
4. The emf $E'$ behind the transient reactance retains constant magnitude.
5. We neglect damping torque.

In view of assumptions 3 and 5, the swing equation (12-5) will be of the form

$$P_T^0 - P_G = \frac{H}{\pi f^0}\frac{d^2\delta}{dt^2} \tag{12-19}$$

### 12-3.1 SMALL-SCALE OSCILLATIONS

Let us first consider the case when the generator, running initially in a nominal steady state, is subject to *relatively small* disturbances. For example, a local load of 5 percent may suddenly be dropped from the generator bus (this bus is not shown in the figure). This permits us to *linearize* the nonlinear equation (12-19), and thus make it solvable.

**Example 12-3** Let us assume the following generator and network data:

$H = 2.00$ s

$X_d = X_q = 0.90$ pu

$X_d' = 0.30$ pu

$X_{\text{transformer+line}} = 0.10$ pu

The initial nominal operating state is characterized by

$|E^0| = 1.50$ pu

$P_G^0 = P_T^0 = 0.75$ pu

The static power formula is thus†

$$P_{G,\text{stat}} = \frac{1.50 \times 1.00}{0.90 + 0.10}\sin\delta = 1.50\sin\delta \tag{12-20}$$

We then compute the following initial variable values:

$$\delta^0 = \sin^{-1}\frac{0.75}{1.50} = 30°$$

$$V_q^0 = 1.00\cos 30° = 0.866 \text{ pu}$$

$$|E'| = \frac{0.40 \times 1.50 + 0.60 \times 0.866}{1.00} = 1.12 \text{ pu}$$

† Note that when an *external* reactance (0.10 pu, in our case) is added between the generator bus and the network bus $V$, then this reactance must be added to *all* reactances in our preceding formulas.



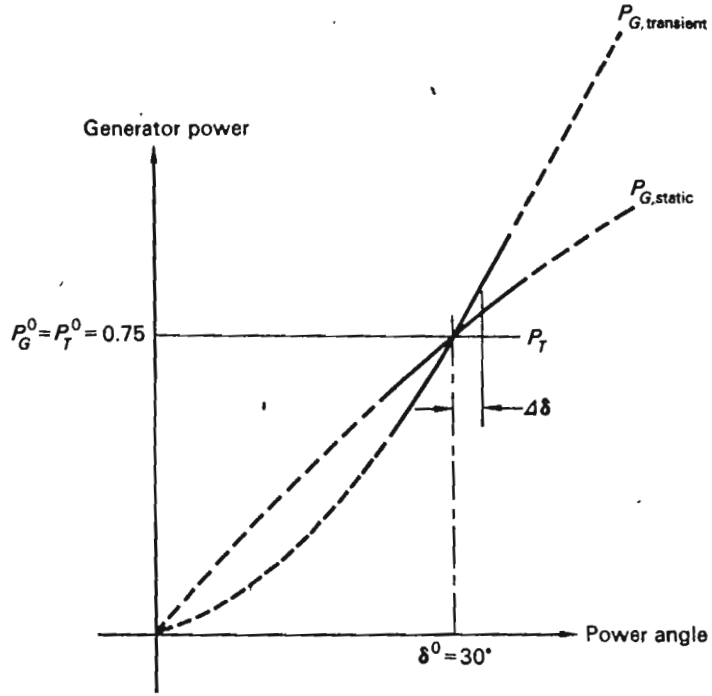


**Fig. 12-8** Static and transient generator powers for generator in Example 12-3.

From Eq. (12-13) we get

$$P_{G,\text{transient}} = \frac{1.00 \times 1.12}{0.40}\sin\delta + \frac{(1.00)^2}{2}\left(\frac{1}{1.00} - \frac{1}{0.40}\right)\sin 2\delta$$

$$= 2.80\sin\delta - 0.75\sin 2\delta \tag{12-21}$$

In Fig. 12-8 we have plotted the static and transient generator powers versus $\delta$. We show only a small region around the nominal operating point to stress the *linear* features in the neighborhood of this point. For a small angular deviation $\Delta\delta$, we have

$$P_{G,\text{transient}} \approx P_G^0 + \left(\frac{\partial P_G}{\partial\delta}\right)^0\Delta\delta \tag{12-22}$$

We compute from Eq. (12-21)

$$\left(\frac{\partial P_G}{\partial\delta}\right)^0 = 2.80\cos 30° - 1.50\cos 60° = 1.67 \text{ pu MW/rad}$$

For the transient generator power we thus have

$$P_{G,\text{transient}} \approx 0.75 + 1.67\,\Delta\delta$$

Upon substitution into Eq. (12-19), the swing equation therefore attains the following *linear* form:

$$\frac{d^2}{dt^2}\Delta\delta + 157\Delta\delta \approx 0 \tag{12-23}$$

We recognize this as the differential equation for an undamped harmonic oscillator swinging at the frequency

$$f = \frac{1}{2\pi}\sqrt{157} = 2.1 \text{ Hz}$$

The amplitude depends, of course, upon the type and magnitude of disturbance. Assume, for example, that we drop a local load corresponding to 1° in the static power angle $\delta$. The rotor will now assume the new static angle, 29°, in the transient fashion indicated in Fig. 12-9.

### 12-3.2 LARGE-SCALE OSCILLATIONS

Let us clarify by a typical example the kind of situation that will lead to *large-scale* dynamics.

**Example 12-4** The line between the generator and network in Fig. 12-7 is suddenly subject to a solid three-phase short circuit. The protective relaying will command the line to be disconnected. A fraction of a second later the line will be "reclosed," and assuming that the fault is now removed, we will back to "normal" operation.

However, for the period of the fault, the generator output $P_G$ will be zero, and the turbine power, which is unchanged, will accelerate the rotor.

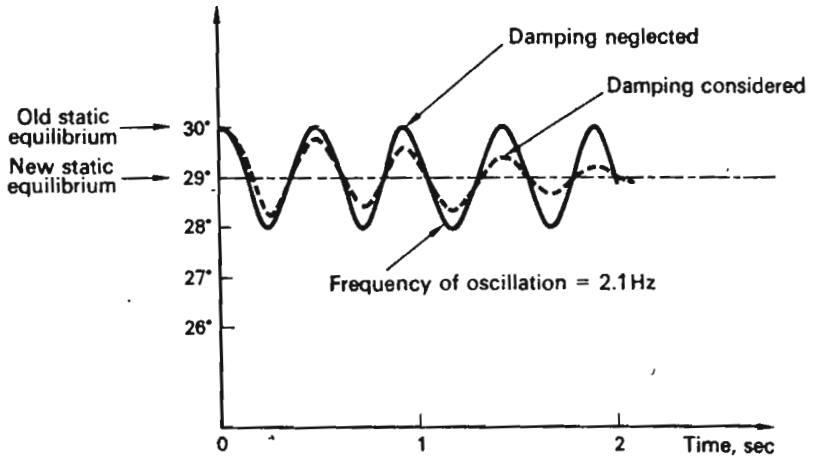


**Fig. 12-9** Small-scale generator oscillations caused by sudden small load drop.



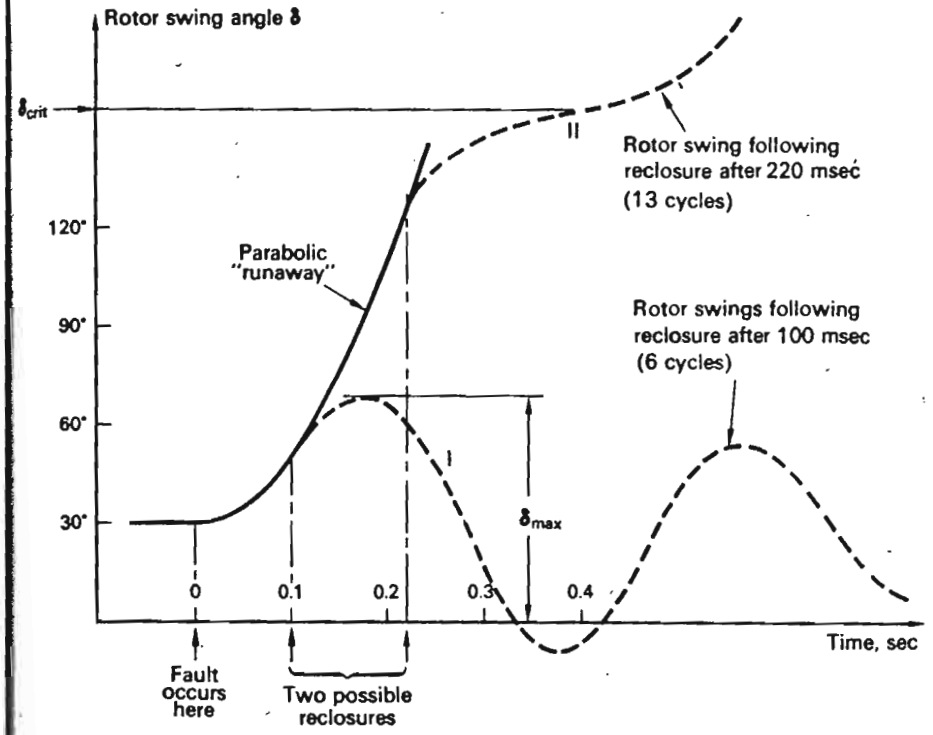


**Fig. 12-10** Rotor angular swings following the fault discussed in Example 12-4.

During this "acceleration" period the swing equation (12-19) will be of the form

$$P_{acc} = P_T{}^0 = \frac{H}{\pi f^0}\frac{d^2\delta}{dt^2} \tag{12-24}$$

or with our specific numerical values,

$$\frac{d^2\delta}{dt^2} = 70.6 \text{ rad/s}^2$$

We easily integrate this *linear* equation and obtain

$$\delta(t) = 30 + 2020t^2 \quad \text{electrical degrees} \tag{12-25}$$

The rotor position increases as the square of $t$; that is, we experience a "runaway" situation, as depicted in Fig. 12-10.

In Fig. 12-11 the situation is further clarified by means of a $P\delta$ graph. Note that during the acceleration period the accelerating power $P_{acc}$ is independent of $\delta$. [This explains why we could integrate Eq. (12-24) so simply.]

At the moment of reclosure, the generator power instantaneously jumps to the value given by Eq. (12-21). For the subsequent "deceleration" period the swing equation takes on the form

$$P_{dec} = 0.75 - (2.80 \sin\delta - 0.75 \sin 2\delta) = \frac{H}{\pi f^0}\frac{d^2\delta}{dt^2} = 0.0106\frac{d^2\delta}{dt^2} \tag{12-26}$$

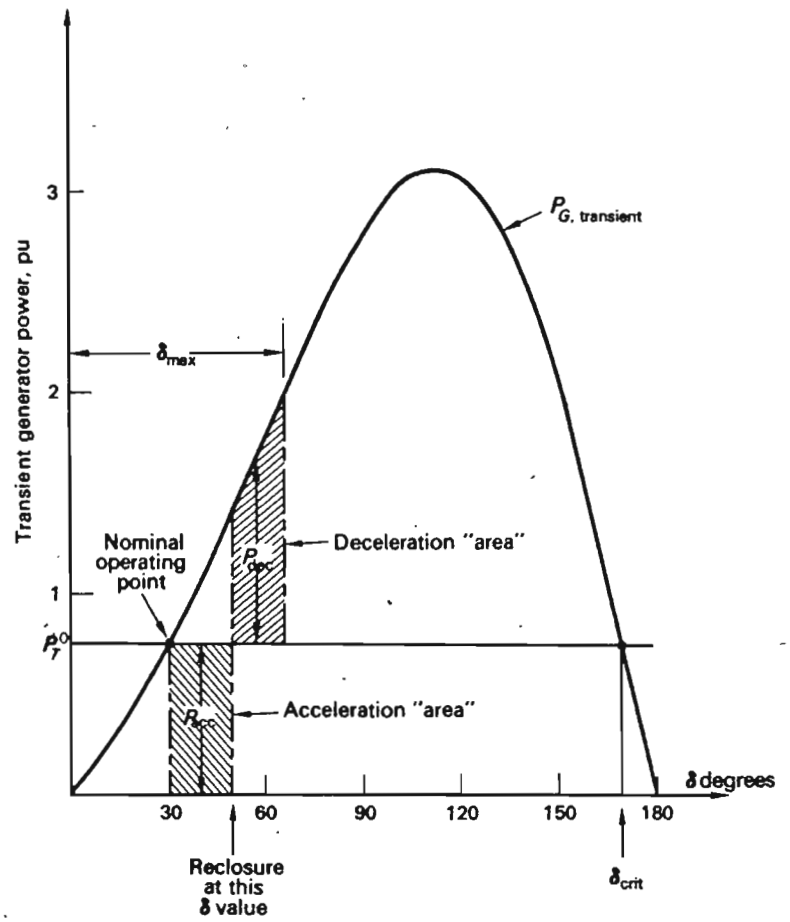


**Fig. 12-11** A $P\delta$ graph of the transients in Fig. 12-10.

As shown in Fig. 12-11, the positive accelerating power changes instantaneously to a negative decelerating power, *which is dependent on* $\delta$.

This $\delta$ dependency has one immediate result: Eq. (12-26) does not, like Eq. (12-24), integrate into any simple elementary function.† We shall discuss numerical integration methods in the next section: at present we describe a qualitative picture of the rotor dynamics following the reclosing of the line.

The immediate effect of the torque reversal is a speed reduction. The dotted portions of the swing curves in Fig. 12-10 indicate how the velocity $\dot{\delta}$ begins to decrease at the moment of reclosure. If the reclosure does not occur too late, the speed of the "runaway" rotor is halted, and then reversed. This case is shown by the curve marked *1*. The rotor will settle down to the old steady state following a series of swings; i.e., the system is transient stable.

† We can actually obtain a solution in terms of so-called *elliptic integrals*.



If the reclosure takes place too late, the rotor will have attained too high a speed, and the torque reversal will only slow down the rotor, altough not enough to stop it before it reaches the critical angle $\delta_{crit}$ identified in Fig. 12-11. If the rotor is permitted to swing beyond this angle, the power difference, $P_T - P_G$, will again turn positive, the deceleration will change to acceleration, and now we lose the rotor for good. This case is exemplified by graph II in Fig. 12-10.

### 12-3.3 DIRECT STABILITY ANALYSIS METHODS

In the preceding example there is, obviously, a critical time limit beyond which the line must not remain open if stability is to be preserved. How do we find this limit?

In practice, two methods are used:

1. The *indirect solution* method is presently by far the most useful approach, indeed the *only* practical one in the case of realistic-size systems. The swing equations are solved during and after the fault either by analog simulation or by some numerical, digital, computer-oriented, step-by-step integration method. Stability or the lack of it is determined from the looks of the resulting swing curves.
2. By *direct analysis* methods the question of stability can be settled *without actually solving* the differential equations.

   Direct analysis methods, as of this writing, have found little use beyond the single-generator case. The author believes strongly that in view of the universal availability of digital computers, the indirect solution methods will dominate over the direct for some time to come. Direct methods, particularly the popular (in other fields) *Liapunov method*, presently are of only academic interest in power system analysis. There is no reason why this situation could not rapidly change, however. Judged from the very few published reports, only scant interest has been shown in the application of the Liapunov method to power system stability. This area should prove very promising for research.

   Of great historical interest is the fact that a direct stability analysis method, the so-called *equal-area method*, proved to be very useful in the first attempts that were made to explain transient stability phenomena in power systems. It is true that it can be applied with real success only to a single machine system. Since the method has great tutorial value, the author feels that it nevertheless has a place in a 1970 text, and consequently it will serve as our point of departure.

**The equal-area method** Consider the swing equation (12-24) written in the following form:

$$P_{acc} = \frac{H}{\pi f^0}\frac{d^2\delta}{dt^2} = \frac{H}{\pi f^0}\dot{\delta}\frac{d\dot{\delta}}{d\delta} \tag{12-27}$$

By separation of variables and integrating once, we get

$$\tfrac{1}{2}[\dot{\delta}^2(t) - \dot{\delta}^2(0)] = \frac{\pi f^0}{H} \int_{\delta(0)}^{\delta(t)} P_{acc}\, d\delta \tag{12-28}$$

The right-side integral obviously equals in magnitude the shaded "acceleration area" depicted in Fig. 12-11. *Equation (12-28) therefore tells us that the velocity increase attained during the acceleration interval is measured by this area.*

We can similarly conclude that the velocity decrease attained during the deceleration period is measured by the "deceleration area." Since the rotor swing will attain an amplitude ($\delta_{max}$) characterized by zero total velocity change, we conclude, therefore, immediately that *the two areas must be equal.*

This *equal-area criterion* can be conveniently used to determine the critical reclosure time that we earlier spoke of. Figure 12-12 shows the

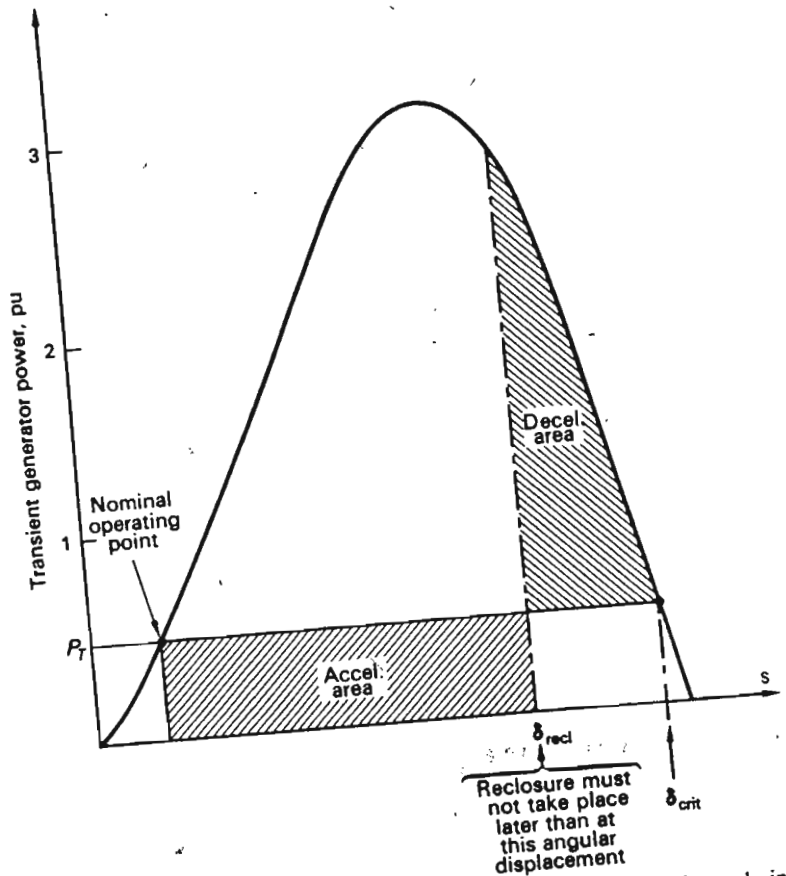


**Fig. 12-12** Application of the equal-area criterion to the $P\delta$ graph in Fig. 12-11. The two shaded areas are of equal size.



procedure. We concluded that the angular swing must not be permitted to go beyond the value $\delta_{crit}$. By trial and error we thus find the reclosure angle $\delta_{recl}$ that corresponds to equal areas. Reclosure must take place before the rotor reaches this position, and Eq. (12-25) gives us, then, directly the maximum permissible reclosure time,

$$t_{max} = \sqrt{\frac{\delta_{recl} - 30^\circ}{2020}}$$

The reader should note that we thus have been able to find $t_{max}$ without having obtained an *explicit* solution of the swing equations.

### 12-3.4 COMPUTER SOLUTION OF SWING EQUATION ("INDIRECT" STABILITY ANALYSIS)

The most practical method for solution of the swing equation is integration by means of either analog or digital computer. We discuss both briefly.

**Analog simulation** In using the analog or digital computer it is convenient to write, first, the second-order swing equation (12-5) in a different form. For that purpose we introduce the two dynamic *state variables* $x_1$ and $x_2$, defined as follows:

$x_1 \triangleq \delta$ rotor angular position in electrical radians

$x_2 \triangleq \dot{\delta}$ rotor angular velocity in electrical radians per second

These state variables constitute the components of the state vector

$$\mathbf{x} = \begin{bmatrix} x_1 \\ x_2 \end{bmatrix} \triangleq \begin{bmatrix} \delta \\ \dot{\delta} \end{bmatrix} \tag{12-29}$$

In terms of these state variables the second-order swing equation can be written as two coupled first-order *state differential equations:*

$$\begin{aligned} \dot{x}_1 &= x_2 \\ \dot{x}_2 &= \frac{\pi f^0}{H}(P_T - P_G - Dx_2) \end{aligned} \tag{12-30}$$

The generator power $P_G$ is a function of $\delta(= x_1)$, and we can therefore write these equations in the following more general† form:

$$\begin{aligned} \dot{x}_1 &= f_1(x_1, x_2) \\ \dot{x}_2 &= f_2(x_1, x_2) \end{aligned} \tag{12-31}$$

† In our specific case, the function $f_1(\cdot\,\cdot)$ is linear in $x_2$ and independent of $x_1$, whereas $f_2(\cdot\,\cdot)$ is linear in $x_2$ and nonlinear in $x_1$. Compare, also, the nonlinear equations (12-31) with the linear equations (9-88). The latter contain control forces $u$, missing in Eqs. (12-31). The presence of control forces implies that the state can be controlled; the absence, that the state is uncontrolled. See also comments on page 478.

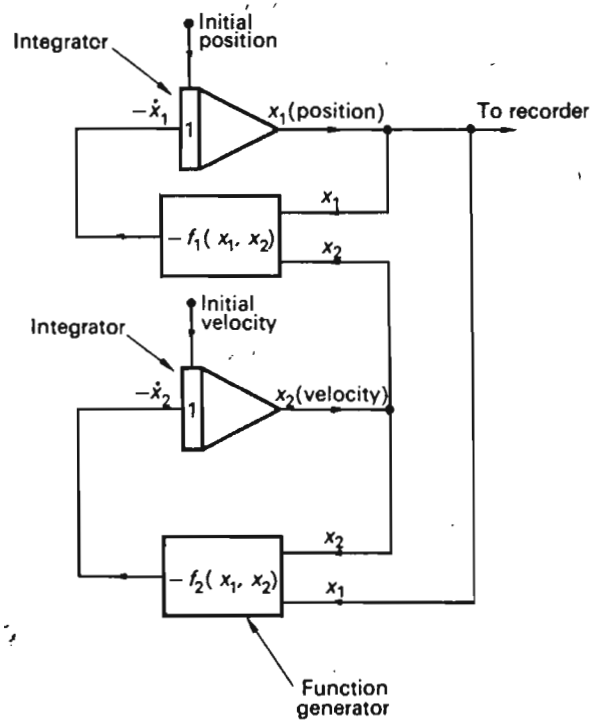


**Fig. 12-13** Analog setup for study of rotor transients.

or in vector form,

$$\dot{\mathbf{x}} = \mathbf{f}(\mathbf{x}) \tag{12-32}$$

In terms of accepted analog computer symbolism these differential equations would be simulated by the programming setup depicted in Fig. 12-13. Note that we need two integrators per generator. The nonlinear "function generator" must generate with sufficient accuracy nonlinear functions of the type of Eq. (12-21). Figure 12-14 shows the recordings of the swing curves in Example 12-4. The various curves correspond to different line reclosing times.

The beauty of analog simulation lies in the fact that once the programming is done and "debugged," the solution of the swing equation is obtained by all integrators and function generators working simultaneously in "parallel." As a result, the solution time is the same for a single-generator as for a multigenerator system.

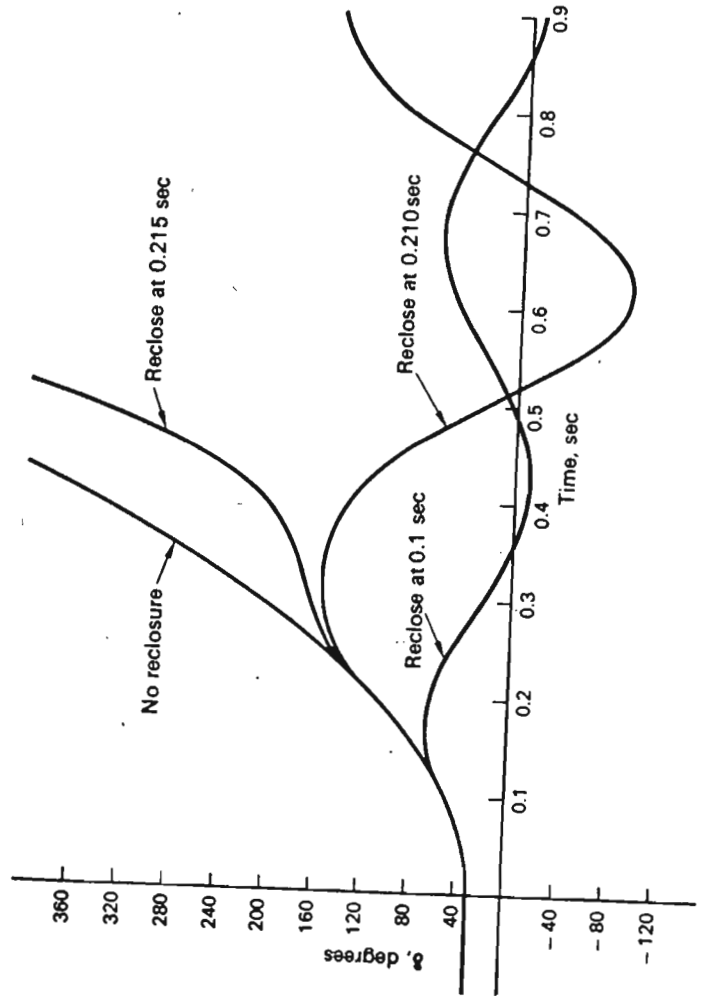


**Fig. 12-14** Swing curves of Example 12-4 obtained by analog computer. (Compare Fig. 12-10.)

**Digital simulation** The parallel-operation feature of the analog computer stands in sharp contrast with integration by means of the digital computer (*digital simulation*).

The general procedure of digital simulation is as follows: The independent variable $t$ is discretized into time elements $t^{(0)}, t^{(1)}, \ldots, t^{(\nu)}, \ldots$, not necessarily equidistant. Starting with the known initial state $\mathbf{x}^{(0)}$, we compute by means of some appropriate algorithm the new states $\mathbf{x}^{(1)}, \mathbf{x}^{(2)}, \ldots, \mathbf{x}^{(\nu)}, \ldots$.

As always in numerical analysis, the accuracy of the method depends upon the quality of the algorithm used. We shall discuss a couple of algorithms, and start, appropriately, with the simplest of them all.

*The Euler numerical integration method* Preparatory to discussing the digital solution of the vector equations (12-32), let us consider the scalar case

$$\dot{x} = f(x) \tag{12-33}$$

For $t = t^{(\nu)}$, we can set with some accuracy

$$\dot{x}^{(\nu)} \approx \frac{\Delta x^{(\nu)}}{\Delta t} = f(x^{(\nu)}) \tag{12-34}$$

Using this formula, we would perform the integration of Eq. (12-33) in the following steps (Fig. 12-15):

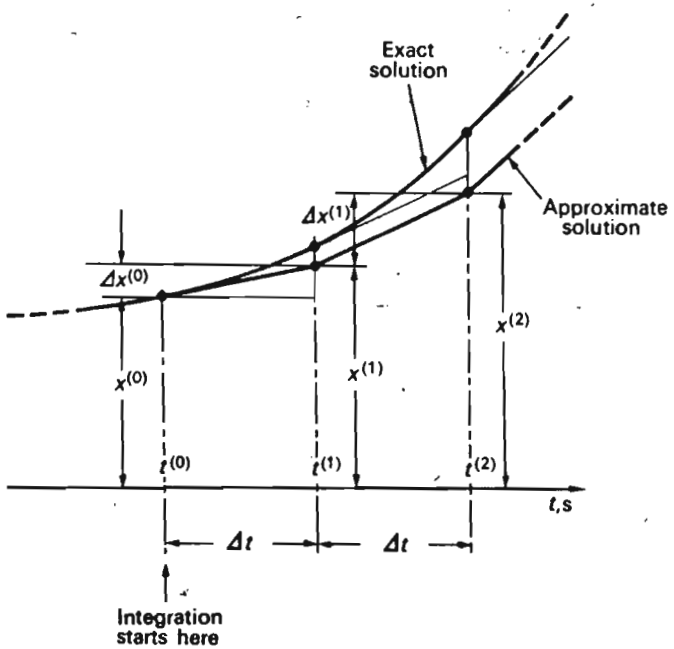


**Fig. 12-15** Graphical display of Euler's integration method.



*Step* 0 For $t = t^{(0)}$ and $x = x^{(0)}$, compute the state increment $\Delta x^{(0)}$:

$$\Delta x^{(0)} = f(x^{(0)})\,\Delta t$$

*Step* 1 For $t^{(1)} = t^{(0)} + \Delta t$, we therefore have the new state

$$x^{(1)} = x^{(0)} + f(x^{(0)})\,\Delta t$$

*Step* 2 For $t^{(2)} = t^{(1)} + \Delta t$ we similarly obtain

$$x^{(2)} = x^{(1)} + f(x^{(1)})\,\Delta t$$

etc.

Clearly, the computational algorithm is

$$x^{(\nu+1)} = x^{(\nu)} + f(x^{(\nu)})\,\Delta t \qquad \text{for } \nu = 0, 1, \ldots \tag{12-35}$$

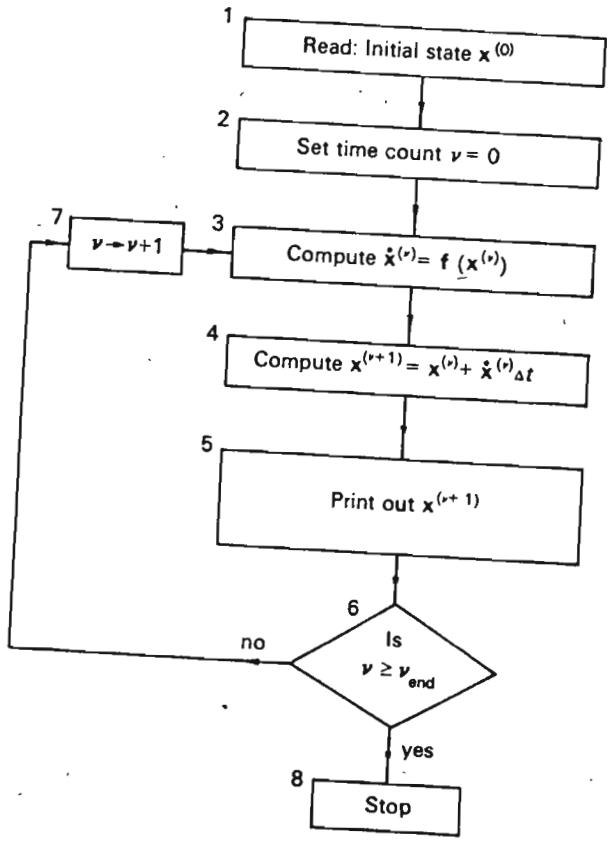


**Fig. 12-16** Computational flow graph for Euler's integration method.

We may readily extend this algorithm to the vector case. For the $i$th component of the $\mathbf{x}$ vector we have

$$x_i^{(\nu+1)} = x_i^{(\nu)} + f_i(x_1^{(\nu)}, x_2^{(\nu)}, \ldots, x_n^{(\nu)})\,\Delta t \qquad \text{for } i = 1, 2, \ldots, n \tag{12-36}$$

or in vector form,

$$\mathbf{x}^{(\nu+1)} = \mathbf{x}^{(\nu)} + \mathbf{f}(\mathbf{x}^{(\nu)})\,\Delta t \tag{12-37}$$

Figure 12-16 depicts a flow diagram for the computations involved in Euler's method. The diagram should be self-explanatory.

Euler's method is simple, but not particularly accurate. Figure 12-15 shows why. Since the state variables at the end of an interval are computed

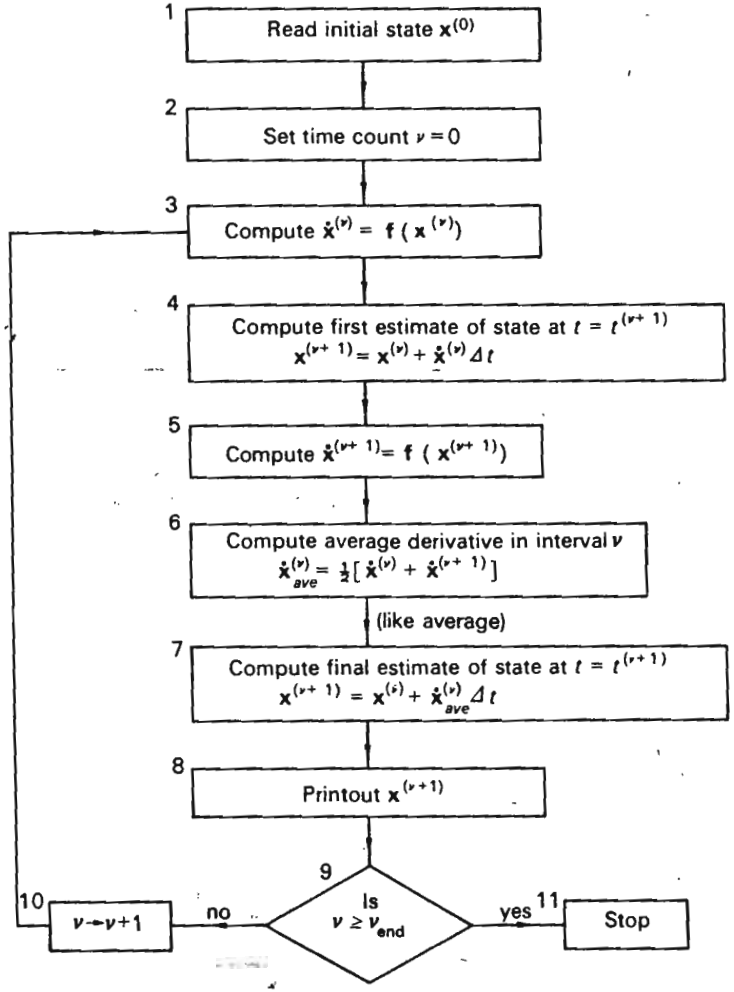


**Fig. 12-17** Computational flow graph for Euler's modified method.



on the basis of the derivative in the beginning of the interval, an error will be introduced which is the more pronounced the faster the derivative is changing within the interval $\Delta t$.

*The modified Euler method* The accuracy of the Euler method can be improved remarkably by the obvious modification of using an *average* value for the derivative throughout each time interval. The computational algorithm given in the preceding flow graph will now be modified in accordance with Fig. 12-17. Let us discuss the changes introduced.

The computations proceed as before up to and including block 4. Based upon the *tentative* value of $\mathbf{x}^{(\nu+1)}$ obtained in block 4, we compute in block 5 the derivative at the *end* of interval $\nu$.

In the next block 6, we then compute an *average value* for the derivative in interval $\nu$, and based upon this average derivative, we then proceed to recompute an *upgraded* value for $\mathbf{x}^{(\nu+1)}$ in block 7. This new value is better than the one previously computed in block 4. We may decide now that the improvement obtained in $\mathbf{x}^{(\nu+1)}$ is sufficient and proceed to the next time interval. This is often done in stability analyses. We may, alternatively, decide to repeat the upgrading sequence of $\mathbf{x}^{(\nu+1)}$ $N$ times, or until no further

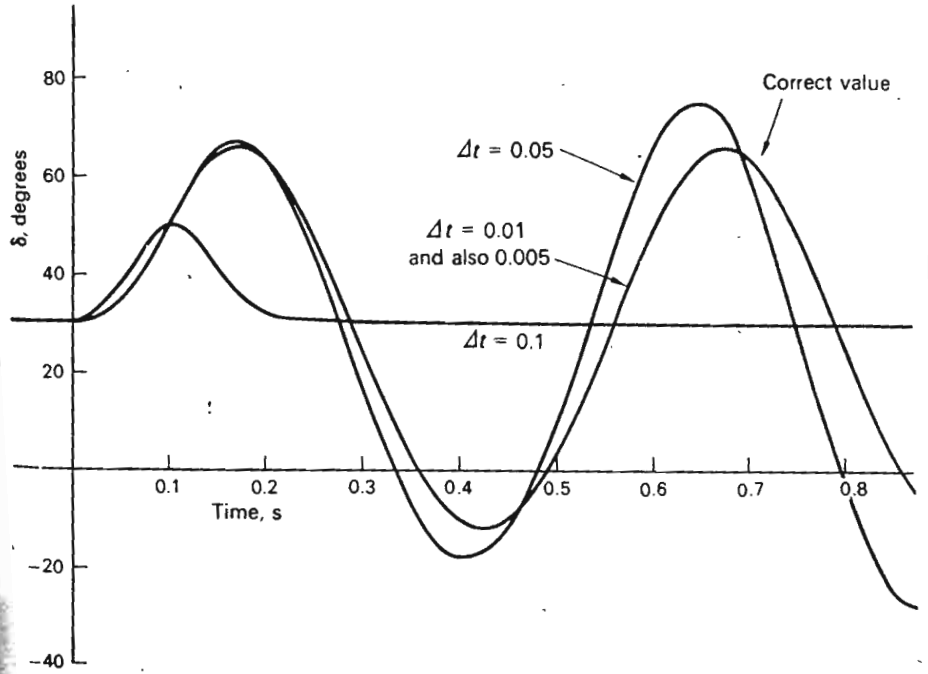


**Fig. 12-18** Euler modified approach used to find one swing curve in Example 12-4. Note that if $\Delta t < 0.01$ s, no discernible improvement can be detected. For $\Delta t > 0.05$, we obtain totally unacceptable accuracy.

improvement in $\mathbf{x}^{(\nu+1)}$ can be detected. For this purpose we must introduce an iterative loop (not shown in Fig. 12-17) around blocks 4 to 7.

Figure 12-18 shows a digitally computed swing curve for our Example 12-4, using the modified Euler method. (The same curve, corresponding to a reclosure after 0.1 s, was earlier obtained by analog computer in Fig. 12-14.) We used four widely different $\Delta t$ values. Note that no discernible difference is obtained if $\Delta t$ is chosen below the value 0.01.

*Other algorithms* There is a large variety of integration algorithms in addition to those detailed above. None of them possess the inherent simplicity of the Euler methods, and most of them require a vast amount of computation per time interval. (The reader may consult Ref. 4)

## 12-4 SOLUTION OF SWING EQUATIONS—THE MULTIGENERATOR CASE

We now turn our attention to the practically important multigenerator case. Rather than try to develop computational procedures for an entirely general case, we choose to study a specific fault condition occurring in our old sample three-bus system. However, the procedure presented has applicability to a general $n$-generator system.

### 12-4.1 SYSTEM DESCRIPTION

The system we consider is depicted in Fig. 7-2*a*. We assume that it is being operated in a prefault steady-state condition, as defined in Fig. 12-19. The

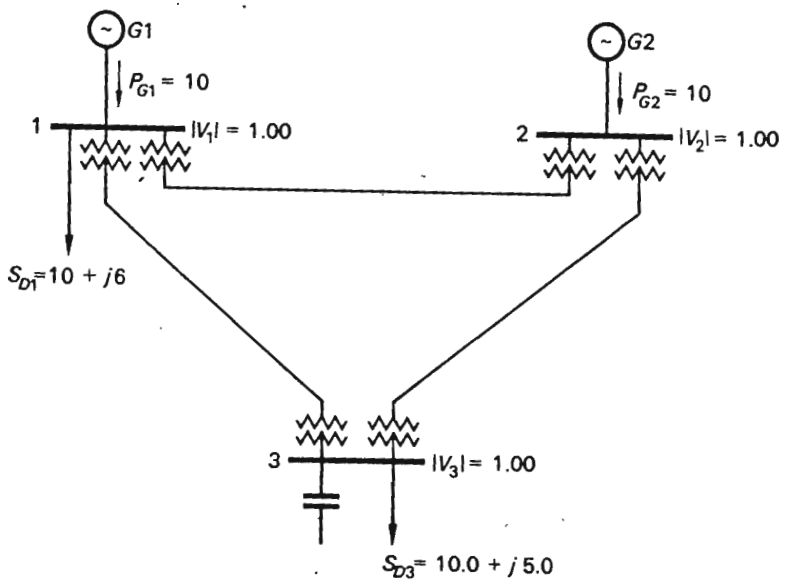


**Fig. 12-19** Prefault bus power and voltage specifications in example system.



prefault voltage profile is flat. The two bus loads are specified, and the generators carry half the real load each.

Here follow the pertinent component data. (All impedances and inertias are given in per units of 50-MVA base.)

**Lines and transformers** The impedance of each line, *including* the transformers, equals $j0.050$ pu. (We will neglect the resistive parts of all impedances. Their inclusion would not mean any added complexity, but we wish to consider all reasonable simplifications.)

**Generators** The transient reactance of each generator equals $X_d' = j0.054$ pu. The inertia constants of the generators are

$H_1 = 30$ s on 50-MVA base
$H_2 = 300$ s on 50-MVA base

The generators have a rating of 600 MVA each. (We have chosen the inertia of generator 2 ten times larger than in generator 1 so as to obtain fairly small angular swings in the former machine. The low-inertia machine will therefore, in effect, swing around the high-inertia machine, and we shall find it fairly easy to distinguish between stable and unstable cases.)

### 12-4.2 FAULT SEQUENCE

We shall consider the following sequence of abnormal events:

1. The generator $G1$ is tripped and will remain disconnected from the network for a period of $T$ s. We refer to this as "postfault period $I$" in the following analysis.
2. When the generator is reconnected to the network after $T$ s, we enter "postfault period II."

During postfault period I the generator $G1$ will obviously experience an acceleration. The generator $G2$, with its relatively high inertia, will remain fairly fixed in angular reference. The two generators are obviously going apart, and the question therefore is whether, upon reclosure, the system has sufficient synchronizing "glue" to hold them together. Our study will be aimed at finding this out.

### 12-4.3 ASSUMPTIONS

The subsequent analysis will be based upon the following assumptions:

1. Generator saliency will be neglected, and the transient generator models will therefore be chosen in accordance with Fig. 12-6.
2. The turbine powers $P_{T1}$ and $P_{T2}$ will be constant throughout the postfault period (their values are $P_{T1} = P_{T2} = P_G^0 = 10$ pu).

3. The emfs behind the transient reactances will retain constant magnitude throughout the postfault period.
4. All resistances are neglected.
5. All damping torques are likewise neglected. (Assumptions 4 and 5 render solutions which are on the safe side.)
6. The bus voltages will undergo major changes during the postfault period. These changes will strongly affect the bus loads (Chap. 3). The nature of the load determines the voltage dependency. We shall assume that our two bus loads are of "impedance type"; i.e., we may represent both by *constant* shunt admittances $Y_{D1}$ and $Y_{D3}$, which will not change throughout the analysis. The loads will thus vary as the square of the voltage, but the load power factors will be fixed.
7. The frequency will change only slightly, and we will therefore neglect the change of load with frequency.

### 12-4.4 DETERMINATION OF INITIAL SYSTEM STATE

In order to be able to solve the postfault swing equations, it is necessary to determine the initial prefault state of the generators. Also, we must find the voltages behind the transient reactances.

**Prefault load flow** The stage is fully set for a load flow study of the type discussed in Chap. 7. All impedances are given so that the prefault $\mathbf{Y}_{\text{bus}}$ can be found. Bus power and voltage specifications are complete (Fig. 12-19).

We perform such a study (by digital computer, of course) and obtain the prefault load flows given in Fig. 12-20. Since we will need them in our further analysis, we compute the prefault generator currents $I_{G1}{}^0$ and $I_{G2}{}^0$ and also the equivalent load admittances $Y_{D1}$ and $Y_{D3}$.

$$I_{G1}{}^0 = \left(\frac{S_{G1}{}^0}{V_1{}^0}\right)^* = 10 - j6.57$$
$$I_{G2}{}^0 = \left(\frac{S_{G2}{}^0}{V_2{}^0}\right)^* = 9.82 - j3.09 \qquad (12\text{-}38)$$

$$Y_{D1} = \frac{(S_{D1}{}^0)^*}{|V_1{}^0|^2} = 10 - j6 \quad \text{pu}$$
$$Y_{D3} = \frac{(S_{D3}{}^0)^*}{|V_3{}^0|^2} = 10 + j1.415 \quad \text{pu} \qquad (12\text{-}39)$$

Note that $Y_{D3}$ includes the shunt capacitor at bus 3.



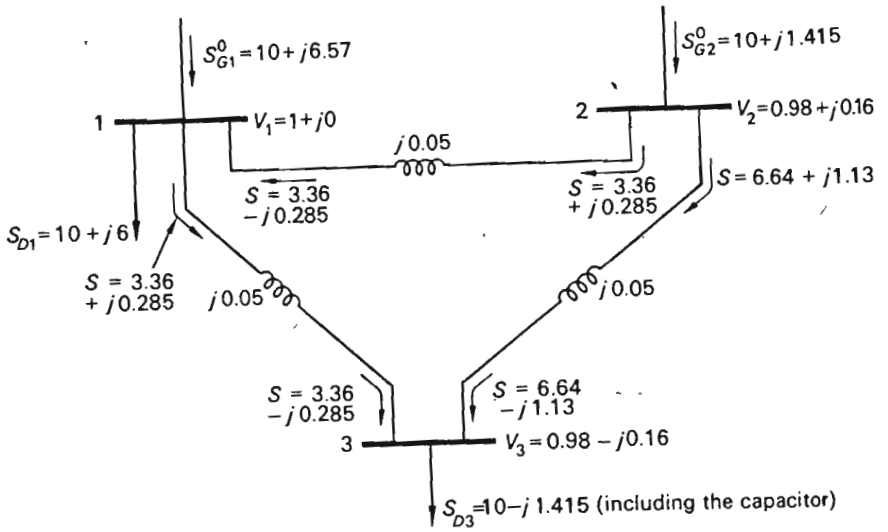


**Fig. 12-20** Prefault load flow picture in example system.

**Emfs behind transient reactances** Using the equivalent network of Fig. 12-6, we now compute the prefault values of emfs $E_1'$ and $E_2'$.

$$(E_1')^0 = V_1{}^0 + I_{G1}{}^0 jX_d' = 1.35 + j0.54$$
$$(E_2')^0 = V_2{}^0 + I_{G2}{}^0 jX_d' = 1.15 + j0.69 \qquad (12\text{-}40)$$

Note that the magnitudes of these emfs are

$$|E_1'|^0 = 1.46$$
$$|E_2'|^0 = 1.34 \qquad (12\text{-}41)$$

These magnitudes will be retained throughout the analysis.

As the phasors $E_1'$ and $E_2'$ coincide with the $d$ axes, the initial rotor positions are

$$\delta_1{}^0 = \underline{/E_1'} = 21.8° = 0.38 \text{ rad}$$
$$\delta_2{}^0 = \underline{/E_2'} = 30.9° = 0.54 \text{ rad} \qquad (12\text{-}42)$$

We summarize the initial voltage and angular position state in Fig. 12-21. Note that $V_1{}^0$ has been chosen as reference for the angular positions of *both* generator rotors. In the postfault state, $V_1{}'$ will not coincide with $V_1{}^0$, but the postfault angles $\delta_1{}'$ and $\delta_2{}'$ will still be measured relative to the *prefault synchronous* reference.

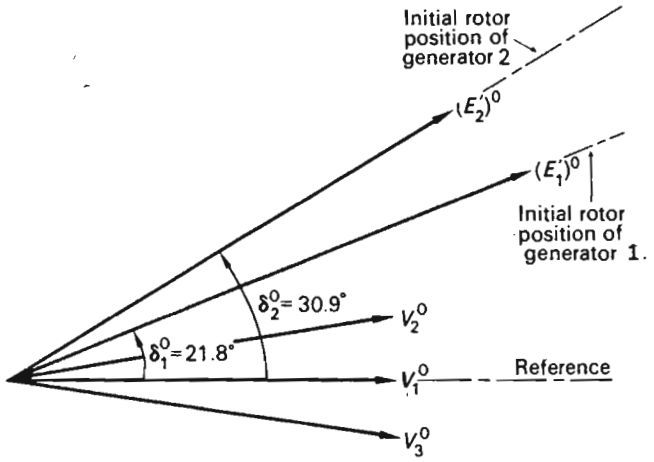


**Fig. 12-21** Prefault generator rotor angular positions.

#### 12-4.5 POSTFAULT SYSTEM MODELS (POSTFAULT PERIOD I)

At the moment when the fault sets in, the three bus voltages will change instantaneously ("inertialess") to new values. *The emfs $E_1'$ and $E_2'$, however, will remain unchanged in both magnitude and phases.*† The magnitudes will be constant, for reasons previously explained. The phase angles will remain *initially* constant because of the rotor inertias, but will immediately start to change due to the torque imbalance resulting from the fault.

**Network equations (postfault period I)** By making use of the generator model in Fig. 12-6, we can represent the system in the postfault state as shown in Fig. 12-22. Two fictitious buses (coded 4 and 5) have been added, each held at the "bus voltages" $V_4 \triangleq E_1'$ and $V_5 \triangleq E_2'$, respectively.

Note that all network elements have been represented as admittances. The "transient admittances" $Y_{d1}'$ and $Y_{d2}'$ are, of course, defined by

$$Y_{d1}' \triangleq \frac{1}{jX_{d1}'} = -j18.5 \quad \text{pu}$$
$$Y_{d2}' \triangleq \frac{1}{jX_{d2}'} = -j18.5 \quad \text{pu} \tag{12-43}$$

We had assumed that the bus loads were of "impedance type." They have therefore been represented by the shunt admittances computed earlier in Eq. (12-39).

† In order not to clutter up our symbols, we will, in the following discussion, delete the postfault superscript *f* in our symbol notations. No confusion should result.



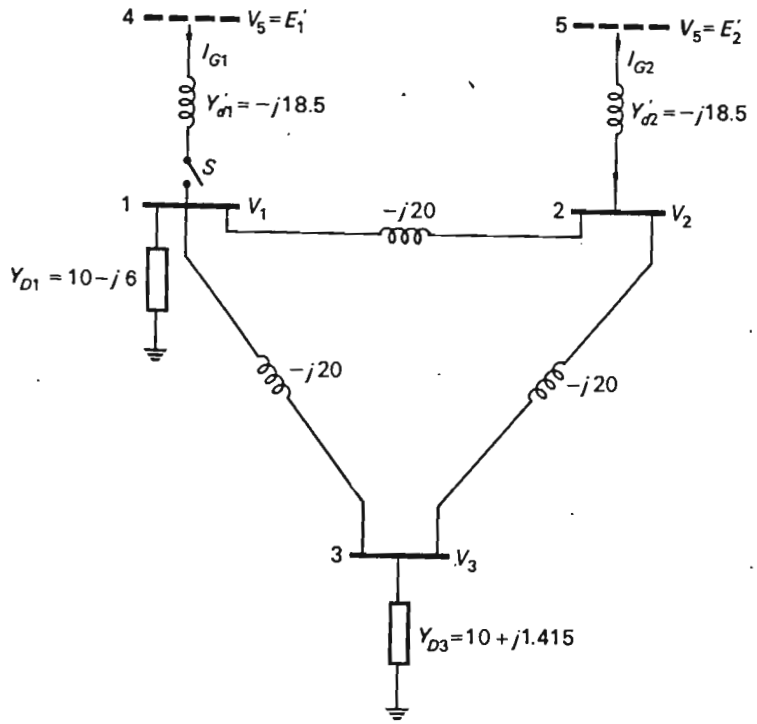


**Fig. 12-22** Equivalent postfault system representation.

The bus admittance matrix for the three-bus system can be obtained by using Eqs. (7-34). We get by inspection

$$\mathbf{Y}_{\text{bus}} = \begin{bmatrix} y_{11} & y_{12} & y_{13} \\ y_{21} & y_{22} & y_{23} \\ y_{31} & y_{32} & y_{33} \end{bmatrix} = \begin{bmatrix} 10 - j46 & j20 & j20 \\ j20 & -j40 & j20 \\ j20 & j20 & 10 - j38.585 \end{bmatrix} \tag{12-44}$$

(Note that this is *not* the same $\mathbf{Y}_{\text{bus}}$ as was used in the prefault load flow study.)

The load currents having been accounted for by the load admittances, the bus currents consist of only the generator currents, and the network equations therefore read

$$\begin{bmatrix} I_{G1} \\ I_{G2} \\ 0 \end{bmatrix} = \begin{bmatrix} y_{11} & y_{12} & y_{13} \\ y_{21} & y_{22} & y_{23} \\ y_{31} & y_{32} & y_{33} \end{bmatrix} \begin{bmatrix} V_1 \\ V_2 \\ V_3 \end{bmatrix} \tag{12-45}$$

The generator currents must satisfy the following additional constraint equations.

Since the onset of the fault is characterized by the disconnection of $G1$, that is, by the opening of switch $S$ in Fig. 12-22, we must have

$$I_{G1} = 0 \tag{12-46}$$

From Fig. 12-22 we realize that $I_{G2}$ must satisfy the relation

$$I_{G2} = Y'_{d2}(E'_2 - V_2) = -j18.5(E'_2 - V_2) \tag{12-47}$$

By substitution of these current values into Eq. (12-45), we obtain the following algebraic network equations *valid in postfault period I:*

$$\begin{aligned} V_1 &= -\frac{1}{y_{11}}(y_{12}V_2 + y_{13}V_3) \\ V_2 &= -\frac{1}{y_{22} + Y'_{d2}}(y_{21}V_1 + y_{23}V_3 - Y'_{d2}E'_2) \\ V_3 &= -\frac{1}{y_{33}}(y_{31}V_1 + y_{32}V_2) \end{aligned} \tag{12-48}$$

These three complex equations suffice to solve for the three complex voltages $V_1$, $V_2$, and $V_3$ *if the emf* $E'_2$ *is known.* If we use the Gauss-Seidel iterative method for solving the above equations, the computational algorithm will be

$$\begin{aligned} V_1^{(k+1)} &= -\frac{1}{y_{11}}(y_{12}V_2^{(k)} + y_{13}V_3^{(k)}) \\ V_2^{(k+1)} &= -\frac{1}{y_{22} + Y'_{d2}}(y_{21}V_1^{(k+1)} + y_{23}V_3^{(k)} - Y'_{d2}E'_2) \\ V_3^{(k+1)} &= -\frac{1}{y_{33}}(y_{31}V_1^{(k+1)} + y_{32}V_2^{(k+1)}) \end{aligned} \tag{12-49}$$

(We have used the iteration index $k$ rather than $\nu$ so as not to risk confusion with the discrete time index used in the Euler method.)

**Swing equations (postfault period I)** In analogy with Eq. (12-29), we define the following four-dimensional state vector:

$$\mathbf{x} = \begin{bmatrix} x_1 \\ x_2 \\ x_3 \\ x_4 \end{bmatrix} \triangleq \begin{bmatrix} \delta_1 \\ \dot{\delta}_1 \\ \delta_2 \\ \dot{\delta}_2 \end{bmatrix} \tag{12-50}$$



If we neglect the damping torques, and if we remember that the turbine powers are constant and equal to the prefault value 10 pu, we obtain in analogy with Eq. (12-30) the following swing equations:

$$\begin{aligned} \dot{x}_1 &= x_2 \\ \dot{x}_2 &= 2\pi(10 - P_{G1}) \\ \dot{x}_3 &= x_4 \\ \dot{x}_4 &= 0.2\pi(10 - P_{G2}) \end{aligned} \tag{12-51}$$

In the postfault period I we have

$$\begin{aligned} P_{G1} &= 0 \\ P_{G2} &= \text{Re}\,\{E'_2 I^*_{G2}\} \end{aligned} \tag{12-52}$$

By substitution of Eq. (12-47) into (12-52), we get

$$\begin{aligned} P_{G2} &= \text{Re}\,\{j18.5E'_2(E'^*_2 - V^*_2)\} = \text{Re}\,\{j18.5(|E'_2|^2 - E'_2V^*_2)\} \\ &= \text{Re}\,\{-j18.5E'_2V^*_2\} = \text{Im}\,\{18.5E'_2V^*_2\} \end{aligned} \tag{12-53}$$

Upon substitution of $P_{G1}$ and $P_{G2}$ into Eq. (12-51), we obtain the following swing equations, *valid in postfault period I:*

$$\begin{aligned} \dot{x}_1 &= x_2 \\ \dot{x}_2 &= 20\pi \\ \dot{x}_3 &= x_4 \\ \dot{x}_4 &= 0.2\pi(10 - \text{Im}\,\{18.5E'_2V^*_2\}) \end{aligned} \tag{12-54}$$

In accordance with Eqs. (12-42), the initial state is

$$\mathbf{x}^{(0)} = \begin{bmatrix} \delta_1^0 \\ \dot{\delta}_1^0 \\ \delta_2^0 \\ \dot{\delta}_2^0 \end{bmatrix} = \begin{bmatrix} 0.38 \\ 0 \\ 0.54 \\ 0 \end{bmatrix} \tag{12-55}$$

### 12-4.6 POSTFAULT SYSTEM MODELS (POSTFAULT PERIOD II)

Upon reclosure of which $S$ in Fig. 12-22, we enter the postfault period II. This network change does not affect the bus admittance matrix as given by Eq. (12-44). It will, however, change the value of the bus current at bus 1 from zero to the new value

$$I_{G1} = Y'_{d1}(E'_1 - V_1) = -j18.5(E'_1 - V_1) \tag{12-56}$$

This will change the generator power $P_{G1}$ from zero to the new value

$$P_{G1} = \text{Re}\,\{E'_1 I^*_{G1}\} \tag{12-57}$$

This equation can be written, in analogy with Eq. (12-53), in the form

$$P_{G1} = \text{Im}\,\{18.5E_1'V_1^*\} \tag{12-58}$$

By substitution of the expression for $I_{G1}$ into Eq. (12-45), the network equations (12-49) change to

$$\begin{aligned} V_1^{(k+1)} &= -\frac{1}{y_{11} + Y_{d1}'}(y_{12}V_2^{(k)} + y_{13}V_3^{(k)} - Y_{d1}'E_1') \\ V_2^{(k+1)} &= -\frac{1}{y_{22} + Y_{d2}'}(y_{21}V_1^{(k+1)} + y_{23}V_3^{(k)} - Y_{d2}'E_2') \\ V_3^{(k+1)} &= -\frac{1}{y_{33}}(y_{31}V_1^{(k+1)} + y_{32}V_2^{(k+1)}) \end{aligned} \tag{12-59}$$

Upon substitution of the expression for $P_{G1}$ into Eqs. (12-51), the swing equations (12-54) will change to the new set

$$\begin{aligned} \dot{x}_1 &= x_2 \\ \dot{x}_2 &= 2\pi(10 - \text{Im}\,\{18.5E_1'V_1^*\}) \\ \dot{x}_3 &= x_4 \\ \dot{x}_4 &= 0.2\pi(10 - \text{Im}\,\{18.5E_2'V_2^*\}) \end{aligned} \tag{12-60}$$

We do not at this time know the initial state $\mathbf{x}^{(0)}$ for period II. The initial state in period II equals the final state in period I, and we have not yet computed the latter.

### 12-4.7 COMPUTATIONAL SEQUENCE

All necessary mathematical models, including algebraic network equations and state differential ("swing") equations, have been assembled at this stage. We need now to settle for a proper sequence in which to solve these equations, using methods that we have discussed earlier. Figure 12-23 shows one possible approach.

The following explanatory remarks should help the reader understand this chart:

1. The computations prescribed in the three first blocks provide us with sufficient data to determine the initial state $\mathbf{x}^{(0)}$, that is, the *prefault* angular rotor positions measured in *electrical* radians relative to our chosen reference. (Note, in particular, the change in block 3 of $\mathbf{Y}_{\text{bus}}$ as was explained in the text.)



2. The postfault period is divided into discrete time intervals $t^{(0)}, t^{(1)}, \ldots,$ spaced $\Delta t$ s apart. A typical interval size may be
   $\Delta t = 0.02$ s
   Let us follow the sequence of computations that will take us from $t = t^{(0)}$ to $t = t^{(1)}$.
3. In block 5, distinction is first made between the postfault periods I and II. Assume that we are in period I.
4. Upon arriving at the solution of the *algebraic* network equations in block 7, we will specifically have obtained knowledge of $V_2$. This permits us to compute the term $E_2'V_2^*$ in the swing equations as specified in block 8. (Note that $E_2'$ has not changed from the value we computed in block 3.)
5. Having computed the initial rate of change of the state vector in block 8, we can perform a rough linear extrapolation to $t = t^{(1)}$ in block 9. Upon exit from this block, we therefore have a *rough* idea about the state at $t = t^{(1)}$.
6. Since we thus know the approximate value of $\delta_1(= x_1)$ and $\delta_2(= x_3)$ at $t = t^{(1)}$, we can simply determine the *rough* value of $E_1'$ and $E_2'$ for $t = t^{(1)}$. The magnitude of these phasors are *constant*, and the phasor tips therefore move on circles. This fact (visualized by Fig. 12-24) explains the formula in block 10.
7. Having now a rough idea about $E_1'$ and $E_2'$ for $t = t^{(1)}$, we can again solve the algebraic network equations, and thus obtain the rough voltage state for $t = t^{(1)}$ (block 11).
8. Data are now available to compute the rate of change of the state vector for $t = t^{(1)}$ (block 12).
9. With the knowledge of the derivatives at both ends of the interval, we can compute an average value for the rate of change in the interval (block 13).
10. From a knowledge of the average derivative, we compute an upgraded (and also final) value for the state at $t = t^{(1)}$ (block 14).
11. Finally, we "polish up" the values for the emfs $E_1'$ and $E_2'$ at $t = t^{(1)}$ (block 15).
12. At this stage we print out the result and proceed to the next time interval.

### 12-4.8 COMPUTER RESULTS

A computer program was developed, based on the flow chart in Fig. 12-23. The program was run for several values of reclosure times $T$. The results are shown in Fig. 12-25. In Fig. 12-25*a* we depict the swing curves for a transient *stable* case corresponding to $T = 0.1$ s. In Fig. 12-25*b* we have an *unstable* case corresponding to $T = 0.18$ s.

In both charts we have also included the variations in the bus voltage of bus 1.

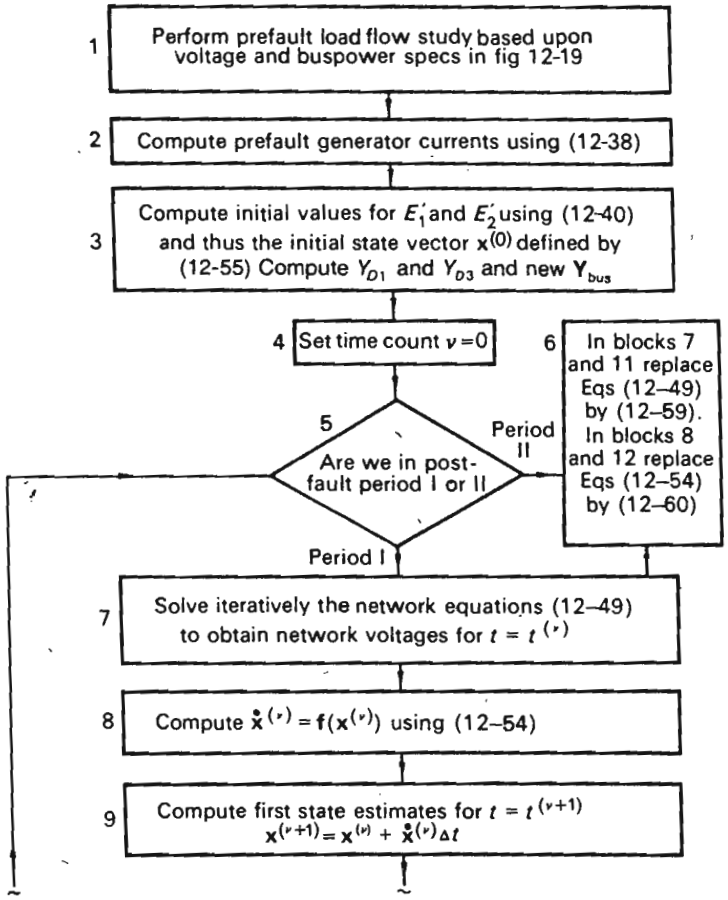


**Fig. 12-23** Computational sequence for obtaining swing curves.



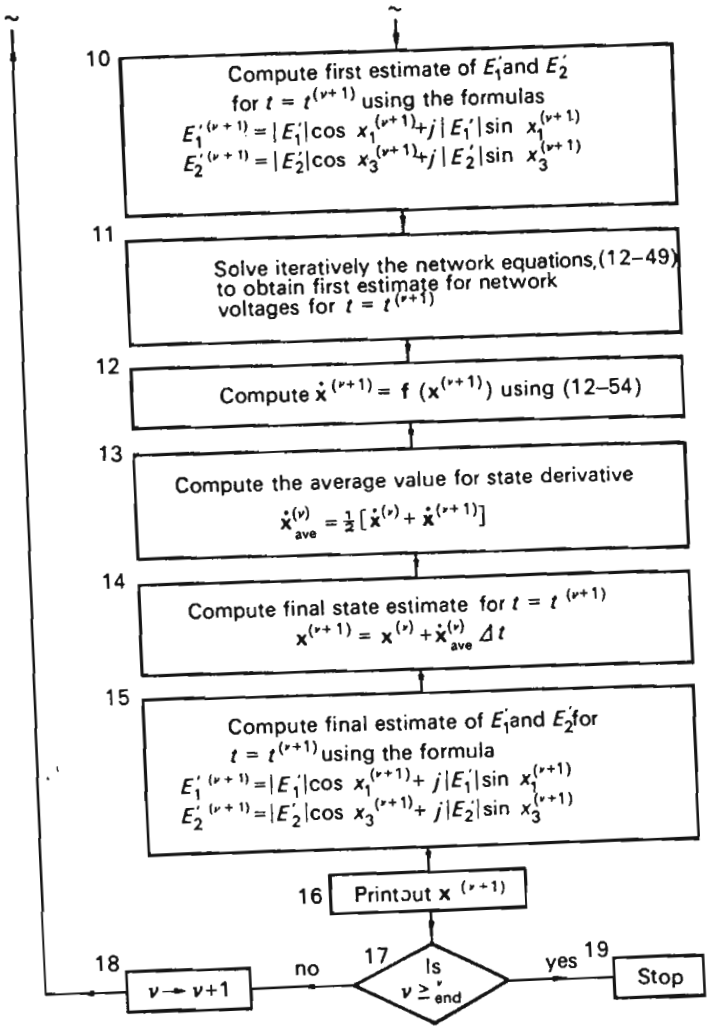


**Fig. 12-23** (*Continued*)

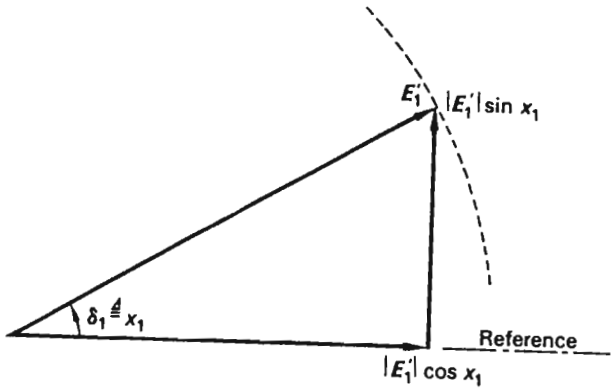


**Fig. 12-24** The tips of phasors $E_1'$ and $E_2'$ must move on the peripheries of circles.

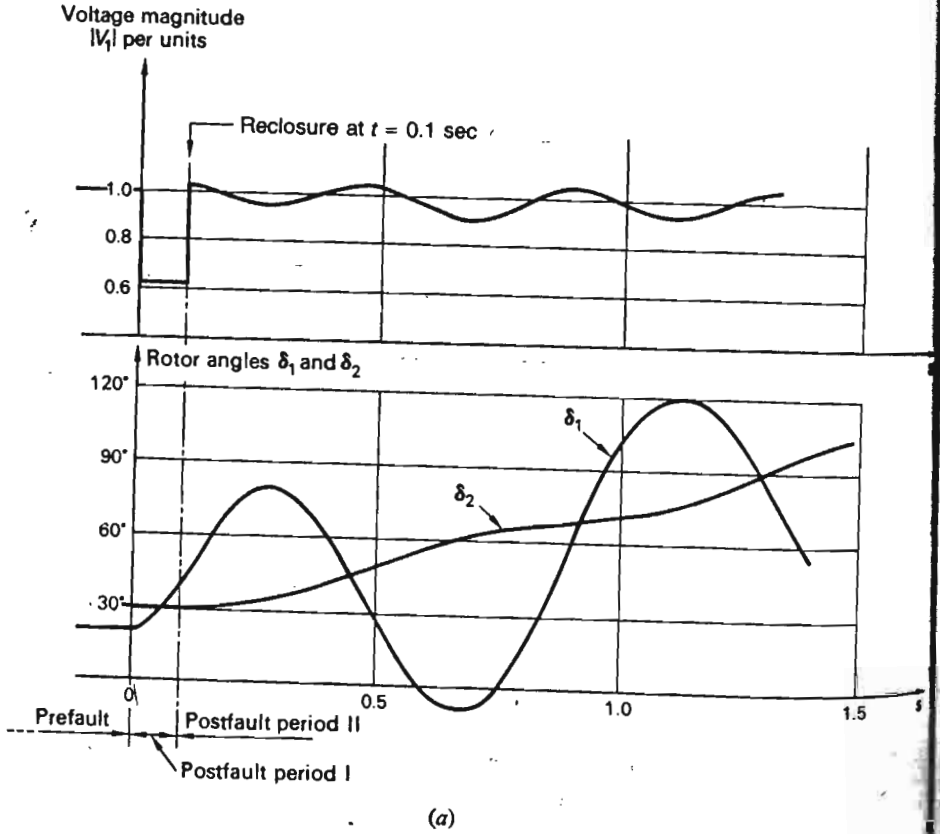


(*a*)

**Fig. 12-25** Computed swing curves. The upper curves show the variation of the voltage on bus 1 (= the fault bus). The lower curves represent the transient rotor positions. (*a*) Reclosure at $T = 0.1$ s; (*b*) reclosure at $T = 0.18$ s. [Note the different angular scales used in parts (*a*) and (*b*).]



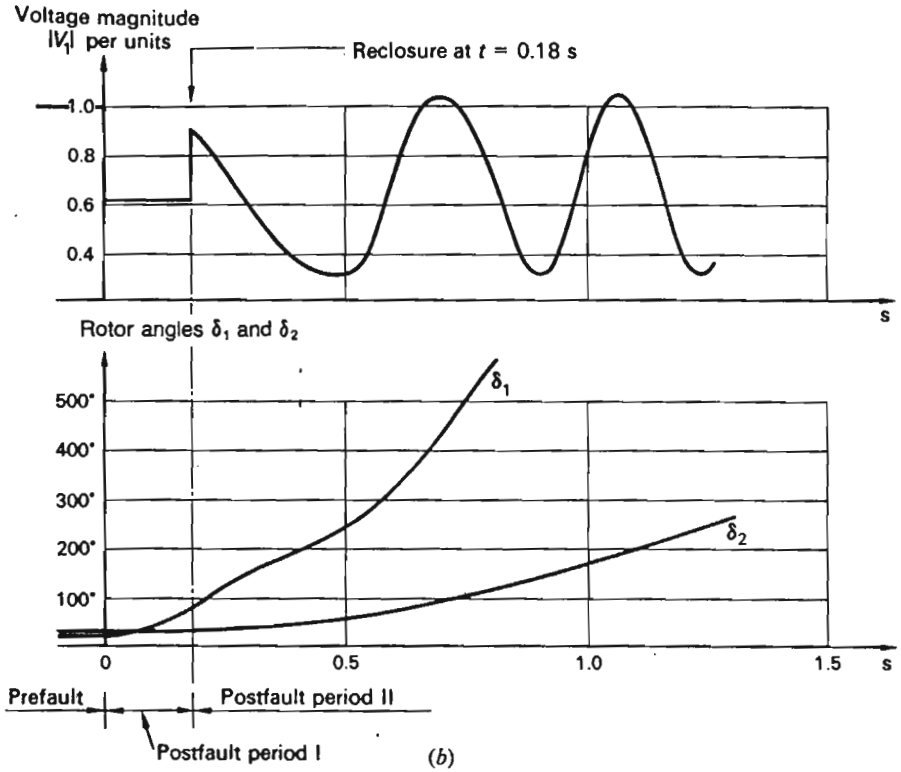


(*b*)

**Fig. 12-25** (*Continued*)

We note the following features from those graphs:

1. The onset of the fault results in a 40 percent dip of $|V_1|$.
2. Generator 1 performs "livelier" angular rotor swings than generator 2 because of its lower inertia.
3. We have not computed the swing curves beyond about 1 s because our models lose their validity beyond this time.
4. The generator rotor positions will *not* return to their original values even in the stable case (Fig. 12-25*a*). Why?

## 12-5 THE LOAD FREQUENCY AND VOLTAGE CONTROLLERS—THEIR EFFECT ON TRANSIENT STABILITY

In our preceding analysis we neglected the influence of both the load frequency ($Pf$) and voltage ($QV$) controllers. We assumed that the turbine power $P_T$ and the emf $E'$ behind the transient reactance would retain constant magnitudes throughout the transient period. This is a fair assumption to make, if, as often is the case, the transient stability is determined by the events within the "initial" transient period.

Should our study extend into the "intermediate" transient interval, then the controller effects will be felt, and we must take them into account in our analysis.

It is important to realize that both the load frequency and voltage control systems that we discussed in great detail in Chap. 9 are designed, basically, to keep frequency, tie line powers, and bus voltages at specified nominal values by counteracting relatively *small* but *normal* perturbations in the real and reactive loads. The synthesis of the control systems therefore centered around *linear perturbation* models, and their response and stability characteristics, in the strictest sense, apply only to *small-scale* dynamics.

We do not, in fact, have any real guarantee that the control systems will perform in an optimum fashion for the *large-scale* disturbances that we are concerned with in this chapter. *As a matter of fact, we can easily conceive of situations where the actions taken by the control systems will tend to deteriorate, rather than improve, the transient stability characteristics.* This follows as a consequence of the structural system changes often associated with the faults.

The obvious design objective should be directed toward development of a control system that will perform *optimally* during small-scale *and* large-scale dynamics; i.e., the control systems should be designed to operate in two distinctly different modes (*dual-mode* control systems). It is safe to state that as of this writing (1970) very little knowledge has accumulated in this important area. The author believes this to be the most promising and deserving area for research in EESE.

The treatment that follows will reflect the rather unsatisfactory present state of affairs. The effect of the control loops on the transient stability is discussed solely from an analysis point of view. We thus assume a priori a control system structure of the type introduced in Chap. 9. The effect of the control loop upon the rotor angle dynamics is then investigated simply by amending our previously used models to account for the presence of the control loop.

The only originality we claim is the full usage of the state-variable technique, which permits optimum systematization of the computational process. The *only* change that will be experienced in the computational flow chart in Fig. 12-23 is an increased dimensionality in the state vector $\mathbf{x}$. This means that the presence of the *Pf* and *QV* control loops do not add any principal computational difficulties, but will result in increased computer time.

### 12-5.1 EFFECTS OF *Pf* CONTROL LOOP

Consider the single-unit *Pf* controller shown in Fig. 9-12. Its block diagram is redrawn in Fig. 12-26 in somewhat more detail. Note, in particular, that we make a distinction between $P_T$ and $P_G$ (compare comments on page 325)



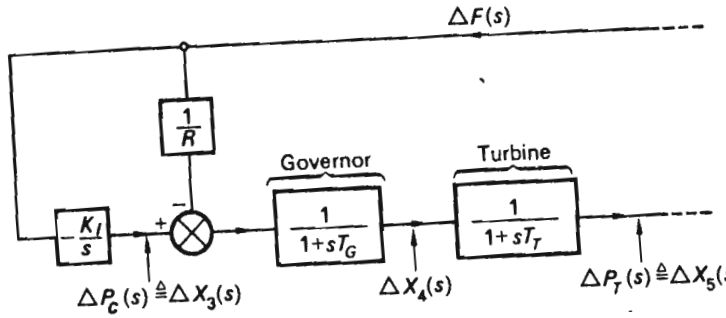


**Fig. 12-26** The *Pf* controller of single-generator unit. (See also Fig. 9-12.)

and, in addition, we introduce a new intermediate variable, $\Delta X_4$. The reader may easily confirm that this new variable has dimension of power and is proportional to (but not identical with) the valve position $\Delta X_E$ in Fig. 9-3.

From the block diagram in Fig. 12-26 we directly obtain the following relations:

$$\Delta P_c(s) = -\frac{K_I}{s}\Delta F(s)$$

$$\Delta X_4(s) = \frac{1}{1+sT_G}\left[\Delta P_c(s) - \frac{1}{R}\Delta F(s)\right] \tag{12-61}$$

$$\Delta P_T(s) = \frac{1}{1+sT_T}\Delta X_4$$

Inverse transformation of these equations results in the following three differential equations:

$$\frac{d}{dt}\Delta P_c = -K_I\,\Delta f$$

$$\frac{d}{dt}\Delta x_4 = \frac{1}{T_G}\left(\Delta P_c - \frac{1}{R}\Delta f - \Delta x_4\right) \tag{12-62}$$

$$\frac{d}{dt}\Delta P_T = \frac{1}{T_T}(\Delta x_4 - \Delta P_T)$$

The frequency deviation $\Delta f$ is related to the rotor position angle $\delta$ through the equation

$$\Delta f = \frac{1}{2\pi}\dot{\delta} = \frac{1}{2\pi}x_2 \tag{12-63}$$

**State-variable description of *Pf* controller** At this time we define the following *secondary*† *state variables:*

$$\begin{aligned} x_3 &\triangleq x_3^0 + \Delta x_3 \triangleq P_c^0 + \Delta P_c = P_c \\ x_4 &\triangleq x_4^0 + \Delta x_4 \\ x_5 &\triangleq x_5^0 + \Delta x_5 \triangleq P_T^0 + \Delta P_T = P_T \end{aligned} \tag{12-64}$$

$P_c^0$, $x_4^0$, and $P_T^0$ are the *constant prefault* values of $x_3$, $x_4$, and $x_5$, respectively, and we can easily confirm, from Fig. 12-26, that they are all equal and have a magnitude corresponding to the prefault turbine (or generator) power; i.e.,

$$x_3^0 = x_4^0 = x_5^0 = P_T^0 = P_c^0 = P_G^0 \tag{12-65}$$

If we substitute the state variables (12-64) into Eqs. (12-62) and make use of the identity equation (12-63), we obtain

$$\begin{aligned} \dot{x}_3 &= -\frac{K_I}{2\pi} x_2 \\ \dot{x}_4 &= \frac{1}{T_G}\left(x_3 - \frac{1}{2\pi R} x_2 - x_4\right) \\ \dot{x}_5 &= \frac{1}{T_T}(x_4 - x_5) \end{aligned} \tag{12-66}$$

These, then, are the additional three state equations that must be added to the previous two [Eqs. (12-30)] if we wish to include the effects of the *Pf* controller. The initial values of the new state variables are

$$\begin{bmatrix} x_3^0 \\ x_4^0 \\ x_5^0 \end{bmatrix} = \begin{bmatrix} P_T^0 \\ P_T^0 \\ P_T^0 \end{bmatrix} \tag{12-67}$$

We make at this time the following observations:

1. The above state vector adequately describes the behavior of the *Pf* controller only in the time region for which the model in Fig. 12-26 applies, i.e., approximately the first few seconds following the disturbance. It is possible to extend the "validity region" by including additional state variables which account for the slower dynamics of the steam system.
2. It is quite possible that the turbine command signal during a transient swing would be of such a magnitude as to command a turbine power beyond the capability of the turbine. The valve position $x_4$ must lie within the limits

$$0 < x_4 < P_{\max} \tag{12-68}$$

and we must make sure, in our computer program, that $x_4$ never can exceed these limits.

3. The first one of Eqs. (12-61) applies only to the single-generator case. In a multiarea case the ACE will contain additional signals which must be added to the equations.

† The "primary" ones being $x_1$ and $x_2$, defined by Eqs. (12-29).



### 12-5.2 EFFECTS OF VOLTAGE CONTROL LOOP

The emf $E'$, which in our earlier analysis was assumed to retain constant magnitude, will in actuality change, as a result of the automatic actions taken by the voltage control loop in Fig. 9-24.

These effects can be described in terms of four additional state variables.

**State-variable description of voltage controller** From Fig. 9-24 we obtain by inspection

$$\begin{aligned} \frac{V_r(s)}{V_2(s)} &= \frac{K_E}{1 + sT_E} \\ \frac{V_2(s)}{V_1(s)} &= \frac{K_A}{1 + sT_A} \\ \frac{V_{st}(s)}{V_r(s)} &= \frac{sK_{st}}{1 + sT_{st}} \\ V_1(s) &= |V|_{\text{ref}}(s) - |V|(s) - V_{st}(s) \end{aligned} \tag{12-69}$$

By inverse transformation the following three differential equations are obtained:

$$\begin{aligned} \dot{v}_r &= \frac{1}{T_E}(K_E v_2 - v_r) \\ \dot{v}_2 &= \frac{1}{T_A}[K_A(|V|_{\text{ref}} - |V| - v_{st}) - v_2] \\ \dot{v}_{st} &= \frac{1}{T_E T_{st}}(K_{st}K_E v_2 - K_{st}v_r - T_E v_{st}) \end{aligned} \tag{12-70}$$

We can write these equations in the standard state-variable form

$$\begin{aligned} \dot{x}_6 &= \frac{1}{T_E}(K_E x_7 - x_6) \\ \dot{x}_7 &= \frac{1}{T_A}[K_A(|V|_{\text{ref}} - |V| - x_8) - x_7] \\ \dot{x}_8 &= \frac{1}{T_E T_{st}}(K_{st}K_E x_7 - K_{st}x_6 - T_E x_8) \end{aligned} \tag{12-71}$$

The three new secondary state variables, $x_6$, $x_7$, and $x_8$, have been defined as follows:

$$\begin{aligned} x_6 &\triangleq v_r \\ x_7 &\triangleq v_2 \\ x_8 &\triangleq v_{st} \end{aligned} \tag{12-72}$$

Under static prefault conditions the voltage $v_{st}$ is zero and the voltages $v_r$ and $v_2$ have values $v_r^0$ and $v_2^0$ that depend upon the known excitation state in question. Therefore the initial values of the new state variables are

$$\begin{bmatrix} x_6^0 \\ x_7^0 \\ x_8^0 \end{bmatrix} = \begin{bmatrix} v_r^0 \\ v_2^0 \\ 0 \end{bmatrix} \tag{12-73}$$

**The effect of finite field time constant $T_r$** There is an additional important link missing in model (12-70). We must establish the relationship between the field voltage $v_r = x_6$ and the emf $E'$. To accomplish this we choose the last of Eqs. (4-36) as our point of departure.

If this equation is multiplied by the factor $\omega L_5/\sqrt{2}\,L_4$, it takes on the form

$$\frac{\omega L_5}{\sqrt{2}\,L_4} v_r - \frac{\omega L_5 r_r}{\sqrt{2}\,L_4} i_r = \frac{d}{dt}\left(\frac{\omega L_5}{\sqrt{2}} i_r - \frac{3}{2}\frac{L_5^2}{\sqrt{2}\,L_4} i_d\right) \tag{12-74}$$

Let us momentarily set

$$\begin{aligned} r_r &= 0 \\ v_r &= 0 \end{aligned} \tag{12-75}$$

which causes the left side of the equation to vanish. Equations (12-75) mean the assumption of a lossless and short-circuited field winding.† By integrating Eq. (12-74) and observing Eq. (12-75), we obtain the solution

$$\frac{\omega L_5}{\sqrt{2}} i_r - \frac{3}{2}\frac{L_5^2}{\sqrt{2}\,L_4} i_d = \frac{\omega L_5}{\sqrt{2}} i_r^0 - \frac{3}{2}\frac{L_5^2}{\sqrt{2}\,L_4} i_d^0 = \text{const} \tag{12-76}$$

This equation tells us that whenever a change occurs in $i_d$, a corresponding change immediately takes place in the rotor current.

† Setting $v_r = 0$ is necessary in order to prevent the rotor current to take on unlimited values in the resistanceless winding.



In view of Eqs. (4-46), (4-56), (10-23), and (12-11) we can write Eq. (12-76) as follows:

$$|E| - (X_d - X_d')\,|I_d| = |E^0| - (X_d - X_d')\,|I_d^0| \doteq |E'|^0 = \text{const} \tag{12-77}$$

This last equation confirms the constancy of the magnitude of $E'$ in the case of resistanceless field winding, i.e., for $T_r = \infty$.

Let us now see what happens for *finite* $T_r$. Having just identified the expression within parentheses in Eq. (12-74) as $|E'|$, we can write the latter equation in the form

$$\frac{1}{T_r}(|E_v| - |E_i|) = \frac{d}{dt}|E'| \tag{12-78}$$

where

$$T_r \triangleq \frac{L_4}{r_r} \qquad \text{field time constant}$$

$$\begin{aligned} |E_v| &\triangleq \frac{\omega L_5}{\sqrt{2}}\frac{v_r}{r_r} \triangleq K_v v_r \\ |E_i| &\triangleq \frac{\omega L_5}{\sqrt{2}} i_r \triangleq K_i i_r \end{aligned} \tag{12-79}$$

The new variables $E_v$ and $E_i$ have the physical dimension of emf, and in view of Eq. (4-46), we can give them the following interpretation:

$E_v(E_i)$ is the *steady-state* stator emf we would get if the field voltage (current) were held at the *constant* value $v_r(i_r)$.

At this point we introduce our final state variable,

$$x_9 \triangleq |E'| \tag{12-80}$$

and obtain from Eq. (12-78) our last state equation,

$$\dot{x}_9 = \frac{1}{T_r}(K_v x_6 - |E_i|) \tag{12-81}$$

The initial value of $x_9$ is, of course,

$$x_9^0 = |E'|^0 \tag{12-82}$$

### 12-5.3 SUMMARY OF MODEL

In summarizing our results, we conclude that the effects on the transient stability of the $Pf$ and $QV$ control loops can be accounted for by characterizing

each generator unit by the following nine-dimensional state equations:

$$\begin{aligned}
\dot{x}_1 &= x_2 \\
\dot{x}_2 &= \frac{\pi f^0}{H^0}(x_5 - P_G - Dx_2) \\
\dot{x}_3 &= -\frac{K_I}{2\pi}x_2 \\
\dot{x}_4 &= \frac{1}{T_G}\left(x_3 - \frac{1}{2\pi R}x_2 - x_4\right) \\
\dot{x}_5 &= \frac{1}{T_T}(x_4 - x_5) \\
\dot{x}_6 &= \frac{1}{T_E}(K_E x_7 - x_6) \\
\dot{x}_7 &= \frac{1}{T_A}[K_A(|V|_{\text{ref}} - |V| - x_8) - x_7] \\
\dot{x}_8 &= \frac{1}{T_E T_{st}}(K_{st}K_E x_7 - K_{st}x_6 - T_E x_8) \\
\dot{x}_9 &= \frac{1}{T_r}(K_r x_6 - |E_i|)
\end{aligned} \tag{12-83}$$

We make the following concluding remarks:

1. Accounting for the effect of the control loops has increased the dimensionality of the state vector *per generator* from 2 to 9.
2. No change in the flow chart of Fig. 12-23 is needed, except, of course, that consideration be given in blocks 10 and 15 to the *changing* values $|E_i'|$.
3. During the transient swings the field voltage $v_r(= x_6)$ will with great probability "hit the ceiling", i.e., reach the limit values of the exciter.

   In the computer program we must therefore see to it that $x_6$ cannot reach values beyond this saturation limit.
4. The value for $|V|$ in the seventh of Eqs. (12-83) is obtained from the solution of network equations in block 7.
5. The value of $|E_i|$ in the ninth of Eqs. (12-83) is computed as follows:

   From the definition of $E_i$ as a *steady-state* emf proportional to the instantaneous current value, we can interpret this emf from the phasor diagram in Fig. 12-27.



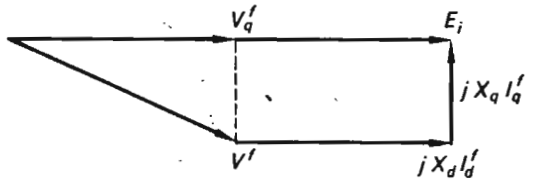


**Fig. 12-27** Phasor diagram for finding $E_i$.

From this diagram we get

$$|E_i| = |V_q| + X_d|I_d| \tag{12-84}$$

If $X_d = X_q$ (that is, nonsaliency) we have the alternative formula

$$|E_i| = |V + jX_d I_G| \tag{12-85}$$

## 12-6 SUMMARY

In this final chapter we have introduced the reader to the basic theory of electromechanical transients in power systems. The electromechanical torques that exist within the synchronous machines tend, under normal operation, to hold the network together in a stable equilibrium state, characterized by a perfect torque and power balance within each machine.

As a result of disturbances, which usually take the form of sudden structural network changes, the torque balance is upset within each machine. The individual machines, as a consequence, will be subject to accelerations or decelerations, causing angular rotor swings of such large magnitudes that certain machines may pull out of synchronism.

The differential equations describing the swing dynamics are of nonlinear type and lack, generally, analytical solutions. Numerical solutions can always be found, and we have discussed the modified Euler method for digital simulation of the swing equations. The differential equations have been expressed in standard "state" form. The advantage of this approach is that we can achieve a great measure of systematization and also make use of the compact vector notation features.

During approximately the first second following a disturbance, the turbine torque and the emf behind the transient reactance remain fairly constant. In this time interval the dynamic state of each generator can be adequately characterized by two state variables. As the voltage and turbine controllers come into play, the dynamics grows more complex, and we need now about 10 state variables to model the machine behavior adequately.

In all our examples we neglected the damping torques and also the resistances in the network. This procedure has the advantage of rendering results which are on the safe side and thus compensating for uncertain factors in our models.

It should be noted, however, that the computational procedures presented can accommodate with ease both these effects if we wish to do so.

All fault situations that were exemplified were of the symmetrical variety. Unbalanced faults will not offer any principal difficulties, but will, of course, necessitate our taking into account separately the three sequence systems, as was discussed in Chap. 11. It must be noted, however, that *only the positive sequence system will determine the transient generator power.* (The negative and zero sequence systems are associated with pulsating generator torques.)

## EXERCISES

**12-1.** Using the swing equation (12-5), prove that if the damping is neglected, the speed of the generator, when subject to a constant decelerating power of 1 pu, will be reduced from rated value to zero in $2H$ s. (This gives a good feel for the physical meaning of $H$.)

**12-2.** Consider Eqs. (12-24) and (12-26). If the saliency term is neglected, we can write the two equations in the following forms:

$$\ddot{\delta} = \frac{\pi f^0}{H} P_T^0 \tag{12-86}$$

$$\ddot{\delta} = \frac{\pi f^0}{H} (P_T^0 - P_{a,\max} \sin \delta) \tag{12-87}$$

(*a*) Turn your attention now to the mechanical system in Fig. 12-28. Prove that the dynamics of this system is described by an equation of the form of Eq. (12-87). If you remove the pendulum, the differential equation will be of the form of Eq. (12-86).

(*b*) The system in Fig. 12-28 evidently is a mechanical analog of the generator in Example 12-4.

Assign proper values to $m_1$, $m_2$, $L$, and $I_w$ so that the differential equations for the system in Fig. 12-28 turn out numerically identical with Eqs. (12-86) and (12-87).

(*c*) What numerical value must you assign to $m_2$ to make the analog apply to the prefault static case, characterized by $\ddot{\delta} = 0$?

(*d*) How would you use the analog thus obtained to study the fault situation in the text? Would it be a convenient experiment?

**12-3.** Equation (12-86) can be written in state-variable form thus:

$$\dot{x}_1 = x_2$$

$$\dot{x}_2 = \frac{\pi f^0}{H} P_T^0$$

By dividing these two equations we have

$$\frac{dx_2}{dx_1} = \frac{\pi f^0 P_T^0}{H} \frac{1}{x_2} \tag{12-88}$$



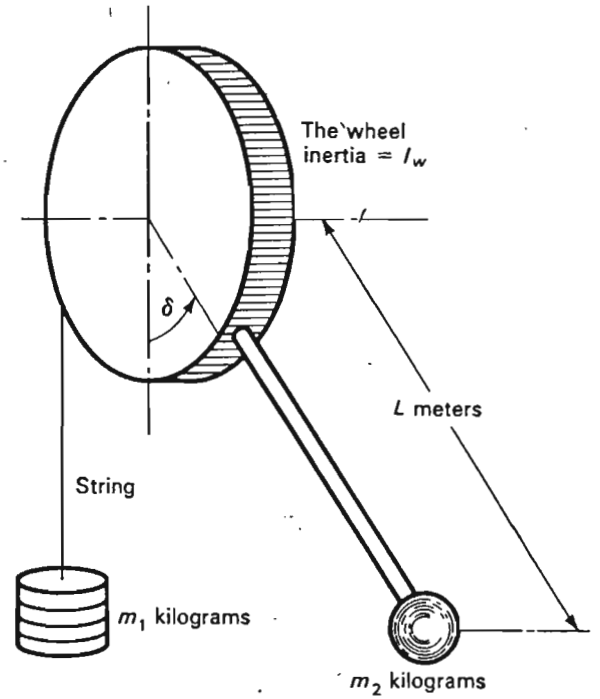


**Fig. 12-28** Analog of single generator operated onto infinite bus.

Time $t$ does not appear explicitly in this equation. Upon integrating Eq. (12-88), we obtain

$$x_2^2 = 2 \frac{\pi f^0 P_T^0}{H} x_1 + C \tag{12-89}$$

Depending upon the value of the integration constant $C$, the curves defined by Eq. (12-89) are parabolas, as shown in Fig. 12-29. The $x_2x_1$ coordinate system is referred to as a *state*, or *phase*, *plane*. The parabolas are called *state trajectories*, and give the relationship between the velocity ($x_2$) and position ($x_1$) states before reclosure.

(*a*) Start with Eq. (12-87) and prove that the trajectories after reclosure look as shown dotted in Fig. 12-29.

(*b*) Prove that there are two groups of trajectories after reclosure, separated by the so-called *separatrix*. The trajectories inside the separatrix are *stable*; those outside are *unstable*.

(*c*) Find the equation for the separatrix.

(*d*) The generator in Example 12-4 is in the initial state

$$\mathbf{x}^0 = \begin{bmatrix} \frac{\pi}{6} \\ 0 \end{bmatrix}$$

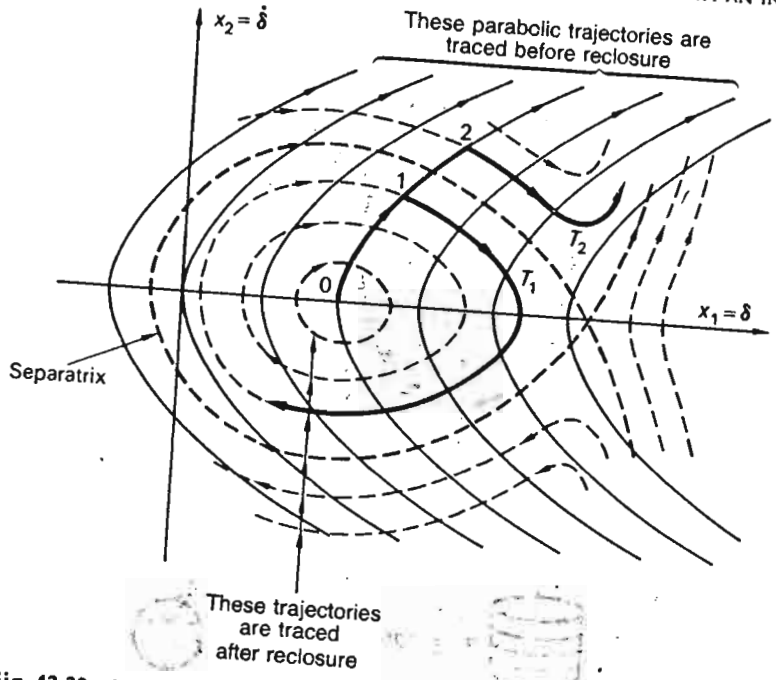


**Fig. 12-29** State trajectories for Exercise 12-3.

This state is marked 0 in Fig. 12-29. Following the onset of the fault, the generator state traces the boldface trajectory. An early reclosure in state 1 means a switchover onto a stable trajectory $T_1$. A late reclosure in state 2 results in the unstable trajectory $T_2$. Correlate these trajectories with the swing curves in Fig. 12-10.

(*e*) If we take the damping term into account, how will this change the trajectories?

**12-4.** Seek, graphically, the value for the reclosure angle $\delta_{recl}$ in Fig. 12-12.

**12-5.** Consider the single-generator system in Example 12-3. Assume that the 0.10-pu external reactance is the combined impedance of two parallel lines having a reactance of 0.125 and 0.50 pu, respectively. Assume that the stronger line suddenly is opened and stays open.

(*a*) Use the equal-area criterion to prove that the ensuing rotor swings are stable. Work the problem on the assumption that the initial loading is 0.75 pu as in the text.

(*b*) If the generator had been initially full-loaded (1 pu), would the system now be transient stable following the same fault?

**12-6.** You probably concluded, in Exercise 12-2, that the analog in Fig. 12-28 would be quite unwieldy to use if we were to simulate the opening-reclosure fault sequence in Example 12-4. Prove, however, that it is easy to use it to simulate the fault in Exercise 12-5 (assuming of course, that we are permitted to neglect the saliency term).

**12-7.** Simulate the swing equations you derived in Exercise 12-5 on an analog computer and confirm your previous results.

**12-8.** Simulate the swing equations in Exercise 12-5 on a digital computer, using the Euler modified method. Use a time step of $\Delta t = 0.02$ s.



**12-9.** Consider the five-bus three-generator system described in Exercise 8-3. Develop a computer program for studying the transient stability of the system following a solid three-phase short circuit of load bus 4, and subsequent clearing of the fault.

Use the prefault conditions specified in Table 8-3. Make reasonable assumptions regarding the generator inertia constants and transient reactances. Neglect generator saliency, and confine your study to the initial period, where $P_{Ti}$ and $|E_i'|$ are constants. Find, in particular, the critical fault clearing time, i.e., the maximum time that the fault may persist.

## REFERENCES


### Books

1. Crary, S. B.: "Power System Stability," vols. I and II, John Wiley & Sons, Inc., New York, 1945–1947.
2. Kimbark, E. W.: "Power System Stability," John Wiley & Sons, Inc., New York, 1948.
3. Venikov, V. A. (ed.): "Transient Phenomena in Electrical Power Systems," Pergamon Press, New York, 1965.
4. Collatz, L.; "The Numerical Treatment of Differential Equations," Springer-Verlag OHG, Berlin, 1966.
5. Stagg, G. W., and A. H. El-Abiad: "Computer Methods in Power Systems Analysis," McGraw-Hill Book Company, New York, 1968.
6. Elgerd, O.: "Control Systems Theory," McGraw-Hill Book Company, New York, 1967.

(References 1 and 2 give comprehensive treatment of the "transient stability problem" on power systems. Although aged, they still are valuable reference sources. Reference 3 gives insight into the Russian methods of solving stability problems. Reference 4 presents, in an excellent fashion, numerical solution of differential equations. Reference 5 gives examples on computer solutions of rotor swing dynamics. Reference 6 presents the state-variable method made use of in this chapter.)

### Technical papers and reports

7. Olive, D. W.: New Techniques for the Calculation of Dynamic Stability, *Proc. Power Ind. Computer Appl.*, Clearwater, Fla., 1965, pp. 212–229.
8. Lokay, H. E., and J. W. Skooglund: Power System Stability: Digital Analysis Showing Effect of Generator Representation, Types of Voltage Regulators, and Speed Governor, *Proc. Power Ind. Computer Appl.*, Clearwater, Fla., 1965, pp. 230–241.
9. Dyrkacz, M. S., and C. C. Young: Automatic System Reduction for Transient Stability Studies, *Proc. Power Ind. Computer Appl.*, Clearwater, Fla., 1965, pp. 242–246.
10. Smith, R. R.: The Effect of Regulating Devices on the Steady-state Stability of a Synchronous Machine, *Proc. Power Systems Computation Conf.*, rept. 5.4, Stockholm, Sweden, 1966.
11. Dineley, J. L., et al.: Factors Affecting Automatic Excitation Control on a Synchronous Machine, *Proc. Power Systems Computation Conf.*, rept. 5.5, Stockholm, Sweden, 1966.
12. Roy, J. C.: Effect of Synchronous Machine Parameters on Dynamic and Transient Stability, *Proc. Power Systems Computation Conf.*, rept. 5.9, Stockholm, Sweden, 1966.
13. Gustavson, H., et al.: A Computer Program for Stability Calculations in AC Networks Including Voltage and Prime Mover Regulation and Containing DC Links, *Proc. Power Systems Computation Conf.*, rept. 5.10, Stockholm, Sweden, 1966.

14. Dineley, J. L., et al.: Optimized Transient Stability from Excitation Control of Synchronous Generators, *Proc. Power Ind. Computer Appl. Conf.*, Pittsburgh, Pa., 1967, pp. 1–12.
15. Olive, D. W.: Digital Simulation of Synchronous Machine Transients, *Proc. Power Ind. Computer Appl. Conf.*, Pittsburgh, Pa., 1967, pp. 13–20.
16. Webler, R. M., and C. C. Young: A New Digital Computer Program for Predicting Dynamic Performance of Electric Power Systems, *Proc. Power Ind. Computer Appl. Conf.*, Pittsburgh, Pa., 1967, pp. 21–30.
17. Byerly, R. T., and D. G. Ramey: Dynamic Simulation of Interconnected Systems, *Proc. Power Ind. Computer Appl. Conf.*, Pittsburgh, Pa., 1967, pp. 31–40.
18. Baba, J., et al.: Load Shedding and System Splitting, *Proc. Second Power Systems Computation Conf.*, pt. 4, rept. 6.1, Stockholm, Sweden, June–July, 1966.
19. Hicks, K. L.: Coordination of Disaster Control Procedures for Large Interconnected Systems, *IEEE Spectrum*, November, 1967, pp. 52–55.
20. Specifications for Tomorrow's Power Flow and Dynamic Stability Programs, Western Systems Coordinating Council Committee Report, *Proc. Power Ind. Computer Appl. Conf.*, Denver, Colo., 1969.
21. Chang, A., and M. M. Adibi: Power System Dynamics Equivalents, *Proc. Power Ind. Computer Appl. Conf.*, Denver, Colo., 1969.
22. Teichgraeber, R. D., et al.: A New Stability Measure for Multimachine Power Systems, *Proc. Power Ind. Computer Appl. Conf.*, Denver, Colo., 1969.
23. Tuel, W. G., and M. M. Adibi: Some Considerations on Power Systems Stability Studies, *Proc. Power Ind. Computer Appl. Conf.*, Denver, Colo., 1969.
24. Byerly, R. T., and T. M. McCanley: Mathematical Models and Computing Techniques for Generator and Transmission Line Voltages Following Load Rejection, *Proc. Power Ind. Computer Appl. Conf.*, Denver, Colo., 1969.
25. Computer Representation of Excitation Systems, IEEE Committee Report, *IEEE Trans.*, vol. PAS-87, pp. 1460–1464, June, 1968.
26. Mittelstadt, W. A.: Four Methods of Power System Damping, *IEEE Trans.*, vol. PAS-87, no. 5, pp. 1323–1329, May, 1968.
27. El-Abiad, A. H., and K. Nagappan: Transient Stability Regions of Multi-machine Power Systems, *IEEE Trans.*, vol. PAS-85, no. 2, pp. 169–178, February, 1966.
28. Gless, G. E.: The Direct Method of Liapunov Applied to Transient Power System Stability, *IEEE Trans.*, vol. PAS-85, no. 2, pp. 159–168, February, 1966.
29. Kimbark, E. E.: Improvement of System Stability by Switched Series Capacitors, *IEEE Trans.*, vol. PAS-85, no. 2, pp. 180–188, February, 1966.
30. Undrill, J. M.: Power System Stability Studies by the Method of Liapunov, *IEEE Trans.*, pts. I and II, vol. PAS-86, no. 7, pp. 791–811, July, 1967.
31. Undrill, J. M.: Structure in the Computation of Power System Response, *IEEE Trans.*, vol. PAS-88, no. 1, pp. 1–6, January, 1969.
32. Smith, O. J. M.: Power System Transient Control by Capacitor Switching, *IEEE Trans.*, vol. PAS-88, no. 1, pp. 28–35, January, 1969.
33. Brown, H. E., et al.: A Study of Stability Equivalents, *IEEE Trans.*, vol. PAS-88, no. 3, pp. 200–207, March, 1969.
34. Kent, M. H., et al.: Dynamic Modeling of Loads in Stability Studies, *IEEE Trans.*, vol. PAS-88, no. 5, pp. 756–763, May, 1969.
35. Kimbark, E. W.: Improvement of Power System Stability by Changes in the Network, *IEEE Trans.*, vol. PAS-88, no. 5, pp. 773–781, May, 1969.

# appendix A
# Elements of Vector and Matrix Algebra

## A-1 VECTORS

We define a vector $\mathbf{x}$ as an ordered set of numbers, the *components* $x_1$, $x_2, \ldots, x_n$,

$$\mathbf{x} \triangleq \begin{bmatrix} x_1 \\ x_2 \\ \cdot \\ \cdot \\ \cdot \\ x_n \end{bmatrix} \tag{A-1}$$

The numbers $x_i$ may be real or complex.

$n$ defines the *dimensionality* of the vector.

Although the above column arrangement will be used most commonly, it proves convenient sometimes to use the *row*, or *transposed*, representation

$$\mathbf{x}^T \triangleq [x_1 \quad x_2 \quad \cdots \quad x_n] \tag{A-2}$$

### A-1.1 SPECIAL VECTORS

The *null vector* $\mathbf{0}$ and the *sum vector* $\mathbf{1}$ are defined as follows:

$$\mathbf{0} \triangleq \begin{bmatrix} 0 \\ 0 \\ \cdot \\ \cdot \\ \cdot \\ 0 \end{bmatrix} \qquad \mathbf{1} \triangleq \begin{bmatrix} 1 \\ 1 \\ \cdot \\ \cdot \\ \cdot \\ 1 \end{bmatrix}$$

The unit vector $\mathbf{e}_i$ is defined as the vector

$$\mathbf{e}_i \triangleq \begin{bmatrix} 0 \\ \cdot \\ \cdot \\ \cdot \\ 1 \\ \cdot \\ \cdot \\ \cdot \\ 0 \end{bmatrix} \leftarrow i\text{th component}$$

### A-1.2 ELEMENTARY VECTOR OPERATIONS

Two vectors $\mathbf{x}$ and $\mathbf{y}$ are said to be equal if and only if $x_i = y_i$ for $i = 1, 2, \ldots, n$. In such a case, we write

$$\mathbf{x} = \mathbf{y}$$

By the product of a vector $\mathbf{x}$ with the scalar $\lambda$, we define a new vector $\lambda\mathbf{x}$, having each component amplified by the same scalar; i.e.,

$$\lambda\mathbf{x} = \mathbf{x}\lambda \triangleq \begin{bmatrix} \lambda x_1 \\ \lambda x_2 \\ \cdot \\ \cdot \\ \cdot \\ \lambda x_n \end{bmatrix} \tag{A-3}$$

*Addition* and *subtraction* of two vectors $\mathbf{x}$ and $\mathbf{y}$ result in new vectors

$$\mathbf{x} \pm \mathbf{y} \triangleq \begin{bmatrix} x_1 \pm y_1 \\ x_2 \pm y_2 \\ \cdot \\ \cdot \\ \cdot \\ x_n \pm y_n \end{bmatrix} \tag{A-4}$$



Clearly, these two last operations make sense only with vectors of the *same* dimensionality.

The following properties apply to the defined operations:

$$\begin{aligned} \mathbf{x} + \mathbf{y} &= \mathbf{y} + \mathbf{x} \\ \mathbf{x} + (\mathbf{y} + \mathbf{z}) &= (\mathbf{x} + \mathbf{y}) + \mathbf{z} \\ \lambda_1(\lambda_2\mathbf{x}) &= (\lambda_1\lambda_2)\mathbf{x} \\ (\lambda_1 + \lambda_2)\mathbf{x} &= \lambda_1\mathbf{x} + \lambda_2\mathbf{x} \\ \lambda(\mathbf{x} + \mathbf{y}) &= \lambda\mathbf{x} + \lambda\mathbf{y} \\ 0\mathbf{x} &= \mathbf{0} \end{aligned}$$

### A-1.3 THE INNER VECTOR PRODUCT

The so-called *inner*, or *scalar*, multiplication of two vectors $\mathbf{x}$ and $\mathbf{y}$ *of equal dimension* results in a very useful product. This multiplication is defined by

$$\mathbf{x}^T\mathbf{y} \triangleq \sum_{i=1}^{n} x_i y_i \tag{A-5}$$

Our chosen symbol $\mathbf{x}^T\mathbf{y}$ will be explained later in connection with matrix multiplication. In addition to this symbol, one often finds one of the following:

$$\mathbf{x} \cdot \mathbf{y}$$
$$(\mathbf{x},\mathbf{y})$$
$$\langle \mathbf{x},\mathbf{y} \rangle$$

(It should be noted that other *useful* vector products exist, for instance, the so-called *cross product* in three-dimensional space. However, for our present objectives, the inner product will suffice.)

Consider the two vectors $\mathbf{x}$ and $\mathbf{y}$ in ordinary two-space, defined by

$$\mathbf{x} = \begin{bmatrix} x_1 \\ x_2 \end{bmatrix} \triangleq \begin{bmatrix} |\mathbf{x}| \cos\alpha \\ |\mathbf{x}| \sin\alpha \end{bmatrix}$$

$$\mathbf{y} = \begin{bmatrix} y_1 \\ y_2 \end{bmatrix} \triangleq \begin{bmatrix} |\mathbf{y}| \cos\beta \\ |\mathbf{y}| \sin\beta \end{bmatrix}$$

and shown in Fig. A-1. $|\mathbf{x}|$ and $|\mathbf{y}|$ represent here the geometric length of each vector.

From the definition of inner product, we have

$$\begin{aligned} \mathbf{x}^T\mathbf{y} \triangleq x_1y_1 + x_2y_2 &= |\mathbf{x}|\,|\mathbf{y}|\,(\cos\alpha\cos\beta + \sin\alpha\sin\beta) \\ &= |\mathbf{x}|\,|\mathbf{y}|\cos(\alpha - \beta) = |\mathbf{x}|\,|\mathbf{y}|\cos\theta \end{aligned}$$

We also note that

$$\mathbf{x}^T\mathbf{x} = x_1x_1 + x_2x_2 = |\mathbf{x}|^2$$

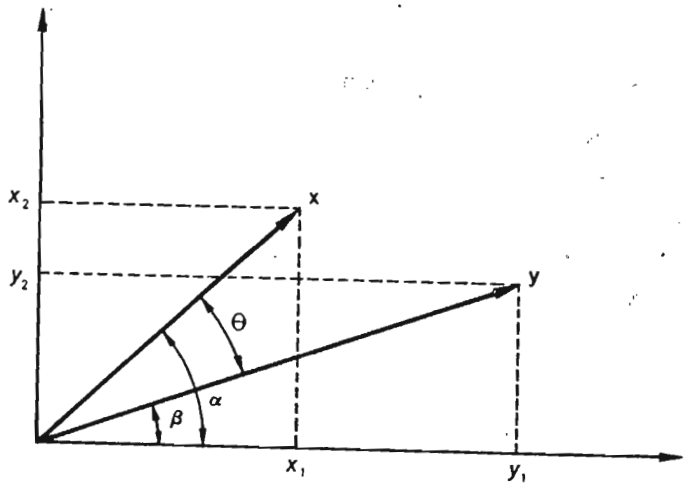


**Fig. A-1** Two-dimensional vectors.

and

$$\mathbf{y}^T\mathbf{y} = |\mathbf{y}|^2$$

We conclude, therefore, that the inner product between $\mathbf{x}$ and $\mathbf{y}$ indicates the *degree of parallelism* between the two vectors, and the inner product of $\mathbf{x}$ by itself gives information about the length of the vector.

By extending the concepts of *length* $|\mathbf{x}|$ and *angle* $\theta$ between vectors to $n$-dimensional space, we get

$$|\mathbf{x}|^2 \triangleq \mathbf{x}^T\mathbf{x}$$

$$\cos\theta \triangleq \frac{\mathbf{x}^T\mathbf{y}}{|\mathbf{x}|\,|\mathbf{y}|} \tag{A-6}$$

It is not possible to visualize these concepts beyond $n = 3$.

Note that if $\mathbf{x}$ is *normalized* (i.e., the length $|\mathbf{x}|$ equals unity), then we have

$$|\mathbf{y}|\cos\theta = \mathbf{x}^T\mathbf{y}$$

*In words*, the inner product gives us the *projection of* $\mathbf{y}$ *on* $\mathbf{x}$.

Two *nonzero* vectors are said to be *orthogonal* if

$$\mathbf{x}^T\mathbf{y} = 0 \tag{A-7}$$

(The scalar product of the "sum vector" and $\mathbf{x}$ equals

$$\mathbf{1}^T\mathbf{x} = \sum_{i=1}^{n} x_i$$

and this explains the name.)



The following rules for scalar products are easily verified:

$$\begin{aligned}
\mathbf{x}^T(\mathbf{y}+\mathbf{z}) &= \mathbf{x}^T\mathbf{y} + \mathbf{x}^T\mathbf{z}\\
(\mathbf{x}+\mathbf{y})^T\mathbf{z} &= \mathbf{x}^T\mathbf{z} + \mathbf{y}^T\mathbf{z}\\
\mathbf{x}^T(\lambda\mathbf{y}) &= \lambda\mathbf{x}^T\mathbf{y}\\
(\lambda\mathbf{x}^T)\mathbf{y} &= \lambda(\mathbf{x}^T\mathbf{y})
\end{aligned} \tag{A-8}$$

**Example A-1** In a rectangular three-dimensional coordinate system we have the two vectors

$$\mathbf{x} = \begin{bmatrix}1\\2\\3\end{bmatrix} \quad \text{and} \quad \mathbf{y} = \begin{bmatrix}1\\1\\1\end{bmatrix}$$

Find the angle $\theta$ between these vectors. We have

$$|\mathbf{x}| = \sqrt{1+4+9} = \sqrt{14}$$

$$|\mathbf{y}| = \sqrt{1+1+1} = \sqrt{3}$$

$$\mathbf{x}^T\mathbf{y} = 1+2+3 = 6$$

$$\therefore \cos\theta = \frac{6}{\sqrt{14}\times\sqrt{3}} = 0.928$$

and

$$\theta = 68.0°$$

## A-2 MATRICES

An $m \times n$ matrix $\mathbf{A}$ is defined as a rectangular array of $mn$ numbers

$$\mathbf{A} \triangleq \begin{bmatrix} a_{11} & a_{12} & \cdots & a_{1n}\\ a_{21} & a_{22} & \cdots & a_{2n}\\ \cdots & \cdots & \cdots & \cdots\\ a_{m1} & a_{m2} & \cdots & a_{mn}\end{bmatrix} \triangleq [a_{ij}] \tag{A-9}$$

The $mn$ numbers $a_{ij}$ are referred to as the *matrix elements*.

The integers $m$ and $n$ associated with an $m \times n$ matrix refer to the numbers of rows and columns, respectively.

An $n \times n$ matrix is called a *square matrix*, of *order n*.

An $m \times 1$ matrix is a *column vector* obeying all the rules of the preceding section.

A $1 \times n$ matrix is a *row vector*.

## A-2.1 ELEMENTARY MATRIX OPERATIONS

Two matrices **A** and **B** are said to be equal if and only if

$$a_{ij} = b_{ij} \qquad \text{for } i = 1, 2, \ldots, m, \quad j = 1, 2, \ldots, n$$

In such a case, we write

$$\mathbf{A} = \mathbf{B}$$

A matrix is multiplied by a scalar $\lambda$ if all $mn$ elements are multiplied by $\lambda$, that is,

$$\lambda\mathbf{A} = \mathbf{A}\lambda \triangleq \begin{bmatrix} \lambda a_{11} & \cdots & \lambda a_{1n} \\ \cdots & \cdots & \cdots \\ \lambda a_{m1} & \cdots & \lambda a_{mn} \end{bmatrix} \tag{A-10}$$

*Addition* and *subtraction* of two matrices result in new matrices in accordance with

$$\mathbf{A} \pm \mathbf{B} \triangleq \begin{bmatrix} a_{11} \pm b_{11} & \cdots & a_{1n} \pm b_{1n} \\ \cdots & \cdots & \cdots \\ a_{m1} \pm b_{m1} & \cdots & a_{mn} \pm b_{mn} \end{bmatrix} \tag{A-11}$$

Clearly, these operations apply only to matrices with the same number of rows and columns.

*Matrix multiplication* is defined to facilitate the operations necessary in connection with *linear transformations*. Consider the linear transformation

$$\begin{aligned} y_1 &= a_{11}x_1 + a_{12}x_2 + \cdots + a_{1n}x_n \\ y_2 &= a_{21}x_1 + a_{22}x_2 + \cdots + a_{2n}x_n \\ &\cdots\cdots\cdots\cdots\cdots\cdots\cdots \\ y_m &= a_{m1}x_1 + a_{m2}x_2 + \cdots + a_{mn}x_n \end{aligned} \tag{A-12}$$

or

$$y_i = \sum_{j=1}^{n} a_{ij}x_j \qquad \text{for } i = 1, 2, \ldots, m \tag{A-13}$$

We now can consider *formally* the $a_{ij}$'s as elements in an $m \times n$ matrix **A** and write the above equations in *compact* form:

$$\mathbf{y} = \mathbf{A}\mathbf{x} \tag{A-14}$$

This symbolism will have no meaning, of course, *until we prescribe that the product* **Ax** *will mean an m vector whose ith component will be defined by* (A-13).

This fully defines the *matrix-vector product*. In itself, this new concept would be useful only as a shorthand notation. The full power of the concept of matrix multiplication will be evident only upon definition of a



*matrix-matrix product*. Consider for that purpose a new linear transformation

$$\begin{aligned} x_1 &= b_{11}z_1 + b_{12}z_2 + \cdots + b_{1p}z_p \\ x_2 &= b_{21}z_1 + b_{22}z_2 + \cdots + b_{2p}z_p \\ &\cdots\cdots\cdots\cdots\cdots\cdots\cdots \\ x_n &= b_{n1}z_1 + b_{n2}z_2 + \cdots + b_{np}z_p \end{aligned} \tag{A-15}$$

or

$$x_k = \sum_{r=1}^{p} b_{kr}z_r \qquad \text{for } k = 1, 2, \ldots, n \tag{A-16}$$

Using the accepted shorthand notation, we can also write the last equations

$$\mathbf{x} = \mathbf{B}\mathbf{z} \tag{A-17}$$

where **B** is an $n \times p$ matrix, and **z** a $p$ vector.

By substituting Eq. (A-16) into Eq. (A-13), we can eliminate the $x$ components, and we end up with the following $m$ relations between **y** and **z**:

$$y_i = \sum_{j=1}^{n} a_{ij} \sum_{r=1}^{p} b_{jr}z_r \qquad \text{for } i = 1, 2, \ldots, m \tag{A-18}$$

We rearrange the summation signs in this last expression:

$$y_i = \sum_{r=1}^{p} \left( \sum_{j=1}^{n} a_{ij}b_{jr} \right) z_r \qquad \text{for } i = 1, 2, \ldots, m \tag{A-19}$$

and by introduction of the $mp$ new $c$ coefficient, defined by

$$c_{ir} \triangleq \sum_{j=1}^{n} a_{ij}b_{jr} \qquad \text{for } i = 1, 2, \ldots, m, \; r = 1, 2, \ldots, p \tag{A-20}$$

we can write the $m$ equations (A-19) as

$$y_i = \sum_{r=1}^{p} c_{ir}z_r \qquad \text{for } i = 1, 2, \ldots, m \tag{A-21}$$

Suppose that, instead, we *formally* had eliminated the **x** vector in Eq. (A-14) by using the vector equation (A-17), i.e.,

$$\mathbf{y} = \mathbf{A}\mathbf{B}\mathbf{z} \tag{A-22}$$

Since we can consider Eq. (A-21) a vector equation,

$$\mathbf{y} = \mathbf{C}\mathbf{z} \tag{A-23}$$

where the $m \times p$ matrix **C** is defined by Eq. (A-20); it is at this point quite obvious *that we have indeed defined a matrix product*

$$\mathbf{C} \triangleq \mathbf{A}\mathbf{B} \tag{A-24}$$

*where the mp equations* (A-20) *constitute the rule for multiplication of* **A** *and* **B**.

We note immediately that this product matrix is defined only if the number of columns in **A** equals the number of rows in **B**.

We note also from the definition that, in general,

$$\mathbf{AB} \neq \mathbf{BA}$$

(Indeed, unless $p$ equals $m$, the product **BA** is not even defined.)

If **AB** and **BA** are both defined and if

$$\mathbf{AB} = \mathbf{BA}$$

then the matrices are said to *commute*.

The associative and distributive laws hold for matrix multiplication (when the appropriate operations are defined); i.e.,

$$\begin{aligned} (\mathbf{AB})\mathbf{C} &= \mathbf{A}(\mathbf{BC}) = \mathbf{ABC} \\ \mathbf{A}(\mathbf{B} + \mathbf{C}) &= \mathbf{AB} + \mathbf{AC} \end{aligned} \tag{A-25}$$

**Example A-2** Given the two matrices

$$\mathbf{A} = \begin{bmatrix} 2 & 0 \\ 3 & 1 \\ 1 & 1 \end{bmatrix} \qquad \mathbf{B} = \begin{bmatrix} 1 & 3 & 1 \\ 0 & -1 & 2 \end{bmatrix}$$

Find **AB** and **BA**.

From the definition we have

$$\mathbf{AB} = \begin{bmatrix} 2 & 0 \\ 3 & 1 \\ 1 & 1 \end{bmatrix} \begin{bmatrix} 1 & 3 & 1 \\ 0 & -1 & 2 \end{bmatrix} = \begin{bmatrix} 2 & 6 & 2 \\ 3 & 8 & 5 \\ 1 & 2 & 3 \end{bmatrix}$$

$$\mathbf{BA} = \begin{bmatrix} 1 & 3 & 1 \\ 0 & -1 & 2 \end{bmatrix} \begin{bmatrix} 2 & 0 \\ 3 & 1 \\ 1 & 1 \end{bmatrix} = \begin{bmatrix} 12 & 4 \\ -1 & 1 \end{bmatrix}$$

### A-2.2 SPECIAL MATRICES

The *null matrix* **0** is defined by

$$\mathbf{0} \triangleq \begin{bmatrix} 0 & \cdots & 0 \\ \cdots & \cdots & \cdots \\ 0 & \cdots & 0 \end{bmatrix} \tag{A-26}$$

For a mull matrix, we have

$$\begin{aligned} \mathbf{A} + \mathbf{0} &= \mathbf{A} \\ \mathbf{A0} = \mathbf{0A} &= \mathbf{0} \\ \mathbf{A} - \mathbf{A} &= \mathbf{0} \end{aligned} \tag{A-27}$$



*Note:* In the *scalar* case, we know that the equation $ab = 0$ implies that either $a$ or $b$ or both are zero.

The matrix equation $\mathbf{AB} = \mathbf{0}$ does *not* imply the same thing, as is exemplified by the product

$$\begin{bmatrix} 1 & 4 \\ 0 & 0 \end{bmatrix} \begin{bmatrix} 4 & 0 \\ -1 & 0 \end{bmatrix} = \begin{bmatrix} 0 & 0 \\ 0 & 0 \end{bmatrix}$$

A matrix is referred to as *diagonal* if it is square ($m = n$) and if $a_{ij} = 0$ for $i \neq j$.

A diagonal matrix of special importance is the *identity matrix* **I**.

$$\mathbf{I} \triangleq \begin{bmatrix} 1 & & & 0 \\ & 1 & & \\ & & \cdot & \\ & & & \cdot \\ 0 & & & 1 \end{bmatrix} \tag{A-28}$$

For the **I** matrix, we have

$$\begin{aligned} \mathbf{IA} &= \mathbf{AI} = \mathbf{A} \\ \underbrace{\mathbf{II} \cdots \mathbf{I}}_{n \text{ times}} &\triangleq \mathbf{I}^n = \mathbf{I} \end{aligned} \tag{A-29}$$

The *transpose* $\mathbf{A}^T$ of a matrix **A** is formed by interchanging rows and columns.

Transposition follows the easily confirmed rules

$$\begin{aligned} (\mathbf{A} + \mathbf{B})^T &= \mathbf{A}^T + \mathbf{B}^T \\ (\mathbf{AB})^T &= \mathbf{B}^T\mathbf{A}^T \\ (\mathbf{A}^T)^T &= \mathbf{A} \end{aligned} \tag{A-30}$$

We now can explain better why we earlier denoted the inner vector product of **x** and **y** by the symbol $\mathbf{x}^T\mathbf{y}$.

The reason is, simply, that the two vectors $\mathbf{x}^T$ and **y**, viewed as $1 \times n$ and $n \times 1$ matrices, respectively, can be multiplied, and result in the $1 \times 1$ matrix (a scalar) defined by Eq. (A-5).

A matrix is *symmetric* if it satisfies the equation

$$\mathbf{A} = \mathbf{A}^T \tag{A-31}$$

### A-2.3 DETERMINANTS AND ADJUGATE (ADJOINT) MATRICES

Consider the $n \times n$ matrix **A**. Now select an element from each row and column of this matrix and form the following product of $n$ elements:

$$a_{1i}a_{2j}a_{3k} \cdots a_{nr}$$

The set of second subscripts $(i, j, k, \ldots, r)$ is a *permutation* of the set of integers $(1, 2, \ldots, n)$. We can form $n!$ different products of the above type. For example, in the case of a $3 \times 3$ matrix, the six products are

$$a_{11}a_{22}a_{33}$$
$$a_{12}a_{23}a_{31}$$
$$a_{13}a_{21}a_{32}$$
$$a_{11}a_{23}a_{32}$$
$$a_{12}a_{21}a_{33}$$
$$a_{13}a_{22}a_{31}$$

We define now the determinant $|\mathbf{A}|$:

$$|\mathbf{A}| \triangleq \sum (\pm)\, a_{1i}a_{2j}a_{3k} \cdots a_{nr} \tag{A-32}$$

The sum has to be extended over the $n!$ different permutations of the second subscripts. Each term will be assigned a sign (+ or −) in accordance with the following rule: If the permutation is *even*, use the + sign; if *odd*, use the − sign. [A permutation is even or odd depending upon the number of integer interchanges in the set $i, j, k, \ldots, r$. For example, the sequence 132 has one interchange, (3-2), and is therefore odd, whereas the sequence 231 has two, (2-1) and (3-1), and is thus even.]

For example, returning to the example of the $3 \times 3$ matrix, we find the determinant, in that case,

$$|\mathbf{A}| = a_{11}a_{22}a_{33} + a_{12}a_{23}a_{31} + a_{13}a_{21}a_{32} - a_{11}a_{23}a_{32} - a_{12}a_{21}a_{33} - a_{13}a_{22}a_{31}$$

The following properties of determinants can be deduced directly from the definition

$$\begin{aligned} |\mathbf{A}| &= |\mathbf{A}^T| \\ |\lambda\mathbf{A}| &= \lambda^n |\mathbf{A}| \qquad n \text{ is the order of } \mathbf{A} \\ |\mathbf{AB}| &= |\mathbf{A}|\,|\mathbf{B}| \end{aligned} \tag{A-33}$$

Another useful property is that an interchange of two columns or rows changes the sign of $|\mathbf{A}|$. We see that this follows directly from the definition when we realize that such an interchange changes all odd permutations to even, and vice versa. As a corollary, it follows that $|\mathbf{A}|$ must equal zero if the matrix has two equal rows or columns.

*Any* element $a_{ij}$ of $\mathbf{A}$ will appear as a factor in $(n-1)!$ of the $n!$ terms of $|\mathbf{A}|$. Furthermore, *each* of the $n$ elements of *any* particular row or column of $\mathbf{A}$ is a factor in *all* the $n!$ terms of $|\mathbf{A}|$. It is therefore possible to rearrange Eq. (A-32) into either of the following two alternative forms:

$$|\mathbf{A}| = \sum_{j=1}^{n} a_{ij}A_{ij} \qquad \text{or} \qquad \sum_{i=1}^{n} a_{ij}A_{ij} \tag{A-34}$$



where $i$ can be *any* row and $j$ *any* column. The $A_{ij}$'s, the so-called *cofactors*, will each contain a sum of $(n-1)!$ terms involving those $(n-1)^2$ elements not to be found in row $i$ and column $j$. By simple reasoning, we find that the rule for computing $A_{ij}$ is

$A_{ij} = (-1)^{i+j}$ times the determinant of the submatrix formed by deleting row $i$ and column $j$

From Eq. (A-34), we can derive an extremely useful relationship.

Consider the $n$ cofactors $A_{i1}, A_{i2}, \ldots, A_{in}$. They are evidently *completely independent* of the elements of row $i$. If, therefore, we replace these elements with those in row $k (k \neq i)$, we have, in effect, a matrix with two equal rows and therefore zero determinant. From Eq. (A-34), we thus obtain the relationship

$$\sum_{j=1}^{n} a_{kj}A_{ij} = 0 \qquad \text{for } k \neq i \tag{A-35}$$

By applying the same discussion to a column, we similarly get

$$\sum_{i=1}^{n} a_{ik}A_{ij} = 0 \qquad \text{for } k \neq j \tag{A-36}$$

At this time, we define an $n \times n$ matrix $\mathbf{A}^+$, having as elements the $A_{ji}$'s (note, *not* the $A_{ij}$'s) and referred to as the *adjugate*, or *adjoint*, of matrix $\mathbf{A}$, that is,

$$\mathbf{A}^+ \triangleq \begin{bmatrix} A_{11} & A_{21} & \cdots & A_{n1} \\ A_{12} & A_{22} & \cdots & A_{n2} \\ \cdots & \cdots & \cdots & \cdots \\ A_{1n} & A_{2n} & \cdots & A_{nn} \end{bmatrix} \tag{A-37}$$

Equations (A-34) to (A-36) represent a total of $2n^2$ scalar equations. By recalling the definition of a matrix product (A-20), we can summarize them all in the compact matrix formulas

$$\mathbf{AA}^+ = \mathbf{A}^+\mathbf{A} = |\mathbf{A}|\,\mathbf{I} \tag{A-38}$$

The reader will easily confirm this statement by simply writing the $2n^2$ scalar equations defined by Eq. (A-38) and noting that they are identical with Eqs. (A-34) to (A-36).

### A-2.4 THE MATRIX INVERSE

Consider the linear transformation

$$\mathbf{y} = \mathbf{Ax} \tag{A-39}$$

where $\mathbf{A}$ is a square matrix of order $n$, having a *nonzero* determinant.

Assume that we desire to solve the $x_i$'s from the $n$ Eqs. (A-39).

Intuitively, we feel that the solution should read

$$\mathbf{x} = \mathbf{B}\mathbf{y} \tag{A-40}$$

where $\mathbf{B}$ is one as yet unknown matrix.

If this solution is substituted back into Eq. (A-39), we obtain

$$\mathbf{y} = \mathbf{A}\mathbf{B}\mathbf{y}$$

On the other hand, if the original y vector is substituted into the solution equation (A-40), we have

$$\mathbf{x} = \mathbf{B}\mathbf{A}\mathbf{x} \tag{A-41}$$

In either case, if the solution is correct, we evidently must require that the $\mathbf{B}$ matrix satisfy

$$\mathbf{A}\mathbf{B} = \mathbf{B}\mathbf{A} = \mathbf{I} \tag{A-42}$$

A matrix $\mathbf{B}$ possessing this property is called the *inverse of* $\mathbf{A}$ and is designated with the special symbol $\mathbf{B} \triangleq \mathbf{A}^{-1}$.

By comparing Eqs. (A-42) with Eqs. (A-38), we find a matrix that satisfies our requirements, i.e.,

$$\mathbf{A}^{-1} = \frac{1}{|\mathbf{A}|}\mathbf{A}^{+} \tag{A-43}$$

It is simple to prove that the inverse is *unique*, so that indeed this $\mathbf{A}^{-1}$ is *the* one.

We can deduce the following properties characterizing the inverse:

$$\begin{aligned} &(\mathbf{AB})^{-1} = \mathbf{B}^{-1}\mathbf{A}^{-1} \\ &(\mathbf{A}^{-1})^{T} = (\mathbf{A}^{T})^{-1} \\ &(\mathbf{A}^{-1})^{-1} = \mathbf{A} \end{aligned} \tag{A-44}$$

**Example A-3** Given the matrix

$$\mathbf{A} = \begin{bmatrix} 1 & 2 \\ 3 & 4 \end{bmatrix}$$

Find its inverse.

We first compute the determinant

$$|\mathbf{A}| = 1 \times 4 - 3 \times 2 = -2$$

Then we compute the $n^2 = 4$ cofactors.

$$\begin{bmatrix} A_{11} & A_{12} \\ A_{21} & A_{22} \end{bmatrix} = \begin{bmatrix} 4 & -3 \\ -2 & 1 \end{bmatrix}$$



The adjoint matrix thus equals

$$\mathbf{A}^{+} = \begin{bmatrix} 4 & -2 \\ -3 & 1 \end{bmatrix}$$

From Eq. (A-43) we finally get

$$\mathbf{A}^{-1} = \frac{1}{-2}\begin{bmatrix} 4 & -2 \\ -3 & 1 \end{bmatrix} = \begin{bmatrix} -2 & 1 \\ 1.5 & -0.5 \end{bmatrix}$$

## REFERENCES

1. G. Hadley: "Linear Algebra," Addison-Wesley Publishing Company, Inc., Reading, Mass., 1961.
2. R. Bellman: "Introduction to Matrix Analysis," McGraw-Hill Book Company, New York, 1960.

# appendix B
# Computer Program For Solution of SLFE

We present a detailed computer program for solution of the SLFE and subsequent computation of line power flows. The actual computational results of an eight-bus example system are given. The system is presented in Fig. B-1.

Each line is represented by a $\pi$ link (Fig. B-2). The 14 lines of our example system are characterized by the series and shunt data shown on page 547.

The program converts (statements 0012 and 0013) the per mile data (YSHT and ZSER) into total line data (SHTY and SERZ) by multiplication by line length. (In our example system the data in Table B-1 are given as total data, and the LENGTH is thus set equal to unity.)

In statement 0014 the impedance data are converted to admittance.

Assembly of the bus admittance matrix (statements 0017 through 0020) follows the rule set out on page 223. Note that the network structure is given by the integers SB and EB, which carry the information about the terminal buses for the lines.







**Table B-1 Line data**

| *Line* | $Z_{ser}$, % | $Y_{sh}$, pu |
|---|---|---|
| 1 | $1.0 + j7.0$ | $j0.05$ |
| 2 | $0.2 + j1.0$ | 0 |
| 3 | $0.3 + j3.0$ | 0 |
| 4 | $0.8 + j6.5$ | $j0.03$ |
| 5 | $0.35 + j2.0$ | 0 |
| 6 | $0.75 + j6.3$ | $j0.06$ |
| 7 | $0.1 + j1.5$ | 0 |
| 8 | $0.25 + j2.3$ | 0 |
| 9 | $1.1 + j8.1$ | $j0.08$ |
| 10 | $0.32 + j3.0$ | 0 |
| 11 | $0.21 + j1.0$ | 0 |
| 12 | $0.2 + j1.3$ | 0 |
| 13 | $0.16 + j2.1$ | 0 |
| 14 | $0.21 + j3.11$ | 0 |

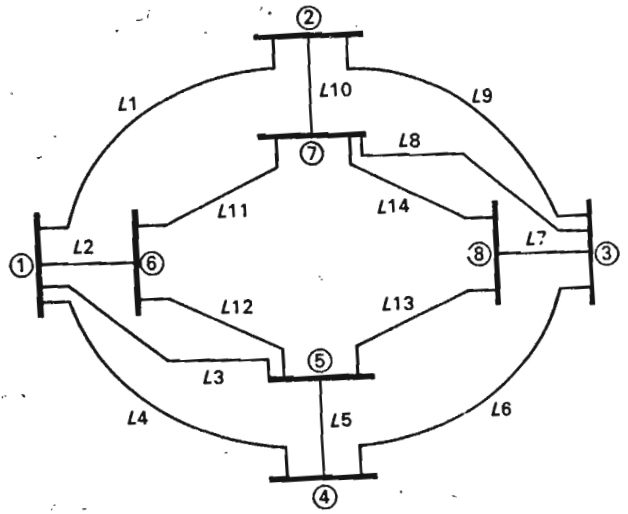


**Fig. B-1** Eight-bus example system.

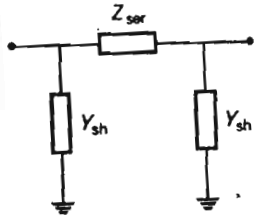


**Fig. B-2** $\pi$-representation of transmission lines.

Before the iterative computation can start, we must read in the bus power and voltage specifications (statements 0032 through 0035). In our example system these data are as follows

**Table B-2 Bus power and voltage specification**

| *Bus* | *Type* | *Bus power* | *Voltage* | $Q_{min}$ | $Q_{max}$ |
|---|---|---|---|---|---|
| 1 | 3 | Unspec. | $1.0 + j0.0$ | | |
| 2 | 2 | $-23.30 + j$ (Unspec.) | $\|V_2\| = 1.0$ | −10.00 | 10.00 |
| 3 | 2 | $15.00 + j$ (Unspec.) | $\|V_3\| = 1.0$ | −10.00 | 10.00 |
| 4 | 2 | $-20.00 + j$ (Unspec.) | $\|V_4\| = 1.0$ | −10.00 | 10.00 |
| 5 | 1 | $25.00 + j\,20.00$ | Unspec. | | |
| 6 | 1 | $-22.00 - j\,13.00$ | Unspec. | | |
| 7 | 1 | $25.00 + j\,00.00$ | Unspec. | | |
| 8 | 1 | $00.00 - j\,10.00$ | Unspec. | | |

The iterative computations of the SLFE follow closely the flow graph in Fig. 7-18 (statements 0037 through 0091). Gauss iterative technique is used.

When the iterations have converged the line powers are computed (statements 0094 through 0098).

Here follows the detailed program. At the end of the program is a printout showing the computer results for our example system.

**Computer program**

```
0001        COMPLEX YSHT,YSER,SERY,SHTY,Y,A,B,V,VI,VII,SUM,S,R,DX,ZSER,SERZ,
          1 VN
0002        INTEGER SB,EB
0003        REAL LENGTH,MAGV
0004        DIMENSION LINE(14),SB(14),EB(14),LENGTH(14),YSHT(14),YSER(14),
          1 SERY(14),SHTY(14),A(14),B(8,8),V(14),P(14),Q(14),QMAX(14),
          2 QMIN(14),VSPEC(14),Y(8,8),ZSER(14),SERZ(14),VN(8)
          C READ NUMBER OF BUSSES, NUMBER OF LINES, NUMBER OF VOLTAGE
          C CONTROL BUSSES INCLUDING SLACK BUS, ACCELERATION FACTOR
          C (1.0 IF NOT USED).
0005        READ(5,100) NB,NL,MB,ALPHA
0006        DO 1 I = 1,NB
0007        DO 1 J = 1,NB
0008      1 Y(I,J) = CMPLX(0.0,0.0)
0009        DO 2 I = 1,NL
          C READ LINE NUMBER, STARTING BUS, END BUS, LENGTH, SHUNT
          C ADMITTANCE AND SERIES IMPEDANCE IN P.U. — PER UNIT LENGTH.
0010        READ(5,100) LINE(I),SB(I),EB(I),LENGTH(I),YSHT(I),ZSER(I)
0011      100 FORMAT(3I5,F5.1,4E10.3)
0012        SHTY(I) = YSHT(I) * LENGTH(I)
0013        SERZ(I) = ZSER(I) * LENGTH(I)
0014        SERY(I) = 1.0/SERZ(I)
          C ASSEMBLE THE BUS ADMITTANCE MATRIX.
0015        L = SB(I)
```



**Computer program** *(Continued)*

```
0016        M = EB(I)
0017        Y(L,L) = Y(L,L) + SERY(I) + SHTY(I)/2.
0018        Y(M,M) = Y(M,M) + SERY(I) + SHTY(I)/2.
0019        Y(L,M) = Y(L,M) − SERY(I)
0020      2 Y(M,L) = Y(M,L) − SERY(I)
          C WRITE OUT THE INPUT LINE DATA AND THE Y BUS MATRIX.
0021        WRITE(6,101)
0022      101 FORMAT('1',T38,'LINE DATA'//T8,'LINE',T15,'SB',T19,'EB',T24,
          1 'LENGTH',T36,'SHUNT ADMITTANCE',T58,'SERIES IMPEDANCE'/)
0023        DO 3 I = 1,NL
0024      3 WRITE(6,102) LINE(I),SB(I),EB(I),LENGTH(I),SHTY(I),SERZ(I)
0025      102 FORMAT(' ',T6,3I5,F8.1,4X,2F9.4,4X,2F9.4)
0026        WRITE(6,103)
0027      103 FORMAT(////T10,'BUS ADMITTANCE MATRIX'//)
0028        DO 4 I = 1,NB
0029      4 WRITE(6,104) (Y(I,J),J=1,NB)
0030      104 FORMAT(2(4(F9.4,1X,F9.4,3X)/))
0031        K = MB + 1
          C READ IN SPECIFIED BUS DATA, REAL POWER, REACTIVE POWER,
          C REFERENCE VOLTAGE V1, VOLTAGE CONTROL BUS MAGNITUDES AND
            REACTIVE POWER LIMITS.
0032        READ(5,105) (P(I),I=2,NB)
0033        READ(5,105) (Q(I),I=K,NB)
0034        READ(5,105) V(1),(VSPEC(I),I=2,MB)
0035        READ(5,105) (QMIN(I),QMAX(I),I=2,MB)
0036      105 FORMAT(8F10.3)
          C INITIALIZE UNKNOWN VOLTAGES AND REACTIVE POWERS.
0037        DO 5 I = 2,NB
0038        IF(I.LT.K) Q(I) = 0.0
0039        V(I) = CMPLX(1.0,0.0)
          C CALCULATE NECESSARY CONSTANTS A(I) AND B(I).
0040        IF(I.GT.MB) A(I) = (CMPLX(P(I),−Q(I)))/Y(I,I)
0041        DO 5 J = 1,NB
0042      5 IF(I.NE.J) B(I,J) = Y(I,J)/Y(I,I)
          C INITIALIZE CONSTANTS AND BEGIN VOLTAGE ITERATIONS.
0043        N = 0
0044      6 DVMAX = 0.0
0045        I = 2
0046      7 VII = V(I)
0047        IF(I − MB) 8,8,15
          C FOR VOLTAGE CONTROL BUSSES ADJUST VOLTAGE TO SPECIFIED
          C MAGNITUDE AND CALCULATE REACTIVE POWER, IF Q LIMITS ARE
          C EXCEEDED SET Q EQUAL TO THE LIMIT AND RETURN VOLTAGE TO
          C PREVIOUS VALUE, CALCULATE A(I).
0048      8 V(I) = (V(I)/CABS(Y(I))) * VSPEC(I)
0049        SUM = CMPLX(0.0,0.0)
0050        DO 9 L = 1,NB
0051      9 SUM = SUM + Y(I,L) * V(L)
0052        Q(I) = −AIMAG(SUM * CONJG(V(I)))
0053        IF(Q(I) − QMAX(I)) 10,14,11
0054      10 IF(Q(I) − QMIN(I)) 12,14,14
0055      11 Q(I) = QMAX(I)
0056        GO TO 13
```

**Computer program** *(Continued)*

```
0057      12 Q(I) = QMIN(I)
0058      13 V(I) = VII
0059      14 A(I) = (CMPLX(P(I), — Q(I)))/Y(I,I)
          C CALCULATE NU + 1 VOLTAGES.
0060      15 SUM = CMPLX(0.0,0.0)
0061         VI = V(I)
0062         DO 16 L = 1,NB
0063      16 IF(L.NE.I) SUM = SUM + B(I,L) * V(L)
0064         VN(I) = A(I)/CONJG(V(I)) — SUM
0065         DX = VN(I) — VI
0066         VN(I) = VI + ALPHA * DX
          C DETERMINE MAXIMUM VOLTAGE DIFFERENCE BETWEEN ITERATIONS.
0067         DELV = CABS(VN(I) — VII)
0068         IF(DELV.GE.DVMAX) DVMAX = DELV
0069         I = I + 1
0070         IF(I.LE.NB) GO TO 7
          C UPDATE VOLTAGES BY ONE ITERATION.
0071         DO 17 I = 2,NB
0072      17 V(I) = VN(I)
0073         N = N + 1
          C COMPARE MAXIMUM VOLTAGE DIFFERENCE AGAINST CONVERGENCE
          C CRITERIA.
0074         IF(DVMAX.LE.1.0E—04) GO TO 19
          C LIMIT ITERATIONS AS A PROTECTION AGAINST DIVERGENCE.
0075         IF (N.LT.50) GO TO 18
0076         WRITE(6,106) N
0077      106 FORMAT(////,T10,'CONVERGENCE NOT OBTAINED IN',I3,' ITERATIONS')
0078         GO TO 23
0079      18 GO TO 6
          C CONVERGENCE OBTAINED — CALCULATE SLACK BUS POWER.
0080      19 SUM = CMPLX(0.0,0.0)
0081         DO 20 I = 1,NB
0082      20 SUM = SUM + Y(1,I) * V(I)
0083         P(1) = REAL(SUM * CONJG(V(1)))
0084         Q(1) = —AIMAG(SUM * CONJG(V(1)))
          C WRITE OUT BUS DATA.
0085         WRITE(6,107) N
0086      107 FORMAT('1',T6,'GAUSS ITERATIVE TECHNIQUE CONVERGED IN',I3,
            1 'ITERATIONS'//T6,'BUS',T16,'VOLTAGE',T30,'MAGNITUDE',T42,
            2 'DELTA(DEGS)',T57,'REAL POWER',T69,'REACTIVE POWER'/)
0087         DO 21 I = 1,NB
0088         DELTA = ATAN2(AIMAG(V(I)),REAL(V(I))) * 57.29578
0089         MAGV = CABS(V(I))
0090      21 WRITE(6,108) I,V(I),MAGV,DELTA,P(I),Q(I)
0091      108 FORMAT(' ',I7,2X,2F8.4,4X,F7.4,4X,F9.5,6X,F8.4,6X,F8.4)
          C CALCULATE AND WRITE OUT LINE FLOWS.
0092         WRITE(6,109)
0093      109 FORMAT(////T25,'LINE FLOW'//T8,'LINE',T15,'SB',T20,'EB',T27,
            1 'REAL POWER',T39,'REACTIVE POWER'/)
0094         DO 22 I = 1,NL
0095         L = SB(I)
0096         M = EB(I)
0097         S = V(L) * CONJG((V(L) — V(M))*SERY(I) + V(L)*(SHTY(I)/2.))
```



**Computer program** *(Continued)*

```
0098         R = V(M) * CONJG((V(M) — V(L))*SERY(I) + V(M)*(SHTY(I)/2.))
0099         WRITE(6,110) LINE(I),L,M,S
0100      22 WRITE(6,110) LINE(I),M,L,R
0101      110 FORMAT(' ',T7,3I5,5X,F8.4,6X,F8.4)
0102      23 STOP
0103         END
```

**Printouts**

GAUSS ITERATIVE TECHNIQUE CONVERGED IN 40 ITERATIONS

| BUS | VOLTAGE | | MAGNITUDE | DELTA(DEGS) | REAL BUS POWER | REACTIVE BUS POWER |
|---|---|---|---|---|---|---|
| 1 | 1.0000 | 0.0 | 1.0000 | 0.0 | 3.4386 | 5.6820 |
| 2 | 0.9515 | —0.3077 | 1.0000 | —17.92220 | —23.3000 | 9.7960 |
| 3 | 0.9827 | 0.1853 | 1.0000 | 10.67595 | 15.0000 | 6.9111 |
| 4 | 0.9900 | —0.1413 | 1.0000 | —8.12036 | —20.0000 | 2.8630 |
| 5 | 1.0509 | 0.1152 | 1.0572 | 6.25464 | 25.0000 | 20.0000 |
| 6 | 0.9276 | 0.0057 | 0.9276 | 0.35247 | —22.0000 | —13.0000 |
| 7 | 0.9435 | 0.1414 | 0.9540 | 8.52400 | 25.0000 | 0.0 |
| 8 | 0.9235 | 0.1465 | 0.9350 | 9.01675 | 0.0 | —10.0000 |

LINE FLOW

| LINE | SB | EB | REAL POWER | REACTIVE POWER |
|---|---|---|---|---|
| 1 | 1 | 2 | 4.4052 | 0.0388 |
| 1 | 2 | 1 | —4.2111 | 1.2699 |
| 2 | 1 | 6 | 0.8435 | 7.0708 |
| 2 | 6 | 1 | —0.7421 | —6.5638 |
| 3 | 1 | 5 | —3.9695 | —1.3010 |
| 3 | 5 | 1 | 4.0219 | 1.8245 |
| 4 | 1 | 4 | 2.1594 | —0.1267 |
| 4 | 4 | 1 | —2.1220 | 0.4006 |
| 5 | 4 | 5 | —12.9387 | 1.0583 |
| 5 | 5 | 4 | 13.5286 | 2.3123 |
| 6 | 3 | 4 | 5.1424 | 0.2043 |
| 6 | 4 | 3 | —4.9436 | 1.4051 |
| 7 | 3 | 8 | 2.0862 | 4.2198 |
| 7 | 8 | 3 | —2.0640 | —3.8874 |
| 8 | 3 | 7 | 1.7573 | 1.8378 |
| 8 | 7 | 3 | —1.7411 | —1.6891 |
| 9 | 2 | 3 | —5.6017 | 2.2269 |
| 9 | 3 | 2 | 6.0034 | 0.6510 |
| 10 | 2 | 7 | —13.4908 | 6.2998 |
| 10 | 7 | 2 | 14.2002 | 0.3507 |
| 11 | 6 | 7 | —12.3592 | 1.0452 |
| 11 | 7 | 6 | 12.7347 | 0.7426 |
| 12 | 5 | 6 | 9.2223 | 9.5216 |
| 12 | 6 | 5 | —8.9079 | —7.4779 |
| 13 | 5 | 8 | —1.7851 | 6.3434 |
| 13 | 8 | 5 | 1.8473 | —5.5275 |
| 14 | 7 | 8 | —0.2063 | 0.5979 |
| 14 | 8 | 7 | 0.2072 | —0.5842 |

(The line flows are defined positive when flowing out from the bus.)

# Index

# Index